DOCTOR OF PHILOSOPHY

Multiorgan imaging and multimorbidity prevention: Evidence from the heart-brain-liver axis in UK Biobank



Celeste M. A. McCracken
BCom, MCom, PGDipCom, MSc

Linacre College
Oxford Centre for Clinical Magnetic Resonance Research (OCMR)
Division of Cardiovascular Medicine, Radcliffe Department of Medicine
University of Oxford

Supervisors
Professor Stefan Neubauer, Professor Thomas Nichols, Professor Steffen Petersen

First submission: 12/09/2024; Final submission 13/01/2025
This thesis is submitted to the Division of Cardiovascular Medicine, University of Oxford in partial fulfilment of the requirements for the degree of Doctor of Philosophy

Declaration

I declare that this thesis is entirely my own work, and describes my own research, that I, myself have undertaken.

C. McCracken
Linacre College

Abstract

As populations age globally, multimorbidity (the coexistence of multiple chronic conditions) presents increasing challenges to clinicians, policymakers and patients. Despite widespread interest in addressing this issue, strategies for multimorbidity prevention are scarce, often targeting individual organ systems rather than considering the interconnections between them. This thesis uses the UK Biobank health research database to answer a series of questions regarding population-level multimorbidity prevention, expanding the traditional focus on atherosclerotic cardiovascular disease to include disease risk across the heart, brain, liver and kidneys. By taking an explicitly multiorgan approach, this research gathers evidence that could inform and elevate multi-disease prevention efforts.

We used multiorgan magnetic resonance imaging (MRI) in 30,444 participants to describe the significant cross-organ relationships between the heart, brain and liver. We found that liver impairment (in the form of elevated liver fat, fibrosis and liver iron) was linked to poorer cardiovascular function and adverse brain features (such as reduced brain volume and poorer white matter microstructure). Conversely, markers of healthy heart function were associated with larger brain volumes and fewer cerebrovascular plaques. Multiorgan modelling suggests that liver and heart health affect brain health directly and indirectly, in conjunction with common risk factors like diabetes, hypertension, and obesity.

Building on these findings, we evaluated the effectiveness of primary care health checks in preventing multiorgan disease. We analysed the multiorgan outcomes of 48,602 participants who received an NHS Health Check between 2009 and 2016, compared with extensively-matched controls, over an average follow-up of 9 years. Adjusted survival models demonstrated that NHS Health Check recipients experienced lower rates of heart, liver, and kidney disease, likely due to the earlier detection and management of risk factor conditions.

While the NHS Health Check showed benefits, our analysis also revealed limitations in its ability to predict, and therefore prevent, multimorbidity. Consequently, we explored the feasibility of expanding the NHS Health Check protocol to more effectively predict multiorgan risk. In a proof-of-concept analysis with 228,240 participants, we showed how the same information currently available as part of the NHS Health Check could be reconfigured to produce multiple risk estimates for diseases across the

heart, brain, liver and kidneys. This approach places multiorgan risk information at the fingertips of primary care physicians, enhancing prevention efforts by targeting multiple diseases simultaneously.

Finally, the thesis explores the role of imaging for multiorgan risk stratification. We showed that risk models incorporating imaging information were better at identifying people at risk for multiorgan disease than non-imaging methods. Cost-effectiveness analysis indicated that while imaging is expensive, there may be certain subgroups for whom such imaging could be cost effective. We develop and present a "first-in-line" methodology for modelling effectiveness scenarios of this type.

Altogether, these findings highlight the importance of a multiorgan awareness in healthcare delivery and prevention of disease in the heart-brain-liver-kidney cluster. We provide large-scale evidence and actionable recommendations for expanding existing preventive frameworks to better preserve multiorgan health. Further research is needed to refine these strategies and facilitate their practical implementation within the National Health Service.

Acknowledgements

I offer sincere thanks to my supervisory team; Stefan Neubauer, Thomas Nichols and Steffen Petersen, particularly Stefan Neubauer and all others involved in securing the funding for this project. This work is fully funded by the Imaging theme, within the NIHR Oxford Biomedical Research Centre. Group collaboration was also provided by Betty Raman, Michele Veldsman, Anya Topiwala, Masud Husain, Andrea Dennis and Adriana Roca-Fernandez. Many thanks to my collaborators at Barts Health and Queen Mary University of London, Steffen Petersen, the brilliant Zahra Raisi-Estabragh, Liliana Szabo and Jacqueline Cooper. And thank you to the half a million UK Biobank participants who have kindly donated their data.

Publications associated with this DPhil:

1 **McCracken C,** Raisi-Estabragh Z, Veldsman M, et al. Multi-organ imaging demonstrates the heart-brain-liver axis in UK Biobank participants. *Nature Communications*. 2022;**13**:7839.

2 **McCracken C**, Raisi-Estabragh Z, Raman B, et al. Healthier CMR phenotypes are linked to favourable brain MRI structure and function metrics in the UK Biobank. *Heart*. 2021;**107**:A4–5.

3 **McCracken C**, Raisi-Estabragh Z, Szabo L, et al. NHS Health Check attendance is associated with reduced multiorgan disease risk: a matched cohort study in the UK Biobank. *BMC Medicine*. 2024;**22**:1.

4 **McCracken C**, Raisi-Estabragh Z, Szabo L, et al. Feasibility of multiorgan risk prediction with routinely collected diagnostics: a prospective cohort study in the UK Biobank. *BMJ Evidence-Based Medicine*. Published Online First: 6 May 2024.

Other relevant publications:

5 **McCracken, C**, Condurache DG, Szabo L, et al, Predictive Performance of Cardiovascular Risk Scores in Cancer Survivors from the UK Biobank. JACC: *CardioOncology.* 2024;6(4): 575-588.

6 **McCracken C**, Szabo L, Abdulelah ZA, et al. Ventricular volume asymmetry as a novel imaging biomarker for disease discrimination and outcome prediction'. *European Heart Journal Open* 2024; 4(4): oeae059.

7 Ardissino M, **McCracken C**, Bard A, et al. Pericardial adiposity is independently linked to adverse cardiovascular phenotypes: a CMR study of 42 598 UK Biobank participants. *European Heart Journal - Cardiovascular Imaging*. 2022;jeac101.

8 Elghazaly H, **McCracken C**, Szabo L, et al. Characterizing the hypertensive cardiovascular phenotype in the UK Biobank. *European Heart Journal - Cardiovascular Imaging*. 2023;24:1352–60.

9 Jaggi A, Conole ELS, Raisi-Estabragh Z, **McCracken C**, et al. A structural heart-brain axis mediates the association between cardiovascular risk and cognitive function. *Imaging Neuroscience*. 2024;2:1–18.

10 Mahmood A, Simon J, Cooper J, **McCracken C**, et al. Neuroticism personality traits are linked to adverse cardiovascular phenotypes in the UK Biobank. *European Heart Journal - Cardiovascular Imaging*. 2023;jead166.

11 Pujadas ER, Raisi-Estabragh Z, Szabo L, **McCracken C**, et al. Prediction of incident cardiovascular events using machine learning and CMR radiomics. *European radiology.* 2023;33(5):3488-500.

12 Raisi-Estabragh Z, Cooper J, **McCracken C**, et al. Incident cardiovascular events and imaging phenotypes in UK Biobank participants with past cancer. *Heart*. 2023;109:1007–15.

13 Raisi-Estabragh Z, M'Charrak A, **McCracken C**, et al. Associations of cognitive performance with cardiovascular magnetic resonance phenotypes in the UK Biobank. *European Heart Journal - Cardiovascular Imaging*. 2022;**23**:663–72.

14 Raisi-Estabragh Z, **McCracken C**, Bethell MS, et al. Greater risk of severe COVID-19 in Black, Asian and Minority Ethnic populations is not explained by cardiometabolic, socioeconomic or behavioural factors, or by 25(OH)-vitamin D status: study of 1326 cases from the UK Biobank. *Journal of Public Health*. 2020;**42**:451–60.

15 Raisi-Estabragh Z, **McCracken C**, Condurache D-G, et al. Left atrial structure and function are associated with cardiovascular outcomes independent of left ventricular measures: a UK Biobank CMR study. *European Heart Journal - Cardiovascular Imaging*. 2021;jeac119.

16 Raisi-Estabragh Z, **McCracken C**, Cooper J, et al. Adverse cardiovascular magnetic resonance phenotypes are associated with greater likelihood of incident coronavirus disease 2019: findings from the UK Biobank. *Aging Clinical and Experimental Research*. 2021;**33**:1133–44

17 Raisi-Estabragh Z, **McCracken C**, Gkontra P, et al. Associations of Meat and Fish Consumption with Conventional and Radiomics Cardiovascular Magnetic Resonance Phenotypes in the UK Biobank. *Frontiers in Cardiovascular Medicine*. 2021;8:667849.

18 Raisi-Estabragh Z, **McCracken C**, Hann E, et al. Incident Clinical and Mortality Associations of Myocardial Native T1 in the UK Biobank. *JACC: Cardiovascular Imaging*. 2023;**16**:450–60.

19 Raisi-Estabragh Zahra, Szabo L, **McCracken C**, et al. Cardiovascular Magnetic Resonance Reference Ranges from the Healthy Hearts Consortium. *JACC: Cardiovascular Imaging*. 2024;**17**: 746-762

20 Raman B, **McCracken C**, Cassar MP, et al. Multiorgan MRI findings after hospitalisation with COVID-19 in the UK (C-MORE): a prospective, multicentre, observational cohort study. *The Lancet Respiratory Medicine*. 2023;**11**:1003-1019.

21 Roca-Fernandez A, Banerjee R, Thomaides-Brears H, **McCracken C**, et al. Liver disease is a significant risk factor for cardiovascular outcomes – A UK Biobank study. *Journal of Hepatology*. 2023;**79**:1085–95.

22 Samat AHA, Cassar MP, Akhtar AM, **McCracken C**, et al. Diagnostic utility of electrocardiogram for screening of cardiac injury on cardiac magnetic resonance in post-hospitalised COVID-19 patients: A prospective multicenter study. *International Journal of Cardiology*. 2024;132415.

23 Szabo L, **McCracken C**, Cooper J, et al. The role of obesity-related cardiovascular remodelling in mediating incident cardiovascular outcomes: a population-based observational study. *European Heart Journal - Cardiovascular Imaging.* 2023;jeac270.

24 Szabo L, Raisi-Estabragh Z, Salih A, **McCracken C**, et al. Clinician's guide to trustworthy and responsible artificial intelligence in cardiovascular imaging. *Frontiers in Cardiovascular Medicine*. 2022; 9:1016032.

Table of Contents

Declaration....2
Abstract....3
Acknowledgements....5
Publications associated with this DPhil:....6
Other relevant publications:....6
Table of Contents....8
List of Tables....10
List of Figures....11
Abbreviations....12

Chapter 1: Introduction....13

1.1 Multimorbidity....13
1.2 Preventive medicine and big data....15
1.3 Multimorbidity prevention in primary care....16
1.4 The heart-brain-liver-kidney (HBLK) cluster....17
1.5 Problem definition....19
1.6 Terms and assumptions....23

Chapter 2: Large-scale data, imaging biomarkers and prevention of multiorgan disease....25

2.1 The UK Biobank....26
2.2 The NHS Health Check....26
2.3 Magnetic resonance imaging (MRI) biomarkers of organ health....27
2.4 Relationships between the heart, brain, liver and kidney....30
2.5 The use of imaging in disease prevention....34

Chapter 3: Methods....38

3.1 Introduction....38
3.2 The UK Biobank Imaging Study....38
3.3 Study variables and data handling....39
3.4 Statistical analysis....48
3.5 Custom tools....51

Chapter 4: Multiorgan imaging and cross-organ associations....54

4.1 Introduction....54
4.2 Methods....56
4.3 Results....59
4.4 Discussion....72

Chapter 5: Prevention of multimorbidity: The NHS Health Check....77

5.1 Introduction....77
5.2 Methods....78
5.3 Results....84
5.4 Discussion....91

Chapter 6: Multiorgan risk assessment in primary care....95

6.1 Introduction....95
6.2 Methods....97
6.3 Results....106
6.4 Discussion....112

Chapter 7: The incremental value of imaging....115

7.1 Introduction....115
7.2 Methods....116
7.3 Results....122
7.4 Discussion....134

Chapter 8: The potential cost-effectiveness of imaging....139

8.1 Introduction....139
8.2 Methods....140
8.3 Results....144
8.4 Discussion....155

Chapter 9: Discussion....157

9.1 Summary of findings relating to research questions....157
9.2 Reflection on findings in the context of existing work....158
9.3 Limitations....162
9.4 Implications for clinical practice....166
9.5 Future research directions....170
9.6 Conclusion....174

References....176

Appendices....208

Appendix 1: Magnetic resonance imaging details....209
Appendix 2: Condition codes from UK Biobank records....211
Appendix 3: Published risk indices for heart-brain-liver-kidney risk....223
Appendix 4: Chapter 4 - Missingness in imaging variables....226
Appendix 5: Chapter 4 - Imaging variable orthogonalisation....227
Appendix 6: Chapter 5 - Codes for NHS Health Check exposure....228
Appendix 7: Chapter 5 - Missing value imputation details....228
Appendix 8: Chapter 5 - Visualisation of time-varying hazard effects....229
Appendix 9: Chapter 5 - Hazard ratios for NHS Health Check....230
Appendix 10: Chapter 5 - Sensitivity analysis with stratified time periods....231
Appendix 11: Chapter 5 - E-value lower bounds for significant hazard ratios....232
Appendix 12: Chapter 6 - Covariate handling, descriptive statistics and source IDs....233
Appendix 13: Chapter 6 - Biochemistry handling, descriptive statistics and source IDs....234
Appendix 14: Chapter 6 - Missing value imputation details....235
Appendix 15: Chapter 6 - Stability retention threshold evaluations....236
Appendix 16: Chapter 6 - Details of pairwise Cox analysis....237
Appendix 17: Chapter 6 - Performance of existing risk indices in the whole sample....240
Appendix 18: Chapter 6 - Model performance in the validation cohort....243
Appendix 19: Chapter 6 - Calibration plots....246
Appendix 20: Chapter 6 - Reclassification indices....247
Appendix 21: Chapter 6 - Remote model coefficients....248
Appendix 22: Chapter 6 - Standard model coefficients....249
Appendix 23: Chapter 6 - Extended model coefficients....250
Appendix 24: Chapter 7 - Hazard ratios (imaging vs non-imaging)....251
Appendix 25: Chapter 7 - Global performance scores....254
Appendix 26: Chapter 7 - Why is the sensitivity lower than expected?....256
Appendix 27: Chapter 7 - Decomposition of effects (AUC)....257
Appendix 28: Chapter 7 - Decomposition of effects (True positives)....258
Appendix 29: Chapter 7 - Decomposition of effects (Sensitivity)....259
Appendix 30: Chapter 8 - Subgroup structure....260
Appendix 31: Subgroup CE results for Combined HBLK (single model), with no filter....264
Appendix 32: Subgroup CE results for Combined HBLK (single model), above median risk....265
Appendix 33: Subgroup CE results for Aggregated HBLK risk (multi-model), with no filter....266
Appendix 34: Subgroup CE results for Aggregated HBLK risk (multi-model), risk ≥ 8....267
Appendix 35: Subgroup CE results for Aggregated HBLK risk (multi-model), risk ≥ 12....268

List of Tables

Table 3.1: Study outcomes across the heart-brain-liver-kidney (HBLK) cluster 42
Table 3.2: Summary of multiorgan imaging variables 44
Table 3.3: Existing population-level tools for HBLK disease risk 46
Table 3.4: Principles of the SPROUT framework 53
Table 4.1: Chapter 4 - Imaging metrics 56
Table 4.2: Chapter 4 - Sample characteristics 61
Table 4.3: Chapter 4 - Liver–brain associations 63
Table 4.4: Chapter 4 - Heart–brain associations 64
Table 4.5: Chapter 4 - Liver–heart associations 65
Table 4.6: Chapter 4 - Simultaneous liver-heart associations 66
Table 4.7: Chapter 4 - Simultaneous three-organ network models 67
Table 5.1: Chapter 5 - Sample characteristics 87
Table 6.1: Chapter 6 - Easily-collected features 100
Table 6.2: Chapter 6 - Sample characteristics 107
Table 7.1: Chapter 7 - Study variables 120
Table 7.2: Chapter 7 - Sample characteristics 123
Table 7.3: Chapter 7 - Imaging characteristics (selected variables) 124
Table 7.4: Chapter 7 - Multiorgan outcomes 125
Table 8.1: Chapter 8 - Health utility weights for multiorgan outcomes 141
Table 8.2: Chapter 8 - Subgroup grouping factors 144
Table 8.3: Chapter 8 - Global QALYs picked by imaging vs non-imaging risk models 145
Table 8.4: Chapter 8 - Global QALYs in aggregated risk models 149
Table 8.5: Chapter 8 - Example cost-effectiveness scenarios 154

List of Figures

Figure 1.1: Thesis roadmap overview 21
Figure 3.1: UK Biobank data schema for this project 40
Figure 3.2: Schema overview for the UK Biobank Outcomes Database 52
Figure 4.1: Chapter 4 - Roadmap location 54
Figure 4.2: Chapter 4 - Conceptual overview of the heart-brain-liver axis 55
Figure 4.3: Chapter 4 - Alternative forms considered for three-organ path analysis 58
Figure 4.4: Chapter 4 - Sample selection 60
Figure 4.5: Chapter 4 - Pairwise associations between heart, brain and liver 62
Figure 4.6: Chapter 4 - Simultaneous liver/heart associations with brain health 71
Figure 5.1: Chapter 5 - Roadmap location 77
Figure 5.2: Chapter 5 - Study sample selection 79
Figure 5.3: Chapter 5 - NHS Health Check records by year and record type 81
Figure 5.4: Chapter 5 - Summary of NHS Health Check in UK Biobank participants 85
Figure 5.5: Chapter 5 - Outcomes during follow-up in NHS Health Check recipients vs controls 89
Figure 5.6: Chapter 5 - Associations between NHS Health Check and incident outcomes 90
Figure 6.1: Chapter 6 - Roadmap location 95
Figure 6.2: Chapter 6 - What can existing information tell us about multiorgan disease risk? 98
Figure 6.3: Chapter 6 - Study sample and workflow 99
Figure 6.4: Chapter 6 - Existing risk scores and their constituents 102
Figure 6.5: Chapter 6 - Hazard ratios for incident outcomes by existing disease diagnoses at baseline 108
Figure 6.6: Chapter 6 - Performance of multiorgan risk scores in the validation set 111
Figure 7.1: Chapter 7 - Roadmap location 115
Figure 7.2: Chapter 7 - Comparison method overview 116
Figure 7.3: Chapter 7 - Sample selection 122
Figure 7.4: Chapter 7 - Significant imaging predictors – Brain outcomes 126
Figure 7.5: Chapter 7 - Significant imaging predictors – Arterial outcomes 127
Figure 7.6: Chapter 7 - Significant imaging predictors – Heart outcomes 129
Figure 7.7: Chapter 7 - Significant imaging predictors – Liver outcomes 131
Figure 7.8: Chapter 7 - Significant imaging predictors – Kidney outcomes 131
Figure 7.9: Chapter 7 - Significant imaging predictors - Combined HBLK outcomes 133
Figure 7.10: Chapter 7 - Discriminative accuracy (AUC) of imaging vs non-imaging models 133
Figure 7.11: Chapter 7 - Decomposition plots (AUC) 135
Figure 8.1: Chapter 8 - Roadmap location 139
Figure 8.2: Chapter 8 - Comparison method overview 143
Figure 8.3: Chapter 8 - Differences in QALYs picked up by imaging vs non-imaging models 146
Figure 8.4: Chapter 8 - Global incremental cost-effectiveness ratios (ICERS) 146
Figure 8.5: Chapter 8 - Differences in QALYs picked up in aggregated models 150
Figure 8.6: Chapter 8 - ICERs for aggregated risk models 150
Figure 8.7: Chapter 8 - Subgroup ICERs below £30,000 per QALY 152

Abbreviations

Abbreviation	Definition
ACVD	Arteriosclerotic cardiovascular disease
AoD	Aortic distensibility
BMI	Body mass index (kg/m2)
CIMT	Carotid intima-medial thickness
cT1	Corrected T1 relaxation time (ms)
EDV	End diastolic volume (e.g. LVEDV)
EF	Ejection fraction (e.g. LVEF)
eGFR	Estimated glomerular filtration rate
ESV	End systolic volume (e.g. LVESV)
FA	Fractional anisotropy
GLS	Global longitudinal strain
HBL	Heart-brain-liver
HBLK	Heart, brain, liver and kidney (including arterial disease)
ICVF	Intracellular volume fraction
ISOVF	Isotropic volume fraction
LV GFI	Left ventricular global function index
LV, RV	Left ventricular / right ventricular
LVM	Left ventricular mass
LVM/LVEDV	Left ventricular mass-to-volume ratio
MD	Mean diffusivity
MRI	Magnetic resonance imaging
NHS	National Health Service
PDFF	Proton density fat fraction (%)
SBP	Systolic blood pressure
SV	Stroke volume (e.g. LVSV)
WB-MRI	Whole-body MRI
WHR	Waist-hip ratio
WMH	White matter hyperintensities

Chapter 1: Introduction

This chapter lays out the literature supporting the foundation and general context for the thesis and presents the key objectives and research questions.

1.1 Multimorbidity

Non-communicable diseases are central to the global health burden of ageing populations [1]. Conditions such as heart disease, diabetes, cancer, and chronic respiratory diseases are now the leading causes of death worldwide, representing about 74% of all global mortalities [2]. These conditions also form the core of multimorbidity - the co-occurrence of two or more chronic conditions in one individual [3]. As populations age and lifestyle-related health conditions become more common, the global prevalence of multimorbidity has risen significantly [4, 5]. Currently, it affects an estimated 30% of adults aged 45-64 years, 65% of those aged 65-84 years, and up to 82% of individuals aged 85 years or above [6]. By 2050, the global population aged 60 and above is expected to double, reaching over 2 billion, further exacerbating the burden of multimorbidity [7].

The implications of multimorbidity are profound. At the individual level, multimorbidity is associated with a 2- to 4-fold increase in mortality risk [8, 9], a sharp decline in quality of life [10], and substantial increases in physical disability [11], psychological distress, and social isolation [12]. At the healthcare system level, multimorbidity drives up health expenditure, with affected individuals incurring costs that are two to three times higher than age-matched comparators [13]. It accounts for a disproportionate share of hospitalisations, frequent healthcare visits and polypharmacy, while also placing growing demands on social care services [13, 14]. For example, in the United Kingdom, treating patients with multimorbidity consumes over 50% of general practitioner consultations and nearly 80% of all prescription costs in primary care settings [15]

The urgency of addressing multimorbidity is well-recognised by key healthcare agencies, including the National Health Service (NHS) [16], the National Institute for Health and Care Research (NIHR) [17], the National Institute for Health and Care Excellence (NICE)[18] and the Academy of Medical Sciences UK [7]. Indeed, many organisations have identified multimorbidity as a strategic priority, with calls for innovative, evidence-based solutions to mitigate its impact [4, 19–21]. Despite the high level of interest, there remains a lack of research and consensus around effective strategies for multimorbidity

prevention. Therefore, at a high level, the research gap for this project is very broad, with supporting evidence needed in multiple aspects.

Researching multimorbidity in real-world populations is unusually difficult due to its inherent complexity. Considering the 'curse of dimensionality' already present in single-organ work (widely acknowledged as the main challenge to data interpretation [22, 23]), adding a multiorgan dimension can feel almost prohibitive. There is no accepted method for measuring multimorbidity risk. Multimorbidity itself can be measured using simple or weighted counts of conditions [24–27], including the recently developed Cambridge Multimorbidity Score [28]. However, the criteria used to measure multimorbidity can vary widely across studies, with variation that is also present in research detailing multimorbidity trajectories over time [29–31].

The interactions between multiple chronic conditions can be complex and poorly understood. Conditions may influence each other in ways that exacerbate health outcomes, complicate access to health services, or affect the efficacy of treatments [32]. The development of multimorbidity can be latent, lengthy and highly variable. A wide range of conditions can co-occur in countless combinations. Although there has been significant work in identifying commonly occurring clusters of conditions [33–35] (see Section 1.4 below), there is variation in commonly observed multimorbidity combinations. This lack of standardisation complicates the comparison of research findings, hampers the accumulation of a coherent body of evidence, and makes it difficult to draw broad conclusions about best practices [36]. In addition, we argue that the complexity and longer-term nature of multimorbidity development signal a potentially growing role for evidence derived from big data registry research [37], rather than randomised control trials, which are currently considered the gold standard.

In summary, multimorbidity is an important but highly challenging research area that is currently substantively and methodologically underserved. An understanding of multiorgan health is essential to the design of multimorbidity prevention strategies. By leveraging tools like multiorgan imaging and integrating them with population-level data, researchers can be better placed to identify at-risk individuals, elucidate disease mechanisms, and evaluate the impact of preventative interventions.

1.2 Preventive medicine and big data

Benjamin Franklin's 1735 assertion that "an ounce of prevention is worth a pound of cure" [38] is broadly accepted by both physicians [39] and the general public [40]. Nevertheless, nearly three hundred years later, there is still significant tension around preventive spending in a health system that is resource-constrained and built mainly around reactive care [41]. At its core, it is (and likely always will be) notoriously challenging to assess the effectiveness of preventive interventions by measuring outcomes and costs that don't eventuate, particularly long-term benefits that may be even less quantifiable [42].

Even so, disease prevention is a core objective of public health, according to the often-cited first definition given by Charles-Edward Winslow (1877-1957):

> *"Public health is the science and the art of preventing disease, prolonging life, and promoting physical health and efficiency through organised [societal], community [and individual] efforts ... for the early diagnosis and preventive treatment of disease" ([43]p. 30)*

These themes were echoed by Professor Sir Richard Doll (1912-2005), for whom the objectives of preventive medicine were "to prolong life, reduce disability, and to take those specific measures to reduce the incidence of disease" ([44], p.3). Dr Gerald Caplan (1917-2008) further proposed the three-tier preventive model that is still in use today: primary prevention aims to prevent disease before it occurs, secondary prevention focuses on early detection and treatment to slow the progression of disease, and tertiary prevention seeks to minimise and manage the consequences of existing disease [45, 46]. These definitions were comprehensively expanded by Geoffrey Rose (1926-1993), who described in detail the tension between the "high-risk strategy", wherein health interventions are targeted towards those perceived to be at highest risk, and a "population strategy", which aims to lift health conditions incrementally across the entire population [47]. First published in 1993, Rose's highly influential work emphasised that the motivations for disease prevention are both economic and moral and that in any health system, there are inefficiencies and inequalities that can be translated into tangible benefits.

Since these beginnings, academic work at all levels of preventive medicine has proliferated, providing voluminous evidence on the mechanisms of disease development, the epidemiological understanding of risk factors, the effectiveness of early detection screenings, and the complex interface between health belief and behaviour change [48].

In the mid-2010s, advanced computing and big data capabilities began to transform the landscape of research in all areas of population health [49, 50], with vast quantities of health-related information collected and computerised as part of routine care. In the past ten years, new streams of research have emerged, examining the ways that big data is revolutionising preventive medicine by integrating population statistics, electronic health records (EHRs), medical imaging, genetic profiling, and biometric monitoring [49]. These disciplines are set to become even more sophisticated in coming years, enabling early detection of epidemics and environmental hazards [51], optimisation of resource allocation across different population groups [52], the personalisation of preventive strategies [53, 54] and the iterative improvement of health programmes, ensuring that preventive measures are safe, effective and efficient [50, 55, 56].

Despite the long-recognised conceptual value of disease prevention, significant challenges and tensions remain in effectively planning, implementing and evaluating preventive interventions. On the other hand, advancements in health data science and big data analytics are creating new avenues for complex, real-world preventive research [49]. In particular, large-scale health research database resources amplify research opportunities by bringing multiple data streams together and following specific cohorts of people across time [37, 57]. Such databases allow researchers to derive a more detailed understanding of relationships between risk factors and disease, the effectiveness of interventions, and ultimately support policy decision-making. The UK Biobank is one example of such a resource and is discussed further in Section 2.1 below.

1.3 Multimorbidity prevention in primary care

Multimorbidity prevention is a challenge that requires proactive action within health systems historically set up to be reactive [58, 59]. Similarly, effective handling of multimorbidity requires a multi-system approach within a health system that has historically focused on single diseases [21, 60].

Specific to the current study, some authors argue that primary care is ideally placed to take the leading role in multimorbidity prevention [42, 46]. Primary care practitioners are uniquely qualified to guide lifestyle modifications that address modifiable risk factors [61]. Alcohol, exercise, smoking cessation, and weight management can all have a significant impact on chronic disease prevention. These interventions can be provided by allied primary care health professionals [62] or supported with

technology [63], in ways that align with the recently described concepts of lifestyle medicine [64] and proactive health support [65].

Primary care teams provide a generalist, close-to-home, patient-centred access point that (ideally) maintains a continuous, longer-term care relationship while facilitating comprehensive care planning, medication regimen management, coordination of specialist care services, and referrals to community-based support [20, 66, 67]. Such an approach aligns closely with the concept of patient- or person-centred care [68]. Keen readers will recognise that the primary care remit already encompasses these functions and is already overburdened within the UK NHS [69].

1.4 The heart-brain-liver-kidney (HBLK) cluster

A multiorgan approach is superior to focusing on a single organ when addressing multimorbidity prevention because multimorbidity often arises from interconnected pathophysiological processes across multiple organ systems [60]. Single-organ approaches fail to capture these systemic interactions and the cascading effects of dysfunction in one organ on others. For example, cardiovascular disease, chronic kidney disease, and diabetes often co-occur due to shared risk factors such as hypertension, inflammation, and metabolic dysregulation. A multiorgan approach allows researchers and clinicians to identify these shared pathways, detect early signs of organ interplay (e.g., subclinical changes in the heart, kidneys, or liver), and intervene before the disease spreads or worsens. At the same time, multiorgan work that includes all possible organs quickly becomes too large and complex to yield meaningful, detailed insights.

As Professor Sir Chris Whitty and Professor Fiona Watt argue, multiorgan or multi-disease work can be difficult to fund and publish because current medical training, funding, and publishing frameworks have historically focused on single organ systems [70]. Their advice to researchers is to tackle multimorbidity prevention by focusing on common clusters of conditions. This thesis follows the call made by Whitty and Watt (2020) and considers multimorbidity prevention within a cluster of conditions arising from the heart, brain, liver and kidney.

There are several compelling reasons for selecting the heart-brain-liver-kidney (HBLK) cluster for this project. First, the UK Biobank has made available detailed magnetic resonance imaging (MRI) data for the heart, brain and liver in the same set of participants [71]. This dataset offers a unique opportunity

for detailed analysis of the interrelations between these organs and their associated dysfunctions. Second, the HBLK cluster is featured in existing prior research on multimorbidity clusters [33, 34, 72] establishing the population-level relevance of this cluster in the broader context of multimorbidity research.

Thirdly, this cluster can be thought of as the natural expansion to the traditionally central focus on arteriosclerotic cardiovascular disease (ACVD), which remains the leading cause of mortality worldwide [73]. Diseases of the brain (stroke and dementia), the liver and kidneys are all already known to be connected to ACVD via shared risk factors and shared underlying mechanisms [74–76] (See Section 2.4 below). This expanded focus from ACVD to related conditions allows us to leverage the already well-established links and derive incrementally better preventive strategies that have benefits across multiple organs.

Fourth, the conditions arising within the HBLK cluster align closely with the objectives of existing preventive healthcare interventions, such as the NHS Health Check programme (Section 2.2). The primary targets of the NHS Health Check are heart disease, diabetes, stroke, dementia, kidney and liver disease, as laid out in the official guidance [77], the website [78] and patient information [79].

Finally, while other organ systems such as the lungs, pancreas, and musculoskeletal system also play critical roles in multimorbidity, the HBLK cluster was prioritised for its combination of systemic relevance, population-level burden, and existing resources for research. Diseases affecting these four organs are among the leading causes of mortality and morbidity worldwide [4], with high societal and healthcare costs. Additionally, their interconnectedness makes them particularly suited to multiorgan imaging and risk prediction approaches, allowing this project to generate meaningful insights into multimorbidity prevention while maintaining a focused scope.

Specific routine screenings and preventive services are already present in primary care [80]. Primary clinicians are given limited powers to treat known risk factors and disorders before they progress to more complicated, linked health problems [59, 70]. However, more research is needed on the ways that primary care prevention efforts can be expanded to anticipate and prevent health issues rather than just reacting to them after they occur [19, 81]. By focusing on the heart, brain, liver, and kidney, the work

of this thesis builds directly on existing ACVD research and leads into the practical aspects of identifying and mitigating risks of multimorbidity with a special focus on the primary care setting.

In summary, the heart-brain-liver-kidney (HBLK) cluster is prioritised for multimorbidity prevention in this project because these organ systems are highly interconnected through shared risk factors and mechanisms, making them critical drivers of multimorbidity. They also represent significant population health burdens, align closely with existing healthcare frameworks like the NHS Health Check, and are supported by unique data opportunities from the UK Biobank, including multiorgan imaging. Focusing on the HBLK cluster allows for a manageable, impactful scope that balances feasibility and relevance, providing a strong foundation for future expansion to other organ systems.

1.5 Problem definition

In contrast to a traditional hypothesis-driven approach, this thesis gathers evidence across a series of studies addressing various aspects of multimorbidity prevention within the HBLK cluster with a special focus on primary care. We reflect on current disease prevention efforts and consider potential adjustments to the existing system to yield the greatest multiorgan benefits for the smallest cost. These questions echo and directly respond to recent calls for the expansion of preventive efforts within the NHS [82–84]. By leveraging the 'big data' of the UK Biobank, this thesis iterates over questions around multimorbidity prevention in a way that gathers the evidence required to inform future prevention strategy-building efforts.

1.5.1 Research gap

Multimorbidity prevention requires interventions that address multiple diseases simultaneously, enabling early intervention and treatment. Existing frameworks, such as the NHS Health Check, represent a significant effort in disease prevention, but there is insufficient evidence on their effectiveness in reducing disease burden or how they could be adapted to incorporate a multiorgan or multi-disease approach. Furthermore, the potential role of multiorgan imaging in preventing multimorbidity remains largely unexplored.

For the first time, this research leverages the unique combination of detailed multiorgan magnetic resonance imaging (MRI) data (covering the heart, brain, and liver), extensive demographic and

lifestyle characterisation, and longitudinal electronic health records from the UK Biobank cohort [57]. This approach provides an unprecedented opportunity to investigate cross-organ relationships, evaluate current prevention strategies, and explore the utility of multiorgan imaging for predicting and preventing multimorbidity. By addressing these gaps, this research advances the field by providing a catalogue of evidence to inform the next generation of multimorbidity prevention strategies.

1.5.2 Overall research objective

This thesis aims to use the UK Biobank to gather and assess evidence for strategies that effectively predict or prevent diseases within the heart-brain-liver-kidney (HBLK) cluster, including evaluating the potential role of imaging in preventing multimorbidity.

1.5.3 Research questions

The following research questions are designed to address key challenges in multimorbidity prevention and align closely with the overall research objective.

A. What are the significant cross-organ relationships within the HBLK cluster, as identified via multiorgan imaging, and how can they inform multimorbidity prevention strategies?
B. To what extent is the current NHS Health Check effective in preventing disease within the HBLK cluster?
C. How feasible is it to expand the NHS Health Check to include accurate risk assessments for multiorgan disease?
D. What is the incremental value of multiorgan imaging for risk stratification, and how cost-effective is this approach for specific patient subgroups?

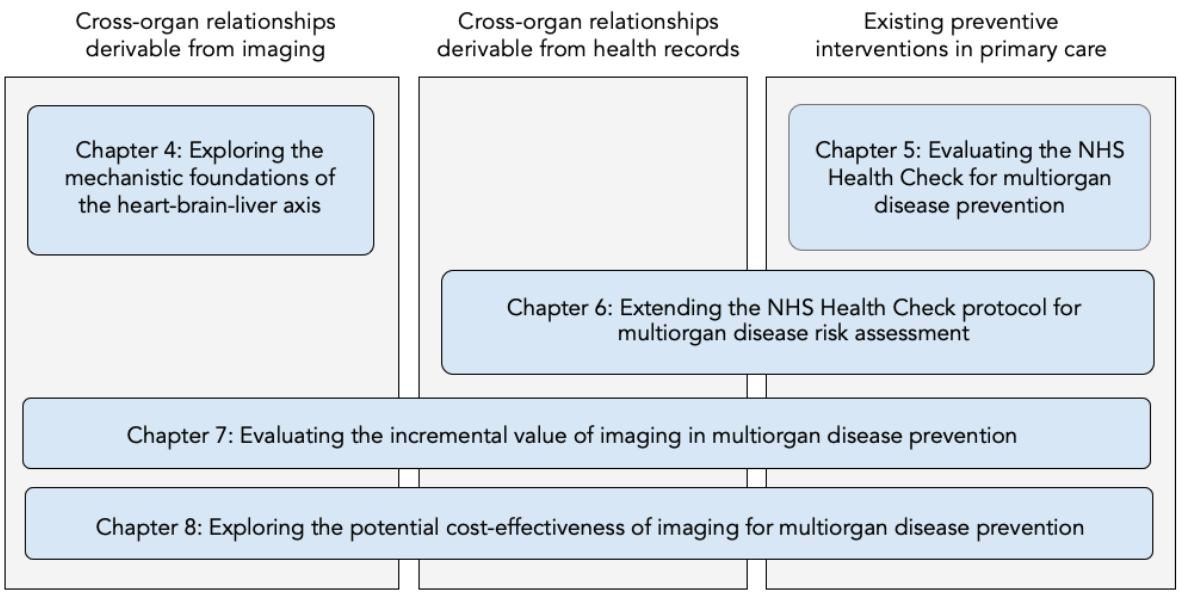


Figure 1.1: Thesis roadmap overview

1.5.4 Thesis outline

In this thesis, Chapter 2 provides the reader with an overview of the literature relating to the UK Biobank, the NHS Health Check, multiorgan imaging and cross-organ relationships. Chapter 3 provides details of the methods applicable to all studies within the project. Chapters 4 through 8 present specific methods and results of four self-contained studies, each addressing a distinct research question (Figure 1.1).

A. What are the significant cross-organ relationships within the HBLK cluster, as identified via multiorgan imaging, and how can they inform multimorbidity prevention strategies?

In Chapter 4, we examine the cross-organ associations found in imaging data from the heart, brain, and liver. The purpose of this analysis is to describe the ways that dysfunctions or alterations in one organ are associated with others, even after adjusting for known risk factors and before any conditions are diagnosed. These results provide the mechanistic links that can explain shared risk factors, inform potential targets for therapy, and support the substantive elements of multimorbidity tracking and prevention.

B. To what extent is the current NHS Health Check effective in preventing disease within the HBLK cluster?

In Chapter 5, we evaluate the effectiveness of the NHS Health Check, a cornerstone of the UK's preventive health strategy, in reducing adverse outcomes across the HBLK cluster. Using UK Biobank data, we compare long-term heart, brain, liver, and kidney outcomes in participants who received the NHS Health Check to those who did not. This analysis assesses the utility of the current preventive framework and identifies opportunities to enhance its impact through a multiorgan focus.

C. How feasible is it to expand the NHS Health Check to include accurate risk assessments for multiorgan disease?

In Chapter 6, we assess the feasibility of adapting the NHS Health Check to include multiorgan risk assessment. We analyse the information currently collected within the NHS Health Check framework and evaluate whether it could reasonably support multiorgan risk prediction. The purpose of this analysis is to determine whether preventive multiorgan risk assessment in primary care is (or is not) feasible, given current constraints, and whether existing risk assessment tools could have multiorgan risk prediction potential.

D. What is the incremental value of multiorgan imaging for risk stratification, and how cost-effective is this approach for specific patient subgroups?

In Chapter 7, we quantify the added value of multiorgan imaging in predicting multiorgan disease risk compared to standard non-imaging risk scores that use demographic, lifestyle, and clinical data. In Chapter 8, we build on this by conducting a cost-effectiveness analysis to evaluate whether the higher costs of imaging are justified by improvements in risk stratification. This includes subgroup analyses and the application of health economic principles to identify scenarios where imaging may provide the greatest benefit.

Together, this portfolio of studies integrates diverse evidence to enhance our understanding of multimorbidity and develop actionable strategies for its prevention. Chapter 9 synthesises the findings, discusses their implications for policy and practice, and proposes directions for future research.

1.6 Terms and assumptions

1.6.1 Heart-brain-liver-kidney (HBLK)

One of the difficult parts of communicating multiorgan work is the cumbersome naming. As this project is focused on diseases of the heart, brain, liver and kidney, we will often refer to the cluster of these organs using the abbreviation HBLK. Arterial health is implicitly included within this definition.

1.6.2 Cis-organ vs cross-organ

In the context of this project, it is helpful to add some terms. Cis- is a Latin prefix meaning "*on this side of*" or for our needs "*on the same side of*" [85]. Commonly used in gender studies (cisgender) and chemistry (cis isomer), we will use the term **cis-organ** in this thesis to describe relationships where both parts of the dyad relate to the same organ. The following would be examples of cis-organ relationships: An association between a liver fat imaging biomarker and later liver disease, or an association between a brain volume biomarker and later cognitive decline. On the other hand, **cross-organ** relationships are where an aspect of one organ (e.g. biomarker or diagnosis) is associated with an aspect of a different organ. This could include, for example, associations between diseases in different organs (such as between atrial fibrillation and stroke) or associations between biomarkers in one organ and disease in another organ (such as high liver inflammation associated with kidney disease risk).

Generally speaking, there is already substantial research behind all the cis-organ relationships that feature in this project. For example, the association between brain atrophy and neurocognitive decline is already well-known and well-described [86]. Where this thesis aims to advance the body of knowledge is by looking at cross-organ relationships, of multiple kinds, from multiple directions, and determining where such knowledge could be useful for multiorgan disease prevention.

1.6.3 Preventive (vs preventative)

Although both spellings have equivalent meanings, in this thesis, I intend to use the term "preventive" rather than "preventative" because the former term is said to be more widely used and is less likely to cause confusion [87].

1.6.4 Multiorgan (vs multi-organ)

Similarly, in this thesis, we will prefer the use of multiorgan (rather than multi-organ). A PubMed search at the time of writing indicates that the former term appears approximately twice as frequently as the latter in the titles of indexed articles. In the context of the current study, we use the term “multiorgan imaging” to refer to the multiorgan UK Biobank imaging protocol, including MRI of the heart, brain and liver, including a full cardiac MRI protocol and carotid intima-media thickness by ultrasound. Similarly, this study uses the term “multiorgan disease” to mean disease outcomes across the heart, brain, liver, kidney and vascular system.

Chapter 2: Large-scale data, imaging biomarkers and prevention of multiorgan disease

This chapter provides the foundational context for the thesis by reviewing key themes and existing literature relevant to the study of multimorbidity prevention within the heart-brain-liver-kidney (HBLK) cluster. Specifically, it examines the UK Biobank as a unique resource for multiorgan research, the NHS Health Check as an existing preventive framework, and imaging biomarkers as tools to explore organ health and cross-organ relationships. The chapter also addresses the evidence for the interconnected nature of the HBLK cluster and the potential of imaging and multiorgan approaches to inform disease prevention strategies. The chapter is organized into five sections:

- **The UK Biobank (Section 2.1):** This section introduces the UK Biobank as the primary data source for this thesis and highlights its unique contribution to multiorgan and multimorbidity research, underpinning all research questions.

- **The NHS Health Check (Section 2.2):** This section reviews the NHS Health Check as a key preventive health framework and discusses its current limitations. It sets the stage for Research Question B, which evaluates the effectiveness of the NHS Health Check in preventing multiorgan disease, and Research Question C, which examines the feasibility of expanding its scope to include multiorgan risk prediction.

- **Magnetic Resonance Imaging (MRI) Biomarkers (Section 2.3):** This section reviews imaging biomarkers for the heart, brain, and liver, focusing on their ability to detect subclinical changes and cross-organ relationships. This literature provides the foundation for Research Question A and informs later analysis of the incremental value of imaging in Research Question D.

- **Cross-Organ Relationships (Section 2.4):** This section synthesises the existing evidence for pairwise and multiorgan interactions, supporting Research Question A, which identifies cross-organ relationships relevant to multimorbidity prevention, and Questions C and D, where these relationships are used to produce more accurate risk multiorgan risk models.

- **The Use of Imaging in Disease Prevention (Section 2.5):** This section evaluates the potential role of imaging in prevention, with attention to its cost-effectiveness. It provides critical context for Research Question D, which examines the incremental value and cost-effectiveness of multiorgan imaging in risk stratification.

2.1 The UK Biobank

The work of this thesis takes place within the UK Biobank - a large-scale, prospective biomedical database and research resource comprising genetic and health information from approximately 500,000 UK participants, established to support and enable research of all kinds to improve health outcomes [57]. Population-dwelling people aged 40-69 years were initially selected from National Health Service (NHS) registers and were invited to register. Initial recruitment took place between 2006 and 2010, where participants voluntarily provided physical measurements, biological samples (blood, urine, and saliva), detailed health information, and consent for regular updates from their medical records. Since its inception, the UK Biobank has had a huge positive impact on health research [88]. This rich dataset has enabled researchers all over the world to conduct diverse and complex studies aimed at understanding the relationships between genetics, environment, and health.

2.2 The NHS Health Check

The NHS Health Check programme is a preventive public health intervention launched in England in 2009 to identify individuals at risk for cardiovascular diseases such as heart disease, stroke, diabetes, and kidney disease [77, 89]. This initiative offers free routine cardiovascular risk assessments along with treatment for risk factor conditions and support for behavioural changes to reduce the burden of cardiovascular morbidity [90]. Briefly, under the NHS Health Check protocol, healthy adults aged 40-74 are invited to visit their primary care team for basic physical measurements, blood tests, and health behaviour questions; after which attendees are offered follow-up support and services according to NICE guidelines [77]. With a similar and slightly expanded protocol, the Scottish version ("Keep Well") was launched in 2006 and is specifically targeted towards areas of socio-economic deprivation [91, 92].

Despite initial criticism for lack of a sufficient evidence base [93], the NHS Health Check was implemented across England on the strength of successful similar protocols elsewhere (notably in Japan

[94], Canada [95], Germany [96] and South Korea [97]). In the 15 years since then, a modest body of evidence has developed documenting the administration and uptake of the NHS Health Check [98, 99]. This literature provides important details about various aspects of the health check, including patient experience [99], service delivery [100], follow-up activities [101], communication of risk [102] organisational perspectives [103] and health inequalities [104]. However, there is much less research on associations between NHS Health Check and subsequent health outcomes and the effectiveness of the programme in disease prevention. Although there is some existing work documenting the short-term effects of NHS Health Check [101, 105], evidence regarding longer-term outcomes is proving to be particularly challenging to find.

2.3 Magnetic resonance imaging (MRI) biomarkers of organ health

The multiorgan imaging featured in this thesis is primarily magnetic resonance imaging (MRI). MRI has emerged as a pivotal tool in clinical diagnosis and management due to its ability to provide non-invasive and detailed images of various body tissues. With sequences that are highly customisable, MRI excels in the early detection of abnormalities, allowing for timely intervention that can potentially slow disease progression [106]. This is particularly crucial in latent disease processes that might go unnoticed until symptomatic. In our analysis of the heart-brain-liver axis, we include a range of MRI biomarkers that have been developed and validated in previous research.

2.3.1 Cardiovascular magnetic resonance (CMR)

Standard CMR metrics are imaging-derived measures of cardiovascular structure and function derived from measurements taken from each frame of the heart scan [107]. These include blood pool volumes of the four chambers of the heart, including right and left ventricles (RV, LV) and right and left atria (RA, LA), along with their associated ejection fractions (the volume of blood that moves through with each pump on average). In general, chamber volumes have a healthy size and symmetry relative to age, sex and body surface area, with abnormal size (either small or enlarged) indicating possible cardiac risk [107, 108].

Cardiac output, left ventricular (LV) ejection fraction, LV strain and global function index are measures of cardiac function shown to have prognostic value in population cohorts [109–111]. Size of the heart (LV mass), thickness of the heart wall and LV mass to LV end-diastolic volume ratio (LVM/LVEDV)

[112] are important biomarkers associated with higher risk for ischaemic heart disease [113]. Increased LVM/LVEDV indicates increased heart muscle mass relative to the blood volume, reflecting a concentric remodelling pattern in the left ventricle. Asymmetry in ventricular volumes (LV/RV) is a potential risk signal for heart failure or valvular heart disease [114]. We also include a measure of pericardial fat accumulation [115], which is known to be associated with hypertension, diabetes and high cholesterol [116]. Native T1 relaxation times, derived from T1-weighted maps of the CMR, are thought to reflect potential fibrosis in the heart muscle [117] and have been shown to be associated with risk for adverse cardiac events [117]. Aortic distensibility is a measure of local bio-elastic function derived from systolic and diastolic measurements of the aorta and is an important indicator of overall arterial health [118] and a protective factor in risk for cardiac events [119].

2.3.2 Brain MRI

Structural T1-weighted and T2-weighted imaging of the brain separates brain tissue from cerebrospinal fluid (CSF), facilitating the quantification of overall brain volume, grey matter volume, and peripheral cortical grey matter volume [120, 121]. Brain atrophy or loss of brain volume is known to be associated with neurocognitive decline [122], as well as other less obvious conditions such as Type 2 diabetes [123], hearing loss [124], depression [125] and exposure to vascular risk factors [126, 127]. Brain volume is only one aspect of brain health that is visible in MRI. Plaques, micro-bleeds and micro-ischaemia appear as areas of increased brightness in T2*-weighted imaging. These are known as white matter hyperintensities (WMH) and are the most widely-used imaging indicator of incipient cerebral small vessel disease burden and neurodegenerative disease [128–130].

Diffusion MRI scanning uses the movement of water molecules in the brain in response to magnetic stimuli to provide information about the white matter microstructure in each voxel of brain tissue. Neurite orientation dispersion and density imaging (NODDI) [131] is an advanced diffusion analysis methodology from which we derive brain health metrics, including intracellular volume fraction (ICVF) and isotropic volume fraction (ISOVF). ICVF is a measure of healthy neurite density, whilst ISOVF is an adverse health metric, a measure of free-water movement suggestive of brain oedema, breakdown in myelin and increased permeability of axonal membranes [132]. Changes in white matter microstructure, including reduced neurite density, increased ISOVF or both, have been observed with

neurodegenerative conditions [133], adult autism [134], epilepsy [135] and, in larger samples, vascular risk factors such as hypertension [136].

Large-scale studies have shown that, on average, brain ageing over time has a predictable pattern, including decreasing brain volume, accumulation of white matter hyperintensities, decreasing neurite density /ICVF, and increasing ISOVF [121]. This has developed into an active field of study around brain age gap analysis [137], but in cross-organ work, this pattern helps us identify adverse brain alterations in brain imaging data and recognise negative associations when we observe them.

2.3.3 Liver MRI

MRI is a highly effective non-invasive method to assess the accumulation of fat, iron and fibrosis in liver tissue. Proton density fat fraction (PDFF) is an MRI-derived measure of liver fat calculated with imaging masks that separate water from fat signals in the liver tissue [138]. PDFF has been validated against histology studies (the gold standard) [139] and has been shown to be a sensitive and robust metric for tracking the progression or improvement in fatty liver disease [140, 141].

Elevated liver iron levels are associated with conditions such as fibrosis, cirrhosis, and hepatocellular carcinoma [142]. The iron concentration in the liver can be derived from the T2* signal and converted into milligrams per gram of liver tissue [143]. More recently, iron-corrected T1 (cT1) has been developed as a composite marker of liver fibrosis and inflammation derived from both T1 and T2* images [144]. Corrected T1 has also been shown to correlate with histopathologic features [145] and is linked to adverse liver-related health events [146]. All three liver imaging metrics have been previously assessed for reproducibility [147] and used to identify liver differences in healthy and mixed cohorts [148].

In this thesis, we use the term "fatty liver disease" to denote either a diagnosis or a disease outcome. Much of the existing research uses the older term “nonalcoholic fatty liver disease” (NAFLD), which seeks to separate fatty liver damage according to levels of alcohol consumption [149]. Recently, there has been a shift towards using the term “metabolic-associated fatty liver disease” (MAFLD) to describe cases of fatty liver that coexist with metabolic disorders such as hypertension, diabetes, obesity, or hyperlipidaemia [150] whether or not there is alcohol consumption. However, we use the more general term "fatty liver disease" in this thesis due to limitations in the specificity of clinical coding in our data

and the time period covered. This term encompasses any diagnosed excess fat accumulation in the liver, regardless of the underlying cause. It is also worth noting that because a large segment of liver disease is undiagnosed in the general population [151, 152], we expect it to also be true within the UK Biobank.

2.4 Relationships between the heart, brain, liver and kidney

Cross-organ relationships are not a new concept in the literature. In fact, there is a very wide and diverse range of commentary and empirical evidence that fall into the 'multiorgan' category. A dyad or two-part relationship is the simplest and easiest type of connection to understand, aligning well with the form of evidence we can gather with established statistical methods. However, as we progress towards multiorgan systems thinking, which more accurately reflects the complexities of the human body, the research and communication challenges increase significantly.

Emerging research that explicitly addresses multiorgan syndromes will be addressed in Section 2.4.5. While the multiorgan approach is gaining traction in the academic discourse, most existing research primarily focuses on pairwise relationships, laying the groundwork for the specific connections underlying multimorbidity.

2.4.1 Heart and brain

It is well-established that cardiovascular diseases (CVD) and cerebrovascular events are closely connected through shared threats to the vascular system, such as smoking, hypertension, diabetes, and hyperlipidaemia [153, 154]. Research has consistently shown that these risk factors contribute to both coronary artery disease and cerebrovascular alterations, with multiple shared mechanistic pathways [155]. From a multimorbidity perspective, atrial fibrillation is a well-known risk factor for stroke [156], and increased risk for cognitive decline has been linked with coronary heart disease [157], atrial fibrillation [158] and heart failure [159].

The cerebral hypoperfusion hypothesis [160] states that ageing, combined with vascular risk factors, reduces cardiac pumping efficiency and decreases blood flow from the heart, leading to chronically reduced blood flow to the brain. This mechanism is thought to underlie the reduced brain volume and adverse microstructural alterations observed in people with reduced cardiac output [161, 162], dilated cardiomyopathy [163], and heart failure [160, 164]. The accumulation of white matter hyperintensities,

together with microstructural changes, are associated with coronary artery calcium [165], arterial stiffness [166, 167], arrhythmias [168], and atherosclerosis in general [169].

While these studies support an effect in the heart-to-brain direction, there is other evidence that suggests bi-directionality. In their review of 20 human neuroimaging studies, Kimmerly and colleagues [170] summarise the ways that cardiovascular homeostasis (including regulation of heart rate, the force of heart contractions and the dilation of blood vessels) is regulated via specific brain regions (including the insular cortex, anterior cingulate cortex, medial prefrontal cortex, amygdala, and cerebellum). This brain-to-heart influence finds fuller expression in the form of Takotsubo syndrome, a stress-induced cardiomyopathy that has been linked to imaging-based alterations in the limbic system [171], particularly the amygdala [172].

2.4.2 Heart and liver

The connection between the heart and liver is also well-documented, with numerous studies linking liver disease with CVD [173–175]. Literature review articles report significant associations between fatty liver disease and coronary artery calcification [176], ischaemic heart disease [177], epicardial fat accumulation [178], cardiac arrhythmias [179, 180], heart failure [181], and liver cirrhosis with ischaemic heart disease [182]. A 2019 state-of-the-art review posited that both NAFLD and CVD reflect end-organ damage of metabolic syndrome risk factors such as hypertension, diabetes and dyslipidaemia [177].

Due to the maturity of research examining the heart-liver axis, some studies have used imaging biomarkers to observe aspects of the liver, the heart or both, with Borges-Canha and colleagues providing a review of studies up to 2019 [183]. In these and more recent studies, liver disease (either fatty liver or cirrhosis) has been shown to associate with; adverse cardiac remodelling features such as greater cardiac mass, greater wall thickness, concentric remodelling [184–186], cardiac function such as left ventricular strain, diastolic or systolic dysfunction [186, 187], right atrial pressure [188] and possible myocardial fibrosis shown by greater late gadolinium enhancement, longer myocardial T1 relaxation times, and higher extracellular volume [189].

2.4.3 Liver and brain

The liver and brain are closely connected due to the liver's crucial role in detoxifying the blood [190]. Infection, accumulated fat, toxins, alcohol and other insults can impair the liver in carrying out this vital function such that higher levels of toxic lipids, ammonia, tau amyloid, metals and other neurotoxins remain in the blood. These compounds then have the potential to cross the blood-brain barrier into the brain tissue, influencing brain health, cognitive function and longer-term risk for neurodegenerative disease. Several recent review articles summarise the imaging-based mechanisms at the liver-brain interface. The most frequently observed effects are reduced cerebral blood flow, brain volume atrophy, and, ultimately, loss of cognitive function [191]. Another liver-brain pathway includes inflammation, pro-coagulation/increased platelet activity and endothelial dysfunction in the micro-vessel wall [192–194]. These factors are known to exacerbate atherosclerosis and lead directly to cerebrovascular changes such as micro-haemorrhage, micro-ischaemia, white matter lesions, and stroke [195, 196]. There is also a growing evidence base documenting the important role of gut health in liver-brain interactions [197].

The liver-brain connection is most clearly seen in hepatic encephalopathy, a dementia-like illness that accompanies serious liver dysfunction or liver failure [193]. In these cases, liver transplantation has proven somewhat effective in restoring both liver and cognitive function, suggesting that certain liver-driven neurological impairments may be modifiable with appropriate liver disease treatment. Imaging research has been instrumental in describing changes in the brain associated with hepatic encephalopathy, for example, reduced brain volume [198], white matter lesions [199] and alterations in white matter microstructure [200]. Other research has shown stenosis of the intracranial main artery [201] or calcification of the carotid artery [202, 203] in individuals with serious liver disease.

There is also evidence that liver-brain associations similar to those described above are sometimes present in less severe liver diseases such as viral hepatitis [204], liver cirrhosis [197], alcoholic liver disease [205] and (the very common) nonalcoholic fatty liver disease [192]. Cardiovascular risk factors such as hypertension, hyperlipidaemia, obesity, alcohol use disorder, diabetes and smoking also play a significant role [206] in the liver-brain relationship. A better understanding of these intersecting scenarios could improve the management of risk factors for both liver and brain disorders, potentially preventing the progression of silent liver changes to major cerebrovascular events [192].

2.4.4 Associations with kidney disease

We have no imaging data for the kidneys in this thesis, although they play a potentially important role in the HBLK multimorbidity cluster. Patients with cirrhosis or severe liver disease sometimes also develop chronic kidney disease (CKD), at which point it is called hepatorenal syndrome [207]. At the milder end, fatty liver disease is also associated with higher odds of developing CKD [175].

The relationship between heart failure and kidney function is bidirectional, with each condition influencing the other. Heart failure can lead to reduced kidney perfusion, resulting in kidney damage, a phenomenon known as cardiorenal syndrome type 1 [208]. Conversely, CKD can contribute to cardiovascular disease through mechanisms such as hypertension, fluid overload, and dysregulated mineral metabolism [209]. Imaging studies of the heart have shown associations between higher right heart work index and estimated glomerular filtration rate (eGFR) [210] and right heart failure with CKD [211].

It was initially thought that renal dysfunction was associated with an increased risk of all-cause dementia and stroke, primarily through mechanisms involving white matter hyperintensities (WMH) and silent brain infarcts [212]. More recent imaging studies have shown that renal dysfunction, as shown by reduced eGFR, has been linked to lower white matter fractional anisotropy (FA) and decreased cortical volume, in addition to white matter hyperintensities [213]. One Mendelian randomisation study has shown a causal association between poorer eGFR and reduced cortical brain thickness [214].

2.4.5 Explicitly multiorgan syndromes

There is an increasing recognition of the interconnectedness among cardiovascular, cerebrovascular, metabolic, and kidney diseases, which share common pathological mechanisms and often require integrated therapeutic strategies [215]. This movement is reflected in the emergence of multi-word syndrome definitions, which aim to encapsulate the multiorgan nature of these conditions and advance clinical approaches accordingly. Some examples are metabolic syndrome (heart, liver and pancreas [216]), hepatic encephalopathy (liver and brain), cardiorenal syndrome (heart and kidneys [208]) and hepatorenal syndrome (mentioned above). More recently, the American Heart Association issued a consensus statement on cardiovascular-kidney-metabolic syndrome (2023, [217]), and other researchers have described cardiac-kidney-liver syndrome as the “real entity” of Type 2 diabetes [218].

While these approaches have the potential to be highly beneficial for streamlining clinical experiences and providing better patient-centred care, there are potential drawbacks. One concern is the number of possible combinations of organ systems that can be involved. This complexity could lead to the creation of numerous similar multi-word syndromes, which could further complicate diagnostic criteria and treatment protocols, thus increasing confusion and inconsistency in clinical practice.

2.5 The use of imaging in disease prevention

At the time of writing, we could not find any previous research linking multiorgan imaging with multimorbidity prevention, nor studies that have used imaging for an explicitly multi-disease preventive purpose. Generally, the vast majority of research looking at imaging biomarkers for early disease focuses on cis-organ relationships.

2.5.1 Single-organ imaging

The most widely cited publications in this area are guidelines or consensus statements describing the role of imaging in the prevention of dementia [219], stroke [220], heart disease [221], sudden cardiac death [222], steatohepatitis [223] and liver cancer [224]. These documents lay out the principles guiding the limited use of imaging for risk stratification based on specific clinical parameters and other risk factors.

In addition, there is a very large body of research in imaging biomarker development, where novel imaging metrics are assessed for utility in predicting adverse outcomes. All of the multiorgan imaging metrics which are described in Section 2.3 (above) are featured in these types of studies.

Despite extensive research in single-organ imaging (whether cardiovascular, neurological or hepatic imaging) it remains evident that disease events still occur in individuals considered to be at low risk [225]. There is significant optimism that imaging can help bridge this gap as new biomarkers are developed [226, 227], although the design of imaging-based preventive strategies requires further investigation [228].

2.5.2 Evidence for cost-effectiveness

The cost-effectiveness of primary, secondary, and tertiary disease prevention is a crucial consideration. While scattered evidence supports the cost-effectiveness of preventive measures for heart, brain, and liver diseases, the role of imaging remains underexplored. This section reviews the current evidence on the cost-effectiveness of imaging in preventing these conditions, with a focus on dementia, stroke, heart disease, and liver disease. It is important to note that imaging itself is not a form of treatment, and most cost-effectiveness studies focus on the relationship between treatment interventions and disease reduction rather than on imaging. Some studies below consider the role of imaging as part of a two-stage process.

Brain imaging is essential for diagnosing early-stage dementia/Alzheimer's disease and tracking neurodegenerative markers over time [229]. A 2022 systematic review by Walsh et al. [230] examined 45 studies and found that interventions, particularly those targeting smoking, educational attainment, and physical inactivity, were highly cost-effective in preventing all-cause dementia. Another 2023 review [231] analysed 11 studies and concluded that physical activity interventions implemented before or during early cognitive impairment stages could be cost-effective in reducing the total dementia burden.

Mukadam and colleagues [232] highlighted that interventions aimed at preventing late-onset dementia — such as smoking cessation, hypertension treatment, and the provision of hearing aids — can be cost-effective. Braun et al. [233] reviewed seven studies in 2024 and concluded that dementia prevention programmes targeting well-defined at-risk populations might be cost-effective, particularly when addressing lifestyle-related risk factors in middle-aged cohorts. Although brain imaging was mentioned as part of the screening process, the primary focus was preventing dementia by improving risk factors.

Early imaging plays a pivotal role in stroke detection. Bhagia et al. [234] conducted a record review of 828 emergency room patients with suspected stroke and found that early MRI screening for cerebrovascular events in appropriately screened patients can be cost-effective by reducing hospitalisation length and total healthcare costs. However, they emphasised the need for further studies to refine patient screening criteria. Martinez et al. [235] used a decision-simulation model based on the American Heart Association’s recommendations for acute ischaemic stroke, revealing that both computed tomography (CT) and MRI provide benefits in terms of quality-adjusted life-years (QALYs),

but CT was more cost-effective than MRI in acute stroke assessment. Importantly, Lechtman and colleagues [236] found carotid plaque MRI to be a cost-effective first-line strategy for identifying asymptomatic patients at high risk of stroke in people over 70 years old in Canada. Finally, research by Puhr-Westerheide et al. [237] demonstrated the cost-effectiveness of a shortened MRI protocol for improving stroke detection in a two-stage process following an initial CT scan.

Cardiac magnetic resonance (CMR) imaging has shown promise in managing heart disease cost-effectively. A 2010 systematic review [238] of 32 studies found cardiovascular imaging interventions more cost-effective than observation, medical treatment, or non-intervention. An updated review in 2022 found that CMR was a cost-effective option for assessing significant coronary artery disease in low-to-intermediate-risk patients with suspected coronary artery disease in 10 out of 15 studies reviewed. Walker et al. [239] demonstrated that CMR-guided management was cost-effective in 1,202 UK patients with stable coronary heart disease compared to usual care per UK NICE guidelines. Ge et al. [240] concluded that stress CMR could serve as a cost-effective screening step before invasive angiography in patients with stable chest pain. Other research has reflected on the optimisation of CMR scanning [241] highlighting the development of shorter cardiac MRI protocols aimed at enhancing cost-effectiveness.

Liver function tests with blood biomarkers are the standard first-line liver screening approach in primary care [242, 243]. Several studies demonstrate the cost-effectiveness of risk stratification for patients with non-alcoholic fatty liver disease (NAFLD) using non-imaging biomarkers or risk scores in primary care clinics [244, 245]. Crossan and colleagues [246] found that liver MRI was more cost-effective than liver biopsy for staging established liver disease, but the most cost-effective approach was treatment without diagnostic imaging. Srivastava et al. [247] suggested that a two-stage process of non-imaging risk scoring followed by transient elastography was more cost-effective for identifying cirrhosis in NAFLD patients than either method alone.

The literature suggests there is reasonable evidence that disease prevention efforts can be cost-effective. While imaging can be highly effective in the management of established dementia, stroke, heart disease, and liver disease, the cost-effectiveness of imaging for prevention is less clear. Further research is needed to refine the parameters around the use of imaging in disease prevention in a way that can be cost-effective.

2.5.3 Whole-body MRI

Whole-body MRI (WB-MRI) is a multiorgan imaging approach to detect early-stage diseases and conditions before symptoms appear, allowing for timely intervention and better prognosis [248]. With some variation, most WB-MRI protocols include the heart, brain, liver and kidneys [249]. This thesis is not necessarily about WB-MRI as it is currently applied, but there are some relevant similarities. The main advantage of WB-MRI is its ability to detect many potential abnormalities and conditions in one scan, making it especially efficient for multifactorial diseases and comorbidities [250]. It can also be a highly effective modality for asymptomatic early cancer screening [251]. Whole-body MRI's non-invasiveness and lack of ionising radiation make repeated screenings safer, especially in younger or high-risk populations [250]. On the other hand, critics argue that the high cost and limited accessibility of WB-MRI limit its potential utility for widespread preventive screening [248]. In addition, WB-MRI is known to regularly identify false-positive and indeterminate incidental findings, causing anxiety and triggering potentially unnecessary additional investigations [252]. WB-MRI can be cost-effective for the early detection of asymptomatic cancers and more cost-effective than conventional imaging for staging metastatic cancer [248]

Chapter 3: Methods

3.1 Introduction

In this chapter, we describe the data sources, study variables, and statistical methods used to address the research questions of this thesis. We begin by introducing the UK Biobank Imaging Study, which serves as the primary data source, and outline the imaging protocols and population-level variables incorporated into our analyses. We then detail the covariates, study outcomes, imaging biomarkers, and population risk scores used across studies. The approaches to handling missing data, statistical analysis, and feature selection are explained, with explicit justification for the methods chosen. Finally, we highlight several novel methodologies developed during the course of this work.

This study complies with the Declaration of Helsinki; the work was covered by the ethical approval for UK Biobank studies from the National Health Service (NHS) National Research Ethics Service on 17th June 2011 (Ref 11/NW/0382) and extended on 18 June 2021 (Ref 21/NW/0157) with written informed consent obtained from all participants.

3.2 The UK Biobank Imaging Study

As part of an ongoing programme of enrichment, the UK Biobank resource has been augmented with the addition of multiorgan imaging for a large subset of the original participants. To date, approximately 50,000 participants have completed the standardised UK Biobank imaging protocol, which includes MRI of the brain, heart, and liver. Image acquisition was in accordance with pre-defined standard operating procedures using uniform equipment and staff training. The UK Biobank imaging protocol is detailed in published sources [71, 107, 121]. First-visit imaging from which the data in this thesis was drawn took place between May 2014 and March 2019.

3.2.1 Liver imaging

Liver MRI scans were performed using a Siemens 1.5T scanner as part of the UK Biobank abdominal imaging protocol [138]. A single transverse slice was taken through the centre of the liver above the porta hepatis, in end-expiration breath-hold without contrast [144]. Scanning sequences included shortened modified Look-Locker inversion recovery (ShMOLLI) T1 and multi-echo spoiled-gradient-echo T2* acquisition. Three 15mm circular regions of interest were identified as representative

parenchymal tissue, from which the following summary statistics were calculated: proton density fat fraction (PDFF), liver iron concentration and iron-corrected T1 (cT1, see Section 3.3.4 below).

3.2.2 Brain imaging

Multi-modal brain MRI was conducted using a Siemens 3T scanner [121, 253] using three acquisition types; T1-weighted magnetisation-prepared rapid acquisition with gradient echo for overall brain segmentation and volumes, T2-weighted fluid-attenuated inversion recovery for white matter lesion detection, and diffusion-weighted imaging acquisition with100 diffusion-encoding directions over two shells. A range of standardised brain imaging-derived phenotypes were produced via an extensive data processing and quality control pipeline [254]. Further details of brain MRI acquisition and processing are provided in Appendix 1.

3.2.3 Cardiac imaging

Cardiovascular magnetic resonance (CMR) was performed using Siemens 1.5T scanners, including long-axis cines (horizontal long axis, vertical long axis, left ventricular outflow tract) with a complete short-axis stack and a transverse aortic cine slice at the intersection of the pulmonary trunk and right pulmonary artery. The UK Biobank CMR protocol is available in a separate publication [255], along with details of image processing and metric derivation [107, 256].

The imaging metrics used in this thesis were selected based on their established validity, clinical relevance, and ability to detect subclinical changes indicative of organ dysfunction. A detailed description of MRI acquisition parameters is provided in Appendix 1.

3.3 Study variables and data handling

All data for the current study was sourced from the UK Biobank via Access Application 59867. Figure 3.1 provides an overview of the data sources relevant to the current project and how they fit together.

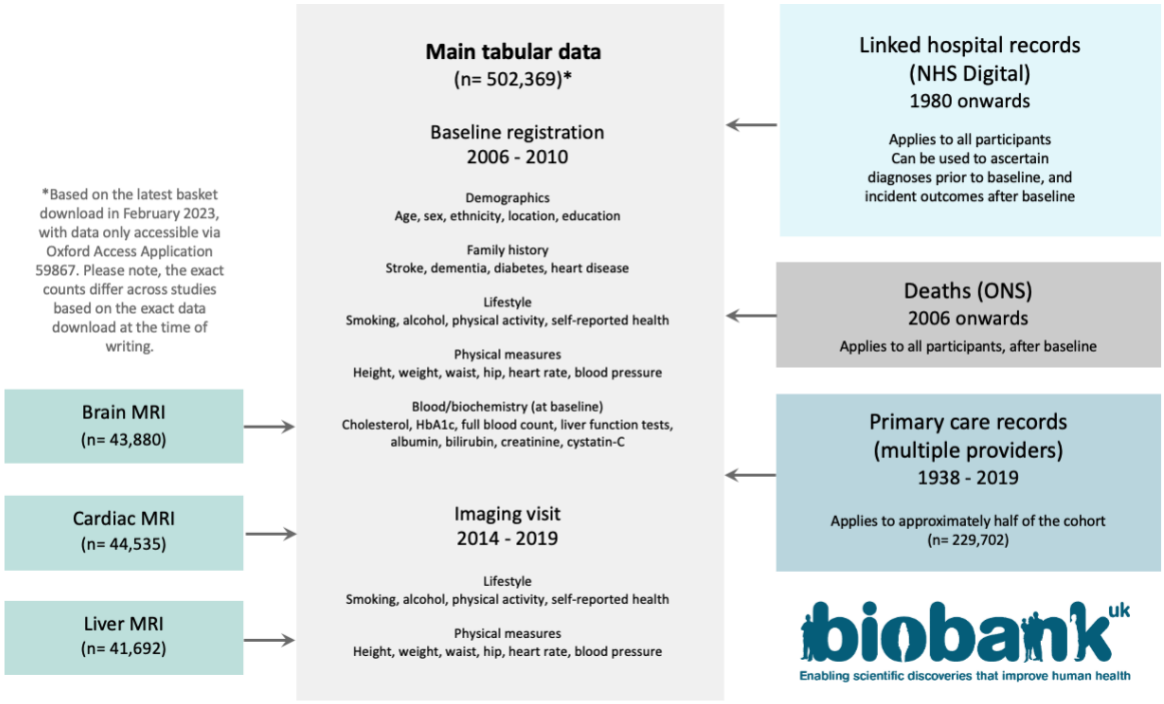


Figure 3.1: UK Biobank data schema for this project

Generally speaking, the main UK Biobank dataset holds the core features supporting the analyses, with other datasets (such as imaging and linked health records) that were joined to the main set and incorporated into research samples. The main variable groups are covariates, outcomes, multiorgan imaging and population risk scores.

3.3.1 Covariates

The main tabular data is the backbone of the UK Biobank, and from here we draw the wide variety of participant characteristics of the study sample. Whilst many variables such as age and sex feature in every study, in this section we lay out all covariate variables that have been used for the DPhil, although they might not feature in every study.

Participants' sex at birth, month of birth, year of birth, educational level, rounded geographical location and Townsend deprivation score were obtained from the baseline visit. Age at various timepoints was calculated from reported year and month of birth. Education level was converted to years of education for use in some risk scores, and binarised to post-secondary education (yes/no) in several studies. Rounded geographical location was clustered into regions using the nearest main city in Chapter 5. Self-reported ethnicity was gathered primarily from the baseline visit with missing values updated at later visits. Due to the large majority of "White" ethnicity in the sample (96%), non-white ethnicity

(yes/no) was sometimes included as a binary variable. Townsend deprivation index at baseline was assigned based on participant postcode.

A range of physical measurements and self-reported health behaviours were recorded at the baseline assessment and again at the imaging visit. These were height, weight, waist circumference, hip circumference, heart rate, systolic blood pressure, diastolic blood pressure, self-reported health status, self-reported family history, smoking status, alcohol consumption frequency, and physical activity. Additional physical quantities such as body surface area, body mass index (BMI) and waist-hip ratio were calculated from their constituents at the same two timepoints. According to UK Biobank guidance, physical activity was quantified from responses to the simplified International Physical Activity Questionnaire (IPAQ) into summed metabolic equivalent (MET)-minutes per week [257]. In Chapters 6-8, physical activity was dichotomised to greater than or equal to 600 summed MET-minutes per week, approximately equivalent to 20 minutes exercise per day [258]. Family history was drawn from self-reported illnesses of mother, father and siblings, where age of illness was not specified. Clinical diagnoses for hypertension, diabetes and high cholesterol were gathered from a combination of self-report and linked health records.

There were several blood biomarkers that were highly relevant to our studies, including total cholesterol, high-density lipoprotein (HDL) cholesterol, red blood cell count and glycated haemoglobin (HbA1c). A much broader range of laboratory tests was considered in Chapter 6 (see Section 6.2.6). Finally, as per published recommendations, we included the following de-confounding variables in brain analyses: head size, imaging site, site by age/sex interactions and de-meaned scanner table coordinates (X, Y, Z and table position) [259].

3.3.2 Outcomes

Multiorgan disease outcomes are a major feature of this project, with specific study outcomes provided in Table 3.1. Study outcomes were selected following discussion within the supervisory team and were shaped by the target messages of published work, and by event counts in the dataset that potentially limit the statistical power.

Table 3.1: Study outcomes across the heart-brain-liver-kidney (HBLK) cluster

Organ/System	Chapters 5-6	Chapters 7-8
Brain	Stroke All-cause dementia	Stroke All-cause dementia
Arterial	-	Atherosclerosis / peripheral artery disease Venous thromboembolism
Heart	Myocardial infarction Atrial fibrillation Heart failure	Myocardial infarction Atrial fibrillation Non-ischaemic cardiomyopathies Valvular heart disease Heart failure
Liver	Fatty liver disease Liver cirrhosis Liver failure	Combined liver disease Fatty liver disease Liver cirrhosis
Kidney	Chronic kidney disease (Stage 3+)	Combined kidney disease Chronic kidney disease (stage 3+)
Combined	-	Combined outcomes (heart, brain, arterial, liver and kidney)
Mortality	All-cause mortality	
Linked health records	Hospital records, deaths and primary care records	Hospital records and deaths only

Disease diagnoses (and dates thereof) were collated across multiple UK Biobank data sources including self-report, linked hospital records and deaths. Linked primary care records [260] were also used to support diagnosis ascertainment in Chapters 5 and 6. The main reason for excluding primary care records from Chapters 7 and 8 is the poor data coverage for the period following multiorgan imaging. Incident outcomes were defined by first occurrence of disease after the index date, which was baseline recruitment for Chapters 6-7 and date of imaging for Chapters 7-8. As per normal practice with survival modelling, participants with a record of a particular disease at the index date were excluded from time-to-event modelling for that disease. For all disease outcomes, code definitions were drawn from published resources where available, including the published UK Biobank outcome code lists [261], from the phenotype library maintained by Health Data Research UK [262] and the primary care code repository maintained by University of Cambridge [263]. Code definition lists were reviewed by clinical members of the advisory team. A UK Biobank-specific code list for main outcomes is provided in Appendix 2.

Because health outcomes are critical to health research beyond the current project and medical records were updated periodically throughout the work, I developed a custom module for extracting and updating clinical diagnoses from the UK Biobank. This is described in Section 3.5.2 below.

3.3.3 Additional health conditions

In addition to the study outcomes, a wide selection of other potentially relevant diagnoses were ascertained from the UK Biobank resource using the same multi-source approach. These include core risk factor conditions (diabetes, hypertension, high cholesterol), diagnoses required for calculating risk scores (transient ischaemic attack, migraine, erectile dysfunction, coronary heart disease, angina, rheumatoid arthritis, systemic lupus erythematosus, depression, bipolar disorder, schizophrenia, anti-hypertensive medication, atypical antipsychotics and regular steroid tablets), and additional potentially important factors identified in prior research, including family history of heart/brain/liver/kidney disease, dizziness, fainting, shortness of breath, chronic obstructive pulmonary disease, cancer, epilepsy, Parkinson's disease, multiple sclerosis, traumatic brain injury, sleep disorder, rarer cardiac arrhythmias, acute kidney injury, kidney stones, hypertensive renal disease, infective/viral hepatitis, ascites, liver cancer, gout, anxiety disorder, insulin medication, and statins.

3.3.4 Multiorgan imaging variables

In this section, we outline the specific imaging variables used in this study, further to the substantive multiorgan imaging concepts described in the previous chapter (Section 2.3).

Brain imaging was conducted at three dedicated imaging centres with identical scanners, using T1 structural, T2-weighted FLAIR structural and diffusion-weighted sequences. Imaging-derived phenotypes were extracted from the images and were made available as part of the general UK Biobank data release. Phenotype extraction was carried out primarily by the Oxford Centre for Functional MRI of the Brain (FMRIB) using tools from the now-open source FSL, FMRIB Software Library [264]. Brain volume metrics are segmented into grey matter, white mater and cerebrospinal fluid (CSF), all measured in cubic millimetres and normalised for head size. Volume of white matter hyperintensities was scaled by cube root to correct a strong right-skew. Hippocampus volume was extracted using ASEG Freesurfer volumetric segmentation [265], and averaged between left and right hemispheres. In this study we used mean brain diffusion MRI values derived at the FA skeleton [266].

Table 3.2: Summary of multiorgan imaging variables

Organ/System	Imaging-derived metric	Chapter 4	Chapters 7-8
Structural T1 Brain	Total brain volume (mm3)	✓	✓
	White matter volume (mm3)		✓
	Grey matter volume (mm3)	✓	✓
	Peripheral grey matter volume (mm3)		✓
	Volume of cerebrospinal fluid (mm3)		✓
	Volume of white matter hyperintensities (WMH, mm3)	✓	✓
Subcortical	Volume of hippocampus (mm3)		✓
Diffusion	Fractional anisotropy (FA)		✓
	Mean diffusivity (MD)		✓
	Intracellular volume fraction (ICVF)	✓	✓
	Isotropic volume fraction (ISOVF)	✓	✓
	Orientation dispersion (OD)		✓
Arterial	Aortic distensibility (AoD, 10-3mmHg)	✓	✓
	Carotid intima-medial thickness (left and right)		✓
Standard cardiac*	End diastolic volumes (LVEDV, RVEDV, mL),		✓
	End systolic volumes (LVESV, RVESV, mL),		✓
	Stroke volumes (LVSV, RVSV, mL),	LVSVi	✓
	Ejection fractions (LVEF, RVEF, %),		✓
	LV global function index (LV GFI, %),	✓	✓
	LV mass (LVM, g)		✓
	LV mass-to-volume ratio (LVM/LVEDV)	✓	✓
	LV wall thickness (mm)		✓
	Atrial volumes (RAV, LAV)		✓
	Atrial ejection fractions (RAEF, LAEF, %)		✓
Additional cardiac	Pericardial adipose tissue (PAT, mm2)		✓
	Left ventricular T1 (ms, global LV, free wall, septal)		✓
	Ventricular volume ratio		✓
Liver	Liver fat (Proton density fat fraction, PDFF, %)	✓	✓
	Liver iron (mg/g dry tissue weight)	✓	✓
	Corrected T1 (cT1, ms)	✓	✓

* LV= left ventricular, RV = right ventricular

These were scaled for normality with ordered quantile normalisation [267] and whole-brain averages were derived across white matter tracts excluding the brain stem. Susceptibility-weighted imaging of the subcortical structures was initially included in analyses, but was later removed due to lack of incremental interpretability.

The standard cardiac MRI (CMR) variables used in this study were extracted from images by Bai and colleagues [256], using deep convolutional networks trained on an initial set of 5,000 scans that were manually contoured by an Oxford-London clinical team [107]. Aortic distensibility measures were also part of this data return. Standard CMR chamber volumes can be analysed as raw variables, or indexed to body surface area (indicated with the subscript i). For example, in Chapter 4, left ventricular stroke volume was included as an indexed metric (LVSVi). The analysis in Chapters 7-8 allowed for feature

selection from both raw and indexed CMR features, along with a novel metric, ventricular volume ratio (LVEDV/RVEDV) which has been shown in our earlier work to be a potentially useful biomarker [114].

Pericardial fat was extracted by Bard and colleagues [115], and cardiac native T1 measures returned by Puyol-Anton et al. [268]. Carotid intima-medial thickness (CIMT) was measured at the end of the imaging visit by ultrasound, at two pre-defined angles for each carotid artery, that were then reduced into two independent CIMT variables by principal components analysis [269].

Liver imaging metrics were produced from abdominal MRI scans by the research team at Perspectum Ltd (Oxford), including proton density fat fraction (PDFF) [138], liver iron content [143], and corrected T1 (cT1), a novel biomarker of combined fibrosis and inflammation [144]. PDFF was scaled with natural log to correct a right-skew. A summary of the multiorgan imaging variables and where they feature in the thesis is provided in Table 3.2.

3.3.5 Population risk scores

Population-level risk scores are the final category of variables that feature prominently in this work (Chapters 6-8). This is driven by two motivations: a) it is incumbent upon all researchers to consider the potential applicability of existing risk tools before creating new ones [270], and b) in order to evaluate the incremental value of multiorgan imaging, we need a non-imaging baseline for comparison. To fulfil both these requirements, we considered a range of published risk scores tracking conditions across the heart, brain, liver and kidney. The 22 risk scores included for analysis were chosen after conducting a literature search for the most widely used metrics for each outcome, as well as the availability of published formulae and online calculators for quality verification. A summary is provided in Table 3.3, and more detailed information for all published indices is provided in Appendix 3.

For incident stroke risk we considered QStroke [271] and CHA2DS2-VASc [272]. For all-cause dementia we included a risk score from the Cardiovascular Risk Factors, Aging and Dementia study (CAIDE) [273], the Lifestyle for Brain Health score (LIBRA) [274], and a recently-developed UK Biobank Dementia Risk Score (UKB-DRS) [275].

Table 3.3: Existing population-level tools for HBLK disease risk

Organ/ System	Risk score	Target disease (optional description)
Brain	QStroke	Stroke (developed by QResearch)
	CHA2DS2-VASc	Stroke (an aggregate score assigning points for heart failure, hypertension, age, diabetes mellitus, prior stroke/TIA, vascular disease, and sex)
	UKB-DRS	All-cause dementia (a dementia risk score recently developed in the UK Biobank with external validation)
	CAIDE	All-cause dementia (developed in the Cardiovascular Risk Factors, Aging and Dementia study)
	LIBRA	All-cause dementia (Lifestyle for Brain Health score)
Heart	QRISK3	Atherosclerotic CVD (myocardial infarction, stroke or CVD death)
	Framingham Risk Score (2 versions)	Atherosclerotic CVD (one version using BMI, and the other using cholesterol)
	SCORE2/SCORE-OP	Atherosclerotic CVD (developed by the European SCORE2 working group)
	PCP-HF	Heart failure (the Pooled Cohort Equations to Prevent Heart Failure)
	CHARGE-AF	Atrial fibrillation (developed from the Cohorts for Heart and Aging Research in Genomic Epidemiology model for atrial fibrillation)
Kidney	QKidney (2 versions)	Chronic kidney disease (developed by QResearch)
	Kidney risk score	Chronic kidney disease (developed by CKD Prognosis Consortium across 28 countries)
Liver	Fatty liver index	Fatty liver disease (developed in a small study but widely used)
	Dallas Steatosis Index	Fatty liver disease (from the Dallas Heart Study)
	QDiabetes (2 versions)	Undiagnosed current Type 2 diabetes (developed by QResearch)
	Cambridge Diabetes Score	Undiagnosed current Type 2 diabetes
	AUDIT-C	Alcohol use disorder (the Alcohol Use Disorders Identification Test)
	FIB-4	Liver fibrosis /cirrhosis (The Fibrosis-4 Index)
	NAFLD Fibrosis Score	Liver fibrosis /cirrhosis
	AST/Platelet ratio (APRI)	Liver fibrosis /cirrhosis (Aspartate aminotransferase/platelet ratio)
	ALBI (albumin/bilirubin)	Severity grading in liver cancer

For myocardial infarction and heart failure we considered Framingham Risk Score (with and without blood lipids) [276], PCP-HF heart failure equations [277] and QRISK3 [278]. The European-derived SCORE2 and SCORE-OP were added as additional candidate risk scores for ACVD in Chapter 7. CHARGE-AF [279] was included as a risk score for atrial fibrillation; developed in the Cohorts for Heart and Aging Research in Genomic Epidemiology model for atrial fibrillation. Chronic kidney disease risk (Stage 3+) was predicted by two versions of QKidney [280] and (Nelson) Kidney Risk Score [281]. For fatty liver disease we implemented the Fatty Liver Index [282] and the Dallas Steatosis Index [283]. Three diabetes risk scores (two versions of QDiabetes [284] and the Cambridge Diabetes Score [285]) were included as possibly useful predictors.

AUDIT-C [286] (the Alcohol Use Disorders Identification Test) is a questionnaire designed to assess risk for alcoholic liver disease, however only the first AUDIT question was available in the UK Biobank

with a high degree of data completeness. Liver fibrosis was represented by three candidate scores (FIB-4 [287], NAFLD Fibrosis Score [288] and AST/Platelet ratio [289]). All published risk scores have been separately validated in their own studies.

Risk estimates for all these risk scores were calculated from their constituent components using published formulae across all participants. Online risk calculators were used to perform systematic checks for calculation accuracy.

3.3.6 Missing value handling

Missing data were addressed using a combination of complete case analysis and multiple imputation. The choice between complete case analysis and multiple imputation in this thesis was driven by the specific objectives and data characteristics of each chapter. In Chapters 4-5, complete case analysis was used due to the low level of missing data (less than 5%) in key variables, ensuring straightforward exploratory analyses of cross-organ relationships without introducing potential biases from imputation. In contrast, Chapters 6-8 employed multiple imputation to address higher levels of missingness (up to 15%) in imaging variables, which would have significantly reduced sample size and statistical power in predictive modelling. Multiple imputation minimised bias by leveraging relationships among variables and preserving data representativeness, particularly in high-dimensional analyses. Sensitivity analyses confirmed that the results were robust to the choice of missing data approach, supporting the validity of both methods in their respective contexts.

Our standard protocol was to filter to complete cases across age, sex, height and weight. Next, in our data, Townsend deprivation index has a unimodal continuous distribution, a very small rate of missingness, and its value cannot reasonably be estimated from other variables. Therefore, we replaced these with the mean so that the results of any analysis, including imputed values, will not be significantly different from analysis without them. For the categorical ethnicity variable, there was again a very small degree of missingness, which cannot be predicted from age, sex, and body size, and it has a very large majority category (95.5% “White”). Therefore, we assigned missing ethnicity values to the overwhelming majority group to have a much smaller chance of introducing bias than assigning them to the minority category.

Finally, the remaining set of variables were continuous health metrics that contained some native associations between them and associations with our foundational variables of age, sex, BMI and waist-to-hip ratio. Therefore, for this set, multiple imputation with chained equations (MICE) with the ***mice*** package [290] was the ideal method to produce imputed values that reflect the underlying pattern of correlations and allowed the use of all present data whilst introducing the least possible amount of bias. The MICE algorithm makes iterative predictions of the missing value given all other predictors and then reviews the overall variation introduced by imputation. This is refined over 20 iterations until we arrive at a set of imputations for missing values that sit very nicely within the correlation context of the overall data. In all published work (Chapters 4-6), multiple imputation is used only for covariates, not for exposures or outcomes. In Chapters 7-8, imputation is used to complete the imaging set with less than 15% average missingness.

3.4 Statistical analysis

3.4.1 Software

All statistical analysis was conducted with R Statistical Computing software versions 4.1.0 to 4.3.2 [291] and RStudio version 1.4.1717 to 2023.12.1 [292]. Custom analysis pipelines were written by myself in R for all analyses presented in this thesis, with the additional use of my own package (***UKBTools***, Section 3.5.1) and other open-source packages as mentioned in the text.

3.4.2 Modelling

Statistical modelling is present in all results chapters chosen to address specific research questions. Standard linear regression models were used in Chapter 4 to quantify associations between cross-organ imaging metrics with substantial, flexible scope for covariate adjustment (Research Question A). Linear regression was appropriate for its simplicity and interpretability in the context of continuous imaging variables

Survival models (Cox proportional hazards) were used in Chapters 5-8 to evaluate influences on time-to-event outcomes, such as disease incidence or mortality. Survival analysis was relevant for assessing the effectiveness of NHS Health Checks (Research Question B) and for developing risk prediction models (Research Questions C and D). The proportional hazards assumption was tested for all models.

The ***survival*** package [293] provided the core time-to-event modelling functions. The ***pec*** package [294] was used to generate individual-level risk prediction estimates, the ***car*** package was used to calculate variance inflation scores for multicollinearity monitoring [295].

Additional specialised modelling techniques will be described in their respective chapters. Results are typically presented as standardised beta coefficients with 95% confidence intervals (CIs) and p-values where significance thresholds were adjusted for multiple testing using the Benjamini-Hochberg method [296] with a false discovery rate of 0.05.

Stability selection (see Section 3.4.3) was the primary feature selection method used in Chapters 6 and 7 due to its robustness in handling high-dimensional data and its ability to penalise overfitting while identifying stable predictors. Alternative methods, such as stepwise regression, LASSO, and ridge regression, were considered but not selected. Stepwise regression was excluded due to its susceptibility to overfitting and issues with multicollinearity, while single-sample LASSO, although effective at penalising model complexity, does not explicitly focus on predictor stability across bootstraps. Ridge regression, which retains all predictors by shrinking coefficients, was less appropriate for developing sparse models where a limited set of variables was preferred. Stability selection, therefore, offered a well-balanced approach, combining simplicity, predictive accuracy, and robustness to address the research objectives.

3.4.3 Stability selection

Stability selection is the core feature selection method that is used for model-building in Chapters 6 and 7. Stability selection is a model-agnostic method for building a stable, simple model from a large pool of possible predictors [297]. The aim is to obtain the best model fit possible, with the simplest model possible (a small number of predictors) and minimise the risk of overfitting. In this case, overfitting occurs when the final models are so tightly tuned to the UK Biobank dataset that they perform poorly on any other dataset. Stability selection is a method developed to identify features that consistently contribute to the predictive power of the model across various subsets of the data and to penalise the inclusion of non-informative variables that could otherwise lead to overfitting.

The process begins by creating 100 bootstrapped samples of 50% of the training set. Each subset is then subjected to a feature selection process that incorporates modelling with regularisation to favour sparser

models, thereby implicitly penalising the selection of superfluous features. In this study, within each bootstrapped sample, we applied lasso regression with an underlying Cox model, using 5-fold cross-validation to tune for the local minimum lambda. In this way, each subsample produces its own penalised (simplified) Cox model, with only a reduced set of predictors chosen out of the total pool.

The essence of stability selection lies in the subsequent aggregation phase, where the selection frequencies of features across all subsamples are compiled. This frequency data serves as the basis for determining the stability of each feature's selection, highlighting those consistently deemed important.

A critical step in the stability selection method is the establishment of a frequency threshold to discern stable features. Features surpassing this predetermined threshold are considered sufficiently stable and are thus selected for inclusion in the final model. In this study, we evaluated model fit and parsimony across stability retention thresholds between 50% and 100%. We found that using a conservative 80% cut-off resulted in models with a much smaller set of predictors, but with discriminative accuracy that was not significantly different from the much larger better-fitting models. The overall stability selection pipeline was coded manually in R. The ***glmnet*** package [298] was used to fit lasso Cox models and the ***rsample*** package [299] was used for bootstrapping. Haftorn and colleagues [300] provide a published example of stability selection implementation, predicting gestational age from newborn DNA using only 5 methylation sites.

3.4.4 Model scoring

There are a number of model performance metrics that were used to assess and compare the performance of risk prediction models. Area under the receiver operating curve (AUC) [301] provides a single scalar value that summarises a model's ability to distinguish between positive and negative classes independent of any specific decision threshold, making it a robust measure for comparing models. AUC is also relatively robust to class imbalance [302], providing an accurate reflection of a model's discriminative ability even when predicted outcomes are rare. Receiver operating curve statistics were calculated with the ***pROC*** package [303], with AUC confidence intervals calculated using the ***ROCR*** package [304].

Sensitivity (true positive rate) measures the proportion of actual disease/diagnosis outcomes correctly identified by the model. Specificity (true negative rate) assesses the proportion of non-event outcomes

correctly identified, important for minimising false positives. Balanced accuracy is the mean value of sensitivity and specificity, offering a single performance measure that is particularly useful for imbalanced datasets by providing an equal consideration of both positive and negative classes. Sensitivity and specificity were calculated using the ***caret*** package [305], and model calibration statistics were calculated using the ***rms*** [306] and ***PredictABEL*** packages [307]. ***PredictABEL*** was also used to calculate reclassification statistics (the integrated discrimination index (IDI) and the net reclassification index (NRI)) used in Chapter 6. Reclassification indices are distinct from accuracy measures, and reflect the degree to which a new model produces better individual classifications than existing models. Bootstrapping was used in Chapters 7 and 8 to derive confidence intervals for sensitivity and specificity estimates, with permutation testing to calculate p-values for differences in these quantities.

When we were developing our model scoring pipelines, we conducted a sensitivity analysis implementing a time-dependent AUC metric using ***survAUC*** [308] and ***timeROC*** [309] packages. Due to our large sample sizes, this analysis was significantly more computationally intensive and did not provide AUC estimates that were materially different from simple binary AUC values.

3.5 Custom tools

3.5.1 UKBTools

Since I began working with the UK Biobank in 2019, many tasks have appeared repetitively in my work. I have developed an original R package to facilitate easy interaction with UK Biobank data (***UKBTools***), including many of the core functions that I use day-to-day and have been instrumental in this DPhil. Like all good toolboxes, ***UKBTools*** is under continuous improvement.

3.5.2 UK Biobank Outcomes Database

Similarly, health outcomes are highly relevant to this and many other projects, and outcome information is dispersed throughout the UK Biobank data, not confined to a single column. Furthermore, due to regular updates of linked health records, this extraction process is iterative. Since 2019, I have developed, refined, and maintained an outcome extraction pipeline that now includes a variety of multiorgan features, as mentioned in Sections 3.3.2 and 3.3.3. The pipeline operates using a code driver

file, which contains reference lists for each intended outcome based on published resources. The software sequentially accesses various UK Biobank data sources to identify participants with codes matching each outcome. Finally, the pipeline compiles these results and produces analysis-ready columns formatted for time-to-event modelling.

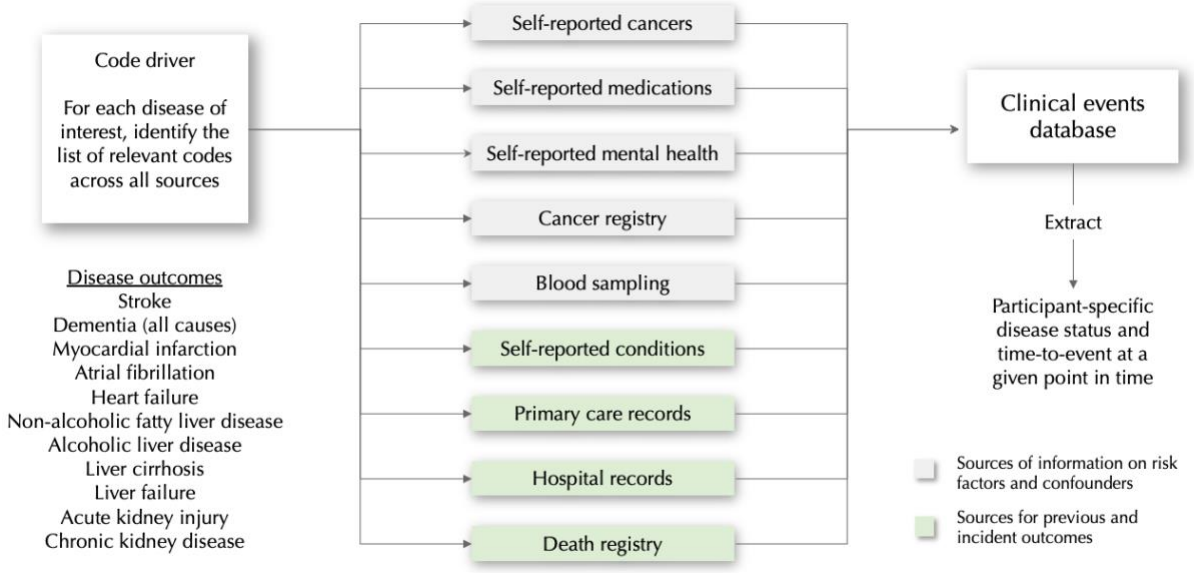


Figure 3.2: Schema overview for the UK Biobank Outcomes Database

3.5.3 SPROUT

I am fortunate to have many years of experience using R as a programming language for both academic and industry applications. During the years of my DPhil, I have been called upon frequently to provide advice and training to various research teams, causing me to reflect on and distil the most important elements of reproducible R programming that students will not learn in *DataCamp* or *Codecademy*. The resulting framework is ***SPROUT***, which combines some guiding principles with a set of R notebook templates that can "clip on" to any programming language and help even beginner researcher-programmers build reproducible analysis pipelines that are simple, functional and highly effective for reducing analysis-associated headaches. These principles apply in addition to existing best practices and principles of clean code.

Table 3.4: Principles of the SPROUT framework

	Principle	What this means	Why this is important	How it shows up
S	Self-contained	All inputs and code are contained within a single project folder	If your code links to an external file that changes or moves, your code will break no matter how well-written it is	In your CreateData script, provide source references, but copy source data to Inputs folder
P	Process-based	Script files are written, laid out, and named to reflect a standard process	This helps you come back later and easily locate the piece of code you need. Also protects against accidental code changes, facilitates code versioning and sharing.	Use SPROUT layout and naming of files Follow script content and output rules Use a Process Driver
R	Reproducible	The code will produce the same results one year from now	This is important when changes or additional details are requested by reviewers, co-authors or external parties.	Set seed when randomness is present Ensure your pipeline connects properly Check data before and after edits Annotate code with row counts and checksums.
O	Open source	Commitment to giving back to the community	We gladly use the work of others (packages)	Be willing to publish your code publicly. (Sometimes required by journals)
U	User-friendly	Use plenty of signposting Use external drivers where appropriate	Help yourself remember what you did and why Helps others understand your work	Write informative comments in your code Use a Process Driver for collaboration with and sign-off from non-technical colleagues
T	Traceable	Create external outputs along the way that contain maximum necessary information	Allows you to look up details of the results at a later date without needing to run the code. Necessary for tracing back errors.	Check all inputs against external values / ranges Document these checks Indicate in your code what the outputs are and where they live

Chapter 4: Multiorgan imaging and cross-organ associations

4.1 Introduction

All strategies for multimorbidity prevention need to be underpinned by a sound understanding of cross-organ relationships. In this chapter, we use multiorgan imaging data to examine the imaging-level relationships between the heart, brain and liver in UK Biobank participants.

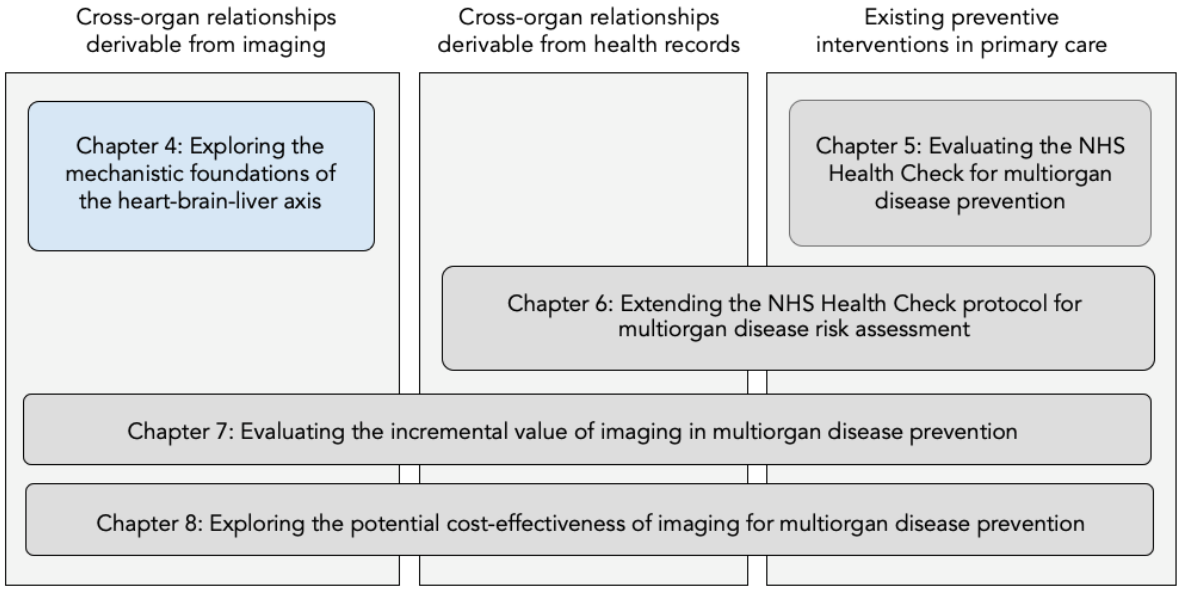


Figure 4.1: Chapter 4 - Roadmap location

The analysis and results of this chapter have been published under open access at

> *McCracken, Celeste, Zahra Raisi-Estabragh, Michele Veldsman, Betty Raman, Andrea Dennis, Masud Husain, Thomas E. Nichols, Steffen E. Petersen, and Stefan Neubauer. 'Multi-Organ Imaging Demonstrates the Heart-Brain-Liver Axis in UK Biobank Participants'. Nature Communications 13, no. 1 (21 December 2022): 7839. https://doi.org/10.1038/s41467-022-35321-2.*

This chapter addresses a significant gap in current research by providing an empirical analysis of cross-organ imaging relationships using a large, population-based cohort. Medical imaging technology has provided a range of biomarkers that offer significant prognostic value [110, 128, 146]. Many of the cis-organ relationships within the heart-brain-liver axis are well described in existing literature, for example, heart metrics that signal risk for heart disease, or brain imaging metrics that identify risk for cognitive decline. Cross-organ relationships have received much less attention, especially where such associations are shown by multiorgan imaging. Where imaging-derived cross-organ associations have

been published (Section 2.4), this has usually been drawn from either small samples or specific clinical cohorts rather than the general population. There has also been a lack of standardisation in existing literature, in imaging protocols, biomarker handling and confounding control.

In this study, we analyse state-of-the-art MRI biomarkers across the heart, brain and liver in a large, population-based sample enriched with deep characterisation of potential confounders. This analysis provides an essential understanding of the organ-level differences associated with shared risk factors and could point to potential therapeutic targets with multiorgan benefits. Figure 4.2 provides a conceptual overview of where this analysis fits within the broader heart-brain-liver axis.

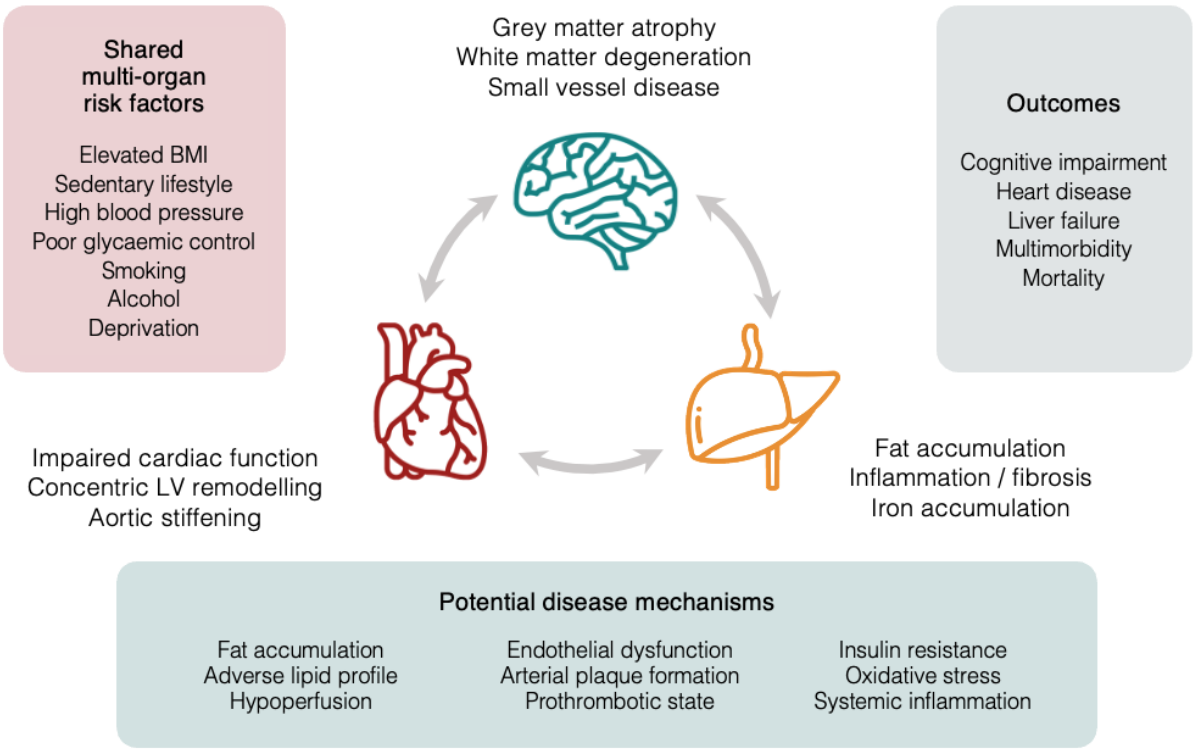


Figure 4.2: Chapter 4 - Conceptual overview of the heart-brain-liver axis

Heart, brain and liver systems co-exist within a context of shared multiorgan risk factors. In this study, we identify the ways that subclinical changes in each organ associate with others in the heart-brain-liver axis, relevant to a range of possible underlying disease mechanisms. A detailed understanding of multiorgan interaction could potentially improve our ability to predict and prevent connected complex outcomes. BMI= body mass index, LV = left ventricular. Please note, this is a conceptual figure and not all elements displayed are explicitly tested in this study.

4.2 Methods

This study was conducted within the UK Biobank (Section 2.1) and using the subset of the UK Biobank who had received multiorgan imaging by February 2020 (Section 3.2).

4.2.1 Imaging metrics

Table 4.1 summarises the imaging metrics used in this study. Section 3.3.4 provides details of image acquisition and metric handling, with additional information provided in Appendix 1. A summary of the missingness present in multiorgan imaging variables in this study is provided in Appendix 4.

Table 4.1: Chapter 4 - Imaging metrics

Organ	Imaging metric	Reflects
Heart	Left ventricular stroke volume (LVSV)	Quantity of blood ejected by the left ventricle of the heart in one contraction. Reflects both cardiac structure and function
	Left ventricular global function index (LV GFI)	A modified version of LV ejection fraction, which incorporates LV structure, has been shown to have superior prognostic value in population cohorts [109, 110]
	Left ventricular mass to end-diastolic volume ratio (LVM/LVEDV)	A measure of LV structural remodelling [112]. Higher LVM/LVEDV indicates predominance of a more concentric pattern of LV remodelling, which typically represents an unhealthy structural phenotype.
	Aortic distensibility (AoD)	A measure of local aortic bioelastic function, as an indicator of arterial health [118, 119].
Brain	Overall brain volume Grey matter volume	Structural measures of brain tissue volume, normalised for head size [120]
	Volume of white matter hyperintensities (WMH)	was included as a measure of incipient cerebral small vessel disease burden previously linked to neurodegenerative disease [129, 130]
	Intracellular volume fraction (ICVF)	ICVF refers to the proportion of restricted movement of water diffusion, with higher values of ICVF thought to reflect higher neurite density [131]
	Isotropic volume fraction (ISOVF)	ISOVF represents the proportion of water moving in a free-moving or unrestricted motion, with higher values associated with brain oedema, breakdown in myelin and increased permeability of axonal membranes [132].
Liver	Proton density fat fraction (PDFF)	PDFF is a reliable measure of liver fat, with PDFF>5% indicative of fatty liver disease [138]
	Liver iron	Liver iron is a key biomarker of liver health with high levels linked to fibrosis, cirrhosis, and hepatocellular carcinoma [143, 310]
	Corrected T1 (cT1)	Finally, cT1 is a novel measure, developed as a composite marker of liver fibrosis and inflammation and linked in recent work to adverse liver-related health events [146].

4.2.2 Cognitive function

We also calculated the associations of the brain imaging metrics with cognitive function to clarify the directionality of their impact on brain health, particularly when the brain health implications of these metrics were not initially clear. The battery of cognitive function tests administered by UK Biobank has been previously evaluated for reliability and validity [311, 312]. A subset of these was administered at the imaging visit, from which we included fluid intelligence, (inverted) reaction time, and prospective memory. These tests were selected as they had high data availability (administered to greater than 90% of the imaging participants) and their coverage of multiple cognitive functions (problem-solving, working memory and processing speed). An overall measure for cognitive performance was obtained by calculating the average z-score across the three measures.

4.2.3 Covariates and confounders

Participants' sex at birth, date of birth, educational level, and Townsend deprivation score were obtained from the baseline visit. Physical measures (height, weight, waist circumference, and systolic blood pressure) were recorded at the imaging visit. Body surface area and body mass index (BMI) were calculated from height and weight measurements taken at the imaging visit, with BMI $\geq 30 kg/m^2$ classified as obese. Self-reported smoking status, alcohol consumption frequency, and physical activity were recorded at imaging.

Physical activity was quantified from responses to the simplified International Physical Activity Questionnaire (IPAQ) [313] into summed metabolic equivalent (MET)-minutes per week according to UK Biobank guidance [257]. Red blood cell count, total cholesterol and glycated haemoglobin (HbA1c) were taken from blood sampling at baseline. Clinical diagnoses for diabetes, high cholesterol and hypertension were ascertained via a combination of self-report, biochemistry, and linked hospital episode statistics data, as described in Section 3.3.3 with status at the time of imaging. A full listing of UKB fields and codes is given in Appendix 2. In addition, as per published recommendations, we included the following de-confounding variables in brain analyses: head size, imaging site, site by age/sex interactions and de-meaned scanner table coordinates (X, Y, and Z) [259].

4.2.4 Pairwise association models

We conducted a series of multivariable linear regression analyses to examine pairwise associations between heart, brain and liver features. All models were adjusted by the following covariates: age, sex, height, diabetes, high cholesterol, hypertension, smoking, physical activity, alcohol consumption, Townsend deprivation index, education, obesity, systolic blood pressure, red blood cell count, total cholesterol, and glycated haemoglobin. Results are presented as standardised beta coefficients with 95% confidence intervals (CIs) and p-values where significance thresholds were adjusted for multiple testing using a false discovery rate of 0.05 across exposure variables across all pairwise models.

4.2.5 Three-organ models

Following pairwise analysis, we sought to identify the relationships between heart, brain and liver that persisted when modelled simultaneously, to identify the empirically strongest pathways between organs and potential indirect effects. Features with the greatest number of significant cross-organ links in the pairwise analysis were carried forward into three-organ modelling, including all heart variables, liver fat and liver cT1 and three brain outcomes (total grey matter volume white matter hyperintensities and ISOVF). We modelled simultaneous relationships with path analysis using the ***lavaan*** package in R [314]. For each brain outcome, liver and heart exposures were modelled together in two forms: (a) Brain ~ heart + liver, Heart ~ liver, and (b) Brain ~ heart + liver, Liver ~ heart, as depicted in Figure 4.3.

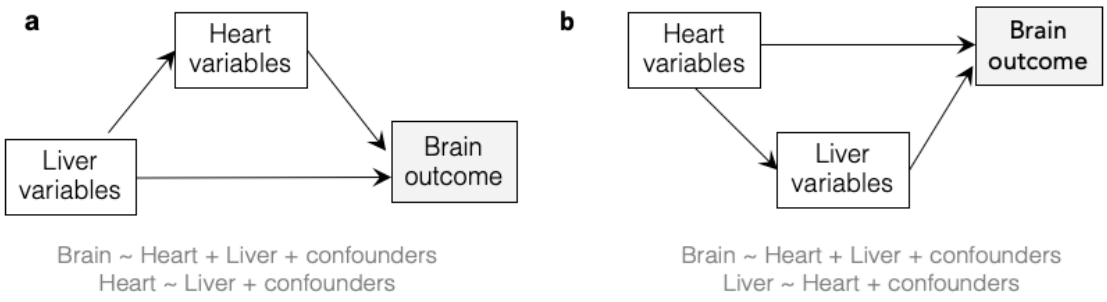


Figure 4.3: Chapter 4 - Alternative forms considered for three-organ path analysis

In the first step, all variables were included together in the model, along with all confounders described above as linear (not latent) covariates. The additional imaging confounders were included in paths for

the brain outcome. In the second step, non-significant variables were removed one at a time from each formulation, leading to a final model for each outcome in forms (a) and (b). From these, the best fitting model (a or b) was selected based on the lowest root mean squared error and highest brain outcome r-squared (R^2) and highest Tucker-Lewis index [315]. Prior to simultaneous modelling, heart and liver variables were orthogonalised with principal components analysis rotation using the ***psych*** R package [316] to remove within-organ correlation while retaining more than 90% of the original signal. Details of this within-organ adjustment are shown in Appendix 5.

4.3 Results

4.3.1 Study sample

Within the total UK Biobank cohort at the time of analysis (n= 502,462), 48,996 participants had attended an imaging appointment (Figure 4.4). Of these, 31,174 participants had at least one piece of imaging data across heart, brain and liver. We excluded 730 (2%) participants with missing covariate data, leaving a maximum analysis sample of 30,444 participants. There are three nested data sets in this study. The pairwise heart-brain analyses are based on the main set of 30,444 participants. A subset of 15,097 participants had at least one piece of liver imaging data. We refer to this as the liver subset and this forms the basis of the pairwise liver-brain and liver-heart analyses. Even so, there is remaining variation in sample sizes across heart, brain and liver imaging metrics, described in detail in Supplementary Table 1. In the three-organ path analyses, we use only complete rows across all imaging metrics, which includes 6,865 participants referred to as the three-organ subset.

4.3.2 Sample characteristics

Our sample included 15,905 female participants (52.2%) and 14,539 male participants (47.8%, Table 4.2). The average age was 63.2 (±7.5) years, with median BMI of 25.9 kg/m^2. The proportion of participants with diabetes, hypertension and BMI ≥ 30 kg/m2 was 5.7%, 32.4%, and 18.0% respectively (Table 1). The three study samples (main set, liver subset and the three-organ set) were similar in terms of age, sex, average blood pressure, alcohol intake, smoking and physical activity. Participants in the three-organ set (n= 6,865) had slightly lower levels of diabetes, hypertension and elevated BMI than the maximum set (4.9%, 29.8% and 15.3%, respectively).

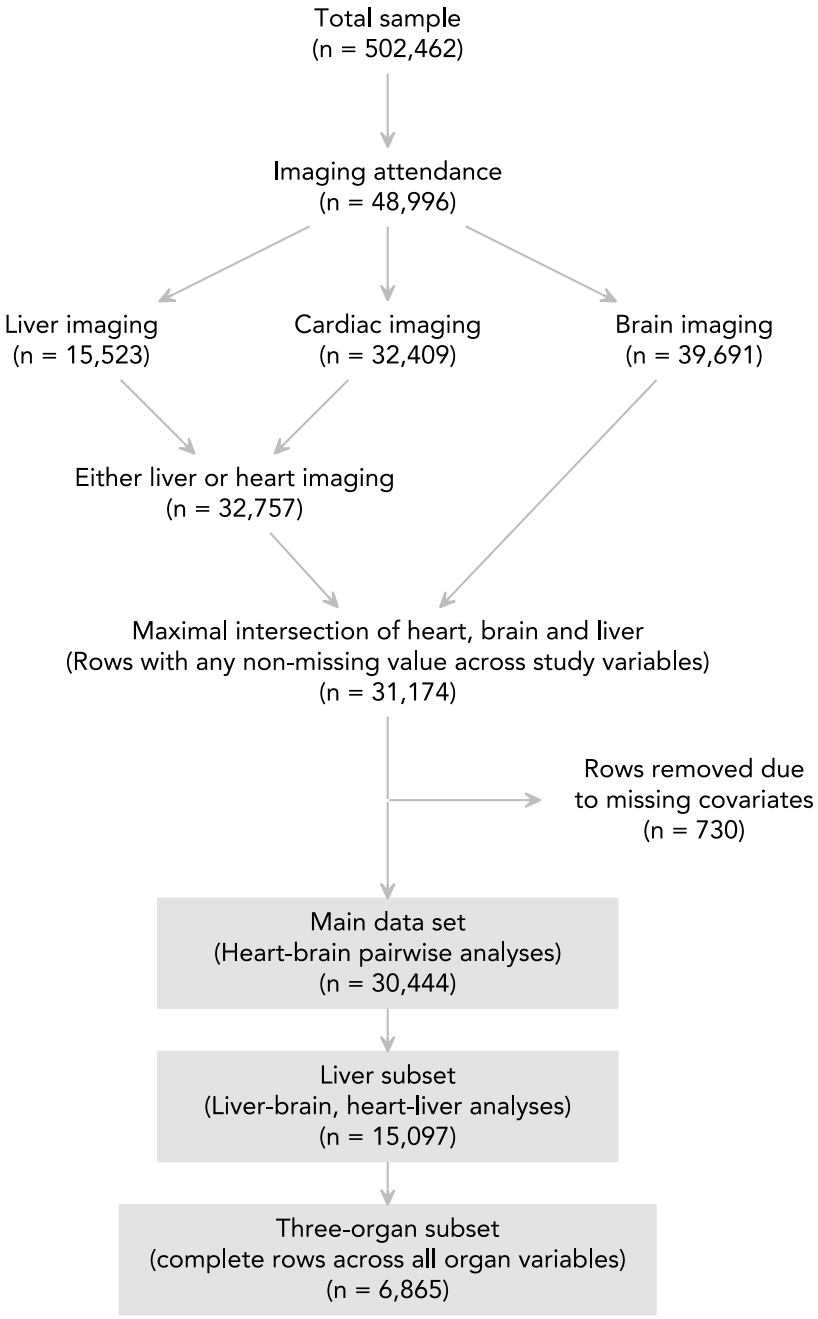


Figure 4.4: Chapter 4 - Sample selection

Table 4.2: Chapter 4 - Sample characteristics

Characteristic	Main set (n= 30,444)	Liver subset (n= 15,097)	Three-organ set (n= 6,865)
Female	15,905 (52.2%)	8,145 (54.0%)	3,736 (54.4%)
Male	14,539 (47.8%)	6,952 (46.0%)	3,129 (45.6%)
Age at imaging (years)	63.2 (±7.5)	62.6 (±7.5)	62.7 (±7.4)
SBP (mmHg)	137.8 (±18.2)	137.0 (±17.9)	136.8 (±17.3)
BMI (Kg/m2)	25.9 [23.5, 28.8]	25.7 [23.4, 28.5]	25.7 [23.5, 28.4]
BMI ≥ 30 kg/m^2	5,469 (18.0%)	2,446 (16.2%)	1,052 (15.3%)
Smoking status			
Never smoked	18,962 (62.3%)	9,462 (62.7%)	4,346 (63.3%)
Previous smoker	10,160 (33.4%)	4,953 (32.8%)	2,232 (32.5%)
Current smoker	1,095 (3.6%)	566 (3.7%)	241 (3.5%)
Physical activity (total MET-minutes/week)			
Highly active (>3,000)	9,635 (31.6%)	4,557 (30.2%)	2,082 (30.3%)
Moderately active (600-2,999)	15,551 (51.1%)	7,833 (51.9%)	3,605 (52.5%)
Inactive (<600)	5,008 (16.4%)	2,573 (17.0%)	1,126 (16.4%)
(Missing)	250 (0.8%)	134 (0.9%)	52 (0.8%)
Alcohol consumption frequency			
Never	1,963 (6.4%)	955 (6.3%)	418 (6.1%)
Less than once per week	6,547 (21.5%)	3,212 (21.3%)	1,453 (21.2%)
Once per week or more	21,704 (71.3%)	10,814 (71.6%)	4,948 (72.1%)
(Missing)	230 (0.8%)	116 (0.8%)	46 (0.7%)
Diagnosed status at imaging			
Diabetes	1,737 (5.7%)	753 (5.0%)	336 (4.9%)
Hypertension	9,855 (32.4%)	4,649 (30.8%)	2,043 (29.8%)
High cholesterol	10,541 (34.6%)	5,048 (33.4%)	2,280 (33.2%)
Cardiac imaging			
LVSVi (ml/m2)	46.9 (±8.4)	46.8 (±8.0)	46.8 (±7.9)
LV GFI (%)	47.6 (±6.9)	47.8 (±6.7)	48.0 (±6.6)
LVM/LVEDV (g/ml)	0.57 [0.52, 0.63]	0.57 [0.52, 0.63]	0.57 [0.52, 0.63]
Aortic distensibility (x10^{-3} mmHg^{-1})	2.23 [1.60, 3.03]	2.27 [1.62, 3.07]	2.24 [1.61, 3.04]
(Missing all cardiac metrics)	581 (1.9%)	443 (2.9%)	-
Liver imaging			
Liver fat (PDFF, %)	2.87 [2.00, 4.76]	2.87 [2.00, 4.76]	3.02 [2.12, 5.22]
Fatty liver (PDFF > 5%)	3,503 (23.2%)	3,503 (23.2%)	1,825 (26.6%)
Liver cT1 (ms)	693 [662, 729]	693 [662, 729]	691 [661, 727]
Liver iron (mg/g)	1.22 [1.13, 1.36]	1.22 [1.13, 1.36]	1.22 [1.12, 1.36]
(Missing all liver metrics)	15,347 (50.4)	-	-
Brain imaging			
Total brain volume (mL)	1,498.4 (±72.9)	1,504.4 (±72.6)	1,502.3 (±71.9)
Grey matter volume (mL)	794.1 (±47.8)	797.3 (±47.9)	797.4 (±47.0)
White matter hyperintensities (mL)	2.74 [1.48, 5.57]	2.58 [1.40, 5.08]	2.68 [1.46, 5.17]
(Missing all brain metrics)	1,317 (4.3%)	1,317 (8.7%)	-

Entries are either count (percent) or mean (± standard deviation) or median [25th percentile, 75th percentile]. BMI = body mass index, MET = metabolic equivalent task, SBP = systolic blood pressure, HbA1c = glycated haemoglobin, LVSVi = left ventricular stroke volume indexed to body surface area, LVEF= left ventricular ejection fraction, LV GFI = left ventricular global function index, LVM/LVEDV = left ventricular mass to volume ratio (left ventricular mass / left ventricular end diastolic volume), PDFF = proton density fat fraction, cT1 = corrected T1 relaxation time.

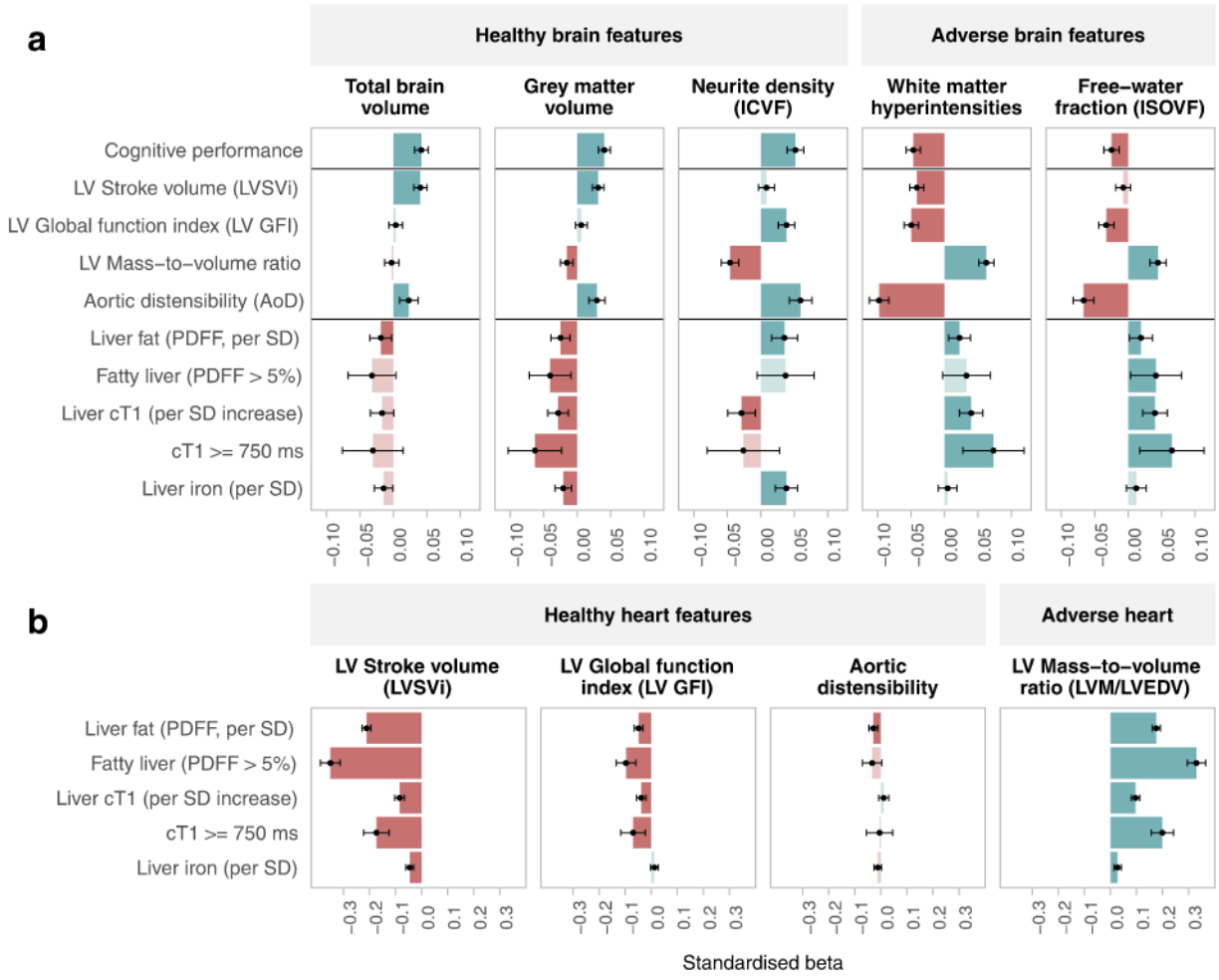


Figure 4.5: Chapter 4 - Pairwise associations between heart, brain and liver

The size of the bars and interval centre dot represent standardised beta coefficients, error bars represent 95% confidence intervals for the standardised beta coefficient from multivariable linear regression models. Red bars reflect negative associations, green bars reflect positive associations. **a** Heart and liver imaging metrics in pairwise associations with brain imaging metrics. **b** Pairwise associations between liver and heart imaging metrics. Models are adjusted by age, sex, diabetes, hypertension, BMI ≥ 30 kg/m2, high cholesterol, smoking, physical activity, alcohol consumption, deprivation, educational level, red blood count, total cholesterol, and glycosylated haemoglobin. Brain analyses are additionally adjusted by head size, imaging site, scanner coordinates and date of scanning. Each bar is from a separate model. Coefficient significance is assessed with a two-sided T-test, and p-values were considered significant after adjustment for multiple testing with a 5% false discovery rate. Where the p-value is not significant, the bar is shown in transparent colour. PDFF = proton density fat fraction, cT1 = corrected T1 relaxation time, ICVF = intracellular volume fraction, ISOVF = isotropic volume fraction, LVSVi = left ventricular stroke volume indexed to body surface area, LV GFI = left ventricular global function index, LVM/LVEDV = left ventricular mass to volume ratio (left ventricular mass / left ventricular end-diastolic volume), AoD = aortic distensibility. Associations between cognitive performance and brain imaging were calculated across a minimum of 25,280 participants. Liver-brain associations are from a minimum of 9,649 participants, heart-brain associations are from a minimum of 20,610 participants, liver-heart associations are from a minimum of 8,234 participants.

Table 4.3: Chapter 4 - Liver–brain associations

		Total brain volume	Grey matter volume	Neurite density (ICVF)	White matter hyperintensities (WMH)	Free-water fraction (ISOVF)
Cognitive performance	Std. beta	0.042*	0.041*	0.052*	-0.047*	-0.025*
	95% CI	[0.032, 0.052]	[0.032, 0.050]	[0.039, 0.064]	[-0.057, -0.036]	[-0.036, -0.013]
	p-value	1.00×10^{-15}	3.97×10^{-19}	4.94×10^{-16}	1.89×10^{-17}	2.18×10^{-5}
	n	27,113	27,113	25,280	25,983	25,280
Liver fat (PDFF, per SD increase)	Std. beta	-0.019*	-0.025*	0.036*	0.023*	0.019*
	95% CI	[-0.035, -0.003]	[-0.039, -0.011]	[0.016, 0.055]	[0.006, 0.039]	[0.002, 0.037]
	p-value	0.0234	6.32×10^{-4}	3.42×10^{-4}	0.0067	0.0308
	n	13,747	13,747	12,727	13,258	12,727
Fatty liver (PDFF > 5%)	Std. beta	-0.032	-0.040*	0.037	0.033	0.042*
	95% CI	[-0.068, 0.004]	[-0.072, -0.009]	[-0.005, 0.080]	[-0.003, 0.069]	[0.004, 0.080]
	p-value	0.0793	0.0113	0.0876	0.0704	0.032
	n	13,747	13,747	12,727	13,258	12,727
Liver cT1 (per SD increase)	Std. beta	-0.017	-0.029*	-0.029*	0.040*	0.040*
	95% CI	[-0.034, 0.000]	[-0.044, -0.013]	[-0.050, -0.008]	[0.022, 0.057]	[0.022, 0.058]
	p-value	0.0565	2.72×10^{-4}	0.0062	8.53×10^{-6}	1.86×10^{-5}
	n	10,403	10,403	9,649	10,138	9,649
Liver cT1 >= 750 ms	Std. beta	-0.031	-0.063*	-0.026	0.073*	0.065*
	95% CI	[-0.076, 0.015]	[-0.103, -0.023]	[-0.080, 0.028]	[0.027, 0.119]	[0.017, 0.113]
	p-value	0.1843	0.002	0.3439	0.0017	0.0076
	n	10,403	10,403	9,649	10,138	9,649
Liver iron (per SD increase)	Std. beta	-0.015	-0.021*	0.038*	0.005	0.012
	95% CI	[-0.029, -0.001]	[-0.033, -0.008]	[0.022, 0.055]	[-0.009, 0.019]	[-0.003, 0.027]
	p-value	0.0402	8.91×10^{-4}	6.53×10^{-6}	0.512	0.110
	n	13,761	13,761	12,741	13,273	12,741

Entries are standardised beta coefficients, 95% confidence intervals and p-values from linear regression models. Each cell represents one model, with the brain variable placed as the outcome/response and the liver variable placed as the exposure/predictor. Models are adjusted by age, sex, diabetes, hypertension, BMI ≥ 30 kg/m^2, high cholesterol, smoking, physical activity, alcohol consumption, deprivation, educational level, red blood count, total cholesterol, glycosylated haemoglobin, and imaging confounders (including head size, imaging site, scanner coordinates, date of scanning and interactions). P-values are from two-sided T-tests for each coefficient. An asterisk indicates significance after adjustment for multiple testing with a false discovery rate of 5%. PDFF = proton density fat fraction, cT1 = corrected T1 relaxation time, ICVF = intracellular volume fraction, ISOVF = isotropic volume fraction.

Table 4.4: Chapter 4 - Heart–brain associations

		Total brain volume	Grey matter volume	Neurite density (ICVF)	White matter hyperintensities (WMH)	Free-water fraction (ISOVF)
Cognitive performance	Std. beta	0.042*	0.041*	0.052*	-0.047*	-0.025*
	95% CI	[0.032, 0.052]	[0.032, 0.050]	[0.039, 0.064]	[-0.057, -0.036]	[-0.036, -0.013]
	p-value	1.00×10^{-15}	3.97×10^{-19}	4.94×10^{-16}	1.89×10^{-17}	2.18×10^{-5}
	n	27,113	27,113	25,280	25,983	25,280
LV Stroke volume (LVSVi)	Std. beta	0.040*	0.031*	0.009	-0.041*	-0.007
	95% CI	[0.030, 0.050]	[0.023, 0.040]	[-0.003, 0.021]	[-0.052, -0.031]	[-0.019, 0.004]
	p-value	7.27×10^{-16}	5.52×10^{-13}	0.1615	4.42×10^{-15}	0.1833
	n	28,561	28,561	26,653	27,438	26,653
LV Global function index (LV GFI)	Std. beta	0.003	0.006	0.038*	-0.050*	-0.033*
	95% CI	[-0.007, 0.014]	[-0.002, 0.015]	[0.026, 0.051]	[-0.060, -0.039]	[-0.044, -0.021]
	p-value	0.5039	0.1554	1.01×10^{-9}	6.73×10^{-20}	1.68×10^{-8}
	n	28,561	28,561	26,653	27,438	26,653
LV Mass-to-volume ratio (LVM/LVEDV)	Std. beta	-0.003	-0.016*	-0.046*	0.063*	0.045*
	95% CI	[-0.013, 0.008]	[-0.025, -0.006]	[-0.059, -0.033]	[0.051, 0.074]	[0.033, 0.057]
	p-value	0.6398	0.0011	5.60×10^{-12}	1.92×10^{-27}	3.82×10^{-13}
	n	28,561	28,561	26,653	27,438	26,653
Aortic distensibility (AoD)	Std. beta	0.023*	0.030*	0.060*	-0.098*	-0.067*
	95% CI	[0.009, 0.037]	[0.018, 0.042]	[0.043, 0.076]	[-0.112, -0.083]	[-0.082, -0.051]
	p-value	0.0011	1.44×10^{-6}	5.02×10^{-12}	8.66×10^{-40}	3.26×10^{-17}
	n	22,080	22,080	20,610	21,166	20,610

Entries are standardised beta coefficients, 95% confidence intervals and p-values from linear regression models. Each cell represents one model, with the brain variable placed as the outcome/response and the heart variable placed as the exposure/predictor. Models are adjusted by age, sex, diabetes, hypertension, BMI ≥ 30 kg/m^2, high cholesterol, smoking, physical activity, alcohol consumption, deprivation, educational level, red blood count, total cholesterol, glycosylated haemoglobin, and imaging confounders (including head size, imaging site, scanner coordinates, date of scanning and interactions). P-values are from two-sided T-tests for each coefficient. An asterisk indicates significance after adjustment for multiple testing with a false discovery rate of 5%. LVSVi = left ventricular stroke volume indexed to body surface area, LV GFI = left ventricular global function index, LVM/LVEDV = left ventricular mass to volume ratio (left ventricular mass / left ventricular end-diastolic volume), AoD = aortic distensibility, ICVF = intracellular volume fraction, ISOVF = isotropic volume fraction.

Table 4.5: Chapter 4 - Liver–heart associations

		LV Stroke volume (LVSVi)	LV Global function index (LV GFI)	LV Mass-to-volume ratio (LVM/LVEDV)	Aortic distensibility (AoD)
Liver fat	Std. beta	-0.211*	-0.048*	0.176*	-0.029*
(PDFF, per SD increase)	95% CI	[-0.228, -0.195]	[-0.065, -0.031]	[0.160, 0.192]	[-0.046, -0.012]
	p-value	8.65×10^{-136}	1.76×10^{-8}	1.65×10^{-107}	6.16×10^{-4}
	n	14,618	14,618	14,618	11,428
Fatty liver	Std. beta	-0.350*	-0.096*	0.330*	-0.033
(PDFF > 5%)	95% CI	[-0.388, -0.313]	[-0.134, -0.059]	[0.295, 0.365]	[-0.071, 0.004]
	p-value	4.43×10^{-74}	4.83×10^{-7}	2.75×10^{-75}	0.0798
	n	14,618	14,618	14,618	11,428
Liver cT1	Std. beta	-0.084*	-0.038*	0.097*	0.011
(per SD increase)	95% CI	[-0.103, -0.066]	[-0.056, -0.020]	[0.080, 0.113]	[-0.008, 0.031]
	p-value	6.21×10^{-19}	3.38×10^{-5}	4.10×10^{-31}	0.2511
	n	11,175	11,175	11,175	8,234
Liver cT1 >= 750 ms	Std. beta	-0.174*	-0.070*	0.199*	-0.005
	95% CI	[-0.222, -0.125]	[-0.117, -0.022]	[0.157, 0.242]	[-0.055, 0.046]
	p-value	2.96×10^{-12}	0.0038	5.94×10^{-20}	0.852
	n	11,175	11,175	11,175	8,234
Liver iron	Std. beta	-0.045*	0.012	0.028*	-0.012
(per SD increase)	95% CI	[-0.060, -0.030]	[-0.002, 0.027]	[0.013, 0.042]	[-0.026, 0.003]
	p-value	4.06×10^{-9}	0.0996	1.27×10^{-4}	0.1086
	n	14,635	14,635	14,635	11,438

Entries are standardised beta coefficients and p-values from linear regression models. Each beta coefficient represents one model, with the heart variable as the outcome/response and the liver variable as the exposure/predictor. Models are adjusted by age, sex, diabetes, hypertension, BMI ≥ 30 kg/m^2, high cholesterol, smoking, physical activity, alcohol consumption, deprivation, educational level, red blood count, total cholesterol, and glycosylated haemoglobin. P-values are from two-sided T-tests for each coefficient. An asterisk indicates significance after adjustment for multiple testing with a false discovery rate of 5%. PDFF = proton density fat fraction, cT1 = corrected T1 relaxation time, LVSVi = left ventricular stroke volume indexed to body surface area, LV GFI = left ventricular global function index, LVM/LVEDV = left ventricular mass to volume ratio (left ventricular mass / left ventricular end-diastolic volume), AoD = aortic distensibility.

Table 4.6: Chapter 4 - Simultaneous liver-heart associations

Left hand side		Right hand side	Standard. beta	Lower CI	Upper CI	p-value	Fit measures
Reduced LVSV	~	Liver fat (PDFF)	0.227	0.205	0.249	$< 1.00 \times 10^{-250}$	Chi-square =
	~	Liver cT1	0.042	0.022	0.063	5.74×10^{-5}	6.76 (df = 3)
	~	Liver iron	0.051	0.036	0.066	2.91×10^{-11}	RMSEA = 0.021
		R^2	0.160				(95% CI= 0.000,
Reduced LV GFI	~	Liver fat (PDFF)	0.066	0.044	0.087	2.34×10^{-9}	0.025)
	~	Liver cT1	0.021	0.001	0.042	0.0415	TLI = 0.994
		R^2	0.190				N = 8,165
LVM/LVEDV	~	Liver fat (PDFF)	0.185	0.166	0.204	$< 1.00 \times 10^{-250}$	
	~	Liver cT1	0.054	0.036	0.072	4.39×10^{-9}	
	~	Liver iron	0.024	0.009	0.039	0.0023	
		R^2	0.332				
Aortic stiffening	~	Liver fat (PDFF)	0.030	0.011	0.049	0.0020	
		R^2	0.397				

Entries are standardised beta coefficients and p-values from a single path analysis containing four heart outcomes modelled by all liver exposures entered together. Model was fitted using the *sem* function in the *lavaan* package in R. Initially all liver variables were included for each outcome, then non-significant variables were removed one at a time to arrive at the final model. Liver variables were orthogonalized prior to modelling (see Appendix 5 for details). P-values are from two-sided Z-tests for each coefficient, and p-values were considered significant after adjustment for multiple testing with a 5% false discovery rate. Paths are adjusted by age, sex, diabetes, hypertension, BMI $\geq 30 kg/m^2$, high cholesterol, smoking, physical activity, alcohol consumption, deprivation, educational level, red blood count, total cholesterol, and glycosylated haemoglobin. PDFF = proton density fat fraction, cT1 = corrected T1 relaxation time, LVSV = left ventricular stroke volume, LV GFI = left ventricular global function index, LVM/LVEDV = left ventricular mass to volume ratio (left ventricular mass / left ventricular end-diastolic volume).

Table 4.7: Chapter 4 - Simultaneous three-organ network models

Model	Equation	Left hand side		Right hand side	Standard. beta	Lower CI	Upper CI	p-value	Fit measures	Reported in Figure 4.6
1a	1	Grey matter volume	~	Reduced LVSV	-0.024	-0.043	-0.006	0.0106	Chi-square = 147.70 (df = 9)	Yes
		Grey matter volume	~	Aortic stiffening	-0.038	-0.060	-0.017	$4.56x10^{-4}$	RMSEA = 0.047 [0.041, 0.054]	
		Grey matter volume	~	Liver ct1	-0.029	-0.046	-0.011	0.0018	TLI = 0.881	
	2	Reduced LVSV	~	Liver fat (PDFF)	0.229	0.206	0.252	$< 1.00 \times 10^{-250}$	$R^2 = 0.503$	
		Reduced LVSV	~	Liver cT1	0.037	0.015	0.059	$9.01x10^{-4}$		
1b	1	Grey matter volume	~	Reduced LVSV	-0.025	-0.044	-0.006	0.0112	Chi-square = 529.27 (df = 20)	No
		Grey matter volume	~	Aortic stiffening	-0.038	-0.060	-0.017	$4.96x10^{-4}$	RMSEA = 0.061 [0.056, 0.065]	
		Grey matter volume	~	Liver cT1	-0.030	-0.048	-0.012	$8.86x10^{-4}$	TLI = 0.737	
	2	Liver fat (PDFF)	~	LVSVi	0.213	0.189	0.237	$< 1.00 \times 10^{-250}$	$R^2 = 0.502$	
		Liver fat (PDFF)	~	LV_GFI	-0.038	-0.062	-0.014	0.0021		
		Liver fat (PDFF)	~	LVM/LVEDV	0.152	0.127	0.177	$< 1.00 \times 10^{-250}$		
		Liver fat (PDFF)	~	Aortic stiffening	0.050	0.023	0.076	$2.14x10^{-4}$		
	3	Liver cT1	~	LVM/LVEDV	0.026	0.001	0.052	0.0457		
2a	1	White matter hyperintensities	~	LV_GFI	0.031	0.009	0.052	0.0046	Chi-square = 480.2 (df= 10)	No
		White matter hyperintensities	~	LVM/LVEDV	0.072	0.050	0.094	$1.58x10^{-10}$	RMSEA = 0.083 [0.077, 0.089]	
		White matter hyperintensities	~	Aortic stiffening	0.071	0.046	0.095	$1.11x10^{-8}$	TLI = 0.554	
		White matter hyperintensities	~	Liver cT1	0.032	0.011	0.052	0.0021	$R^2 = 0.363$	
	2	LVM/LVEDV	~	Liver fat (PDFF)	0.184	0.162	0.207	$< 1.00 \times 10^{-250}$		
		LVM/LVEDV	~	Liver cT1	0.048	0.026	0.069	1.36x10-5		
2b	1	White matter hyperintensities	~	Reduced LV GFI	0.031	0.009	0.052	0.0056	Chi-square = 107.59 (df= 9)	Yes
		White matter hyperintensities	~	LVM/LVEDV	0.072	0.049	0.094	$5.91x10^{-10}$	RMSEA = 0.040 [0.033, 0.047]	
		White matter hyperintensities	~	Aortic stiffening	0.071	0.046	0.095	$1.45x10^{-8}$	TLI = 0.855	
		White matter hyperintensities	~	Liver cT1	0.032	0.012	0.052	0.0020	$R^2 = 0.363$	
	2	Liver ct1	~	LVM/LVEDV	0.026	0.001	0.052	0.0046		
3	1	ISOVF	~	Aortic stiffening	0.068	0.042	0.094	$3.41x10^{-7}$	Chi-square = 0.00 (df = 0)	Yes
		ISOVF	~	Liver cT1	0.042	0.020	0.064	$1.87x10^{-4}$	RMSEA = 0.000 , TLI = 1.000	(Both forms reduced
		ISOVF		(R^2)	0.251				$R^2 = 0.251$	to these paths)

Final results from multiorgan path analysis for simultaneous liver/heart associations with grey matter volume, white matter hyperintensities and free-water fraction (ISOVF), in the subset with complete cases across three organs (N= 6,865). Results show test paths only – not showing confounder coefficients. Path analysis models were fitted using the *sem* function in the *lavaan* package in R. All paths are adjusted by age, sex, height, diabetes, hypertension, high cholesterol, smoking, physical activity, alcohol intake frequency, Townsend deprivation score, education, systolic blood pressure, BMI ≥ 30 kg/m^2, total cholesterol, glycated haemoglobin and red blood cell count. Paths featuring the brain are additionally adjusted by head size, imaging site, scanner coordinates and imaging date. P-values are from two-sided Z-tests for each coefficient, and p-values were considered significant after adjustment for multiple testing with a 5% false discovery rate. The chi-square in model 3 is zero as this has reduced to a single fitted linear equation. Prior to simultaneous modelling, heart and liver predictors were orthogonalized to remove within-organ correlation (see Appendix 5 for details).

4.3.3 Associations between liver and brain indices

In fully adjusted models, greater liver fibro-inflammation (cT1) was associated with significantly smaller grey matter brain volumes (standardised beta = -0.029, 95% confidence interval = [-0.044, -0.013]), larger volumes of white matter hyperintensities (0.040, [0.022, 0.057]), and adverse white matter microstructural measurements (Figure 4.5a, Table 4.3). Specifically, higher levels of liver fibro-inflammation (higher cT1) were associated with lower neurite density (lower ICVF, -0.029, [-0.050, -0.008]) and a greater proportion of free-moving water (higher ISOVF, 0.040, [0.022, 0.058]). In sense checks against cognitive function, higher values across the healthy brain features (total brain volume, grey matter volume and neurite density, ICVF) were associated with better cognitive performance, while the reverse was true for adverse brain features (white matter hyperintensities and free-water fraction, ISOVF). Greater liver iron was associated with smaller total brain and grey matter volumes (-0.015, [-0.029, -0.001] and -0.021, [-0.033, -0.008] respectively) but was positively associated with neurite density (higher ICVF, 0.038, [0.022, 0.055]).

In fully adjusted models, greater liver fat (higher PDFF) was significantly associated with adverse macroscale structural brain changes; specifically, smaller total brain and grey matter brain volumes (standardised beta = -0.019, 95% confidence interval = [-0.035, -0.003], and -0.025, [-0.039, -0.011] respectively) and larger white matter hyperintensity volumes (0.023, [0.006, 0.039]). However, the associations between brain microstructure and liver fat were mixed, in that higher PDFF was associated with both higher free-water fraction (higher ISOVF, 0.019, [0.002, 0.037]) and higher neurite density (higher ICVF, 0.036, [0.016, 0.055]). In participants with PDFF above the 5% threshold, however, the effect for neurite density was not significant (ICVF, 0.037, [-0.005, 0.080]) while the effect for free-water fraction was strengthened (higher ISOVF, 0.042, [0.004, 0.080]; Figure 4.5a, Table 4.3).

4.3.4 Associations between heart and brain indices

We observed a number of significant associations between adverse brain and cardiac image-derived phenotypes (Figure 4.5a, Table 4.4). Specifically, greater total brain and grey matter volumes were associated with greater cardiac LV stroke volume (0.040, [0.030, 0.050] and 0.031, [0.023, 0.040] respectively). Accumulation of white matter hyperintensities was linked to significantly poorer cardiac function in the form of lower LVSV (-0.041, [-0.052, -0.031]), lower LV global function index (-0.050,

[-0.060, -0.039]), a more concentric LV remodelling pattern (higher LVM/LVEDV, 0.063, [0.051, 0.074]), and lower aortic distensibility (-0.098, [-0.112, -0.083]).

Similarly, microstructural aspects of brain health were associated with adverse cardiac phenotypes. In particular, lower neurite density (ICVF) and a higher proportion of free-moving water (lower ISOVF) were linked to LV global function index (ICVF, 0.038, [0.026, 0.051]; ISOVF, -0.033, [-0.044, -0.021]), concentric LV remodelling (ICVF, -0.046, [-0.059, -0.033]; ISOVF, 0.045, [0.033, 0.057]), with aortic distensibility showing the strongest effects (ICVF, 0.060, [0.043, 0.076]; ISOVF, -0.067, [-0.082, -0.051]).

4.3.5 Associations between liver and heart indices

In fully-adjusted pairwise models, higher values of all three liver features (PDFF, cT1, liver iron) were associated with poorer cardiac structure and function metrics (Figure 4.5b, Table 4.5), with the strongest signal observed for liver fat (PDFF). Larger LV stroke volumes were associated with lower levels of liver fibro-inflammation (lower cT1, -0.084, [-0.103, -0.066]), lower liver fat (PDFF, -0.211, [-0.228, -0.195]), and lower liver iron (-0.045, [-0.060, -0.030]). Greater global function index was also protective for the accumulation liver fat (-0.048, [-0.065, -0.031]) and liver cT1 (-0.038, [-0.056, -0.020]). Concentric LV remodelling (higher LVM/LVEDV) was associated with all three adverse liver features; higher liver cT1 (0.097, [0.080, 0.113] , higher liver fat (0.176, [0.160, 0.192]), and liver iron (0.028, [0.013, 0.042]). Greater liver fat (higher PDFF) was associated with greater aortic stiffening (lower aortic distensibility, -0.029, [-0.046, -0.012]), whereas the relationship between liver cT1 and aortic distensibility was not significant (0.011, [-0.008, 0.031]).

In simultaneous liver-heart modelling (Table 4.6), higher liver fat (PDFF) had significant adverse associations with all heart features and had a stronger effect on the heart (larger coefficient) than liver cT1 or liver iron. The heart imaging metrics most strongly associated with liver fat were reduced LV stroke volume (0.227, [0.205, 0.249]) and increased concentric LV remodelling (higher LVM/LVEDV, 0.185, [0.166, 0.204]).

4.3.6 Multiorgan models

Three-organ path analysis modelling found direct and indirect associations with both heart and liver for all three brain outcomes (Figure 4.6, Table 4.7). Aortic stiffening (AoS, lower aortic distensibility) and liver cT1 were the strongest heart and liver features respectively, both directly associated with smaller grey matter volumes (AoS, -0.038, [-0.060, -0.017]; liver cT1, -0.029, [-0.046, -0.011]), greater white matter hyperintensities (AoS, 0.071, [0.046, 0.095]; liver cT1, 0.032, [0.012, 0.052]) and higher ISOVF (AoS, 0.068, [0.042, 0.094]; liver cT1, 0.042, [0.020, 0.064]), even after adjustment for confounders. For all three brain outcomes, aortic stiffening had a stronger signal than liver cT1.

In addition to the features mentioned above, reduced LV stroke volume was also associated with smaller grey matter volumes (-0.024, [-0.043, -0.006]) with LVSV in turn strongly associated with higher liver fat (0.229, [0.206, 0.252]). In addition to aortic stiffening and liver cT1, the accumulation of white matter hyperintensities was associated with greater concentric LV remodelling (higher LVM/LVEDV, 0.072, [0.049, 0.094]) and reduced LV global function index (0.031, [0.009, 0.052]). While the variance explained in brain outcomes (R^2) was comparable between alternative model forms (see Figure 4.3), the final three-organ models reported in Figure 4.6 had better overall fit (lower root mean squared error, higher Tucker-Lewis index) than their alternative form counterparts (see Fit measures, Table 4.7).

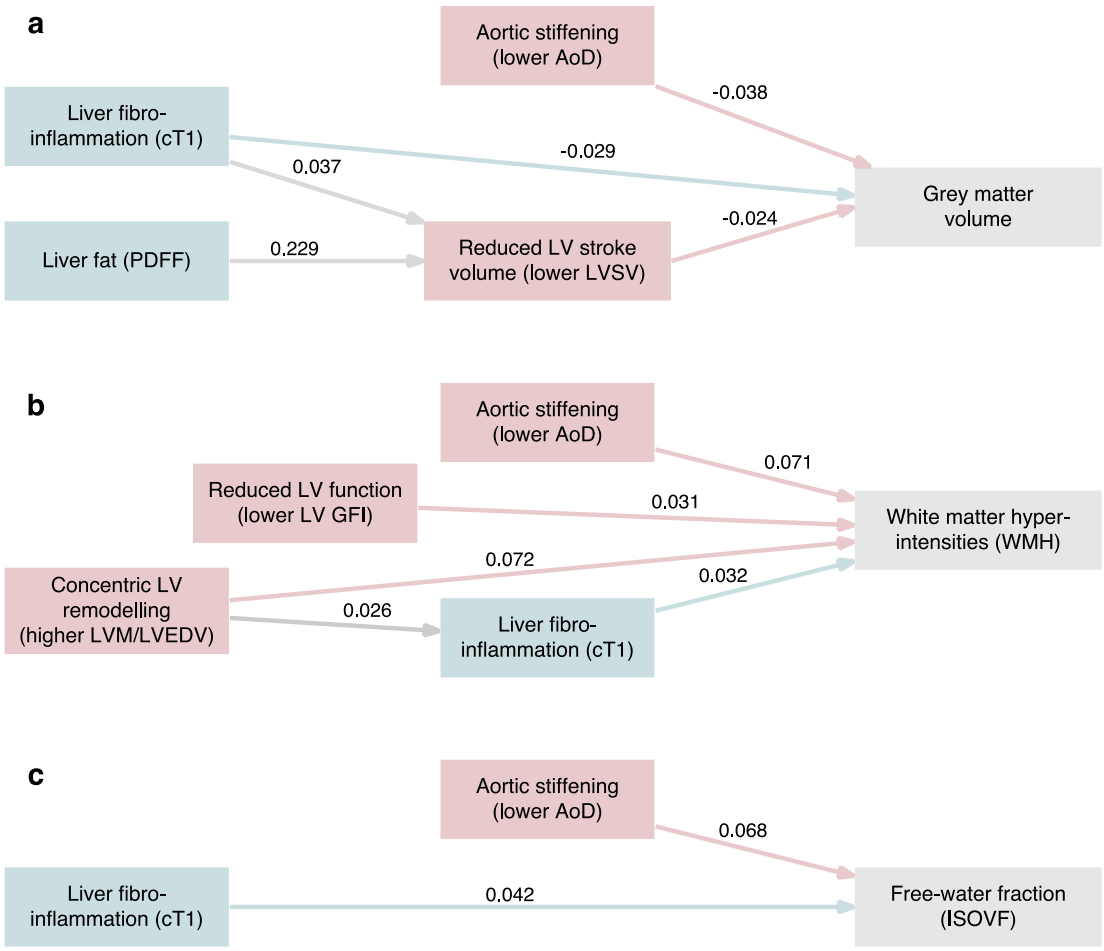


Figure 4.6: Chapter 4 - Simultaneous liver/heart associations with brain health

Final models and standardised beta coefficients from path analyses fitted using the *lavaan* package in R. All path analysis models are calculated with 6,865 participants. **a** Simultaneous heart and liver associations with grey matter volume. **b** Simultaneous heart and liver associations with accumulation of white matter hyperintensities. **c** Simultaneous heart and liver associations with increased free-water fraction. Brain measures are in grey, heart measures are in pink and liver measures are in teal. Models are built for a single brain outcome, and initially include two liver variables as predictors (liver PDFF and cT1) and all heart variables together in two alternative forms (i) Brain ~ Heart + Liver, Heart ~ Liver, and (ii) Brain ~ Heart + Liver, Liver ~ Heart (see Supplementary Figure 1 for detail).Non-significant paths were removed one at a time to reach the final model, then the best fitting form based on highest Tucker-Lewis fit index and lowest root mean squared error. All paths are adjusted by age, sex, height, diabetes, hypertension, high cholesterol, smoking, physical activity, alcohol frequency, Townsend deprivation score, education, systolic blood pressure, BMI ≥ 30 kg/m^2, total cholesterol, glycated haemoglobin, red blood cell count. Paths connecting to the brain are additionally adjusted by imaging confounders. Coefficient significance was assessed with a two-sided Z-test, and p-values were considered significant after adjustment for multiple testing with a 5% false discovery rate. Prior to simultaneous modelling, liver and heart variables were orthogonalized to remove within-organ correlation (see Supplementary Table 4 for details). LV= left ventricular, PDFF= proton density fat fraction, cT1 = corrected T1 relaxation time, ISOVF = isotropic volume fraction, AoD= aortic distensibility.

4.4 Discussion

4.4.1 Summary of findings

In this extensive cohort study involving 14,539 men and 15,905 women from the UK Biobank, we identified multiple significant patterns of association across the heart-brain-liver axis using multiorgan imaging. Elevated liver fat, increased liver fibro-inflammation, and higher liver iron levels were associated with reduced total brain and grey matter volumes, increased brain microvascular injury volumes, and poorer white matter microstructure, as indicated by diffusion metrics. Similar correlations were noted between brain and heart imaging metrics. Unfavourable liver characteristics were linked to compromised cardiovascular structure and function, including reduced left ventricular function, more concentric left ventricular remodelling, and decreased aortic compliance. The most consistent markers in liver-brain, liver-heart, and heart-brain associations were liver fibro-inflammation (cT1), liver fat (PDFF), and aortic distensibility, respectively. Notably, these relationships were independent of a variety of shared demographic, lifestyle, environmental, and vascular risk factors such as diabetes mellitus, hypertension, high cholesterol, high BMI, and smoking. Structural equation modelling demonstrated both direct and indirect relationships between the three organ systems, further supporting the interdependencies of the heart-brain-liver axis.

4.4.2 Associations Between Liver and Brain

Elevated liver tissue cT1 is linked to increased inflammation and fibrosis and serves as an indicator of liver fibro-inflammation [144]. Our research showed that liver fibro-inflammation (higher cT1 values) primarily influences adverse brain characteristics, including reduced brain volume, increased white matter hyperintensities, lower neurite density (ICVF), and higher free-water fraction (ISOVF).

Previous studies with smaller sample sizes have established connections between fatty liver disease and brain atrophy [198, 317–319] as well as a higher burden of white matter hyperintensities [199, 320, 321]. While our findings corroborate these associations, our analysis of microscale imaging metrics revealed a more complex relationship between liver fat and white matter integrity. Specifically, within the lower/healthy liver fat range (0 – 4.9%), we observed an association with higher neurite density. This atypical finding could be attributed to phenotypic variations in individuals with normal liver fat

levels [322, 323], or the role of fatty acids in forming and maintaining axonal myelin, which is predominantly composed of lipids [324, 325].

However, when liver fat exceeded the 5% threshold, the beneficial effects on the brain were negated, and adverse impacts, such as increased ISOVF, became more prominent. In simultaneous modelling, liver fat did not directly correlate with negative brain phenotypes in the presence of liver cT1, suggesting that fibro-inflammation is the main driver of these associations. It is important to note that most UK Biobank participants fall within the healthy liver fat range, and our results might not fully represent individuals with significantly higher liver fat levels, implying that these relationships could differ in less healthy populations.

4.4.3 Associations Between Heart and Brain

Our study reveals significant associations between cardiac and cerebral metrics across all structural and functional parameters, independent of well-known shared risk factors. Aortic distensibility emerged as the most robust marker, corroborating previous smaller studies that linked aortic stiffness with brain ageing [166, 326, 327]. Our findings support the cerebral hypoperfusion hypothesis, showing that reduced left ventricular (LV) function and decreased arterial compliance are associated with adverse brain characteristics, such as cerebral atrophy and microvascular plaque accumulation [328].

A prior UK Biobank analysis identified a correlation between lower LV ejection fraction and negative structural brain changes, such as decreased grey matter volume and increased white matter hyperintensities [329]. This research extends these findings by examining a broader spectrum of cardiovascular and brain features, including both structural and functional metrics.

Research on the relationship between cardiac imaging metrics and white matter microstructure is limited. One small-scale study (n=318) reported that increased LV mass was linked to compromised white matter in several brain regions, including the superior frontal gyrus and the anterior and superior corona radiata [330]. The current study presents associations between various heart imaging metrics and advanced neuronal microstructure metrics, indicating a consistent pattern of mutual reinforcement between more favourable cardiac and brain imaging outcomes, particularly through aortic distensibility. While previous studies have connected vascular risk factors like hypertension and smoking to brain atrophy, white matter hyperintensities, and white matter microstructure [136, 331–334], our findings

show significant brain-heart metric associations even after adjusting for these shared vascular risk factors. Another small study of 406 participants [335] found an association between adverse CMR (enlarged left atrium) and brain diffusion metrics (reduced white matter fractional anisotropy) independent of risk factors.

4.4.4 Associations Between Liver and Heart

We found a consistent pattern of associations between liver and heart metrics across all imaging parameters considered. The most notable associations were between liver fat and heart metrics, where higher PDFF was strongly linked to reduced left ventricular (LV) stroke volume and more concentric LV remodelling. This cardiac profile is consistently associated with poorer mortality and clinical outcomes [112]. Although previous research has linked clinically diagnosed fatty liver disease to poorer heart health and LV hypertrophy in particular [183], our study confirms this relationship at the organ level in a large, population-based sample predominantly free from clinical disease.

Additionally, higher levels of liver fibro-inflammation (cT1) and liver iron were associated with adverse cardiac features, though these associations were less pronounced than those with liver fat. It is important to consider that elevated liver fat often precedes liver fibrosis in many individuals. Consequently, the stronger associations between liver fat and cardiac health in the UK Biobank population may be due to the greater magnitude of fat changes compared to fibro-inflammation changes. Therefore, it is possible that associations between cardiac health and liver fibro-inflammation may become more prominent in populations with more advanced liver disease.

4.4.5 Three-Organ Network Analysis

Beyond pairwise associations, our simultaneous three-organ path analysis highlighted key aspects of the heart-brain-liver axis. Among the studied heart and liver features, aortic distensibility and liver fibro-inflammation (cT1) emerged as significant factors influencing brain health. These features consistently correlated with adverse brain changes at both macro and micro levels. This suggests that therapies aimed at enhancing vascular health and reducing liver inflammation may also benefit brain health.

Moreover, the analysis revealed interactions between the liver and heart, potentially exacerbating negative impacts on the brain. For instance, higher liver fat was linked to reduced LV stroke volume, which in turn was associated with decreased grey matter volume. Although the effect sizes were small, the presence of both direct and indirect effects suggests a potentially cumulative burden of multiorgan dysfunction.

4.4.6 Conclusion

The UK Biobank's multiorgan imaging, using standardised methods, provides an ideal framework for this study. By using imaging measures of organ structure and function, our assessments avoid the biases and subjectivity inherent in clinical diagnoses or cognitive function tests used in prior research. Our imaging analysis included only previously validated, fully automated, quality-controlled metrics published in other work, to reduce the risk of information bias from image translation. The extensive characterisation of the UK Biobank cohort allowed for adjustments for a wide range of potential confounders. However, there might be imperfections in the measurement of these covariates (e.g., physical activity is self-reported), leading to residual confounding. This study's analysis reflects cross-sectional relationships, and in our three-organ models, we assigned brain metrics as model outcomes. This choice does not imply a specific direction of relationships, which we believe is likely bidirectional, but rather ensures consistency and ease of interpretation. Furthermore, the presented three-organ model structures are not exhaustive of all possible combinations but highlight the most prominent simultaneous heart-brain-liver associations among the metrics studied. Future research might explore other approaches to address more specific questions. Our model structures assume that clinical diagnoses drive organ-level remodelling represented by imaging metrics; for instance, hypertension leading to LV hypertrophy. This direction seems most probable, making clinical diagnoses confounders in the model. However, we cannot rule out the possibility that changes in imaging metrics also drive clinical diagnoses, in which case the diagnoses would be colliders. While we consider this less likely, further investigation into these points could raise very interesting questions.

The UK Biobank imaging study is unique in its inclusion of multiorgan imaging data for a large population cohort, allowing analyses of large samples of predominantly healthy individuals. Available evidence supports the technical and clinical validity of the image-derived phenotypes used in our study. Increasing evidence demonstrates the clinical validity and trends of the CMR-derived metrics in the UK

Biobank [336]. Regarding brain imaging metrics, we provided a "sense check" against cognitive function to aid the interpretation of health direction. Overall, further research is needed to fully understand these measures' clinical validity in population cohorts. Lastly, due to the study's observational nature, we cannot rule out residual confounding or infer causation from the results presented.

In conclusion, we have outlined the connections between the heart, brain, and liver, demonstrating that many cross-organ associations identified in smaller clinical studies also appear in a large, mostly healthy population sample. We showed that multiorgan relationships persist after adjusting for dominant shared risk factors and that multiple cross-system associations can coexist within the same individuals. Our work adds to the mounting body of evidence suggesting that adverse features in one organ (e.g., the liver) may have implications for other organs. In this context, physicians should consider how other organs might be at risk and identify treatments with potential multi-system benefits.

As this is a hypothesis-generating study, further mechanistic research is needed to investigate the multiorgan impact of known risk factors (e.g., diabetes, hypertension) and the pathophysiological processes underpinning the identified associations (whether vascular, inflammatory, nutritional, infection-related, or toxin-related). A detailed examination of multiorgan mechanisms could help identify potential therapeutic strategies to maximise multiorgan benefits (e.g., statins, ACE inhibitors, blood-sugar-lowering medications).

In summary, the empirical evidence base for multiorgan interdependence is required to inform population-level risk stratification and disease prevention efforts. These findings show that the detection of abnormalities in any of the three organs may present an opportunity for early intervention and improved preservation of multiorgan health. The future insights gained from multi-system imaging are expected to significantly impact our ability to predict and prevent complex diseases, thus improving quality of life and delaying multimorbidity.

Chapter 5: Prevention of multimorbidity: The NHS Health Check

5.1 Introduction

In the previous chapter, we laid out the evidence for cross-organ relationships that are derivable from multiorgan imaging. In this chapter, we turn our attention to practical questions around the prevention of multimorbidity. The NHS Health Check programme (described in Section 2.2), is an intervention that already exists in primary care in the United Kingdom. The NHS Health Check aims to identify individuals at risk for several target conditions (heart disease, stroke, diabetes, and kidney disease) among adults aged 40-74. Participants undergo physical checks, blood tests, and health behaviour assessments, followed by support to prevent these conditions [77].

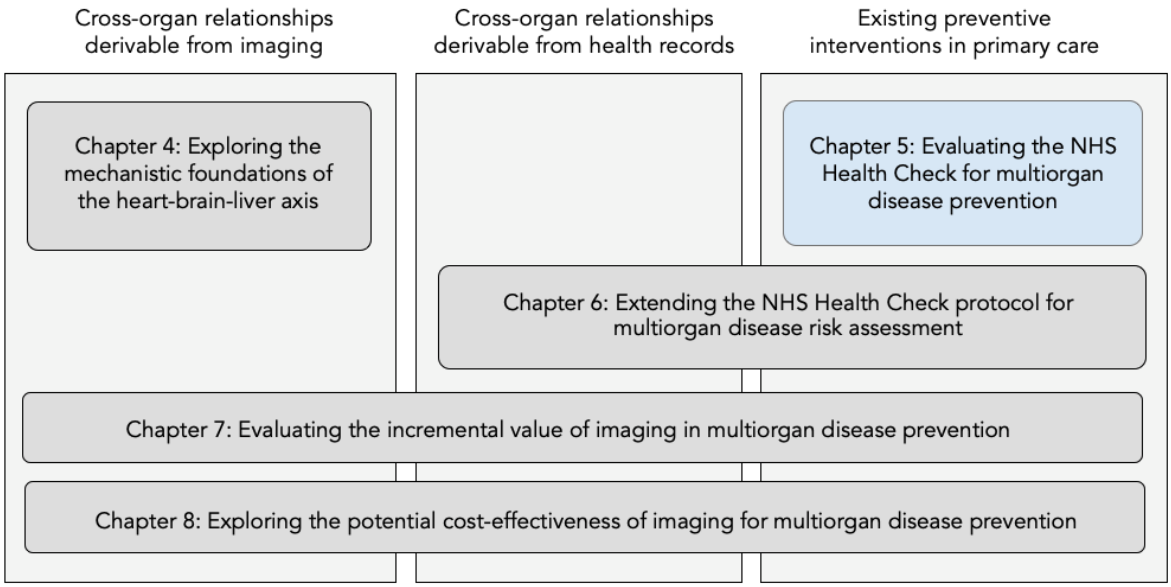


Figure 5.1: Chapter 5 - Roadmap location

The analysis and results of this chapter have been published under open access at

> *McCracken, Celeste, Zahra Raisi-Estabragh, Liliana Szabo, John Robson, Betty Raman, Anya Topiwala, Adriana Roca-Fernández, et al. 'NHS Health Check Attendance Is Associated with Reduced Multiorgan Disease Risk: A Matched Cohort Study in the UK Biobank'. BMC Medicine 22, no. 1 (23 January 2024): 1. https://doi.org/10.1186/s12916-023-03187-w.*

Because this intervention is already in place in the NHS, it is important to understand its effectiveness in preventing or delaying disease outcomes. While there is considerable evidence on the administration and uptake of the NHS Health Check [98], research on its long-term effectiveness in disease prevention is limited [101, 105, 337], often lacking data on multiple disease outcomes and longer-term follow-up.

The objective of this study is to compare the health outcomes of participants with and without evidence of receiving an NHS Health Check, with a view to establishing the evidence base for the NHS Health Check as an effective intervention for multimorbidity prevention.

5.2 Methods

5.2.1 Study sample

In this study, we drew upon the UK Biobank resource (Section 2.1) to identify participants who have received an NHS Health Check and to observe any new diagnoses received during the follow-up period. At the time of this study, there were 227,297 participants who had completed consent for their primary care records to be made available, and who had confirmed primary care records in the database (Figure 5.2). From this pool of participants, 7 participants had missing geographical location or were outside the age range for the NHS Health Check. A further 20,256 participants (9%) were excluded as ineligible for an NHS Health Check due to an existing diagnosis of heart, brain, liver or kidney disease and 66,135 participants (31%) were excluded due to statins prescription, or an existing diagnosis of diabetes or hypertension. The NHS Health Check criteria specifically exclude people with these conditions as they are considered to be already identified and managed by their NHS providers. Thus, 140,899 participants were used as the study sample.

5.2.2 Case-control matching

In order to reduce confounding from known sources, we applied an extensive case-control matching algorithm, to produce a control group that was matched 1-to-1 with NHS Health Check recipients using nearest neighbour propensity score matching with a calliper width of 0.2, as per published recommendations [338]. The iterative precision matching pipeline was custom coded using the central functionality of the ***MatchIt*** R package [339]. We conducted matching with respect to demographic features (geographical region, age, sex, ethnicity, Townsend deprivation index, education), family history of disease (stroke, heart disease, dementia), physical measures (body mass index, waist-to-hip ratio, systolic blood pressure at baseline) and health behaviours (smoking, alcohol intake frequency, physical activity and daily vegetable intake). More than 95% of cases (NHS Health Check recipients) received a high-quality match, and non-matching participants were dropped from the analysis. A review of the excluded participants indicated that although they tended to be younger, more deprived and more

obese, the main reason for matching failure was the strict requirement for 1-to-1 matching within geographical region. In other words, the matched control for a London health check recipient must also be from London. From this process, we derived a matched sample of 97,204 participants, with 48,602 participants in each exposure group (Figure 5.2).

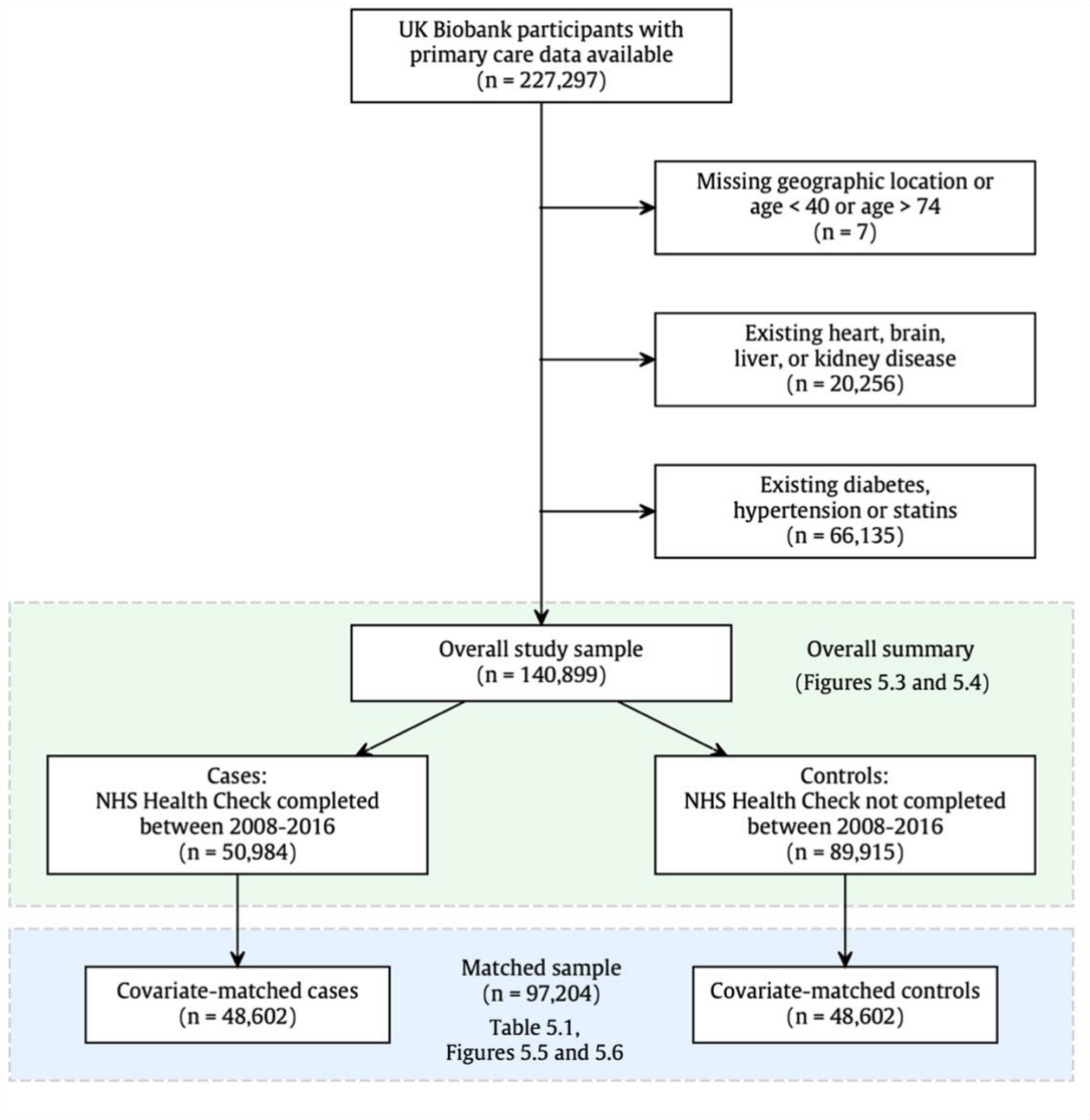


Figure 5.2: Chapter 5 - Study sample selection

5.2.3 The intervention: NHS Health Check

To identify participants who had received an NHS Health Check (or its Scottish equivalent), we performed a text search of primary care clinical records, for the following phrases "*keep well, health check, check up, healthy start, healthy lifestyle, diabetes prevent, well man, well woman, well adult*". This search returned 283,536 records between April 2006 and December 2022. From here, we reviewed the record text to exclude other types of health checks (healthy lifestyle, diabetes management, carer health checks and unspecified check-ups), and records that did not indicate NHS Health Check completion, for example invitations (terms including invitation, email, letter), neutral descriptors (not appropriate, indicated, status), and health check refusal (declined, refused, did not attend). The remaining codes that were used to confirm NHS Health Checks are provided in Appendix 6.

Although the official nation-wide launch took place in April 2009, there were some areas who participated in a pilot programme in the year leading up to this date [340]. Within the UK Biobank resource, coverage for primary care records was high up to mid-2016, when the availability of records dropped sharply. Therefore, the exposure window was set between 1st January 2008 and 30th June 2016. The count of records for health check exposure by year are illustrated in Figure 5.3. For modelling purposes, we considered the date of exposure to be the date of the first completed NHS Health Check.

5.2.4 Ascertainment of outcomes

Existing disease at baseline was assessed via both self-report and linked records (hospital and primary care). Incident disease after baseline was ascertained via primary care linked records, hospital records and death registry (Appendix 2) using published code lists where available [341–343]. We included the following outcomes; hypertension, diabetes, hyperlipidaemia, stroke (any type), all-cause dementia, myocardial infarction, atrial fibrillation, heart failure, acute kidney injury, chronic kidney disease (Stage 3, 4 or 5), fatty liver disease, alcoholic liver disease, liver cirrhosis, liver failure, cardiovascular mortality (death with a primary cause between ICD I00- I80), and all-cause mortality. Participants were followed up until the end of October 2022. All patient consent procedures were completed by UK Biobank, and details of record linkage in UK Biobank have been published previously [344].

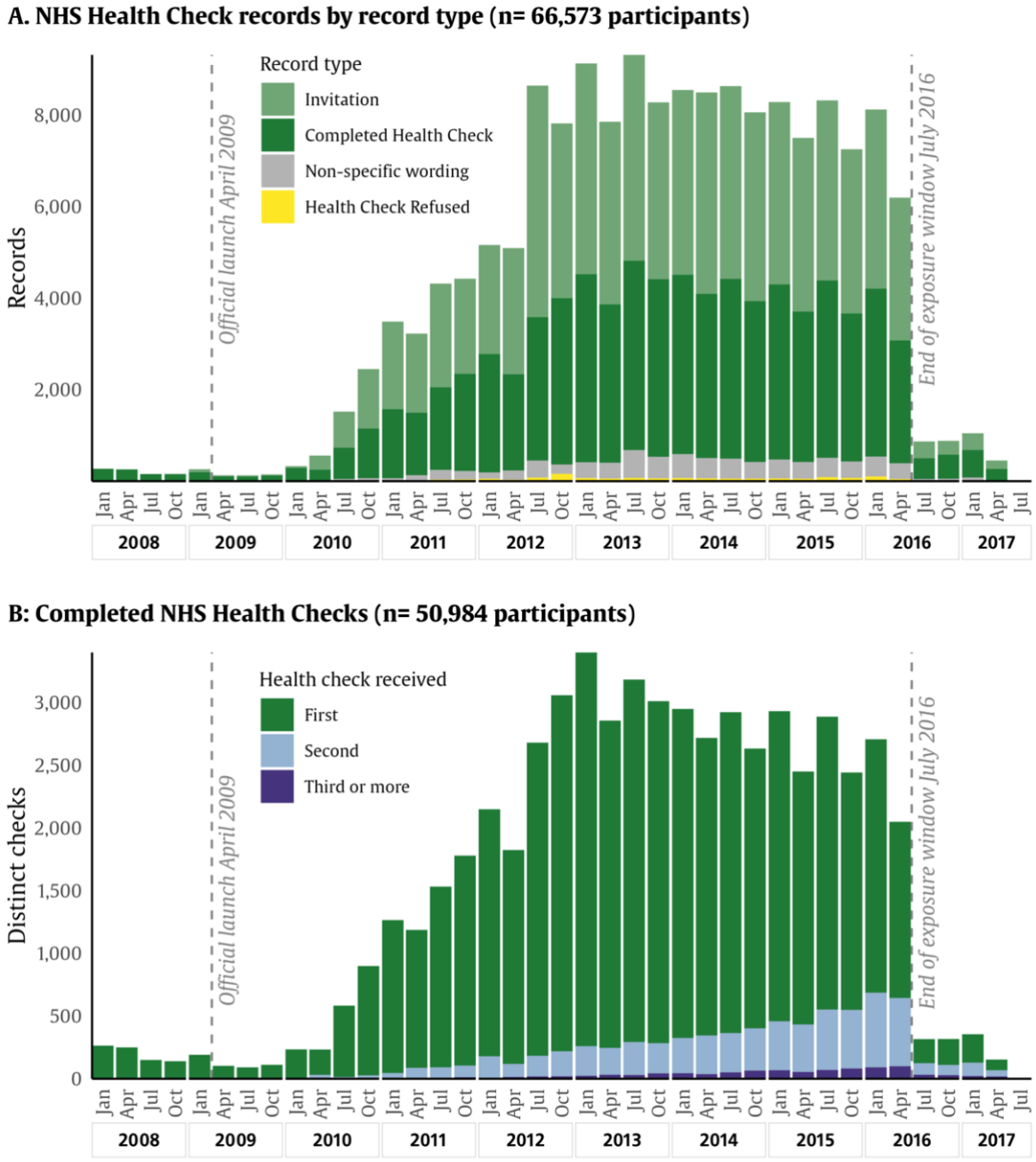


Figure 5.3: Chapter 5 - NHS Health Check records by year and record type

Distributions describing NHS Health Check records in the UK Biobank. **A**: The distribution of records tagged with NHS Health Check identifiers, coloured by record type, whether the record describes a completed health check, an invitation, a refusal, or a descriptive tag (not necessarily implying completion or refusal). **B**: The distribution of completed health checks, with blue showing the first recorded NHS Health Check, with green and yellow showing follow-up health checks. Participants are included from January 2008 until July 2016.

5.2.5 Definition of covariates

Age, sex, and all other covariates were recorded at baseline. Modelling covariates were selected based on their known associations with outcome risk in previous research, these include age, sex, geographical region, Townsend deprivation score, ethnicity (White / non-White), post-secondary education (yes/no), body mass index, waist-to-hip ratio, current smoking (yes/no), systolic blood pressure, Charlson comorbidity index, alcohol intake frequency, physical activity and fresh vegetable intake. Charlson comorbidity index – a widely-validated multiorgan comorbidity metric - was coded from existing conditions at baseline [345]. Physical activity was coded in summed metabolic equivalent task-minutes per week, based on aggregation of physical activity fields according to published guidance [257]. To partition participants into geographical region, we identified the coordinates of six major cities in the mainland UK (London, Bristol, Birmingham, Manchester, Newcastle upon Tyne and Edinburgh), and then allocated each participant to their nearest city based on the rounded east and north coordinate provided at baseline. Some of the covariates had a small amount of missing values (less than 2%) that were imputed together using multiple imputation with chained equations [290] as summarised in Appendix 7.

5.2.6 Statistical analysis

We used graphical illustration and simple descriptive statistics to outline the features of UK Biobank participants with primary care data and the uptake of the NHS Health Check. To assess the covariate-adjusted differences in outcomes between health check recipients and non-recipients, we used two main modelling approaches.

1) Time-varying Cox regression: We applied Cox survival modelling with the intervention (NHS Health Check date) coded in time-varying fashion following the method outlined by Therneau and colleagues [346–348]. In this method, follow-up begins at baseline registration, and all participants begin the follow-up period with intervention-negative status, in other words, no NHS Health Check. Then, across time, some participants receive an NHS Health Check, so at that date, they acquire intervention-positive status. Survival models were adjusted by the full complement of covariates outlined above, as recorded at baseline. This analysis makes use of the most amount of data and allows

time-based differences in exposure effect to be observed more easily, but could still be biased due to residual confounding.

2) Aligned-start Cox regression: In this analysis, we aligned the intervention window between cases and controls in a manner similar to Sebuødegård and colleagues [349] and then applied proportional hazards regression in the conventional sense. Here, the follow-up period is defined to begin at the date of the completed NHS Health Check, with outcome times aligned accordingly. Each control participant (without an NHS Health Check) is followed up from the intervention date of his or her matched pair. Full follow-up lengths were compared and were not significantly different between groups. In aligned-start analyses, ages were updated to be consistent with the intervention date, with the remainder of covariates as measured at baseline. This method provides better quality control for known confounding, but involves the loss of data, and hence loss in power.

Survival models in both approaches above were adjusted by age, sex, geographical region, Townsend deprivation score, ethnicity, post-secondary education, body mass index, waist-to-hip ratio, current smoking, systolic blood pressure, Charlson comorbidity index, alcohol intake frequency, physical activity, and fresh vegetable intake. Aligned-start models were additionally adjusted by length of time since registration. Multiple testing correction using a false discovery rate of 5% was applied to identify significant p-values across all models.

3) Further time adjustments: Prior research has identified that NHS Health Check receipt was associated with an increased detection and diagnosis of prevalent (but unrecognised) diabetes, hypertension, cardiovascular and kidney disease [98]. Therefore, we conducted the survival modelling with three-time exclusion settings; a) include all outcomes b) exclude outcome events in the first 12 months after NHS Health Check, and c) exclude outcome events in the first 24 months after NHS Health Check. In epidemiological research, it is common to exclude events that occur in the first few years of follow-up when studying the relationship between an exposure and a disease outcome. This latency period intends to reduce bias from reverse causation, which occurs when the main biological processes creating the disease outcome precede the exposure. By removing events that occur in the early years of follow-up, we hope to observe associations between the exposure and disease outcome that are not due to pre-existing disease influencing exposure status (see Rothman and colleagues, p.218-219 [350], and examples [351, 352]. We tested the proportional hazards assumption for the effect of NHS Health Check

on outcome risk using a chi-square test and graphical display of Schoenfeld residuals. In sensitivity analysis we re-ran the aligned start Cox models with stratified time periods (Therneau and colleagues [346], Section 4 of the referenced document). This approach has the lowest power of all, as each coefficient is calculated only using the outcomes within each time stratum.

4) Unmeasured confounding: Finally, we applied the e-value methodology described by VanderWeele and colleagues [353] to evaluate the potential nullifying impact of unobserved confounding variables. We calculated e-values and their lower bounds for each significant result and provided a translation of these into "years of ageing equivalent" to aid intuitive understanding of their relative strength.

5.3 Results

5.3.1 Description of NHS Health Check in UK Biobank

Within the overall sample (n= 140,899), 66,573 participants (47%) received at least one invitation for an NHS Health check between January 2008 and June 2016 (Figure 5.2). Of those who were invited, 50,984 participants (77% of those invited, 36% of full sample) received an NHS Health Check. Within recipients, most received only one NHS Health Check (44,910, 88%), 10.5% received a second NHS Health Check, and 1.4% received three or more.

In the full sample, there were more women than men (59% compared to 41%), with participants fairly evenly spread across the age range from 40 to 70 years at baseline (Figure 5.4). Eighteen percent of participants were obese (with body mass index > 30kg/m^2), and 10.6% were current smokers. Overall, 29.3% of participants had Townsend Deprivation index above the 2011 UK median indicating lower than average deprivation in the study sample [354]. This varied by geographical region, with London participants having the most nationally representative deprivation with 52.3% of participants above the UK median. NHS Health Check uptake rates also varied by geographical region, with the highest uptake in Birmingham, Manchester and Newcastle regions (all above 40%), with lowest uptake observed in Scotland (8.2%).

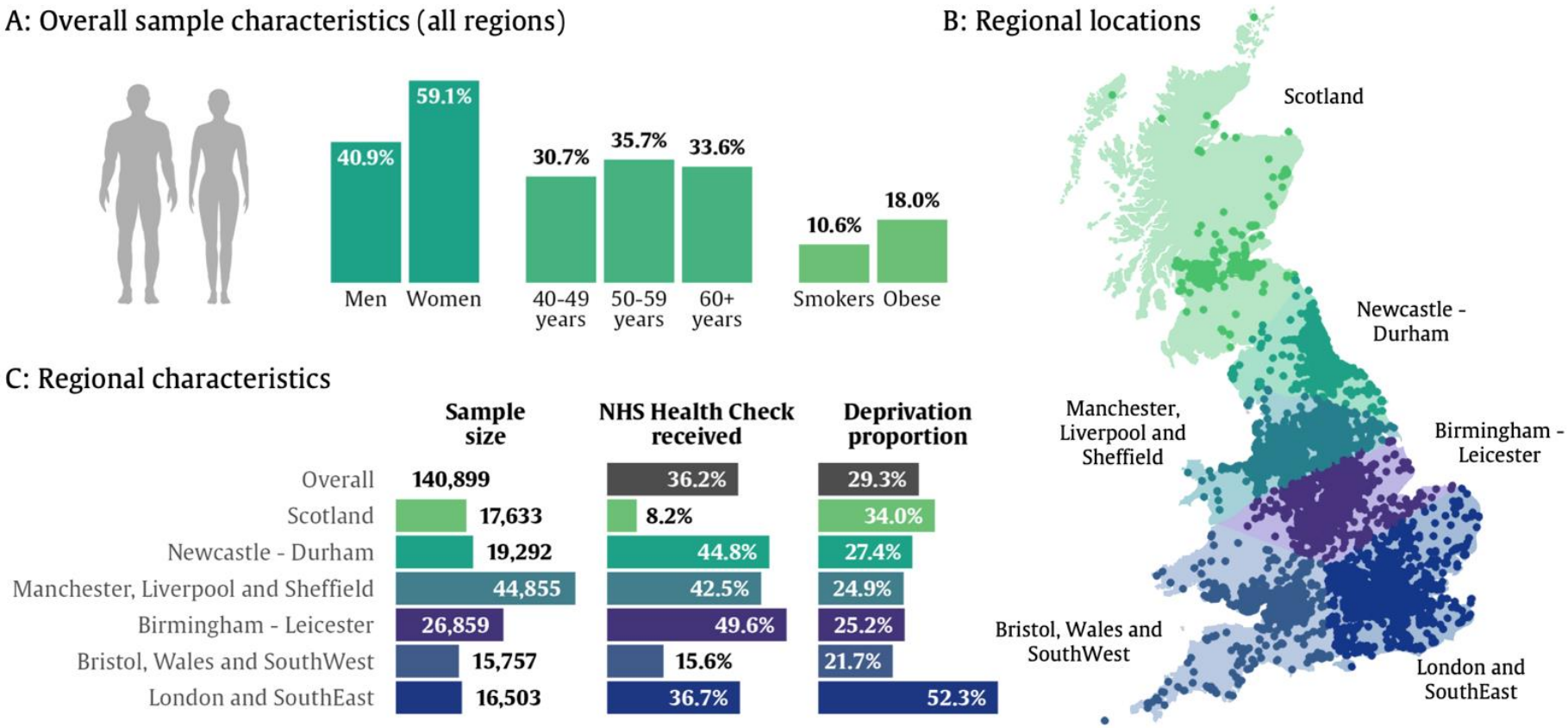


Figure 5.4: Chapter 5 - Summary of NHS Health Check in UK Biobank participants

A: Overall summaries for the sample of UK Biobank participants with primary care available (n= 140,772). **B:** Summary of geographical locations, **C:** Sample characteristics by geographical region. Deprivation proportion refers to the proportion of the sample that fall above the UK median for socioeconomic deprivation according to reported Townsend deprivation scores and quintiles from the 2011 Census.

5.3.2 The matched modelling set and observed outcomes

The matched subset used for modelling was very similar in profile to the overall study set, with 95% of NHS Health Check recipients (48,602 / 50,984) receiving a high-quality matched control pair (Table 5.1).

Characteristic of the UK Biobank more generally, the sample was mostly White ethnicity (4% other ethnicities), mostly physically active (23% inactive), with 19% of the sample consuming alcohol at least once per day. Table 5.1 also reports the outcome counts observed in the matched groups, along with their percentage rates. Many of the reported outcome rates are similar between groups (hypertension, diabetes, stroke, heart failure, chronic kidney disease). For several outcomes, there are larger differences between cases and controls, for example, all-cause dementia (1.2% vs 1.4%), myocardial infarction (1.9% vs 2.2%), and acute kidney injury (4.0% vs 5.3%). In Figure 5.5, histogram plots of outcome counts in NHS Health Check recipients are overlaid with the time-aligned outcome counts observed in their matched counterparts. Interestingly, for some outcomes (hypertension, diabetes, high cholesterol, chronic kidney disease, fatty liver disease and liver failure), more new diagnoses were recorded in NHS Health Check recipients in the initial two-year period following the health check than in their matched pairs. On the other hand, following the two-year mark, outcome counts were more likely to be equal or slightly higher in people who did not receive the NHS Health Check.

Table 5.1: Chapter 5 - Sample characteristics

Category	Variable	NHS Health Check recipients (n= 48,602)	Matched controls (n= 48,602)
Demographics	Age 40-49 years	13,536 (27.9%)	13,536 (27.9%)
	Age 50-59 years	17,998 (37.0%)	17,998 (37.0%)
	Age 60+ years	17,068 (35.1%)	17,068 (35.1%)
	Women	29,040 (59.8%)	29,040 (59.8%)
	Men	19,562 (40.2%)	19,562 (40.2%)
	Townsend deprivation index > UK median	13,950 (28.7%)	14,152 (29.1%)
	Non-white ethnicity	2,048 (4.2%)	2,046 (4.2%)
	Post-secondary education	29,986 (61.7%)	30,135 (62.0%)
Family history	Family history of stroke	12,664 (26.1%)	12,650 (26.0%)
	Family history of heart disease	20,280 (41.7%)	20,272 (41.7%)
	Family history of dementia	7,226 (14.9%)	7,229 (14.9%)
Health parameters	Obesity (Body mass index ≥30 kg/m2)	7,957 (16.4%)	8,130 (16.7%)
	Waist-hip ratio≥ 1	2,073 (4.3%)	2,082 (4.3%)
	SBP at baseline ≥ 140 mmHg	15,309 (31.5%)	15,889 (32.7%)
	Current smoker	4,640 (9.5%)	4,738 (9.7%)
	Daily alcohol intake	9,376 (19.3%)	9,325 (19.2%)
	Inactive (< 600 MET-minutes/week)	11,326 (23.3%)	11,307 (23.3%)
	Salad/raw vegetables daily (< 2 Tbsp)	21,134 (43.5%)	21,099 (43.4%)
Geographical region	Birmingham - Leicester	11,564 (23.8%)	11,564 (23.8%)
	Bristol, Wales and Southwest	2,411 (5.0%)	2,411 (5.0%)
	London and Southeast	5,979 (12.3%)	5,979 (12.3%)
	Manchester, Liverpool and Sheffield	18,790 (38.7%)	18,790 (38.7%)
	Newcastle - Durham	8,427 (17.3%)	8,427 (17.3%)
	Scotland	1,431 (2.9%)	1,431 (2.9%)
Exposure	NHS Health Check completed	48,602 (100.0%)	-
	Average follow-up time (years)	9.1 (±1.9)	9.0 (±2.0)
Measured outcomes			
Metabolic	Hypertension	5,603 (11.5%)	5,398 (11.1%)
	Diabetes	1,144 (2.4%)	1,187 (2.4%)
	High cholesterol	3,690 (7.6%)	3,487 (7.2%)
Brain	Stroke	708 (1.5%)	770 (1.6%)
	All-cause dementia	562 (1.2%)	694 (1.4%)
Heart	Myocardial infarction	913 (1.9%)	1,052 (2.2%)
	Atrial fibrillation	1,660 (3.4%)	1,759 (3.6%)
	Heart failure	739 (1.5%)	796 (1.6%)
Kidney	Acute kidney injury	1,924 (4.0%)	2,572 (5.3%)
	Chronic kidney disease	973 (2.0%)	946 (1.9%)
Liver	Fatty liver disease	502 (1.0%)	492 (1.0%)
	Alcoholic liver disease	67 (0.1%)	93 (0.2%)
	Liver cirrhosis	109 (0.2%)	161 (0.3%)
	Liver failure	43 (0.1%)	60 (0.1%)
Mortality	Cardiovascular mortality	279 (0.6%)	360 (0.7%)
	All-cause mortality	1,989 (4.1%)	2,568 (5.3%)

MET = metabolic equivalent task. Cardiovascular mortality refers to any death with a primary cardiovascular cause (ICD I00- I80)

5.3.3 NHS Health Check associations with outcomes

Because the smoothed Schoenfeld residual curves and chi-square tests indicated departures from proportionality for several of the outcomes studied (Appendix 8), we applied time stratification and two types of time-dependent modelling. In time-varying survival models, the time effect is demonstrated clearly. When including all outcomes, the fully-adjusted diagnosis rate was significantly higher in NHS Health Check recipients (Figure 5.6, Appendix 9). When early events (in the first 12 months) were included, diagnoses of hypertension were 6% higher in the NHS Health Check group, with additional higher rates for high cholesterol (11%), chronic kidney disease (15%) and fatty liver disease (17%). However, when the initial 12 or 24 months were excluded from the model, the overall hazard across all outcomes were significantly lower in NHS Health Check recipients, with average risk reductions between 20 and 40% (hazard ratios between 0.6 and 0.8).

In aligned-start regression models, early-event time effects are much less pronounced (Figure 5.6, Appendix 9). In these fully-adjusted models, NHS Health Check recipients had significantly lower diagnosis rates for all-cause dementia (19% lower, hazard ratio (HR) 0.81), myocardial infarction (15% lower, HR 0.85), atrial fibrillation (9% lower, HR 0.91), acute kidney injury (23% lower, HR 0.77), alcoholic liver disease (30% lower, HR 0.70), liver cirrhosis (44% lower, HR 0.66), all-cause mortality and cardiovascular mortality (both 23% lower, with HR 0.77).

The significant early effects observed in the main analysis were confirmed in sensitivity analysis applying time stratification to the aligned-start models (Appendix 10), with the addition of significantly higher rates of diabetes diagnosed in the first year of follow-up. Time-stratified models characterised significantly reduced longer-term risk for the same disease outcomes identified in the main aligned-start models

Application of e-values to the regression results (Appendix 11) found moderate robustness of most observed hazard ratios to unmeasured confounding. Results for acute kidney injury, liver cirrhosis, and myocardial infarction had stronger e-values (less likely to be rendered insignificant by unmeasured confounders), while the e-values for all-cause dementia and atrial fibrillation were weak, meaning that even quite a weak unmeasured confounding variable could render our result non-significant.

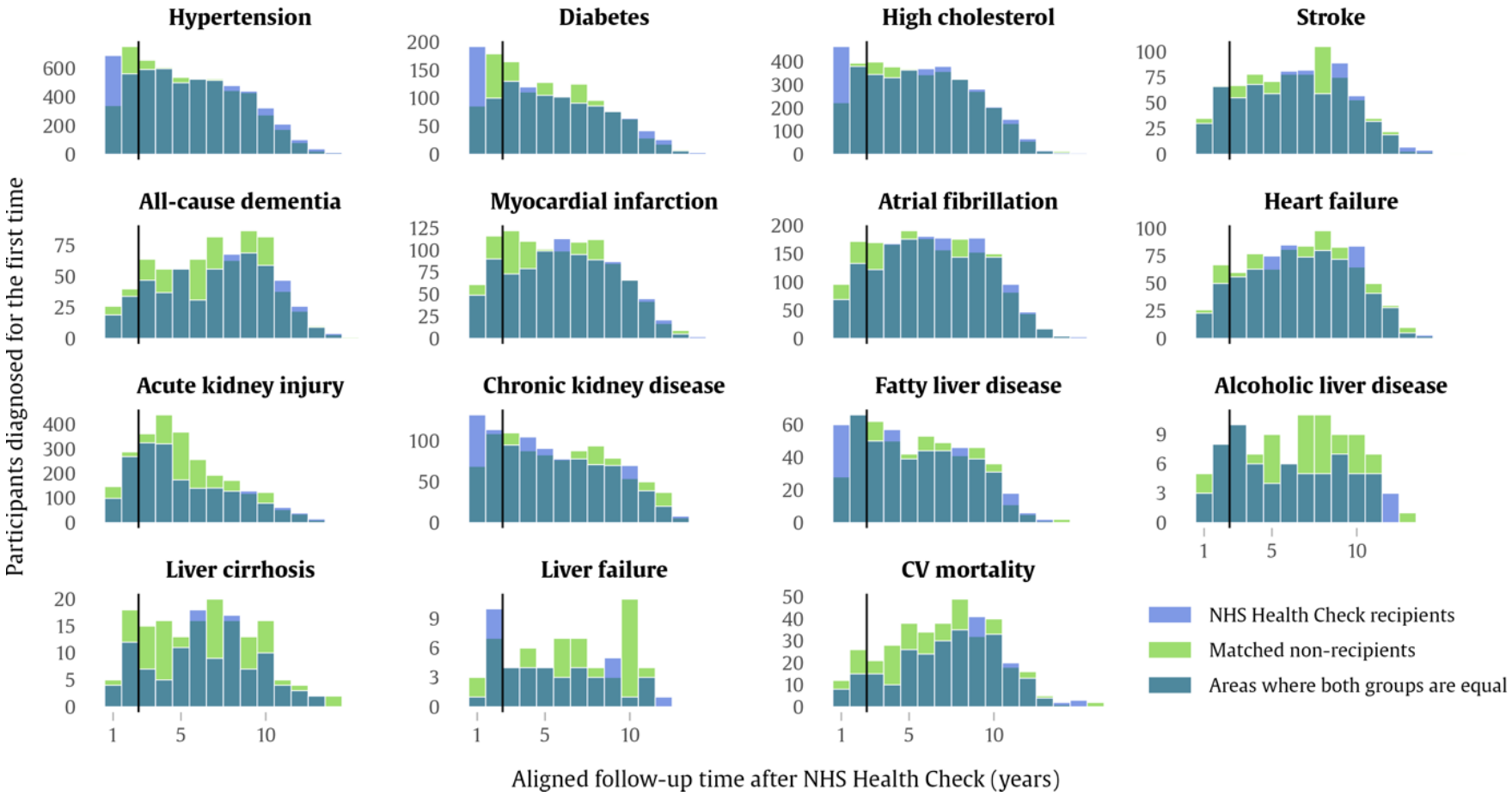


Figure 5.5: Chapter 5 - Outcomes during follow-up in NHS Health Check recipients vs controls

Bars show counts of participants receiving condition diagnoses for the first time, in the years following the NHS Health Check in health check recipients, and in the aligned exposure window in the covariate-matched control cohort. The dark teal shows the counts where both groups are equal, the bright purple indicates where health check group counts are greater, and the bright green indicates where control counts are greater. The two- year initial period following the health check is marked with a black vertical line.

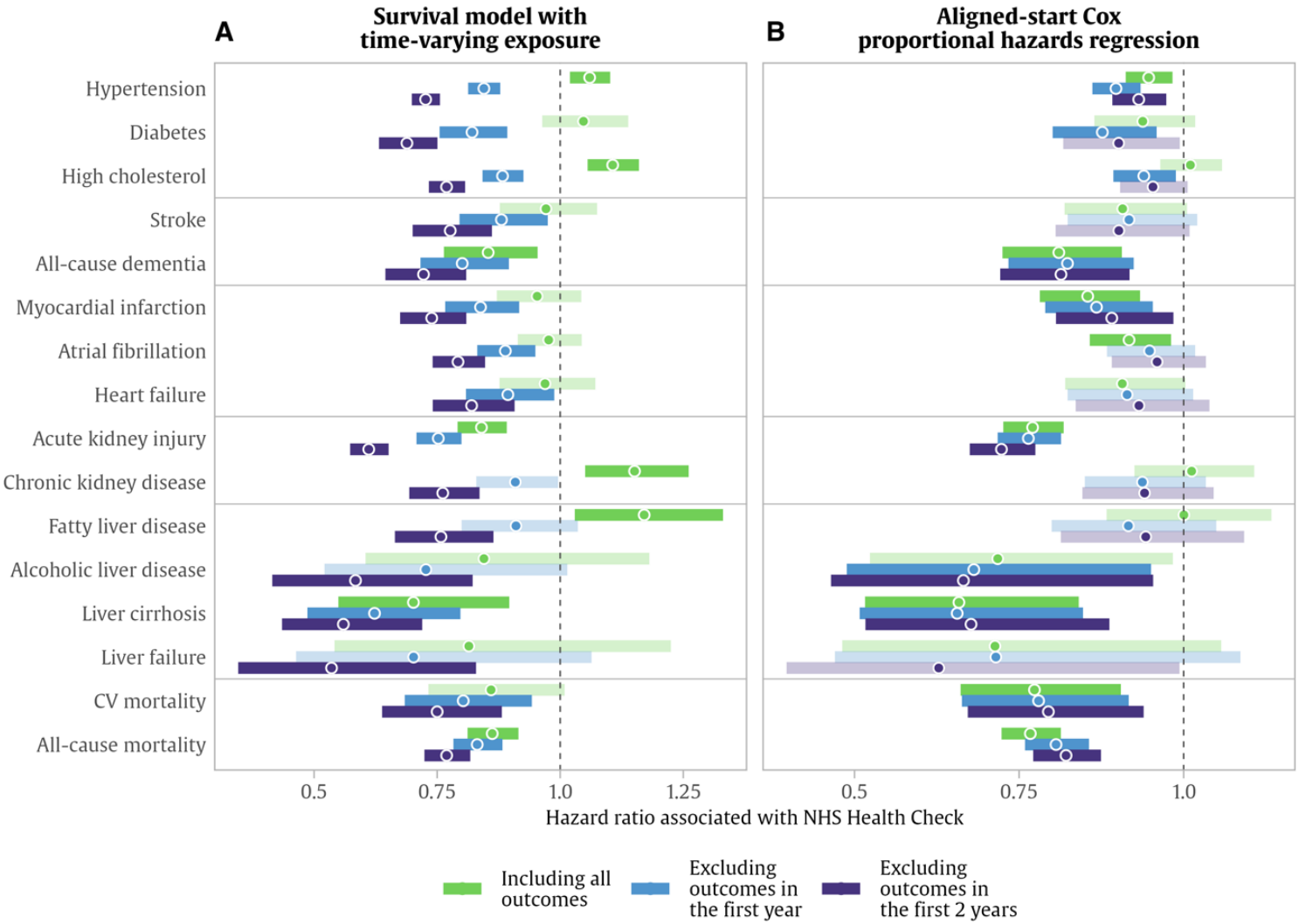


Figure 5.6: Chapter 5 - Associations between NHS Health Check and incident outcomes

Points represent hazard ratios and horizontal bars represent 95% confidence intervals for hazard ratios from Cox proportional hazards models associating completed NHS Health Check with new diagnoses received during follow-up. **Panel A** shows hazard ratios from models with time-varying exposure, and **Panel B** shows hazard ratios from models with aligned follow-up start times. Results shown in faded/greyed out colour were not significant after applying multiple testing correction with a 5% false discovery rate. Colours indicate that models were computed with three outcome exclusion settings (green (0) =including all outcomes, aqua blue (12) = excluding outcomes in the first 12 months after NHS Health Check, navy blue (24)= excluding outcomes in the first 24 months after NHS Health Check). Models are adjusted by age, sex, geographical region, Townsend deprivation score, ethnicity, body mass index, waist-hip ratio, smoking, systolic blood pressure, alcohol intake frequency, physical activity, daily vegetable/salad intake and Charlson comorbidity index.

5.4 Discussion

In this large community-based sample from the UK Biobank across an average 9 years of prospective follow-up, receipt of the NHS Health Check was related to reduced long-term risk of all-cause and cardiovascular disease mortality, and reduced incidence of disease across the liver, kidney, heart, and brain organ systems. In analyses including the early follow-up period, those who had the NHS Health check had increased detection of hypertension, high cholesterol, and chronic kidney disease. This effect was not observed in analyses restricting follow-up to beyond 24 months after the Health Check, indicating that these increased diagnoses indicate heightened detection of undiagnosed or quiescent pre-clinical disease, the treatment of which likely contributes to the reduction in health outcomes observed in the longer term.

5.4.1 Comparison with existing work

The existing evidence on the effect of the NHS Health Check programme so far is mixed [98]. Some studies have found that the programme is associated with small reductions in the risk of cardiovascular disease and diabetes, while others have found no significant benefit. In a 5-year study of electronic health records from several London commissioning groups, Robson et al. found that NHS Health Check attendees had a higher short-term likelihood of diagnosis of type 2 diabetes, hypertension, and chronic kidney disease, and to receive treatment with statins and antihypertensives [355]. These findings were subsequently confirmed in a large nationally representative sample (QDatabase) [104].

Using a similar approach to the current work, Chang and colleagues [356] used a matched sample from the Clinical Practice Research Datalink (CPRD, with n= 29,672 in each group) to find evidence of an overall reduction in cardiovascular risk as computed by QRISK2 in NHS Health Check participants, and a significant increase in diagnoses for hypertension and diabetes. This study was unable to detect differences in longer-term outcomes with a median follow-up time of two years.

Our findings corroborate these observations in a much larger independent cohort by demonstrating an increased diagnosis rate for incident hypertension, high cholesterol, and chronic kidney disease in the immediate period after the NHS Health Check. These conditions are typically asymptomatic with a long pre-clinical phase. As such, they are almost always identified through screening or opportunistic

diagnosis. The longer follow-up duration in our study enabled us to extend existing knowledge by demonstrating that this apparent increase in diagnosis is confined to the first two years after the NHS Health Check, after which the risk of incident health events is significantly lower in recipients.

Our study is the first to demonstrate an association between receipt of the NHS Health Check and reduction in long-term risk of multiorgan outcomes. We do not assert that significant changes flow directly from a single 15-minute appointment. It is more plausible that longer-term trajectory changes arise from 1) increased detection and treatment of risk factors (such as diabetes, hypertension and high cholesterol), 2) more regular face-to-face reinforcement towards healthy behaviour change (like exercise and smoking cessation) and 3) better management of underlying active disease processes like atherosclerosis and atrial fibrillation. These processes work together to reduce the risk of long-term illnesses in NHS Health Check recipients. The initial health check visit sets up a relationship with the primary healthcare team, which may not otherwise occur in ostensibly healthy people. Although a recent review has found wide variation in practice, [101] the health check system is specifically designed to facilitate access to further healthcare services, increasing subsequent healthcare utilisation and providing further opportunities for appropriate screening and risk factor optimisation.

Uptake of the NHS Health Check is an active area of research. Several recent studies [357, 358] have identified a range of factors influencing health check uptake. In 2018/2019 Public Health England published an uptake rate for England at 45.9% of those invited [98]. This figure is corroborated by a study of primary care records in England over a similar time period as our study, which reports an uptake rate of 52.6% of those invited [359]. The overall health check rate of 36.2% observed in this study is in line with an invitation rate of 80% of those eligible, and an uptake rate of 45%.

Some studies have also found that NHS Health Check is associated with improvements in health behaviours such as smoking cessation, physical activity, and diet, and with better management of hypertension and hypercholesterolaemia [105, 360]. But also, it has been found that the programme has not reached everyone who would benefit, particularly those in more deprived areas, and that the programme's effectiveness may have been limited by a lack of follow-up and support for lifestyle changes [98]. Using a health economics modelling approach, Thomas and colleagues [361] did not report significant differences in outcomes but still found that NHS Health Check would generate cost savings from improved detection of cardiovascular risk factors such as diabetes and high cholesterol.

5.4.2 Limitations

We recognise that the UK Biobank cohort is known to be healthier on average than the general UK population [362, 363], meaning that the rates of incident disease observed in the current study are likely to be lower than UK average incidence rates [364]. Similarly, while this study found significant differences in outcome rates overall, the exact size of any effects would need to be validated in a nationally representative cohort.

In addition, self-selection bias is a very important factor to consider when assessing the effectiveness of any voluntary intervention like the NHS Health Check. People who engage with health screening programmes are systematically different in important ways from those who do not. They tend to have a more favourable social, lifestyle, and health profile compared to non-attenders. Studies evaluating the clinical value of screening programmes for the prevention of health outcomes are highly susceptible to confounding by these factors, which can be challenging to capture and include in modelling adjustments [104]. In our study, we created a comparator cohort of health check non-attenders matched to recipients on an extensive range of social, demographic, and clinical factors, with descriptive analyses confirming high-quality matching on variables considered. The observed associations in our study may be inflated, but not fully explained, by self-selection bias in the NHS Health Check recipient group.

The UK Biobank is subject to participation bias [365]. The extensive measurements taken at baseline recruitment is likely to have made all participants more aware of their cardiovascular risk and in turn influenced their decision to independently take part in the NHS Health Check programme. For the purposes of this study however, all participants (both cases and controls) would be subject to this bias equally.

Finding evidence linking any intervention with longer-term outcomes can be challenging, due to differences in implementation times and the abundance of potentially confounding factors. Although we have adjusted for a number of important confounders, there could still be residual uncaptured confounding associated with UK Biobank membership and attendance at NHS Health Checks. While we have explored several regression methods, future work could study a larger matched cohort of participants receiving their first NHS Health Check at the same time, to remove potential confounding associated with time differences. And lastly, the intervention and outcomes variables in this study are

both defined via electronic health records, therefore the accuracy of both measures is limited by the quality and timeliness of the data coding, and the integrity of data linkage [260].

5.4.3 Conclusions

This study demonstrates that proactive, well-designed preventive programmes such as the NHS Health Check can be effective in reducing longer-term disease outcomes, across multiple organ systems. Overall, our results suggest that the NHS Health Check has a role in preventing long-term diseases through risk factor modification and that this effect is independent of any risk modifying behaviours the participants may pursue otherwise. While it remains challenging to gather evidence-based data to evaluate screening programmes, our work goes some way in addressing methodological issues that have hampered previous studies and provides further evidence in support of the NHS Health Check as a preventive public health programme. This research is an important addition to a growing body of work supporting the long-term benefits of a programme such as NHS Health Check, and its effectiveness for potential multimorbidity prevention.

Chapter 6: Multiorgan risk assessment in primary care

6.1 Introduction

This thesis examines multimorbidity prevention efforts by considering both cross-organ relationships and preventive strategies. While earlier chapters covered relationships via imaging, and a reflection on the existing NHS Health Check, this chapter explores the incremental approaches in primary care that could have potential for more effectively predicting and delaying multiorgan disease. The current NHS Health Check [16, 77], designed to identify and mitigate risk factors for cardiovascular disease among adults in England, offers a well-established protocol for atherosclerotic cardiovascular disease (CVD) prevention. However, as the prevalence of multimorbidity rises, there is a growing need to broaden the scope of these checks to encompass a wider range of organ systems, thus enabling earlier detection and intervention for multiple interconnected conditions.

Whilst the previous chapter examined the effectiveness of the existing NHS Health Check programme, this chapter focuses on the feasibility of expanding the health check protocol to incorporate multiorgan risk assessment.

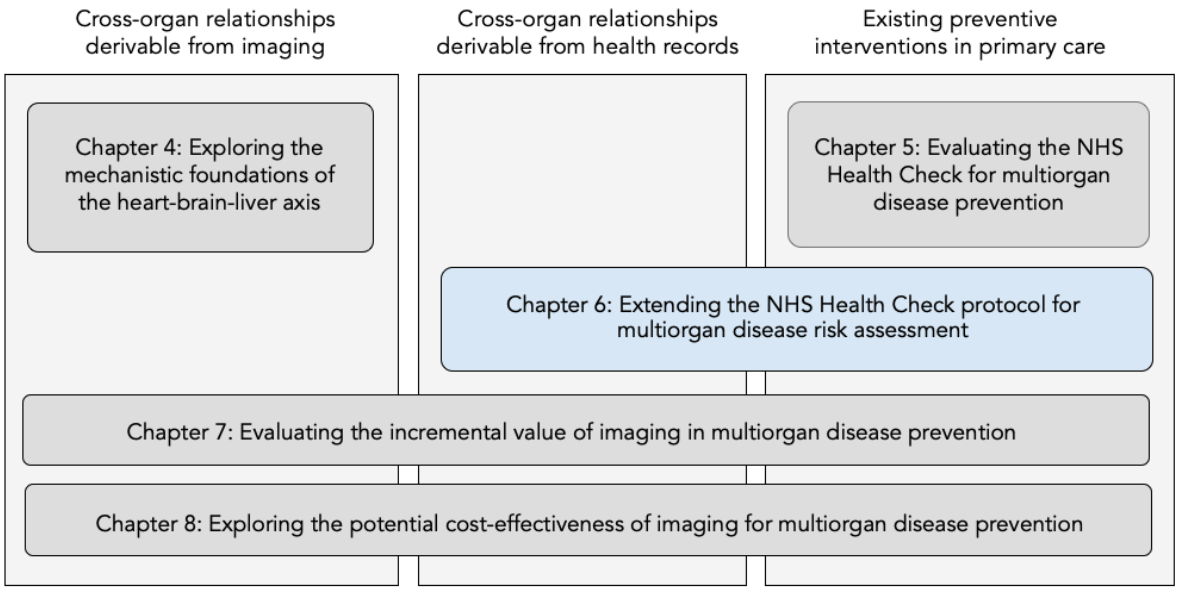


Figure 6.1: Chapter 6 - Roadmap location

The analysis and results of this chapter have been published under open access at

McCracken, Celeste, Zahra Raisi-Estabragh, Liliana Szabo, Michele Veldsman, Betty Raman, Anya Topiwala, Adriana Roca-Fernández, et al. 'Feasibility of Multiorgan Risk Prediction with

Routinely Collected Diagnostics: A Prospective Cohort Study in the UK Biobank'. BMJ Evidence-Based Medicine, 6 May 2024. https://doi.org/10.1136/bmjebm-2023-112518.

Assessment of CVD risk in primary care is now quick and easy, due to widely available risk calculator tools such QRISK3 [278] and Framingham Risk Score [276]. At the NHS Health Check visit, a number of clinical parameters are collected, CVD risk is assessed, and the general practitioner directs personalised interventions that influence the long-term health trajectory of the patient. Despite urgent calls for more preventative attention to other diseases [366, 367] there are currently no existing methods for multi-disease risk prediction in primary care.

The objective of this study is to examine the feasibility of expanding the primary care health check to include risk assessment across multiple diseases. We focus on the ten most commonly occurring serious conditions across the heart, brain, kidney and liver, namely, myocardial infarction, atrial fibrillation, heart failure, stroke, all-cause dementia, chronic kidney disease, fatty liver disease, alcoholic liver disease, liver cirrhosis and liver failure. Having access to a wider panel of risk information could lead to earlier disease detection, more targeted interventions, and more effective prevention of longer-term multimorbidity.

However, there are several important challenges to consider. Firstly, although risk scores have previously been developed for each additional condition (e.g. dementia) there is simply not enough time within a 10–15-minute consultation to gather all the required inputs and to calculate each risk score separately [368]. A preferred solution would involve a single pool of inputs, and a single data entry page, from which multiple risk estimates could be calculated simultaneously.

Secondly, individual risk scores differ by the people they exclude, depending on the cohort in which they were developed [369]. This leads to shifting sets of calculators (and required inputs) in the hands of the physician depending on the existing comorbidities of the patient. Instead, future solutions would include a person's medical history and existing diagnoses, and adjust risk estimates accordingly [370, 371].

Thirdly, not all health measures are equally accessible. NHS England is actively exploring ways that remote healthcare solutions can be used effectively to ease health service usage and make primary care

services more accessible to all [372–374]. These objectives call us to reflect on information that is easily obtained and consider whether simple metrics can be potentially powerfully combined.

In this study, we use the UK Biobank data resource to emulate the information available within the primary care setting. Our objective is to explore the feasibility of multi-disease risk estimation with easily collected diagnostics (Figure 6.2) setting the minimum acceptable performance of 0.70 area under the receiver operating curve (AUROC) across all outcomes (as per Hosmer and colleagues [375] p.177). We begin by evaluating a range of published risk scores and assessing their performance in the UK Biobank cohort.

We review the component inputs for each of those risk indices and identify scores that can be applied fully remotely (i.e., without direct in-person contact) and those with a standard set of in-person inputs. Finally, we re-use the standard set of inputs to develop new risk scores compare their performance with existing risk scores.

6.2 Methods

6.2.1 Setting and study population

This study uses the UK Biobank data set (Section 2.1) with baseline data collection that took place between 2006 and 2010, where the registration date was used as the index date for the study. Follow-up events were ascertained via linked health records with latest censor date of 31st October 2022. Comprehensive details regarding linked primary care and hospital records are provided in official UK Biobank resources [376, 377]. To focus on 10-year risk estimation for all outcomes, follow-up was truncated at 10 years following baseline, giving a median follow-up time of 10 years (IQR= [10, 10]). The clinical and demographic parameters collected in UK Biobank mimic those available in primary care, and permit population-based modelling of multiorgan risk from baseline features.

From the overall UK Biobank cohort (n=502,386), 1,298 participants were removed due to self-withdrawal or loss to follow-up, and 271,386 participants did not have primary care data available.

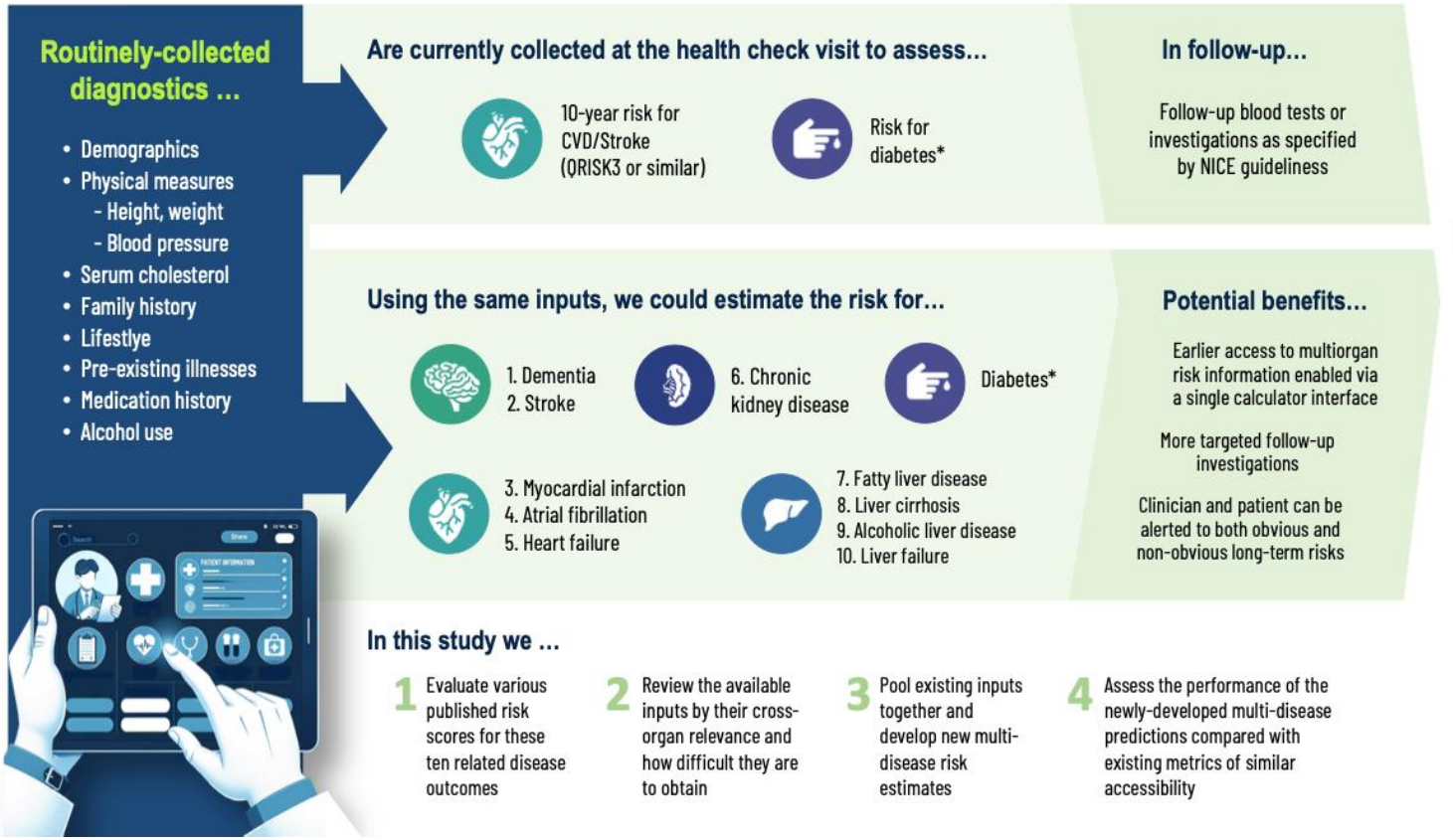


Figure 6.2: Chapter 6 - What can existing information tell us about multiorgan disease risk?

In the context of increasing multimorbidity, we examine the feasibility of extending the existing primary care health check framework to include risk assessment for multiple diseases within the heart-brain-liver-kidney cluster. We evaluate a range of existing risk scores and consider whether and how they could be blended, and whether information already being collected could be effectively re-used. If successful, this expansion could lead to earlier disease detection, more effective prevention, and better resource allocation for multimorbidity prevention. NICE = National Institute for Health and Care Excellence. *The diabetes screening component of the NHS Health Check protocol is not part of this analysis and would exist unchanged in both versions.

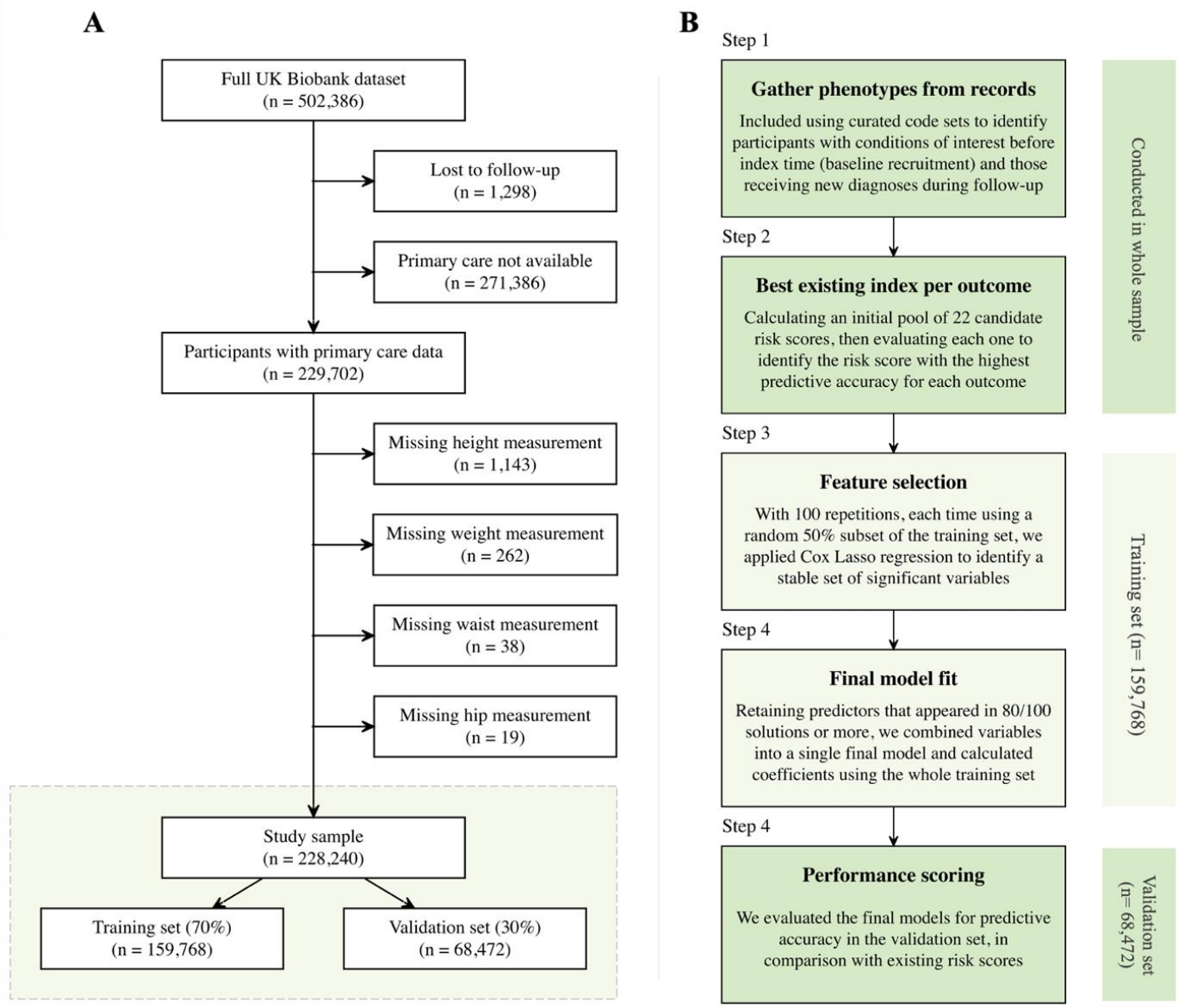


Figure 6.3: Chapter 6 - Study sample and workflow

There were 229,702 remaining participants who were confirmed to be present in both the main dataset and the primary care dataset. From these, a further 1,462 participants were excluded due to missing values for height, weight, waist or hip circumference, leaving a final sample of 228,240 participants (see Figure 6.3A).

6.2.2 NHS Health Check and easily collected diagnostics

The NHS Health Check (Section 2.2) forms the situational anchor for our study. Briefly, healthy people aged between 40-74 years are invited to visit their primary care team, where an inexpensive set of diagnostics are collected and 10-year risk of CVD is calculated using the widely-validated QRISK3 calculator [278] (https://qrisk.org/three/) or similar tool (Figure 6.2).

Table 6.1: Chapter 6 - Easily-collected features

	1. Remote features*		2. Standard features	3. Extended features
	Features expected as part of the NHS Health Check	**Features that could be added with minimal additional cost**	**In-person metrics that are specified as part of NHS Health Check**	**Features that are extra but may help detect / predict disease**
Demographics	Age, sex, ethnicity, postcode[1]	Self-reported education level		
Family history	Family history of heart disease	Family history of dementia, diabetes, or stroke		
Lifestyle	Smoking, alcohol use General self-reported health	Physical activity, household occupancy (living alone)	All remote features plus …	Both other categories plus…
Physical measures	BMI (height, weight),	Waist-hip ratio (waist, hip in cm), resting pulse rate	SBP, DBP SBP variability[2]	
Blood/ biochemistry			Total cholesterol, HDL cholesterol	Blood glucose, HbA1c, RBC, platelet count, CRP, GGT, AST, ALT, ALP, cystatin-C, serum creatinine, albumin, bilirubin, total protein, urate, urine creatinine
Existing diagnoses / medical history				
Vascular/general risk factors	Diabetes, hypertension, high cholesterol	Dizziness, fainting, shortness of breath, COPD, any cancer		
Brain	[Stroke, transient ischaemic attack][3] Migraine	Other cerebrovascular disease, dementia (any cause), epilepsy, Parkinson's disease, multiple sclerosis, traumatic brain injury, sleep disorder		
Arterial	Erectile dysfunction	Atherosclerosis, peripheral artery disease, venous thromboembolism		
Heart	[Coronary heart disease including angina and myocardial infarction][3] Atrial fibrillation (AF)	Other (non-AF) cardiac arrhythmias, valvular heart disease, non-ischaemic cardiomyopathies, heart failure		
Kidney	Chronic kidney disease	Acute kidney injury, kidney stones		
Liver		NAFLD, hepatitis, alcoholic liver disease, cirrhosis		
Systemic inflammation	Rheumatoid arthritis, systemic lupus erythematosus	Gout		
Mental health	Depression, bipolar disorder, schizophrenia	Anxiety		
Medications	Anti-hypertensive medication, atypical antipsychotics, regular steroid tablets	Insulin, statins		

*The term "remote" features is used to convey that remote collection of these parameters is possible, whether by phone or via an online form. Remote features can also be collected in person as part of the primary care visit.1 Townsend deprivation score via postcode was dropped from the set of predictors, as this feature is difficult to implement in a simple portable spreadsheet and applies only to the UK. [2.] SBP variability was dropped from the set of predictors, as this feature is difficult to obtain in a single in-person visit. [3] These are diagnoses that the primary care physician would typically already be aware of, and would preclude attendance at an NHS Health Check. *Abbreviations:* BMI= body mass index, SBP = systolic blood pressure, NAFLD= non-alcoholic fatty liver disease, HDL= high-density lipoprotein, HbA1c = glycated haemoglobin, RBC= red blood cell count, CRP = C-reactive protein, GGT = gamma glutamyl transferase, AST = aspartate aminotransferase, ALT = alanine aminotransferase.

Simple self-reported measures such as age, sex, family history, lifestyle factors, current medications and medical history are features that can be reported verbally and can be collected fully remotely (i.e. without in-person contact). Physical measures such as height, weight, waist and hip circumference are easily measured oneself without specialised technology. These are categorised as "***remote features***" and are shown in the first two columns of Table 6.1. The term 'remote' is used to convey that remote collection of these parameters is possible, whether by phone or via an online form. Remote features can also be collected in person as part of the primary care visit.

Best practice guidelines [77] specify a minimum set of parameters to be collected as part of the standard NHS Health Check protocol, consistent with the use of QRISK3. These include a number of remote features, with the addition of blood pressure measurement and blood tests for total and HDL cholesterol. In this study, we include all remote features plus the required NHS Health Check parameters (blood pressure and cholesterol) under the category of "***standard features***".

Finally, there are various blood/biochemistry tests that are widely available but are not part of the existing first-line health check protocol. These measures were identified based on their inclusion in existing research or risk scores (discussed below) and have been included as an additional analysis to evaluate their potential incremental utility. These are shown in the fourth column of Table 6.1, and the full set of features including additional blood tests are referred to as "***extended features***".

6.2.3 Ascertainment of outcomes

Diagnoses and dates for the ten disease outcomes (itemised above) were collated across multiple UK Biobank sources including self-report, linked hospital and primary care records and deaths, using published code lists where available [275, 341, 378]. Incident outcomes were defined by first occurrence of disease after baseline recruitment. Participants with record of the same disease at baseline were excluded from modelling for that disease, and follow-up was censored at either death or the study end date. In addition to the defined outcomes, a wide selection of other potentially relevant diagnoses were collected using the same multi-source approach (Section 3.3.3). A full listing of UK Biobank codes for outcomes ascertainment is provided in Appendix 2.

6.2.4 Existing risk scores

We calculated QRISK3 for all study participants, along with 21 other published risk scores targeting disease risk across heart, brain, liver and kidney (Figure 6.4). These risk scores were selected based on literature search for most frequently used metrics for each outcome, availability of published equations, and availability of online calculators for quality checking. Detailed information for all published indices is provided in Appendix 3. For incident stroke risk we considered QStroke [271] and CHA2DS2-VASc [272], and for all-cause dementia we included CAIDE [273], LIBRA [274], and a recently-developed UK Biobank Dementia Risk Score (UKB-DRS) [275]. For myocardial infarction and heart failure we considered Framingham Risk Score (with and without blood lipids) [276], PCP-HF heart failure equations [277] and QRISK3 [278]. CHARGE-AF [279] was included as a risk score for atrial fibrillation. Chronic kidney disease risk (Stage 3+) was predicted by two versions of QKidney [280] and (Nelson) Kidney Risk Score [281].

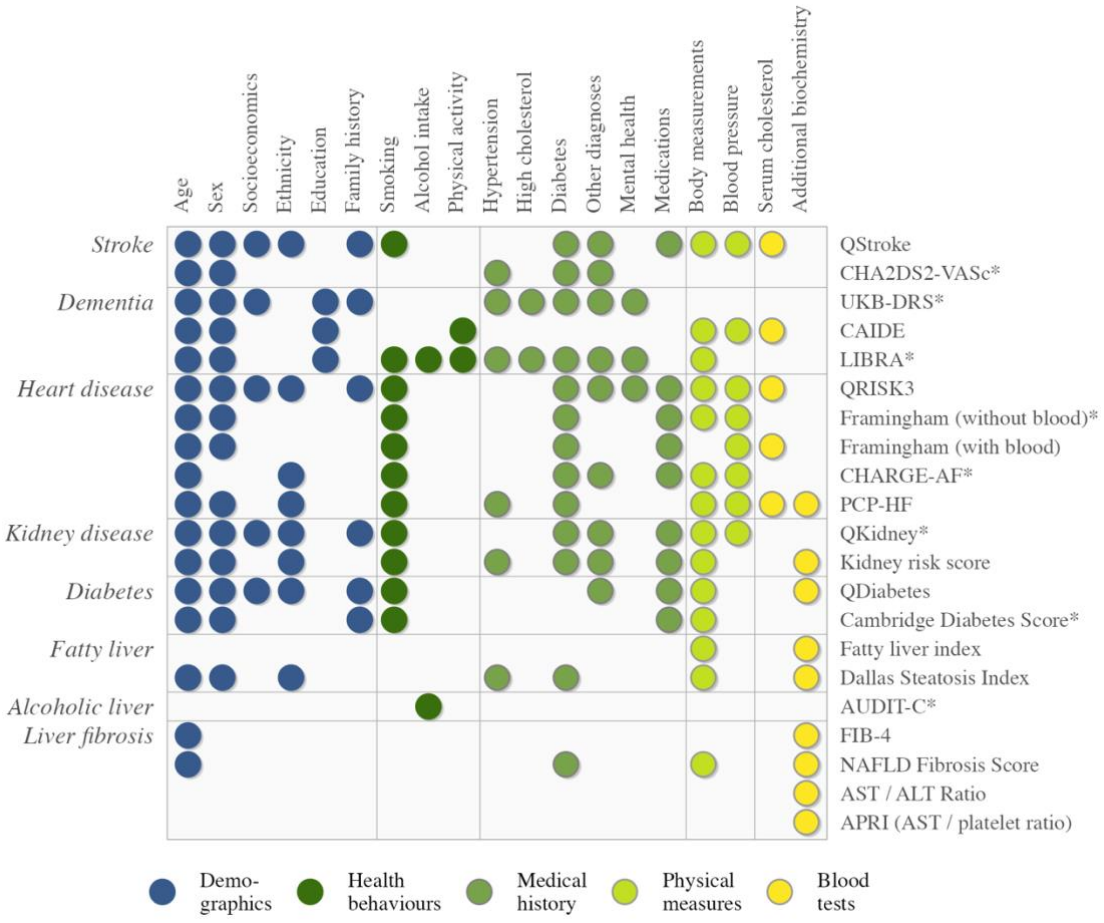


Figure 6.4: Chapter 6 - Existing risk scores and their constituents

For fatty liver disease we considered Fatty Liver Index [282] and the Dallas Steatosis Index [283]. Three diabetes risk scores (two versions of QDiabetes [284] and Cambridge Diabetes Score [285]) were included as possibly useful predictors. AUDIT-C [286] is a questionnaire designed to assess risk for alcoholic liver disease, however only the first AUDIT question was available in the UK Biobank with a high degree of data completeness. Liver fibrosis was represented by three candidate scores (FIB-4 [287], NAFLD Fibrosis Score [288] and AST/Platelet ratio [289]). All published risk scores have been separately validated in their own studies. To assess their general utility, all risk scores were applied to the whole sample and to 10-year follow-up regardless of restrictions present in each respective derivation cohort.

6.2.5 Existing risk scores inherit their type from their inputs

At the high level, examination of score inputs (Figure 6.4) shows significant overlap in feature topics, however the finer level detail (Appendix 3) reveals significant variability in input requirements. Moreover, the inputs to each risk score differ by accessibility, in other words, risk score inputs are often a mixture of remote and standard features, with occasional additional blood tests. Extending the health information framework described above, we categorise any risk score that is comprised only of inputs that can be collected remotely as a remote risk score. UKB-DRS [275] (dementia) and Framingham risk score (using BMI) [276] are examples of this. With the most restricted set of inputs, we would expect these models to be least powerful and have the lowest predictive performance. Risk scores that include remote and standard features are considered standard risk scores (e.g. QRISK [278], QStroke [271]), whilst risk scores that require additional blood tests fall into the category of extended risk scores (e.g. Nelson Kidney Risk Score [281], Fatty Liver Index [282]). We would expect risk models with access to the extended set of inputs (standard inputs plus additional biochemistry) to have the highest predictive performance. These categories are relevant to the process of building and comparing risk scores, such that performance comparisons are between models of the same type.

6.2.6 Ascertainment of other features

Age at baseline, self-reported sex, systolic blood pressure, pulse rate and anthropomorphic measurements were taken at baseline, along with a touchscreen questionnaire collecting information about ethnicity, education, family history, smoking, alcohol use and physical activity. Townsend

deprivation index at baseline was assigned based on participant postcode. Ethnic groups and smoking categories were recoded to match QRISK3 specifications. Education was coded as binary - “Do you have any post-secondary / college / university qualifications?” Physical activity was dichotomised to greater than or equal to 600 summed MET-minutes per week [257], approximately equivalent to 20 minutes exercise per day [258]. Family history was drawn from self-reported illnesses of mother, father and siblings, where age of illness was not specified. Descriptive statistics and source information for study features are provided in Appendix 12. Blood sampling was carried out as part of the baseline assessment, providing measures of total cholesterol, HDL cholesterol and additional biochemistry. The additional blood markers were; blood glucose, glycated haemoglobin, red blood cell count, platelet count, C-reactive protein, gamma glutamyl transferase, aspartate aminotransferase, alanine aminotransferase, alkaline phosphatase, cystatin-C, serum creatinine, albumin, bilirubin, total protein, urate and urine creatinine (see Appendix 13 for more details). Missingness among remote features was very small (<1%), while missingness among blood test variables ranged between 3% and 14%. Covariate missingness was handled with multiple imputation, with details provided in Appendix 14 and Section 3.3.6.

6.2.7 Statistical analysis

Statistical analysis was with R version 4.1.2, and RStudio 2022.02.0. We randomly stratified the data to create a training set (70%, 159,768 participants) and an internal validation set (30%, 68,472 participants). Standard checks confirmed that the characteristics of the training and validation cohorts were not significantly different.

6.2.7.1 Pairwise modelling of cross-disease associations

Prior to full-scale modelling, we sought to describe the associations between diseases. We examined the association of prevalent conditions with risk of incident conditions using Cox proportional hazards regression, adjusting by age, sex, post-secondary education, ethnicity, smoking, physical activity, alcohol intake frequency, body mass index, Townsend deprivation index, family history (of heart disease, stroke and dementia), any cancer diagnosis, hypertension, high cholesterol and diabetes. Proportionality was checked with visualisation of residuals across all models. This analysis was performed using the whole cohort (n= 228,240). Due to the large number of tests in this section, all

coefficient tests were adjusted for multiple testing via the Benjamini-Hochberg method [296] with a false discovery rate of 5%.

6.2.7.2 Evaluation of existing risk scores

From the initial set of 22 published risk indices described above, we identified the best-performing score for each outcome across the 10 years of follow-up in the whole sample. Importantly, we evaluated all risk-score-outcome combinations, checking for potential predictive utility of each index beyond its original derivation cohort and intended outcome. We identified the risk score with highest discriminative performance, as measured by area under the receiver operating curve (AUROC). AUROC was selected as the primary criterion for risk score performance, because it does not depend on a specific prediction threshold and is more effective than simple accuracy in situations where rare events are being predicted.

6.2.7.3 New models for heart, brain, liver and kidney disease

Then, new models were developed for each of the ten outcomes in the training set, and their performance for 10-year prediction was assessed in the internal validation set (Figure 6.3B). Model fitting was carried out 1) using remote features, and 2) using standard features and 3) using the extended set of features. Crucially, at each level we restricted all models (across the 10 related outcomes) to draw from the same pool of predictors. Feature selection was conducted using a stability selection approach [297], combining lasso Cox regression with bootstrapping to systematically identify the predictors that show consistent importance, thereby simplifying the final model and mitigating the risk of overfitting (see Section 3.4.3).

For each outcome, the final set of predictors were placed into a single survival model, with coefficients and prediction thresholds calculated using the training set, and predictions scored for discriminative accuracy in the validation set.

6.2.7.4 Model performance metrics

Across all models, prediction performance was assessed with multiple metrics including AUROC, sensitivity, specificity, Somers' Dxy (the rank correlation between predicted risk and outcomes [379]) and Brier score (the mean squared differences between predicted risk and outcomes). Calibration plots

were used to visually assess the alignment of predicted probabilities with actual outcomes. Differences in performance metrics were further bootstrapped with 1000 bootstrapped samples to derive uncertainty estimates. To calculate sensitivity and specificity, the prediction thresholds were set to maximise balanced accuracy, given by (sensitivity + specificity)/2 [380].

Reclassification indices, such as IDI (integrated discrimination improvement) and NRI (net reclassification improvement), were applied to help assess small improvements in predictive performance when comparing two or more models [301, 381]. These indices help us discern whether a new model improves the classification of risk beyond the existing model.

Integrated Discrimination Improvement (IDI) measures the improvement in the discrimination slope between a reference model and a new model. It is defined by the difference in the discrimination slopes (the difference between the average predicted probabilities of the events occurring versus non-occurring) between the new and the reference model. The IDI is a continuous measure that does not require predefined risk categories and can capture improvements in model performance even if the improvements do not change the risk category of individuals.

Continuous Net Reclassification Improvement (NRI) quantifies how well a new model assigns risk to subjects compared to an existing model. It is calculated by examining changes in the predicted risk (e.g., low, intermediate, high risk) and assesses whether individuals who experienced events (e.g., disease occurrence) are appropriately moved to higher risk values, and those who did not experience events are moved to lower risk values in the new model, when compared to the reference model.

6.3 Results

6.3.1 Participant characteristics

Overall, the study sample (n= 228,240) was 45.3% male and 54.7% female, with an average age of 56.5 years at baseline (SD 8.1 years, Table 6.2). Prevalence of hypertension, high cholesterol and diabetes at baseline was 32.6%, 20.8% and 5.5% respectively. The most common incident event was atrial fibrillation (n=9,997; 4.4%), and liver failure was the least common (n=340 events; 0.1%). Training and internal validation sets were similar across baseline variables and outcomes.

.

Table 6.2: Chapter 6 - Sample characteristics

Characteristic	Whole sample (n= 228,240)	Training set (n= 159,768)	Internal validation set (n=68,472)
Age (years)	56.5 (±8.1)	56.5 (±8.1)	56.5 (±8.1)
Sex: Female	124,891 (54.7%)	87,563 (54.8%)	37,328 (54.5%)
Sex: Male	103,349 (45.3%)	72,205 (45.2%)	31,144 (45.5%)
Townsend deprivation index	-1.34 (±3.03)	-1.34 (±3.03)	-1.35 (±3.03)
Post-secondary education			
No	91,042 (39.9%)	63,739 (39.9%)	27,303 (39.9%)
Yes	135,207 (59.2%)	94,625 (59.2%)	40,582 (59.3%)
(Missing)	1,991 (0.9%)	1,404 (0.9%)	587 (0.9%)
White ethnicity	217,863 (95.5%)	152,469 (95.4%)	65,394 (95.5%)
All other ethnicity groups	10,377 (4.5%)	7,299 (4.6%)	3,078 (4.5%)
Current smoker	23,934 (10.5%)	16,716 (10.5%)	7,218 (10.5%)
Physically active (METS ≥ 600)	169,005 (74.0%)	118,544 (74.2%)	50,461 (73.7%)
Alcohol intake less than once per week	70,489 (30.9%)	49,341 (30.9%)	21,148 (30.9%)
Alcohol intake once a week or more	157,751 (69.1%)	110,427 (69.1%)	47,324 (69.1%)
Physical measurements			
Body mass index (BMI kg/m^2)	26.8 [24.2, 30.0]	26.8 [24.2, 30.0]	26.8 [24.2, 30.0]
Obesity (BMI >= 30 kg/m^2)	57,469 (25.2%)	40,375 (25.3%)	17,094 (25.0%)
Waist circumference (cm)	90.3 (±13.5)	90.4 (±13.5)	90.3 (±13.5)
Resting heart rate (bpm)	69.4 (±11.3)	69.4 (±11.3)	69.4 (±11.2)
Systolic blood pressure (SBP, mmHg)	138.2 (±18.7)	138.2 (±18.6)	138.2 (±18.7)
Total/HDL cholesterol ratio	4.14 (±1.13)	4.14 (±1.13)	4.14 (±1.13)
Risk factors			
Hypertension	74,503 (32.6%)	52,240 (32.7%)	22,263 (32.5%)
High cholesterol	47,471 (20.8%)	33,315 (20.9%)	14,156 (20.7%)
Diabetes	12,543 (5.5%)	8,917 (5.6%)	3,626 (5.3%)
Chronic obstructive pulmonary disease	5,288 (2.3%)	3,706 (2.3%)	1,582 (2.3%)
Any cancer	21,896 (9.6%)	15,307 (9.6%)	6,589 (9.6%)
Existing conditions at baseline			
Stroke	4,284 (1.9%)	2,994 (1.9%)	1,290 (1.9%)
Alzheimer's disease / dementia	346 (0.2%)	246 (0.2%)	100 (0.1%)
Myocardial infarction	6,664 (2.9%)	4,719 (3.0%)	1,945 (2.8%)
Atrial fibrillation	4,232 (1.9%)	2,964 (1.9%)	1,268 (1.9%)
Heart failure	1,677 (0.7%)	1,194 (0.7%)	483 (0.7%)
Chronic kidney disease	5,610 (2.5%)	3,886 (2.4%)	1,724 (2.5%)
Fatty liver disease	1,063 (0.5%)	718 (0.4%)	345 (0.5%)
Alcoholic liver disease	434 (0.2%)	298 (0.2%)	136 (0.2%)
Liver cirrhosis	498 (0.2%)	326 (0.2%)	172 (0.3%)
Liver failure	255 (0.1%)	170 (0.1%)	85 (0.1%)
Diagnoses after baseline			
Stroke	3,953 (1.7%)	2,728 (1.7%)	1,225 (1.8%)
Dementia	2,720 (1.2%)	1,911 (1.2%)	809 (1.2%)
Myocardial infarction	5,953 (2.6%)	4,122 (2.6%)	1,831 (2.7%)
Atrial fibrillation	9,997 (4.4%)	6,977 (4.4%)	3,020 (4.4%)
Heart failure	4,988 (2.2%)	3,500 (2.2%)	1,488 (2.2%)
Chronic kidney disease (Stages 3, 4 and 5)	8,698 (3.8%)	6,116 (3.8%)	2,582 (3.8%)
Fatty liver disease	3,585 (1.6%)	2,534 (1.6%)	1,051 (1.5%)
Alcoholic liver disease	561 (0.2%)	402 (0.3%)	159 (0.2%)
Liver cirrhosis	951 (0.4%)	685 (0.4%)	266 (0.4%)
Liver failure	340 (0.1%)	236 (0.1%)	104 (0.2%)
Follow-up time (years, median, IQR)	10 [10, 10]	10 [10, 10]	10 [10, 10]

Entries are either counts (percentages), mean (standard deviation) or median (25th percentile, 75th percentile). METS = metabolic equivalent task, summed per week. BMI= body mass index.

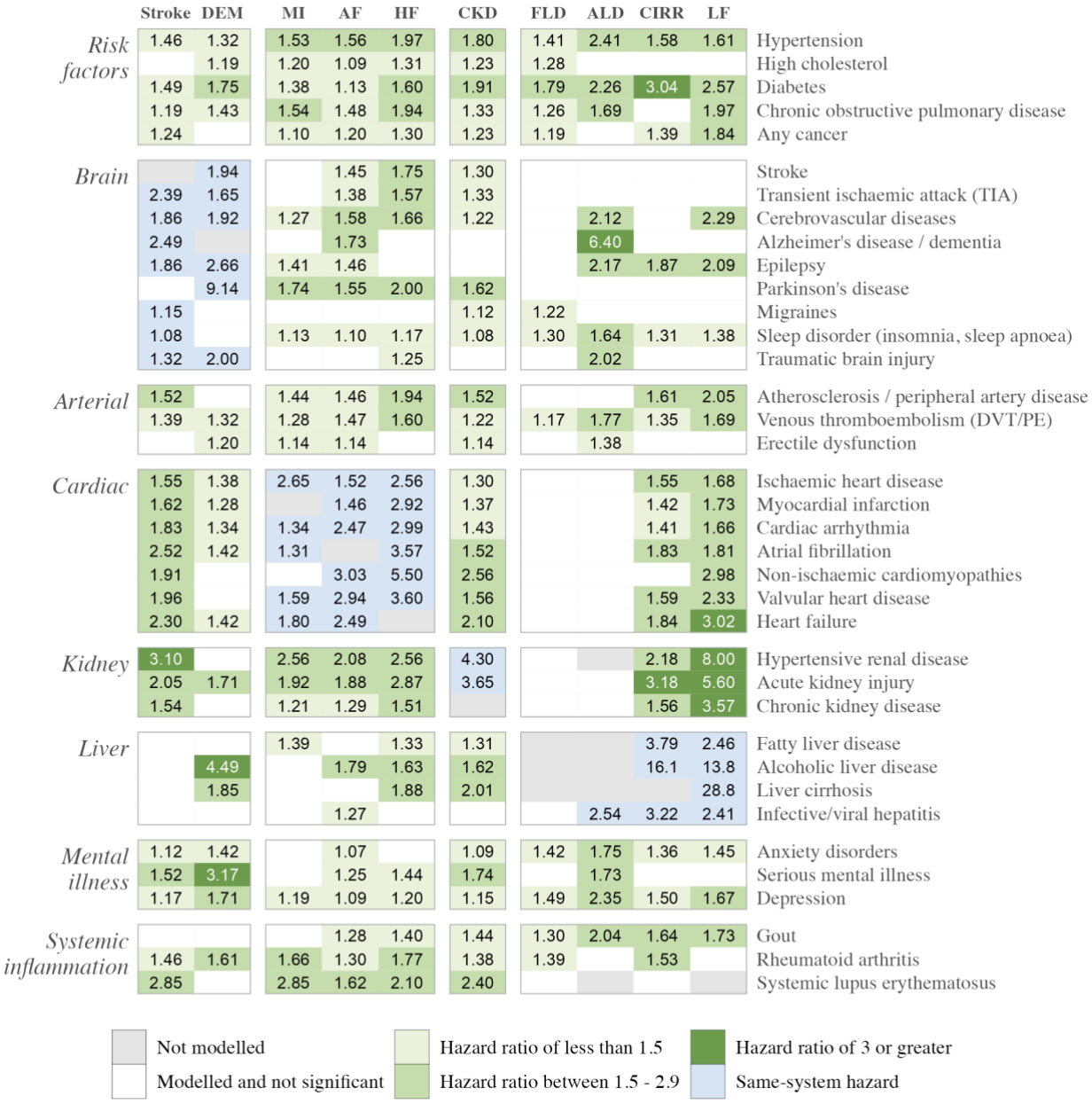


Figure 6.5: Chapter 6 - Hazard ratios for incident outcomes by existing disease diagnoses at baseline

Each entry shows the hazard ratio for incident outcomes (shown along the top) associated with the presence of existing risk factors, diagnoses and medication at baseline (shown down the right-hand side) in the whole cohort (n= 228,240), using Cox-proportional hazards regression. For example, pre-existing hypertension increases the 10-year risk of stroke by 46%. Models are adjusted by age, sex, post-secondary education, ethnicity, smoking, physical activity, alcohol intake frequency, body mass index, Townsend deprivation index, family history (of heart disease, stroke and dementia), any cancer diagnosis, hypertension, high cholesterol and diabetes. Hazard ratio significance was adjusted for multiple testing with a false discovery rate of 5%, where non-significant results are shown as empty white cells. Each result is from a different model. See Supplementary Table 8 for detailed results. DEM = all-cause dementia, MI = myocardial infarction, AF= atrial fibrillation, HF = heart failure, CKD = chronic kidney disease (stage 3, 4 or 5), FLD= fatty liver disease, ALD = alcoholic liver disease, CIRR = cirrhosis, LF = liver failure.

6.3.2 Associations between existing disease and future disease risk

Pairwise Cox analysis between heart-brain-liver-kidney outcomes and existing disease diagnoses revealed multiple cross-organ associations (Figure 6.5, Appendix 16). All major heart diseases were significantly associated with increased risk of stroke, liver failure and the development of chronic kidney disease. All non-infective liver diseases at baseline were associated with increased risk of heart disease within ten years, with an 88% increased risk of heart failure in participants with cirrhosis (hazard ratio = 1.88, 95% confidence interval = [1.31, 2.71], p = 7.05×10^{-4}), and a 39% increased risk of myocardial infarction in participants with fatty liver disease at baseline (1.39, [1.08, 1.80], p= 0.012).

Participants with alcoholic liver disease at baseline had a 4.5-fold risk for all-cause dementia (4.49, [3.10, 6.49], p= 1.46×10^{-15}), while rheumatoid arthritis at baseline conferred a 61% increased risk (1.61, [1.30, 1.99], p= 1.50×10^{-5}). Diagnosis of kidney or systemic inflammatory disease at baseline was associated with increased ten-year risk for disease across heart, brain and liver. Depression diagnosis at baseline had significant associations with disease across all four organs, while serious mental illness (bipolar/schizophrenia/other psychosis) was associated with increased risk of alcoholic liver disease (HR 1.73 [1.04, 2.85], p= 0.032), chronic kidney disease (HR 1.74, [1.49, 2.02], p= 6.78×10^{-13}) and all-cause dementia (HR 3.17, [2.58, 3.90], p= 9.66×10^{-28}).

6.3.3 Best existing risk scores

Details of the three best-performing existing risk scores of each type (by highest sample AUROC) for each level of accessibility are shown in Appendix 17. From here, the one risk score with the highest AUROC was applied as the comparator in the validation sample, shown by dark blue bars in Figure 6.6 with additional details in Appendix 18. At least one existing risk score surpassed the minimum adequate AUROC (0.70) for all outcomes except liver failure, with CHARGE-AF providing the best performance for atrial fibrillation across all levels (AUROC= 0.759, 95% CI= [0.751, 0.767]), and UKB-DRS performing best for all-cause dementia (0.807, [0.793, 0.820]). Please note, that where a lower-level (remote or standard) model performs better than all more complex (extended) models for the same outcome, it will be retained as the best model at that level. Within the remote models, QKidney 5 had the highest AUROC for stroke (0.701, [0.687, 0.715]), and a surprisingly high remote model AUROC for heart failure (0.798, [0.787, 0.809]). Within standard models, we found several expected risk-score-

outcome pairings, namely QStroke for stroke (0.727, [0.714, 0.741]), QRISK3 for myocardial infarction (0.757, [0.747, 0.767]), and QKidney 3 for chronic kidney disease (0.760, [0.751, 0.769]). Unexpectedly, QStroke also had the highest AUROC for 10-year heart failure (0.806, [0.795, 0.817]).

6.3.4 Multiorgan risk prediction

The prediction performance of the newly developed risk scores are presented as green bars in Figure 6.6 with additional details in Appendix 18). In general, the new risk score models performed as well or better than existing risk scores for all outcomes, with all new models achieving AUROC above 0.70.

Using standard health check predictors, newly-developed models performed significantly better than existing risk scores for some outcomes, with higher AUROC for myocardial infarction of 0.785 with 95% CI= [0.775, 0.795]), atrial fibrillation (0.777, [0.768, 0.785]), heart failure (0.828, [0.818, 0.838]), fatty liver disease (0.766, [0.753, 0.779]), alcoholic liver disease (0.864, [0.835, 0.894]) and liver cirrhosis (0.763, [0.734, 0.793]). Newly developed risk models had similar performance to existing scores for stroke (0.727, [0.713, 0.740]), dementia (0.823, [0.810, 0.836]), and chronic kidney disease (0.774, [0.765, 0.783]).

Importantly, for all outcomes studied, newly developed models using only remote features were able to achieve similar discriminative accuracy (AUROC) to their respective standard models. When the set of additional biochemistry was added to the pool of potential predictors (in the extended models), there was very little incremental increase in predictive performance for heart and brain outcomes. In contrast, extended model features produced significantly better predictions for chronic kidney disease (AUROC = 0.875, 95% CI= [0.868, 0.881]), fatty liver (0.809 [0.797, 0.822]), alcoholic liver (0.922 [0.899, 0.944]) and cirrhosis (0.862 [0.837, 0.888]).

This improvement is substantial compared to existing risk scores and standard model estimates, suggesting that an approach with more blood biomarkers might be better at picking up these abnormalities. As expected, calibration statistics (Appendix 19) and reclassification indices (Appendix 20) showed better calibration and significantly improved reclassification in the newly developed risk scores compared with existing risk scores, for example standard myocardial infarction IDI =0.014, 95% CI= [0.011, 0.017], and cNRI = 0.633 [0.588, 0.677].

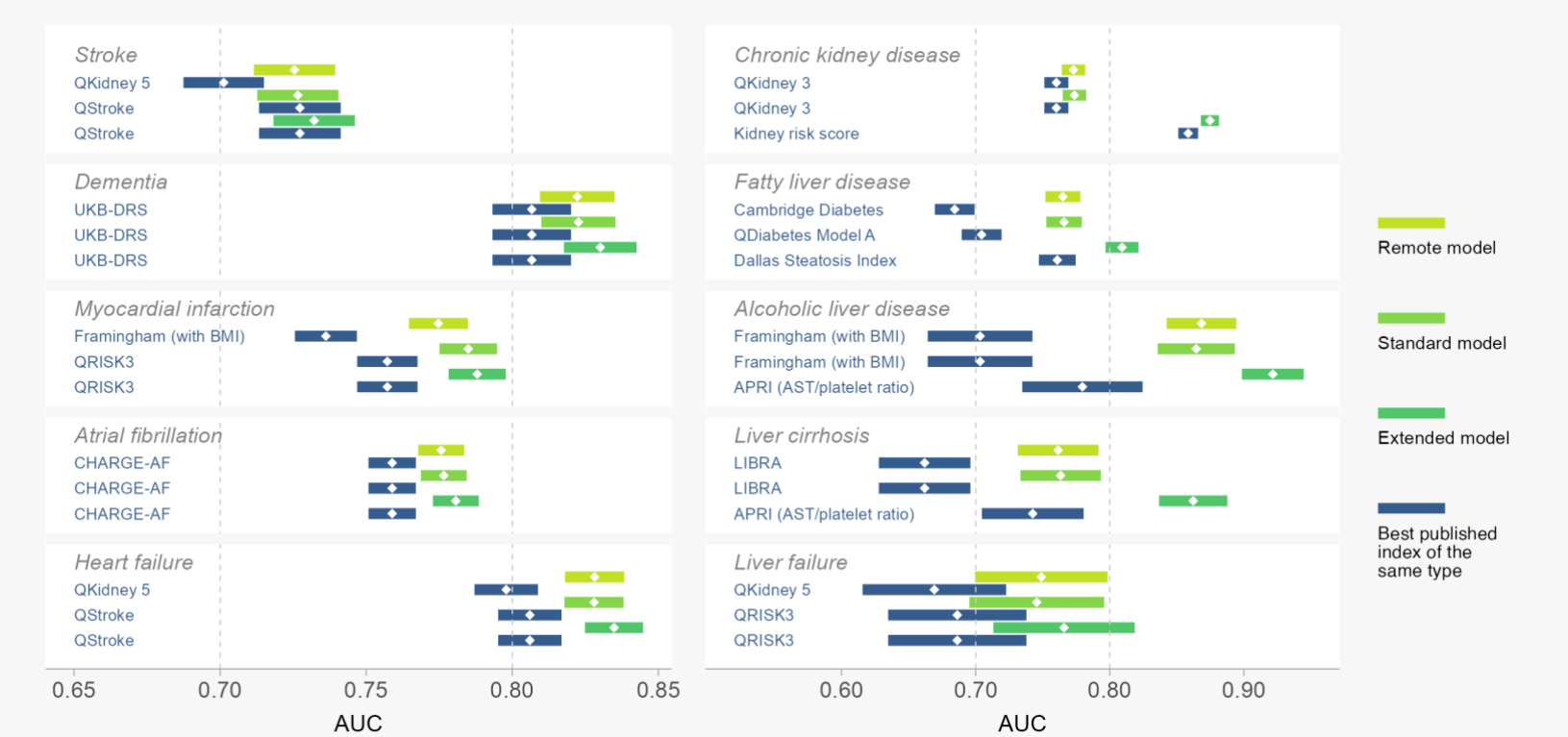


Figure 6.6: Chapter 6 - Performance of multiorgan risk scores in the validation set

Comparison of area under the curve (AUC, also known as concordance or C-statistic) for 10-year risk prediction across 10 outcomes. horizontal bars show the 95% confidence interval for validation set AUC with uncertainty estimated from 1000 bootstrapped samples. Predictions from existing risk scores are shown in dark blue, whilst newly developed risk scores are shown in green. Remote models contain health metrics that can be answered verbally or self-measured easily by the patient. Standard models contain all remote metrics plus blood pressure and serum cholesterol tests. Extended models contain further blood tests. See Appendix 18 for detailed results.

In nearly all comparisons, newly developed models had lower Brier scores (less average squared error) and higher Somers' Dxy (better rank correlation) than existing models. While there were some instances of improved sensitivity in the newer models (stroke, myocardial infarction, chronic kidney disease, alcoholic liver and cirrhosis), overall, the improvements in discrimination were mainly driven by better specificity (fewer false positives, Appendix 18). Final model coefficients (hazard ratios) are presented visually in Appendices 21-23.

6.4 Discussion

In this proof-of-concept analysis with 228,240 UK Biobank participants, we demonstrated that easily collected diagnostics can be used to assess risk across multiple disease outcomes. We have shown how this can be done without specialist computing or invasive biomarkers.

Pairwise modelling showed a complex pattern of cross-system associations, building on prior efforts to understand multimorbidity in the heart-brain-liver-kidney cluster [34], We confirmed that disease risk across all four organs was significantly associated with well-known risk factors such as hypertension, diabetes and high cholesterol; as well as other factors that have not yet been incorporated into standard risk paradigms beyond QRISK3, such as mental illness, systemic inflammation, sleep quality, arterial health and medication use [343, 382].

Recent studies have shown significant improvements in cardiovascular risk prediction using large data sets and machine learning methods [343, 383–385]. However, these studies still only target one organ (the heart), and when compared to conventional statistical models, deep learning or other "black box" methods are not as readily explainable, or easily translatable to clinical use [386]. Several studies have tackled multi-disease prediction. Bayati and colleagues [387] used multi-task learning and group dimensionality reduction to identify a reduced pool of health check features to predict heart-brain-liver-kidney outcomes across two years follow-up. Most similarly to the current work, Mahajan et al. [388] used electronic health records to derive multiple organ-specific risk scores, with a high degree of discrimination (AUROC > 0.80 across heart, brain, lung, kidney and digestive disease). However, this study predicted hospital readmission using previous admissions for the same disease, whereas our models predict risk of new onset disease.

The current study has several important limitations. We recognise the importance of thoroughly evaluating existing risk instruments before moving forward with new risk score development. We have begun this process, but there is more work to be done. On the other hand, by restricting the pool of input variables, new risk score development may well be required to meet this constraint, particularly where remote risk scores of adequate quality do not yet exist.

We acknowledge that the internal validation performance of our scores (developed within UK Biobank) is not directly comparable with external validation performance of published risk scores developed outside UK Biobank. Furthermore, each published risk score has a range of validation values across published work. For example, the validation AUROC provided by the original QRISK3 paper [278] was 0.88 for women and 0.86 for men. Since then other external validation performance has varied in a numerical range consistent with the current work, with values of 0.707 for women and 0.681 for men reported for the 45-64 age group in the Clinical Practice Research Datalink [389], and values of 0.722 for women and 0.697 for men in a recent validation in UK Biobank [390].

It may seem unconventional to apply existing risk score instruments outside their intended cohort (for example including people with comorbidities) and outside their intended outcome (for example using QRISK3 to predict myocardial infarction rather than combined CVD). Our study is not the first to explore this approach [369, 391], and to provide essential evidence for whether existing scores hold unrealised potential in additional contexts.

The UK Biobank participants are subject to self-selection bias, and they are known to be healthier and less ethnically diverse than the UK population [392]. This means that the observed associations may not hold or may be different in a population with greater socioeconomic deprivation, or greater ethnic diversity. Because the UK Biobank are known to be healthier, the risk equations derived in this chapter may systematically under-represent the health outcome risks if applied to the general UK population.

Furthermore, we caution that this study is small compared to larger risk score development projects, and we have not provided an external validation cohort. Therefore, any final models with this approach will require further recalibration and validation in large nationally-representative cohorts. We acknowledge that there are some variables that are not well-measured in the UK Biobank. Where these

come up in multi-disease risk equations, these are likely to be more accurately captured in a primary care-specific database.

In conclusion, this analysis demonstrates the feasibility of using standard health check predictors to produce multi-disease risk estimates of reasonable quality. Such an approach has the potential to ease pressure on primary care, allowing physicians more time to focus on interpretation and follow up [393] thus providing new opportunities for multimorbidity prevention.

Chapter 7: The incremental value of imaging

7.1 Introduction

In Chapter 6, we evaluated the feasibility of expanding risk stratification in primary care to include multiorgan disease risk, enabling earlier identification of individuals at risk and potentially slowing the progression of multimorbidity [394]. While these methods are valuable, they only provide estimates of population-level average risk based on demographic and behavioural health parameters and do not necessarily reflect the organ-level health of the individual.

In Chapter 4 we demonstrated that multiorgan MRI biomarkers have the potential to reveal subtle pathophysiological differences across one or more organs that are not detectable through conventional health checks [75]. However, multiorgan MRI is costly and is unlikely to be implemented as a universal screening tool. In this chapter, we aim to evaluate the incremental predictive value that imaging information may add to non-imaging multiorgan risk stratification.

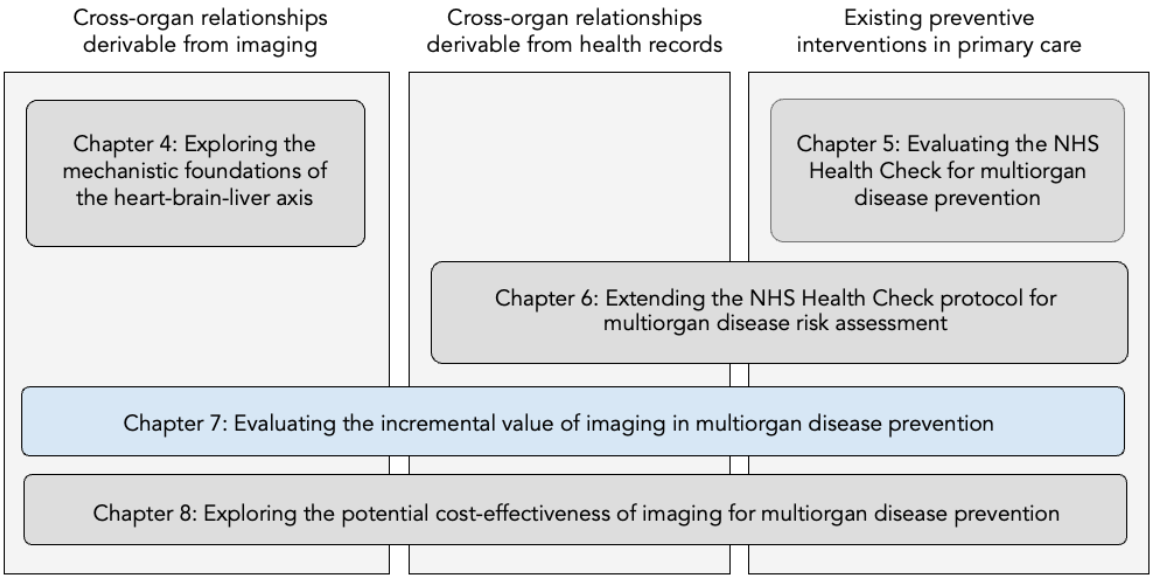


Figure 7.1: Chapter 7 - Roadmap location

The key questions addressed in this chapter are:

1. Which specific imaging biomarkers contribute most significantly to the enhancement of multiorgan risk assessment?

2. How do imaging-based risk stratification models compare with traditional non-imaging models in terms of predictive accuracy?

7.2 Methods

Once again, this study draws upon the UK Biobank data (Section 2.1), this time limiting the analysis to participants that are part of the multiorgan imaging substudy (Section 3.2), and focusing on the outcome events that occur after imaging.

7.2.1 Incremental imaging comparison

Figure 7.2 provides an overview of the components of the comparison setup. The core comparison is between the quality of the risk assessment that includes non-imaging and imaging risk assessment (Method B), compared with only non-imaging risk (Method A). Risk models were used to predict 5-year outcomes across the heart-brain-liver-kidney (HBLK) cluster in the same set of people, comparing imaging with non-imaging risk calculations.

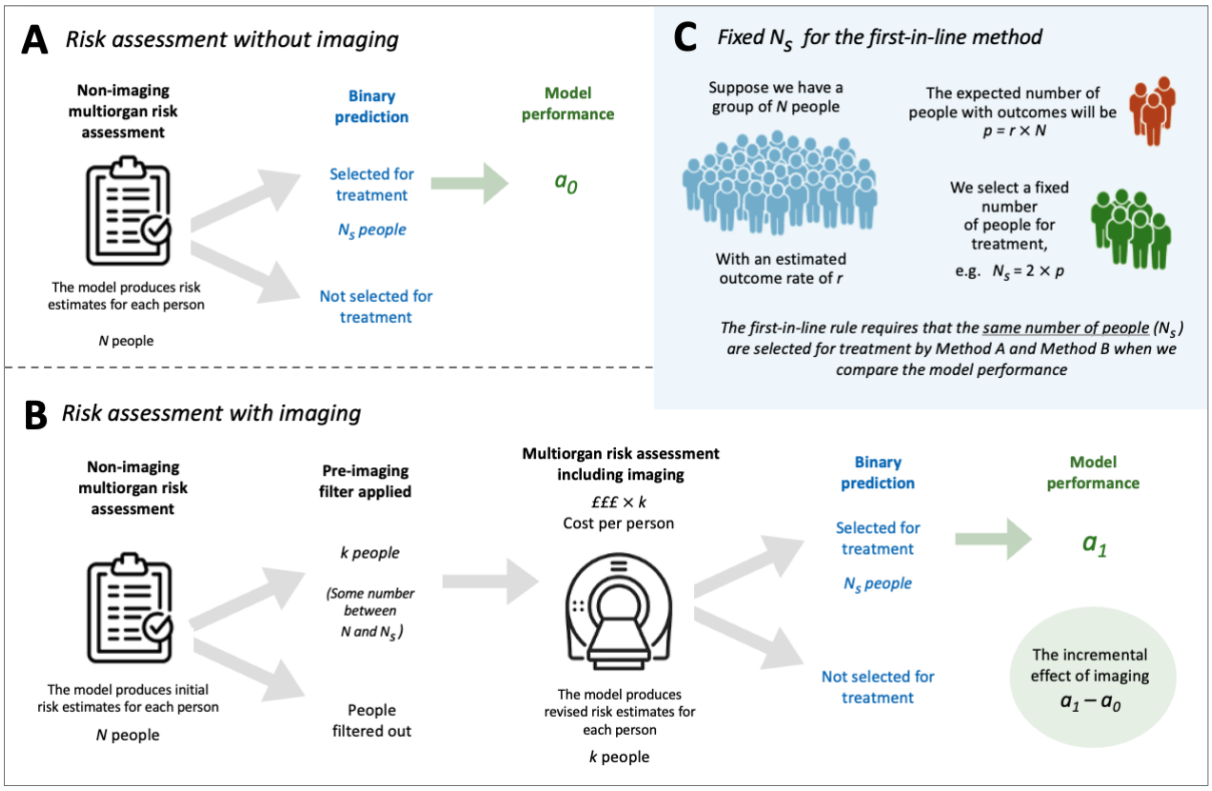


Figure 7.2: Chapter 7 - Comparison method overview

The assumption here is that risk assessment is used to identify a group of people at high risk that would be directed to some treatment that would then improve their longer-term prospects in some way. In this study, we are not considering what that treatment may be but only evaluating the incremental improvement in the quality of risk allocation achieved using imaging models when compared to risk assessment using non-imaging models.

7.2.2 The "first-in-line" method

When running these models, it became clear that there was a need to produce a fair comparison between imaging and non-imaging (Methods A and B) that was traceable back to each individual. The "first-in-line" rule is a simple method for achieving this, ensuring that the comparison reflects real-world scenarios where resources for treatment are limited. The key property of the first-in-line method is that we evaluate the model performance in the same number of people for each method.

7.2.2.1 Explanation

Suppose we have a group of N = 1000 people, and we expect an outcome rate of r = 1.5%. It follows then that we would expect about

$$p = r \times N$$

$$p = 1.5\% \times 1000$$

$$p = 15 \text{ people}$$

in the group to have outcome events during the follow-up period (Figure 7.2, Panel C). With the first-in-line method, the key constraint is that we "select for treatment" the same number of people (N_S) using each method and then compare the accuracy or quality of these selections. The value of N_S is arbitrary, and in this study, we decided to choose a small number (due to the expected high cost of specialised treatment per person) that scales relative to outcome prevalence *(r)*. Other values are equally possible, but in this study, we have chosen to set $N_S = 2 \times p$ (= 30 people in this example).

Once the value of N_S is fixed, applying the first-in-line method is very simple. First, we build best-fitting models for multiorgan risk, one set of models including multiorgan imaging (Method B) and another set without the inclusion of imaging (Method A). We use both non-imaging and imaging risk models to produce a multiorgan risk estimate (%) for each person. Then, the group of people is sorted

from highest to lowest risk by Method A (non-imaging risk), and the N_S highest-risk individuals are selected. We follow the same process to select another N_S individuals using Method B (imaging-based risk). This is equivalent to making a binary prediction for both models. Then, we evaluate the predictive performance in each group of N_S people who were first in line with the highest predicted risk. We calculate performance measures (Method A = a_0, and Method B = a_1) using standard binary performance metrics such as AUC (area under the curve), AUC-PR (area under the precision-recall curve), sensitivity, specificity, balanced accuracy and positive predictive value (see Section 3.4.4). The incremental difference in performance ($a_1 - a_0$) represents the incremental value of imaging.

7.2.2.2 Rationale for the first-in-line method

This method addresses a critical limitation of traditional model comparison techniques, such as unconstrained AUC or population-wide calibration metrics. While these metrics provide a broad assessment of model performance, they do not reflect the practical realities of clinical decision-making, where prioritisation of high-risk individuals is necessary due to resource constraints. Without the first-in-line constraint, differences in predicted probabilities between models could bias the evaluation, making it unclear whether observed improvements in model performance stem from true incremental value or simply differences in probability distributions.

The first-in-line method achieves fairness by fixing Ns relative to the prevalence of outcomes (r). For example, in a population of 1,000 individuals with an outcome prevalence of 1.5% (r = 0.015), we select Ns = 2 × r × N = 30 individuals for comparison. The method allows us to evaluate the accuracy of models in predicting high-risk individuals under equal conditions, ensuring robust comparison of imaging and non-imaging models.

7.2.2.3 Alternatives to the first-in-line method

Two main alternatives were considered but not used. Comparisons could be made by selecting individuals based on a fixed predicted risk threshold (e.g., >10%). This approach can introduce bias (and cause miscalculations in costs and outcomes) when the thresholds do not align with the natural distribution of risk in the population or where the distributions of risk predictions are different between imaging and non-imaging estimates. This is a serious problem because we need the imaging and non-

imaging risk results to be comparable such that the incremental value can be calculated. Having said that, once the imaging and non-imaging models are calibrated in a particular sample, (whether small or large), appropriate risk thresholds can be obtained for forward clinical use.

Secondly, we could compare models using AUC or calibration metrics across the entire population using non-parametric comparison. Indeed, we have included these metrics in the results. While informative, these metrics lack clinical relevance in contexts where only a subset of individuals can be targeted for follow-up or intervention, and are too flexible when we need to fix the cost point to a specific number of people receiving imaging.

7.2.2.4 Sensitivity Analysis of Ns

The choice of Ns is arbitrary but scaled to reflect realistic clinical scenarios. To assess robustness, sensitivity analyses were conducted with different values of Ns, including Ns = 1 × r × N and Ns = 3 × r × N (where r is the expected outcome prevalence rate). These analyses demonstrated that the incremental value of imaging (a1 – a0) remained consistent across different values of Ns, with similar relative improvements in AUC, sensitivity, specificity, and other performance metrics. The part that did change, however, was the cost ratio (in Chapter 8). Sensitivity analysis showed that the scope for cost-effectiveness was limited to smaller values of Ns relative to the outcome prevalence rate.

7.2.3 Study variables

This study again involves building population-level risk models, but this time, building non-imaging models by evaluating a range of candidate risk scores for discriminative performance in the imaging cohort. A listing of study variables is provided in Table 7.1. For the purposes of this study, the combined heart, brain, liver and kidney (HBLK) model includes all specified outcomes plus rarer conditions within the HBLK cluster of organs. In addition, the model for combined HBLK events includes all participants, so it is a model assessing the risk for an additional HBLK event in the coming five years given current diagnoses.

7.2.4 The best non-imaging risk model for each outcome

We calculated all the risk scores listed in Table 7.1 for all participants, with the covariate values available at the time of imaging (with details found in Appendix 3).

Table 7.1: Chapter 7 - Study variables

Variable Group	Organ/System	Variable
Candidate non-imaging risk scores (Exposures)	Brain	QStroke, UKB-DRS (UK Biobank Dementia Risk Score)
	Heart	QRISK3, Framingham Risk Score, CHARGE-AF, PCP-HF, SCORE2/SCORE-OP
	Liver	Fatty liver index, FIB-4 Index, NAFLD Fibrosis Score
	Kidney	QKidney (V3), QKidney (V5)
Imaging features (Exposures)	Brain	Overall brain volume metrics (all in mm^3) Total brain volume White matter volume Grey matter volume Peripheral grey matter volume Volume of cerebrospinal fluid Volume of white matter hyperintensities (WMH) Volume of hippocampus White matter microstructure via diffusion MRI Fractional anisotropy (FA) Mean diffusivity (MD) Intracellular volume fraction (ICVF) Isotropic volume fraction (ISOVF) Orientation dispersion (OD)
	Arterial	Aortic distensibility (AoD, 10-3mmHg) Carotid intima-medial thickness
	Cardiac	Standard CMR metrics LV= left ventricular, RV = right ventricular, End diastolic volumes (LVEDV, RVEDV, mL), End systolic volumes (LVESV, RVESV, mL), Stroke volumes (LVSV, RVSV, mL), Ejection fractions (LVEF, RVEF, %), LV global function index (LV GFI, %), LV mass (LVM, g) LV mass-to-volume ratio (LVM/LVEDV) LV wall thickness Additional CMR metrics LV T1 (ms, global LV, free wall, septal), Pericardial adipose tissue (PAT, mm^2) Left atrial volume (LAV) Left atrial ejection fraction (LAEF, %)
	Liver	Liver fat (Proton density fat fraction, PDFF, %) Liver iron (mg/g dry tissue weight) Corrected T1 (cT1, ms, a measure of fibroinflammation)
De-confounders	Covariates	Age, sex, age squared, non-white ethnicity, Townsend deprivation index, self-reported health (poor, fair, good or excellent), post-secondary education, family history (heart, brain, liver and kidney disease), hypertension, high cholesterol, diabetes, body mass index, waist-to-hip ratio, systolic blood pressure, red blood cell count, heart rate, total-to-HDL cholesterol ratio, sleep disorder.
	Imaging confounders	(Age, sex, age squared) Imaging site, height, head size scaling factor, date of imaging, imaging table coordinates (X, Y, Z)
Outcomes	Brain	Stroke, all-cause dementia
	Arterial	Atherosclerosis / peripheral artery disease, Venous thromboembolism
	Heart	Myocardial infarction, atrial fibrillation, non-ischaemic cardiomyopathies, valvular heart disease, heart failure
	Liver	Combined liver disease, fatty liver disease, liver cirrhosis.
	Kidney	Combined kidney events, chronic kidney disease (stage 3+)
	Combined HBLK	Combined heart, brain, arterial, liver and kidney disease or death

We created a list of all risk score and outcome combinations and used Cox proportional hazards regression models with risk score entered as the sole predictor in each model. Models were fitted for each combination and scored for accuracy (Section 3.4.4). The best-performing model by highest AUC was selected as the representative non-imaging risk score for each outcome.

As expected, the UKB-DRS was the risk score with the highest AUC for all-cause dementia, CHARGE-AF for atrial fibrillation, QRISK3 for myocardial infarction, Framingham Risk Score (with BMI) for non-ischaemic cardiomyopathy, PCP-HF for combined kidney disease and venous thromboembolism, QKidney for chronic kidney disease, Fatty liver index for all three liver outcomes, and QStroke for stroke, peripheral artery disease, valvular heart disease, heart failure and combined HBLK. Even though a non-imaging risk score may appear more than once, each model's predicted risk distribution is unique as it is tuned to different outcomes.

7.2.5 Model fitting including multiorgan imaging

Then, we applied stability selection (Section 3.4.3) to combine non-imaging risk scores with imaging metrics to produce the best-fitting simplified models for each outcome. In all cases, we forced the model to contain (at minimum) the best-performing non-imaging risk score, along with age, sex, and the required imaging de-confounders. Additional covariates were allowed to be included if selected by the algorithm. Because these models did not need to be translated into a risk calculator, we entered all continuous variables as scaled z-scores, such that model coefficients reflect the hazard ratio associated with a one standard deviation increase in predictor value. Pruning was applied to the final model fits to remove variables causing collinearity and redundancy.

7.2.6 Performance scoring and differences

AUC, AUC-PR, sensitivity, specificity, balanced accuracy and positive predictive value were calculated for imaging models and non-imaging models and the differences between them. Standard errors were calculated using 1000 bootstrapped samples, with p-values ascertained with permutation testing with 1000 replications.

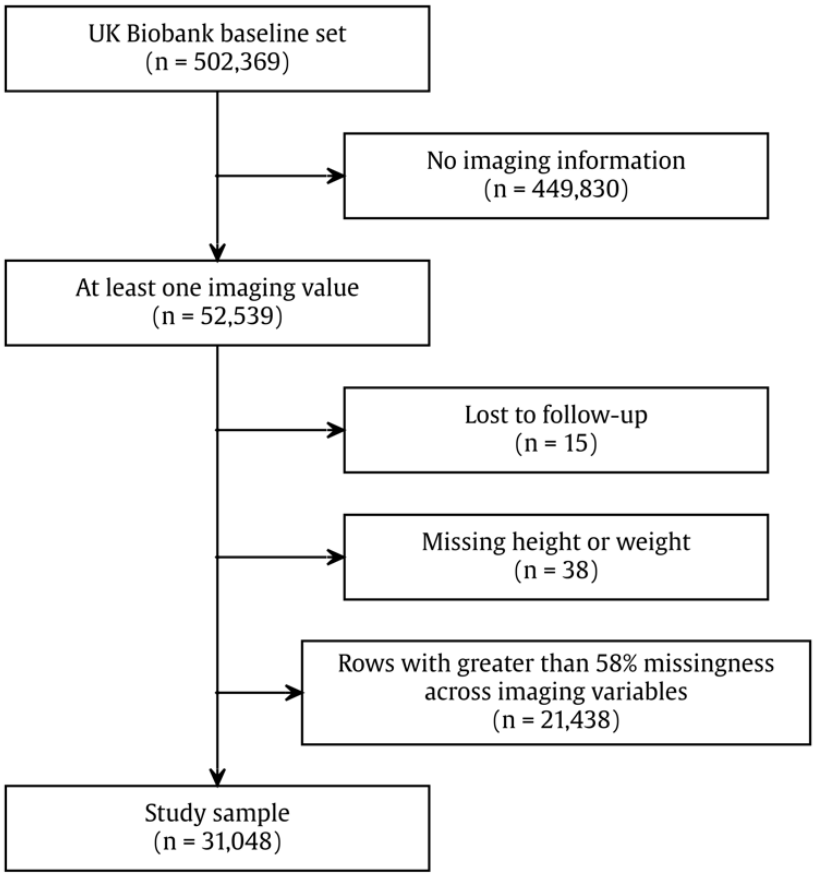


Figure 7.3: Chapter 7 - Sample selection

7.3 Results

7.3.1 Sample selection

For this study, we conducted risk modelling on participants from the time of multiorgan imaging until our maximum study date (31 October 2022) giving an average post-imaging follow-up period of 5.5 years. We identified all UK Biobank participants with at least one form of imaging data available in the downloaded dataset at the study start date (February 2023, see Figure 7.3).

From the 52,539 participants with at least one item of imaging data, 15 participants were lost to follow-up and 38 were excluded due to missing height or weight information. We created a pragmatic data set from the remaining participants by filtering out rows with high missingness, such that the remaining data had less than 15% missingness across all imaging input variables. This process resulted in a final data set with 30,048 participants with imaging records across heart, brain, liver and carotid ultrasound.

Table 7.2: Chapter 7 - Sample characteristics

Characteristic	Whole sample n= 31,048	Women n= 16,178, 52.1%	Men n= 14,870, 47.9%
Age at imaging	63.2 (±7.5)	62.6 (±7.4)	63.8 (±7.6)
Less than 60 years	10,144 (32.7%)	5,709 (35.3%)	4,435 (29.8%)
Age 60 – 69 years	13,780 (44.4%)	7,288 (45.0%)	6,492 (43.7%)
Age 70 or more	7,124 (22.9%)	3,181 (19.7%)	3,943 (26.5%)
Non-white ethnicity	828 (2.7%)	390 (2.4%)	438 (2.9%)
Townsend deprivation index	-2.67 [-3.92, -0.64]	-2.60 [-3.88, -0.59]	-2.72 [-3.95, -0.69]
Self-reported health			
1.Excellent	5,851 (18.8%)	3,098 (19.1%)	2,753 (18.5%)
2.Good	19,420 (62.5%)	10,245 (63.3%)	9,175 (61.7%)
3.Fair	4,869 (15.7%)	2,369 (14.6%)	2,500 (16.8%)
4.Poor	634 (2.0%)	313 (1.9%)	321 (2.2%)
Physical measures			
Body mass index (kg/m2)	25.9 [23.5, 28.8]	25.3 [22.8, 28.5]	26.5 [24.3, 29.1]
Waist-hip ratio (cm/cm)	0.871 (±0.087)	0.816 (±0.067)	0.930 (±0.063)
Systolic blood pressure (mmHg)	138 (±18)	135 (±19)	141 (±17)
Heart rate (bpm)	69.4 (±11.6)	71.2 (±11.0)	67.5 (±12.0)
Lifestyle factors			
Current smoker	1,122 (3.6%)	488 (3.0%)	634 (4.3%)
Physically active	25,656 (82.6%)	13,164 (81.4%)	12,492 (84.0%)
Sleep disorder (yes)	9,683 (31.2%)	5,617 (34.7%)	4,066 (27.3%)
Risk factors			
Diabetes	1,790 (5.8%)	653 (4.0%)	1,137 (7.6%)
Hypertension	10,350 (33.3%)	4,361 (27.0%)	5,989 (40.3%)
High cholesterol	8,847 (28.5%)	3,330 (20.6%)	5,517 (37.1%)

The sample characteristics for the sample of 31,048 participants are provided in Table 7.2. Consistent with previous results, the sample was slightly more female (52.1%), of predominantly white ethnicity, (97.2%) with low socioeconomic deprivation. Overall, men in the sample had a poorer health profile with higher rates of diabetes, hypertension and high cholesterol.

Table 7.3: Chapter 7 - Imaging characteristics (selected variables)

Metric	Whole sample n= 31,048	Women n= 16,178 (52.1%)	Men n= 14,870 (47.9%)
Cardiac imaging			
LVM (g)	86.2 (±22.2)	70.9 (±12.2)	103 (±18)
Max wall thickness (mm)	7.08 (±1.08)	6.48 (±0.79)	7.74 (±0.96)
LVEDV (mL)	148 (±34)	130 (±22)	169 (±32)
LV cardiac output (L/min)	5.45 (±1.26)	5.00 (±1.08)	5.94 (±1.27)
LAV max (mL)	70.1 [57.0, 85.3]	65.9 [54.4, 78.7]	76.0 [61.1, 92.6]
LVEF (%)	59.6 (±6.1)	61.1 (±5.6)	57.8 (±6.1)
Global function index (%)	47.7 (±6.8)	50.4 (±6.2)	44.8 (±6.2)
GCS	-22.3 (±3.3)	-23.4 (±3.1)	-21.1 (±3.2)
GLS	-18.5 (±2.7)	-19.1 (±2.7)	-17.8 (±2.6)
LAEF (%)	61.3 (±9.1)	61.9 (±8.6)	60.5 (±9.7)
Pericardial fat (cm^2)	22.5 [16.2, 31.5]	18.4 [14.1, 24.5]	28.5 [20.8, 38.5]
LV interventricular septum T1 (ms)	933 (±51)	950 (±51)	915 (±45)
Liver imaging			
Liver PDFF (%)	3.00 [2.10, 5.50]	2.60 [1.90, 4.40]	3.60 [2.50, 6.62]
Very low liver fat (< 2%)	5,755 (18.5%)	4,082 (25.2%)	1,673 (11.3%)
Liver iron (mg/g)	1.20 [1.10, 1.40]	1.20 [1.10, 1.30]	1.20 [1.10, 1.40]
Very low liver iron (< 1.1mg)	2,626 (8.5%)	1,559 (9.6%)	1,067 (7.2%)
Liver iron > 1.5 mg/g	4,855 (15.6%)	2,063 (12.8%)	2,792 (18.8%)
Liver cT1 (ms)	693 [662, 730]	685 [656, 720]	701 [669, 741]
Liver cT1 > 700 ms	13,713 (44.2%)	6,243 (38.6%)	7,470 (50.2%)
Brain imaging (normalised for head size)			
Total brain volume (mm^3)	1,498,844 (±72,961)	1,510,206 (±73,193)	1,486,154 (±70,572)
Grey matter volume (mm^3)	794,405 (±47,822)	809,248 (±45,937)	777,827 (±44,312)
Peripheral brain volume (mm^3)	619,807 (±40,653)	630,777 (±39,999)	607,553 (±37,777)
CSF volume (mm^3)	41,773 [32,096, 54,802]	37,892 [29,334, 49,418]	46,655 [36,092, 60,766]
Hippocampus volume (mm^3)	4,050 (±401)	3,925 (±356)	4,189 (±402)
White matter hyperintensities (mm^3)	2,736 [1,469, 5,542]	2,498 [1,360, 4,930]	3,031 [1,615, 6,213]

LVM = left ventricular mass, LVEDV= left ventricular end-diastolic volume, LAV = left atrial volume, LVEF = left ventricular ejection fraction, GCS = global circumferential strain, GLS = global longitudinal strain, LAEF = left atrial ejection fraction, PDFF = proton density fat fraction, cT1 = corrected T1 relaxation time, CSF = cerebrospinal fluid.

Table 7.3 provides a summary of the imaging characteristics observed in study participants. These values are consistent with published results of the same data [115, 121, 138, 143, 268, 395, 396]. As expected, we observe that men have larger hearts, with greater pericardial fat, greater liver fat, and more liver inflammation (cT1 > 700 ms). On the other hand, women have higher cardiac T1, with higher LV ejection fraction and are more likely to have very low liver iron (< 1.1mg/g).

Table 7.4: Chapter 7 - Multiorgan outcomes

Outcomes	Whole sample n= 31,048	Women n= 16,178, 52.1%	Men n= 14,870, 47.9%
Combined HBLK outcomes	3,193 (10.3%)	1,241 (7.7%)	1,952 (13.1%)
Brain			
Stroke	298 (1.0%)	129 (0.8%)	169 (1.1%)
All-cause dementia	145 (0.5%)	64 (0.4%)	81 (0.5%)
Arterial			
Peripheral artery disease	359 (1.2%)	122 (0.8%)	237 (1.6%)
Venous thromboembolism	308 (1.0%)	125 (0.8%)	183 (1.2%)
Heart			
Myocardial infarction	406 (1.3%)	117 (0.7%)	289 (1.9%)
Atrial fibrillation	749 (2.4%)	241 (1.5%)	508 (3.4%)
Non-ischaemic cardiomyopathy	93 (0.3%)	28 (0.2%)	65 (0.4%)
Valvular heart disease	608 (2.0%)	243 (1.5%)	365 (2.5%)
Heart failure	337 (1.1%)	111 (0.7%)	226 (1.5%)
Kidney			
Combined kidney events	1,026 (3.3%)	396 (2.4%)	630 (4.2%)
Chronic kidney disease	447 (1.4%)	188 (1.2%)	259 (1.7%)
Liver			
Combined liver disease	357 (1.1%)	186 (1.1%)	171 (1.1%)
Fatty liver disease	221 (0.7%)	124 (0.8%)	97 (0.7%)
Liver cirrhosis	45 (0.1%)	13 (0.1%)	32 (0.2%)
Mortality			
All-cause mortality	648 (2.1%)	225 (1.4%)	423 (2.8%)
Mortality with cardiac cause	121 (0.4%)	29 (0.2%)	92 (0.6%)
HBLK mortality	185 (0.6%)	52 (0.3%)	133 (0.9%)
Follow-up time	5.45 (±1.36)	5.47 (±1.35)	5.44 (±1.36)

HBLK = heart, brain, liver or kidney

Table 7.4 summarises the multiorgan outcomes recorded in the study. Overall, we observed 3,193 events relating to the heart, brain, liver and kidney cluster across an average 5.45 years of follow-up, including 185 deaths with an HBLK primary cause. Atrial fibrillation was the most commonly observed outcome (n= 749), with liver cirrhosis being the rarest (n=45).

In the upcoming section, we provide a description of the multiorgan imaging metrics that were included in final models by the stability selection process, indicating significant incremental predictive value over and above the best-performing non-imaging risk score. The results in these sections address the first research question by identifying the specific imaging biomarkers that contribute most significantly to multiorgan risk assessment. The corresponding numerical results are included in Appendix 24.

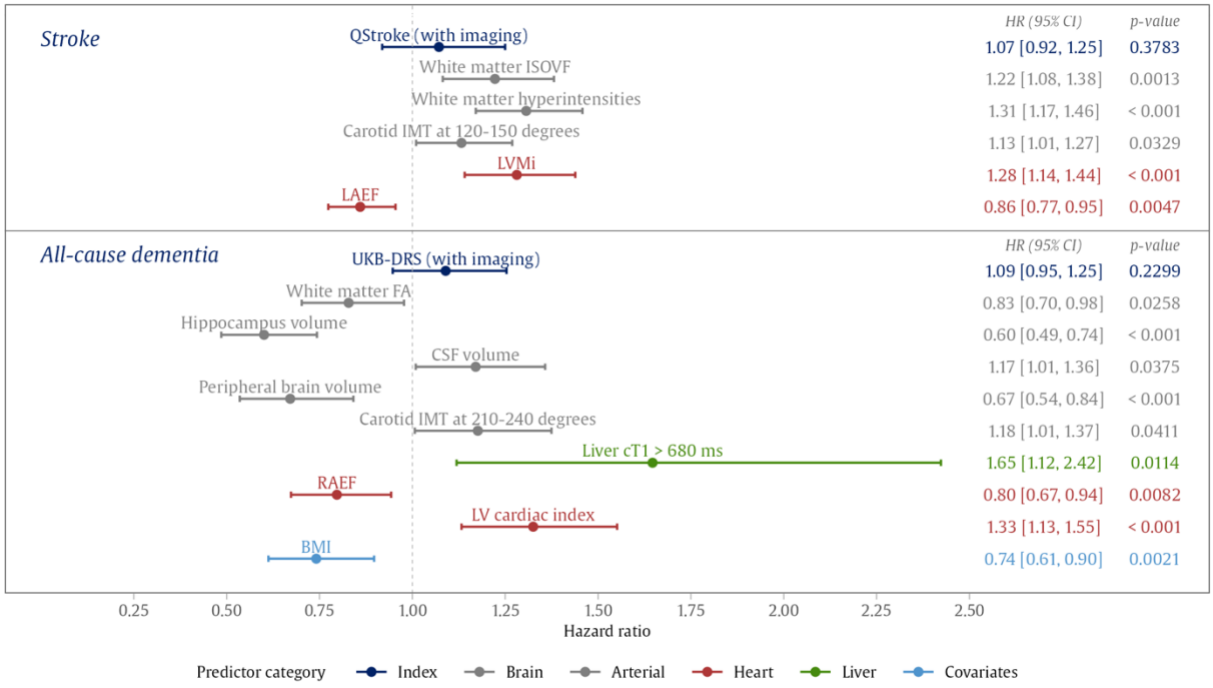


Figure 7.4: Chapter 7 - Significant imaging predictors – Brain outcomes

Points represent hazard ratios of the significant imaging variables selected in final models by stability selection, along with significant covariate variables. Each rectangle represents a single Cox proportional hazards model for 5-year risk for the disease outcome indicated on the left-hand side. Unless binary (eg. liver cT1 > 680 ms), hazard ratios are from standardised beta coefficients, meaning that the hazard ratio represents the increase in outcome hazard associated with one standard deviation increase in the predictor variable observed from multiorgan imaging. Error bars indicate the 95% confidence intervals for hazard ratios, with numerical results and p-values shown on the right-hand side. Colours identify model variables by category, with cardiac imaging variables in red, liver imaging in green, brain/arterial imaging in grey, and additional covariates in bright blue. All models are additionally adjusted by age, sex, brain imaging coordinates and imaging site (coefficients not shown). See Appendix 24 for additional details.

7.3.2 Brain outcomes (stroke and dementia)

In the non-imaging model for stroke, every standard deviation increase in QStroke score was associated with a 54% increase in risk for stroke with HR= 1.54, 95% CI= [1.43, 1.66]. When multiorgan imaging was added to the model, the QStroke score became non-significant (1.07, [0.92, 1.25], Figure 7.4). Instead, increased stroke risk was associated with greater volume of white matter hyperintensities (1.31, [1.17, 1.46]), white matter inflammation (1.22, [1.08, 1.38]), greater carotid intima-media thickness (1.13, [1.01, 1.27]), greater LV mass indexed to body surface area (1.28, [1.14, 1.44]) and reduced LA ejection fraction (0.86, [0.77, 0.95]).

In the case of all-cause dementia, in the non-imaging model, a standard deviation increase in UKB-DRS was associated with a 49% increase in dementia risk (1.49, [1.40, 1.58]). When imaging was added, 5-year risk of dementia was instead associated with reduced fractional anisotropy of the brain white matter (0.83, [0.70, 0.98]), greater carotid thickness (1.18, [1.01, 1.37]), reduced hippocampus

volume (0.60, [0.49, 0.74]), reduced volume of peripheral grey matter (0.67, [0.54, 0.84]) and increased volume of cerebrospinal fluid (1.17, [1.01, 1.36]). Interestingly, having a liver cT1 of greater than 680 milliseconds was associated with a 65% increase in five-year hazard for dementia (1.65, [1.12, 2.42]) along with reduced right atrial ejection fraction (0.80, [0.67, 0.94]). Given the values of all other coefficients, a higher-than-average LV cardiac index was associated with increased dementia risk (1.33, [1.13, 1.55]).

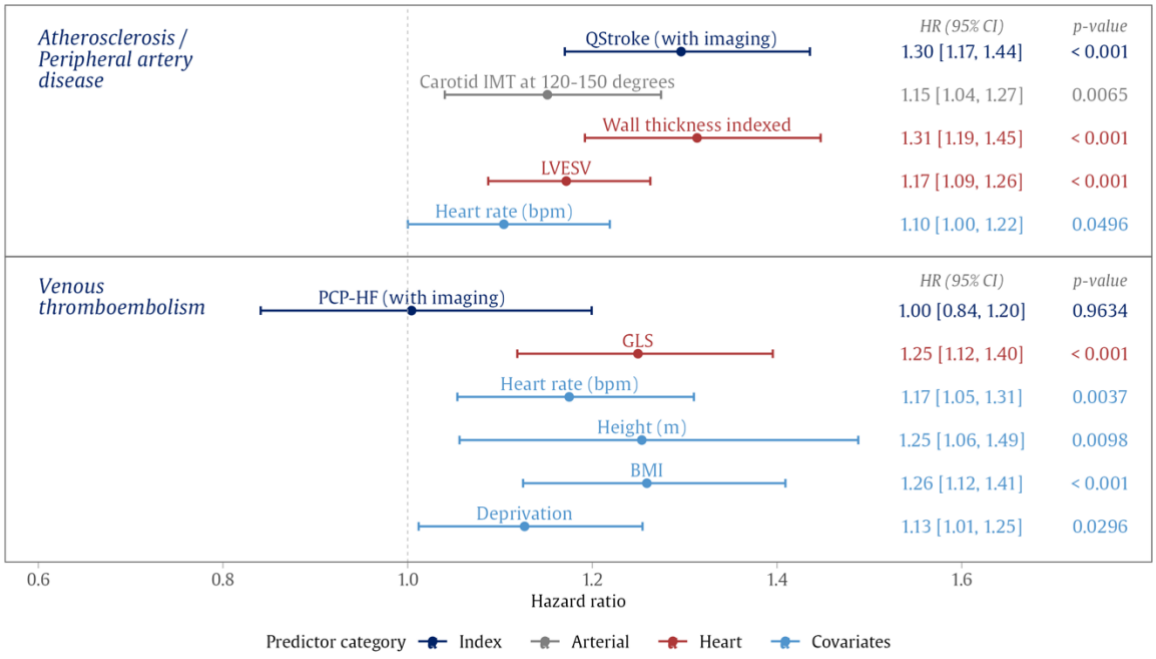


Figure 7.5: Chapter 7 - Significant imaging predictors – Arterial outcomes

Points represent hazard ratios of the significant imaging variables selected in final models by stability selection, along with significant covariate variables. Each rectangle represents a single Cox proportional hazards model for 5-year risk for the disease outcome indicated on the left-hand side. Hazard ratios are from standardised beta coefficients, meaning that the hazard ratio represents the increase in outcome hazard associated with one standard deviation increase in the predictor variable observed from multiorgan imaging. Error bars indicate the 95% confidence intervals for hazard ratios, with numerical results and p-values shown on the right-hand side. Colours identify model variables by category, with cardiac imaging variables shown in red, liver imaging variables shown in green, and brain/arterial imaging variables shown in grey, and additional covariates in bright blue. All models are additionally adjusted by age, sex, and imaging site (coefficients not shown). See Appendix 24 for additional details.

7.3.3 Arterial/vascular outcomes

In non-imaging models for a five-year diagnosis of atherosclerosis or peripheral arterial disease, a standard deviation increase in QStroke was associated with a 59% increased risk (HR= 1.59, 95% CI = [1.51, 1.68]). In the presence of multiorgan imaging (Figure 7.5), QStroke was still significant but only indicated a 30% increased risk (1.30, [1.17, 1.44]). Arterial disease was associated with greater carotid thickness (1.15, [1.04, 1.27]), greater LV end-systolic volume (1.17, [1.09, 1.26]), greater cardiac wall

thickness indexed to body surface area (1.31, [1.19, 1.45]), and slightly higher heart rate (1.10, [1.01, 1.22]).

A standard deviation increase in PCP-HF risk score was initially associated with a 26% increase in five-year risk of venous thromboembolism (HR=1.26, 95% CI= [1.17, 1.37]), but when imaging was added this coefficient became non-significant (1.00, [0.84, 1.20]). In imaging models, increased 5-year risk for venous thromboembolism was associated with increased cardiac strain (GLS, 1.25, [1.12, 1.40]), higher heart rate (1.17, [1.05, 1.31]) along with several other factors.

7.3.4 Heart outcomes

In non-imaging models for myocardial infarction, one standard deviation increase in QRISK3 score was associated with 89% increased risk (HR= 1.89, 95% CI= [1.76, 2.02]). With the addition of imaging (Figure 7.6). QRISK3 was still significant with a hazard ratio of 1.22 (95% CI= [1.07, 1.40]). However, increased myocardial infarction risk was also associated with greater carotid thickness (1.14, [1.04, 1.26]), reduced cardiac index (0.78, [0.69, 0.87]), and greater LV mass index (1.27, [1.15, 1.41]). Liver cT1 greater than 680 ms was associated with a 25% risk for myocardial infarction within 5 years (1.25, [1.00, 1.56]).

Initially, one standard deviation increase in CHARGE-AF score was associated with a 51% increased risk for atrial fibrillation. When multiorgan imaging was added, this effect was not significant (1.02, [0.94, 1.11]). Instead, increased atrial fibrillation risk was associated with greater myocardial wall thickness (1.26, [1.17, 1.37]), greater right and left atrial volumes (1.10, [1.02, 1.18] and 1.39, [1.28, 1.50] respectively), and reduced LA ejection fraction (0.84, [0.75, 0.94]). Interestingly, having a liver cT1 of greater than 720 milliseconds was associated with a 31% increased risk for atrial fibrillation (1.31, [1.13, 1.53]).

Framingham risk score was the best-performing score for non-ischaemic cardiomyopathies within 5 years, with an 80% increase in risk with each standard deviation (1.80, [1.54, 2.09]). In imaging models, this was not significant, instead, risk for non-ischaemic cardiomyopathies was associated with greater cardiac wall thickness indexed to body surface area (1.65, [1.44, 1.91]), greater LV end-systolic volume (1.22, [1.05, 1.43]), greater LA volume (1.15, [1.05, 1.27]) and greater left-to-right ventricular volume asymmetry (volume ratio, 1.23, [1.05, 1.44]).

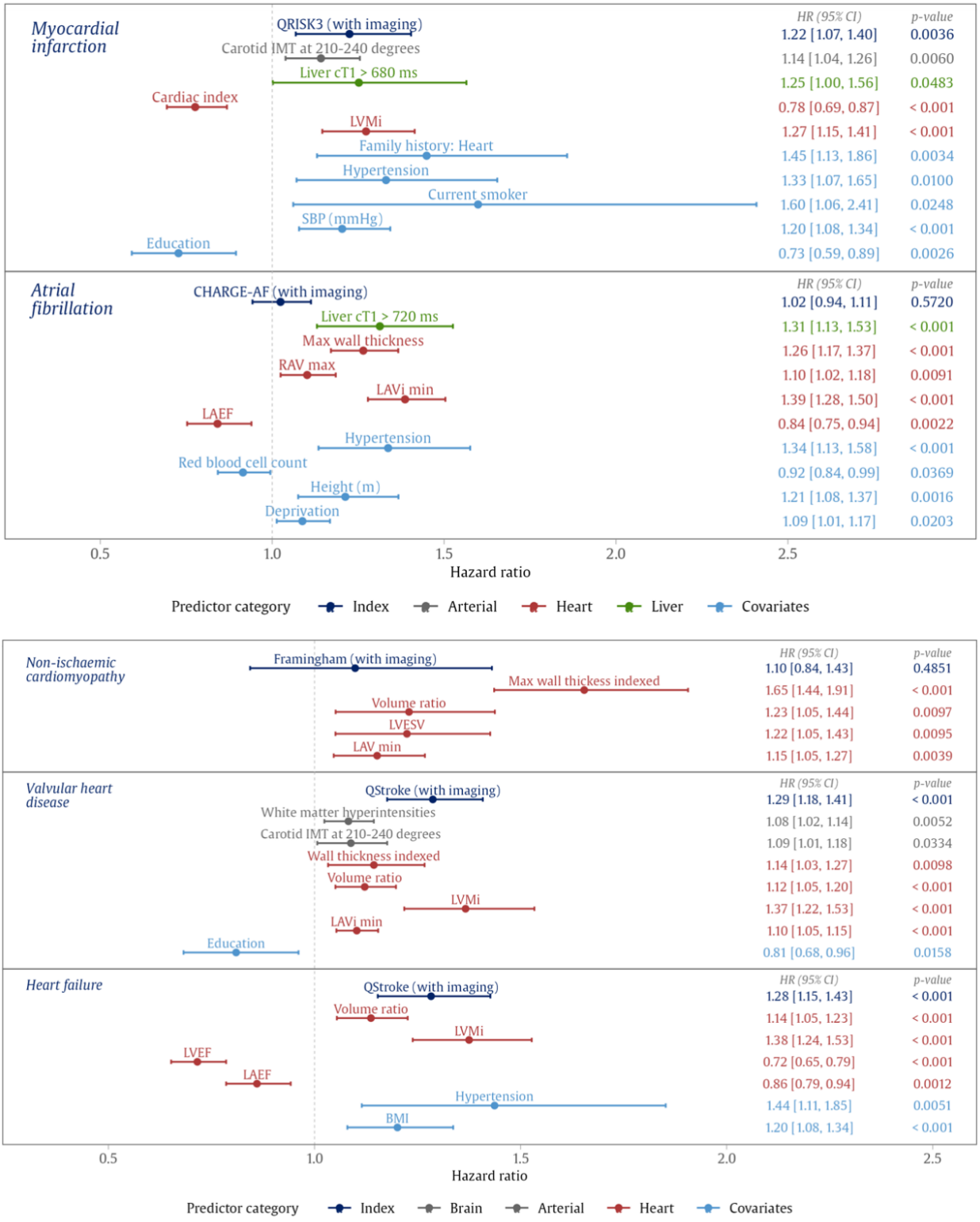


Figure 7.6: Chapter 7 - Significant imaging predictors – Heart outcomes

Points represent hazard ratios of the significant imaging variables selected in final models by stability selection, along with significant covariate variables. Each rectangle represents a single Cox proportional hazards model for 5-year risk for the disease outcome indicated on the left-hand side. Unless binary, hazard ratios are from standardised beta coefficients, meaning that the hazard ratio represents the increase in outcome hazard associated with one standard deviation increase in the predictor variable observed from multiorgan imaging. Error bars indicate the 95% confidence intervals for hazard ratios, with numerical results and p-values shown on the right-hand side. Colours identify model variables by category, with cardiac imaging variables shown in red, liver imaging variables shown in green, and brain/arterial imaging variables shown in grey, and additional covariates in bright blue. All models are additionally adjusted by age, sex, and imaging site (coefficients not shown). See Appendix 24 for additional details.

One standard deviation increase in QStroke was associated with an 81% increased risk for valvular heart disease (combined types) in non-imaging models (1.81, [1.73, 1.89]). When multiorgan imaging was added, the QStroke score was still significant, conferring 29% increased risk (1.29, [1.18, 1.41]). In addition, greater risk for valvular heart disease was associated with greater white matter hyperintensities (1.08, [1.02, 1.14]), greater carotid thickness (1.09, [1.01, 1.18]), greater wall thickness indexed to body size (1.14, [1.03, 1.27]), greater LV mass indexed (1.37, [1.22, 1.53]), greater LA volume (1.10, [1.05, 1.15]) and left-side asymmetry (1.12, [1.05, 1.20]).

QStroke was also the best-performing index in our sample for 5-year risk of heart failure, associated with 78% increased risk in the non-imaging setting (1.78, [1.70, 1.86]). In the presence of imaging information, QStroke was still significant, conferring a 28% increased risk (1.28, [1.15, 1.43]). In addition, increased heart failure risk was associated with greater LV mass indexed to body size (1.38, [1.24, 1.53]), reduced LV ejection fraction (0.72, [0.65, 0.79]), reduced LA ejection fraction (0.86, [0.79, 0.94]), and left-side volume asymmetry (1.14, [1.05, 1.23]).

7.3.5 Liver outcomes

For all three liver outcomes (fatty liver disease, liver cirrhosis and combined liver disease), the Fatty Liver Index was the best-performing non-imaging risk score. In all three cases (Figure 7.7), the non-imaging score remained significant after the addition of imaging with high-risk ratios: for combined liver disease (2.13, [1.71, 2.67]), fatty liver (2.34, [1.79, 3.05]), and liver cirrhosis (4.19, [2.26, 7.78]). As expected, fatty liver disease risk was associated with greater liver fat by imaging (PDFF, 1.51, [1.32, 1.72]), and five-year risk for diagnosed liver cirrhosis was associated with elevated liver cT1 (1.53, [1.20, 1.96]). Reduced volume of the right ventricle was associated with fatty liver risk (RVEDVi, 0.81 [0.69, 0.96]) and risk of liver disease generally (RVSV, 0.87, [0.77, 0.99]).

7.3.6 Kidney outcomes

The PCP-HF risk score was the best-performing index for combined kidney events, with a 47% increase in risk associated with a one standard deviation increase in risk score (1.47, [1.42, 1.51]). In the presence of imaging (Figure 7.8) this remained significant but with only a 10% increased risk (1.10, [1.03, 1.18]). Instead, the risk for combined kidney outcomes was associated with a range of heart, brain and liver imaging metrics including greater white matter hyperintensities (1.11, [1.04, 1.18]), higher

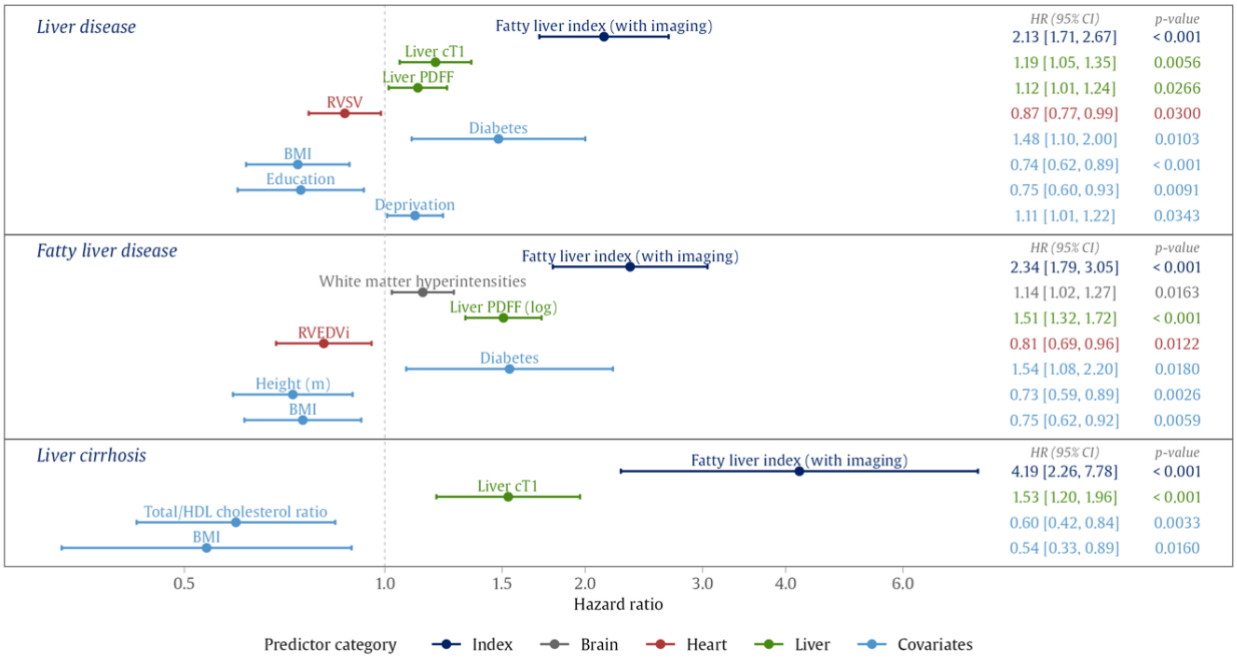


Figure 7.7: Chapter 7 - Significant imaging predictors – Liver outcomes

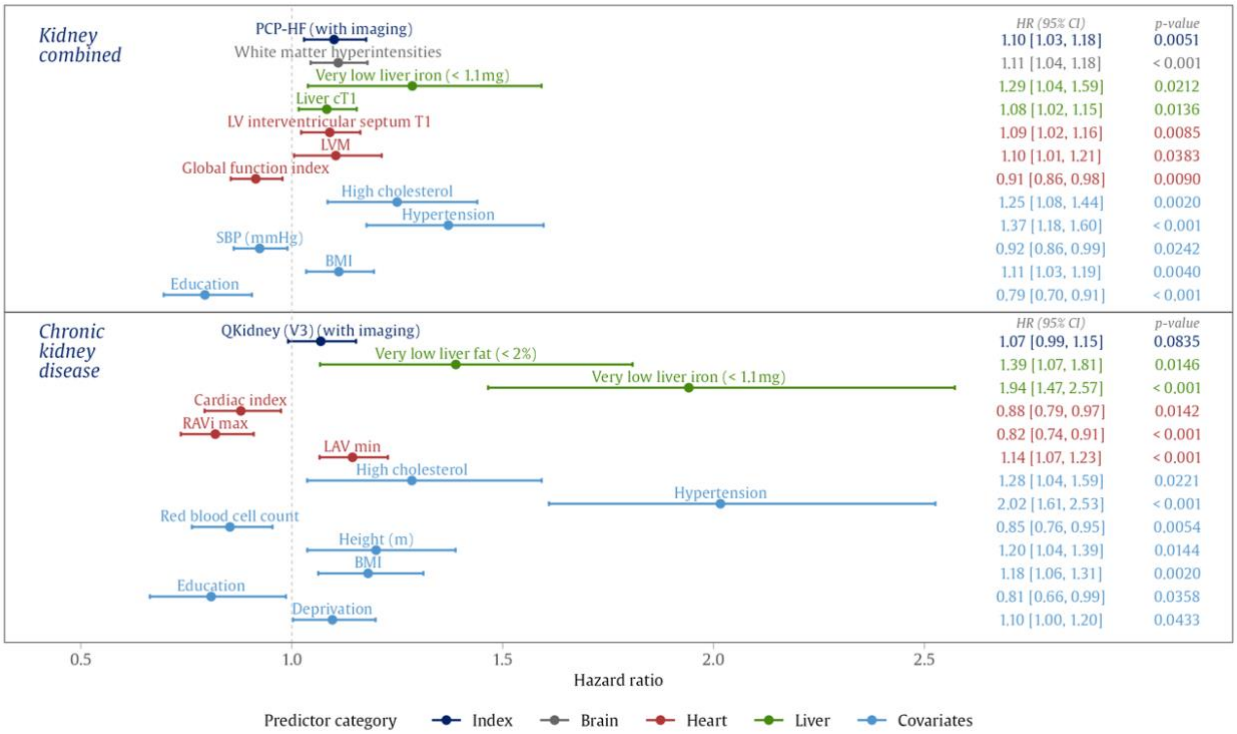


Figure 7.8: Chapter 7 - Significant imaging predictors – Kidney outcomes

Points represent hazard ratios of the significant imaging variables selected in final models by stability selection, along with significant covariate variables. Each rectangle represents a single Cox proportional hazards model for 5-year risk for the disease outcome indicated on the left-hand side. Unless binary, hazard ratios are from standardised beta coefficients, meaning that the hazard ratio represents the increase in outcome hazard associated with one standard deviation increase in the predictor variable observed from multiorgan imaging. Error bars indicate the 95% confidence intervals for hazard ratios, with numerical results and p-values shown on the right-hand side. Colours identify model variables by category, with cardiac imaging variables shown in red, liver imaging variables shown in green, and brain/arterial imaging variables shown in grey, and additional covariates in bright blue. All models are additionally adjusted by age, sex, and imaging site (coefficients not shown). See Appendix 24 for additional details.

interventricular septum T1 (1.09, [1.02, 1.16]), greater LV mass (1.10, [1.01, 1.21]), reduced global cardiac function index (0.91, [0.86, 0.98]), higher liver cT1 (1.08 [1.02, 1.15]) and very low liver iron (1.29, [1.04, 1.59]).

With chronic kidney disease (CKD), the best performing score was QKidney (V3), which was associated with a 49% increased risk in the non-imaging setting (1.49, [1.44, 1.54]). When imaging was added, QKidney score was not significant (1.07, [0.99, 1.15]). People with very low liver iron - less than 1.1mg/g - had a nearly two-fold increased risk for CKD (1.94, [1.47, 2.57]). CKD risk was also associated with very low liver fat (< 2%, 1.39, [1.07, 1.81]), reduced cardiac index (0.88, [0.79, 0.97]), smaller right atrial volume (0.82, [0.74, 0.91]), and larger left atrial volume (1.14, [1.07, 1.23]).

7.3.7 Combined heart, brain, liver and kidney (HBLK)

When fitting a model to combined HBLK events, one standard deviation increase in QStroke score was associated with a 55% increase in risk (1.55, [1.52, 1.58]). When multiorgan imaging was added (Figure 7.9), QStroke score was still a significant predictor for HBLK events but was weaker (1.10, [1.05, 1.15]). Greater risk of an additional HBLK event within 5 years was associated with greater white matter hyperintensities (1.10, [1.06, 1.14]), greater carotid thickness (1.05, [1.01, 1.08]), liver cT1 greater than 700 ms (1.15, [1.07, 1.24]), greater maximum cardiac wall thickness (1.17, [1.12, 1.22]), ventricular volume asymmetry (1.06, [1.03, 1.09]), larger LV end-diastolic volume (1.12, [1.08, 1.17]), reduced left atrial ejection fraction (0.91, [0.88, 0.94]) and reduced global function index (0.94, [0.90, 0.98]).

7.3.8 Overall incremental performance

For all outcomes studied, we found that the discriminative accuracy (AUC) was significantly higher in models including both imaging and non-imaging, compared with models only containing the non-imaging index. These results address the second research question for this chapter, by comparing the predictive accuracy of imaging-based risk models with non-imaging models. Figure 7.10 provides a visual summary of these results, with additional performance metrics provided in Appendix 25. Non-imaging risk scores produced risk estimates above 70% AUC for all outcomes except stroke, venous thromboembolism, combined kidney disease, combined liver disease and combined HBLK.

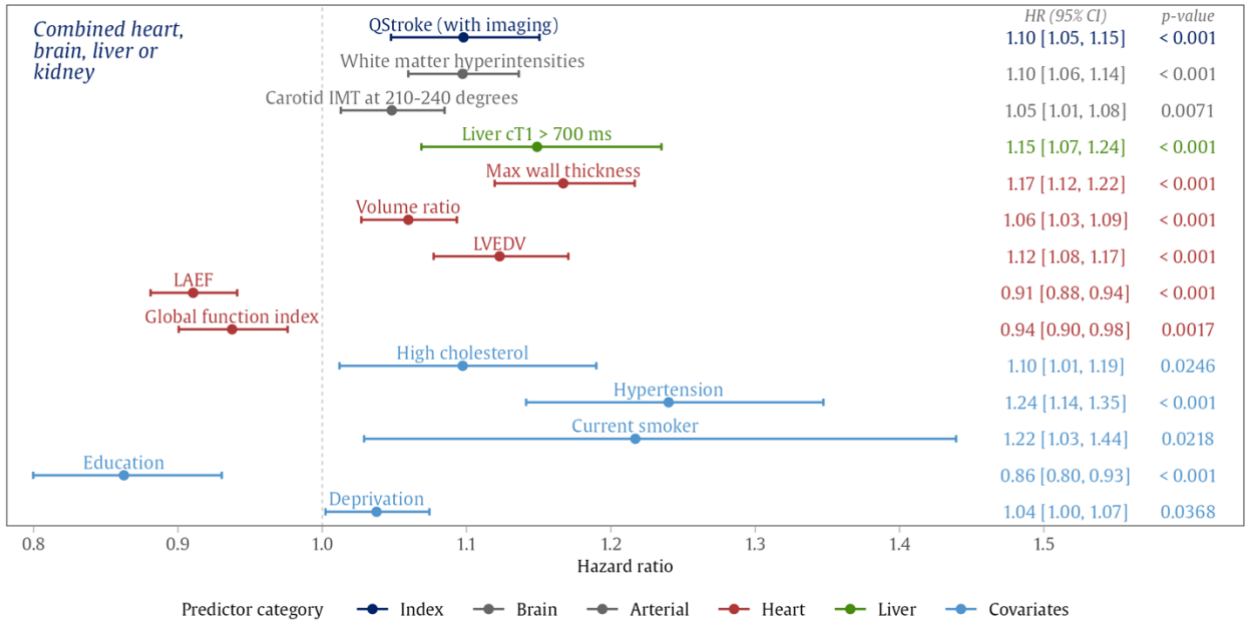


Figure 7.9: Chapter 7 - Significant imaging predictors - Combined HBLK outcomes

Points represent hazard ratios of the significant imaging variables selected in final models by stability selection, along with significant covariate variables. Each rectangle represents a single Cox proportional hazards model for 5-year risk for the disease outcome indicated on the left-hand side. Unless binary, hazard ratios are from standardised beta coefficients, meaning that the hazard ratio represents the increase in outcome hazard associated with one standard deviation increase in the predictor variable observed from multiorgan imaging. Error bars indicate the 95% confidence intervals for hazard ratios, with numerical results and p-values shown on the right-hand side. Colours identify model variables by category, with cardiac imaging variables shown in red, liver imaging variables shown in green, and brain/arterial imaging variables shown in grey, and additional covariates in bright blue. All models are additionally adjusted by age, sex, and imaging site (coefficients not shown). See Appendix 24 for additional details

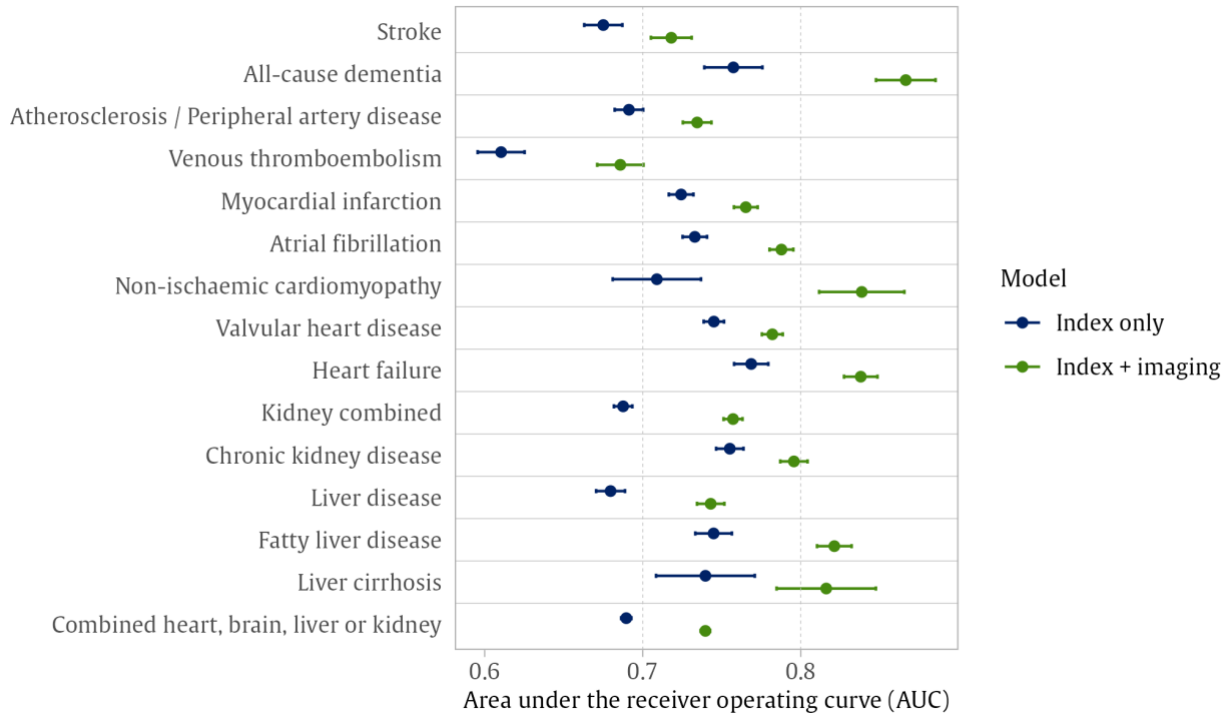


Figure 7.10: Chapter 7 - Discriminative accuracy (AUC) of imaging vs non-imaging models

Points represent AUC for models using best non-imaging index (in dark blue), compared with AUC for Cox proportional hazards models including both non-imaging index and imaging information (in green). Error bars are 95% confidence intervals for model performance (AUC). Each row represents two competing final models (imaging vs non-imaging) for each outcome.

All models that included imaging had AUC greater than 70% except venous thromboembolism. Imaging models for dementia, non-ischaemic cardiomyopathy, heart failure and fatty liver disease achieved AUC greater than 80%. Notwithstanding, keen readers will note that although the sensitivity of the imaging model is significantly higher than the non-imaging model, all sensitivity values are considerably lower than we would normally observe in analyses of this type. This is because the first-in-line method constrains the value of the sensitivity by limiting the prediction threshold (Appendix 26). With the first-in-line method, the same number of positive predictions are made with each model (imaging vs non-imaging), which allows a fair comparison, but because we have set our "pick rate" of N_S to a relatively small number ($2 \times p$), this places a rather low upper bound on our sensitivity.

7.3.9 Decomposition of effects

Another intuitively appealing property of the first-in-line method is that it allows for the decomposition of AUC or any other metric across the series of nested models. In this way, we can empirically quantify the incremental contribution of each additional set of predictors. This is illustrated visually in Figure 7.11 with more granular results in Appendices 27-29.

This property allows us to pinpoint the cases and outcomes where the unique information from imaging is the strongest, or whether the observed improvement could potentially come from better non-imaging covariate tuning. This has important implications as we apply the method to different metrics. For example, if we look at true positives in the combined HBLK outcome (people who were identified as high-risk who then had an event, Appendix 28), we can attribute 74 additional true positive events to the effect of covariate tuning and 168 additional events to imaging information. This property makes it straightforward to link tangible incremental effects to the cost of the imaging information.

7.4 Discussion

In this chapter, we demonstrated that imaging information offered significant incremental value beyond the best non-imaging risk scores available in the current literature. This means that for all outcomes studied, multiorgan imaging can significantly increase the discriminative accuracy of 5-year disease risk assessment. For four outcomes, the addition of imaging elevated the AUC above the 80% mark (all-cause dementia, non-ischaemic cardiomyopathy, heart failure and fatty liver disease).

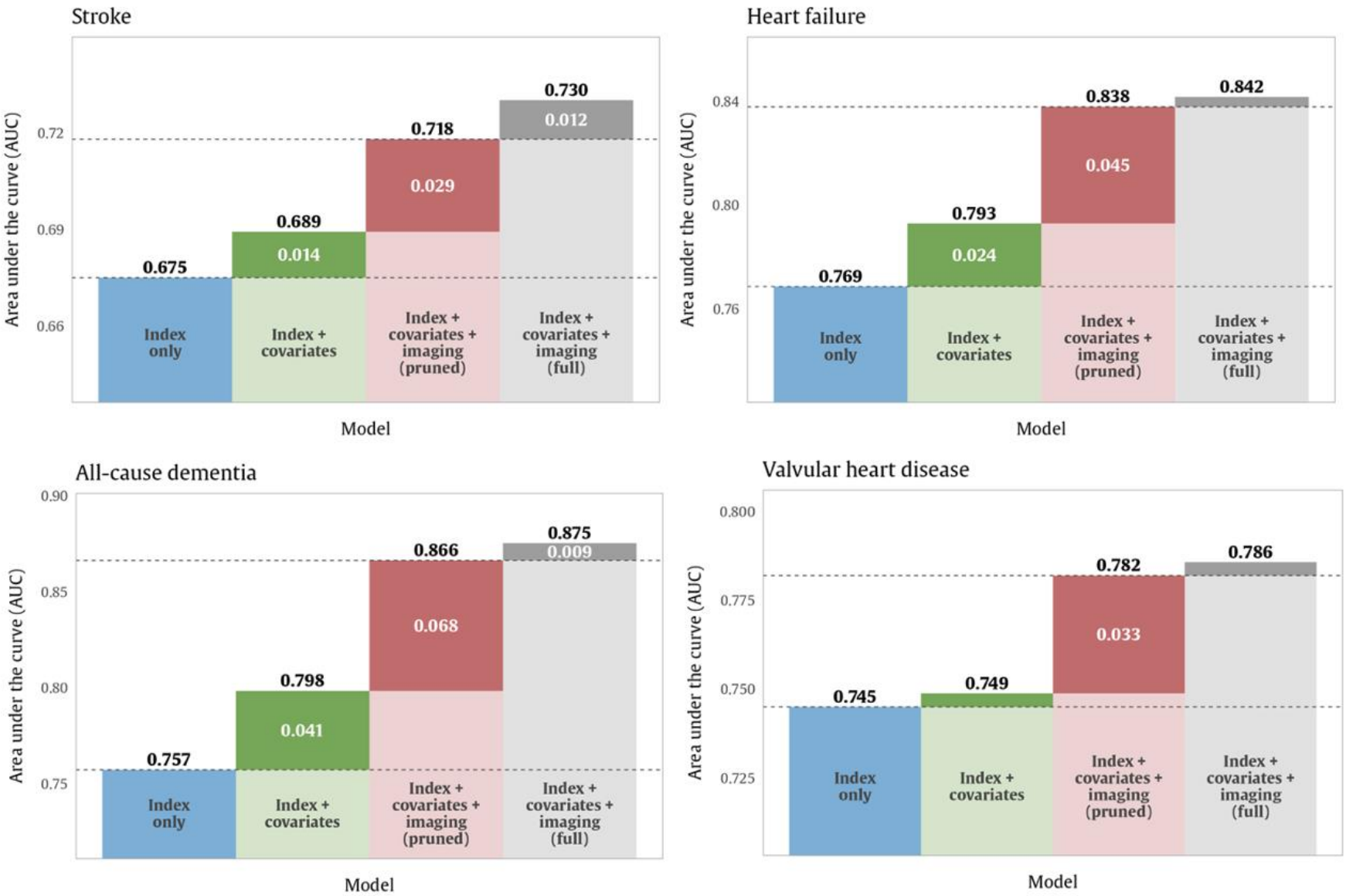


Figure 7.11: Chapter 7 - Decomposition plots (AUC)

Illustrating the decomposition property of the first-in-line method. Where you have a series of nested models, it is possible to determine the incremental effect of subsequent models. Here we have illustrated AUC, but this could apply to any other performance metric. For all outcomes shown in the plots, imaging information (in red) contributed a significant additional portion of AUC that did not come from finer tuning of covariates (in green). In all cases, the effect of pruning (in grey) was small.

In these results, we observed many expected cis-organ associations, including heart diseases associated with adverse cardiac features (larger cardiac mass, wall thickness, and reduced cardiac function), and brain conditions (stroke and dementia) associated with reduced brain volumes and adverse microstructural changes (lower FA, higher ISOVF). Liver imaging metrics of fat accumulation (PDFF) and fibroinflammation (cT1) were central to the assessment of liver disease risk and elevated the AUC of liver disease risk above the 80% mark. We also observed many cross-organ associations, for example, heart imaging metrics associating with brain and liver conditions, liver imaging metrics associating with brain and heart conditions, and all three organs relating to chronic kidney disease.

Although left ventricular ejection fraction (LVEF) is often seen as the 'cornerstone' heart health metric in clinical practice ([397], p.1301), LVEF only appeared in one of our risk models (heart failure). The very large pool of imaging predictors available meant that impaired ventricular function was able to appear in a range of ways, for example, reduced global function index (HBLK, combined kidney disease), cardiac index (myocardial infarction, CKD), global longitudinal strain (venous thromboembolism), and reduced right ventricular volumes (fatty liver disease, and combined liver disease). Measures of atrial structure and function were also significant indicators of future disease risk in the form of reduced left atrial ejection fraction (stroke, atrial fibrillation, heart failure and combined HBLK), right atrial ejection fraction (all-cause dementia), enlarged left atrium (non-ischaemic cardiomyopathy, atrial fibrillation, valvular heart disease, chronic kidney disease), enlarged right atrium (atrial fibrillation) and reduced right atrium (chronic kidney disease).

Some of the cross-organ associations can be traced back to known relationships or mechanisms, others suggest associations that have not yet been described in the literature. The risk of stroke was associated with various adverse heart features such as elevated cardiac mass and reduced left atrial ejection fraction [398]. Liver fibrosis and inflammation (elevated cT1) was associated with a significantly increased risk for dementia, confirming similar findings in several other studies [399, 400]. Beyond this, liver fibroinflammation was also associated with myocardial infarction, atrial fibrillation, and combined kidney disease, suggesting that liver cT1 may be a useful multi-disease biomarker.

The volume of white matter hyperintensities was central to risk assessment for stroke, as found in previous work [401]. We also found cross-organ associations, meaning that elevated white matter

hyperintensities were also associated with increased risk for valvular heart disease, fatty liver disease, combined kidney disease and combined HBLK. Carotid intima-medial thickness (CIMT) emerged as an important metric in stroke, dementia, artery disease, myocardial infarction, valvular heart disease and HBLK. In contrast to Chapter 4 where aortic distensibility was an important biomarker of arterial health, in all final models, CIMT was more significant than aortic distensibility.

Right-heart weakness (in the form of smaller right ventricular volumes) was associated with risk of liver disease. This relationship has previously been described in small, clinical cohorts [402–404]; we now show that a subtle form of this can be found pre-disease in the population setting. We found that people with very low liver iron (less than 1.1mg/g) had an approximately two-fold increased risk for a diagnosis of chronic kidney disease within 5 years. These relationships could reflect the association between anaemia and kidney disease that has been found and described in previous research [405]. Our model-building did not provide any evidence of adverse risk associations with excess liver iron accumulation.

The main limitation of this study relates to the known healthy participant bias of the UK Biobank [362, 363], a bias which is even stronger in the imaging sub-cohort [71]. If this work was re-run in a less healthy and more diverse cohort that is more representative of the UK population, we would expect a larger number of disease outcomes during the follow-up period, and a higher frequency of abnormalities at the time of imaging. It is uncertain whether the difference in discriminative accuracy between imaging and non-imaging models would hold in the general population, or whether the differences would be larger or smaller. The scarcity of large-scale imaging studies means that there is somewhat limited opportunity to validate these findings in a larger, more representative sample.

These results highlight several key implications for clinical practice. Firstly, consistent with previous work [406], the addition of multiorgan imaging has the potential to significantly enhance the accuracy of multi-disease risk prediction, enabling clinicians to better identify people at risk. Secondly, specific imaging biomarkers, such as cT1 and CIMT, may offer valuable insights that inform multiorgan health and risk for multimorbidity. Further work is required to narrow down the pool of imaging predictors, to identify the minimum imaging protocol that would deliver the greatest information.

The combination of imaging and covariate information did not always fully replace non-imaging risk scores. For five outcomes (stroke, dementia, VTE, atrial fibrillation, and chronic kidney disease), the non-imaging risk score was no longer significant in the presence of imaging information. On the other hand, the non-imaging risk score was still informative alongside imaging variables for peripheral artery disease, myocardial infarction, valvular heart disease, heart failure, liver disease, kidney disease and combined HBLK. This finding confirms the face validity of a two-stage methodology similar to approaches taken in previous work [237, 247]. Despite the substantial benefits of imaging, validated non-imaging risk scores remain relevant and should be used as a first assessment.

The abundance of cross-organ relationships underscores the utility of a multiorgan approach in clinical practice [70, 215]. This raises important questions about the current use of diagnostic imaging data and whether clinical teams are fully realising the potential of the information contained therein. For example, when a person undergoes clinically indicated cardiac MRI, this information could be used to inform multiorgan health as well as heart health.

In this study, we describe and implement the 'first-in-line' methodology, a constrained form of prediction comparison where we ensure that existing and new diagnostics are compared on an equal footing. This is an important extension to existing work and a potential answer to calls for improved methods for identifying those at greatest risk in the context of limited resources [407].

Finally, the many results found in this chapter signal significant future potential for multiorgan risk assessment when integrated with artificial intelligence (AI). By combining population-level trends and multiorgan imaging data, there is a future potential for sophisticated, relatively low-cost multiorgan health monitoring. Such a system could facilitate early detection and prevention by identifying subtle pre-disease conditions and effectively prioritising high-risk individuals. This form of predictive, personalised and proactive healthcare could be one way to improve patient outcomes and tackle multimorbidity in an overburdened health system.

Chapter 8: The potential cost-effectiveness of imaging

8.1 Introduction

This final analysis chapter is an extension to the study conducted in the previous chapter. In Chapter 7 we explored the ways that risk assessment using imaging yielded a significant improvement upon risk models using only non-imaging risk information. In this chapter, we take the first steps towards exploring this question through the lens of cost-effectiveness.

Considering the cost-effectiveness of imaging is crucial for several reasons. Imaging of any type, and multiorgan imaging in particular, is a scarce, somewhat expensive diagnostic. The current NHS does not have the capacity or the resources to offer it to everyone alongside general health checks [408, 409]. On the other hand, there is substantial evidence that multimorbidity imposes a significant economic burden in the longer term [13, 14]. Therefore, a well-targeted, cost-effective imaging strategy could help reduce longer-term costs by identifying those at highest risk, or ruling out people with high risk scores that are actually healthy.

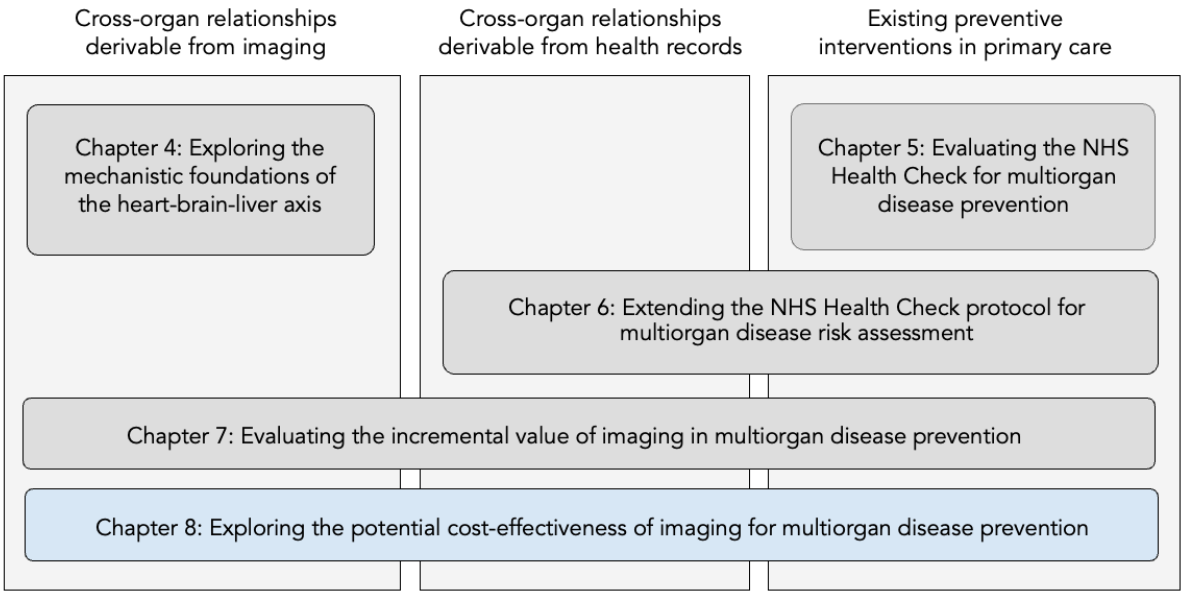


Figure 8.1: Chapter 8 - Roadmap location

The key research questions for this chapter are:

1. Is imaging cost-effective for risk stratification in the general sample?

2. For which population subgroups are the costs of imaging outweighed by better detection of future health outcomes?

Traditional cost-effectiveness analysis (CEA) models can be extremely complex and designed to evaluate the cost and effectiveness of health outcomes to a high degree of rigour. Applying a traditional CEA approach to an analysis with 14 or so outcomes would present substantial challenges. Scaling up these models by a factor of 14 would exponentially increase model complexity, requiring additional time, modelling parameters, and computational resources. We are also aware that communicating the complex message of this work is already a difficult task. Whilst we plan to move in this direction in future work, we have developed, in this chapter, a simplified cost-effectiveness method tailored to the time and computing constraints of this DPhil. This provides an overall assessment and lays the groundwork for further refinement in future studies.

The analysis approach here was developed with several key objectives in mind. Firstly, we needed an approach that was built with conventional statistical and epidemiological tools rather than black-box machine learning. This was important to ensure full explainability and full scrutiny of the processes and assumptions involved. Secondly, we needed a method that was consistent with established health economic literature, adhering to NICE guidelines and rules regarding willingness-to-pay thresholds. By aligning with these standards, we ensured that our findings would be consistent with the broader context of health economics. Thirdly, we wanted a method that could be flexible, such that it could be easily tuned to different health targets and budgetary constraints and easily updated to incorporate newly developed imaging biomarkers as new research emerges.

8.2 Methods

The dataset for this study is the same sample as Chapter 7, in other words, 31,048 participants drawn from the multiorgan imaging cohort (Section 7.2), with all risk models (imaging and non-imaging) as previously described. In this section, we describe the study elements that were added for the purposes of cost-effectiveness evaluation.

8.2.1 QALYs (Quality-adjusted life years)

Quality-Adjusted Life Years (QALYs) are a measure used to assess the value of health outcomes in the health economics literature. QALYs combine both the quantity and quality of life lived to provide a metric upon which to evaluate the benefits of medical interventions [410]. One QALY represents one year of life in perfect health. When an individual becomes ill or disabled, the QALY score is adjusted proportionally using health utility weights. For example, suppose that severe osteoarthritis carries a health utility weight of 0.5; then, one year lived with severe osteoarthritis would equal 0.5 QALYs (with 0.5 QALYs lost due to illness). Using a custom-designed metric like QALYs is highly beneficial in our context, where we are evaluating health effects across multiple organs. Aggregating these effects into a single number simplifies comparisons significantly.

Table 8.1 provides the health utility weights that were drawn from the literature for each of the 14 outcomes. We agree that this is a relatively simplistic first step into cost-effectiveness analysis. Future work could standardise these utilities by quality-of-life schema and could consider severity levels and whether participants experienced mild, moderate or severe illness.

Table 8.1: Chapter 8 - Health utility weights for multiorgan outcomes

Condition	Average Utility	Reference
Peripheral artery disease	0.81	Kim et al. (2021) [411]
Venous thromboembolism	0.81	Hogg et al. (2013) [412]
Stroke	0.58	Luengo-Fernandez et al (2013) [413]
All-cause dementia	0.84	Ormeus et al (2014) [414]
Myocardial infarction	0.76	Brandão et al (2017) [415]
Atrial fibrillation	0.82	Witassek et al. (2019) [416]
Non-ischaemic cardiomyopathies	0.83	Wiethoff et al (2023) Xie et al. (2022) [417, 418]
Valvular heart disease	0.74	Dyer et al. (2010) [419]
Heart failure	0.68	Di Tanna et al. (2021) [420]
Chronic kidney disease	0.74	Cooper et al. (2020) [421]
Fatty liver disease	0.66	Sayiner et al. (2016) [422]
Cirrhosis	0.55	Sayiner et al. (2016) [422]

For the entire sample, we calculated QALYs lost across the heart, brain, liver and kidney in two steps. In the first step, we collated years of life lost to early death with an HBLK primary cause where that death occurred prior to the sex-specific life expectancy. In the second step, we collated QALYs lost across the years of life lived with reduced quality of life due to illness. To do this, we identified the time periods between disease diagnosis and either death or study end date, then multiplied this by one minus the health utility weight for the specific illness in Table 8.1. The QALYs lost from both steps were added together to produce a total QALYs lost value for each person. Participants who reached the study end date with no disease diagnoses within the HBLK cluster were recorded to have zero QALYs lost.

8.2.2 Cost of imaging

The representative cost of imaging was drawn from the 2021/22 NHS National Cost Collection Data Publication. The sum of two health resource groups (RD04Z Magnetic resonance imaging scan of two or three areas, without contrast, £180.73, and RD08Z Cardiac magnetic resonance imaging scan without contrast, £400.18) gives a total cost of £580.91 per person scanned [423]. Further research could add additional cost elements such as scan reading, reporting and follow-up due to incidental findings. The associated costs of the in-person appointment are not included as this is a comparative analysis and that cost would apply in both imaging and non-imaging settings.

8.2.3 NICE Willingness-to-pay

The National Institute for Health and Clinical Excellence (NICE) has published a cost-effectiveness threshold to guide researchers who examine costs and QALYs [424]. They have indicated that an incremental cost-effectiveness ratio (ICER) of between £20,000 to £30,000 per QALY gained is the range where options have the potential to be cost-effective. A smaller ICER is better, so interventions with ICERs less than £20,000 would be considered more cost-effective, while interventions with ICERs greater than £30,000 will only be considered in special circumstances.

8.2.4 Incremental imaging comparison

Figure 8.2 provides an updated overview of the components of the comparison setup. The overall setup is the same. However, the core comparison is now between the total QALYs picked up via a risk assessment process that includes both non-imaging and imaging risk assessment (Method B), compared

with only non-imaging risk (Method A). The comparison is still being made between the quality of the binary prediction (shown in blue font in panels A and B), but this is quantified in QALYs. Please refer to Section 7.2.1 - 7.2.2 for the foundational setup of the comparison, as these aspects are identical in both Chapters 7 and 8.

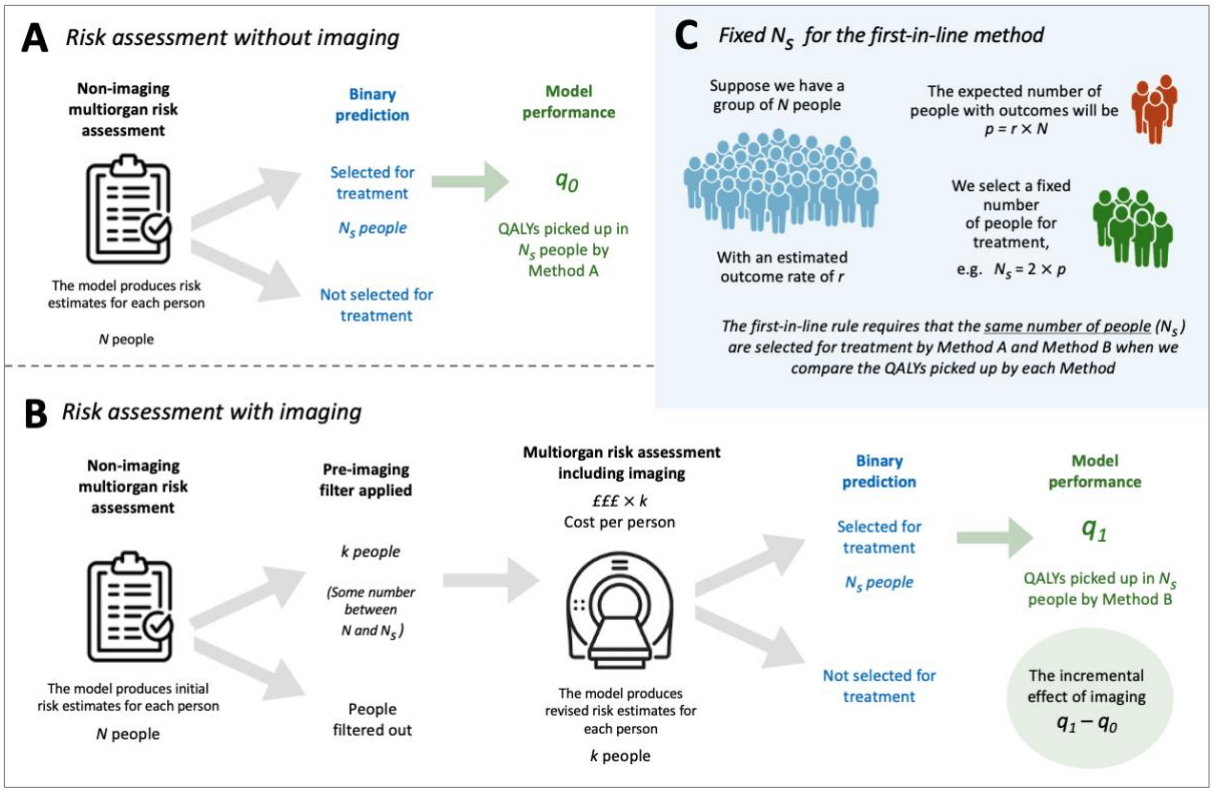


Figure 8.2: Chapter 8 - Comparison method overview

This formulation does not include the costs of the non-imaging risk assessment as this cost would apply equally in both options and would belong to the NHS Health Check process or something similar. Our assessment ends with an evaluation of the people identified as high-risk. Although this is an important part of the process, we agree that this is not the same thing as providing treatment to these individuals, and as such, we cannot claim the actual treatment or improvement of health as part of this calculation.

For the purposes of this study, the formula for the ICER then becomes: the cost of imaging / (the difference in QALYs picked up by imaging models compared with non-imaging models). In this study, we do not penalise or assign costs to the QALYs that are not picked up by either method; this could be a potential avenue for future work.

8.2.5 Subgroup grouping variables

In order to explore cost-effectiveness across subgroups within the dataset, we created a subgroup framework. We identified 11 grouping factors (shown in Table 8.2) and then created a factorial structure, making all possible combinations of groupings from length 1 (one grouping factor) to length 3 (with an intersection of three grouping factors). The full subgroup structure is provided in Appendix 30. Most of the grouping variables are self-explanatory, with the exception of metabolic syndrome. Metabolic syndrome is a diagnosis that represents a specific cluster of symptoms, including high blood pressure, high blood sugar, excess body fat around the waist, and abnormal cholesterol or triglyceride levels, that together increase the risk of heart disease, stroke, liver and kidney disease [216]. We included metabolic syndrome as a grouping factor to represent a potential 'step up' in severity from either diabetes or hypertension alone. Family history is defined as having a parent or a sibling with a history of heart disease, dementia or stroke.

Table 8.2: Chapter 8 - Subgroup grouping factors

Subgroup	Subgroup description	Participants	HBLK events	QALYs*
001	Men	14,870	1,952	1,846
002	Women	16,178	1,241	1,173
003	People aged less than 60yrs	10,144	546	482
004	People aged from 60 to 69yrs	13,780	1,398	1,370
005	People aged 70rs or more	7,124	1,249	1,167
006	People with hypertension	10,350	1,670	1,673
007	People with diabetes	1,790	357	379
008	People with high cholesterol	8,847	1,431	1,357
009	People with higher local deprivation	7,074	766	731
010	People with metabolic syndrome	5,301	829	801
011	People with family history	12,821	1,370	1,317

*Total QALYs within the follow-up period associated with illness and early death attributable to a heart, brain, liver or kidney cause.

8.3 Results

8.3.1 Overall cost-effectiveness

The total QALYs picked up by imaging vs non-imaging models, using the first-in-line method, are presented in Table 8.3, with the incremental differences visually displayed in Figure 8.3 and corresponding ICERS in Figure 8.4.

Table 8.3: Chapter 8 - Global QALYs picked by imaging vs non-imaging risk models

	QALYs picked up in *Ns* positive predictions					
Risk prediction model	**Non-imaging index only**	**Index + imaging + covariates**	**Difference in QALYs picked up**	**p-value**	**Significant difference**	**N**
Stroke	178 [155, 202]	216 [191, 240]	37 [-2, 77]	0.0609		30,441
All-cause dementia	62 [43, 80]	93 [74, 111]	31 [1, 61]	0.0309	*	31,004
Athero/ Peripheral artery disease	209 [187, 232]	297 [275, 319]	87 [51, 124]	$< 1.0x10^{-20}$	*	30,400
Venous thromboembolism	167 [140, 194]	232 [205, 260]	65 [21, 110]	0.0040	*	30,007
Myocardial infarction	197 [174, 220]	256 [233, 278]	58 [22, 94]	0.0030	*	30,225
Atrial fibrillation	359 [327, 392]	532 [498, 566]	172 [119, 226]	$< 1.0x10^{-20}$	*	30,160
Non-ischaemic cardiomyopathy	63 [41, 84]	143 [121, 166]	81 [44, 117]	$< 1.0x10^{-20}$	*	30,976
Valvular heart disease	325 [293, 357]	460 [429, 492]	135 [82, 188]	$< 1.0x10^{-20}$	*	30,465
Heart failure	197 [169, 226]	357 [329, 385]	160 [114, 206]	$< 1.0x10^{-20}$	*	30,840
Kidney combined	465 [429, 501]	721 [685, 757]	256 [197, 316]	$< 1.0x10^{-20}$	*	29,109
Chronic kidney disease	247 [224, 270]	285 [262, 309]	38 [1, 76]	0.0519		30,456
Liver disease	128 [107, 149]	184 [163, 204]	55 [22, 89]	$9.98x10^{-4}$	*	30,306
Fatty liver disease	87 [71, 104]	110 [92, 127]	22 [-6, 50]	0.1208		30,816
Liver cirrhosis	17 [7, 28]	40 [30, 51]	23 [6, 40]	0.0060	*	30,975
Combined heart, brain, liver or kidney	1,280 [1,240, 1,321]	1,632 [1,592, 1,672]	352* [286, 418]	$< 1.0x10^{-20}$	*	31,048

Entries are point predictions with 95% confidence intervals derived from 1000 bootstrapped replicates, with p-values derived from 1000 permutation replicates. An asterisk (*) indicates a significant difference in QALYs in predictions made by risk models incorporating imaging compared with the best non-imaging risk score, in this sample.

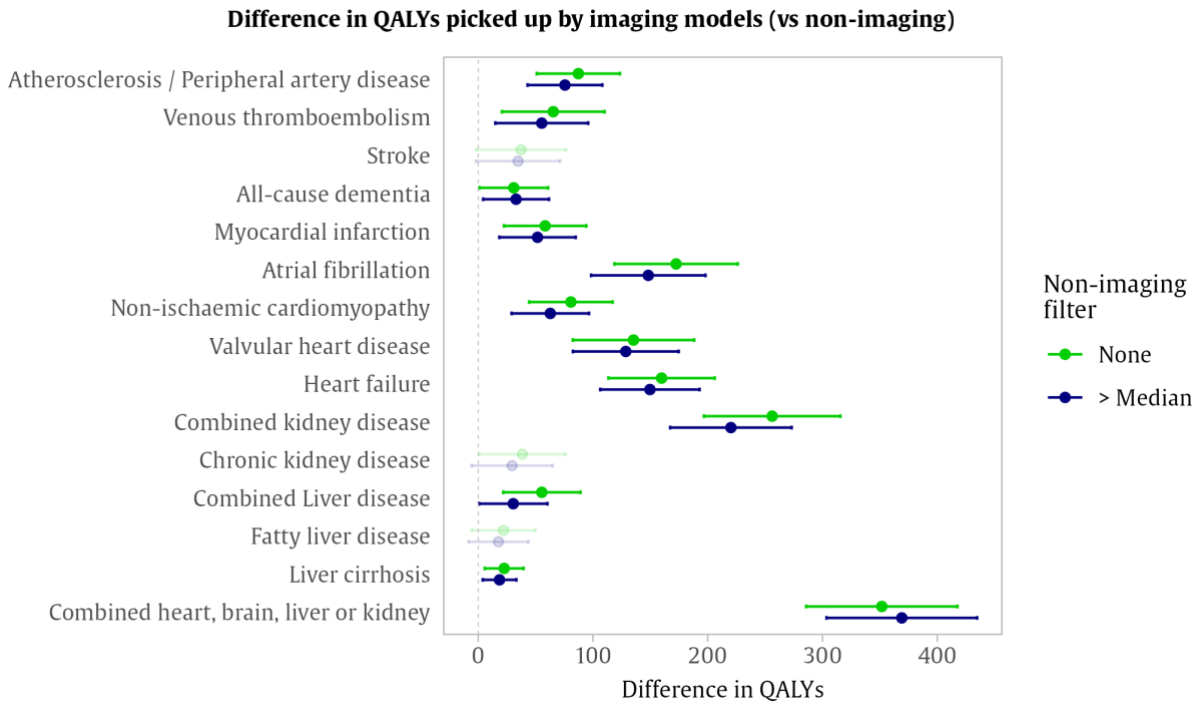


Figure 8.3: Chapter 8 - Differences in QALYs picked up by imaging vs non-imaging models

Points represent differences in QALYs identified in positive model predictions, comparing imaging models with non-imaging models. In other words, if each model identifies a certain number of people as high risk, the difference in QALYs associated with imaging = QALYs found in high-risk people identified by imaging-based prediction models - QALYs found in high-risk people identified by non-imaging prediction models. The error bars represent 95% confidence intervals of the difference in QALYs, assessed using 1000 bootstrapped replicates. Results in green show where no pre-imaging/non-imaging filter was applied to the sample (reducing overall costs), whereas results in dark blue show the difference in QALYs where this filter was applied.

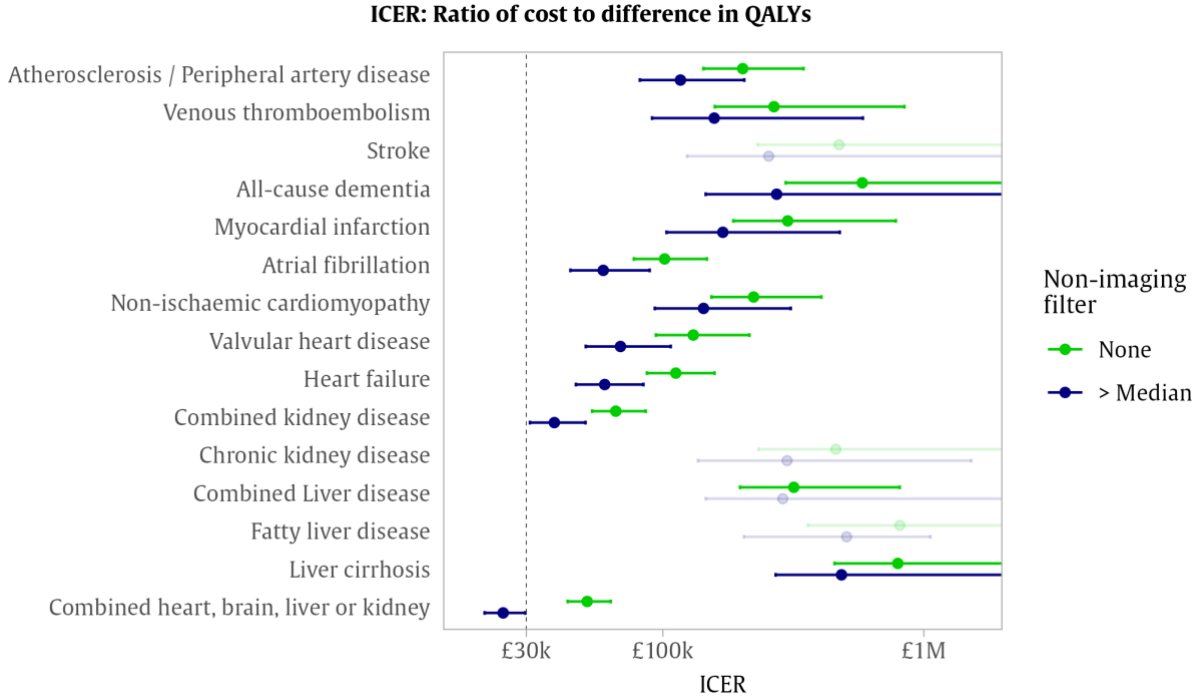


Figure 8.4: Chapter 8 - Global incremental cost-effectiveness ratios (ICERS)

The underlying data for Figure 8.4 is the same as Figure 8.3, except that the points in Figure 8.4 present ICERs (incremental cost-effectiveness ratios), in other words, the total cost of imaging (in £) divided by the difference in QALYs shown in Figure 8.3. The error bars represent 95% confidence intervals assessed using 1000 bootstrapped replicates. Results in green show where no pre-imaging, non-imaging filter is applied to the sample (reducing overall costs), whereas results in dark blue show the difference in QALYs where this filter was applied. The x-axis is presented in log scale, and is truncated after £1M. A dotted vertical line at £30k indicates the threshold where interventions begin to be considered by NICE to be cost-effective. We see that combined heart-brain-liver-kidney is the only result to approach this threshold, because it takes into account the greatest number of outcomes (and therefore a greater difference in QALYs) relative to the costs of imaging.

These results show that similar to the significant incremental accuracy differences found in Chapter 7, there are also significant differences in the QALYs identified in true positives from imaging models compared with non-imaging models. These differences are significant with all underlying risk models except stroke, chronic kidney disease and fatty liver disease. This means that for these three outcomes, although the model might have shown a significant increase in other accuracy metrics, when we examine the cumulative value of health outcomes in the positive predictions, the model containing imaging metrics was not significantly different from the best non-imaging risk index. In Figure 8.3, if there is no difference between imaging and non-imaging, the point lies near the zero vertical line. Figure 8.4 displays the same results, but as ICERs, taking the cost of imaging into account. Additionally, in both figures, the scenario where imaging is applied to everyone is shown in bright green. The navy blue results indicate what the QALYs and ICERs would be if imaging was only offered to people who were above the non-imaging median risk score in the first step.

What immediately becomes obvious from the results in these two figures, is that analyses with single outcomes rarely have the power to gather enough QALYs or differences in QALYs to counterbalance the sizable costs of imaging. This is the case even if we only offer imaging to the upper 50% of the sample. In this case, only the model profiling risk for combined HBLK events was able to accrue a difference in QALYs sufficiently high, bringing the ICER into the ballpark of consideration with an upper 50% filter.

8.3.2 Aggregated multiorgan risk

This result led us to consider a new modelling scenario that had an explicitly multiorgan approach from the outset. In this scenario, all participants would receive 14 itemised outcome risk estimates using non-imaging risk equations, then the results would be aggregated to create a non-imaging filter. The 14 outcomes include the 12 outcomes shown previously, plus acute kidney injury and death with HBLK primary cause. The “non-imaging filter” then is the number of times (out of 14) each person has appeared in the upper 50% (above the median) for non-imaging risk score. A person with a filter value of 0 was identified as low risk by all non-imaging risk equations, whilst a person with a value of 10 has non-imaging risk above the median for 10 out of 14 risk equations. We can use this non-imaging filter

(alone or in conjunction with subgroupings) to tune or titrate the number of people who progress to multiorgan imaging.

In the second stage of the scenario, multiorgan risk is assessed again, this time using imaging-informed models, and the aggregation of those scores is used to identify our "first-in-line" predictions. From there, QALYs from all HBLK outcomes are evaluated. In this step, we explored imaging risk aggregation in two forms – mean aggregated risk across all outcomes and count of high-risk flags across all outcomes.

These results indicate that aggregated risk models work well in identifying participants with overall higher QALYs associated with multiorgan outcomes in the HBLK cluster. Risk count is a more effective overall model for identifying first-in-line predictions (compared with average risk), and the non-imaging filter works well to control the costs associated with imaging. Using the combination of these two mechanisms, it is possible to identify imaging scenarios that are cost-effective based on the incremental identification of future HBLK outcomes, relative to the costs of imaging.

Specifically, Figure 8.6 indicates a range of ICERs beneath the upper cost-effectiveness threshold of £30,000 per QALY. In words, the most cost-effective scenario (aggregate risk count, non-imaging filter >= 12) can be described by the following: all non-imaging risk scores are calculated, and we identify the pool of people with above-median risk for 12 out of the 14 different scores (i.e. the non-imaging filter). These people then receive multiorgan imaging, after which their multiorgan risk is calculated again with their imaging parameters informing their new risk scores. A composite score is then formed using their aggregated multiorgan risk and this is used to identify the small group of people that are first-in-line for follow-up or treatment. In doing so, the incremental QALYs identified in this small group of people using imaging (compared with the information without imaging) is large enough to counterbalance the cost of imaging in the larger group.

Table 8.4: Chapter 8 - Global QALYs in aggregated risk models

		QALYs picked up in *Ns* positive predictions				
Overall risk model	**Non-imaging filter**	**Non-imaging index only**	**Index + imaging + covariates**	**Difference in QALYs picked up**	**p-value**	**Imaging k**
Aggregated risk by counting times the person is in the upper 50% of risk across outcomes	None	824 [784, 865]	1,256 [1,215, 1,298]	432* [365, 499]	$< 1.0x10^{-20}$	31,048
	Risk count ≥ 2	824 [782, 866]	1,255 [1,213, 1,296]	431* [362, 499]	$< 1.0x10^{-20}$	23,157
	Risk count ≥ 4	813 [772, 854]	1,236 [1,196, 1,276]	423* [356, 489]	$< 1.0x10^{-20}$	18,358
	Risk count ≥ 6	807 [767, 847]	1,213 [1,172, 1,254]	406* [340, 473]	$< 1.0x10^{-20}$	16,406
	Risk count ≥ 8	798 [759, 837]	1,204 [1,165, 1,242]	405* [341, 470]	$< 1.0x10^{-20}$	15,319
	Risk count ≥ 10	769 [729, 808]	1,170 [1,132, 1,208]	402* [338, 465]	$< 1.0x10^{-20}$	13,988
	Risk count ≥ 12	636 [601, 671]	994 [957, 1,030]	357* [299, 416]	$< 1.0x10^{-20}$	10,497
Aggregated risk by average risk across outcomes	None	1,297 [1,256, 1,338]	1,607 [1,567, 1,647]	310* [243, 376]	$< 1.0x10^{-20}$	31,048
	Risk count ≥ 2	1,208 [1,167, 1,249]	1,537 [1,497, 1,577]	328* [263, 394]	$< 1.0x10^{-20}$	23,157
	Risk count ≥ 4	1,106 [1,066, 1,145]	1,412 [1,374, 1,449]	306* [244, 367]	$< 1.0x10^{-20}$	18,358
	Risk count ≥ 6	1,064 [1,027, 1,102]	1,337 [1,298, 1,376]	272* [210, 335]	$< 1.0x10^{-20}$	16,406
	Risk count ≥ 8	1,022 [982, 1,061]	1,303 [1,263, 1,344]	282* [215, 349]	$< 1.0x10^{-20}$	15,319
	Risk count ≥ 10	959 [922, 997]	1,246 [1,210, 1,283]	287* [226, 347]	$< 1.0x10^{-20}$	13,988
	Risk count ≥ 12	767 [733, 802]	1,012 [977, 1,048]	245* [188, 301]	$< 1.0x10^{-20}$	10,497

Entries are point predictions with 95% confidence intervals derived from 1000 bootstrapped replicates, with p-values derived from 1000 permutation replicates. An asterisk (*) indicates a significant difference in QALYs in predictions made by risk models incorporating imaging compared with the best non-imaging risk score, in this sample.

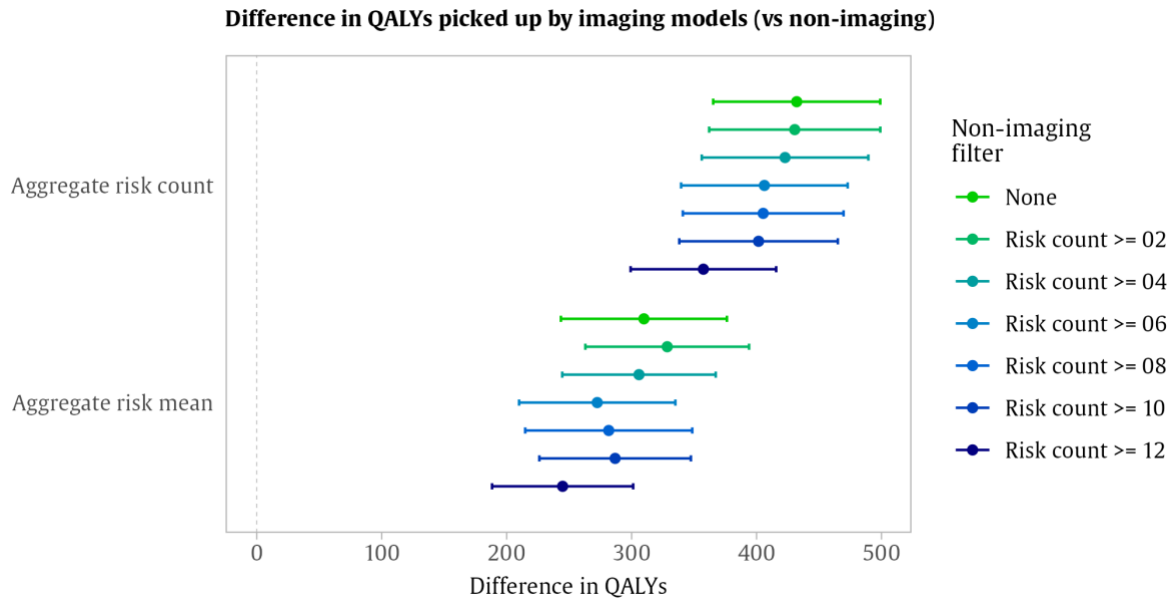


Figure 8.5: Chapter 8 - Differences in QALYs picked up in aggregated models

Points represent differences in QALYs identified in positive model predictions, comparing imaging models with non-imaging models. In other words, if each model identifies a certain number of people as high risk, the difference in QALYs associated with imaging = QALYs found in high-risk people identified by imaging-based prediction models - QALYs found in high-risk people identified by non-imaging prediction models. The error bars represent 95% confidence intervals of the difference in QALYs, assessed using 1000 bootstrapped replicates. Colours show the sensitivity tuning to different pre-imaging/non-imaging filters applied to the sample (reducing overall costs), whereas the y-axis indicates different types of pre-imaging/non-imaging filters (aggregate risk vs aggregate mean risk).

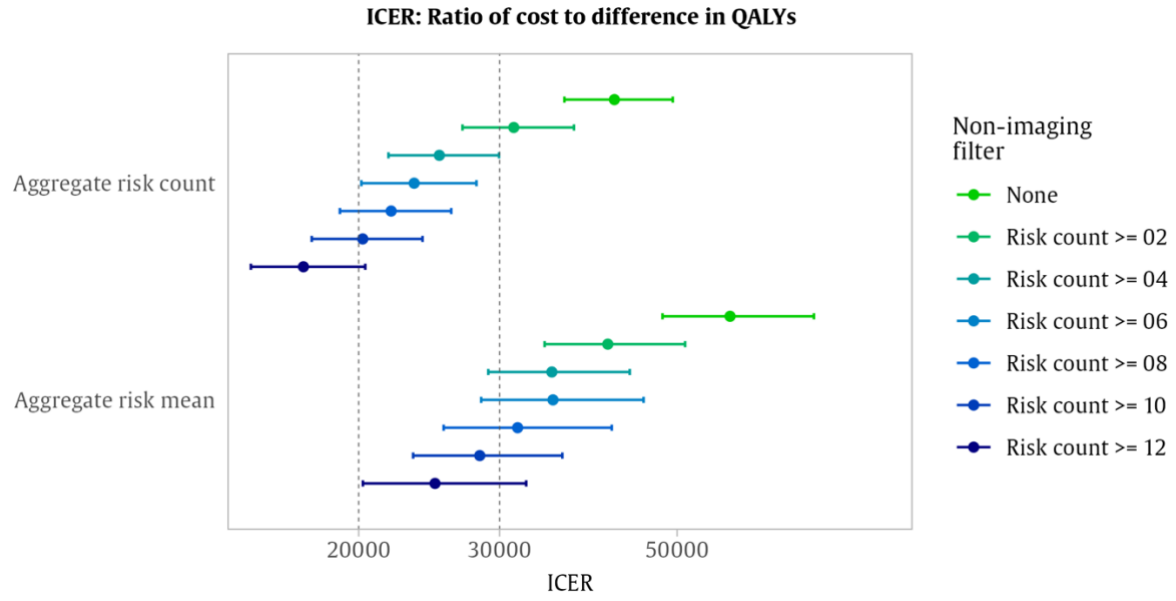


Figure 8.6: Chapter 8 - ICERs for aggregated risk models

The underlying data for Figure 8.6 is the same as Figure 8.5, except that the points in Figure 8.6 present ICERs (incremental cost-effectiveness ratios), in other words, the total cost of imaging (in £) divided by the difference in QALYs shown in Figure 8.5. The error bars represent 95% confidence intervals assessed using 1000 bootstrapped replicates. Colours show the sensitivity tuning to different pre-imaging/non-imaging filters applied to the sample (reducing overall costs), whereas the y-axis indicates different types of pre-imaging/non-imaging filters (aggregate risk count vs aggregate mean risk). The x-axis is presented in log scale. A dotted vertical line at £30k indicates the threshold where interventions begin to be considered by NICE to be cost-effective. Therefore, multiorgan imaging can be potentially cost-effective using aggregate HBLK models, using an aggregated risk count non-imaging filter, and by filtering to people with risk count of 6 or more.

8.3.3 Multiorgan risk and imaging in subgroups

Subgroup analysis is another approach to targeting imaging and treatment to people who might benefit most. We applied imaging vs non-imaging cost-effectiveness analysis for all outcomes and all 193 subgroups in the subgroup framework. The 30 most cost-effective subgroups for four composite outcomes are provided in Appendices 31-35. Without additional constraints (for example, a total budget or total number of possible scans), the subgroup results become quite difficult to summarise and communicate. Selected subgroup cost-effectiveness results for groups with ICERs with 95% confidence intervals fully below the £30,000 per QALY cutoff are presented in Figure 8.7.

The multi-model for aggregated heart-brain-liver-kidney risk (HBLK, shown with a triangle point) features more prominently among the most cost-effective subgroups than the single model assessing HBLK risk (shown with a filled circle). Notably, many cost-effective subgroups are age-based (e.g., individuals aged 60-69 and those aged 70 or older), with some focusing specifically on men. In the current sample, adding a third subgroup grouping factor, such as narrowing from "Men aged 70 or older" to "Men aged 70 or older with high cholesterol," often only slightly affects cost-effectiveness but still reduces the overall imaging budget. This effect is not visible in Figure 8.7 but can be observed in Table 8.5.

Figure 8.7 clearly shows that for younger (ages 60-69) and unselected age subgroups (people with hypertension), there is a greater effect of adding a pre-imaging risk filter (results shown in green or blue) compared with providing imaging to the whole subgroup (results shown with thicker grey line). Such a filter has very little effect on the cost-effectiveness in groups that are over 70 years old, as most members of these subgroups will already be scoring above-median risk based on non-imaging risk calculators. In the “men with higher local deprivation” subgroup, the results were only cost-effective when the high-risk non-imaging filter was applied (no results in grey).

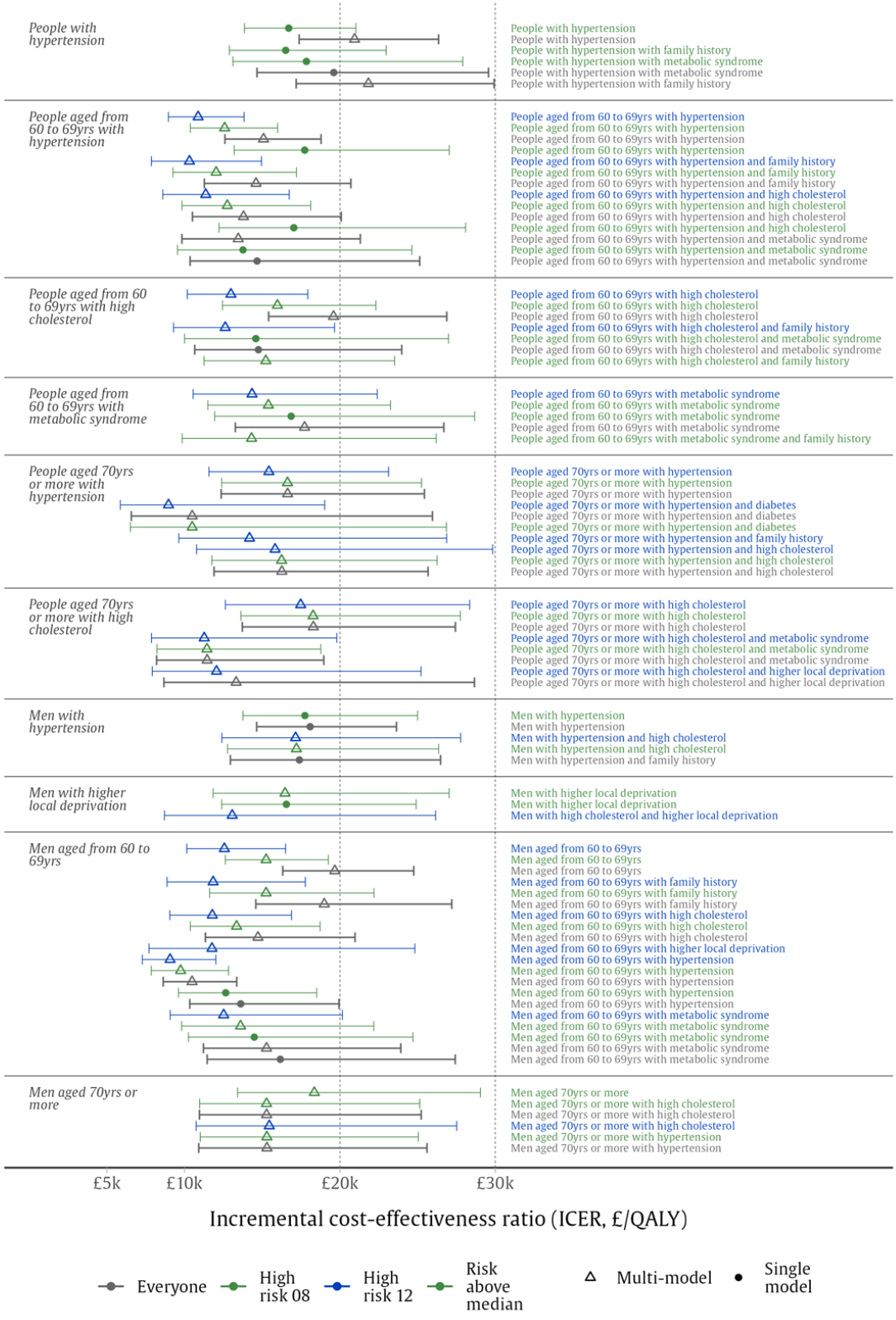


Figure 8.7: Chapter 8 - Subgroup ICERs below £30,000 per QALY

Points show incremental cost-effectiveness ratios (ICERs) for the most cost-effective population subgroups found in our sample. Error bars indicate 95% confidence intervals from 1000 bootstrapped replicates. Colours and shapes indicate sensitivity results around various tuning parameters. In particular, triangle points show results where multiorgan risk is assessed using the individual disease risk models aggregated together, where the circle points show results where HBLK risk is assessed using the single HBLK combined model. Colours refer to the type of pre-imaging/non-imaging filter applied to the subgroup sample.

8.3.4 Scenario-driven decision-making

Looking at these results in a different way, Table 8.5 presents the same data but in the form of scenarios. These tables illustrate in detail another property of the first-in-line method, wherein the successive application of additional constraints reduces the overall imaging cost and progressively identifies nested subgroups with increasing cost-effectiveness.

Each scenario starts with a large group, with the number receiving imaging. Multiorgan risk is assessed using both the best non-imaging index and models incorporating imaging biomarkers. The first-in-line method predicts outcomes based on each risk model, nominating a fixed number of individuals for further treatment. The QALYs for 5-year heart, brain, liver, kidney, and arterial outcomes from each model's nominated individuals are Table 8.5 in Column D (non-imaging model) and Column E (imaging model), with differences shown in Column F. The ICER (Column I) is calculated as the cost of imaging (Column H) divided by the difference in QALYs (Column F). The tables illustrate the impact of each successive scenario filter. As N decreases, the cost of imaging decreases, and the ICER becomes more cost-effective, while the difference in QALYs remains proportionally consistent. This approach combines standard statistical and cost-effectiveness principles with the first-in-line method to support targeted, budget-specific decision-making.

Table 8.5: Chapter 8 - Example cost-effectiveness scenarios

Scenario 1

				QALYs picked up in positive predictions						
Risk model	**A Non-imaging filter**	**B Word label**	**C Imaging k**	**D Non-imaging index only**	**E Index + imaging**	**F Difference**	**H Cost of imaging**	**I ICER**	**J Event r%**	**K Picked Ns**
Combined	None	People aged less than 60yrs	10,144	143 [129, 157]	169 [154, 184]	26* [2, 49]	£5,893,664	£230,664	5%	1092
HBLK	HBLK > median	People aged less than 60yrs	498	34 [27, 40]	38 [31, 45]	4.5 [-6.5, 15.4]	£289,338	£64,648	16%	162
	HBLK > median	People aged less than 60yrs with family history	211	9 [5, 13]	15 [11, 19]	5.9 [-0.6, 12.4]	£122,591	£20,708	16%	66
	HBLK > median	People aged less than 60yrs with family history and diabetes	70	6 [1, 10]	13 [9, 17]	7.2* [0.5, 13.9]	£40,670	£5,682	21%	30

Scenario 2

				QALYs picked up in positive predictions						
Risk model	**A Non-imaging filter**	**B Word label**	**C Imaging k**	**D Non-imaging index only**	**E Index + imaging**	**F Difference**	**H Cost of imaging**	**I ICER**	**J Event %**	**K Picked Ns**
Aggregated	Count >= 12	People with diabetes	1,297	126 [110, 142]	166 [150, 182]	40* [14, 67]	£753,557	£18,719	22%	417
risk	Count >= 12	Women with diabetes	401	26 [18, 35]	43 [35, 50]	16.3* [3.1, 29.6]	£232,981	£14,270	18%	99
	Count >= 12	Women with diabetes and higher local deprivation	131	13 [6, 20]	25 [18, 32]	11.7* [0.1, 23.2]	£76,111	£6,529	21%	38

Scenario 3

				QALYs picked up in positive predictions						
Risk model	**A Non-imaging filter**	**B Word label**	**C Imaging k**	**D Non-imaging index only**	**E Index + imaging**	**F Difference**	**H Cost of imaging**	**I ICER**	**J Event %**	**K Picked Ns**
Aggregated	None	People with higher local deprivation	7,074	243 [221, 265]	355 [335, 376]	113* [79, 147]	£4,109,994	£36,477	11%	888
risk	Count >= 8	People with higher local deprivation	3,448	236 [217, 255]	336 [316, 355]	100* [69, 131]	£2,003,288	£20,057	16%	826
	Count >= 8	People aged less than 60yrs with higher local deprivation	197	13 [9, 18]	18 [14, 23]	5.3 [-2.0, 12.5]	£114,457	£21,786	19%	68
	Count >= 8	People aged less than 60yrs with higher local deprivation and high chol.	125	6 [2, 10]	16 [12, 20]	9.8* [3.5, 16.2]	£72,625	£7,382	19%	34

These scenarios illustrate a further way the first-in-line method enables cost-effectiveness decision-making. In each case, we begin with a large group of people, with the number receiving imaging shown in column C. The cost of imaging (Column H) is £581 per person. In each case, multiorgan risk is assessed with the best possible non-imaging index, and also with models incorporating imaging biomarkers. The first-in-line method makes positive predictions based on each risk model, nominating a fixed number of people for further treatment (Column K = 2 x Event % x N = 2 x Column J x Column C). The QALYs associated with 5-year heart, brain, liver, kidney and arterial outcomes from each model's nominated people are shown in Column D (for the non-imaging model), Column E (for the imaging model), with the difference between imaging and non-imaging shown in Column F. An asterisk (*) in Column F indicates where the difference in QALYs was significantly different between imaging and non-imaging models based on permutation testing with 1000 replicates. The ICER (in Column I) is equal to the cost of imaging (Column H) divided by the difference in QALYs picked up (Column F). The point of these tables is to illustrate the effect in each successive row of the scenario. In each case, we apply an additional filter to the people receiving imaging. In doing so, N becomes successively smaller, the cost of imaging becomes cheaper, and because the difference in QALYs is proportionally maintained, the ICER becomes successively more cost-effective. In this way, standard statistical and cost-effectiveness principles are combined with the first-in-line method to support meaningful budget and target-specific decision-making.

8.4 Discussion

In this chapter, we have extended the methodology of the previous chapter to encompass cost-effectiveness elements (cost of imaging, QALYs, ICERs and willingness-to-pay) and extensive consideration of population subgroups. We have demonstrated that the significant incremental discriminative accuracy described in Chapter 7 does not always translate directly into cost-effective solutions, due to the substantial per-person cost of imaging. Similarly, models that focus on targeting risk for single outcomes are much less likely to be cost-effective, compared with approaches that assess risk and count outcomes across multiple related diseases.

The first-in-line method presents a valuable, simple approach for deciding who should receive multiorgan imaging, balancing the overall budget, cost-effectiveness and target health outcomes. This method can be used to make comparisons between risk assessment models of any type, provided that each produces a percentage risk estimate per person. This is a "clip-on" methodology that could potentially be used to compare, for example, black box models with current care. Any incremental differences in accuracy can be analysed to reverse-identify the subgroups that are most likely to benefit, and how this benefit can be balanced against any incremental costs. This targeted approach ensures that scarce and costly imaging resources are allocated where they can have the greatest impact, thereby enhancing the efficiency of healthcare delivery.

We accept that the current study took a significantly simpler approach to cost-effectiveness modelling than would traditionally be required. This was done in order to reach a set of results that aggregate risk differences across 14 outcomes. Future research could take a more conventional approach to this research question by accounting for treatment costs and effect, adding scan analysis costs, adding granularity to the distribution of health utilities used, adding time-discounted cost and benefits for serious outcomes, and by building a multi-outcome model that incorporates all possible transition probabilities and the interactions between them.

Once again, we need to acknowledge the healthy participant bias that exists within the UK Biobank. If this section of the analysis was undertaken in a more diverse, less healthy population, we would expect to see a higher number of adverse outcomes in the 5-year follow-up period, and potentially more abnormalities at the time of imaging. This increases the overall level of QALYs observable. It is uncertain whether the difference in QALY detection between imaging and non-imaging models would

hold, or whether the effect would be larger or smaller. Potentially, a substudy of the existing data using a population-weighted sample could be used to create a sensitivity analysis to address this question. Furthermore, it could be that more sophisticated machine learning models could be applied to make population-weighted forecasts.

It will always be crucial to quantifiably understand the cost-effectiveness of new diagnostic risk models compared to existing ones. This task becomes exponentially more complex as we move into a multi-system or multiorgan setting. Nevertheless, as researchers we need to be developing approaches that can connect population-level insight with clinical decision-making and pragmatic cost-effectiveness. Policymakers rely on this data to develop guidelines and recommendations, ensuring effective, equitable outcomes, and supporting the long-term sustainability of the healthcare system.

In summary, the first-in-line method ensures the judicious use of multiorgan imaging by focusing on those most likely to benefit, compared with a non-imaging risk strategy. This approach maximises health outcomes while minimising costs, making it an invaluable strategy for enhancing the effectiveness of imaging interventions aimed at preventing multimorbidity.

Chapter 9: Discussion

This thesis has used the UK Biobank as a multidimensional resource to gather statistical evidence supporting various strategic aspects of multimorbidity prevention. In this chapter, we summarise the findings, reflect on the limitations, discuss the implications for clinical practice, and identify avenues for future research.

9.1 Summary of findings relating to research questions

Research Question A. What are the significant cross-organ relationships within the HBLK cluster, as identified via multiorgan imaging, and how can they inform multimorbidity prevention strategies?

The findings from Chapter 4 addressed Research Question A by identifying significant cross-organ relationships between the heart, brain, and liver using multiorgan imaging. Adverse cardiac features such as increased cardiac mass and reduced cardiac function were associated with markers of brain atrophy and white matter hyperintensities, supporting the cerebral hypoperfusion hypothesis. Similarly, liver fibroinflammation (measured via cT1) was associated with brain atrophy and microstructural changes in white matter, while liver fat levels were associated with adverse cardiac features. These findings confirm the heart-brain-liver axis as a clinically relevant system and point to shared risk factors such as hypertension, obesity, and vascular health as possible levers for multimorbidity prevention.

Research Question B. To what extent is the current NHS Health Check effective in preventing disease within the HBLK cluster?

Chapter 5 demonstrated that the NHS Health Check is associated with reduced or delayed multiorgan disease outcomes in the long term, confirming its effectiveness as a preventive tool for the HBLK cluster. Using a matched cohort design, the analysis found that participants who received the NHS Health Check had fewer longer-term disease events related to the heart, brain, liver, and kidneys compared to controls. These findings provide empirical evidence that supports the continuation and refinement of the NHS Health Check as a central strategy for multimorbidity prevention in primary care.

Research Question C. How feasible is it to expand the NHS Health Check to include accurate risk assessments for multiorgan disease?

Chapter 6 explored the feasibility of expanding the NHS Health Check to incorporate multiorgan disease risk assessments. These results demonstrated that by using existing NHS Health Check inputs (e.g., age, BMI, blood pressure, and lipid levels), it is possible to develop multiorgan risk calculators with acceptable discriminative accuracy (AUC ≥ 70%) for diseases across the heart, brain, liver, and kidneys. We further demonstrated that including additional blood biomarkers (e.g., glycated haemoglobin and liver function tests) significantly improved risk predictions for specific outcomes such as fatty liver disease, liver cirrhosis, and chronic kidney disease. These results show that multiorgan risk information can be derived without major disruptions to current NHS protocols, making it a feasible and scalable enhancement to the existing prevention framework.

Research Question D. What is the incremental value of multiorgan imaging for risk stratification, and how cost-effective is this approach for specific patient subgroups?

Chapter 7 addressed the incremental value of multiorgan imaging by demonstrating that imaging-based models had significantly higher discriminative accuracy for heart-brain-liver-kidney outcomes compared to the best-performing non-imaging risk scores. Imaging-derived metrics such as liver fibroinflammation (cT1), carotid intima-media thickness, and cardiac function measures contributed variously to significantly higher predictive value for all outcomes studied. Chapter 8 extended this analysis by incorporating cost-effectiveness considerations. Developing a "first-in-line" methodology, these results showed that imaging is most cost-effective when targeted at specific subgroups, such as younger individuals (ages 60–69) with elevated multimorbidity risk trajectories. While multiorgan imaging offers significant potential incremental value, its routine use must be prioritised for specific patient populations to remain cost-effective in a resource-constrained healthcare system.

9.2 Reflection on findings in the context of existing work

In Chapter 4, we conducted one of the largest-ever studies to simultaneously assess underlying associations between the heart, brain and liver using multiorgan imaging. This study demonstrated that many of the cross-organ relationships that have been previously identified in smaller, clinical cohorts (described in Section 2.4) still hold in the general mostly healthy population, although the effect is more

subtle. Even after adjusting for known risk factors such as hypertension, high cholesterol and diabetes, there were organ-level effects, with differential patterns of associated pathology in each cross-organ relationship. Poorer vascular health was associated with adverse features in all three organs.

Relationships between the liver and the brain that have previously been observed in cases of severe liver disease were also observed (more subtly) in the general population. Elevations in liver fibro-inflammation were associated with lower brain volume, more white matter lesions and poorer white matter microstructure (Section 2.4.3). Our findings confirmed associations from earlier, smaller studies linking fatty liver disease to brain atrophy and white matter hyperintensities but showed a more complex relationship between white matter integrity and liver fat. Below the 5% threshold, liver fat was associated with higher neurite density, possibly due to phenotypic differences or fatty acids' role in axonal myelin maintenance. However, excess liver fat over 5% negated these benefits, manifesting in poorer white matter health. There is some emerging evidence around the complex interplay between healthy fats and the maintenance of brain health in older age [325, 425]. It will be interesting to see how future research teases out these effects, potentially challenging long-held beliefs around blood lipids and potential brain effects of lipid-lowering treatments. In simultaneous modelling, it was liver fibro-inflammation, not liver fat, that appeared to drive negative brain phenotypes, along with vascular health which affected all three organs.

This analysis brought together and confirmed a number of cross-organ relationships that had already been described in clinical cohorts, but can now be shown together in the same set of participants in a population-based cohort. Associations found with the more novel MRI metrics such as liver cT1, ICVF and ISOVF expanded the evidence base (Section 2.3), supporting the further use of these metrics in non-invasive health assessments.

The results presented in Chapter 4 represent a much smaller subset of the analysis that was undertaken. Initial results included principal components analysis of diffusion metrics across brain regions, additional cardiac metrics and additional brain metrics. These findings had to be greatly scaled back to create a coherent and understandable message for publication. Interesting incidental findings that were not included related to; regions of the brain differentially associated with cardiac function and liver inflammation, liver-heart associations with susceptibility-weighted measures of the brain, and a potential non-linear relationship between liver iron and healthy neurite density.

The question of the directionality of association came up in many in-person discussions of these results. The available data does not permit a direct assessment of relationship directionality, as it is observational and from a single point in time. However, analysis with direction dependence analysis [426] indicated evidence of relationships in both directions, depending on the metric. Previous anatomical research concerning the fibres of the vagus nerve has shown that 80-90% of the fibres are afferent – meaning heading from the body towards the brain [427].

In Chapter 5 we changed track and evaluated the NHS Health Check as a potential intervention for multimorbidity prevention. We used an extensively matched cohort within the UK Biobank to show that the NHS Health Check, as it is currently applied, was associated with significantly reduced or delayed multiorgan outcomes in the longer term. These results support the use of the NHS Health Check as an intervention in primary care that plays a significant role in preventing the progression of multimorbidity. Although there has been a substantial amount of research on various aspects of the NHS Health Check (see Section 2.2), this is the first analysis to produce evidence that the protocol effectively prevents or delays disease outcomes in the longer term.

These results were met with scepticism from some quarters. The most commonly-received criticism was that the observed results must be due to uncontrolled confounding. Although one can never remove all confounding in observational work, we took several steps to reduce this, including extensively matching the cases and controls, model adjustment for known confounders and adjustment for time-varying hazards. We also applied post-hoc e-value analysis to identify the results most at risk of nullification from potential unmeasured confounding. This question brings to mind the scepticism and debate around insufficient evidence exhibited at the launch of NHS Health Check [93, 428]. It is difficult to produce 'sufficient evidence' for any preventive intervention unless changes are made in tiny incremental steps. At the time, the introduction of the NHS Health Check was an optimistic move [429]; based on 'sound principles'[428] but fraught with inherent political complexities [430]. Looking back, we can now identify this as an important foundational strategy for multimorbidity prevention and progression towards sustainable healthcare.

In Chapter 6 we examined the feasibility of expanding the NHS Health Check to assess risk for multiorgan disease. In that study, we showed how the same information currently available as part of the NHS Health Check could be reconfigured to produce multiple risk estimates for diseases across the

heart, brain, liver and kidneys, with performance comparison to existing risk metrics (Section 3.3.5). We explored this at three levels of information restriction: remote models that use only health parameters that could be collected remotely, standard models that include all health parameters already part of the existing NHS Health Check protocol, and extended models that include additional blood tests that are widely available but are not part of the existing protocol. At all levels, multiorgan risk scores of acceptable quality were possible, using a discriminative accuracy cut-off of 70% area under the curve.

Pairwise analysis demonstrated that existing diagnoses play a major role in predicting future risk for related disease, describing several novel and several previously observed relationships (Section 2.4). Rather than creating ever-more-specific risk calculators for people with existing comorbidities, we demonstrated one way that existing comorbidities could be built into multiorgan risk calculations.

In Chapter 7 we found that risk stratification models that included multiorgan imaging had significantly higher discriminative accuracy than the best non-imaging risk scores found in the literature. Reviewing the imaging components of best-fit models, we found a number of expected cis-organ relationships, as well as novel cross-organ relationships that help improve the multiorgan risk stratification across 5 years of follow-up. Cardiac function, carotid intima-medial thickness and liver fibroinflammation were key metrics that contributed significantly to improved multiorgan risk assessment.

To our knowledge, this is the only study of its type, integrating and building upon large bodies of research looking at cis-organ associations. In prior studies, individual biomarkers are evaluated based on cis-organ outcomes and analyses are often produced in ways that showcase the potential of new biomarkers rather than strictly measuring incremental effects. In this study, we used the best possible non-imaging risk scores and required all imaging parameters to compete with each other for inclusion in final models. In this way, we could identify the most powerful biomarkers for multiorgan risk given our sample.

In Chapter 8, we reconsidered the role of imaging in risk stratification, taking the considerable costs of imaging into account. Here we found that, in our sample, multi-outcome models were necessary to identify sufficient incremental benefit. In other words, if we only viewed the incremental effect of imaging using a single outcome, there was not enough benefit to make the imaging cost-effective. We

used the UK Biobank data to set up a simplified cost-effectiveness analysis and developed a "first-in-line" method for deriving cost-effective imaging allocation within the context of limited resources. This analysis found that demographic and risk-based subgroupings can be used to prioritise the use of imaging given a specific budget or scanning capacity. We showed that finding and treating younger people (aged 60-69) who have high multimorbidity trajectory risk could have more long-term benefits than scanning all people over 70. This analysis confirmed that non-imaging information still has an important role to play in this determination.

9.3 Limitations

9.3.1 Selection bias and healthy participant effect in the UK Biobank

The UK Biobank has several limitations that may influence the conclusions drawn in this thesis, reflecting broader challenges associated with observational studies in general [431], and the UK Biobank in particular. Analyses conducted with observational data can be affected by confounding variables (measured and unmeasured), which may lead to incorrect conclusions about relationships between factors. We have conducted all studies in this thesis with a careful awareness of and best-efforts approach to deconfounding. Fortunately, the UK Biobank provides an extensive array of clinical variables that allow confounding factors to be included in matching and modelling. Unlike randomised controlled trials, observational studies cannot establish causality, therefore we have been cautious throughout to report associations and observed effects and we do not make any claims about causality.

The UK Biobank participants are known to be healthier, wealthier, better educated, and more health-conscious compared to the general UK population [362, 363]. This is a form of selection bias meaning that the rates of incident disease observed in the current study are known to be lower than the UK average incidence rates, lower prevalence of multimorbidity, and reduced variability in health outcomes within the cohort [364]. Such skewed sampling reduces the generalisability of findings, particularly to higher-risk groups such as individuals with lower socioeconomic status or those burdened with multiple comorbidities [365]. For instance, the associations observed in this thesis between multiorgan imaging biomarkers and disease outcomes may differ in populations with higher baseline disease burden. In such groups, pre-existing conditions might overshadow or complicate the observed relationships, potentially leading to overestimation of the predictive utility of imaging biomarkers.

9.3.2 Ethnic and socioeconomic homogeneity

This selection bias has also meant that the UK Biobank is significantly less ethnically and socioeconomically diverse than the UK population [365, 432]. This aspect poses the most significant threat to the conclusions of the current work. Many diseases within the heart-brain-liver-kidney (HBLK) cluster, such as stroke, diabetes, and liver disease, disproportionately affect ethnic minority groups and individuals from lower socioeconomic backgrounds. As a result, the findings of this thesis may not fully capture the appropriate risk factors, cross-organ relationships, and disease trajectories that are more common in these groups. For instance, liver fibro-inflammation or carotid intima-media thickness may behave differently in populations with higher prevalence of diabetes or obesity, potentially altering the conclusions about their utility as predictive biomarkers.

9.3.3 Self-report, recall bias and information bias

All information that was provided by participants solely by self-report is subject to recall bias. This bias especially applies to health behaviours such as smoking, physical activity and alcohol consumption [433]. This effect cannot be remedied by the researcher and is likely to bias reported values downward (e.g. reporting less alcohol consumption than actual levels), potentially leading to under-correction for confounding. This could lead to an underestimation of the role of lifestyle factors in cross-organ relationships and disease risk. For example, if alcohol consumption is underreported, the observed association between liver fibro-inflammation and disease outcomes may overestimate the direct impact of the imaging biomarker while underestimating the role of alcohol-related liver damage.

Where values are measured and reported by the UK Biobank personnel, measurement errors and missing data can compromise the reliability of the results. Nevertheless, all UK Biobank staff received standardised training on the assessment protocol, and standard machines were used for imaging and blood pressure. Where study variables are defined via electronic health records, the accuracy of measures is limited by the quality and timeliness of the data coding, and the integrity of data linkage [260]. As researchers, we rely on the reported timing of outcomes and exposures to establish the time order of events. Information bias in this case is likely to be worse for conditions that do not necessarily coincide with immediate secondary care. For example, we might expect coding for myocardial infarction or ischaemic stroke to be well-coded based on prompt admission to hospital, compared with mild cognitive impairment or fatty liver disease, which may not be recorded in any records. Although

we apply best possible efforts, there is always a limit to how correct our analyses can be when working with real-world data.

9.3.4 Feasibility and scalability of integrating imaging into the NHS

A key limitation of this thesis lies in the feasibility and scalability of integrating multiorgan imaging into routine NHS practice. Although the results demonstrate the incremental value of imaging for multiorgan risk stratification, significant practical barriers remain. First, the high cost of imaging, both in terms of equipment and operational expenses, presents a major challenge for routine implementation. Second, the availability of trained radiologists and standardised reporting frameworks varies widely across NHS trusts, which may limit the uniform application of these methods.

Additionally, NHS imaging services are already under pressure due to increasing demand for diagnostic scans, raising questions about whether preventive imaging could be incorporated without overburdening existing infrastructure. Scalability would require not only additional resources but also strategic prioritisation, such as targeting high-risk subgroups as described in Chapter 8. Investments in automation, including artificial intelligence (AI) for image analysis, could potentially reduce costs and alleviate workforce constraints. However, implementing such systems at scale would require extensive validation, training, and regulatory oversight, which may delay adoption.

9.3.5 Chapter format and publication

There is a limit to how much material can be effectively communicated in a single published article. With Chapter 4, we initially conducted a much more lengthy and detailed analysis. The academic publishing process required that the message be greatly simplified, resulting in a much more pared-back analysis that is now found in Chapter 4. This problem is ever-present in multiorgan work. The existing normal structure of scientific studies requires a particular layout that examines specific hypotheses. Journals and readers are often attuned to a particular speciality or organ. This standard format does not always fit well with multiorgan work, which is cross-disciplinary by definition.

9.3.6 Small sample size post-imaging

When building risk prediction models, it is ideal to have a training set (sometimes called a development set) and an external test set (sometimes called a validation set). In Chapter 6, we used random splitting

of the set to create a training set and an internal test set. For the risk prediction work carried out in Chapter 7, the dataset was significantly smaller, as we were only using those UK Biobank participants who had received multiorgan imaging, and there were also significantly fewer events, as the follow-up period since imaging is much shorter. Therefore, we did not have sufficient data to conduct a train-test split. Therefore, all results presented in Chapter 7 are observational associations in a single set of data.

9.3.7 The important role of blood biomarkers

Blood and urine tests can be highly efficient for detecting underlying disease or risk. It makes sense that lab tests would form an intermediate step between non-imaging health risk and imaging. In the UK Biobank, however, blood tests were primarily taken at the baseline recruitment. There was insufficient blood test data from the imaging visit to adequately include these parameters alongside the imaging. We gave blood/biochemistry predictors some consideration in Chapter 6 where we found that including common laboratory tests enabled significantly higher discriminative accuracy for chronic kidney disease, fatty liver disease, alcoholic liver disease and liver cirrhosis. On the other hand, the commonly available blood/biochemistry predictors tested in our study did not offer significantly higher discriminative accuracy for brain or heart outcomes.

9.3.8 Cost-effectiveness with more rigorous costs and trajectories

The cost-effectiveness analysis conducted in Chapter 8 represents an important first step but is based on simplified assumptions regarding costs and outcomes. This analysis did not account for critical downstream factors, such as the costs associated with clinical follow-up, incidental imaging findings, or the potential for overtreatment. For example, incidental findings — which are common in imaging — may lead to additional diagnostic tests or interventions, which could drive up costs significantly, causing the cost-effectiveness of multiorgan imaging to be overstated. Moreover, the analysis did not incorporate long-term trajectories of health outcomes, which could further affect the cost-benefit balance. A more rigorous cost-effectiveness framework would include these variables, along with extensive sensitivity analyses to explore how changes in assumptions influence the results.

Beyond cost considerations, the feasibility of implementing imaging-based risk stratification within the NHS was not fully explored. Practical factors such as scanner availability, workforce shortages, and patient acceptability present significant barriers to scaling imaging approaches. These challenges could

limit the real-world applicability of our stated findings, particularly in resource-constrained settings. For example, even if imaging demonstrates clear clinical benefit, the lack of trained radiographers and scanners might prevent equitable access, potentially undermining the broader healthcare implications. Future analyses should incorporate these logistical barriers into the analysis, to assess the true feasibility and sustainability of multiorgan imaging within routine clinical practice.

9.3.9 Impact of limitations on conclusions

The biases and limitations outlined above could undermine the generalisability and validity of the thesis conclusions. The numerous findings presented here should be interpreted with caution, particularly when extrapolating to diverse populations, longer time horizons, or routine clinical practice. For validation and comparison, future work could look to other important research resources such as the German National Cohort [434], the Rotterdam Study (from the Netherlands [435]), or the China Kadoorie Biobank [436]. Further research using such resources has the potential to address the above limitations by gathering evidence across more diverse cohorts and incorporating longer follow-up periods, thus allowing for more robust sensitivity analyses and more rigorous effectiveness analyses.

9.4 Implications for clinical practice

The findings of this research have significant clinical implications for understanding and managing multimorbidity risk within the heart-brain-liver-kidney cluster.

9.4.1 Systems thinking

Our research supports the need for a multiorgan focus, or at least a multiorgan awareness in clinical practice [215]. Such an awareness has the potential to guide clinical decision-making in ways that enhance longer-term multiorgan health and reduce health service costs. This work invites clinicians to consider the multiorgan effects of any observed dysfunctions or planned interventions by providing evidence for significant cross-organ relationships. Although this perspective aligns well with the national-level NHS mandate [16, 429], individual people within the NHS are often restricted to quite a strict statutory framework for how health services are to be delivered. The multiorgan shift applies to both physicians and administration. In their 2022 systematic review of 33 studies, Bhat and colleagues

reported that ‘systems leadership’ was the vital factor in successfully integrating health and social care and achieving the goals of the NHS Long Term Plan [437]. At the systems level, this could look like better collaboration between care home staff and primary care, and better information sharing between secondary providers. At the individual level, the standard 10-15 minute primary care appointment could be seen as insufficient and potentially unsafe for people with multimorbidity [368]. Our research would suggest that there is some problem-solving required to close the gap between the crucial health preventive functions needed in general practice appointments and how these appointments are designed and commissioned.

9.4.2 Multiorgan disease prevention with the basics

Many findings in this thesis are unsurprising. One theme running throughout this work is that a significant portion of multimorbidity prevention comes down to the management of the basic known risk factors. These include smoking, hypertension, insulin resistance, obesity, systemic inflammation, alcohol use and lack of physical activity. Although these risk factors were not an explicit focus of this work, our results showed that they consistently affect all four organs.

For example, good management of hypertension is crucial in preventing disease and damage within the heart, brain, liver and kidneys. Hypertension is a known risk factor for ischaemic heart disease, heart failure, stroke and dementia. Chronic high blood pressure can damage the blood vessels in the kidneys, which can impair kidney function and can progress to chronic kidney disease. Similarly, hypertension can exacerbate liver conditions by contributing to fatty liver disease, increasing portal pressure, and worsening liver inflammation and fibrosis [438]. Effective hypertension control managed between the patient and the primary care team helps protect these vital organs, minimising the risk of related complications in the longer term. In this way, over time, Bi and Liu (2023) show how general practitioners in the UK have become much more involved with maintaining the health of all their registered patients rather than simply acting as ‘gatekeepers’ [439] for those who fall ill. Our research suggests that renewed enthusiasm for risk factor detection, screening and management could pay significant dividends in terms of lower longer-term multimorbidity.

9.4.3 Support for the NHS Health Check

This research supports continued focus and potential strengthening of the NHS Health Check in preventing the progression of multimorbidity. The primary care setting provides the ideal opportunity and infrastructure for face-to-face contact, routine screenings, and the central launchpad from which to orchestrate specialist referrals. Although the NHS Health Check is not currently part of the NHS Quality and Outcomes Framework (QOF [440]), it overlaps with several QOF metrics, including smoking cessation and control of hypertension and obesity. Given the multiorgan utility of the NHS Health Check demonstrated in our work, we agree with a recent review recommending that central support for the NHS Health Check should be increased. The six recommendations from the governmental review were: 1. build sustained engagement (with the NHS Health Check); 2. launch a digital service; 3. start younger; 4. improve participation; 5. address more conditions, and 6. create a learning system [441].

The results of this thesis support the expansion of the NHS Health Check in a multi-disease direction. In this thesis we have described the protocol adjustments that could have minimal impact on the delivery but could significantly benefit multiorgan disease prevention. These include a more detailed handling of mental health (multiorgan outcomes), laboratory tests for liver and kidney function (for liver and kidney health), and referrals to treat hearing loss (for dementia prevention)[1].

Any expanded delivery of the NHS Health Check will be seen as burdensome if the entire work falls upon the general practitioner. If this work can be spread out more sensibly, it is possible to make it less so. For example, health check electronic invitations can be done through an automated system, removing the costs associated with administration, paper and postage. Systems like eConsult [442] can be used to collect self-reported health parameters online prior to the in-person appointment. We strongly support such approaches. Physical measurements and interviewing can be done by practice nurses or allied health professionals. All these measures would make the best possible use of the time the patient spends with the general practitioner.

We demonstrated that multiorgan risk assessment is feasible and immediately applicable in clinical practice, potentially improving patient outcomes and healthcare efficiency. In Chapter 6 we

[1] The other commonly mentioned facets not mentioned in the current work are cancer, respiratory function, frailty and chronic pain.

demonstrated how a multiorgan risk calculator could work using new models and a single set of inputs. Clinicians can then use this risk information to follow up with patients based on their multiorgan risk profile, enabling better quality resource allocation and more timely preventative care. In the absence of such software in clinical practice, existing online risk calculators could be prepared and applied prior to meeting with the general practitioner.

9.4.4 Strategic use of multiorgan imaging

In this thesis, we have developed a method for identifying people who are 'first-in-line' for multiorgan imaging based on available scanning capacity, assessment of multiorgan risk and the number of people overall. This is an approach that could be calibrated for either large- or small-scale settings. Once calibrated, the day-to-day preventive imaging decisions can be reverse-engineered by fitting together the puzzle pieces of cost, increased accuracy, and differential rates of expected multiorgan outcomes in specific subgroups. This is an example of a data-driven clinical decision support algorithm that does not fall into the category of artificial intelligence, as it is built with conventional models, with each component being fully explainable [443]. One way this could work would be to compile a waiting list of 'first-in-line' candidates, who could be called upon at short notice to fill empty spots when clinical patients make cancellations, or to fill time slots that are less preferred by the elderly and very ill.

Substantively, preventive imaging could be applied for risk screening in two main ways. Imaging could be used in younger people (less than 70 years) who have scored higher than usual using non-imaging multiorgan disease risk scores. In this group, we would be identifying higher-risk younger people with a potentially longer lead time for disease prevention. On the other hand, our data shows that when offered to older people (70 years or older), imaging tends to identify more current undiagnosed dysfunction with a shorter lead time for intervention.

9.4.5 Better data, better health

This research also illustrates the benefits of a paradigm shift in clinical practice towards a more integrated and data-driven approach to managing multimorbidity and multiorgan risk. As health data systems improve, the information contained therein becomes more powerful. There is huge untapped potential, even at the practice level, to better use the data being collected. Incremental progress could

include health check reminders for non-attenders, expansion of remote information collection and background health tracking over time.

9.4.6 Self-pay or private health prevention

This work also has potential implications for private health insurers. Although the NHS is the main health provider in the United Kingdom, there is still some scope for private health organisations to be interested in this type of methodology. A more personalised risk assessment profile offers enhanced underwriting accuracy, allowing for fairer and more precise premium rates. By identifying high-risk policyholders early, insurers can also trigger targeted preventive strategies, reducing the incidence of costly claims and improving overall cost management. As a potential drawback of this, if such preventive services are only offered by private sectors (and not the NHS) the unintended consequence would be worsening inequality of healthcare and population health.

9.5 Future research directions

Building on the findings of this thesis, several high-priority areas for future academic research emerge, each critical for advancing the understanding of multimorbidity prevention. These directions aim to refine current approaches, develop new strategies, and ultimately improve patient outcomes.

9.5.1 Multisystem vernacular: clusters, syndromes and axes

Integrating data from multiple organ systems can be exciting and useful when identifying underlying patterns and relationships that might otherwise be overlooked, but complexity is difficult to communicate. The central question here would be, what are the multiorgan clusters that provide a high level of academic and clinical utility in ways that reduce more confusion than they create? The significant pairwise and multiorgan associations found in this thesis provide support for the heart-brain-liver-kidney cluster as a valid object of study, but this is by no means the only answer.

We have previously spoken about metabolic-associated fatty liver [150], cardiovascular-kidney-metabolic syndrome [217] and cardiac-kidney-liver syndrome [218] which have arisen, in part, from clinical experience and clinical associations. On the other hand, systematic reviews from health

databases provide important insight into commonly occurring multimorbidity clusters. From 51 studies gathered in 2019, Busija and colleagues [444] used dimension reduction to identify two consistent groupings: mental health and cardiometabolic disease – a cluster including heart disease, stroke, diabetes, hypertension, obesity and, to a lesser extent, liver and kidney disease. Another systematic review of 97 studies gathered in 2023 [445] found that cardiometabolic, musculoskeletal, mental, and respiratory patterns were the most commonly found. From a health system cost perspective, a systematic review of 59 studies in 2022 [14] identified the most costly condition dyads to be 1) cardiometabolic (diabetes + cardiovascular) and 2) cancer plus mental health.

Future work could reflect on this situation and consider the dimensions of clustering that hold priority for different users, and seed for consensus around the multimorbidity cluster partitioning that emerges. For example, for clinicians it makes sense to group conditions and organs together based on shared risk factors and underlying mechanisms, but economists and planners may want to group conditions based on population trends and community needs. Data specialists are very comfortable grouping conditions together by prevalence, even when such groupings seem incongruous to clinicians. At this time, I am unsure whether it is possible to agree on a non-overlapping set of multimorbidity clusters for general use, or whether such a solution would be significantly more efficient than the (primarily) single - specialty focus we have currently.

9.5.2 Integration and optimisation of big data in multiorgan research

It is a very exciting time to work in health data science. The analyses presented in this thesis using the (relatively small) UK Biobank present a compelling case for further research into the integration and optimisation of large-scale health datasets. Models for health check effectiveness and multiorgan risk will need to be validated and calibrated within a larger, more representative dataset like the Clinical Practice Research Datalink (CPRD [446]). Unfortunately, CPRD does not include imaging information, so that portion will not be extendable.

In general, due to the availability of large-scale health records, there is an opportunity to apply a range of analytical tools to learn population-level associations that can help inform and support clinicians in their decision-making. Such datasets could offer novel scope to understand the interactions between conditions and outcomes and how multimorbidity progresses over time. For example, the OPTIMISE

study [447] is a recent example of a large-scale study using electronic health records from over two million UK participants to develop risk scores for incident cardio-renal-metabolic disease and cardiovascular death. Further research could also significantly extend the cost-effectiveness analysis presented here with a real-world cost and outcome substrate of CPRD, allowing extensive comparative scenario modelling.

While this thesis presents associations from single-timepoint imaging, and follow-up outcomes over time, more truly longitudinal studies are needed to understand the long-term effects and sustainability of these preventative measures. Future research should investigate the multiorgan impact of lifestyle interventions, regular screenings, and preventive medication taken over extended periods. Such studies could help identify the most effective strategies for different patient populations and conditions.

Currently, there is a high level of enthusiasm around artificial intelligence (AI) for disease diagnosis and prediction [448, 449]. While this certainly represents the general direction of travel, progression is complicated by several factors. Traditionally, disease risk scores needed to be publishable in simple, easy-to-read equations. This was the standard open-source format so that other entities or researchers could key in the values and reproduce the risk score with relatively little effort. This standard format places upper limits on the number of predictors that can be reasonably used in the model. On the other hand, machine learning and AI models can ingest thousands of parameters. Conventional statistical models are highly explainable, which is a property that is prioritised in any technology under consideration for adoption within the NHS [443, 450, 451]. On the other hand, AI models (even ones considered ‘explainable’) have inner decision-workings that are not directly examinable by stakeholders.

Therefore, in my opinion, the advancements in multiorgan risk assessment enabled through big data and AI should be incremental rather than revolutionary. Future research should focus on creating more sophisticated and accurate risk stratification models that can be easily implemented in clinical settings, but always leaving actual decision-making in the hands of trained clinicians. Additionally, future studies should include diverse populations to ensure the tools are universally applicable and should include an examination of patient outcomes and costs.

9.5.3 Advancements in multiorgan imaging techniques

There is already substantial ongoing work developing new imaging biomarkers [452], new imaging sequences and image analysis software. Further work following this thesis could identify the minimum set of imaging inputs that have the greatest impact for multimorbidity risk prediction. This work has been developed using multiorgan MRI, but potentially there could be much lower-cost ways to glean similar information.

MRI is not the only option for imaging in cardiometabolic disease including liver, pancreas, and microcirculation [453]. Ultrasound is a well-known approach for transient elastography of the liver [454], and echocardiography preceded MRI for cardiac imaging [455]. For example, according to some, whole-body MRI (WB-MRI) is poised to be a crucial tool for multiorgan disease detection and prevention due to its ability to provide comprehensive, high-resolution, and non-invasive imaging of the entire body [249, 250]. We acknowledge that WB-MRI is not the same as the imaging that was done in this study. However, if we are imagining future application of the current work, it would probably not look too different from existing WB-MRI approaches. Given that there is already some existing infrastructure around WB-MRI, future research might find a fruitful overlap between population-level risk profiling and (potentially simplified) WB-MRI.

Total-body CT/PET is another well-known approach to multiorgan imaging [456, 457]. Total-body CT/PET offers rapid, comprehensive imaging with high sensitivity for active disease processes, atherosclerotic plaques and cancers, but involves significant radiation exposure and is less effective in soft tissues. WB-MRI provides superior soft tissue contrast and functional imaging without ionizing radiation, making it a safer modality for repeated screenings. WB-MRI is more costly, requires longer scan times and is less widely available. Both CT/PET and MRI can be conducted in mobile units as a potential option for reaching people in remote locations. Future research in multiorgan imaging could consider the mix of imaging modalities that provide the most efficient solution.

9.5.4 Other areas of disciplinary overlap

Given the complexity and variability of multimorbidity, future research could explore personalised medicine approaches that tailor interventions to individual patient characteristics. Emerging 'omics' datasets, including genomics and proteomics, hold significant promise for multiorgan risk prediction

and multimorbidity prevention [458, 459]. Ongoing efforts are identifying various genetic or metabolite signatures that signal multimorbidity risk [460, 461].

Secondly, the effectiveness of the NHS Health Check relies, in part, on healthy behaviour change. Under the 'Health Belief Model', people are more likely to make behaviour changes when the perceived benefits and barriers are counterbalanced by perceived severity and susceptibility [48]. Arlene Bierman provides an illuminating review of behaviour change studies [67] connected with primary care and multimorbidity, once again advocating for integration between clinical medicine, social care and community support. Several studies have demonstrated the positive effect that local "community champions" can have in healthy behaviour change [462, 463]. Community champions are members of the local community who "promote health and wellbeing or improve conditions in their local community" ([462], p.6). It can be significantly easier for people to access health services or change health behaviour when there is appropriate support within their local social network.

Finally, research in healthcare policy is essential to translate these findings into practice. Further studies could explore the ways that risk information at the point of assessment then interacts with the existing NICE guidelines framework, whether there are gaps that could have potential impact for multimorbidity prevention, and whether policies could be adjusted or integrated for smoother administration.

9.6 Conclusion

In this thesis, we have explored multimorbidity prevention through a series of analyses covering cross-organ relationships, preventative interventions, population-level risk stratification tools, and multiorgan imaging. Our research demonstrates that a multiorgan focus to long-term population health is both reasonable and feasible, using large-scale real-world health data. We show that interventions in primary care, lifestyle changes and regular screenings can significantly reduce the progression of multimorbidity over time. We show that a data-driven approach to multiorgan risk assessment is immediately possible, even with limited resources in primary care. Furthermore, multiorgan imaging offers significant incremental benefit, with certain parameters being more useful than others. Although imaging is a relatively high-cost option, there are specific subgroups of patients for whom multiorgan imaging can be cost-effective in the longer term.

Taken together, this collection of studies produces interesting new evidence that meaningfully adds to the field of multimorbidity prevention. This research provides a hopeful outlook for the future. Continued focus and cross-disciplinary collaboration are the engines needed to ultimately drive progress towards multimorbidity prevention, optimisation of scarce healthcare resources and overall improvement in patient outcomes.

References

1. Wagner, K.-H. & Brath, H. A global view on the development of non communicable diseases. *Preventive Medicine* **54**, S38–S41 (2012).

2. World Health Organization (WHO). Fact Sheets: Non communicable diseases. https://www.who.int/news-room/fact-sheets/detail/noncommunicable-diseases.

3. Skou, S. T. *et al.* Multimorbidity. *Nature Reviews Disease Primers* **8**, 1–22 (2022).

4. Vetrano, D. L. *et al.* An international perspective on chronic multimorbidity: approaching the elephant in the room. *The Journals of Gerontology: Series A* **73**, 1350–1356 (2018).

5. Willadsen, T. G. *et al.* The role of diseases, risk factors and symptoms in the definition of multimorbidity – a systematic review. *Scandinavian Journal of Primary Health Care* **34**, 112–121 (2016).

6. Fortin, M., Stewart, M., Poitras, M.-E., Almirall, J. & Maddocks, H. A Systematic Review of Prevalence Studies on Multimorbidity: Toward a More Uniform Methodology. *The Annals of Family Medicine* **10**, 142–151 (2012).

7. The Academy of Medical Sciences. Multiple Long-Term Conditions (Multimorbidity): a priority for global health research. https://acmedsci.ac.uk/policy/policy-projects/multimorbidity (2018).

8. Canoy, D. *et al.* Association between cardiometabolic disease multimorbidity and all-cause mortality in 2 million women and men registered in UK general practices. *BMC Medicine* **19**, 258 (2021).

9. Jani, B. D. *et al.* Relationship between multimorbidity, demographic factors and mortality: findings from the UK Biobank cohort. *BMC Medicine* **17**, (2019).

10. Tooth, L., Hockey, R., Byles, J. & Dobson, A. Weighted multimorbidity indexes predicted mortality, health service use, and health-related quality of life in older women. *Journal of Clinical Epidemiology* **61**, 151–159 (2008).

11. Dugravot, A. *et al.* Social inequalities in multimorbidity, frailty, disability, and transitions to mortality: a 24-year follow-up of the Whitehall II cohort study. *The Lancet Public Health* **5**, e42–e50 (2020).

12. Ronaldson, A. *et al.* Associations between physical multimorbidity patterns and common mental health disorders in middle-aged adults: A prospective analysis using data from the UK Biobank. *The Lancet Regional Health. Europe* **8**, 100149 (2021).

13. Soley-Bori, M. *et al.* Impact of multimorbidity on healthcare costs and utilisation: A systematic review of the UK literature. *British Journal of General Practice* **71**, E39–E46 (2021).

14. Tran, P. B. *et al.* Costs of multimorbidity: a systematic review and meta-analyses. *BMC Medicine* **20**, 234 (2022).

15. Cassell, A. *et al.* The epidemiology of multimorbidity in primary care: a retrospective cohort study. *British Journal of General Practice* **68**, e245–e251 (2018).

16. NHS. The NHS Long Term Plan. https://www.longtermplan.nhs.uk/wp-content/uploads/2019/08/nhs-long-term-plan-version-1.2.pdf (2020).

17. NIHR Strategic Framework for Multiple Long-Term Conditions (Multimorbidity) MLTC-M Research. https://www.nihr.ac.uk/documents/nihr-strategic-framework-for-multiple-long-term-conditions-multimorbidity-mltc-m-research/24639.

18. NICE. Multimorbidity: clinical assessment and management (NG56). https://www.nice.org.uk/guidance/ng56 (2016).

19. Tan, K. Prevention and management of multimorbidity to ensure healthcare sustainability. *Annals of the Academy of Medicine, Singapore* **50**, 807–808 (2021).

20. Pearson-Stuttard, J., Ezzati, M. & Gregg, E. W. Multimorbidity—a defining challenge for health systems. *The Lancet Public Health* **4**, e599–e600 (2019).

21. Hajat, C. & Stein, E. The global burden of multiple chronic conditions: A narrative review. *Preventive Medicine Reports* **12**, 284–293 (2018).

22. Bellman, R. *Dynamic programming*. (Princeton University Press, 1957).

23. Tukey, J. *Exploratory data analysis*. vol. 2 (Addison-Wesley, 1977).

24. Johnston, M. C., Crilly, M., Black, C., Prescott, G. J. & Mercer, S. W. Defining and measuring multimorbidity: a systematic review of systematic reviews. *European Journal of Public Health* **29**, 182–189 (2019).

25. Stirland, L. E. *et al.* Measuring multimorbidity beyond counting diseases: systematic review of community and population studies and guide to index choice. *BMJ* **368**, m160 (2020).

26. Ho, I. S. S. *et al.* Measuring multimorbidity in research: Delphi consensus study. *BMJ Medicine* **1**, e000247 (2022).

27. Lee, E. S. *et al.* Systematic review on the instruments used for measuring the association of the level of multimorbidity and clinically important outcomes. *BMJ Open* **11**, (2021).

28. Payne, R. A. *et al.* Development and validation of the Cambridge Multimorbidity Score. *Canadian Medical Association Journal* **192**, E107–E114 (2020).

29. Cezard, G., McHale, C. T., Sullivan, F., Bowles, J. K. F. & Keenan, K. Studying trajectories of multimorbidity: A systematic scoping review of longitudinal approaches and evidence. *BMJ Open* **11**, (2021).

30. Jensen, A. B. *et al.* Temporal disease trajectories condensed from population-wide registry data covering 6.2 million patients. *Nature Communications* **5**, 4022 (2014).

31. Faruqui, S. H. A., Alaeddini, A., Jaramillo, C. A., Potter, J. S. & Pugh, M. J. Mining patterns of comorbidity evolution in patients with multiple chronic conditions using unsupervised multi-level temporal Bayesian network. *PLOS ONE* **13**, e0199768 (2018).

32. Hughes, L. D. Understanding the processes behind the decisions – GPs and complex multimorbidity decision making. *BMC Primary Care* **23**, 162 (2022).

33. Soley-Bori, M. *et al.* Identifying multimorbidity clusters with the highest primary care use: 15 years of evidence from a multi-ethnic metropolitan population. *British Journal of General Practice* **72**, e190–e198 (2021).

34. Bisquera, A. *et al.* Identifying longitudinal clusters of multimorbidity in an urban setting: A population-based cross-sectional study. *The Lancet Regional Health. Europe* **3**, 100047 (2021).

35. Zhu, Y., Edwards, D., Mant, J., Payne, R. A. & Kiddle, S. Characteristics, service use and mortality of clusters of multimorbid patients in England: A population-based study. *BMC Medicine* **18**, 1–11 (2020).

36. Kastner, M. *et al.* Underlying mechanisms of complex interventions addressing the care of older adults with multimorbidity: a realist review. *BMJ Open* **9**, e025009 (2019).

37. Kinkorová, J. & Topolčan, O. Biobanks in the era of big data: objectives, challenges, perspectives, and innovations for predictive, preventive, and personalised medicine. *EPMA Journal* **11**, 333–341 (2020).

38. Founders Online, National Archives. On Protection of Towns from Fire, 4 February 1735. *Original source: The Papers of Benjamin Franklin, vol. 2, January 1, 1735, through December 31, 1744, ed. Leonard W. Labaree. New Haven: Yale University Press, 1961, pp. 12–15.*

39. Stange, K. C. *et al.* Physician Agreement with US Preventive Services Task Force Recommendations. *The Journal of Family Practice* **34**, 409–416 (1992).

40. Cogswell, B. & Eggert, M. S. People want doctors to give more preventive care: a qualitative study of health care consumers. *Archives of Family Medicine* **2**, 611 (1993).

41. Pencheon, D. Making health care more sustainable: the case of the English NHS. *Public Health* **129**, 1335–1343 (2015).

42. Hensrud, D. D. Clinical Preventive Medicine in Primary Care: Background and Practice: 1. Rationale and Current Preventive Practices. *Mayo Clinic Proceedings* **75**, 165–172 (2000).

43. Winslow, C.-E. A. The Untilled Fields of Public Health. *Science* **51**, 23–33 (1920).

44. Doll, R. Preventive medicine: the objectives. *Ciba Foundation Symposium* **110**, 3–21 (1985).

45. Caplan, G. *Principles of Preventive Psychiatry.* (Basic Books, 1964).

46. AbdulRaheem, Y. Unveiling the significance and challenges of integrating prevention levels in healthcare practice. *Journal of Primary Care & Community Health* **14**, 1–6 (2023).

47. Rose, G. The objectives of preventive medicine. in *Rose's Strategy of Preventive Medicine* (eds. Rose, G., Khaw, K.-T. & Marmot, M.) (Oxford University Press, 2008). doi:10.1093/acprof:oso/9780192630971.003.0001.

48. Rosenstock, I. M. The health belief model and preventive health behavior. *Health Education Monographs* **2**, 354–386 (1974).

49. Raghupathi, W. & Raghupathi, V. Big data analytics in healthcare: promise and potential. *Health Information Science and Systems* **2**, 3 (2014).

50. Khoury, M. J. & Ioannidis, J. P. A. Big data meets public health. *Science* **346**, 1054–1055 (2014).

51. Shah, P. & Patel, C. R. Prevention is Better than Cure: An Application of Big Data and Geospatial Technology in Mitigating Pandemic. *Transactions of the Indian National Academy of Engineering* **5**, 187–192 (2020).

52. Chen, M., Hao, Y., Hwang, K., Wang, L. & Wang, L. Disease Prediction by Machine Learning Over Big Data From Healthcare Communities. *IEEE Access* **5**, 8869–8879 (2017).

53. Alyass, A., Turcotte, M. & Meyre, D. From big data analysis to personalized medicine for all: challenges and opportunities. *BMC Medical Genomics* **8**, 33 (2015).

54. Andreu-Perez, J., Poon, C. C. Y., Merrifield, R. D., Wong, S. T. C. & Yang, G.-Z. Big Data for Health. *IEEE Journal of Biomedical and Health Informatics* **19**, 1193–1208 (2015).

55. Luo, J., Wu, M., Gopukumar, D. & Zhao, Y. Big Data Application in Biomedical Research and Health Care: A Literature Review. *Biomedical Informatics Insights* **8**, BII.S31559 (2016).

56. Khoury, M. J., Iademarco, M. F. & Riley, W. T. Precision Public Health for the Era of Precision Medicine. *American Journal of Preventive Medicine* **50**, 398–401 (2016).

57. Sudlow, C. *et al.* UK Biobank: An open access resource for identifying the causes of a wide range of complex diseases of middle and old age. *PLOS Medicine* **12**, e1001779 (2015).

58. World Health Organization. Multimorbidity: Technical Series on Safer Primary Care. https://iris.who.int/bitstream/handle/10665/252275/9789241511650-eng.pdf (2016).

59. Head, A., Fleming, K., Kypridemos, C., Pearson-Stuttard, J. & O'Flaherty, M. Multimorbidity: the case for prevention. *J Epidemiol Community Health* **75**, 242–244 (2021).

60. Barnett, K. *et al.* Epidemiology of multimorbidity and implications for health care, research, and medical education: a cross-sectional study. *The Lancet* **380**, 37–43 (2012).

61. Noordman, J., van der Weijden, T. & van Dulmen, S. Communication-related behavior change techniques used in face-to-face lifestyle interventions in primary care: A systematic review of the literature. *Patient Education and Counseling* **89**, 227–244 (2012).

62. Morris, M., Halcomb, E., Mansourian, Y. & Bernoth, M. Understanding how general practice nurses support adult lifestyle risk reduction: An integrative review. *Journal of Advanced Nursing* **78**, 3517–3530 (2022).

63. Kampmeijer, R., Pavlova, M., Tambor, M., Golinowska, S. & Groot, W. The use of e-health and m-health tools in health promotion and primary prevention among older adults: a systematic literature review. *BMC Health Services Research* **16**, 290 (2016).

64. Fallows, E. S. Lifestyle medicine: a cultural shift in medicine that can drive integration of care. *Future Healthcare Journal* **10**, 226–231 (2023).

65. Winther, S. *et al.* Exploring patient experiences of participating in a telephone-based self-management support intervention: Proactive Health Support (PaHS). *Journal of Advanced Nursing* **76**, 3563–3572 (2020).

66. Lawrence, W. *et al.* Meeting the UK Government's prevention agenda: primary care practitioners can be trained in skills to prevent disease and support self-management. *Perspectives in Public Health* **142**, 158–166 (2022).

67. Bierman, A. S. Preventing and managing multimorbidity by integrating behavioral health and primary care. *Health Psychology* **38**, 851–854 (2019).

68. Brickley, B. *et al.* A new model of patient-centred care for general practitioners: results of an integrative review. *Family Practice* **37**, 154–172 (2020).

69. Ungoed-Thomas, J. GPs in England treat up to three times more patients than safety limit demands. *The Observer* https://www.theguardian.com/society/2022/nov/20/gps-in-england-treat-up-to-three-times-more-patients-than-safety-limit-demands (2022).

70. Whitty, C. J. M. & Watt, F. M. Map clusters of diseases to tackle multimorbidity. *Nature* **579**, 494–496 (2020).

71. Littlejohns, T. J. *et al.* The UK Biobank imaging enhancement of 100,000 participants: rationale, data collection, management and future directions. *Nature communications* **11**, 2624 (2020).

72. Prados-Torres, A., Calderón-Larrañaga, A., Hancco-Saavedra, J., Poblador-Plou, B. & Van Den Akker, M. Multimorbidity patterns: a systematic review. *Journal of Clinical Epidemiology* **67**, 254–266 (2014).

73. Roth, G. A. *et al.* Global Burden of Cardiovascular Diseases and Risk Factors, 1990-2019: Update From the GBD 2019 Study. *Journal of the American College of Cardiology* **76**, 2982–3021 (2020).

74. El Hadi, H., Di Vincenzo, A., Vettor, R. & Rossato, M. Relationship between Heart Disease and Liver Disease: A Two-Way Street. *Cells* **9**, 567 (2020).

75. McCracken, C. *et al.* Multi-organ imaging demonstrates the heart-brain-liver axis in UK Biobank participants. *Nature Communications* **13**, 7839 (2022).

76. Siriwardhana, C., Lim, E., Davis, J. & Chen, J. J. Progression of diabetes, ischemic heart disease, and chronic kidney disease in a three chronic conditions multistate model. *BMC Public Health* **18**, 1–14 (2018).

77. Hylton, K., Thompson, K., Kearney, M. & Lagord, C. NHS Health Check Best practice guidance: For commissioners and providers (Public Health England). https://www.healthcheck.nhs.uk/seecmsfile/?id=1480 (2019).

78. NHS England. NHS Health Check. *nhs.uk* https://www.nhs.uk/conditions/nhs-health-check/ (2023).

79. Public Health England. NHS Health Check Information Leaflet. https://www.healthcheck.nhs.uk/seecmsfile/?id=401 (2015).

80. Department of Health and Social Care. Population screening programmes. *GOV.UK* https://www.gov.uk/government/collections/population-screening-programmes-document-collection (2023).

81. Coste, J., Valderas, J. M. & Carcaillon-Bentata, L. The epidemiology of multimorbidity in France: Variations by gender, age and socioeconomic factors, and implications for surveillance and prevention. *PLOS ONE* **17**, e0265842 (2022).

82. Neale, E. P., Middleton, J. & Lambert, K. Barriers and enablers to detection and management of chronic kidney disease in primary healthcare: a systematic review. *BMC Nephrology* **21**, 83 (2020).

83. Matthews, J. We need a shift from reactive to proactive care. *BMJ* **344**, e1225 (2012).

84. Department of Health and Social Care. Preventing illness and improving health for all: a review of the NHS Health Check programme and recommendations. *GOV.UK* https://www.gov.uk/government/publications/nhs-health-check-programme-review/preventing-illness-and-improving-health-for-all-a-review-of-the-nhs-health-check-programme-and-recommendations (2021).

85. Loyson, P. Influences from Latin on Chemical Terminology. *Journal of Chemical Education* **87**, 1303–1307 (2010).

86. Sowell, E. R., Thompson, P. M. & Toga, A. W. Mapping changes in the human cortex throughout the span of life. *The Neuroscientist* **10**, 372–392 (2004).

87. Froland, M. Preventive vs. Preventative: What's the Difference? *Two Minute English* https://twominenglish.com/preventive-vs-preventative/ (2023).

88. UK Biobank. Our impact. https://www.ukbiobank.ac.uk/learn-more-about-uk-biobank/our-impact (2024).

89. Artac, M., Dalton, A. R. H., Majeed, A., Car, J. & Millett, C. Effectiveness of a national cardiovascular disease risk assessment program (NHS Health Check): results after one year. *Preventive medicine* **57**, 129–134 (2013).

90. Robson, J. *et al.* The NHS Health Check in England: an evaluation of the first 4 years. *BMJ Open* **6**, e008840 (2016).

91. Muirie, J., McCartney, G., Fischbacher, C., Lewsey, J. & Connolly, J. *The Impact of Keep Well: An Evaluation of the Keep Well Programme from 2006 to 2012*. (NHS Health Scotland, 2014).

92. Public Health Scotlland. Keep Well - NHS Health Scotland. https://www.healthscotland.com/keep-well.aspx.

93. McCartney, M. Where's the evidence for NHS health checks? *BMJ* **347**, f5834 (2013).

94. Lu, J. Ningen Dock: Japan's unique comprehensive health checkup system for early detection of disease. *Global Health & Medicine* **4**, 9–13 (2022).

95. Birtwhistle, R., Bell, N. R., Thombs, B. D., Grad, R. & Dickinson, J. A. Periodic preventive health visits: a more appropriate approach to delivering preventive services: From the Canadian Task Force on Preventive Health Care. *Canadian Family Physician* **63**, 824–826 (2017).

96. Bundesgesundheitsministerium. Gesundheits-Check-up. *BMG* https://www.bundesgesundheitsministerium.de/checkup (2024).

97. Cho, B. & Lee, C. M. Current situation of national health screening systems in Korea. *Journal of the Korean Medical Association* **54**, 666 (2011).

98. Tanner, L. *et al.* NHS Health Check programme: a rapid review update. *BMJ Open* **12**, e052832 (2022).

99. Usher-Smith, J. A. *et al.* Patient experience of NHS health checks: a systematic review and qualitative synthesis. *BMJ Open* **7**, e017169 (2017).

100. Paxton, B., Mills, K. & Usher-Smith, J. A. Fidelity of the delivery of NHS Health Checks in general practice: an observational study. *BJGP Open* **4**, (2020).

101. Duddy, C., Gadsby, E., Hibberd, V., Krska, J. & Wong, G. Understanding what happens to attendees after an NHS Health Check: a realist review. *BMJ Open* **12**, e064237 (2022).

102. Gidlow, C. J. *et al.* Cardiovascular disease risk communication in NHS Health Checks using QRISK®2 and JBS3 risk calculators: the RICO qualitative and quantitative study. *Health technology assessment (Winchester, England)* **25**, VII–102 (2021).

103. Mills, K. *et al.* Views of commissioners, managers and healthcare professionals on the NHS Health Check programme: a systematic review. *BMJ Open* **7**, (2017).

104. Robson, J., Garriga, C., Coupland, C. & Hippisley-Cox, J. NHS Health Checks: an observational study of equity and outcomes 2009–2017. *British Journal of General Practice* **71**, e701–e710 (2021).

105. Debiec, R. *et al.* Evaluating the clinical effectiveness of the NHS Health Check programme: a prospective analysis in the Genetics and Vascular Health Check (GENVASC) study. *BMJ Open* **13**, e068025 (2023).

106. Dale, B. M., Brown, M. A. & Semelka, R. C. *MRI: Basic Principles and Applications*. (John Wiley & Sons, 2015).

107. Petersen, S. E. *et al.* Reference ranges for cardiac structure and function using cardiovascular magnetic resonance (CMR) in Caucasians from the UK Biobank population cohort. *Journal of Cardiovascular Magnetic Resonance* **19**, 1–19 (2017).

108. Elghazaly, H. *et al.* Characterizing the hypertensive cardiovascular phenotype in the UK Biobank. *European Heart Journal - Cardiovascular Imaging* **24**, 1352–1360 (2023).

109. Desai, M. Y. *et al.* LV Global Function Index Provides Incremental Prognostic Value Over LGE and LV GLS in HCM. *JACC: Cardiovascular Imaging* **13**, 2052–2054 (2020).

110. Nwabuo, C. C. *et al.* Left ventricular global function index predicts incident heart failure and cardiovascular disease in young adults: The coronary artery risk development in young adults (CARDIA) study. *European Heart Journal Cardiovascular Imaging* **20**, 533–540 (2019).

111. Patel, H. N. *et al.* Normal Values of Cardiac Output and Stroke Volume According to Measurement Technique, Age, Sex, and Ethnicity: Results of the World Alliance of Societies of Echocardiography Study. *Journal of the American Society of Echocardiography* **34**, 1077-1085.e1 (2021).

112. Tsao, C. W. *et al.* Left ventricular structure and risk of cardiovascular events: A framingham heart study cardiac magnetic resonance study. *Journal of the American Heart Association* **4**, e002188 (2015).

113. Kawel-Boehm, N. *et al.* Left Ventricular Mass at MRI and Long-term Risk of Cardiovascular Events: The Multi-Ethnic Study of Atherosclerosis (MESA). *Radiology* **293**, 107–114 (2019).

114. McCracken, C. *et al.* Ventricular volume asymmetry as a novel imaging biomarker for disease discrimination and outcome prediction | medRxiv. https://www.medrxiv.org/content/10.1101/2023.11.03.23298024v1 (2023).

115. Bard, A. *et al.* Automated quality-controlled cardiovascular magnetic resonance pericardial fat quantification using a convolutional neural network in the UK Biobank. *Frontiers in Cardiovascular Medicine* **8**, 677574 (2021).

116. Ardissino, M. *et al.* Pericardial adiposity is independently linked to adverse cardiovascular phenotypes: a CMR study of 42 598 UK Biobank participants. *European Heart Journal - Cardiovascular Imaging* jeac101 (2022) doi:10.1093/EHJCI/JEAC101.

117. Raisi-Estabragh, Z. *et al.* Incident clinical and mortality associations of myocardial native T1 in the UK Biobank. *JACC: Cardiovascular Imaging* (2022) doi:10.1016/j.jcmg.2022.06.011.

118. Biasiolli, L. *et al.* Automated localization and quality control of the aorta in cine CMR can significantly accelerate processing of the UK Biobank population data. *PLOS ONE* **14**, e0212272 (2019).

119. Redheuil, A. *et al.* Proximal aortic distensibility is an independent predictor of all-cause mortality and incident CV events: The MESA study. *Journal of the American College of Cardiology* **64**, 2619–2629 (2014).

120. Smith, S. M. *et al.* Accurate, robust, and automated longitudinal and cross-sectional brain change analysis. *NeuroImage* **17**, 479–489 (2002).

121. Miller, K. L. *et al.* Multimodal population brain imaging in the UK Biobank prospective epidemiological study. *Nature Neuroscience* **19**, 1523–1536 (2016).

122. Whitwell, J. L. Progression of atrophy in Alzheimer's disease and related disorders. *Neurotoxicity Research* **18**, 339–346 (2010).

123. Moran, C. *et al.* Brain Atrophy in Type 2 Diabetes: Regional distribution and influence on cognition. *Diabetes Care* **36**, 4036–4042 (2013).

124. Chen, X. *et al.* Depression, anxiety and brain volume after hearing loss and tinnitus: cohort study in the UK Biobank. *BJPsych Open* **10**, e37 (2024).

125. Oyarce, D. A. E., Shaw, M. E., Alateeq, K. & Cherbuin, N. Volumetric brain differences in clinical depression in association with anxiety: a systematic review with meta-analysis. *Journal of Psychiatry and Neuroscience* **45**, 406–429 (2020).

126. Debette, S. *et al.* Midlife vascular risk factor exposure accelerates structural brain aging and cognitive decline. *Neurology* **77**, 461–468 (2011).

127. Cox, S. R. *et al.* Associations between vascular risk factors and brain MRI indices in UK Biobank. *European Heart Journal* **40**, 2290–2300 (2019).

128. Jokinen, H. *et al.* Global Burden of Small Vessel Disease-Related Brain Changes on MRI Predicts Cognitive and Functional Decline. *Stroke* **51**, 170–178 (2020).

129. Prins, N. D. & Scheltens, P. White matter hyperintensities, cognitive impairment and dementia: an update. *Nature Reviews Neurology* **11**, 157–165 (2015).

130. Debette, S., Schilling, S., Duperron, M. G., Larsson, S. C. & Markus, H. S. Clinical Significance of Magnetic Resonance Imaging Markers of Vascular Brain Injury: A Systematic Review and Meta-analysis. *JAMA Neurology* **76**, 81–94 (2019).

131. Zhang, H., Schneider, T., Wheeler-Kingshott, C. A. & Alexander, D. C. NODDI: Practical in vivo neurite orientation dispersion and density imaging of the human brain. *NeuroImage* **61**, 1000–1016 (2012).

132. Jones, D. K., Knösche, T. R. & Turner, R. White matter integrity, fiber count, and other fallacies: The do's and don'ts of diffusion MRI. *NeuroImage* **73**, 239–254 (2013).

133. Kamagata, K. *et al.* Diffusion Magnetic Resonance Imaging-Based Biomarkers for Neurodegenerative Diseases. *International Journal of Molecular Sciences* **22**, 5216 (2021).

134. Andica, C. *et al.* Neurite orientation dispersion and density imaging reveals white matter microstructural alterations in adults with autism. *Molecular Autism* **12**, 1–14 (2021).

135. Sone, D. *et al.* Abnormal neurite density and orientation dispersion in unilateral temporal lobe epilepsy detected by advanced diffusion imaging. *NeuroImage: Clinical* **20**, 772–782 (2018).

136. Suzuki, H. *et al.* Abnormal brain white matter microstructure is associated with both pre-hypertension and hypertension. *PLoS ONE* **12**, e0187600 (2017).

137. Franke, K. & Gaser, C. Ten years of brainage as a neuroimaging biomarker of brain aging: What insights have we gained? *Frontiers in Neurology* **10**, 789 (2019).

138. Wilman, H. R. *et al.* Characterisation of liver fat in the UK Biobank cohort. *PLoS ONE* **12**, e0172921 (2017).

139. Noureddin, M. *et al.* Utility of magnetic resonance imaging versus histology for quantifying changes in liver fat in nonalcoholic fatty liver disease trials. *Hepatology* **58**, 1930–1940 (2013).

140. Loomba, R. *et al.* Multicenter Validation of Association Between Decline in MRI-PDFF and Histologic Response in NASH. *Hepatology* **72**, 1219 (2020).

141. Patel, J. *et al.* Association of noninvasive quantitative decline in liver fat content on MRI with histologic response in nonalcoholic steatohepatitis. *Therapeutic Advances in Gastroenterology* **9**, 692–701 (2016).

142. Amin, K., Mileto, A. & Kolokythas, O. MRI for liver iron quantification: concepts and ccurrent methods. *Seminars in Ultrasound, CT and MRI* **43**, 364–370 (2022).

143. McKay, A. *et al.* Measurement of liver iron by magnetic resonance imaging in the UK Biobank population. *PLOS ONE* **13**, e0209340 (2018).

144. Mojtahed, A. *et al.* Reference range of liver corrected T1 values in a population at low risk for fatty liver disease—a UK Biobank sub-study, with an appendix of interesting cases. *Abdominal Radiology* **44**, 72–84 (2019).

145. Dennis, A. *et al.* Correlations Between MRI Biomarkers PDFF and cT1 With Histopathological Features of Non-Alcoholic Steatohepatitis. *Frontiers in Endocrinology* **11**, (2021).

146. Jayaswal, A. N. A. *et al.* Prognostic value of multiparametric magnetic resonance imaging, transient elastography and blood-based fibrosis markers in patients with chronic liver disease. *Liver International* **40**, 3071–3082 (2020).

147. Bachtiar, V. *et al.* Repeatability and reproducibility of multiparametric magnetic resonance imaging of the liver. *PloS One* **14**, e0214921 (2019).

148. Harrison, S. A. *et al.* Prospective evaluation of the prevalence of non-alcoholic fatty liver disease and steatohepatitis in a large middle-aged US cohort. *Journal of Hepatology* **75**, 284–291 (2021).

149. Eslam, M., Sanyal, A. J. & George, J. Toward More Accurate Nomenclature for Fatty Liver Diseases. *Gastroenterology* **157**, 590–593 (2019).

150. Eslam, M. *et al.* MAFLD: A consensus-driven proposed nomenclature for metabolic associated fatty liver disease. *Gastroenterology* **158**, 1999-2014.e1 (2020).

151. Gao, E., Hercun, J., Heller, T. & Vilarinho, S. Undiagnosed liver diseases. *Translational Gastroenterology and Hepatology* **6**, (2021).

152. Koo, S. *et al.* Uncovering undiagnosed liver disease: prevalence and opportunity for intervention in a population attending colonoscopy. *BMJ Open Gastroenterology* **8**, e000638 (2021).

153. Santos, C. Y. *et al.* Pathophysiologic relationship between Alzheimer's disease, cerebrovascular disease, and cardiovascular risk: A review and synthesis. *Alzheimer's & Dementia: Diagnosis, Assessment & Disease Monitoring* **7**, 69–87 (2017).

154. Alloubani, A., Nimer, R. & Samara, R. Relationship between hyperlipidemia, cardiovascular disease and stroke: a systematic review. *Current Cardiology Reviews* **17**, e051121189015 (2021).

155. Manea, M. M., Comsa, M., Minca, A., Dragos, D. & Popa, C. Brain-heart axis--Review Article. *Journal of medicine and life* **8**, 266–271 (2015).

156. Lip, G. Y. & Lim, H. S. Atrial fibrillation and stroke prevention. *The Lancet Neurology* **6**, 981–993 (2007).

157. Liang, X., Huang, Y. & Han, X. Associations between coronary heart disease and risk of cognitive impairment: A meta-analysis. *Brain and behavior* **11**, (2021).

158. Kwok, C. S., Loke, Y. K., Hale, R., Potter, J. F. & Myint, P. K. Atrial fibrillation and incidence of dementia: A systematic review and meta-analysis. *Neurology* **76**, 914–922 (2011).

159. Vogels, R. L. C., Scheltens, P., Schroeder-Tanka, J. M. & Weinstein, H. C. Cognitive impairment in heart failure: A systematic review of the literature. *European Journal of Heart Failure* **9**, 440–449 (2007).

160. Alosco, M. L. & Hayes, S. M. Structural brain alterations in heart failure: a review of the literature and implications for risk of Alzheimer's disease. *Heart Failure Reviews* **20**, 561–571 (2015).

161. Jefferson, A. L. *et al.* Cardiac index is associated with brain aging: The framingham heart study. *Circulation* **122**, 690–697 (2010).

162. Jefferson, A. L. Cardiac output as a potential risk factor for abnormal brain aging. *Journal of Alzheimer's Disease* **20**, 813–821 (2010).

163. Schmidt, R., Fazekas, F., Offenbacher, H., Dusleag, J. & Lechner, H. Brain magnetic resonance imaging and neuropsychologic evaluation of patients with idiopathic dilated cardiomyopathy. *Stroke* **22**, 195–199 (1991).

164. Woo, M. A. *et al.* Global and regional brain mean diffusivity changes in patients with heart failure. *Journal of Neuroscience Research* **93**, 678–685 (2015).

165. Suzuki, H. *et al.* Coronary artery calcium assessed years before was positively associated with subtle white matter injury of the brain in asymptomatic middle-aged men the Framingham heart study. *Circulation: Cardiovascular Imaging* **14**, 621–628 (2021).

166. Pase, M. P. *et al.* Association of Aortic Stiffness with Cognition and Brain Aging in Young and Middle-Aged Adults: The Framingham Third Generation Cohort Study. *Hypertension* **67**, 513–519 (2016).

167. Badji, A. *et al.* Arterial stiffness and brain integrity: A review of MRI findings. *Ageing Research Reviews* **53**, 100907 (2019).

168. Winbo, A. & Paterson, D. J. The brain-heart connection in sympathetically triggered inherited arrhythmia syndromes. *Heart, Lung and Circulation* **29**, 529–537 (2020).

169. Moroni, F. *et al.* Carotid atherosclerosis, silent ischemic brain damage and brain atrophy: A systematic review and meta-analysis. *International Journal of Cardiology* **223**, 681–687 (2016).

170. Kimmerly, D. S. A review of human neuroimaging investigations involved with central autonomic regulation of baroreflex-mediated cardiovascular control. *Autonomic Neuroscience: Basic and Clinical* **207**, 10–21 (2017).

171. Templin, C. *et al.* Altered limbic and autonomic processing supports brain-heart axis in Takotsubo syndrome. *European Heart Journal* **40**, 1183–1187 (2019).

172. Radfar, A. *et al.* Stress-associated neurobiological activity associates with the risk for and timing of subsequent Takotsubo syndrome. *European Heart Journal* **42**, 1898–1908 (2021).

173. de Roos, A. & Lamb, H. J. Exploring the Interaction between Liver and Heart Disease. *Radiology* **297**, 62–63 (2020).

174. Targher, G., Day, C. P. & Bonora, E. Risk of Cardiovascular Disease in Patients with Nonalcoholic Fatty Liver Disease. *New England Journal of Medicine* **363**, 1341–1350 (2010).

175. Tariq, R., Axley, P. & Singal, A. K. Extra-Hepatic Manifestations of Nonalcoholic Fatty Liver Disease: A Review. *Journal of Clinical and Experimental Hepatology* **10**, 81–87 (2020).

176. Jaruvongvanich, V., Wirunsawanya, K., Sanguankeo, A. & Upala, S. Nonalcoholic fatty liver disease is associated with coronary artery calcification: A systematic review and meta-analysis. *Digestive and Liver Disease* **48**, 1410–1417 (2016).

177. Stahl, E. P. *et al.* Nonalcoholic Fatty Liver Disease and the Heart: JACC State-of-the-Art Review. *Journal of the American College of Cardiology* **73**, 948–963 (2019).

178. Emamat, H., Tangestani, H., Nasab, M. B., Ghalandari, H. & Hekmatdoost, A. The association between epicardial adipose tissue and non-alcoholic fatty liver disease: A systematic review of existing human studies. *EXCLI Journal* **20**, 1096 (2021).

179. Ismaiel, A., HA, C., Rusu, F. & DL, D. Cardiac Arrhythmias and Electrocardiogram Modifications in Non-Alcoholic Fatty Liver Disease. A Systematic Review. *Journal of gastrointestinal and liver diseases : JGLD* **28**, 483–493 (2019).

180. Minhas, A. M. *et al.* Link Between Non-Alcoholic Fatty Liver Disease and Atrial Fibrillation: A Systematic Review and Meta-Analysis. *Cureus* **9**, (2017).

181. Mantovani, A. *et al.* Risk of Heart Failure in Patients With Nonalcoholic Fatty Liver Disease: JACC Review Topic of the Week. *Journal of the American College of Cardiology* **79**, 180–191 (2022).

182. Gîrleanu, I. *et al.* Ischemic Heart Disease and Liver Cirrhosis: Adding Insult to Injury. *Life* **12**, 1036 (2022).

183. Borges-Canha, M. *et al.* Association between nonalcoholic fatty liver disease and cardiac function and structure—a meta-analysis. *Endocrine* **66**, 467–476 (2019).

184. Kostka, F. *et al.* Cardiac remodelling in non-alcoholic fatty liver disease in the general population. *Liver International* **44**, 1032–1041 (2024).

185. Fan, N. *et al.* Association of the Non-Alcoholic Fatty Liver Disease Fibrosis Score with subclinical myocardial remodeling in patients with type 2 diabetes: A cross-sectional study in China. *Journal of Diabetes Investigation* **12**, 1035–1041 (2021).

186. VanWagner, L. B. *et al.* Longitudinal association of non-alcoholic fatty liver disease with changes in myocardial structure and function: The CARDIA Study. *Journal of the American Heart Association* **9**, (2020).

187. Dong, Y. *et al.* Assessment of left ventricular function in type 2 diabetes mellitus patients with non-alcoholic fatty liver disease using three-dimensional speckle-tracking echocardiography. *Anatolian Journal of Cardiology* **23**, 41 (2020).

188. Kato, Y. *et al.* Usefulness of Liver Magnetic Resonance Elastography for Estimating Right-Atrial Pressure in Heart Failure Patients. *JACC: Cardiovascular Imaging* **13**, 2050–2052 (2020).

189. Isaak, A. *et al.* Myocardial fibrosis and inflammation in liver cirrhosis: MRI study of the liver-Heart axis. *Radiology* **297**, 51–61 (2020).

190. Butterworth, R. F. The liver–brain axis in liver failure: neuroinflammation and encephalopathy. *Nature Reviews Gastroenterology & Hepatology* **10**, 522–528 (2013).

191. D'Mello, C. & Swain, M. G. Liver-brain inflammation axis. *American Journal of Physiology - Gastrointestinal and Liver Physiology* **301**, 749–761 (2011).

192. Lombardi, R., Fargion, S. & Fracanzani, A. L. Brain involvement in non-alcoholic fatty liver disease (NAFLD): A systematic review. *Digestive and Liver Disease* **51**, 1214–1222 (2019).

193. Hadjihambi, A., Arias, N., Sheikh, M. & Jalan, R. Hepatic encephalopathy: a critical current review. *Hepatology International 2017 12:1* **12**, 135–147 (2017).

194. Airaghi, L. *et al.* Subclinical cerebrovascular disease in NAFLD without overt risk factors for atherosclerosis. *Atherosclerosis* **268**, 27–31 (2018).

195. Wang, M. *et al.* Association between non-alcoholic fatty liver disease and risk of stroke: a systematic review and meta-analysis. *Frontiers in Cardiovascular Medicine* **9**, (2022).

196. Zheng, K. *et al.* Risk of Stroke in Liver Cirrhosis: A Systematic Review and Meta-Analysis. *Journal of Clinical Gastroenterology* **54**, 96–105 (2020).

197. Ahluwalia, V. *et al.* Impaired gut-liver-brain axis in patients with cirrhosis. *Scientific Reports 2016 6:1* **6**, 1–11 (2016).

198. Weinstein, G. *et al.* Association of nonalcoholic fatty liver disease with lower brain volume in healthy middle-aged adults in the Framingham Study. *JAMA Neurology* **75**, 97–104 (2018).

199. Rovira, A. *et al.* Decreased white matter lesion volume and improved cognitive function after liver transplantation. *Hepatology* **46**, 1485–1490 (2007).

200. Chavarria, L. *et al.* Biexponential Analysis of Diffusion-Tensor Imaging of the Brain in Patients with Cirrhosis before and after Liver Transplantation. *American Journal of Neuroradiology* **32**, 1510–1517 (2011).

201. Asakawa, Y. *et al.* Relationship between Fatty Liver Disease and Intracranial Main Artery Stenosis. *Internal Medicine* **53**, 1259–1264 (2014).

202. Targher, G. *et al.* Relations between carotid artery wall thickness and liver histology in subjects with nonalcoholic fatty liver disease. *Diabetes Care* **29**, 1325–1330 (2006).

203. Raman, G. *et al.* Association of Intracranial Artery Stenosis and Carotid Artery Disease in Patients with Non-Alcoholic Fatty Liver Disease and Normal Subjects. *International Journal of Contemporary Medicine Surgery and Radiology* **5**, (2019).

204. Fletcher, N. F. & McKeating, J. A. Hepatitis C virus and the brain. *Journal of Viral Hepatitis* **19**, 301–306 (2012).

205. Anand, S. K., Ahmad, M. H., Sahu, M. R., Subba, R. & Mondal, A. C. Detrimental effects of alcohol-induced inflammation on brain health: from neurogenesis to neurodegeneration. *Cellular and Molecular Neurobiology* **43**, 1885–1904 (2023).

206. Weiss, N. & Thabut, D. Neurological Complications Occurring After Liver Transplantation: Role of Risk Factors, Hepatic Encephalopathy, and Acute (on Chronic) Brain Injury. *Liver Transplantation* **25**, 469–487 (2019).

207. Bucsics, T. & Krones, E. Renal dysfunction in cirrhosis: acute kidney injury and the hepatorenal syndrome. *Gastroenterology Report* **5**, 127–137 (2017).

208. Viswanathan, G. & Gilbert, S. The Cardiorenal Syndrome: Making the Connection. *International Journal of Nephrology* **2011**, 283137 (2011).

209. Jankowski, J., Floege, J., Fliser, D., Böhm, M. & Marx, N. Cardiovascular Disease in Chronic Kidney Disease. *Circulation* **143**, 1157–1172 (2021).

210. Kanjanahattakij, N. *et al.* High right ventricular stroke work index is associated with worse kidney function in patients with heart failure with preserved ejection fraction. *CardioRenal Medicine* **8**, 123–129 (2018).

211.Di Lullo, L. *et al.* Pulmonary Hypertension and Right Heart Failure in Chronic Kidney Disease: New Challenge for 21st-Century Cardionephrologists. *Cardiorenal Medicine* **3**, 96–103 (2013).

212. Bugnicourt, J.-M., Godefroy, O., Chillon, J.-M., Choukroun, G. & Massy, Z. A. Cognitive Disorders and Dementia in CKD: The Neglected Kidney-Brain Axis. *Journal of the American Society of Nephrology* **24**, 353 (2013).

213. Scheppach, J. B. *et al.* Association of Kidney Function Measures With Signs of Neurodegeneration and Small Vessel Disease on Brain Magnetic Resonance Imaging: The Atherosclerosis Risk in Communities (ARIC) Study. *American Journal of Kidney Diseases* **81**, 261-269.e1 (2023).

214. Chen, X. *et al.* Kidney damage causally affects the brain cortical structure: A Mendelian randomization study. *eBioMedicine* **72**, (2021).

215. Oishi, Y. & Manabe, I. Organ system crosstalk in cardiometabolic disease in the age of multimorbidity. *Frontiers in Cardiovascular Medicine* **7**, 64 (2020).

216. Mottillo, S. *et al.* The metabolic syndrome and cardiovascular risk: A systematic review and meta-analysis. *Journal of the American College of Cardiology* **56**, 1113–1132 (2010).

217. Ndumele, C. E. *et al.* Cardiovascular-Kidney-Metabolic Health: A Presidential Advisory From the American Heart Association. *Circulation* **148**, 1606–1635 (2023).

218. Katsiki, N., Kolovou, G., Melidonis, A. & Banach, M. The Cardiac-Kidney-Liver (CKL) syndrome: the “real entity” of type 2 diabetes mellitus. *Archives of Medical Science : AMS* **20**, 207–215 (2024).

219. Livingston, G. *et al.* Dementia prevention, intervention, and care: 2020 report of the Lancet Commission. *The Lancet* **396**, 413–446 (2020).

220. Boehme, A. K., Esenwa, C. & Elkind, M. S. V. Stroke Risk Factors, Genetics, and Prevention. *Circulation Research* **120**, 472–495 (2017).

221. Arnett, D. K. *et al.* 2019 ACC/AHA Guideline on the Primary Prevention of Cardiovascular Disease: A Report of the American College of Cardiology/American Heart Association Task Force on Clinical Practice Guidelines. *Circulation* **140**, e596–e646 (2019).

222. Al, -Khatib Sana M. *et al.* 2017 AHA/ACC/HRS Guideline for Management of Patients With Ventricular Arrhythmias and the Prevention of Sudden Cardiac Death. *Journal of the American College of Cardiology* **72**, e91–e220 (2018).

223. Younossi, Z. *et al.* Global burden of NAFLD and NASH: trends, predictions, risk factors and prevention. *Nature Reviews Gastroenterology & Hepatology* **15**, 11–20 (2018).

224. Yang, J. D. *et al.* A global view of hepatocellular carcinoma: trends, risk, prevention and management. *Nature Reviews Gastroenterology & Hepatology* **16**, 589–604 (2019).

225. Lauer, M. S. Primary Prevention of Atherosclerotic Cardiovascular Disease: The High Public Burden of Low Individual Risk. *JAMA* **297**, 1376–1378 (2007).

226. Ties, D. *et al.* Multi-Modality Imaging for Prevention of Coronary Artery Disease and Myocardial Infarction in the General Population: Ready for Prime Time? *Journal of Clinical Medicine* **11**, 2965 (2022).

227. Meah, M. N., Dweck, M. R. & Newby, D. E. Cardiovascular imaging to guide primary prevention. *Heart* **106**, 1267–1275 (2020).

228. Collij, L. E. *et al.* The amyloid imaging for the prevention of Alzheimer's disease consortium: A European collaboration with global impact. *Frontiers in Neurology* **13**, (2023).

229. Young, P. N. E. *et al.* Imaging biomarkers in neurodegeneration: current and future practices. *Alzheimer's Research & Therapy* **12**, 49 (2020).

230. Walsh, S. *et al.* A systematic review of the cost-effectiveness of community and population interventions to reduce the modifiable risk factors for dementia. *Maturitas* **166**, 104–116 (2022).

231. Li, W. *et al.* Cost-effectiveness of physical activity interventions for prevention and management of cognitive decline and dementia—a systematic review. *Alzheimer's Research & Therapy* **15**, 159 (2023).

232. Mukadam, N. *et al.* Effective interventions for potentially modifiable risk factors for late-onset dementia: a costs and cost-effectiveness modelling study. *The Lancet Healthy Longevity* **1**, e13–e20 (2020).

233. Braun, A., Höfler, M. & Auer, S. Cost-Effectiveness of Prevention for People at Risk for Dementia: A Scoping Review and Qualitative Synthesis. *The Journal of Prevention of Alzheimer's Disease* **11**, 402–413 (2024).

234. Bhagia, G. & Kumar, S. Early MRI versus CT scan for evaluation of cerebrovascular events in a community hospital: a cost minimization analysis. *Cureus* **12**, e12127 (2020).

235. Martinez, G. *et al.* Cost-Effectiveness Study of Initial Imaging Selection in Acute Ischemic Stroke Care. *Journal of the American College of Radiology* **18**, 820–833 (2021).

236. Lechtman, E. *et al.* Cost-effectiveness of magnetic resonance carotid plaque imaging for primary stroke prevention in Canada. *British Journal of Radiology* **91**, 20170518 (2018).

237. Puhr-Westerheide, D. *et al.* Cost-effectiveness of short-protocol emergency brain MRI after negative non-contrast CT for minor stroke detection. *European Radiology* **32**, 1117–1126 (2022).

238. Otero, H. J. *et al.* Cost-effective diagnostic cardiovascular imaging: when does it provide good value for the money? *The International Journal of Cardiovascular Imaging* **26**, 605–612 (2010).

239. Walker, S. *et al.* Cost-effectiveness of cardiovascular imaging for stable coronary heart disease. *Heart* **107**, 381–388 (2021).

240. Ge, Y. *et al.* Cost-Effectiveness Analysis of Stress Cardiovascular Magnetic Resonance Imaging for Stable Chest Pain Syndromes. *JACC: Cardiovascular Imaging* **13**, 1505–1517 (2020).

241. Ibrahim, E.-S. H. *et al.* Value CMR: Towards a Comprehensive, Rapid, Cost-Effective Cardiovascular Magnetic Resonance Imaging. *International Journal of Biomedical Imaging* **2021**, 8851958 (2021).

242. Younossi, Z. M. *et al.* Identification of high-risk patients with nonalcoholic fatty liver disease using noninvasive tests from primary care and endocrinology real-world practices. *Clinical and Translational Gastroenterology* **12**, e00340 (2021).

243. McLeod, A. *et al.* Liver function tests in primary care provide a key opportunity to diagnose and engage patients with hepatitis C. *Epidemiology & Infection* **150**, (2022).

244. Pandyarajan, V., Gish, R. G., Alkhouri, N. & Noureddin, M. Screening for Nonalcoholic Fatty Liver Disease in the Primary Care Clinic. *Gastroenterology & Hepatology* **15**, 357–365 (2019).

245. Tapper, E. B., Hunink, M. G. M., Afdhal, N. H., Lai, M. & Sengupta, N. Cost-effectiveness analysis: Risk stratification of nonalcoholic fatty liver disease (NAFLD) by the primary care physician using the NAFLD Fibrosis Score. *PloS one* **11**, (2016).

246. Crossan, C. *et al.* Cost-effectiveness of non-invasive methods for assessment and monitoring of liver fibrosis and cirrhosis in patients with chronic liver disease: systematic review and economic evaluation. *Health technology assessment* **19**, 1–458 (2015).

247. Srivastava, A. *et al.* Cost-comparison analysis of FIB-4, ELF and fibroscan in community pathways for non-alcoholic fatty liver disease. *BMC Gastroenterology 2019 19:1* **19**, 1–15 (2019).

248. Ahlawat, S. *et al.* Clinical applications and controversies of whole-body MRI: AJR Expert Panel narrative review. *American Journal of Roentgenology* **220**, 463–475 (2023).

249. Kwee, R. M. & Kwee, T. C. Whole-body MRI for preventive health screening: A systematic review of the literature. *Journal of Magnetic Resonance Imaging* **50**, 1489–1503 (2019).

250. Basar, Y., Alis, D., Tekcan Sanli, D. E., Akbas, T. & Karaarslan, E. Whole-body MRI for preventive health screening: Management strategies and clinical implications. *European Journal of Radiology* **137**, 109584 (2021).

251. Zugni, F. *et al.* Whole-body magnetic resonance imaging (WB-MRI) for cancer screening in asymptomatic subjects of the general population: review and recommendations. *Cancer Imaging* **20**, 34 (2020).

252. Schmidt, C. O. *et al.* Psychosocial consequences and severity of disclosed incidental findings from whole-body MRI in a general population study. *European Radiology* **23**, 1343–1351 (2013).

253. Smith, S. M., Alfaro-Almagro, F. & Miller, K. L. UK Biobank - Brain Imaging Documentation (2020). *https://biobank.ctsu.ox.ac.uk/crystal/crystal/docs/brain_mri.pdf* (Date accessed: 29 October 2021).

254. Alfaro-Almagro, F. *et al.* Image processing and Quality Control for the first 10,000 brain imaging datasets from UK Biobank. *NeuroImage* **166**, 400–424 (2018).

255. Petersen, S. E. *et al.* UK Biobank's cardiovascular magnetic resonance protocol. *Journal of Cardiovascular Magnetic Resonance* **18**, 8 (2016).

256. Bai, W. *et al.* Automated cardiovascular magnetic resonance image analysis with fully convolutional networks. *Journal of Cardiovascular Magnetic Resonance* **20**, 1–12 (2018).

257. The IPAQ group. Guidelines for data processing and analysis of the International Physical Activity Questionnaire (IPAQ) – Short and long forms (2005). *https://biobank.ndph.ox.ac.uk/ukb/ukb/docs/ipaq_analysis.pdf* (Date accessed: 21 October 2021).

258. NHS England. Physical activity guidelines for adults aged 19 to 64. *nhs.uk* https://www.nhs.uk/live-well/exercise/exercise-guidelines/physical-activity-guidelines-for-adults-aged-19-to-64/ (2022).

259. Alfaro-Almagro, F. *et al.* Confound modelling in UK Biobank brain imaging. *NeuroImage* **224**, 117002 (2021).

260. Adamska, L. *et al.* Challenges of linking to routine healthcare records in UK Biobank. *Trials* **16**, O68 (2015).

261. UK Biobank. Resource 594: Code lists for algorithmically-defined outcomes. https://biobank.ndph.ox.ac.uk/showcase/refer.cgi?id=594 (2022).

262. HDRUK: Health Data Research United Kingdom. Phenotype Library. http://phenotypes.healthdatagateway.org/ (2024).

263. University of Cambridge. Department of Public Health and Primary Care: CPRD Codelists. https://www.phpc.cam.ac.uk/pcu/cprd_cam/codelists/ (2020).

264. Smith, S. M. *et al.* Advances in functional and structural MR image analysis and implementation as FSL. *NeuroImage* **23**, S208–S219 (2004).

265. Fischl, B. *et al.* Whole Brain Segmentation. *Neuron* **33**, 341–355 (2002).

266. UK Biobank. Brain imaging documentation: Resource 1977. https://biobank.ndph.ox.ac.uk/showcase/refer.cgi?id=1977 (2024).

267. Peterson, R. A. & Cavanaugh, J. E. Ordered quantile normalization: a semiparametric transformation built for the cross-validation era. *Journal of Applied Statistics* **47**, 2312–2327 (2020).

268. Puyol-Antón, E. *et al.* Automated quantification of myocardial tissue characteristics from native T1 mapping using neural networks with uncertainty-based quality-control. *Journal of Cardiovascular Magnetic Resonance* **22**, 60 (2020).

269. UK Biobank. Carotid ultrasound: Resource 511. https://biobank.ndph.ox.ac.uk/showcase/refer.cgi?id=511 (2015).

270. Damen, J. A. A. G. *et al.* Prediction models for cardiovascular disease risk in the general population: systematic review. *BMJ* **353**, i2416 (2016).

271. Hippisley-Cox, J., Coupland, C. & Brindle, P. Derivation and validation of QStroke score for predicting risk of ischaemic stroke in primary care and comparison with other risk scores: a prospective open cohort study. *BMJ* **346**, f2573 (2013).

272. Ntaios, G. *et al.* CHADS2, CHA2DS2-VASc, and long-term stroke outcome in patients without atrial fibrillation. *Neurology* **80**, 1009–1017 (2013).

273. Kivipelto, M. *et al.* Risk score for the prediction of dementia risk in 20 years among middle aged people: a longitudinal, population-based study. *The Lancet Neurology* **5**, 735–741 (2006).

274. Schiepers, O. J. G. *et al.* Lifestyle for Brain Health (LIBRA): a new model for dementia prevention. *International journal of geriatric psychiatry* **33**, 167–175 (2018).

275. Anatürk, M. *et al.* Development and validation of a dementia risk score in the UK Biobank and Whitehall II cohorts. *BMJ Mental Health* **26**, 1–7 (2023).

276. D'Agostino, R. B. *et al.* General cardiovascular risk profile for use in primary care. *Circulation* **117**, 743–753 (2008).

277. Khan, S. S. *et al.* 10-year risk equations for incident heart failure in the general population. *Journal of the American College of Cardiology* **73**, 2388–2397 (2019).

278. Hippisley-Cox, J., Coupland, C. & Brindle, P. Development and validation of QRISK3 risk prediction algorithms to estimate future risk of cardiovascular disease: Prospective cohort study. *BMJ (Online)* **357**, 1–21 (2017).

279. Alonso, A. *et al.* Simple risk model predicts incidence of atrial fibrillation in a racially and geographically diverse population: the CHARGE-AF consortium. *Journal of the American Heart Association* **2**, e000102 (2013).

280. Hippisley-Cox, J. & Coupland, C. Predicting the risk of chronic kidney disease in men and women in England and Wales: prospective derivation and external validation of the QKidney®Scores. *BMC Family Practice* **11**, 49 (2010).

281. Nelson, R. G. *et al.* Development of risk prediction equations for incident chronic kidney disease. *JAMA* **322**, 2104–2114 (2019).

282. Bedogni, G. *et al.* The fatty liver index: A simple and accurate predictor of hepatic steatosis in the general population. *BMC Gastroenterology* **6**, 33 (2006).

283. McHenry, S., Park, Y., Browning, J. D., Sayuk, G. & Davidson, N. O. Dallas Steatosis Index identifies patients with nonalcoholic fatty liver disease. *Clinical Gastroenterology and Hepatology* **18**, 2073-2080.e7 (2020).

284. Hippisley-Cox, J. & Coupland, C. Development and validation of QDiabetes-2018 risk prediction algorithm to estimate future risk of type 2 diabetes: cohort study. *BMJ* **359**, j5019 (2017).

285. Griffin, S. J., Little, P. S., Hales, C. N., Kinmonth, A. L. & Wareham, N. J. Diabetes risk score: Towards earlier detection or type 2 diabetes in general practice. *Diabetes/Metabolism Research and Reviews* **16**, 164–171 (2000).

286. Bush, K., Kivlahan, D. R., McDonell, M. B., Fihn, S. D. & Bradley, K. A. The AUDIT Alcohol Consumption Questions (AUDIT-C): An Effective Brief Screening Test for Problem Drinking. *Archives of Internal Medicine* **158**, 1789–1795 (1998).

287. Vallet-Pichard, A. *et al.* FIB-4: An inexpensive and accurate marker of fibrosis in HCV infection. comparison with liver biopsy and fibrotest. *Hepatology* **46**, 32–36 (2007).

288. Angulo, P. *et al.* The NAFLD fibrosis score: A noninvasive system that identifies liver fibrosis in patients with NAFLD. *Hepatology* **45**, 846–854 (2007).

289. De Matteis, C. *et al.* AST to Platelet Ratio Index (APRI) is an easy-to-use predictor score for cardiovascular risk in metabolic subjects. *Scientific reports* **11**, 14834 (2021).

290. van Buuren, S. & Groothuis-Oudshoorn, K. mice: Multivariate imputation by chained equations in R. *Journal of Statistical Software* **45**, 1–67 (2011).

291. R Core Team. R: A language and environment for statistical computing. R Foundation for Statistical Computing. in *R Version 4.0.3* Vienna, Austria. URL https://www.R-project.org/ (2019).

292. RStudio: Integrated Development for R. Boston, MA URL http://www.rstudio.com/ Preprint at (2021).

293. Therneau, T. M. survival: A Package for Survival Analysis in R. *R package version 2.38* https://cran.r-project.org/web/packages/survival/index.html (2020).

294. Gerds, T. A. pec: Prediction Error Curves for Risk Prediction Models in Survival Analysis. (2023).

295. Fox, J. *et al.* car: Companion to Applied Regression. https://cran.r-project.org/web/packages/car/index.html (2023).

296. Benjamini, Y. & Hochberg, Y. Controlling the false discovery rate: a practical and powerful approach to multiple testing. *Journal of the Royal Statistical Society: Series B* **57**, 289–300 (1995).

297. Meinshausen, N. & Bühlmann, P. Stability selection. *Journal of the Royal Statistical Society: Series B (Statistical Methodology)* **72**, 417–473 (2010).

298. Friedman, J., Hastie, T. & Tibshirani, R. Regularization Paths for Generalized Linear Models via Coordinate Descent. *Journal of statistical software* **33**, 1–22 (2010).

299. Frick, H. rsample 1.2.0: General resampling infrastructure. https://cran.r-project.org/web/packages/rsample/rsample.pdf (2023).

300. Haftorn, K. L. *et al.* Stability selection enhances feature selection and enables accurate prediction of gestational age using only five DNA methylation sites. *Clinical Epigenetics* **15**, 114 (2023).

301. Pencina, M. J., D' Agostino Sr, R. B., D' Agostino Jr, R. B. & Vasan, R. S. Evaluating the added predictive ability of a new marker: From area under the ROC curve to reclassification and beyond. *Statistics in Medicine* **27**, 157–172 (2008).

302. Fawcett, T. An introduction to ROC analysis. *Pattern Recognition Letters* **27**, 861–874 (2006).

303. Robin, X. *et al.* pROC: Display and Analyze ROC Curves. https://cran.r-project.org/web/packages/pROC/index.html (2023).

304. Sing, T., Sander, O., Beerenwinkel, N. & Lengauer, T. ROCR: visualizing classifier performance in R. *Bioinformatics* **21**, 3940–3941 (2005).

305. Kuhn, M. *et al.* caret: Classification and Regression Training. https://cran.r-project.org/web/packages/caret/index.html (2023).

306. Harrell, F. rms: Regression Modeling Strategies. https://cran.r-project.org/web/packages/rms/index.html (2024).

307. Kundu, S., Aulchenko, Y. S., van Duijn, C. M. & Janssens, A. C. J. W. PredictABEL: an R package for the assessment of risk prediction models. *European Journal of Epidemiology* **26**, 261–264 (2011).

308. Potapov, S. & Schmid, W. A. and M. survAUC: Estimators of Prediction Accuracy for Time-to-Event Data. https://cran.r-project.org/web/packages/survAUC/index.html (2023).

309. Blanche, P. timeROC: Time-Dependent ROC Curve and AUC for Censored Survival Data. https://cran.r-project.org/web/packages/timeROC/index.html (2019).

310. Sorrentino, P. *et al.* Liver iron excess in patients with hepatocellular carcinoma developed on non-alcoholic steato-hepatitis. *Journal of Hepatology* **50**, 351–357 (2009).

311. Fawns-Ritchie, C. & Deary, I. J. Reliability and validity of the UK Biobank cognitive tests. *PLOS ONE* **15**, e0231627 (2020).

312. Lyall, D. M. *et al.* Cognitive Test Scores in UK Biobank: Data Reduction in 480,416 Participants and Longitudinal Stability in 20,346 Participants. *PLOS ONE* **11**, e0154222 (2016).

313. Craig, C. L. *et al.* International Physical Activity Questionnaire: 12-Country Reliability and Validity. *Med. Sci. Sports Exerc* **35**, 1381–1395 (2003).

314. Rosseel, Y. Lavaan: An R package for structural equation modeling. *Journal of Statistical Software* **48**, 1–36 (2012).

315. Tucker, L. R. & Lewis, C. A reliability coefficient for maximum likelihood factor analysis. *Psychometrika* **38**, 1–10 (1973).

316. Revelle, W. psych: Procedures for Psychological, Psychometric, and Personality Research. https://cran.r-project.org/web/packages/psych/index.html (2024).

317. Beller, E. *et al.* Hepatic fat is superior to BMI, visceral and pancreatic fat as a potential risk biomarker for neurodegenerative disease. *European Radiology* **29**, 6662–6670 (2019).

318. Gurholt, T. P. *et al.* Population-based body–brain mapping links brain morphology with anthropometrics and body composition. *Translational Psychiatry* **11**, 295 (2021).

319. VanWagner, L. B. *et al.* Nonalcoholic fatty liver disease and measures of early brain health in middle-aged adults: The CARDIA study. *Obesity* **25**, 642–651 (2017).

320. Jang, H. *et al.* Non-alcoholic fatty liver disease and cerebral small vessel disease in Korean cognitively normal individuals. *Scientific Reports* **9**, 1814 (2019).

321. Petta, S. *et al.* The Presence of White Matter Lesions Is Associated With the Fibrosis Severity of Nonalcoholic Fatty Liver Disease. *Medicine* **95**, e3446 (2016).

322. Parisinos, C. A. *et al.* Genome-wide and Mendelian randomisation studies of liver MRI yield insights into the pathogenesis of steatohepatitis. *Journal of Hepatology* **73**, 241–251 (2020).

323. Dekkers, I. A., Jansen, P. R. & Lamb, H. J. Obesity, Brain Volume, and White Matter Microstructure at MRI: A Cross-sectional UK Biobank Study. *Radiology* **291**, 763–771 (2019).

324. Poitelon, Y., Kopec, A. M. & Belin, S. Myelin Fat Facts: An Overview of Lipids and Fatty Acid Metabolism. *Cells* **9**, 812 (2020).

325. Matura, S. *et al.* Association of dietary fat composition with cognitive performance and brain morphology in cognitively healthy individuals. *Acta Neuropsychiatrica* **33**, 134–140 (2021).

326. Pase, M. P. *et al.* Vascular risk at younger ages most strongly associates with current and future brain volume. *Neurology* **91**, e1479 (2018).

327. Singer, J., Trollor, J. N., Baune, B. T., Sachdev, P. S. & Smith, E. Arterial stiffness, the brain and cognition: A systematic review. *Ageing Research Reviews* **15**, 16–27 (2014).

328. Daniele, G., DiLucia, S., Masci, P. G. & del Monte, F. Heart and Brain: Complex Relationships for Left Ventricular Dysfunction. *Current Cardiology Reports* **22**, 72 (2020).

329. van Hout, M. J. P. *et al.* Associations between left ventricular function, vascular function and measures of cerebral small vessel disease: a cross-sectional magnetic resonance imaging study of the UK Biobank. *European Radiology* **31**, 5068–5076 (2021).

330. Moore, E. E. *et al.* Increased Left Ventricular Mass Index Is Associated With Compromised White Matter Microstructure Among Older Adults. *Journal of the American Heart Association* **7**, e009041 (2018).

331. Salerno, J. A. *et al.* Brain atrophy in hypertension: A volumetric magnetic resonance imaging study. *Hypertension* **20**, 340–348 (1992).

332. Dickie, D. A. *et al.* Vascular risk factors and progression of white matter hyperintensities in the Lothian Birth Cohort 1936. *Neurobiology of Aging* **42**, 116–123 (2016).

333. Wassenaar, T. M., Yaffe, K., van der Werf, Y. D. & Sexton, C. E. Associations between modifiable risk factors and white matter of the aging brain: insights from diffusion tensor imaging studies. *Neurobiology of Aging* **80**, 56–70 (2019).

334. Veldsman, M. *et al.* Cerebrovascular risk factors impact frontoparietal network integrity and executive function in healthy ageing. *Nature Communications* **11**, 4340 (2020).

335. Cermakova, P. *et al.* Subclinical cardiac dysfunction and brain health in midlife: CARDIA (Coronary Artery Risk Development in Young Adults) brain magnetic resonance imaging substudy. *Journal of the American Heart Association* **6**, (2017).

336. Raisi-Estabragh, Z. *et al.* Left atrial structure and function are associated with cardiovascular outcomes independent of left ventricular measures: a UK Biobank CMR study. *European Heart Journal - Cardiovascular Imaging* jeac119 (2021) doi:10.1093/EHJCI/JEAB266.

337. Jain, R. *et al.* Canadian Cardiovascular Harmonized National Guideline Endeavour (C-CHANGE) guideline for the prevention and management of cardiovascular disease in primary care: 2022 update. *CMAJ* **194**, E1460–E1480 (2022).

338. Austin, P. C. Optimal caliper widths for propensity-score matching when estimating differences in means and differences in proportions in observational studies. *Pharmaceutical Statistics* **10**, 150–161 (2011).

339. Ho, D. *et al.* MatchIt: Nonparametric preprocessing for parametric causal inference. https://cran.r-project.org/web/packages/MatchIt/index.html (2023).

340. Perry, C., Thurston, M., Alford, S., Cushing, J. & Panter, L. The NHS health check programme in England: a qualitative study. *Health Promotion International* **31**, 106–115 (2016).

341. UK Biobank. Code lists for health outcomes. https://biobank.ndph.ox.ac.uk/showcase/refer.cgi?id=594 (2020).

342. Hagström, H. *et al.* Administrative coding in electronic health care record-based research of NAFLD: an expert panel consensus statement. *Hepatology* **74**, 474–482 (2021).

343. Dolezalova, N. *et al.* Development of an accessible 10-year Digital CArdioVAscular (DiCAVA) risk assessment: a UK Biobank study. *European Heart Journal - Digital Health* **2**, 528–538 (2021).

344. Caleyachetty, R. *et al.* United Kingdom Biobank (UK Biobank): JACC Focus Seminar 6/8. *Journal of the American College of Cardiology* **78**, 56–65 (2021).

345. Charlson, M. E., Pompei, P., Ales, K. L. & MacKenzie, C. R. A new method of classifying prognostic comorbidity in longitudinal studies: Development and validation. *Journal of Chronic Diseases* **40**, 373–383 (1987).

346. Therneau, T., Crowson, C. & Atkinson, E. Using time dependent covariates and time dependent coefficients in the cox model. *Survival Vignettes* **2**, 1–25 (2017).

347. Zhang, Z., Reinikainen, J., Adeleke, K. A., Pieterse, M. E. & Groothuis-Oudshoorn, C. G. M. Time-varying covariates and coefficients in Cox regression models. *Annals of Translational Medicine* **6**, 121 (2018).

348. Shintani, A. K. *et al.* Immortal time bias in critical care research: application of time-varying Cox regression for observational cohort studies. *Critical care medicine* **37**, 2939–2945 (2009).

349. Sebuødegård, S., Botteri, E. & Hofvind, S. Breast cancer mortality after implementation of organized population-based breast cancer screening in Norway. *JNCI: Journal of the National Cancer Institute* **112**, 839–846 (2020).

350. Rothman, K. J. & Lash, T. L. *Modern Epidemiology*. (Wolters Kluwer Health/Lippincott Williams & Wilkins, 2015).

351. Ascherio, A. *et al.* Dietary fat and risk of coronary heart disease in men: cohort follow up study in the United States. *BMJ* **313**, 84–90 (1996).

352. Kivimäki, M. *et al.* Job strain as a risk factor for coronary heart disease: a collaborative meta-analysis of individual participant data. *The Lancet* **380**, 1491–1497 (2012).

353. Van Der Weele, T. J. & Ding, P. Sensitivity analysis in observational research: Introducing the E-Value. *Annals of Internal Medicine* **167**, 268–274 (2017).

354. UK Data Service. 2011 UK Townsend Deprivation Scores. https://statistics.ukdataservice.ac.uk/dataset/2011-uk-townsend-deprivation-scores.

355. Robson, J. *et al.* NHS Health Check comorbidity and management: an observational matched study in primary care. *British Journal of General Practice* **67**, e86–e93 (2017).

356. Chang, K. C.-M. *et al.* Impact of the National Health Service Health Check on cardiovascular disease risk: a difference-in-differences matching analysis. *CMAJ* **188**, E228–E238 (2016).

357. Cook, E. J. *et al.* Who uses NHS health checks? Investigating the impact of ethnicity and gender and method of invitation on uptake of NHS health checks. *International Journal for Equity in Health* **15**, 13 (2016).

358. Bunten, A., Porter, L., Gold, N. & Bogle, V. A systematic review of factors influencing NHS health check uptake: invitation methods, patient characteristics, and the impact of interventions. *BMC public health* **20**, 1–16 (2020).

359. Patel, R. *et al.* Evaluation of the uptake and delivery of the NHS Health Check programme in England, using primary care data from 9.5 million people: a cross-sectional study. *BMJ open* **10**, e042963 (2020).

360. Alageel, S. & Gulliford, M. C. Health checks and cardiovascular risk factor values over six years' follow-up: Matched cohort study using electronic health records in England. *PLOS Medicine* **16**, e1002863 (2019).

361. Thomas, C. *et al.* What are the cost-savings and health benefits of improving detection and management for six high cardiovascular risk conditions in England? An economic evaluation. *BMJ Open* **10**, e037486 (2020).

362. Keyes, K. M. & Westreich, D. UK Biobank, big data, and the consequences of non-representativeness. *The Lancet* **393**, 1297 (2019).

363. Swanson, J. M. The UK Biobank and selection bias. *The Lancet* **380**, 110 (2012).

364. Public Health England. Briefing Document: First Incidence of Stroke—Estimates for England 2007 to 2016. https://assets.publishing.service.gov.uk/government/uploads/system/uploads/attachment_data/file/678444/Stroke_incidence_briefing_document_2018.pdf (2018).

365. Schoeler, T. *et al.* Participation bias in the UK Biobank distorts genetic associations and downstream analyses. *Nature Human Behaviour* **7**, 1216–1227 (2023).

366. Karlsen, T. H. *et al.* The EASL–Lancet Liver Commission: protecting the next generation of Europeans against liver disease complications and premature mortality. *The Lancet* **399**, 61–116 (2022).

367. Shlipak, M. G. *et al.* The case for early identification and intervention of chronic kidney disease: conclusions from a Kidney Disease: Improving Global Outcomes (KDIGO) Controversies Conference. *Kidney International* **99**, 34–47 (2021).

368. Iacobucci, G. Scrap 10 minute consultations, RCGP urges. *BMJ* **365**, l2270 (2019).

369. Badawy, M. A. E. M. D. *et al.* Evaluation of cardiovascular diseases risk calculators for CVDs prevention and management: scoping review. *BMC Public Health* **22**, 1742 (2022).

370. Poppe, K. K. *et al.* Developing and validating a cardiovascular risk score for patients in the community with prior cardiovascular disease. *Heart* **103**, 891–892 (2017).

371. Alonso-Morán, E., Nuño-Solinis, R., Onder, G. & Tonnara, G. Multimorbidity in risk stratification tools to predict negative outcomes in adult population. *European Journal of Internal Medicine* **26**, 182–189 (2015).

372. NHS England. Improving access for all: reducing inequalities in access to general practice services. https://www.england.nhs.uk/publication/improving-access-for-all-reducing-inequalities-in-access-to-general-practice-services/ (2018).

373. Verma, P. & Kerrison, R. Patients' and physicians' experiences with remote consultations in primary care during the COVID-19 pandemic: a multi-method rapid review of the literature. *BJGP Open* **6**, 1–16 (2022).

374. Ladds, E., Khan, M., Moore, L., Kalin, A. & Greenhalgh, T. The impact of remote care approaches on continuity in primary care: a mixed-studies systematic review. *British Journal of General Practice* **73**, e374–e383 (2023).

375. Hosmer, D. W., Lemeshow, S. & Sturdivant, R. *Applied Logistic Regression*. (Wiley, 2013).

376. UK Biobank. Primary Care Linked Data (Version 1.0). https://biobank.ndph.ox.ac.uk/showcase/showcase/docs/primary_care_data.pdf (2019).

377. UK Biobank. Hospital Inpatient Data (Version 4.0). https://biobank.ndph.ox.ac.uk/showcase/showcase/docs/HospitalEpisodeStatistics.pdf (2023).

378. Hayward, K. L. *et al.* Detecting non-alcoholic fatty liver disease and risk factors in health databases: accuracy and limitations of the ICD-10-AM. *BMJ Open Gastroenterology* **8**, e000572 (2021).

379. Somers, R. H. A new asymmetric measure of association for ordinal variables. *American Sociological Review* **27**, 799–811 (1962).

380. Thölke, P. *et al.* Class imbalance should not throw you off balance: Choosing the right classifiers and performance metrics for brain decoding with imbalanced data. *NeuroImage* **277**, 120253 (2023).

381. Pencina, M. J., D'Agostino Sr, R. B. & Steyerberg, E. W. Extensions of net reclassification improvement calculations to measure usefulness of new biomarkers. *Statistics in Medicine* **30**, 11–21 (2011).

382. Correll, C. U. *et al.* Prevalence, incidence and mortality from cardiovascular disease in patients with pooled and specific severe mental illness: a large-scale meta-analysis of 3,211,768 patients and 113,383,368 controls. *World Psychiatry* **16**, 163–180 (2017).

383. Alaa, A. M., Bolton, T., Di Angelantonio, E., Rudd, J. H. F. & van der Schaar, M. Cardiovascular disease risk prediction using automated machine learning: A prospective study of 423,604 UK Biobank participants. *PLOS ONE* **14**, e0213653 (2019).

384. Alsayegh, F. *et al.* Anemia or other comorbidities? using machine learning to reveal deeper insights into the drivers of acute coronary syndromes in hospital admitted patients. *PLOS ONE* **17**, e0262997 (2022).

385. Steinfeldt, J. *et al.* Neural network-based integration of polygenic and clinical information: development and validation of a prediction model for 10-year risk of major adverse cardiac events in the UK Biobank cohort. *The Lancet Digital Health* **4**, e84–e94 (2022).

386. Tu, J. V. Advantages and disadvantages of using artificial neural networks versus logistic regression for predicting medical outcomes. *Journal of Clinical Epidemiology* **49**, 1225–1231 (1996).

387. Bayati, M., Bhaskar, S. & Montanari, A. A low-cost method for multiple disease prediction. *AMIA Annual Symposium Proceedings* **2015**, 329–338 (2015).

388. Mahajan, A., Deonarine, A., Bernal, A., Lyons, G. & Norgeot, B. Developing the total health profile, a generalizable unified set of multimorbidity risk scores derived from machine learning for broad patient populations: retrospective cohort study. *Journal of Medical Internet Research* **23**, e32900 (2021).

389. Livingstone, S. *et al.* Effect of competing mortality risks on predictive performance of the QRISK3 cardiovascular risk prediction tool in older people and those with comorbidity: external validation population cohort study. *The Lancet Healthy Longevity* **2**, e352–e361 (2021).

390. Parsons, R. E. *et al.* Independent external validation of the QRISK3 cardiovascular disease risk prediction model using UK Biobank. *Heart* **109**, 1690–1697 (2023).

391. Zhu, W.-G., Xiong, Q.-M. & Hong, K. Meta-Analysis of CHADS2 versus CHA2DS2-VASc for predicting stroke and thromboembolism in atrial fibrillation patients independent of anticoagulation. *Texas Heart Institute Journal* **42**, 6–15 (2015).

392. Huang, J. Y. Representativeness is not representative: addressing major inferential threats in the UK Biobank and other big data repositories. *Epidemiology* **32**, 189–193 (2021).

393. Atkins, L. *et al.* Influences on NHS Health Check behaviours: a systematic review. *BMC Public Health* **20**, 1359 (2020).

394. McCracken, C. *et al.* Feasibility of multiorgan risk prediction with routinely collected diagnostics: a prospective cohort study in the UK Biobank. *BMJ Evidence-Based Medicine* (2024) doi:10.1136/bmjebm-2023-112518.

395. Bai, W. *et al.* A population-based phenome-wide association study of cardiac and aortic structure and function. *Nature Medicine* **26**, 1654–1662 (2020).

396. Mojtahed, A. *et al.* Reference range of liver corrected T1 values in a population at low risk for fatty liver disease—a UK Biobank sub-study, with an appendix of interesting cases. *Abdominal Radiology* **44**, 72–84 (2019).

397. Russo, C. *et al.* Prevalence and prognostic value of subclinical left ventricular systolic dysfunction by global longitudinal strain in a community-based cohort. *European Journal of Heart Failure* **16**, 1301–1309 (2014).

398. Xu, Y. *et al.* Left atrial enlargement and the risk of stroke: a meta-analysis of prospective cohort studies. *Frontiers in Neurology* **11**, 26 (2020).

399. Parikh, N. S. *et al.* Association of liver fibrosis with cognitive test performance and brain imaging parameters in the UK Biobank study. *Alzheimer's & Dementia* **19**, 1518–1528.

400. Gao, P.-Y. *et al.* Associations of liver dysfunction with incident dementia, cognition, and brain structure: A prospective cohort study of 431 699 adults. *Journal of Neurochemistry* **168**, 26–38 (2024).

401. Debette, S., Markus, H. S. & S Debette, H. M. The clinical importance of white matter hyperintensities on brain magnetic resonance imaging: systematic review and meta-analysis. *BMJ* **341**, 1–9 (2010).

402. Bekler, A. *et al.* Right ventricular function and its relationship with grade of hepatosteatosis in non-alcoholic fatty liver disease: cardiovascular topic. *Cardiovascular Journal Of Africa* **26**, 109–113 (2015).

403. Enenche, A. A. *et al.* Echocardiographic assessment of right ventricular function in patients with liver cirrhosis. *Cureus* **16**, e57410 (2024).

404. Rako, Z. A. *et al.* Liver stiffness is associated with right heart dysfunction, cardiohepatic syndrome, and prognosis in pulmonary hypertension. *The Journal of Heart and Lung Transplantation* **43**, 1105–1115 (2024).

405. Gutiérrez, O. M. Treatment of iron deficiency anemia in ckd and end-stage kidney disease. *Kidney International Reports* **6**, 2261–2269 (2021).

406. Banerjee, A. & Leeson, P. Scoring systems developed by machine learning: intelligent but simple to use? *European Heart Journal* **45**, 937–939 (2024).

407. Nagel, Z. D. *et al.* Towards precision prevention: Technologies for identifying healthy individuals with high risk of disease. *Mutation Research/Fundamental and Molecular Mechanisms of Mutagenesis* **800–802**, 14–28 (2017).

408. Geethanath, S. & Vaughan Jr., J. T. Accessible magnetic resonance imaging: A review. *Journal of Magnetic Resonance Imaging* **49**, e65–e77 (2019).

409. National Institute for Health and Care Excellence. DG50: MRI-based technologies for assessing non-alcoholic fatty liver disease. https://www.nice.org.uk/guidance/dg50 (2023).

410. Drummond, M. F., Sculpher, M. J., Claxton, K., Stoddart, G. L. & Torrance, G. W. *Methods for the Economic Evaluation of Health Care Programmes*. vol. Fourth Edition (Oxford University Press, 2015).

411.Kim, M., Kim, Y., Ryu, G. W. & Choi, M. Functional status and health-related quality of life in patients with peripheral artery disease: a cross-sectional study. *International Journal of Environmental Research and Public Health* **18**, 10941 (2021).

412. Hogg, K. *et al.* Estimating quality of life in acute venous thrombosis. *JAMA Internal Medicine* **173**, 1067 (2013).

413. Luengo-Fernandez, R. *et al.* Quality of life after TIA and stroke. *Neurology* **81**, 1588–1595 (2013).

414. Oremus, M., Tarride, J.-E., Clayton, N. & Raina, P. Health utility scores in Alzheimer's disease: differences based on calculation with American and Canadian preference weights. *Value in Health* **17**, 77–83 (2014).

415. Brandão, S. M. G. *et al.* Utility and quality-adjusted life-years in coronary artery disease. *Medicine* **96**, e9113 (2017).

416. Witassek, F. *et al.* Health-related quality of life in patients with atrial fibrillation: The role of symptoms, comorbidities, and the type of atrial fibrillation. *PLOS ONE* **14**, e0226730 (2019).

417. Wiethoff, I. *et al.* Quality of life and societal costs in patients with dilated cardiomyopathy. *European Heart Journal - Quality of Care and Clinical Outcomes* **10**, 334–344 (2023).

418. Xie, J. *et al.* Assessing health-related quality-of-life in patients with symptomatic obstructive hypertrophic cardiomyopathy: EQ-5D-based utilities in the EXPLORER-HCM trial. *Journal of Medical Economics* **25**, 51–58 (2022).

419. Dyer, M. T., Goldsmith, K. A., Sharples, L. S. & Buxton, M. J. A review of health utilities using the EQ-5D in studies of cardiovascular disease. *Health and Quality of Life Outcomes* **8**, 13 (2010).

420. Di Tanna, G. L. *et al.* Health state utilities of patients with heart failure: a systematic literature review. *Pharmacoeconomics* **39**, 211–229 (2021).

421. Cooper, J. T. *et al.* Health related quality of life utility weights for economic evaluation through different stages of chronic kidney disease: a systematic literature review. *Health and Quality of Life Outcomes* **18**, 310 (2020).

422. Sayiner, M. *et al.* Assessment of health utilities and quality of life in patients with non-alcoholic fatty liver disease. *BMJ Open Gastroenterology* **3**, e000106 (2016).

423. NHS England. 2021/22 National Cost Collection Data Publication. https://www.england.nhs.uk/publication/2021-22-national-cost-collection-data-publication/.

424. McCabe, C., Claxton, K. & Culyer, A. J. The NICE cost-effectiveness threshold: what it is and what that means. *PharmacoEconomics* **26**, 733–744 (2008).

425. Montesinos, J., Guardia-Laguarta, C. & Area-Gomez, E. The fat brain. *Current Opinion in Clinical Nutrition and Metabolic Care* **23**, 68–75 (2020).

426. Wiedermann, W. & Li, X. Direction dependence analysis: A framework to test the direction of effects in linear models with an implementation in SPSS. *Behavior Research Methods* **50**, 1581–1601 (2018).

427. Câmara, R. & Griessenauer, C. J. Chapter 27 - Anatomy of the Vagus Nerve. in *Nerves and Nerve Injuries* (eds. Tubbs, R. S. et al.) 385–397 (Academic Press, 2015). doi:10.1016/B978-0-12-410390-0.00028-7.

428. Price, C. NHS Health Checks programme 'evidence based', public health chief insists. *Pulse Today* https://www.pulsetoday.co.uk/news/referrals/nhs-health-checks-programme-evidence-based-public-health-chief-insists/ (2014).

429. Department of Health. Putting prevention first. https://webarchive.nationalarchives.gov.uk/ukgwa/20130104171449/http://www.dh.gov.uk/en/Publicationsandstatistics/Publications/PublicationsPolicyAndGuidance/DH_083822 (2008).

430. Boswell, J., Cairney, P. & St Denny, E. The politics of institutionalizing preventive health. *Social Science & Medicine* **228**, 202–210 (2019).

431. Colditz, G. A. Overview of the epidemiology methods and applications: strengths and limitations of observational study designs. *Critical Reviews in Food Science and Nutrition* **50**, 10–12 (2010).

432. Lyall, D. M. *et al.* Quantifying bias in psychological and physical health in the UK Biobank imaging sub-sample. *Brain Communications* **4**, fcac119 (2022).

433. Lee, M. M., Whittemore, A. S. & Jung, D. L. Reliability of recalled physical activity, cigarette smoking, and alcohol consumption. *Annals of Epidemiology* **2**, 705–714 (1992).

434. Peters, A. *et al.* Framework and baseline examination of the German National Cohort (NAKO). *European Journal of Epidemiology* **37**, 1107–1124 (2022).

435. Ikram, M. A. *et al.* The Rotterdam Scan Study: design and update up to 2012. *European Journal of Epidemiology* **26**, 811–824 (2011).

436. Chen, Z. *et al.* China Kadoorie Biobank of 0.5 million people: survey methods, baseline characteristics and long-term follow-up. *International Journal of Epidemiology* **40**, 1652–1666 (2011).

437. Bhat, K. *et al.* Identifying and understanding the factors that influence the functioning of integrated healthcare systems in the NHS: a systematic literature review. *BMJ Open* **12**, e049296 (2022).

438. The Mayo Clinic. How high blood pressure can affect the body. *Mayo Clinic* https://www.mayoclinic.org/diseases-conditions/high-blood-pressure/in-depth/high-blood-pressure/art-20045868 (2023).

439. Bi, Y.-N. & Liu, Y.-A. GPs in UK: From health gatekeepers in primary care to health agents in primary health care. *Risk Management and Healthcare Policy* **16**, 1929–1939 (2023).

440. NHS England. QOF 2022-23. https://qof.digital.nhs.uk/ (2022).

441. Office for Health Improvement & Disparities. Preventing illness and improving health for all: a review of the NHS Health Check programme and recommendations. *GOV.UK* https://www.gov.uk/government/publications/nhs-health-check-programme-review/preventing-illness-and-improving-health-for-all-a-review-of-the-nhs-health-check-programme-and-recommendations (2021).

442. Sivarajasingam, V., Tai, M. & Steeghs, K. How eConsult has transformed patient care and staff well-being in an NHS practice. *Primary Health Care* **31**, 16–20 (2021).

443. Rudin, C. Stop explaining black box machine learning models for high stakes decisions and use interpretable models instead. *Nature Machine Intelligence* **1**, 206–215 (2019).

444. Busija, L., Lim, K., Szoeke, C., Sanders, K. M. & McCabe, M. P. Do replicable profiles of multimorbidity exist? Systematic review and synthesis. *European Journal of Epidemiology* **34**, 1025–1053 (2019).

445. Álvarez-Gálvez, J. *et al.* Social determinants of multimorbidity patterns: A systematic review. *Frontiers in Public Health* **11**, 1081518 (2023).

446. Herrett, E. *et al.* Data Resource Profile: Clinical Practice Research Datalink (CPRD). *International Journal of Epidemiology* **44**, 827–836 (2015).

447. Nadarajah, R. *et al.* Development, validation and prospective clinical implementation of a machine learning algorithm for incident cardio-renal-metabolic diseases and cardiovascular death: the OPTIMISE study. *European Journal of Preventive Cardiology* **31**, Supplement_1 (2024).

448. Mehta, N., Pandit, A. & Shukla, S. Transforming healthcare with big data analytics and artificial intelligence: A systematic mapping study. *Journal of Biomedical Informatics* **100**, 103311 (2019).

449. Schwalbe, N. & Wahl, B. Artificial intelligence and the future of global health. *The Lancet* **395**, 1579–1586 (2020).

450. Department of Health and Social Care. A guide to good practice for digital and data-driven health technologies. *GOV.UK* https://www.gov.uk/government/publications/code-of-conduct-for-data-driven-health-and-care-technology/initial-code-of-conduct-for-data-driven-health-and-care-technology (2021).

451. ICO: Information Commissioner's Office. Explaining decisions made with AI. https://ico.org.uk/for-organisations/uk-gdpr-guidance-and-resources/artificial-intelligence/explaining-decisions-made-with-artificial-intelligence/ (2019).

452. Fotaki, A., Velasco, C., Prieto, C. & Botnar, R. M. Quantitative MRI in cardiometabolic disease: From conventional cardiac and liver tissue mapping techniques to multi-parametric approaches. *Frontiers in Cardiovascular Medicine* **9**, 991383 (2023).

453. Kumar, V., Hsueh, W. A. & Raman, S. V. Multiorgan, Multimodality Imaging in Cardiometabolic Disease. *Circulation: Cardiovascular Imaging* **10**, e005447 (2017).

454. Garteiser, P. *et al.* Prospective comparison of transient elastography, MRI and serum scores for grading steatosis and detecting non-alcoholic steatohepatitis in bariatric surgery candidates. *JHEP reports: innovation in hepatology* **3**, 100381 (2021).

455. Zhao, D. *et al.* Systematic comparison of left ventricular geometry between 3D-echocardiography and cardiac magnetic resonance imaging. *Frontiers in Cardiovascular Medicine* **8**, 728205 (2021).

456. Tan, H. *et al.* Total-Body PET/CT: Current applications and future perspectives. *American Journal of Roentgenology* **215**, 325–337 (2020).

457. Alavi, A. *et al.* Potential and most relevant applications of total body PET/CT imaging. *Clinical Nuclear Medicine* **47**, 43 (2022).

458. Tahir, U. A. & Gerszten, R. E. Omics and cardiometabolic disease risk prediction. *Annual Review of Medicine* **71**, 163–175 (2020).

459. Gokuladhas, S. *et al.* Integrating multimorbidity into a whole-body understanding of disease using spatial genomics. in *Nuclear, Chromosomal, and Genomic Architecture in Biology and Medicine* (eds. Kloc, M. & Kubiak, J. Z.) 157–187 (Springer International Publishing, 2022).

460. Deelen, J. Targeting multimorbidity: Using healthspan and lifespan to identify biomarkers of ageing that pinpoint shared disease mechanisms. *eBioMedicine* **67**, 103364 (2021).

461. Pietzner, M. *et al.* Plasma metabolites to profile pathways in noncommunicable disease multimorbidity. *Nature Medicine* **27**, 471–479 (2021).

462. Gilburt, H., Lamming, L., Buck, D. & Mallorie, S. Commissioning Community Champions: Lessons from a pandemic (The King's Fund). https://www.kingsfund.org.uk/insight-and-analysis/reports/commissioning-community-champions-pandemic (2024).

463. Lofters, A., Prakash, V., Devotta, K. & Vahabi, M. The potential benefits of "community champions" in the healthcare system. *Healthcare Management Forum* **36**, 382–387 (2023).

Appendices

Appendix 1: Magnetic resonance imaging details

Organ	Sequence	Acquisition parameters (as reported by [1])	Processing, quality control and analysis	Imaging-derived phenotypes produced	Key references for full protocol
Liver MRI Siemens 1.5T MAGNETOM Aera.	shMOLLI (shortened modified Look-Locker imaging)	Resolution: 1.146 x 1.146 x 8, Matrix: 384 x 288 x 7 TE/TR = 1.93/480.6 ms, α = 35°, R = 2	Main extraction and analysis via Perspectum's LiverMultiScan™ Discover software [2] PDFF maps were constructed, using a three-point DIXON technique [3] Further large-scale phenotyping via a deep learning method [4]	Proton density fat fraction (PDFF) Liver iron Corrected T1 (cT1)	McKay et al. (2018)[5] Mojtahed et al. (2019)[6] Wilman et al. (2017)[7] Perpectum (2016) [2]
	LMS LiverMultiScan	Resolution: 1.719 x 1.719 x 10 Matrix: 256 x 232 x 6 TE/TR = 1.2 (min) TE/TR = 7.2 (max)/14 ms, α = 5°			
	ME GRE (multi-echo spoiled-gradient-echo acquisition)	Resolution: 2.5 x 2.5 x 6 Matrix: 160 x 160 x 10 TE/TR = 2.38(min) TE/TR = 23.8(max)/27 ms, α = 20°			
Cardiac MRI Siemens 1.5T MAGNETOM Aera	LAX Long axis	Resolution: 1.9 x 1.9 x 6 Matrix: 210 x 208 x 50 TE/TR = 1.16/32 ms, α = 65°, R = 2	Imaging-derived markers extracted via a combination of: Automatic scanner-provided values Expert analysis and segmentation of initial set of 5,000 scans Automated image segmentation via deep learning algorithms	LV stroke volume LV mass LV ejection fraction Aortic distensibility Left atrial volume Left atrial ejection fraction Global longitudinal strain	Petersen et al. (2013)[8] Petersen et al. (2016)[9] Petersen et al. (2017)[8] Bai et al. (2017)[10]
	SAX Short axis	Resolution: 1.8 x 1.8 x 8 Matrix: 210 x 208 x 50 TE/TR = 1.1/32 ms, α = 10°, R = 2			
	shMOLLI	Resolution: 0.9375 x 0.9375 x 8 Matrix: variable x 384 x 7 TE/TR = 1.073/400 ms, α = 35°, R = 2			
	Aorta	Resolution: 1.58 x 1.58 x 6 Matrix: 240 x 196 x 100 TE/TR = 1.17/28 ms, α = 66°, R = 2			
Brain MRI Siemens 3.0T Skyra scanner	T1 MPRAGE (magnetization-prepared rapid acquisition with gradient echo)	Resolution: 1.0 x 1.0 x 1.0 Matrix: 256 x 256 x 208 TI/TR = 880/2000 ms, R = 2	Imaging-derived markers extracted via the FMRIB imaging processing pipeline [11] including: Grey and white tissue volumes estimated using a SIENAX-style analysis [12 FSL FAST grey matter segmentation [13] subcortical structure segmentation with FSL FIRST[14], and ASEG [15] White matter hyperintensity volumes with BIANCA [16] Probabilistic tractography analysis with BEDPOSTx / PROBTRACKx [20,21] Diffusion IDP generation with diffusion tensor fitting (DTI) and NODDI [22]	Total brain volume Grey matter volume White matter volume Volume of white matter hyperintensities Regional subcortical volumes Fractional anisotropy (FA) Mean diffusivity (MD) Intracellular volume fraction (ICVF) Isometric volume fraction (ISOVF) Orientation dispersion (OD	Smith, Alfaro-Almagro and Miller (2020)[17] Miller et al. (2016) [18] Alfaro-Amagro et al. (2018)[11] Smith et al. (2004)[19] Zhang et al (2012) [22]
	T2 FLAIR {fluid-attenuated inversion recovery)	Resolution: 1.0 x 1.0 x 1.05 Matrix: 256 x 256 x 192 TI/TR = 1800/5000 ms, R = 2			
	Diffusion MRI	Resolution: 2.0 x 2.0 x 2.0 Matrix: 104 x 104 x 72 TR = 3600 ms, 50 directions/shell, b = 0, 1000, 2000 s/mm2, α = 51°, MB = 3			

1. Littlejohns TJ, Holliday J, Gibson LM, Garratt S, Oesingmann N, Alfaro-Almagro F, Bell JD, Boultwood C, Collins R, Conroy MC, Crabtree N, Doherty N, Frangi AF, Harvey NC, Leeson P, Miller KL, Neubauer S, Petersen SE, Sellors J, Sheard S, Smith SM, Sudlow CLM, Matthews PM, Allen NE. The UK Biobank imaging enhancement of 100,000 participants: rationale, data collection, management and future directions. Nat. Commun. Nature Research; 2020. p. 1–12.
2. Perspectum. LiverMultiScan | Perspectum. 2016. https://perspectum.com/products/livermultiscan (16 July 2021)
3. Glover GH. Multipoint dixon technique for water and fat proton and susceptibility imaging. J Magn Reson Imaging John Wiley & Sons, Ltd; 1991;1:521–530.
4. Irving B, Hutton C, Dennis A, Vikal S, Mavar M, Kelly M, Brady JM. Deep Quantitative Liver Segmentation and Vessel Exclusion to Assist in Liver Assessment. Commun Comput Inf Sci Springer, Cham; 2017;723:663–673.
5. McKay A, Wilman HR, Dennis A, Kelly M, Gyngell ML, Neubauer S, Bell JD, Banerjee R, Thomas EL. Measurement of liver iron by magnetic resonance imaging in the UK Biobank population. Meyre D, ed. PLoS One Public Library of Science; 2018;13:e0209340.
6. Mojtahed A, Kelly CJ, Herlihy AH, Kin S, Wilman HR, McKay A, Kelly M, Milanesi M, Neubauer S, Thomas EL, Bell JD, Banerjee R, Harisinghani M. Reference range of liver corrected T1 values in a population at low risk for fatty liver disease—a UK Biobank sub-study, with an appendix of interesting cases. Abdom Radiol Springer New York LLC; 2019;44:72–84.
7. Wilman HR, Kelly M, Garratt S, Matthews PM, Milanesi M, Herlihy A, Gyngell M, Neubauer S, Bell JD, Banerjee R, Thomas EL. Characterisation of liver fat in the UK Biobank cohort. Lu S-N, ed. PLoS One Public Library of Science; 2017;12:1–14.
8. Petersen SE, Matthews PM, Bamberg F, Bluemke DA, Francis JM, Friedrich MG, Leeson P, Nagel E, Plein S, Rademakers FE, Collins R, Neubauer S. Imaging in population science: Cardiovascular magnetic resonance in 100,000 participants of UK Biobank - Rationale, challenges and approaches. J Cardiovasc Magn Reson 2013;15.
9. Petersen SE, Matthews PM, Francis JM, Robson MD, Zemrak F, Boubertakh R, Young AA, Hudson S, Weale P, Garratt S, Collins R, Piechnik S, Neubauer S. UK Biobank's cardiovascular magnetic resonance protocol. J Cardiovasc Magn Reson 2016;18.
10. Bai W, Sinclair M, Tarroni G, Oktay O, Rajchl M, Vaillant G, Lee AM, Aung N, Lukaschuk E, Sanghvi MM, Glocker B, Rueckert D. Automated cardiovascular magnetic resonance image analysis with fully convolutional networks 08 Information and Computing Sciences 0801 Artificial Intelligence and Image Processing. J Cardiovasc Magn Reson 2018;20.
11. Alfaro-Almagro F, Jenkinson M, Bangerter NK, Andersson JLR, Griffanti L, Douaud G, Sotiropoulos SN, Jbabdi S, Hernandez-Fernandez M, Vallee E, Vidaurre D, Webster M, McCarthy P, Rorden C, Daducci A, Alexander DC, Zhang H, Dragonu I, Matthews PM, Miller KL, Smith SM. Image processing and Quality Control for the first 10,000 brain imaging datasets from UK Biobank. Neuroimage Academic Press Inc.; 2018;166:400–424.
12. Smith SM. Fast robust automated brain extraction. Hum Brain Mapp John Wiley & Sons, Ltd; 2002;17:143–155.
13. Zhang Y, Brady M, Smith S. Segmentation of brain MR images through a hidden Markov random field model and the expectation-maximization algorithm. IEEE Trans Med Imaging 2001;20:45–57.
14. Patenaude B, Smith SM, Kennedy DN, Jenkinson M. A Bayesian model of shape and appearance for subcortical brain segmentation. Neuroimage Academic Press; 2011;56:907–922.
15. Fischl B, Salat DH, Busa E, Albert M, Dieterich M, Haselgrove C, Kouwe A Van Der, Killiany R, Kennedy D, Klaveness S, Montillo A, Makris N, Rosen B, Dale AM. Whole Brain Segmentation: Automated Labeling of Neuroanatomical Structures in the Human Brain. Neuron Cell Press; 2002;33:341–355.
16. Griffanti L, Zamboni G, Khan A, Li L, Bonifacio G, Sundaresan V, Schulz UG, Kuker W, Battaglini M, Rothwell PM, Jenkinson M. BIANCA (Brain Intensity AbNormality Classification Algorithm): A new tool for automated segmentation of white matter hyperintensities. Neuroimage Academic Press Inc.; 2016;141:191–205.
17. Smith SM, Alfaro-Almagro F, Miller KL. UK Biobank - Brain Imaging Documentation. biobank.ctsu.ox.ac.uk/crystal/docs/brain_mri.pdf.
18. Miller KL, Alfaro-Almagro F, Bangerter NK, Thomas DL, Yacoub E, Xu J, Bartsch AJ, Jbabdi S, Sotiropoulos SN, Andersson JLR, Griffanti L, Douaud G, Okell TW, Weale P, Dragonu I, Garratt S, Hudson S, Collins R, Jenkinson M, Matthews PM, Smith SM. Multimodal population brain imaging in the UK Biobank prospective epidemiological study. Nat Neurosci 2016;19:1523–1536.
19. Smith SM, Jenkinson M, Woolrich MW, Beckmann CF, Behrens TEJ, Johansen-Berg H, Bannister PR, Luca M De, Drobnjak I, Flitney DE, Niazy RK, Saunders J, Vickers J, Zhang Y, Stefano N De, Brady JM, Matthews PM. Advances in functional and structural MR image analysis and implementation as FSL. Neuroimage Academic Press; 2004;23:S208–S219.
20. Behrens TEJ, Berg HJ, Jbabdi S, Rushworth MFS, Woolrich MW. Probabilistic diffusion tractography with multiple fibre orientations: What can we gain? Neuroimage Academic Press; 2007;34:144–155.
21. Groot M De, Vernooij MW, Klein S, Ikram MA, Vos FM, Smith SM, Niessen WJ, Andersson JLR. Improving alignment in Tract-based spatial statistics: Evaluation and optimization of image registration. Neuroimage Academic Press; 2013;76:400–411.
22. Zhang H, Schneider T, Wheeler-Kingshott CA, Alexander DC. NODDI: Practical in vivo neurite orientation dispersion and density imaging of the human brain. Neuroimage Academic Press; 2012;61:1000–1016

Appendix 2: Condition codes from UK Biobank records

Disease	Source	Codes
Atherosclerosis / Peripheral artery disease	Self-report (20002)	1067, 1088, 1104, 1492, 1591
	First occurrences	131380, 131382, 131384, 131386, 131388, 131390
	ICD10	I70, I71, I72, I73, I74, I77
	Primary care	.G451, .G6B4, .G81., .G811, .G814, .G82., .G821, .G822, .G823, .G824, .G82Z, 14AE., 2456, 66f3., 7A11., 7A112, 7A113, 7A134, 7A14., 7A144, 7A1B0, 7A1B1, 7A1B2, 7A1B6, 7A1B8, 7A1B9, 7A1BA, 7A1BC, 7A1C0, 7A1C1, 7A1C2, G340., G342., G6732, G6733, G70.., G700., G701., G7010, G702., G7020, G702z, G703., G704., G70y., G70y0, G70z., G71.., G710., G711., G712., G713., G7130, G714., G7140, G7141, G7142, G7143, G715., G7150, G716., G7160, G718., G719., G71A., G71z., G72.., G720., G7200, G7201, G7202, G720z, G721., G7210, G722., G7220, G7221, G7222, G722z, G723., G7230, G7231, G7232, G7233, G7234, G7235, G7236, G723z, G724., G725., G726., G727., G728., G729., G72A., G72B., G72C., G72D., G72D0, G72D1, G72D2, G72E., G72y., G72y0, G72y1, G72y2, G72y3, G72y4, G72y5, G72y6, G72y7, G72y8, G72y9, G72yA, G72yB, G72yC, G72yz, G72z., G73.., G730., G7300, G7301, G730z, G731., G7310, G7311, G731z, G733., G734., G73y., G73y2, G73y4, G73y5, G73y6, G73y7, G73y8, G73yz, G73z., G73z0, G73z1, G73zz, G74.., G740., G741., G742., G7420, G7421, G7422, G7423, G7424, G7425, G7426, G7427, G7428, G7429, G742A, G742B, G742z, G743., G74y., G74y0, G74y1, G74y2, G74y3, G74y5, G74y6, G74y7, G74y8, G74y9, G74yz, G74z., G76.., G760., G761., G762., G7620, G763., G764., G765., G766., G768., G7680, G7681, G768z, G76A., G76B., G76z., G76z0, G76z1, G76z2, G78.., G783., G7830, G7831, G7832, G784., G7840, G7841, G7842, G9..., Gyu70, Gyu71, Gyu72, Gyu73, Gyu74, Gyu75, Gyu76, SP07N, X007n, X00Du, X00Dv, X015i, X015v, X015x, X015y, X104P, X203b, X203c, X203d, X203j, X203K, X203L, X203m, X203n, X203o, X203Q, X203R, X203s, X203S, X203T, X203U, X203w, X203x, X203z, X2040, X2041, X2043, X2045, X2049, X204a, X204b, X204c, X204d, X204e, X204g, X204h, X204k, X204L, X204M, X204N, X204p, X204P, X204Q, X204R, X204T, X204y, X2057, X205D, X205F, X205G, X205H, X205I, X205J, X205K, X205M, X205N, X205O, X205P, X205Q, X205R, X205S, X209F, X209G, X209H, X209I, X209J, X209K, X30KP, X30KV, X40R1, X50BQ, X75If, X76Lk, X76Ll, X77ms, X90Z0, Xa01g, Xa0NF, Xa0NH, Xa1Oi, Xa24I, Xa3fX, Xa3fY, Xa6Yf, Xa6Yh, Xa6Yi, Xa6Yj, Xa6Yk, Xa6Yl, Xa6Ym, Xa6Yn, Xa6Yp, Xa6YQ, Xa6YS, Xa6YU, Xa6YX, Xa6YY, Xa6Yz, Xa6YZ, Xa6ZD, Xa6ZE, Xa6Zh, Xa7lT, Xa7lU, Xa7lV, Xa7lW, Xa7y4, Xa7y5, Xa84U, Xa87l, Xa9Br, Xa9ex, XaAwW, XaB5d, XaB5R, XaB5S, XaB5T, XaB5V, XaB5W, XaB5X, XaBD1, XaBDG, XaBFI, XaBVG, XaBYF, XaD2j, XaDtD, XaDtE, XaDtF, XaDtH, XaDtI, XaDtK, XaDtQ, XaDyM, XaDyN, XaDyP, XaDyQ, XaE3G, XaEed, XaEee, XaEef, XaEeg, XaeVd, XaFsQ, XaFxb, XaG2L, XaIyH, XaJV4, XaLhF, XaLhG, XaLhH, XaMmH, XaMmI, XaMmJ, XaMrD, XaW51, XaX6B, XaYMz, XaYnc, XaYni, XaYnj, XaYnk, XaZV0, XaZV1, XE0Uj, XE0VO, XE0VP, XE0VQ, XE0VS, XE0VT, XE0VW, XE0X8, XM02Q, XM02R, XM02S, XM0rc, XM0rN, XM1Ib, XM1Qi, Y5499
Erectile dysfunction	Self-report (20002)	1518
	Medications (20003)	1140869100, 1140883010, 1141168936, 1141168944, 1141168946, 1141168948, 1141187810, 1141187814, 1141187818, 1141192248, 1141192256, 1141192258, 1141192260
	ICD10	F522, N484
	Primary care	.J3ZB, 1D1B., 7C25E, E2273, Eu522, g16.., gh2.., gh2K., gh2L., gh2M., gh2N., gh3.., gh5.., gh51., gh52., gh53., gh54., gh55., gh56., gh5t., gh5u., gh5v., gh5z., gh6.., gh7.., gh71., gh72., gh73., gh74., gh7w., gh7x., gh7y., gh7z., gh8.., gh81., gh82., gh83., gh84., gh85., gh86., gh87., gh88., pG..., x0092, x04vF, x05kb, x05li, XaMBP, XaXgw, Y0289
Venous thromboembolism (DVT/PE)	Self-report (20002)	1068, 1093, 1094
	First occurrences	131396
	Diagnosed by doctor (6150, 6152)	4012, 4022, 5, 7
	ICD9	4151, 4511, 4512, 4518, 4519, 4538, 4539, 6346, 6356, 6366, 6376, 6386, 673
	ICD10	I260, I269, I801, I802, I803, I808, I809, I828, I829, O082, O223, O229, O871, O879, O882
	OPCS4	L124, L131, L712, L791, L794, L795, L901, L902, L908, L909, L961, L962, L968, L969, L994
	Primary care	14A8., 14A81, 14AC., 14AG., 14Ob0, 14Ob1, 14Ob2, 2I17., 7A093, 7A0A1, 7A0B0, 7A630, 7A633, 7A634, 7A6B., 7A6By, 7A6Ey, 7A6Q., 7A6Q0, 7A6Q1, 7A6Qy, 7A6Qz, 7A6S2, 7A6S3, 88A8., 8CMWA, 8HTm., 8I2G., 8I3L., 8I6E., 9kg.., 9kg0., 9kg1., 9kg2., G40.., G400., G401., G4010, G4011, G402., G40z., G41y1, G740., G7428, G74y5, G80.., G800., G8000, G8001, G8002, G8003, G8004, G8005, G800z, G801., G8010, G8011, G8012, G8013, G8014, G8015, G8016, G8017, G8018, G8019, G801A, G801B, G801C, G801D, G801E, G801F, G801G, G801H, G801J, G801z, G802., G8020, G80y., G80y0, G80y1, G80y2, G80y3, G80y4, G80y5, G80y6, G80y7, G80y8, G80y9, G80yz, G80z., G80z0, G80z1, G80zz, G82.., G820., G821., G822., G8220, G823., G824., G825., G826., G827., G82y., G82z., G82z0, G82z1, G82zz, Gyu80, Gyu81, Gyu82, L0406, L0416, L0426, L0432, L0442, L0452, L0506, L0516, L0526, L0606, L0616, L0626, L0706, L0716, L0726, L086., L09.., L090., L0900, L0901, L0902, L0903, L0904, L090y, L090z, L091., L0910,

Disease	Source	Codes
		L0911, L0912, L091z, L092., L0920, L0921, L0922, L0923, L0924, L0925, L0926, L092z, L093., L0930, L0931, L0932, L0933, L0934, L093z, L094., L095., L096., L0960, L0961, L0962, L0963, L0964, L0965, L0966, L0967, L096z, L09y., L09y0, L09y1, L09y2, L09y3, L09y4, L09yz, L09z., L0A3., L41.., L4105, L4106, L4115, L4116, L4120, L4124, L4125, L4126, L413., L4130, L4131, L4132, L413z, L414., L4140, L4141, L4142, L414z, L415., L4150, L4151, L4152, L4153, L4154, L4155, L4156, L415z, L4170, L4171, L41z5, L41z6, L43.., L432., L4320, L4321, L4322, L4323, L4324, L432z, L433., L4330, L4331, L4332, L4333, L4334, L433z, L43y., L43y0, L43y1, L43y2, L43y3, L43y4, L43yz, L43z., L43z0, L43z1, L43z2, L43z3, L43z4, L43zz, Lyu06, Lyu09, Lyu0A, Lyu0B, Lyu22, Lyu63, Lyu64, SP120, SP121, SP122, SP321, U6045, X00ZU, X012b, X012c, X0178, X017G, X017I, X017J, X017V, X017Y, X202x, X202y, X202z, X203A, X203C, X205a, X205b, X205c, X205d, X205e, X205l, X205m, X205n, X205o, X205s, X205t, X205u, X205Y, X205Z, X40Dc, X40Dd, X40Dg, X40Dh, X70XB, X75Pg, X76Lg, X76Lh, Xa07G, Xa0ga, Xa0Gg, Xa0Gn, Xa0Go, Xa0l8, Xa1aj, Xa1oU, Xa1oV, Xa1oW, Xa6Yr, Xa9Bs, Xaa2K, Xaa2L, XaaBG, XaBDk, XaBDq, XaBDu, XaBJz, XaBK0, XaBMc, XaBMC, XaBMd, XaBMD, XaBME, XaBMG, XaBMH, XaBMI, XaBMJ, XaBMK, XaBML, XaBNh, XaBUk, XaBUu, XaC0s, Xacvd, Xacve, XaDyA, XaDyB, XaDyD, XaDyE, XaIIo, XaJVl, XaJxo, XaLgy, XaLig, XaLih, XaLiM, XaLiN, XaLiv, XaLiw, XaO8G, XaOYV, XaQ8U, XaQHw, XaQHx, XaQHy, XaQIV, XaQmI, XaZ43, XaZHi, XaZHk, XaZht, XC0dZ, XE0Lq, XE0q9, XE0th, XE0Um, XE0Vb, XE0VY, XE0VZ, XE0WI, XE0xI, XE0xK, XE0xL, XE0xM, XE0xN, XE0xq, XE0XS, XE0zm, XM06D, XM1Qq, XM1Qr, XM1RL, XM1RM, ZV128, ZV129
Alzheimer's disease and dementia	Algorithm	42018, 42020, 42022, 42024
	Self-report (20002)	1263
	First occurrences	130836, 130838, 130840, 130842, 131036, 131038
	ICD9	290, 331
	ICD10	F00, F01, F02, F03, F051, G30, G31
	Primary care	.1461, .3AE3, .3AE4, .3AE5, .3AE6, .6AB., .E11., .E111, .E112, .E113, .E114, .E115, .E116, .E11Z, .F21Z, .F371, .G78., 1461, 2233, 38C13, 3AE3., 3AE4., 3AE5., 3AE6., 6AB.., 8BM02, 8BM50, 8BM60, 8BPa., 8CMe0, 8CMG2, 8CMZ., 8CMZ0, 8CMZ1, 8CMZ2, 8CMZ3, 8CSA., 8Hla., 8IAe0, 8IAe2, A411., A4110, E00.., E000., E001., E0010, E0011, E0012, E0013, E001z, E002., E0020, E0021, E002z, E003., E004., E0040, E0041, E0042, E0043, E004z, E012., E02y1, E0300, E0301, E0302, E0303, E0304, E0310, E0311, E0312, E0313, E0314, E041., Eu00., Eu000, Eu001, Eu002, Eu00z, Eu01., Eu010, Eu011, Eu012, Eu013, Eu01y, Eu01z, Eu02., Eu020, Eu021, Eu022, Eu023, Eu024, Eu025, Eu02y, Eu02z, Eu04., Eu040, Eu041, Eu04y, Eu04z, Eu106, Eu107, F1..., F10.., F10y., F10y0, F10y1, F10y2, F10yz, F10z., F11.., F110., F1100, F1101, F111., F112., F116., F118., F11x0, F11x2, F11x7, F11x9, F11xz, F11y., F11y2, F11yz, F11z., F1440, F21y2, Fyu30, Fyu31, Ub1T6, X002m, X002U, X002V, X002W, X002w, X002x, X002y, X002z, X0030, X0031, X0032, X0033, X0034, X0035, X0036, X0037, X0039, X003A, X003B, X003C, X003D, X003E, X003F, X003G, X003H, X003I, X003J, X003l, X003m, X003P, X003R, X003T, X003V, X003W, X003X, X004B, X004E, X005K, X005L, X005M, X005N, X005O, X005P, X00R0, X00R2, X00RI, X00Rk, X77qx, Xa0fZ, Xa0lH, Xa0sC, Xa0sE, Xa1GB, Xa25J, Xa3ez, Xa7nD, XaA1S, XaaBZ, XaaeA, XaaiW, Xabd2, Xabd3, XabEk, XabEl, XabtQ, XabVp, XacIx, XacIy, XacIz, XacJ0, XacLx, Xacly, Xaclz, XacM2, XaE74, Xaefu, XaIKB, XaIKC, XaIRJ, XaJBQ, XaJBU, XaJBV, XaJBW, XaJBX, XaJPy, XaKyY, XaMGF, XaOfZ, XaPws, XaYFR, XaYPX, XaZqJ, XaZWz, XE15F, XE17j, XE1aG, XE1Xr, XE1Xs, XE1Xu, XE1Z6, XE1Z7, XE1Z8
Cerebrovascular diseases	Self-report (20002)	1425
	Self-report (20004)	1106
	First occurrences	131370, 131372, 131374, 131376
	ICD10	I65, I66, I67, I68, I69
	Primary care	.G76., .G763, .G76Z, .G77., .G7Z., 0.1477, 1477, C373M, E0304, E0314, F11x2, F21y2, Fyu57, G6..., G63.., G630., G631., G632., G633., G634., G63y., G63z., G64.., G640., G641., G65z0, G67.., G670., G671., G6710, G6711, G671z, G672., G673., G6730, G6731, G674., G6740, G675., G676., G677., G6770, G6771, G6772, G6773, G6774, G678., G679., G67A., G67B., G67y., G67z., G68.., G680., G681., G682., G683., G68W., G68X., G6y.., G6z.., Gyu6., Gyu65, Gyu66, Gyu67, Gyu68, Gyu69, Gyu6A, Gyu6B, Gyu6C, Gyu6D, L440., N13y1, P7y0., P7y0y, P7y0z, X0025, X00Cz, X00Dm, X00Dt, X00Dw, X00DY, X00E4, X00Ej, X203t, X203W, Xa0Ml, Xa1mP, Xa3fW, Xa6Yd, Xa6Yo, Xa6Ys, Xa6YV, Xa9Bq, XaaJd, XaBL0, XaDyO, XaF4B, XaQZG, XaZq0, XE0VG, XE0VH, XE0VI, XE0VL, XE0VM, XE0X4
Sleep disorder	Self-report (1200)	3
	Self-report (20002)	1123, 1616
	First occurrences	131060
	ICD10	G47
	Primary care	1B1B., 1B1B0, 1B1B1, 1B1B2, 1B1Q., 3148, 8HTn., E274., E2741, E2742, E2746, E274A, E274B, E274E, E274z, Eu51., Eu510, F27.., F270., F271., F27z., Fy0.., Fy00., Fy01., Fy02., Fy03., Fy04., Fy05., Fy06., Fyu58, H5B.., H5B0., R005., R0050, R0051, R0052, R0053, R0054, R0055, R0056, R0057, R0058, R0059, R005z, X007q, X007s, X007x, X0083, X0084, X0085, X0086,

Disease	Source	Codes
		X0087, X0089, X008C, X008D, X008E, X008F, X008G, X76AE, X76AO, X76AR, Xa0Kk, Xa0Kl, Xa7wV, XaEGP, XaFqr, XaIv5, XaJEd, XaN5q, XaOb7, XE0ux, XE2nU, XE2Pv, XE2Q5, XM06j, XM06k, XM0CT, XM0yu
Stroke	Algorithm	42006
	Self-report (20002)	1081, 1086, 1491, 1583
	First occurrences	131360, 131362, 131366, 131368
	Diagnosed by doctor (6150, 6152)	3, 4056
	ICD9	430, 431, 434, 436
	ICD10	I60, I61, I63, I64
	Primary care	G60.., G600., G601., G602., G603., G604., G605., G606., G60X., G60z., G61.., G610., G611., G612., G613., G614., G615., G616., G617., G618., G619., G61X., G61X0, G61X1, G61z., G63y0, G63y1, G64.., G640., G6400, G641., G6410, G64z., G64z0, G64z1, G64z2, G64z3, G64z4, G65z1, G66.., G660., G661., G662., G663., G664., G665., G666., G667., G668., G669., G6760, G6W.., G6X.., Gyu60, Gyu61, Gyu62, Gyu63, Gyu64, Gyu6E, Gyu6F, Gyu6G, X00D3, X00D4, X00D5, X00D6, X00D7, X00D8, X00D9, X00DA, X00DD, X00DE, X00DF, X00Df, X00DG, X00Dg, X00DI, X00DJ, X00DK, X00DM, X00DN, X00DO, X00DP, X00DQ, X00DR, X00DS, X00DT, X204F, Xa00I, Xa00J, Xa00K, Xa01b, Xa01c, Xa01h, Xa01i, Xa01j, Xa01k, Xa01l, Xa01m, Xa01o, Xa0Bj, Xa0kZ, Xa0N3, Xa0NJ, Xa0NK, Xa0NN, Xa0NO, Xa0NQ, Xa0NS, Xa0NV, Xa0NW, Xa0NX, Xa1hE, XaB4Z, XaBE2, XaBEC, XaBED, XaJgQ, XE0VJ, XE2aB
Transient ischaemic attack (TIA)	Self-report (20002)	1082
	First occurrences	131056
	ICD9	435
	ICD10	G45
	Primary care	.G74., 8CRB., EMISNQTR28, F4236, Fyu55, G65.., G650., G651., G6510, G652., G653., G654., G655., G656., G657., G65y., G65z., G65zz, X00DU, X00DV, X00DW, X00E3, XaB5o, XaEGK, XaQve, XaRCF, XaX16, XE0VK, XE0X0, ZV12D
Traumatic brain injury	Self-report (20002)	1240, 1266
	ICD10	S020, S021, S027, S028, S029, S06, S09
	Primary care	14J1., 8A31., 8CAP., E2A2., Eu062, S0..., S03z., S04.., S6..., S60.., S600., S601., S602., S604., S605., S60z., S61xz, S640z, S643., S644., S6z.., SC20., XA004, XA049, XA04L, XA0Fb, XaB4s, XabpV, XaC8Z, XaFCk, XaFCl, XaIwl, XE0kJ, XE1bs, XE1kU, XE1mr, XE1qD, XE2b7, Y0c0c
Atrial fibrillation	Self-report (20002)	1471
	First occurrences	131350
	ICD9	4273
	ICD10	I48, I480, I481, I482, I489
	Primary care	.14AN, .662S, .6A9., .8666, .G67., .G670, 14AN., 662S., 6A9.., 7936A, G573., G5730, G5731, G5732, G5733, G5734, G5735, G5736, G5737, G5738, G5739, G573z, X202R, X202S, Xa2E8, Xa3rp, Xa7nI, XaaUH, XaDv6, XaEga, XaeUP, XaeUQ, XaeUR, Xafis, XaIIT, XaMGD, XaOfa, XaOft, XE0Wk, Y7820
Cardiac arrhythmia	Self-report (20002)	1077, 1471, 1483, 1485, 1486, 1487
	Self-report (20004)	1096, 1550, 1551
	First occurrences	131342, 131344, 131346, 131348, 131350, 131352
	ICD9	426, 427
	ICD10	I44, I45, I46, I47, I48, I49
	OPCS4	K60, K61, K73, K74, U31
	Primary care	.G653, .G654, .G693, 2241, 326.., 3262, 326Z., bb..., bc..., G560., G561., G5610, G5611, G5612, G5613, G5614, G561z, G562., G5620, G5621, G562z, G563., G564., G565., G5650, G5651, G5652, G5653, G5654, G5655, G565z, G566., G5660, G5661, G5662, G566z, G567., G5670, G5671, G5672, G5673, G5674, G567z, G56y., G56y0, G56y1, G56y2, G56y3, G56y4, G56y5, G56yz, G56z., G56z0, G56zz, G57.., G570., G5700, G5701, G5702, G5703, G570z, G571., G572., G5720, G5721, G572z, G573., G5730, G5731, G5732, G5733, G5734, G5735, G5736, G5737, G5738, G5739, G573z, G574., G5740, G5741, G574z, G575., G5750, G5751, G5752, G5753, G575z, G576., G5760, G5761, G5762, G5763, G5764, G5765, G576z, G577., G578., G57y., G57y2, G57y3, G57y4, G57y5, G57y6, G57y9, G57yA, G57yz, G57z., Gyu5a, Gyu5U, Gyu5V, Gyu5W, Gyu5X, Gyu5Y, Gyu5Z, L09y1, SP110, X011a, X011b, X011c, X011d, X011U, X011W, X011X, X011Z, X2025, X2026, X2027, X2028, X2029, X202a, X202A, X202B, X202c, X202C,

Disease	Source	Codes
		X202d, X202D, X202e, X202E, X202F, X202g, X202G, X202h, X202H, X202i, X202j, X202J, X202K, X202L, X202M, X202n, X202N, X202P, X202Q, X202R, X202S, X202T, X202U, X202X, X202Z, X208V, X76Je, X76Jf, X76Jg, X76Jh, X779u, X779v, X779w, X779x, X779y, X77A0, X77A2, X77A3, X77A6, X77Ab, X77Ae, X77AE, X77Af, X77AF, X77Ag, X77AG, X77Ah, X77AN, X77AW, X77AX, X77AY, X77Ba, X77Bb, X77BB, X77BC, X77BD, X77Be, X77BF, X77Bg, X77Bh, X77Bi, X77BI, X77Bj, X77BJ, X77Bk, X77Bl, X77Bm, X77Bo, X77BO, X77Bp, X77Bq, X77BQ, X77Bs, X77BS, X77Bt, X77BT, X77BU, X77Bv, X77BV, X77Bw, X77BW, X77Bx, X77BX, X77By, X77Bz, X77C1, X77C2, X77C3, X77C4, X77C6, X77C7, X77C8, X77C9, X77CA, X90C7, X90CA, X90fZ, Xa0D3, Xa0k6, Xa0kY, Xa0lU, Xa0Ug, Xa0Uh, Xa0Ui, Xa0ZR, Xa0ZT, Xa0ZU, Xa0ZV, Xa0ZW, Xa2E8, Xa2jV, Xa7nI, Xa7nJ, XaaUH, XaBDJ, XaC2K, XaC2L, XaEga, XaeUP, XaeUQ, XaeUR, Xafis, XaOfa, XaOft, XaOgX, XaQia, XaRCI, XaRCJ, XaRCK, XaRCL, XaXGh, XaZxi, XE0V3, XE0V4, XE0V5, XE0V6, XE0V7, XE2QF, XE2xl
Heart failure	Self-report (20002)	1076
	First occurrences	131354
	ICD9	4280, 4281, 4289
	ICD10	I500, I501, I509
	Primary care	.14A6, .14AM, .1O1., .662p, .662T, .662W, .8H2S, .8HBE, .G6A., .G6A1, .G6A2, .G6AZ, 14A6., 14AM., 1O1.., 662p., 662T., 662W., 8H2S., 8HBE., G1yz1, G232., G234., G58.., G580., G5800, G5801, G5802, G5803, G5804, G581., G5810, G582., G583., G584., G58z., G5y4z, SP111, X102Y, X202k, X202l, XaBwi, XaEgY, XafeB, XaIIU, XaIpn, XaIQM, XaIQN, XaKNW, XaLon, XaO5n, XaWyi, XaZIC, XE0V8, XE0V9, XE0Wo, XE2QG, Y27da, Y2b96
Ischaemic heart disease	Algorithm	42000
	Self-report (20002)	1074, 1075
	Self-report (20004)	1070, 1095, 1523
	First occurrences	131296, 131298, 131300, 131302, 131304, 131306
	Diagnosed by doctor (6150, 6152)	1, 2, 3627, 3894
	ICD9	410, 411, 412, 413, 414, 429
	ICD10	I20, I21, I22, I23, I24, I25, I241, I252
	OPCS4	K40, K41, K42, K43, K44, K45, K46, K47, K48, K49, K50, K51, K75
	Primary care	.14A5, .14AJ, .14AL, .662K, .8H2V, .G4.., .G42., .G44., .G440, .G441, .G442, .G443, .G444, .G445, .G446, .G45Z, .G4Z., 14A3., 14A4., 14A5., 14AJ., 14AL., 322.., 3222, 662K., 662K0, 662K1, 662K2, 662K3, 662Kz, 889A.00, 8H2V., EGTON458, EMISAC1, EMISAC3, EMISCAN2, G3..., G30.., G300., G301., G3010, G3011, G301z, G302., G303., G304., G305., G306., G307., G3070, G3071, G308., G309., G30A., G30B., G30X., G30X0, G30y., G30y0, G30y1, G30y2, G30yz, G30z., G31.., G310., G311., G3110, G3111, G3112, G3113, G3114, G3115, G311z, G312., G31y., G31y0, G31y1, G31y2, G31y3, G31yz, G32.., G33.., G330., G3300, G330z, G331., G332., G33z., G33z0, G33z1, G33z2, G33z3, G33z4, G33z5, G33z6, G33z7, G33zz, G34.., G340., G3400, G3401, G341., G3410, G3411, G3412, G3413, G341z, G342., G343., G344., G34y., G34y0, G34y1, G34yz, G34z., G34z0, G35.., G350., G351., G353., G35X., G36.., G360., G361., G362., G363., G364., G365., G366., G37.., G38.., G380., G381., G382., G383., G384., G38z., G39.., G3y.., G3z.., G501., G501.00, G5y2., G704., G72B1, Gyu3., Gyu30, Gyu31, Gyu32, Gyu33, Gyu34, Gyu35, Gyu36, Ua1eH, X2006, X2007, X2008, X2009, X200a, X200A, X200B, X200c, X200d, X200D, X200e, X200G, X200H, X200I, X200J, X200K, X200L, X200M, X200N, X200O, X200P, X200Q, X200R, X200S, X200T, X200U, X200V, X200W, X200x, X200X, X200Y, X200Z, X201u, X2021, X202q, X202r, X203e, X204f, X204q, X77vP, X782C, X782F, Xa0YL, Xa6Yx, Xa7nH, XaAC3, XaAzi, XaBL1, XaBL2, XaBL4, XaEgZ, XaeVd, XaEXt, XaFsG, XaFsH, XaG1Q, XaIf1, XaINF, XaIwM, XaIwY, XaJX0, XaNxN, XaYYq, XC0bX, XE0Ui, XE0Uk, XE0WC, XE0WG, XE2aA, XE2uV, XM0rN, XM1Qk, XSDT6, Y07f2, Y07f3, Y3657
Myocardial infarction	Algorithm	42000
	Self-report (20002)	1075
	First occurrences	131298, 131300, 131302
	Diagnosed by doctor (6150, 6152)	1, 3894
	ICD9	410, 411, 412, 429
	ICD10	I21, I22, I23, I241, I252
	Primary care	14A3., 14A4., 322.., 3222, 889A.00, G30.., G300., G301., G3010, G3011, G301z, G302., G303., G304., G305., G306., G307., G3070, G3071, G308., G309., G30A., G30B., G30X., G30X0, G30y., G30y0, G30y1, G30y2, G30yz, G30z., G31.., G310., G3110, G3115, G312., G31y., G31y0, G31y1, G31y2, G31y3, G31yz, G32.., G34.., G340., G3400, G3401, G341., G3410, G3411, G3412, G3413,

Disease	Source	Codes
		G341z, G342., G343., G344., G34y., G34y0, G34y1, G34yz, G34z., G34z0, G35.., G350., G351., G353., G35X., G36.., G360., G361., G362., G363., G364., G365., G366., G38.., G380., G381., G382., G383., G384., G38z., G3y.., G3z.., G501., G501.00, G5y2., G704., G72B1, Gyu31, Gyu32, Gyu33, Gyu34, Gyu35, Gyu36, X2006, X200a, X200d, X200D, X200e, X200G, X200H, X200I, X200J, X200K, X200L, X200M, X200N, X200O, X200P, X200Q, X200R, X200S, X200T, X200U, X200V, X200W, X200x, X200X, X200Y, X200Z, X201u, X2021, X202q, X202r, X203e, X204f, X204q, X77vP, X782C, X782F, Xa0YL, Xa6Yx, XaAC3, XaAzi, XaBL1, XaEgZ, XaeVd, XaFsH, XaG1Q, XaIf1, XaINF, XaIwM, XaIwY, XaJX0, XC0bX, XE0Uk, XE0WG, XE2aA, XM0rN, XM1Qk, XSDT6
Non-ischaemic cardiomyopathies	Self-report (20002)	1079, 1588
	First occurrences	131288, 131292, 131338, 131340
	ICD9	4020, 4021, 4029, 4040, 4041, 4049, 4250, 4253, 4255
	ICD10	I11, I13, I42, I43
	Primary care	.G32., .G34., .G64., .G642, .G643, .G644, .G645, .G646, .G64Z, A860., C3733, F3919, F391B, G21.., G210., G2100, G2101, G210z, G211., G2110, G2111, G211z, G21z., G21z0, G21z1, G21zz, G23.., G230., G231., G232., G233., G234., G23z., G55.., G550., G551., G552., G553., G554., G5540, G5541, G5542, G5543, G5544, G5545, G554z, G555., G556., G557., G5574, G557z, G558., G5580, G5581, G5582, G5584, G558z, G559., G55A., G55y., G55y0, G55z., G5yy0, G5yy1, G5yy3, G5yy4, Gyu5M, Gyu5N, Gyu5P, Gyu5Q, Gyu5R, Gyu5S, Gyu5T, L1280, L1281, L1865, X201a, X201b, X201c, X201d, X201e, X201f, X201h, X201W, X201Y, X201Z, X708j, X708p, X77tY, X77vE, X77vQ, X77yh, X77yN, Xa1fq, Xa9Bp, XaI9b, XaWye, XaXNg, XaZcx, XE0Ue, XE0Uy, XE0Uz, XE0V0, XE0V1, XE0Wa
Valvular heart disease	Self-report (20002)	1078, 1489, 1490, 1584, 1585, 1586, 1587
	First occurrences	131276, 131278, 131280, 131282, 131322, 131324, 131326, 131328, 131330, 131332
	ICD10	I05, I06, I07, I08, I34, I35, I36, I37, I38, I39
	Primary care	.G21., .G22., .G22Z, .G232, .G6C., 24D5., 24D7., 7910, 79101, 79103, 7910y, 7910z, 7911, 79111, 7911y, 7911z, G11.., G110., G111., G112., G113., G114., G11z., G12.., G120., G121., G122., G12z., G13.., G130., G131., G132., G133., G13y., G13z., G140., G1400, G1401, G1402, G1403, G1404, G1405, G140z, G540., G5400, G5401, G5402, G5403, G540z, G541., G5410, G5411, G5412, G5413, G5414, G5415, G5416, G5417, G541z, G542., G5420, G5421, G5422, G542X, G542z, G543., G5430, G5431, G5432, G5433, G5434, G543z, G544., G5440, G5441, G5442, G544X, G54z., G54z0, G54z1, G54z2, G54z3, G54z4, G54z5, G54zz, Gyu10, Gyu11, Gyu12, Gyu13, Gyu15, Gyu55, Gyu56, Gyu57, Gyu58, Gyu59, Gyu5A, Gyu5B, Gyu5C, Gyu5D, Gyu5E, Gyu5f, X00uF, X00vi, X00vj, X00vk, X00vl, X00vV, X00vW, X200k, X200l, X200m, X200p, X200r, X200u, X200v, X200w, X200y, X200z, X2015, X201G, X201N, X76KE, X76KF, X76KI, X76KK, X76KN, X76KO, X76KP, X76KQ, X76KR, X76KS, X76KT, X76KU, X76KV, X76KX, X777c, X777i, X777k, X777l, X777q, X777r, X777w, X7784, X7786, X7787, X7788, X778A, X778D, X778E, X77zb, Xa0D0, Xa3fK, Xa3fL, Xa3fM, Xa3fN, Xa3fO, Xa3fU, Xa6Zk, XaB0g, XaBXl, XaBXo, XaI9k, XE0Ed, XE0Ef, XE0Vq, XE0Vu, XM00K, XM1IX, XM1LF, XM1LP, XM1LQ, XSDVN
Diabetes	Self-report (20002)	1220, 1222, 1223
	First occurrences	130706, 130708, 130712, 130714
	Diagnosed by doctor	2443, 2976
	Medications (6153, 6177)	3
	ICD10	E10, E11, E13, E14, G590, G632, H280, H360, M142, N083, O240, O241, O243, O244, O249, Y423
	Primary care	C1000, C1001, C100z, C101., C1010, C1011, C101y, C101z, C102., C1020, C1021, C102z, C103., C1030, C1031, C103y, C103z, C104y, C105., C1050, C1051, C105y, C105z, C106., C1060, C1061, C106y, C106z, C107., C1070, C1071, C1072, C1073, C1074, C107y, C107z, C108., C1080, C1081, C1082, C1083, C1084, C1085, C1086, C1088, C1089, C108A, C108E, C108y, C108z, C109., C1090, C1091, C1092, C1093, C1094, C1095, C1097, C1099, C109D, C109J, C109K, C10B., C10B0, C10C., C10D., C10E., C10E0, C10E1, C10E2, C10E3, C10E4, C10E5, C10E6, C10E8, C10E9, C10EA, C10EE, C10EM, C10EN, C10ER, C10F., C10F0, C10F1, C10F2, C10F3, C10F4, C10F5, C10F7, C10F8, C10F9, C10FD, C10FJ, C10FK, C10FN, C10FP, C10FS, C10G., C10G0, C10H., C10H0, C10J., C10J0, C10K., C10K0, C10L., C10L0, C10M., C10M0, C10N., C10N0, C10N1, C10P0, C10P1, C10Q., C10y., C10y0, C10y1, C10yy, C10yz, C10z., C10z0, C10z1, C10zy, C10zz, C11y0, Cyu20, Cyu23, F374., F374z, F4205, F464., F4643, F464z, Fyu6D, Fyu73, Fyu74, Fyu75, Fyu76, Fyu77, Fyu78, Fyu79, FyuE3, FyuE4, FyuE5, FyuF9, K00y0, K01x., K01xz, K02y0, K03y0, K0A6., K0A7., Kyu00, Kyu01, Kyu02, Kyu03, Kyu04, Kyu05, Kyu06, L180., L1800, L1801, L1802, L1803, L1804, L1805, L1806, L1807, L1808, L1809, L180A, L180B, L180X, L180z, Lyu29, M0372, M2710, M2711, M2712, N03.., N030., N0302, N031., N03x., N03x0, N03x1, N03x2, N03x3, N03x4, N03x5, N03x6, N03x7, N03x8, N03x9, N03xA, N03xB, N03xC, N03xD, N03xE, N03xF, N03xG, N03xH, N03xJ, N03xK, N03y., N03z., Nyu1C, Nyu1D,

Disease	Source	Codes
		Nyu1E, Nyu1F, R0542, R0543, X008t, X00cE, X40JI, X40Jj, X40Jk, X40KH, Xaagd, XacoB, XaE69, XaE6A, XaJlL, XaJlN, XaJlO, XaJlR, XaMzI
Gestational diabetes	Diagnosed by doctor	2976, 4041
	ICD9	6480
	ICD10	O244
	Primary care	.C2B., L180., L1800, L1801, L1802, L1803, L1804, L1805, L1806, L1807, L1808, L1809, L180A, L180B, L180X, L180z, Lyu29, X40Jj, X40Jk, X40Jm, XaOPl, XaXZU, ZV13F
Insulin	Diagnosed by doctor	2986
	Medications (20003)	1140883066
	Medications (6153, 6177)	3
	Primary care	.66A5, .66Am, .66Ap, .66AV, .C22., .C2A., 66Am., 66Ap., 66AV., 66Aw., 66o6., 7L100, 7L198, C109J, C10FJ, EMISNQCO166, EMISNQIN19, EMISNQIN49, EMISNQIN92, EMISNQSE45, f111., f12.., f121., f12E., f12W., f12X., f12y., f12z., f13.., f131., f133., f136., f13A., f14.., f14w., f14x., f14y., f14z., f15.., f15x., f15y., f15z., f2..., f21.., f21z., f22.., f221., f22y., f22z., f23.., f23z., f24.., f24z., f25.., f251., f25s., f25W., f25X., f25Y., f25Z., f26.., f26z., f27.., f28.., f29.., f291., f292., f293., f29A., f2A.., f2Ax., f2Ay., f2Az., f2B.., f2B2., f2B4., f2B6., f2C.., f2C2., fw1.., fw2.., ph2.., ph34., ph35., ph36., ph3c., ph3J., ph3K., ph3N., ph3P., ph3Q., ph3T., ph3U., ph3V., X40J6, X71b8, X75XP, Xa5vt, Xa5vu, Xa5XQ, Xa5XR, XaMdq, XaP63, XaR7E, XaXfW, Y1206
Type 1 diabetes	Self-report (20002)	1222
	First occurrences	130706
	ICD10	E10, O240
	Primary care	.66An, .C2C., .C2C0, 66An., C1000, C1010, C1020, C1030, C1050, C1060, C1070, C1073, C108., C1080, C1081, C1082, C1083, C1084, C1085, C1086, C1087, C1088, C1089, C108A, C108B, C108C, C108D, C108E, C108F, C108G, C108H, C108J, C10E., C10E0, C10E1, C10E2, C10E3, C10E4, C10E5, C10E6, C10E7, C10E8, C10E9, C10EA, C10EB, C10EC, C10ED, C10EE, C10EF, C10EG, C10EH, C10EJ, C10EK, C10EL, C10EM, C10EN, C10EP, C10EQ, C10ER, C10P0, C10y0, C10z0, L180., L1800, L1801, L1802, L1803, L1804, L1805, L1806, L1807, L1808, L1809, L180A, L180B, L180X, L180z, Lyu29, X40J4, X40Jj, X40Jk, Xa2h9, Xa4g7, Xaage, XaELP, XaEnn, XaEno, XaF04, XafjT, XaFm8, XaFmK, XaFmL, XaFmM, XaFWG, XaIzM, XaIzN, XaJSr, XaKyW, XaMhJ, XaX49, XaXZv, XM19i
Type 2 diabetes	Self-report (20002)	1223
	First occurrences	130708
	ICD10	E11, O241
	Primary care	.66Ao, .C2A., .C2D., .C2D0, 66Ao., C1001, C1011, C1021, C1031, C1051, C1061, C1071, C1072, C1074, C109., C1090, C1091, C1092, C1093, C1094, C1095, C1096, C1097, C1099, C109A, C109B, C109C, C109D, C109E, C109F, C109G, C109H, C109J, C109K, C10D., C10F., C10F0, C10F1, C10F2, C10F3, C10F4, C10F5, C10F6, C10F7, C10F8, C10F9, C10FA, C10FB, C10FC, C10FD, C10FE, C10FF, C10FG, C10FH, C10FJ, C10FK, C10FL, C10FM, C10FN, C10FP, C10FQ, C10FR, C10FS, C10P1, C10Q., C10y1, C10z1, L180., L1800, L1801, L1802, L1803, L1804, L1805, L1806, L1807, L1808, L1809, L180A, L180B, L180X, L180z, Lyu29, X40J5, X40J6, X40Jj, X40JJ, X40Jk, Xa2hA, XacoB, XaELQ, XaEnp, XaEnq, XaF05, XaFmA, XaFn7, XaFn8, XaFn9, XaFWI, XaIfG, XaIfI, XaIrf, XaIzQ, XaIzR, XaJQp, XaKyX, XaMhK, XaXZR, XM19j
Family history of dementia	Self-report (20107)	10
	Self-report (20110)	10
	Self-report (20111)	10
	Primary care	.1281, .129B, 1281, 129B., XaIkh
Family history of diabetes	Self-report (20107)	9
	Self-report (20110)	9
	Self-report (20111)	9
	Primary care	.1252, .1253, 1252., 12520, 12521, 1253., 12G2., EMISNQFH1, EMISNQFH2, EMISNQFH3, EMISNQFH4, EMISNQFH5, EMISNQFH6, XaKYz, XaVw3, XaVw4, ZV180, ZV198
Family history of heart disease	Self-report (20107)	1
	Self-report (20110)	1
	Self-report (20111)	1

Disease	Source	Codes
	Primary care	.12C., .12C2, .12C3, .12C5, .12CA, .12CB, .12CC, .12CD, .12CI, .12CN, .12CP, .12CV, .12CW, 12C.., 12C2., 12C3., 12C5., 12CA., 12CB., 12CC., 12CD., 12CI., 12CN., 12CP., 12CV., 12CW., EMISNQFH7, EMISNQFH8, Xa6aj, XaI9x, XaI9y, XaI9z, XaIA0, XaILC, XaIya, XaIyb, XaLQq, XaP9K, XaP9M, XaQvx, XaQvy, XE0oF, XE0oG, XE0oH, XE0oI, XE0sZ, XE24Z, XM1Jg, XM1Jx, XM1Jy, XM1XU, XM1Y7, Y1f27, ZV173, ZV174, ZVu66
Family history of kidney disease	Primary care	.12F1, .12FZ, 12F1., 12FZ., ZV186
Family history of liver disease	Primary care	.12E3, 12E3., XE0oN, XM1K5
Family history of stroke	Self-report (20107)	2
	Self-report (20110)	2
	Self-report (20111)	2
	Primary care	.12C4, .12CZ, 12C4., 12CZ., XE2tY, XM1Jf, ZV171
Acute kidney injury	Self-report (20002)	1192
	First occurrences	132030
	ICD9	584
	ICD10	N17
	Primary care	.J15., 14D8., 451L., K034., K035., K04.., K040., K041., K042., K043., K0430, K0431, K0432, K0433, K0434, K044., K045., K046., K0460, K0461, K047., K048., K049., K04A., K04B., K04C., K04D., K04E., K04y., K04z., K13D., Kyu20, L0931, L393., L3930, L3931, L3932, L393z, SK08., X30Im, X30Ir, X30Is, X30Iu, X30J5, X30J6, Xa6nr, Xa85t, Xaa8O, Xaa8P, Xaa8Q, XabmE, XaebJ, XaPwv, XaZ6J, XaZe5, XaZPp, XaZPs, XaZPt, XaZPu, XaZSx, XaZUa, XaZUY, XaZUZ, XaZYv, XaZZ0, XaZZ2, XE1oB, XE2QM
Chronic kidney disease	Algorithm	42026
	Self-report (20002)	1193
	Self-report (20004)	1195, 1580, 1581, 1582
	ICD9	585, 5859
	ICD10	N165, N180, N183, N184, N185, N188, N189, T824, T861, Y602, Y612, Y622, Y841, Z490, Z491, Z492, Z940, Z992
	OPCS4	L741, L742, L743, L744, L745, L746, L748, L749, M012, M013, M014, M015, M018, M019, M023, M084, M172, M174, M178, M179, X401, X402, X403, X404, X405, X406, X407, X408, X409, X411, X412, X418, X419, X421, X428, X429, X431
	Primary care	.1Z12, .1Z13, .1Z14, .1Z15, .1Z16, .1Z1B, .1Z1C, .1Z1D, .1Z1E, .1Z1F, .1Z1G, .1Z1H, .1Z1J, .1Z1K, .1Z1L, 1Z12., 1Z13., 1Z14., 1Z15., 1Z16., 1Z1a., 1Z1b., 1Z1B., 1Z1c., 1Z1C., 1Z1d., 1Z1D., 1Z1e., 1Z1E., 1Z1f., 1Z1F., 1Z1G., 1Z1H., 1Z1J., 1Z1K., 1Z1L., 1Z1T., 1Z1V., 1Z1W., 1Z1X., 1Z1Y., 1Z1Z., K05.., K050., K053., K054., K055., K0D.., X30In, X30J0, X30J1, XacAb, XacAd, XacAe, XacAf, XacAh, XacAi, XacAM, XacAN, XacAO, XacAV, XacAW, XacAX, XaLHI, XaLHJ, XaLHK, XaNbn, XaNbo, XaO3t, XaO3u, XaO3v, XaO3w, XaO3x, XaO3y, XaO3z, XaO40, XaO41, XaO42, XE0df
Early chronic kidney disease	Self-report (20002)	1194
	ICD10	N181, N182
	Primary care	K051., K052., Xac9y, Xac9z, XacA2, XacA4, XacA6, XacA9, XaLHG, XaLHH, XaO3p, XaO3q, XaO3r, XaO3s
Hypertensive renal disease	First occurrences	131290
	ICD10	I12
	Primary care	.G33., G22.., G220., G221., G222., G22z., K138., K1386, L121., L1210, L1211, L1212, L1213, L1214, L121z, XE0Uf, XE0Ug
Kidney stones	Self-report (20002)	1197
	First occurrences	132036
	ICD10	N20
	Primary care	4G41., 4G43., 4G6.., K1006, K12.., K120., K1200, K120z, K121., K122., K12z., X30Pn, X30Ps, XE0dj, XE26Q, XM14o, XM1V2
Other kidney disease	Self-report (20002)	1405

Disease	Source	Codes
	Primary care	K0B.., K0B0., K0B1., K0B2., K0B3., K0B4., K0B5., K10y3, K10y4, Kyu17, Kyu18, Kyu19, Kyu1A, Kyu1B, Kyu1C, Kyu1D, Kyu21, PD01., PD02z, PD03., PD030, PD031, PD032, PE02., X785W, X785X, X785Y, XE1LL
Alcoholic liver disease	First occurrences	131658
	ICD9	5710, 5711, 5712, 5713
	ICD10	K70
	Primary care	.I72., .I722, .I723, G8523, J610., J611., J612., J6120, J613., J6130, J617., J6170, X306r, X3071, X3072, X3073, XaBE3, XaC1d, XE0b4, XE0dD, XE0dF
Ascites	ICD9	7895
	ICD10	R18
Fatty liver disease	ICD10	K758, K760
	Primary care	EMISR4QFA1, J61y1, J61y7, J61y8, XaQIT, J61y9, X307v
Infective/viral hepatitis	Self-report (20002)	1156, 1578, 1579, 1580, 1581, 1582
	First occurrences	130194, 130196, 130198, 130200, 130202
	ICD9	070
	ICD10	B15, B16, B17, B18, B19
	Primary care	.2J23, .43B4, .43M2, .43X3, .A4A., .A4A1, .A4A3, .A4AZ, 2J23., 43B4., 43M2., 43X3., 43XA., 4JQD., 4JQF., A70.., A700., A701., A702., A7020, A703., A7030, A704., A7040, A704z, A705., A7050, A7051, A7052, A7054, A705z, A706., A707., A7070, A7071, A7072, A7073, A707X, A708., A709., A70A., A70B., A70C., A70D., A70E., A70F., A70G., A70z., A70z0, A70z1, AyuB., AyuB0, AyuB1, AyuB2, AyuB3, AyuB4, C13-SHHAPT, C15-SHHAPT, EMISNQHE11, EMISNQHE176, EMISNQHE178, EMISNQHE29, J6315, J633., J633z, X306b, X306c, X306d, X306e, X306f, X306g, X306h, X306i, X306j, X306k, X306l, X306p, X306q, X306Z, Xa9C8, XaCm8, XaFDz, XaQe4, XaXBp, XaYbh, XaYbp, XaYbq, XE0RK, XE0TW, XE0TY, XE2uF, Y096d, Y096f
Liver cirrhosis	Self-report (20002)	1141, 1158
	First occurrences	131666
	ICD9	4560, 4561, 5715, 5722, 5723, 5724
	ICD10	I850, I859, I864, I982, I983, K740, K741, K742, K746, K766, K767
	Primary care	.I725, 2485, G85.., G850., G851., G852., G8520, G8521, G8522, G852z, G857., G858., Gyu94, HNG0090, J61.., J615., J6150, J6151, J6152, J6153, J6154, J6155, J6156, J6157, J6158, J6159, J615A, J615B, J615C, J615D, J615E, J615F, J615G, J615H, J615y, J615z, J616., J6160, J6161, J6162, J616z, J61y., J61y3, J61y4, J61y5, J61y6, J6356, Jyu71, X307L, X307M, X307N, X307O, X307P, X307S, X307T, X307U, X307V, Xa9C7, XaBM6, XE0b5, XE0b7, XE0bA, XE2up
Liver failure	Self-report (20002)	1158
	First occurrences	131662
	ICD9	570
	ICD10	K72, T864, Z944
	OPCS4	J01, X43
	Primary care	.79L8, .I71., 7800, 78000, 78001, 7L1f., 7L1fy, 7L1fz, J60.., J600., J6000, J6001, J6002, J600z, J601., J6010, J6011, J6012, J601z, J60z., J6130, J61y0, J622., J625., J62y., SP086, SP142, X0042, X0058, X20a8, X3073, X3076, X3077, X3078, X3079, X307A, X307C, X307x, X307z, Xa8Df, XaMuG, XaMuH, XaMuI, XE0dB, ZV427
Other liver diseases	Self-report (20001)	1024
	First occurrences	131660, 131664, 131668, 131672
	Cancer register (40006)	C22
	ICD9	155, 572, 573
	ICD10	C22, K71, K73, K75, K77
	Primary care	B15.., B150., B1500, B1501, B1502, B1503, B150z, B151., B1510, B1511, B1512, B1513, B1514, B151z, B152., B15z., B7158, Byu10, Byu11, J614., J6140, J6141, J6142, J6143, J6144, J614y, J614z, J61y., J61yz, J61z., J62.., J620., J6200, J6201, J6202, J6203, J6204, J620z, J621., J623., J624., J62z., J63.., J630., J631., J6311, J631z, J632., J632z, J633., J6330, J633z, J634., J635., J6350, J6351, J6352, J6353, J6354, J6355, J6356, J6357, J635X, J636., J637., J638., J639., J63A., J63B., J63X., J63y., J63y0, J63y1, J63y2, J63yz, J63z., Jyu70, Jyu72, Jyu73, Jyu74, Jyu75, Jyu76, Jyu77,

Disease	Source	Codes
		X205z, X207Y, X306p, X306q, X306s, X306t, X306u, X306U, X306V, X306x, X306y, X307a, X307b, X307c, X307G, X307I, X307J, X307K, X307w, X307Z, X50Aq, X76FK, X76FM, X76LZ, X77nk, X78Oz, X78P0, Xa0lo, Xa7UL, Xa7UM, Xa7UP, Xa8Kk, Xa97q, Xa97r, Xa9C7, Xa9G4, XaFrG, XaJTk, XaJxp, XE0b7, XE0bC, XE1xp, XE1xr, XM1FE
Atypical antipsychotic medication	Medications (20003)	1140867420, 1140867432, 1140867444, 1140927956, 1140927970, 1140928916, 1141152848, 1141152860, 1141153490, 1141167976, 1141177762, 1141195974, 1141202024
	Primary care	d4l.., d4l1., d4l2., d4lC., d4lE., d4lG., d4m3., d4m4., d4p.., d4p1., d4p2., d4p3., d4p4., d4p5., d4p6., d4p7., d4p8., d4p9., d4pA., d4pB., d4pC., d4pD., d4pH., d4pJ., d4pK., d4pL., d4pM., d4pN., d4pO., d4pP., d4pQ., d4pR., d4pS., d4pz., d4q.., d4q1., d4q2., d4q3., d4q4., d4q5., d4q6., d4q7., d4q8., d4r.., d4r1., d4r2., d4r3., d4r4., d4r5., d4r6., d4r7., d4r8., d4r9., d4rA., d4rB., d4rC., d4rE., d4rF., d4rt., d4ru., d4rw., d4rx., d4ry., d4rz., d4s.., d4s1., d4s2., d4s3., d4s4., d4s5., d4s6., d4s7., d4s8., d4s9., d4sA., d4sB., d4sC., d4sD., d4sE., d4sF., d4sG., d4ss., d4st., d4su., d4sv., d4sw., d4sx., d4sy., d4sz., d4t.., d4t1., d4t2., d4tx., d4ty., d4tz., d4v.., d4v1., d4v2., d4v3., d4v4., d4v5., d4v6., d4v7., d4vt., d4vu., d4vv., d4vw., d4vx., d4vy., d4vz., d58.., x02ps, x03hI, x03ik, x03qI, x056z, x05gB, x05gC, x05gE, x05kh, x05Ku, x05te, Y1cbb
Depression 1 (Mild/moderate or single episode)	Self-report (20002)	1286
	Self-report (20544)	11
	First occurrences	130894
	ICD9	3090, 311
	ICD10	F320, F321, F328, F329, F412
	Primary care	1465, 1B17., 1B1U., 1BT.., 2257, 62T1., 9H90., 9H91., 9H92., E112., E1120, E1121, E1122, E1123, E1124, E1125, E1126, E112z, E11y2, E11z2, E135., E2002, E2003, E2004, E204., E2B.., E2B0., E2B1., Eu32., Eu320, Eu321, Eu322, Eu323, Eu324, Eu325, Eu326, Eu327, Eu328, Eu329, Eu32y, Eu32z, Eu41., Eu410, Eu411, Eu412, Eu413, Eu41y, Eu41z, Eu530, X00Sb, X00Sc, X00SO, X00SQ, X00SR, X00SS, X00SU, X40Dl, Xa0wV, XaB9J, XaCHr, XaCHs, XaCIs, XaCIt, XaImU, XaK6d, XaK6e, XaK6f, XaX53, XE0re, XE0uv, XE1Y0, XE1YC, XE1Za, XE1Zb, XE1Zj, XE1ZY, XE1ZZ, XM0CR, XSEGJ, XSGok, XSGol, XSGom, XSGon
Depression 2 (Severe or recurrent)	First occurrences	130896
	ICD9	3091
	ICD10	F322, F330, F331, F332, F334, F338, F339
	Primary care	E1121, E1122, E1123, E1124, E1126, E113., E1130, E1131, E1132, E1133, E1134, E1135, E1136, E1137, E113z, E291., E2B1., Eu32., Eu320, Eu321, Eu322, Eu323, Eu324, Eu325, Eu326, Eu327, Eu328, Eu329, Eu32A, Eu32y, Eu32z, Eu33., Eu330, Eu331, Eu332, Eu333, Eu334, Eu33y, Eu33z, X00SQ, X00SR, X00SS, X00SU, X40Dm, Xa0wV, XaCHo, XaCHr, XaCHs, XaCIs, XaCIu, XaX53, XaX54, XE1Y0, XE1Y1, XE1YC, XE1Za, XE1Zb, XE1Zc, XE1Zd, XE1Ze, XE1Zf, XE1ZY, XE1ZZ, XM1GC, XSEGJ, XSGok, XSGol, XSGom, XSGon
Eating disorder	Self-report (20002)	1470
	Self-report (20544)	12, 13, 16
	ICD10	F50
Serious mental illness	Self-report (20002)	1243, 1289, 1291
	Self-report (20544)	10, 2, 3
	First occurrences	130874, 130880, 130886, 130888, 130892
	ICD9	295, 296
	ICD10	F20, F23, F28, F29, F31, F323, F333
	Primary care	1464, 1464., 146D., 146H., 212V., 9H8.., E01y., E01z., E03y3, E04z., E1…, E10.., E100., E1000, E1001, E1002, E1003, E1004, E1005, E101., E1010, E1011, E1012, E1013, E1014, E1015, E101z, E102., E1020, E1021, E1022, E1023, E1024, E1025, E102z, E103., E1030, E1031, E1032, E1033, E1034, E1035, E103z, E104., E106., E107., E1070, E1071, E1072, E1073, E1074, E1075, E107z, E10y., E10y0, E10y1, E10yz, E10z., E11.., E110., E111., E1110, E1111, E1112, E1113, E1114, E1115, E1116, E111z, E114., E1140, E1141, E1142, E1143, E1144, E1145, E1146, E114z, E115., E1150, E1151, E1152, E1153, E1154, E1155, E1156, E115z, E116., E1160, E1161, E1162, E1163, E1164, E1165, E1166, E116z, E117., E1170, E1171, E1172, E1173, E1174, E1175, E1176, E117z, E11y., E11y0, E11y1, E11y3, E11yz, E11z., E11z0, E11zz, E121., E122., E12z., E13.., E130., E131., E133., E134., E13y., E13y1, E13yz, E13z., E1z.., Eu0z., Eu105, Eu2.., Eu20., Eu200, Eu201, Eu202, Eu203, Eu204, Eu205, Eu206, Eu20y, Eu20z, Eu220, Eu23., Eu230, Eu231, Eu232, Eu233, Eu23y, Eu23z, Eu250, Eu251, Eu26., Eu2y., Eu2z., Eu30., Eu31., Eu310, Eu311, Eu312, Eu313, Eu314, Eu315, Eu316, Eu317, Eu318, Eu319, Eu31y, Eu31z, Eu323, Eu328, Eu329, Eu32A, Eu333, Eu531, X00Qx, X00RN, X00RV, X00S6, X00S8, X00SM, X00SN, X40Dp, X763T, X79ul, Xa0s9, Xa1aD, Xa1Pl, Xa9B0, XaA6j, XaB5v, XaB95, Xabk6, XaIx7, XaL07, XaMwc, XaX53, XaX54, XaY1Y, XE1aM, XE1aO, XE1aQ, XE1aS, XE1Xw, XE1Xx, XE1Y2, XE1Y5, XE1Zc,

Disease	Source	Codes
		XE1Zd, XE1Ze, XE1Zf, XE1ZM, XE1ZQ, XE1ZR, XE1ZS, XE1ZT, XE1ZU, XE1ZW, XE1ZX, XE1ZY, XE1ZZ, XE2un, XE2uT, XM1GC, XM1GG, XM1GH, XSGon, ZV110
Antihypertensive medication	Medications (20003)	1140860334, 1140860336, 1140860338, 1140860340, 1140860342, 1140860348, 1140860352, 1140860356, 1140860358, 1140860380, 1140860382, 1140860386, 1140860390, 1140860394, 1140860396, 1140860398, 1140860402, 1140860404, 1140860406, 1140860410, 1140860418, 1140860422, 1140860426, 1140860434, 1140860492, 1140860498, 1140860562, 1140860564, 1140860580, 1140860590, 1140860610, 1140860654, 1140860658, 1140860690, 1140860696, 1140860706, 1140860714, 1140860728, 1140860736, 1140860738, 1140860750, 1140860752, 1140860758, 1140860764, 1140860776, 1140860784, 1140860790, 1140860802, 1140860806, 1140860878, 1140860882, 1140860892, 1140860904, 1140860912, 1140860918, 1140861088, 1140861090, 1140861106, 1140861110, 1140861114, 1140861120, 1140861128, 1140861130, 1140861136, 1140861138, 1140861166, 1140861176, 1140861190, 1140861194, 1140861202, 1140861276, 1140861282, 1140864950, 1140864952, 1140866072, 1140866078, 1140866090, 1140866092, 1140866094, 1140866096, 1140866102, 1140866104, 1140866122, 1140866128, 1140866132, 1140866136, 1140866138, 1140866140, 1140866144, 1140866146, 1140866156, 1140866158, 1140866162, 1140866164, 1140866168, 1140866226, 1140866232, 1140866236, 1140866244, 1140866262, 1140866306, 1140866308, 1140866312, 1140866318, 1140866324, 1140866328, 1140866330, 1140866340, 1140866352, 1140866354, 1140866360, 1140866396, 1140866400, 1140866402, 1140866404, 1140866410, 1140866416, 1140866420, 1140866440, 1140866446, 1140866450, 1140866460, 1140866466, 1140866484, 1140866546, 1140866554, 1140866692, 1140866704, 1140866712, 1140866724, 1140866726, 1140866738, 1140866756, 1140866758, 1140866764, 1140866766, 1140866778, 1140866782, 1140866784, 1140866798, 1140866800, 1140866802, 1140866804, 1140879760, 1140879762, 1140879778, 1140879782, 1140879786, 1140879794, 1140879798, 1140879802, 1140879806, 1140879810, 1140879818, 1140879824, 1140879830, 1140879834, 1140879842, 1140879866, 1140888510, 1140888552, 1140888556, 1140888560, 1140888578, 1140888646, 1140909368, 1140911698, 1140916356, 1140916362, 1140917428, 1140923572, 1140923712, 1140923718, 1140926778, 1140926780, 1141145658, 1141145660, 1141145668, 1141151016, 1141151018, 1141151382, 1141152600, 1141152998, 1141153006, 1141153026, 1141153032, 1141153328, 1141156754, 1141156808, 1141156836, 1141156846, 1141164148, 1141164154, 1141164276, 1141164280, 1141165470, 1141165476, 1141166006, 1141167822, 1141167832, 1141171152, 1141171336, 1141171344, 1141172682, 1141172686, 1141180592, 1141180598, 1141187788, 1141187790, 1141190160, 1141193282, 1141193346, 1141194794, 1141194800, 1141194804, 1141194808, 1141194810, 1141201038, 1141201040
	Medications (6153, 6177)	2
	Primary care	.8B26, .8B6Q, .8B6T, .8BL0, 8B26., 8B6E., 8B6F2, 8B6F3, 8B6G., 8B6H., 8B6Q., 8B6R., 8B6T., 8BG4., 8BGA., 8BL0., 8BMa1, b21.., b211., b212., b213., b214., b215., b216., b217., b218., b219., b21b., b22.., b221., b22y., b22z., b231., b232., b23z., b25.., b251., b25z., b26.., b261., b262., b263., b264., b26y., b26z., b27.., b27z., b28.., b285., b28z., b2a.., b2az., b2b.., b2b1., b2b2., b2b3., b2bz., b2c.., b2c1., b2cz., b414., b43.., b431., b432., b433., b434., b435., b436., b43a., b43A., b43b., b43c., b43d., b43e., b43f., b43g., b43h., b43j., b43k., b43l., b43m., b43n., b43z., b511., b512., b513., b514., b515., b518., b51a., b51b., b51c., b51E., b51f., b51F., b51G., b51J., b51K., b51r., b51s., b51v., b51w., b913., b915., b916., b919., b91a., b91c., b91e., b91h., bA..., bA1.., bA11., bA12., bA1y., bA1z., bb3.., bb31., bb32., bb33., bb34., bb35., bb36., bb37., bb38., bb39., bb3a., bb3A., bb3b., bb3B., bb3C., bb3d., bb3D., bb3e., bb3f., bb3F., bb3g., bb3h., bb3i., bb3j., bb3k., bb3M., bb3p., bb3q., bb3r., bb3v., bb3w., bb3y., bb3z., bd..., bd1.., bd11., bd12., bd13., bd14., bd15., bd16., bd17., bd18., bd19., bd1a., bd1A., bd1b., bd1B., bd1c., bd1C., bd1D., bd1E., bd1F., bd1G., bd1h., bd1i., bd1I., bd1j., bd1J., bd1k., bd1K., bd1l., bd1L., bd1m., bd1n., bd1o., bd1p., bd1P., bd1Q., bd1r., bd1R., bd1S., bd1t., bd1T., bd1u., bd1U., bd1v., bd1V., bd1w., bd1W., bd1x., bd1X., bd1y., bd1Y., bd2.., bd21., bd22., bd23., bd2w., bd2x., bd2y., bd3.., bd31., bd32., bd34., bd35., bd36., bd37., bd38., bd39., bd3c., bd3d., bd3e., bd3j., bd3x., bd5.., bd51., bd52., bd53., bd5t., bd5u., bd5v., bd5w., bd5x., bd5y., bd6.., bd6w., bd6x., bd6z., bd8.., bd81., bd82., bd83., bd84., bd8u., bd9.., bdd.., bdd1., bdd2., bddz., bde1., bde2., bde3., bde4., bde5., bde6., bde7., bde9., bdea., bdeA., bdeb., bdeB., bdec., bdeC., bdeD., bdeE., bdeF., bdej., bdek., bdeK., bdeL., bdeM., bdeo., bdep., bdeP., bdeq., bder., bdes., bdet., bdev., bdew., bdex., bdey., bdez., bdf.., bdf1., bdf2., bdf3., bdf4., bdf5., bdf6., bdf8., bdf9., bdfA., bdfB., bdfC., bdfD., bdfE., bdfw., bdfx., bdfy., bdfz., bdh.., bdh1., bdh2., bdi.., bdi1., bdj.., bdj1., bdj2., bdj3., bdj4., bdj5., bdl.., bdl3., bdl4., bdl5., bdl6., bdm.., bdm1., bdmy., bdmz., bdn.., bdn6., be..., bf..., bf3c., bh1.., bh11., bh12., bh13., bh14., bh1y., bh1z., bh2.., bh21., bh22., bh2y., bh2z., bh4.., bh41., bh42., bh43., bh44., bh45., bh46., bh47., bh48., bh49., bh4v., bh4w., bh4x., bh4y., bh4z., bh5.., bh51., bh52., bh53., bh54., bh55., bh56., bh57., bh5x., bh5y., bh5z., bh6.., bh61., bh62., bh63., bh64., bh65., bh66., bh67., bh68., bh6y., bh6z., bi..., bi1.., bi11., bi12., bi13., bi14., bi15., bi16., bi17., bi18., bi19., bi1a., bi1A., bi1B., bi1C., bi1I., bi1K., bi1p., bi1q., bi1r., bi1v., bi1w., bi1x., bi1y., bi1z., bi2.., bi21., bi22., bi23., bi24., bi25., bi26., bi27., bi28., bi29., bi2a., bi2A., bi2b., bi2B., bi2C., bi2D., bi2E., bi2F., bi2G., bi2H., bi2t., bi2u., bi2v., bi2w., bi2x., bi2y., bi2z., bi3.., bi31., bi32., bi33., bi34., bi35., bi36., bi37., bi38., bi39., bi3a., bi3b., bi3c., bi3d., bi3e., bi3f., bi3g., bi3h., bi3i., bi3j., bi3k., bi3l., bi3p., bi3q., bi3r., bi3t., bi3y., bi4.., bi41., bi42., bi43., bi47., bi48., bi4A., bi4F., bi5.., bi51., bi52., bi53., bi54., bi55., bi56., bi57., bi58., bi6.., bi61., bi62., bi63., bi67., bi69., bi6B., bi6C., bi6D., bi6E., bi6F., bi6G., bi7.., bi71., bi72., bi73., bi74., bi8.., bi81., bi82., bi83., bi84., bi85., bi86., bi87., bi88., bi89., bi8a., bi9.., bi91., bi92., bi93., bi94., bi95., bi96., bi97., bi98., bi99., bi9A., bi9z., biA.., biA1., biA2., biA3., biA4., biB.., biB1., biB2., biB3., biBx., biBy., biBz., biC.., biC1., biC2., biC3., biC4., biC5., biC6., biC7., biC8., bk..., bk2.., bk3.., bk31., bk32., bk33., bk34., bk35., bk36., bk37., bk38., bk39., bk3A., bk3B., bk3C., bk3D., bk3E., bk3y., bk3z.,

Disease	Source	Codes
		bk4.., bk41., bk42., bk43., bk44., bk45., bk46., bk47., bk48., bk49., bk4A., bk4B., bk4C., bk4s., bk4t., bk4u., bk4v., bk4w., bk4x., bk4y., bk4z., bk5.., bk51., bk52., bk53., bk54., bk55., bk56., bk57., bk58., bk59., bk5x., bk5y., bk5z., bk6.., bk61., bk7.., bk71., bk72., bk73., bk74., bk75., bk76., bk77., bk78., bk79., bk7z., bk8.., bk81., bk82., bk86., bk87., bk88., bk8w., bk8x., bk8y., bk8z., bk9.., bk91., bk92., bk93., bk9x., bk9y., bk9z., bkB.., bkB1., bkB2., bkB3., bkB4., bkB5., bkB6., bkC.., bkC1., bkC2., bkC3., bkCx., bkCy., bkCz., bkD.., bkD1., bkD2., bkD3., bkH.., bkHx., bkHy., bkHz., bkI.., bl5.., bl51., bl53., bl55., bl56., bl57., bl58., bl59., bl5a., bl5A., bl5b., bl5c., bl5d., bl5e., bl5E., bl5f., bl5F., bl5g., bl5G., bl5h., bl5H., bl5i., bl5I., bl5j., bl5J., bl5k., bl5K., bl5L., bl5m., bl5M., bl5n., bl5N., bl5O., bl5P., bl5Q., bl5R., bl5s., bl5S., bl5U., bl5x., bl5y., bl5z., bl5Z., bl7.., bl71., bl72., bl73., bl74., bl7w., bl7x., bl7y., bl7z., bl8.., bl81., bl82., bl83., bl84., bl85., bl86., bl8A., bl8b., bl8B., bl8e., bl8f., bl8F., bl8g., bl8G., bl8h., bl8i., bl8j., bl8k., bl8m., bl8M., bl8P., bl8Q., bl8R., bl8u., bl8v., bl8V., bl8w., bl8W., bl8x., bl8X., bl8y., bl8Y., bl8z., bla.., bla1., bla2., blb.., blb1., blb2., blb3., blb4., blb7., blb8., blc.., blc1., blc2., blc5., blci., blcj., ble.., ble1., ble2., ble3., ble4., blh.., blh1., blh2., blh3., blh4., blj.., blj1., blj2., blj3., blja., bljJ., bljP., bljY., bljZ., bll.., bll3., bll4., bllc., blld., EMISQPR5, gc41., gc5.., gc51., gc52., gc53., gc54., gc55., gc5z., k85.., x0004, x000z, x0010, x001j, x0044, x007H, x007i, x007v, x007w, x008F, x008y, x009B, x00A3, x00B5, x00B6, x00Bb, x00BL, x00Bu, x00Du, x00Te, x00Tl, x00Tm, x01C1, x01C2, x01C4, x01C6, x01C7, x01CA, x01CB, x01CD, x01CE, x01CF, x01CJ, x01CK, x01CN, x01CO, x01CP, x01CR, x01CS, x01CT, x01CU, x01CV, x01CW, x01Qe, x01Qf, x01Qg, x01QU, x01QV, x01QW, x01QX, x02ao, x02aQ, x02at, x02bC, x02bD, x02eC, x02eO, x02eP, x02fa, x02fB, x02fC, x02fG, x02fH, x02fI, x02fl, x02fm, x02fW, x02fX, x02fY, x02fz, x02fZ, x02g6, x02g7, x02im, x02jh, x02ji, x02jj, x02jn, x02jv, x02ke, x02kf, x02kk, x02kW, x02kX, x02lk, x02o9, x02oA, x02oB, x02oV, x02oW, x02Qa, x02Qc, x02Qd, x02Qe, x02qg, x02Qg, x02qh, x02Qh, x02QH, x02Qi, x02QI, x02Qj, x02QJ, x02Qk, x02QK, x02QL, x02QM, x02QO, x02qQ, x02QS, x02QW, x02QY, x02QZ, x02rM, x02rO, x02rP, x02rQ, x02rR, x02rU, x02Sc, x02Sd, x02sK, x02sL, x02Sn, x02So, x02sP, x02sQ, x02T4, x02T5, x02t6, x02tB, x02Tb, x02tC, x02Tc, x02TQ, x02Ty, x02u7, x02UA, x02UD, x02Ug, x02um, x02uP, x02Uy, x02Vc, x02Vm, x02VN, x02VO, x02VQ, x02VR, x02VT, x02VV, x02Wf, x02Wj, x02Wk, x02Wn, x02Wo, x02Wp, x02Wq, x02X3, x02Xf, x02Xg, x02Y2, x02Y4, x02YD, x02YE, x02Yx, x02Za, x03ce, x03df, x03e5, x03h1, x03iy, x03j2, x03jn, x03jo, x03ls, x03lt, x03n3, x03pa, x03qe, x03qf, x03qX, x03vs, x03vt, x03wm, x03xa, x03yR, x03zU, x0411, x0412, x046e, x046f, x047a, x047f, x047g, x047h, x047r, x047s, x047Y, x047Z, x048y, x048z, x049y, x04bN, x04bO, x04bR, x04c7, x04qm, x04qn, x04t2, x04t3, x04t4, x04t8, x04t9, x04tA, x04tB, x04vd, x04vg, x04xj, x04y0, x04yc, x04yd, x051w, x051x, x056B, x056P, x05DC, x05df, x05dg, x05Dq, x05F5, x05hA, x05j2, x05mo, x05rz, x05u2, x05wO, x060W, XaBLq, XaJ5h
High cholesterol	Self-report (20002)	1473
	First occurrences	130814
	Medications (6153, 6177)	1
	ICD10	E780, E782, E783, E784, E785
	Primary care	.C521, C32.., C320., C3200, C3201, C3202, C3203, C3204, C3205, C3206, C320y, C320z, C321., C3210, C322., C3220, C323., C324., C325., C3250, C3251, C3252, C3253, C325z, C328., C329., C32y., C32yz, C32z., Cyu8D, Cyu8E, X003s, X00dK, X20DV, X20DW, X40Vd, X40Vf, X40Vg, X40Vh, X40VH, X40Vi, X40VI, X40Vm, X40Vn, X40Vo, X40Vp, X40Vq, X40Vs, X40Vt, X40VT, X40VW, X40VY, X40Wx, X40Wy, X40Wz, X40X0, X40X1, X40X2, X40X3, X40X5, X40X6, X40X7, X40X9, X40XA, X40XH, X40XI, X40XO, X40XP, X50DQ, X50Fh, X50Fi, X50Fm, X50Fp, X76tz, X78qa, Xa9As, Xa9At, XaL5p, XaR4h, XaR4i, XaR4k, XaRG5, XE11R, XE11T, XE11U, XE11V, XE11W, XE13C
Hypertension	Self-report (20002)	1065, 1072
	First occurrences	131286
	Diagnosed by doctor (6150, 6152)	2966, 4
	Medications (6153, 6177)	2
	ICD10	I10
	Primary care	.14A2, .6627, .6628, .662d, .662F, .662O, .662P, .G3.., .G31., .G35., .G36., 14A2., 6627, 6628, 662d., 662F., 662O., 662P., 662P0, 7Q01., 7Q01z, EMISHGT69, EMISNQST25, G2..., G20.., G200., G201., G202., G203., G20z., G24.., G240., G24z., G24zz, G25.., G250., G251., G26.., G27.., G28.., G2y.., G2z.., HNGZ016, Xa3fQ, Xa8HD, XaIyE, XaM5f, XaM5p, XaXOi, XaZbz, XaZWn, XE0Ub, XE0Uc, XE0Ud, XE0W8, XM1YA, XSDSb
Regular steroid tablets	Medications (20003)	1140857672, 1140857678, 1140862572, 1140868364, 1140868370, 1140873620, 1140874790, 1140874792, 1140874794, 1140874810, 1140874814, 1140874816, 1140874822, 1140874896, 1140874930, 1140874936, 1140874940, 1140874944, 1140874950, 1140874954, 1140874956, 1140874976, 1140874978
Statins	Medications (20003)	1140861958, 1140888594, 1140888648, 1141146234, 1141192410

Disease	Source	Codes
	Primary care	bxd.., bxd1., bxd2., bxd5., bxdu., bxdv., bxdw., bxdx., bxdy., bxdz., bxe.., bxe1., bxe2., bxe5., bxe6., bxe7., bxg3., bxg4., bxgz., bxi.., bxi1., bxi2., bxi3., bxi9., bxiB., bxiy., bxiz., bxk.., bxkw., bxkx., bxky., bxkz., x01R2, x01R3, x05xL
Rheumatoid arthritis	Self-report (20002)	1464
	First occurrences	131848, 131850
	ICD10	M05, M06
	Primary care	14G1., 66HB0, N005., N04.., N040., N0402, N0403, N0404, N0405, N0406, N0407, N0408, N0409, N040A, N040B, N040C, N040D, N040E, N040F, N040G, N040H, N040J, N040K, N040L, N040M, N040N, N040P, N040Q, N040R, N040S, N040T, N041., N042., N0422, N042z, N047., N04X., N04y2, N04z., Nyu10, Nyu11, Nyu12, Nyu1G, X701h, X701i, X701l, X701p, X701s, X705I, X705t, X705u, X705v, Xa3gL, Xa3gP, Xa3wk, XaaWW, XaBMO, XaN2K, XaZdB, XE1DU, XM1XV
Systemic lupus erythematosus	Self-report (20002)	1381
	First occurrences	131894
	ICD9	7100
	ICD10	M32
	Primary care	.M11., H57y4, K01x4, K0B40, N000., N0000, N0002, N0003, N0004, N0005, N000z, Nyu43, X0046, X704b, X704c, X704W, X704X, X705w, XaBE1, XaC1J, XM0ji, XM0jj

Appendix 3: Published risk indices for heart-brain-liver-kidney risk

Risk score	Target disease	References	Score type	Component inputs
QStroke	Stroke	Hippisley-Cox et al. (2013)(1)	Standard	Age, sex, UK postcode / Townsend deprivation index, ethnicity, smoking, BMI, SBP, family history: heart disease, total/HDL cholesterol ratio, diabetes, diabetes, ischaemic heart disease, atrial fibrillation, valvular heart disease, heart failure, chronic kidney disease, antihypertensive medication, rheumatoid arthritis
CHA2DS2-VASc	Stroke	Ntaios et al. (2013)(2)	Remote	Age, sex, diagnoses or history of heart failure, hypertension, diabetes, stroke, transient ischaemic attack, venous thromboembolism, myocardial infarction, peripheral artery disease
QRISK3	Atherosclerotic CVD (myocardial infarction, stroke or CVD death)	Hippisley-Cox et al. (2017a)(3)	Standard	Age, sex, UK postcode / Townsend deprivation index, ethnicity, smoking, BMI, SBP, SBP standard deviation, family history: heart disease, total/HDL cholesterol ratio, diabetes, diabetes, erectile dysfunction, migraines, atrial fibrillation, chronic kidney disease, atypical antipsychotic medication, antihypertensive medication, regular steroid tablets, rheumatoid arthritis, systemic lupus erythematosus, severe mental illness
Framingham Risk Score (2 types)	Atherosclerotic CVD	D'Agostino et al. (2008)(4)	Remote Standard	Age, sex, current smoker, BMI, SBP, diabetes, antihypertensive medication (total cholesterol, HDL cholesterol)
SCORE2/ SCORE-OP	Atherosclerotic CVD	SCORE2 working group and ESC Cardiovascular risk collaboration (5)(6)	Standard	Age, sex, current smoker, SBP, diabetes, total cholesterol, HDL cholesterol
PCP-HF	Heart failure	Khan et al. (2019)(7)	Extended	Age, sex, ethnicity, BMI, SBP, smoking, hypertension, diabetes, blood glucose, total cholesterol, HDL cholesterol
UKB-DRS	All-cause dementia	Anatürk et al. (2020)(8)	Remote	Age, sex, education, family history of dementia, hypertension, diabetes, high cholesterol, stroke, depression, elevated socioeconomic deprivation, lives alone at home.
CAIDE	All-cause dementia	Kivipelto et al. (2006)(9)	Standard	Age, sex, education, physical activity, BMI, SBP, total cholesterol
LIBRA	All-cause dementia	Schiepers et al. (2018)(10)	Remote	Age, sex, education, current smoker, alcohol intake frequency, physical activity, BMI, hypertension, high cholesterol, diabetes, ischaemic heart disease, depression
CHARGE-AF	Atrial fibrillation	Alonso et al. (2013)(11)	Remote	Age, ethnicity, current smoker, height, weight, DBP, SBP, diabetes, myocardial infarction, heart failure, antihypertensive medication
QKidney (2 versions)	Chronic kidney disease	Hippisley-Cox et al. (2010)(12)	Remote	Age, sex, UK postcode / Townsend deprivation index, ethnicity, smoking, BMI, SBP, family history: kidney disease, diabetes, diabetes, atherosclerosis / peripheral artery disease, heart disease, heart failure, kidney stones, antihypertensive medication, NSAID use, rheumatoid arthritis, systemic lupus erythematosus

Kidney risk score	Chronic kidney disease	Nelson et al. (2019)(13)	Extended	Age, sex, ethnicity, smoking, BMI, hypertension, diabetes, heart disease, insulin use, estimated glomerular filtration rate, glycated haemoglobin (hba1c), serum creatinine, urine albumin, urine creatinine
Fatty liver index	NAFLD	Bedogni et al. (2006)(14)	Extended	BMI, waist circumference, GGT, triglycerides
Dallas Steatosis Index	NAFLD	McHenry et al. (2020)(15)	Extended	Age, sex, ethnicity, BMI, hypertension, diabetes, alanine aminotransferase, glucose, triglycerides
QDiabetes (2 versions)	Undiagnosed current	Hippisley-Cox et al (2017b) (16)	Extended	Age, sex, ethnicity, UK postcode / Townsend deprivation index, BMI, smoking, atypical antipsychotic medication, regular steroid tablets, history of heart attack, angina, stroke or TIA, history of gestational diabetes (yes/no), learning difficulties, serious mental illness, polycystic ovarian syndrome, statins, antihypertensive medication, family history of diabetes. [HbA1c, blood glucose]
Cambridge Diabetes	Type 2 diabetes	Griffin et al. (2000)(17)	Remote	Age, sex, smoking, BMI, family history of diabetes, antihypertensive medication, prescribed steroids
AUDIT-C	Alcohol use disorder	Bush et al. (1998)(18)	Remote	Ten-item questionnaire about alcohol use. [Please note only the first question could be implemented in our sample due to high missingness]
FIB-4	Liver fibrosis /cirrhosis	Vallet-Pichard et al. (2007)(19)	Extended	Age, alanine aminotransferase, aspartate aminotransferase, platelet count
NAFLD Fibrosis Score	Liver fibrosis /cirrhosis	Angulo et al. (2007)(20)	Extended	Age, BMI, diabetes, albumin, alanine aminotransferase, aspartate aminotransferase, platelet count
AST/Platelet ratio (APRI)	Liver fibrosis /cirrhosis	Wai et al. (2003)(21)	Extended	Aspartate aminotransferase, platelet count
ALBI (albumin/bilirubin)	Severity grading in liver cancer	Johnson et al (2015)(22)	Extended	Bilirubin, albumin

References for Appendix 3

1. Hippisley-Cox J, Coupland C, Brindle P. Derivation and validation of QStroke score for predicting risk of ischaemic stroke in primary care and comparison with other risk scores: a prospective open cohort study. BMJ. 2013 May 2;346:f2573.
2. Ntaios G, Lip GYH, Makaritsis K, Papavasileiou V, Vemmou A, Koroboki E, et al. CHADS2, CHA2DS2-VASc, and long-term stroke outcome in patients without atrial fibrillation. Neurology. 2013 Mar 12;80(11):1009–17.
3. Hippisley-Cox J, Coupland C, Brindle P. Development and validation of QRISK3 risk prediction algorithms to estimate future risk of cardiovascular disease: Prospective cohort study. BMJ Online. 2017 May 23;357(May):1–21.
4. D'Agostino RB, Vasan RS, Pencina MJ, Wolf PA, Cobain M, Massaro JM, et al. General Cardiovascular Risk Profile for Use in Primary Care. Circulation. 2008 Feb 12;117(6):743–53.
5. SCORE2 working group and ESC Cardiovascular risk collaboration. 'SCORE2 Risk Prediction Algorithms: New Models to Estimate 10-Year Risk of Cardiovascular Disease in Europe'. European Heart Journal 42, no. 25 (2021): 2439–54.
6. SCORE2-OP working group and ESC Cardiovascular risk collaboration. 'SCORE2-OP Risk Prediction Algorithms: Estimating Incident Cardiovascular Event Risk in Older Persons in Four Geographical Risk Regions'. European Heart Journal 42, no. 25 (2021): 2455–67.
7. Khan SS, Ning H, Shah SJ, Yancy CW, Carnethon M, Berry JD, et al. 10-Year Risk Equations for Incident Heart Failure in the General Population. J Am Coll Cardiol. 2019 May;73(19):2388–97.
8. Anatürk M, Patel R, Ebmeier KP, Georgiopoulos G, Newby D, Topiwala A, et al. Development and validation of a dementia risk score in the UK Biobank and Whitehall II cohorts. BMJ Ment Health [Internet]. 2023 Jul 1 [cited 2023 Nov 13];26(1). Available from: https://mentalhealth.bmj.com/content/26/1/e300719
9. Kivipelto M, Ngandu T, Laatikainen T, Winblad B, Soininen H, Tuomilehto J. Risk score for the prediction of dementia risk in 20 years among middle aged people: a longitudinal, population-based study. Lancet Neurol. 2006 Sep 1;5(9):735–41.
10. Schiepers OJG, Köhler S, Deckers K, Irving K, O'Donnell CA, van den Akker M, et al. Lifestyle for Brain Health (LIBRA): a new model for dementia prevention. Int J Geriatr Psychiatry. 2018 Jan 1;33(1):167–75.
11. Alonso A, Krijthe BP, Aspelund T, Stepas KA, Pencina MJ, Moser CB, et al. Simple risk model predicts incidence of atrial fibrillation in a racially and geographically diverse population: the CHARGE-AF consortium. J Am Heart Assoc. 2013 Mar 18;2(2):e000102.
12. Hippisley-Cox J, Coupland C. Predicting the risk of Chronic Kidney Disease in Men and Women in England and Wales: prospective derivation and external validation of the QKidney®Scores. BMC Fam Pract. 2010 Jun 21;11(1):49.
13. Nelson RG, Grams ME, Ballew SH, Sang Y, Azizi F, Chadban SJ, et al. Development of Risk Prediction Equations for Incident Chronic Kidney Disease. JAMA. 2019 Dec 3;322(21):2104–14.
14. Bedogni G, Bellentani S, Miglioli L, Masutti F, Passalacqua M, Castiglione A, et al. The fatty liver index: A simple and accurate predictor of hepatic steatosis in the general population. BMC Gastroenterol. 2006 Nov 2;6(1):33.
15. McHenry S, Park Y, Browning JD, Sayuk G, Davidson NO. Dallas Steatosis Index Identifies Patients With Nonalcoholic Fatty Liver Disease. Clin Gastroenterol Hepatol. 2020 Aug 1;18(9):2073-2080.e7.
16. Hippisley-Cox J, Coupland C. Development and validation of QDiabetes-2018 risk prediction algorithm to estimate future risk of type 2 diabetes: cohort study. BMJ. 2017 Nov 20;359:j5019.
17. Griffin SJ, Little PS, Hales CN, Kinmonth AL, Wareham NJ. Diabetes risk score: towards earlier detection of Type 2 diabetes in general practice. Diabetes Metab Res Rev. 2000;16(3):164–71.
18. Bush K, Kivlahan DR, McDonell MB, Fihn SD, Bradley KA. The AUDIT Alcohol Consumption Questions (AUDIT-C): An Effective Brief Screening Test for Problem Drinking. Arch Intern Med. 1998 Sep 14;158(16):1789–95.
19. Vallet-Pichard A, Mallet V, Nalpas B, Verkarre V, Nalpas A, Dhalluin-Venier V, et al. FIB-4: An inexpensive and accurate marker of fibrosis in HCV infection. comparison with liver biopsy and fibrotest. Hepatology. 2007 Jul 1;46(1):32–6.
20. Angulo P, Hui JM, Marchesini G, Bugianesi E, George J, Farrell GC, et al. The NAFLD fibrosis score: A noninvasive system that identifies liver fibrosis in patients with NAFLD. Hepatology. 2007 Apr 1;45(4):846–54.
21. Wai CT, Greenson JK, Fontana RJ, Kalbfleisch JD, Marrero JA, Conjeevaram HS, et al. A simple noninvasive index can predict both significant fibrosis and cirrhosis in patients with chronic hepatitis C. Hepatology. 2003 Aug 1;38(2):518–26.
22. Johnson P j, Berhane S, Kagebayashi C, Satomura S, Teng M, Hl R, et al. Assessment of liver function in patients with hepatocellular carcinoma: a new evidence-based approach-the ALBI grade. J Clin Oncol Off J Am Soc Clin Oncol [Internet]. 2015 Feb 20 [cited 2023 Nov 21];33(6). Available from: https://pubmed.ncbi.nlm.nih.gov/25512453/

Appendix 4: Chapter 4 - Missingness in imaging variables

	Whole set (n= 30,444)		Liver subset (n= 15,097)		Three-organ set (n= 6,865)	
Heart-brain-liver variables	**Present**	**Missing**	**Present**	**Missing**	**Present**	**Missing**
LV GFI	29,863 (98.1)	581 (1.9)	14,654 (97.1)	443 (2.9)	6,865 (100.0)	-
LVM/LVEDV	29,863 (98.1)	581 (1.9)	14,654 (97.1)	443 (2.9)	6,865 (100.0)	-
LVSVi	29,863 (98.1)	581 (1.9)	14,654 (97.1)	443 (2.9)	6,865 (100.0)	-
AoD	23,079 (75.8)	7,365 (24.2)	11,453 (75.9)	3,644 (24.1)	6,865 (100.0)	-
Liver fat (PDFF)	15,061 (49.5)	15,383 (50.5)	15,061 (99.8)	36 (0.2)	6,865 (100.0)	-
Liver iron	15,077 (49.5)	15,367 (50.5)	15,077 (99.9)	20 (0.1)	6,865 (100.0)	-
Liver cT1 (ms)	11,485 (37.7)	18,959 (62.3)	11,485 (76.1)	3,612 (23.9)	6,865 (100.0)	-
Total brain volume	29,127 (95.7)	1,317 (4.3)	13,780 (91.3)	1,317 (8.7)	6,865 (100.0)	-
Grey matter volume	29,127 (95.7)	1,317 (4.3)	13,780 (91.3)	1,317 (8.7)	6,865 (100.0)	-
White matter hyperintensities	27,954 (91.8)	2,490 (8.2)	13,291 (88.0)	1,806 (12.0)	6,865 (100.0)	-
ICVF	27,148 (89.2)	3,296 (10.8)	12,760 (84.5)	2,337 (15.5)	6,865 (100.0)	-
ISOVF	27,148 (89.2)	3,296 (10.8)	12,760 (84.5)	2,337 (15.5)	6,865 (100.0)	-

LVSVi = left ventricular stroke volume indexed to body surface area, LV GFI = left ventricular global function index, LVM/LVEDV = left ventricular mass to volume ratio (left ventricular mass / left ventricular end-diastolic volume), AoD = aortic distensibility. PDFF = proton density fat fraction, cT1 = corrected T1 relaxation time, ICVF = intracellular volume fraction, ISOVF = isotropic volume fraction.

Appendix 5: Chapter 4 - Imaging variable orthogonalisation

	Rotated components				
Raw liver measures	**Liver fat**	**Liver iron**	**Liver cT1**		**N**
Liver fat (PDFF)	**0.933**	0.145	0.330		11,452
Liver iron	0.117	**0.991**	-0.069		
Liver cT1	0.320	-0.083	**0.944**		
Raw heart measures	**LVM/ LVEDV**	**Aortic stiffening**	**Reduced LVSV**	**Reduced LV GFI**	**N**
LVM/LVEDV	**0.954**	0.101	0.154	0.235	22,798
Aortic stiffening	0.090	**0.993**	0.077	0.022	
Reduced LVSV	0.152	0.085	**0.961**	0.216	
Reduced LV GFI	0.243	0.024	0.227	**0.943**	

Entries are correlation coefficients between the raw features (from liver and heart imaging) and their orthogonalised principal component counterparts. Principal components analysis was performed for each organ, with the number of retained components equal to the number of input variables. Set sizes were determined by complete rows available for each organ. Varimax rotation was applied. For easier interpretability, three original heart variables were reversed so that all heart/liver variables would share the same directionality – these are: aortic stiffening = aortic distensibility * -1, reduced LV stroke volume = LV stroke volume * -1, and reduced LV GFI = LV GFI * -1. LV= left ventricular, SV = stroke volume, GFI = global function index, PDFF= proton density fat fraction, LVM/LVEDV = left ventricular mass to volume ratio.

Appendix 6: Chapter 5 - Codes for NHS Health Check exposure

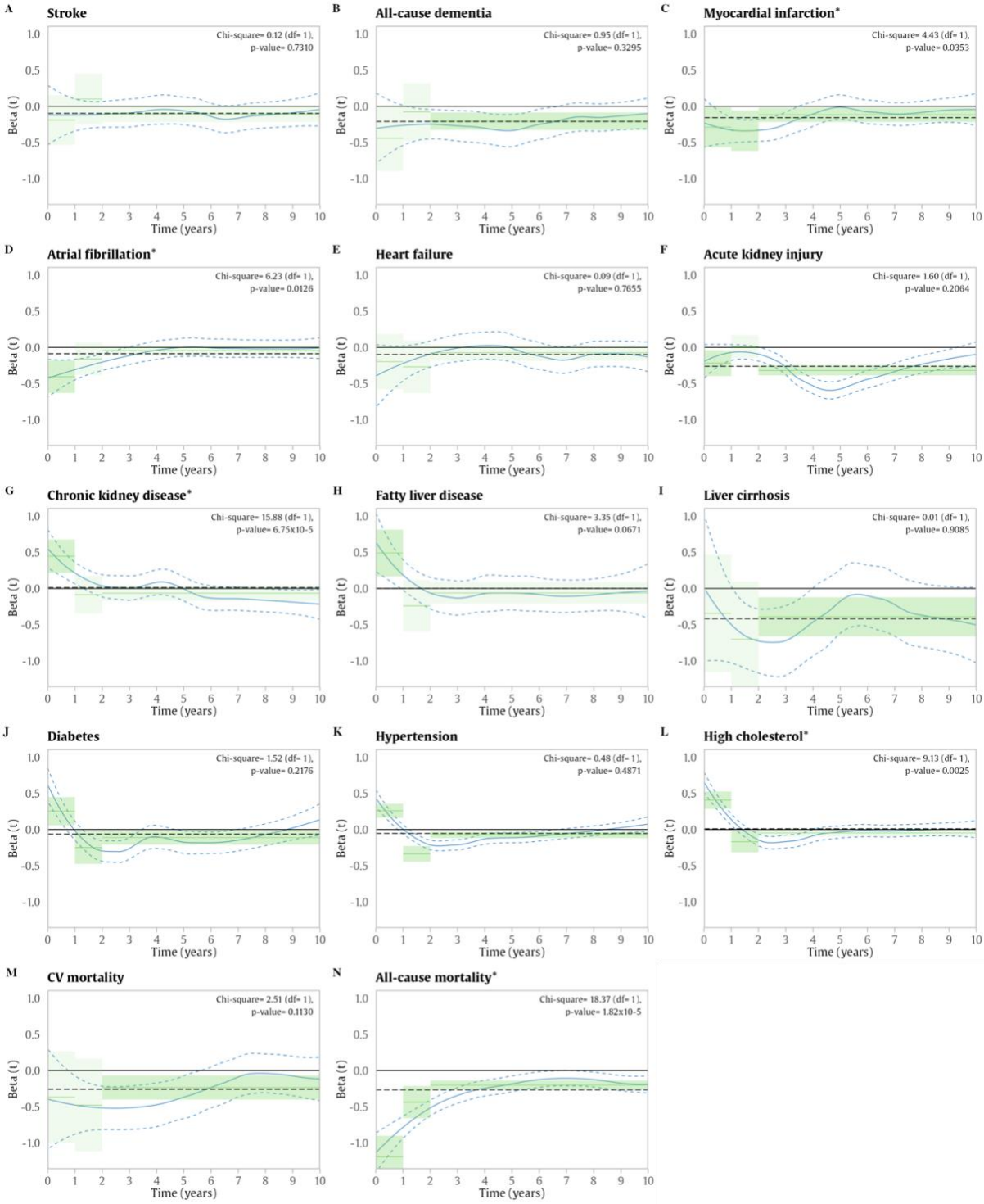
Record text	Codes	Records	Participants
NHS Health Check completed	XaRBQ, 8BAg.	45,500	41,576
NHS Health Check programme	XaR6f, 6B5..	6,379	6,101
NHS Health Check raising awareness about dementia and memory clinics	XaaD1, 67DF.	2,438	2,380
NHS Health Check annual review	XaXIS, 6AH..	1,632	1,397
NHS Health Check completed by third party	XaZPq, 8BAg0	486	479
NHS Health Check follow up	Xab3O, 8HBR.	26	26
NHS Health Check commenced	Xaeab	3	3
Keep well programme	6B3.., XaNPq	1,224	1,152
Keep Well health check	XaZHe, 8BAn.	200	182
Keep Well health check review	XaZHf, 6AM..	72	69
		57,960	50,984

Appendix 7: Chapter 5 - Missing value imputation details

Covariate	Missing count	Missing %
Body mass index	677	0.50%
Waist-hip ratio	493	0.36%
Systolic blood pressure	295	0.22%
Summed MET-minutes per week	770	0.56%
Fresh vegetable/salad daily intake	1,807	1.32%
Alcohol intake frequency	298	0.22%
Educational attainment	1,057	0.77%
Townsend deprivation score	191	0.14%

Missing values in covariate variables in the main data set (n= 140,899). Missing values were imputed together using multiple imputation with chained equations (MICE) using the mice package in R, using 20 iterations to create a single imputed replicate. No imputation was used for exposure or outcomes.

Appendix 8: Chapter 5 - Visualisation of time-varying hazard effects



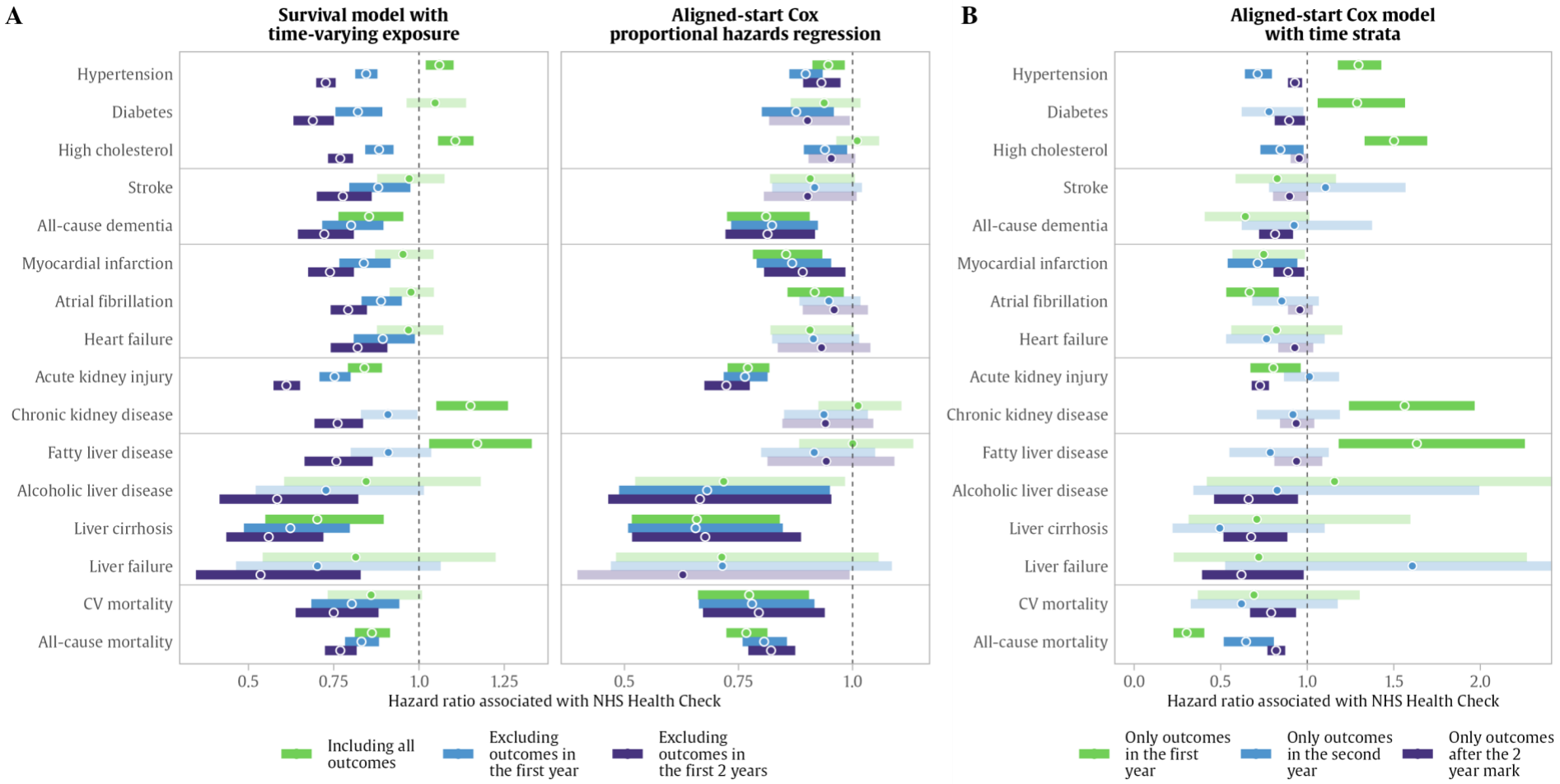
Each panel shows the smoothed curve for Schoenfeld residuals (in blue), for the treatment variable (NHS Health Check) from aligned-start Cox regression models. Where the heading of the panel is marked with an asterisk (*), the test for proportional hazards has failed (p-value < 0.05). The zero line is shown in solid black with the non-stratified treatment effect in dashed black line. Green rectangles indicate the 95% confidence regions for the treatment coefficient in each time strata (the first year, the second year, and time after the 2-year mark). Where the stratified effect is non-significant, this is shown in lighter transparent green.

Appendix 9: Chapter 5 - Hazard ratios for NHS Health Check

Outcome	Ignoring the first (months)	Time-varying Cox regression		Aligned-start Cox regression	
		HR (95% CI)	p-value	HR (95% CI)	p-value
Hypertension	0	1.06* [1.02, 1.10]	0.0031	0.95* [0.91, 0.98]	0.0043
	12	0.84* [0.81, 0.88]	1.15x10-17	0.90* [0.86, 0.93]	1.80x10-7
	24	0.73* [0.70, 0.76]	4.95x10-57	0.93* [0.89, 0.97]	0.0016
Diabetes	0	1.05 [0.96, 1.14]	0.2773	0.94 [0.86, 1.02]	0.1227
	12	0.82* [0.75, 0.89]	3.80x10-6	0.88* [0.80, 0.96]	0.0041
	24	0.69* [0.63, 0.75]	1.99x10-17	0.90 [0.82, 0.99]	0.0376
High cholesterol	0	1.11* [1.06, 1.16]	2.49x10-5	1.01 [0.96, 1.06]	0.6673
	12	0.88* [0.84, 0.93]	2.08x10-7	0.94* [0.89, 0.99]	0.0153
	24	0.77* [0.73, 0.81]	5.96x10-27	0.95 [0.90, 1.01]	0.0813
Stroke	0	0.97 [0.88, 1.07]	0.5722	0.91 [0.82, 1.00]	0.0622
	12	0.88* [0.80, 0.97]	0.0142	0.92 [0.82, 1.02]	0.1124
	24	0.78* [0.70, 0.86]	1.70x10-6	0.90 [0.81, 1.01]	0.071
All-cause dementia	0	0.85* [0.76, 0.95]	0.0053	0.81* [0.72, 0.91]	2.23x10-4
	12	0.80* [0.72, 0.90]	1.01x10-4	0.82* [0.73, 0.92]	9.57x10-4
	24	0.72* [0.64, 0.81]	1.87x10-8	0.81* [0.72, 0.92]	7.88x10-4
Myocardial infarction	0	0.95 [0.87, 1.04]	0.2957	0.85* [0.78, 0.93]	5.21x10-4
	12	0.84* [0.77, 0.92]	1.11x10-4	0.87* [0.79, 0.95]	0.0031
	24	0.74* [0.67, 0.81]	6.67x10-11	0.89 [0.81, 0.98]	0.0233
Atrial fibrillation	0	0.98 [0.91, 1.04]	0.4849	0.92* [0.86, 0.98]	0.0116
	12	0.89* [0.83, 0.95]	4.88x10-4	0.95 [0.88, 1.02]	0.1388
	24	0.79* [0.74, 0.85]	1.12x10-11	0.96 [0.89, 1.03]	0.2775
Heart failure	0	0.97 [0.88, 1.07]	0.5409	0.91 [0.82, 1.00]	0.0561
	12	0.89* [0.81, 0.99]	0.0279	0.91 [0.82, 1.01]	0.0911
	24	0.82* [0.74, 0.91]	1.22x10-4	0.93 [0.84, 1.04]	0.2048
Acute kidney injury	0	0.84* [0.79, 0.89]	9.02x10-9	0.77* [0.73, 0.82]	8.54x10-18
	12	0.75* [0.71, 0.80]	4.02x10-20	0.76* [0.72, 0.81]	5.56x10-17
	24	0.61* [0.57, 0.65]	1.45x10-51	0.72* [0.68, 0.77]	2.63x10-20
Chronic kidney disease	0	1.15* [1.05, 1.26]	0.0025	1.01 [0.93, 1.11]	0.7934
	12	0.91 [0.83, 1.00]	0.0400	0.94 [0.85, 1.03]	0.1944
	24	0.76* [0.69, 0.84]	1.15x10-8	0.94 [0.85, 1.05]	0.256
Fatty liver disease	0	1.17* [1.03, 1.33]	0.0161	1.00 [0.88, 1.13]	0.9961
	12	0.91 [0.80, 1.04]	0.1540	0.92 [0.80, 1.05]	0.2062
	24	0.76* [0.66, 0.86]	3.66x10-5	0.94 [0.81, 1.09]	0.4294
Alcoholic liver disease	0	0.85 [0.60, 1.18]	0.3243	0.72 [0.52, 0.98]	0.0391
	12	0.73 [0.52, 1.01]	0.0608	0.68* [0.49, 0.95]	0.0239
	24	0.58* [0.42, 0.82]	0.0020	0.67* [0.46, 0.95]	0.0265
Liver cirrhosis	0	0.70* [0.55, 0.90]	0.0046	0.66* [0.52, 0.84]	7.94x10-4
	12	0.62* [0.49, 0.80]	1.71x10-4	0.66* [0.51, 0.85]	0.0012
	24	0.56* [0.43, 0.72]	6.19x10-6	0.68* [0.52, 0.89]	0.0047
Liver failure	0	0.81 [0.54, 1.22]	0.3241	0.71 [0.48, 1.06]	0.0923
	12	0.70 [0.46, 1.06]	0.0952	0.71 [0.47, 1.09]	0.1158
	24	0.54* [0.35, 0.83]	0.0051	0.63 [0.40, 0.99]	0.0469
CV mortality	0	0.86 [0.73, 1.01]	0.0643	0.77* [0.66, 0.90]	0.0013
	12	0.80* [0.68, 0.94]	0.0072	0.78* [0.66, 0.92]	0.0026
	24	0.75* [0.64, 0.88]	4.79x10-4	0.79* [0.67, 0.94]	0.007
All-cause mortality	0	0.86* [0.81, 0.92]	1.16x10-6	0.77* [0.72, 0.81]	8.31x10-19
	12	0.83* [0.78, 0.88]	1.48x10-9	0.81* [0.76, 0.86]	2.36x10-12
	24	0.77* [0.72, 0.82]	1.90x10-17	0.82* [0.77, 0.87]	7.21x10-10

Appendix 14 footnote: Entries are hazard ratios, 95% confidence intervals and p-values from Cox proportional hazards models associating completed NHS Health Check with new diagnoses received during follow-up. An asterisk (*) indicates p-value significance after applying multiple testing corrections with a 5% false discovery rate. Columns show models that were computed with three outcome exclusion settings (including all outcomes, excluding outcomes in the first 12 months after NHS Health Check, and excluding outcomes in the first 24 months after NHS Health Check). Models are adjusted by age, sex, geographical region, Townsend deprivation score, ethnicity, body mass index, waist-hip ratio, smoking, systolic blood pressure, alcohol intake frequency, physical activity, daily vegetable/salad intake and Charlson comorbidity index.

Appendix 10: Chapter 5 - Sensitivity analysis with stratified time periods



Panel A is a copy of Figure 5.6. A new panel (B) showing the results from the matched-sample aligned-start Cox model, with stratified time periods. In contrast to Panel A, Panel B divides follow-up time into three parts; the first year (green) the second year (blue) and follow-up time after the 2-year mark (purple). This is another way to deal with hazards that are not necessarily steady across time.

Appendix 11: Chapter 5 - E-value lower bounds for significant hazard ratios

Translated into their nearest "years of ageing" equivalent based on the outcome-specific age coefficient in each model.

		Time-varying Cox regression		Aligned-start Cox regression		Heuristic evaluation of longer-term effect?
Outcome	**Ignoring the first k months**	**HR**	**Years equivalent (E-value lower bound)**	**HR**	**Years equivalent (E-value lower bound)**	
Hypertension	0	1.06*	5 years (1.16)	0.95*	4 years (1.15)	Strong
	12	0.84*	10 years (1.54)	0.90*	8 years (1.34)	7.4
	24	0.73*	10 years (1.98)	0.93*	5 years (1.19)	
Diabetes	0	1.05		0.94		Moderate
	12	0.82*	10 years (1.49)	0.88*	6 years (1.25)	5.2
	24	0.69*	10 years (2.00)	0.9		
High cholesterol	0	1.11*	4 years (1.30)	1.01		Moderate
	12	0.88*	5 years (1.38)	0.94*	2 years (1.12)	3.2
	24	0.77*	9 years (1.78)	0.95		
Stroke	0	0.97		0.91		Weak
	12	0.88*	2 years (1.19)	0.92		1.4
	24	0.78*	5 years (1.59)	0.9		
All-cause dementia	0	0.85*	1 years (1.27)	0.81*	2 years (1.44)	Moderate-weak
	12	0.80*	2 years (1.48)	0.82*	2 years (1.38)	2.2
	24	0.72*	3 years (1.78)	0.81*	2 years (1.40)	
Myocardial infarction	0	0.95		0.85*	5 years (1.35)	Moderate
	12	0.84*	6 years (1.41)	0.87*	5 years (1.28)	5.6
	24	0.74*	9 years (1.78)	0.89*	3 years (1.14)	
Atrial fibrillation	0	0.98		0.92*	1 years (1.16)	Weak
	12	0.89*	2 years (1.29)	0.95		1.6
	24	0.79*	5 years (1.64)	0.96		
Heart failure	0	0.97		0.91		Very weak
	12	0.89*	1 years (1.12)	0.91		0.80
	24	0.82*	3 years (1.44)	0.93		
Acute kidney injury	0	0.84*	7 years (1.49)	0.77*	10 years (1.75)	Strong
	12	0.75*	10 years (1.81)	0.76*	10 years (1.76)	10.00
	24	0.61*	10 years (2.44)	0.72*	10 years (1.90)	
Chronic kidney disease	0	1.15*	2 years (1.28)	1.01		Very weak
	12	0.91		0.94		1.00
	24	0.76*	5 years (1.68)	0.94		
Fatty liver disease	0	1.17*	10 years (1.20)	1		Weak
	12	0.91		0.92		2.00
	24	0.76*	10 years (1.58)	0.94		
Alcoholic liver disease	0	0.85		0.72		Moderate
	12	0.73		0.68*	8 years (1.29)	5.2
	24	0.58*	10 years (1.73)	0.67*	8 years (1.27)	
Liver cirrhosis	0	0.70*	10 years (1.47)	0.66*	10 years (1.66)	Strong
	12	0.62*	10 years (1.82)	0.66*	10 years (1.64)	10.00
	24	0.56*	10 years (2.13)	0.68*	10 years (1.51)	
Liver failure	0	0.81		0.71		Weak
	12	0.70		0.71		2.00
	24	0.54*	10 years (1.71)	0.63		
CV mortality	0	0.86		0.77*	3 years (1.45)	Moderate-weak
	12	0.80*	2 years (1.32)	0.78*	3 years (1.41)	2.8
	24	0.75*	4 years (1.53)	0.79*	2 years (1.33)	
All-cause mortality	0	0.86*	3 years (1.41)	0.77*	6 years (1.76)	Moderate
	12	0.83*	4 years (1.52)	0.81*	5 years (1.61)	4.25
	24	0.77*	5 years (1.75)	0.82*	4 years (1.55)	

E-values measure the strength of the association that an unmeasured confounder would need to have with the outcome in order to nullify the observed hazard ratio. In the interest of space, here we have only reported the e-value lower 95% bound for significant hazard ratios, indicating the strength an unmeasured confounder would need to affect the significance of the measured effect, not necessarily to nullify it. Then we have translated the e-value result into the equivalent effect expressed in terms of years of ageing calculated from the outcome-specific age coefficient from each model. For example, in the time-varying model for hypertension, with a latency period of zero, an unmeasured confounder with the equivalent strength of 7 years of ageing would render our observed hypertension effect non-significant. On the other hand, in our aligned-start model for heart failure, even a weak unmeasured confounder – equivalent to only two years of ageing – could potentially render our observed hazard ratio non-significant. The heuristic evaluation is provided for overview only, and is calculated from the average e-value years (not including time-varying model with k=0), where non-significant effects count as zero, where < 1 = Very weak, 1.1-2.0 = Weak, 2.1-2.9= Moderate-weak, 3.0-6.9 = Moderate, ≥7.0 = strong, i.e., a strong unmeasured confounding factor would be required to render our observed effect non-significant.

Appendix 12: Chapter 6 - Covariate handling, descriptive statistics and source IDs

Category	Variable	Positive	Percent	Mean	SD	Min	25%	50%	75%	Max	N missing	% missing	UKB Field ID
Demographics	All rows	228,240	100%										
	Age (years)	-	0%	56.52	8.07	38	50	58	63	71	0	0.00%	21003
	Sex: Male	103,349	45%	0.45	0.5	0	0	0	1	1	0	0.00%	31
	Townsend deprivation index	-	0%	-1.34	3.03	-6.26	-3.64	-2.15	0.46	11	335	0.15%	189
	Post-secondary education (yes/no)	136,186	60%	0.6	0.49	0	0	1	1	1	1991	0.87%	6138
	Non-white ethnicity (yes/no)	10,377	5%	0.05	0.21	0	0	0	0	1	882	0.39%	21000
Lifestyle	Current smoker (yes/no)	23,934	10%	0.1	0.31	0	0	0	0	1	303	0.13%	20116
	Ex-smoker	78,512	34%	0.34	0.48	0	0	0	1	1	303	0.13%	
	Light smoker <10 per day	10,505	5%	0.05	0.21	0	0	0	0	1	303	0.13%	3456
	Moderate smoker (10 - 19 per day)	7,208	3%	0.03	0.17	0	0	0	0	1	303	0.13%	
	Heavy smoker (>= 20 per day)	6,280	3%	0.03	0.16	0	0	0	0	1	303	0.13%	
	Physical activity (summed MET-minutes per week)	-	0%	2370.47	2643.56	0	578	1493	3213	19278	1498	0.66%	
	Active (METS ≥ 600)	169,005	74%	0.74	0.44	0	0	1	1	1	1498	0.66%	
	Alcohol intake frequency: Times per month	-	0%	11.06	10.5	0	2	6	14	30	406	0.18%	1558
	Alcohol intake daily or nearly daily	44,943	20%	0.2	0.4	0	0	0	0	1	406	0.18%	
	Alcohol intake once a week or more	157,751	69%	0.69	0.46	0	0	1	1	1	406	0.18%	
	Alcohol: Non-drinker	18,631	8%	0.08	0.27	0	0	0	0	1	406	0.18%	
	Health: Excellent	36,458	16%	0.16	0.37	0	0	0	0	1	1248	0.55%	2178
	Health: Poor	10,757	5%	0.05	0.21	0	0	0	0	1	1248	0.55%	
	Lives alone at home	43,037	19%	0.19	0.39	0	0	0	0	1	1668	0.73%	709
Physical measures	Height (m)	-	0%	1.68	0.09	1.22	1.61	1.68	1.75	2.05	0	0.00%	50
	Weight (kg)	-	0%	78.18	15.97	33	66.6	76.5	87.7	197.7	0	0.00%	21002
	Hip circumference (cm)	-	0%	103.49	9.24	39	97	102	108	195	0	0.00%	49
	Waist circumference	-	0%	90.34	13.49	20	80	90	99	197	0	0.00%	48
	BMI: Underweight	1,123	0%	0	0.07	0	0	0	0	1	0	0.00%	
	BMI: Overweight	97,221	43%	0.43	0.49	0	0	0	1	1	0	0.00%	
	BMI: Obese 1 (30-35)	41,097	18%	0.18	0.38	0	0	0	0	1	0	0.00%	
	BMI: Obese 2 (> 35)	16,372	7%	0.07	0.26	0	0	0	0	1	0	0.00%	
	Waist-hip ratio	-	0%	0.87	0.09	0.2	0.8	0.87	0.94	2.13	0	0.00%	
	Pulse rate (bpm)	-	0%	69.4	11.27	30.5	61.5	68.5	76	173	233	0.10%	102, 95
	Pulse rate < 60	43,419	19%	0.19	0.39	0	0	0	0	1	233	0.10%	
	Pulse rate > 90	35,602	16%	0.16	0.36	0	0	0	0	1	233	0.10%	
	Diastolic blood pressure (DBP)	-	0%	82.44	10.15	32	75.5	82	89	147.5	233	0.10%	4079, 94
	Systolic blood pressure (SBP)	-	0%	138.19	18.67	72	125	136.5	150	253	235	0.10%	4080, 93
	SBP standard deviation	-	0%	5.48	4.49	0	2.12	4.24	7.78	84.85	7517	3.29%	
Family history	Family history: Heart disease (yes/no)	142,563	62%	0.62	0.48	0	0	1	1	1	0	0.00%	20110
	Family history: Dementia (yes/no)	27,072	12%	0.12	0.32	0	0	0	0	1	0	0.00%	20107
	Family history: Diabetes (yes/no)	55,756	24%	0.24	0.43	0	0	0	0	1	0	0.00%	20111
	Family history: Stroke (yes/no)	67,127	29%	0.29	0.46	0	0	0	1	1	0	0.00%	

Appendix 13: Chapter 6 - Biochemistry handling, descriptive statistics and source IDs

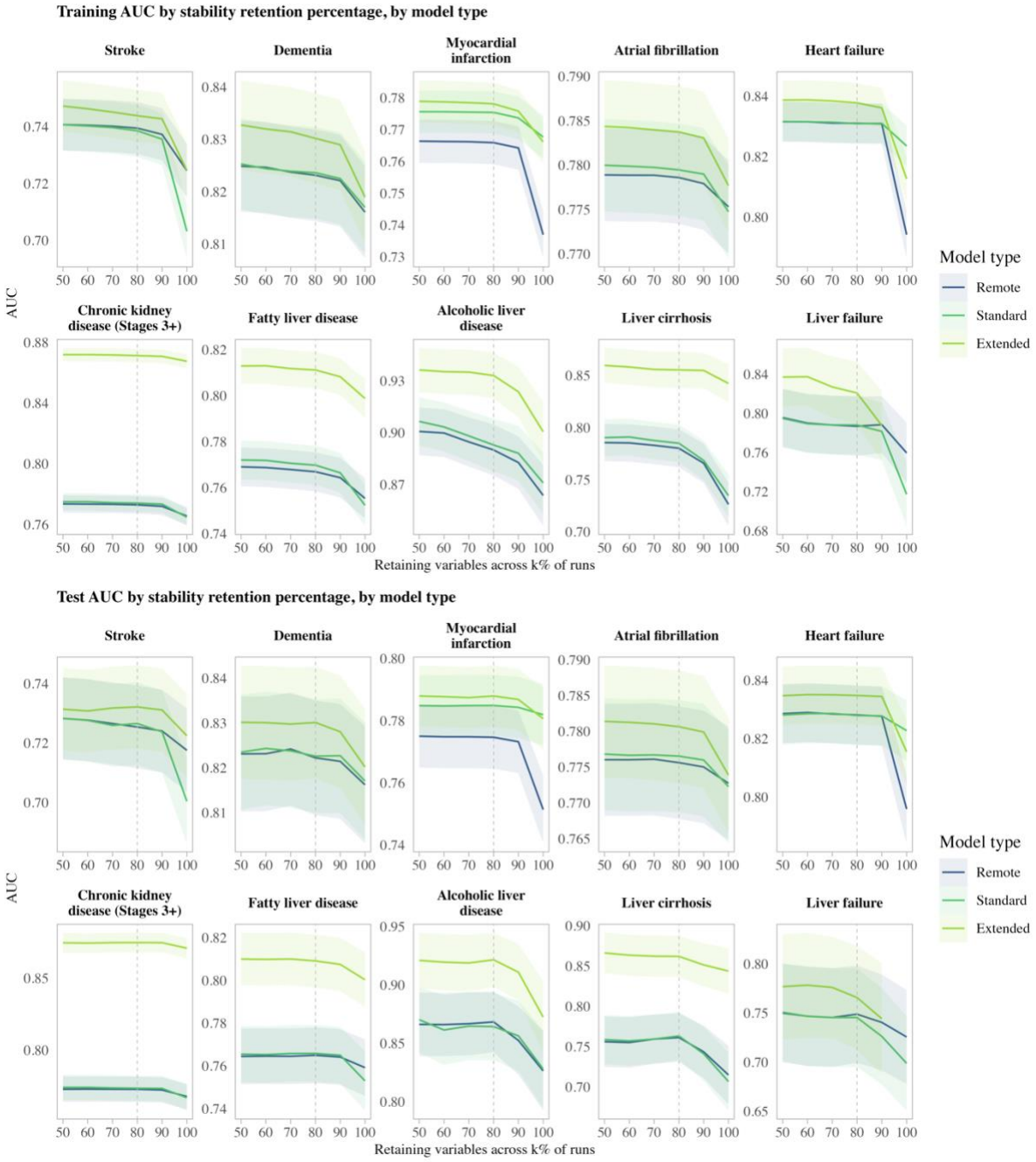
Category	Variable	Mean	SD	Min	25%	50%	75%	Max	UKB Field ID	N missing	% missing
Standard	Total cholesterol (mmol/L)	5.70	1.15	1.43	4.91	5.66	6.44	15.46	30690	13,153	5.8%
biochemistry	HDL cholesterol (mmol/L)	1.45	0.38	0.22	1.17	1.40	1.67	4.40	30760	31,961	14.0%
Additional	Alanine aminotransferase (U/L)	23.67	14.27	3.1	15.49	20.22	27.53	495.19	30620	13,233	5.8%
biochemistry	Albumin (g/L)	45.19	2.63	20.67	43.47	45.17	46.9	59.46	30600	31,839	13.9%
	Alkaline phosphatase (U/L)	83.82	26.3	8.0	67.4	80.5	96.1	1416.7	30610	13,139	5.8%
	Aspartate aminotransferase (U/L)	26.25	10.47	3.3	21	24.4	28.9	500	30650	13,958	6.1%
	C-reactive protein (mg/L)	2.61	4.39	0.08	0.66	1.34	2.78	79.49	30710	13,606	6.0%
	Creatinine (enzymatic) in urine (micromole/L)	8897.91	5823.49	88	4383	7564	12092	60000	30510	6,976	3.1%
	Cystatin C (mg/L)	0.91	0.18	0.38	0.81	0.89	0.98	7.01	30720	13,177	5.8%
	Gamma-glutamyl transferase (U/L)	37.53	41.69	5.0	18.6	26.4	41.2	1167.2	30730	13,274	5.8%
	Glucose (mmol/L)	5.13	1.24	1.1	4.61	4.94	5.32	34.48	30740	32,095	14.1%
	Glycated haemoglobin (HbA1c, mmol/mol)	36.14	6.78	15.0	32.8	35.2	37.9	185	30750	14,066	6.2%
	LDL direct (mmol/L)	3.56	0.88	0.28	2.95	3.53	4.13	9.74	30780	13,564	5.9%
	Platelet count (10^9 cells/Litre)	253.24	60.1	0.3	213.4	248.1	287.2	1402	30080	9,898	4.3%
	Red blood cell count (10^12 cells/Litre)	4.51	0.42	0.01	4.23	4.5	4.79	7.79	30010	9,898	4.3%
	Serum creatinine (umol/L)	72.22	16.99	10.8	61.3	70.3	80.8	500	30700	13,259	5.8%
	Serum phosphate (mmol/L)	1.16	0.16	0.38	1.05	1.16	1.27	4.7	30810	32,174	14.1%
	Total bilirubin (umol/L)	9.11	4.4	1.43	6.41	8.06	10.4	100	30840	14,087	6.2%
	Total protein (g/L)	72.49	4.1	45.99	69.73	72.29	75.02	115.53	30860	32,058	14.0%
	Triglycerides (mmol/L)	1.76	1.03	0.24	1.05	1.49	2.16	11.28	30870	13,324	5.8%
	Urate (umol/L)	308.78	80.5	89.1	250	302.4	360.4	800	30880	13,436	5.9%

Appendix 14: Chapter 6 - Missing value imputation details

Feature	N missing	% missing
Non-biochemistry		
Townsend deprivation index[1]	335	0.15%
Ethnicity	882	0.39%
Pulse rate (bpm)	233	0.10%
Systolic blood pressure (SBP)	235	0.10%
Diastolic blood pressure (DBP)	233	0.10%
Smoking	303	0.13%
Alcohol intake frequency	406	0.18%
Self-reported health	1,248	0.55%
Physical activity	1,498	0.66%
Home occupancy (lives alone)	1,668	0.73%
Post-secondary education	1,991	0.87%
SBP standard deviation	7,517	3.29%
Biochemistry		
Creatinine (enzymatic) in urine	6,976	3.06%
Platelet count	9,898	4.34%
Red blood cell (erythrocyte) count	9,898	4.34%
Alkaline phosphatase	13,139	5.76%
Total cholesterol	13,153	5.76%
Cystatin C	13,177	5.77%
Alanine aminotransferase	13,233	5.80%
Serum creatinine	13,259	5.81%
Gamma-glutamyl transferase	13,274	5.82%
Triglycerides	13,324	5.84%
Urate	13,436	5.89%
LDL direct	13,564	5.94%
C-reactive protein	13,606	5.96%
Aspartate aminotransferase	13,958	6.12%
HbA1cGlycated haemoglobin (HbA1c)	14,066	6.16%
Total bilirubin	14,087	6.17%
Albumin	31,839	13.95%
HDL cholesterol	31,961	14.00%
Total protein	32,058	14.05%
Glucose	32,095	14.06%
Serum phosphate	32,174	14.10%

1. Townsend deprivation index missing values replaced with mean deprivation. 2. Ethnicity missing values were replaced with the overwhelming majority category "White". All other missingness was imputed together using multiple imputation with chained equations (MICE).

Appendix 15: Chapter 6 - Stability retention threshold evaluations



Plots show the Training set and Test set AUC for models by levels of predictor retention from stability selection, for example, x=50 means that we retain predictors that were selected in at least 50% of the sample fits. The vertical dotted line shows the retention cutoff at 80/100

Appendix 16: Chapter 6 - Details of pairwise Cox analysis

Category	Condition	Stroke	Dementia	Myocardial infarction	Atrial fibrillation	Heart failure	CKD (3+)	Fatty liver disease	Alcoholic liver disease	Liver cirrhosis	Liver failure
Risk factors	Hypertension	1.46*	1.32*	1.53*	1.56*	1.97*	1.80*	1.41*	2.41*	1.58*	1.61*
		[1.36, 1.57]	[1.21, 1.44]	[1.45, 1.63]	[1.49, 1.63]	[1.84, 2.11]	[1.71, 1.89]	[1.30, 1.52]	[1.98, 2.93]	[1.36, 1.84]	[1.25, 2.07]
		9.42x10-25	6.02x10-10	4.99x10-47	1.80x10-82	1.45x10-86	3.04x10-121	3.89x10-18	8.64x10-19	2.59x10-9	2.44x10-4
	High cholesterol	1.03	1.19*	1.20*	1.09*	1.31*	1.23*	1.28*	0.83	0.93	1.02
		[0.95, 1.11]	[1.08, 1.30]	[1.13, 1.28]	[1.03, 1.14]	[1.23, 1.40]	[1.16, 1.29]	[1.18, 1.39]	[0.67, 1.03]	[0.79, 1.10]	[0.78, 1.34]
		0.5058	2.45x10-4	8.15x10-9	7.93x10-4	6.08x10-16	5.87x10-15	8.99x10-9	0.0962	0.3988	0.8741
	Diabetes	1.49*	1.75*	1.38*	1.13*	1.60*	1.91*	1.79*	2.26*	3.04*	2.57*
		[1.34, 1.66]	[1.56, 1.97]	[1.27, 1.50]	[1.05, 1.20]	[1.48, 1.73]	[1.79, 2.03]	[1.62, 1.98]	[1.75, 2.91]	[2.54, 3.64]	[1.89, 3.49]
		2.05x10-13	8.07x10-21	5.83x10-14	7.17x10-4	5.78x10-31	6.85x10-90	3.56x10-30	2.80x10-10	9.59x10-34	1.43x10-9
	COPD	1.19*	1.43*	1.54*	1.48*	1.94*	1.33*	1.26*	1.69*	1.26	1.97*
		[1.02, 1.39]	[1.21, 1.68]	[1.37, 1.73]	[1.35, 1.62]	[1.75, 2.16]	[1.20, 1.46]	[1.06, 1.49]	[1.21, 2.37]	[0.94, 1.69]	[1.29, 3.00]
		0.0262	1.85x10-5	3.73x10-13	1.36x10-17	5.34x10-35	3.18x10-8	0.0083	0.0021	0.1261	0.0016
	Any cancer	1.24*	1.08	1.10*	1.20*	1.30*	1.23*	1.19*	1.24	1.39*	1.84*
		[1.13, 1.36]	[0.97, 1.21]	[1.02, 1.20]	[1.13, 1.28]	[1.19, 1.41]	[1.16, 1.31]	[1.07, 1.32]	[0.94, 1.64]	[1.15, 1.68]	[1.37, 2.46]
		5.86x10-6	0.1683	0.0178	1.19x10-9	3.88x10-10	3.50x10-11	0.0017	0.1218	7.11x10-4	4.82x10-5
Arterial	Atherosclerosis / peripheral artery disease	1.52*	1.21	1.44*	1.46*	1.94*	1.52*	0.93	1.39	1.61*	2.05*
		[1.31, 1.77]	[1.01, 1.45]	[1.26, 1.65]	[1.33, 1.61]	[1.74, 2.17]	[1.37, 1.68]	[0.76, 1.14]	[0.93, 2.06]	[1.21, 2.15]	[1.33, 3.17]
		4.47x10-8	0.0438	8.76x10-8	6.37x10-15	7.92x10-32	2.28x10-16	0.4923	0.104	0.0011	0.0011
	Venous thromboembolism (DVT/PE)	1.39*	1.32*	1.28*	1.47*	1.60*	1.22*	1.17*	1.77*	1.35*	1.69*
		[1.23, 1.58]	[1.14, 1.54]	[1.14, 1.43]	[1.36, 1.58]	[1.45, 1.77]	[1.12, 1.33]	[1.02, 1.34]	[1.29, 2.43]	[1.05, 1.73]	[1.14, 2.50]
		2.87x10-7	2.17x10-4	1.32x10-5	1.51x10-22	4.69x10-20	3.05x10-6	0.027	4.35x10-4	0.0193	0.0087
	Erectile dysfunction	1.11	1.20*	1.14*	1.14*	1.1	1.14*	1.12	1.38*	1.09	1.35
		[0.98, 1.25]	[1.05, 1.38]	[1.04, 1.24]	[1.06, 1.22]	[1.00, 1.21]	[1.05, 1.24]	[0.98, 1.28]	[1.06, 1.79]	[0.86, 1.38]	[0.95, 1.91]
		0.0878	0.0077	0.0051	3.85x10-4	0.0468	0.0017	0.1024	0.0173	0.4681	0.0972
Brain	Stroke		1.94*	1.1	1.45*	1.75*	1.30*	1.07	1.12	1.39	1.48
			[1.66, 2.27]	[0.96, 1.27]	[1.31, 1.60]	[1.56, 1.96]	[1.17, 1.44]	[0.88, 1.29]	[0.71, 1.74]	[1.02, 1.90]	[0.90, 2.44]
			7.18x10-17	0.1656	1.36x10-13	3.16x10-22	1.14x10-6	0.4958	0.6311	0.0353	0.1233
	Transient ischaemic attack (TIA)	2.39*	1.65*	1.12	1.38*	1.57*	1.33*	1.19	0.83	1.15	1.25
		[1.89, 3.02]	[1.35, 2.02]	[0.94, 1.33]	[1.22, 1.56]	[1.36, 1.82]	[1.16, 1.51]	[0.94, 1.52]	[0.41, 1.67]	[0.73, 1.79]	[0.61, 2.55]
		4.33x10-13	1.13x10-6	0.2094	3.05x10-7	1.64x10-9	2.43x10-5	0.1568	0.5937	0.5529	0.5362
	Cerebrovascular diseases	1.86*	1.92*	1.27*	1.58*	1.66*	1.22*	1.22	2.12*	1.43	2.29*
		[1.29, 2.69]	[1.53, 2.42]	[1.04, 1.55]	[1.37, 1.83]	[1.40, 1.97]	[1.03, 1.43]	[0.92, 1.60]	[1.28, 3.52]	[0.91, 2.27]	[1.24, 4.23]
		8.62x10-4	2.64x10-8	0.0204	3.02x10-10	5.26x10-9	0.019	0.1651	0.0036	0.1248	0.0079
	Alzheimer's disease / dementia	2.49*		1.6	1.73*	1.18	1.36	1.06	6.40*	1.58	2.73
		[1.54, 4.01]		[1.03, 2.49]	[1.24, 2.43]	[0.70, 2.00]	[0.92, 2.02]	[0.51, 2.23]	[3.02, 13.53]	[0.51, 4.90]	[0.68, 11.00]
		1.81x10-4		0.0355	0.0014	0.529	0.1221	0.8723	1.20x10-6	0.4319	0.1577
	Epilepsy	1.86*	2.66*	1.41*	1.46*	1.18	1.06	1.04	2.17*	1.87*	2.09*
		[1.51, 2.30]	[2.17, 3.25]	[1.18, 1.69]	[1.27, 1.68]	[0.96, 1.46]	[0.90, 1.26]	[0.81, 1.35]	[1.37, 3.44]	[1.27, 2.75]	[1.14, 3.82]
		4.63x10-9	4.36x10-21	1.67x10-4	1.83x10-7	0.1161	0.4814	0.7421	9.46x10-4	0.0014	0.0165
	Parkinson's disease	1.37	9.14*	1.74*	1.55*	2.00*	1.62*	1.6	1.08	1.48	1.59
		[0.88, 2.12]	[7.44, 11.23]	[1.27, 2.38]	[1.21, 2.00]	[1.47, 2.72]	[1.24, 2.10]	[1.01, 2.54]	[0.27, 4.32]	[0.61, 3.56]	[0.39, 6.37]
		0.1643	9.07x10-99	6.03x10-4	6.33x10-4	1.00x10-5	3.53x10-4	0.0469	0.9179	0.385	0.5163
	Migraines	1.15*	1.08	0.99	1.09	0.94	1.12*	1.22*	0.71	0.96	1.38
		[1.02, 1.30]	[0.93, 1.25]	[0.89, 1.10]	[1.00, 1.17]	[0.84, 1.06]	[1.03, 1.21]	[1.09, 1.36]	[0.46, 1.09]	[0.74, 1.25]	[0.94, 2.02]
		0.019	0.2935	0.9031	0.0382	0.3011	0.0049	5.70x10-4	0.1206	0.774	0.0971
	Sleep disorder	1.08*	1.00	1.13*	1.10*	1.17*	1.08*	1.30*	1.64*	1.31*	1.38*

Category	Condition	Stroke	Dementia	Myocardial infarction	Atrial fibrillation	Heart failure	CKD (3+)	Fatty liver disease	Alcoholic liver disease	Liver cirrhosis	Liver failure
	(insomnia, sleep apnoea)	[1.01, 1.15]	[0.92, 1.08]	[1.07, 1.19]	[1.05, 1.14]	[1.10, 1.24]	[1.03, 1.13]	[1.21, 1.39]	[1.39, 1.95]	[1.15, 1.49]	[1.11, 1.72]
		0.0256	0.9907	7.73x10-6	9.04x10-6	9.43x10-8	8.12x10-4	7.65x10-14	9.92x10-9	5.66x10-5	0.0043
	Traumatic brain injury	1.32*	2.00*	1.19	1.11	1.25*	1.01	1.12	2.02*	1.1	1.45
		[1.08, 1.61]	[1.63, 2.44]	[1.01, 1.39]	[0.97, 1.27]	[1.05, 1.48]	[0.87, 1.18]	[0.90, 1.40]	[1.41, 2.90]	[0.72, 1.66]	[0.80, 2.66]
		0.0062	1.45x10-11	0.0353	0.1173	0.0131	0.8897	0.3017	1.24x10-4	0.6645	0.2246
Cardiac	Ischaemic heart disease	1.55*	1.38*	2.65*	1.52*	2.56*	1.30*	1.02	1.27	1.55*	1.68*
		[1.40, 1.71]	[1.23, 1.54]	[2.45, 2.87]	[1.43, 1.62]	[2.38, 2.76]	[1.22, 1.39]	[0.91, 1.15]	[0.97, 1.66]	[1.27, 1.88]	[1.22, 2.31]
		9.30x10-18	2.56x10-8	$2.30x10^{-127}$	9.30x10-42	$2.11x10^{-141}$	8.42x10-16	0.6909	0.0868	1.17x10-5	0.0016
	Myocardial infarction	1.62*	1.28*		1.46*	2.92*	1.37*	0.89	1.1	1.42*	1.73*
		[1.43, 1.83]	[1.11, 1.48]		[1.35, 1.58]	[2.69, 3.17]	[1.27, 1.49]	[0.76, 1.04]	[0.78, 1.56]	[1.11, 1.81]	[1.18, 2.54]
		1.80x10-14	7.76x10-4		2.86x10-22	$3.92x10^{-143}$	1.75x10-14	0.1482	0.5893	0.0055	0.005
	Cardiac arrhythmia	1.83*	1.34*	1.34*	2.47*	2.99*	1.43*	1.03	1.21	1.41*	1.66*
		[1.64, 2.04]	[1.17, 1.54]	[1.21, 1.49]	[2.28, 2.68]	[2.77, 3.23]	[1.32, 1.54]	[0.89, 1.20]	[0.86, 1.71]	[1.11, 1.80]	[1.14, 2.43]
		1.21x10-27	2.17x10-5	1.95x10-8	$7.32x10^{-108}$	$2.91x10^{-168}$	9.49x10-20	0.673	0.275	0.0053	0.0083
	Atrial fibrillation	2.52*	1.42*	1.31*		3.57*	1.52*	0.95	1.37	1.83*	1.81*
		[2.22, 2.85]	[1.19, 1.68]	[1.14, 1.49]		[3.25, 3.91]	[1.38, 1.68]	[0.77, 1.18]	[0.90, 2.09]	[1.38, 2.44]	[1.13, 2.91]
		3.77x10-47	6.90x10-5	1.02x10-4		$9.92x10^{-163}$	1.07x10-16	0.6424	0.1463	2.70x10-5	0.0135
	Non-ischaemic cardiomyopathies	1.91*	1.31	1.24	3.03*	5.50*	2.56*	0.93	1.72	1.27	2.98*
		[1.35, 2.72]	[0.80, 2.15]	[0.86, 1.79]	[2.46, 3.74]	[4.41, 6.84]	[2.09, 3.14]	[0.56, 1.55]	[0.71, 4.15]	[0.57, 2.84]	[1.23, 7.25]
		2.67x10-4	0.2769	0.2478	5.52x10-25	2.44x10-52	1.87x10-19	0.7803	0.2313	0.5602	0.0159
	Valvular heart disease	1.96*	1.22	1.59*	2.94*	3.60*	1.56*	1.07	0.96	1.59*	2.33*
		[1.66, 2.31]	[0.97, 1.53]	[1.36, 1.85]	[2.66, 3.24]	[3.22, 4.04]	[1.39, 1.76]	[0.84, 1.36]	[0.51, 1.79]	[1.10, 2.31]	[1.38, 3.93]
		3.12x10-15	0.0967	3.56x10-9	$3.60x10^{-103}$	$4.85x10^{-109}$	2.10x10-13	0.6039	0.8911	0.0146	0.0015
	Heart failure	2.30*	1.42*	1.80*	2.49*		2.10*	1.14	1.13	1.84*	3.02*
		[1.90, 2.77]	[1.10, 1.82]	[1.44, 2.26]	[2.19, 2.82]		[1.85, 2.38]	[0.87, 1.48]	[0.60, 2.13]	[1.26, 2.69]	[1.80, 5.08]
		7.86x10-18	0.0068	3.27x10-7	2.34x10-44		2.46x10-30	0.3486	0.7067	0.0016	3.05x10-5
Kidney	Hypertensive renal disease	3.10*	1.36	2.56*	2.08*	2.56*	4.30*	0.88		2.18*	8.00*
		[2.16, 4.45]	[0.77, 2.41]	[1.90, 3.45]	[1.58, 2.72]	[1.90, 3.43]	[3.06, 6.03]	[0.47, 1.64]		[1.08, 4.40]	[4.20, 15.27]
		9.27x10-10	0.2868	6.56x10-10	1.31x10-7	4.53x10-10	3.13x10-17	0.6812		0.029	2.76x10-10
	Acute kidney injury	2.05*	1.71*	1.92*	1.88*	2.87*	3.65*	0.84	1.31	3.18*	5.60*
		[1.39, 3.01]	[1.08, 2.72]	[1.41, 2.63]	[1.47, 2.42]	[2.22, 3.70]	[2.82, 4.72]	[0.47, 1.53]	[0.42, 4.08]	[1.83, 5.52]	[2.75, 11.40]
		2.86x10-4	0.0235	4.08x10-5	7.30x10-7	7.16x10-16	4.91x10-23	0.5742	0.6449	3.91x10-5	1.98x10-6
	Chronic kidney disease	1.54*	1.14	1.21*	1.29*	1.51*		1.05	0.82	1.56*	3.57*
		[1.35, 1.77]	[0.97, 1.34]	[1.07, 1.37]	[1.18, 1.41]	[1.36, 1.67]		[0.89, 1.24]	[0.50, 1.37]	[1.20, 2.03]	[2.55, 5.00]
		2.46x10-10	0.1073	0.002	1.14x10-8	1.93x10-14		0.5481	0.4549	7.88x10-4	1.01x10-13
Liver	Fatty liver disease	1.29	1.12	1.39*	1.02	1.33*	1.31*			3.79*	2.46*
		[0.90, 1.84]	[0.72, 1.74]	[1.08, 1.80]	[0.81, 1.30]	[1.03, 1.72]	[1.07, 1.61]			[2.63, 5.45]	[1.16, 5.25]
		0.1596	0.6153	0.0116	0.8429	0.0304	0.0105			7.24x10-13	0.0194
	Alcoholic liver disease	1.6	4.49*	1.42	1.79*	1.63*	1.62*			16.15*	13.79*
		[0.99, 2.58]	[3.10, 6.49]	[0.98, 2.07]	[1.33, 2.41]	[1.13, 2.37]	[1.16, 2.26]			[11.67, 22.34]	[7.97, 23.86]
		0.0534	1.46x10-15	0.0634	1.25x10-4	0.0098	0.0044			3.05x10-63	6.24x10-21
	Liver cirrhosis	1.59	1.85*	1.2	1.34	1.88*	2.01*				28.85*
		[0.99, 2.56]	[1.09, 3.12]	[0.77, 1.86]	[0.95, 1.89]	[1.31, 2.71]	[1.52, 2.66]				[17.81, 46.73]
		0.0569	0.0224	0.4156	0.092	7.05x10-4	8.84x10-7				1.81x10-42
	Infective/viral hepatitis	0.93	0.91	0.96	1.27*	1.12	1	1.18	2.54*	3.22*	2.41*
		[0.69, 1.24]	[0.64, 1.31]	[0.76, 1.21]	[1.08, 1.49]	[0.88, 1.43]	[0.82, 1.21]	[0.89, 1.57]	[1.59, 4.06]	[2.30, 4.49]	[1.28, 4.52]
		0.6035	0.6129	0.7085	0.0035	0.3457	0.987	0.2447	1.03x10-4	6.51x10-12	0.0062
Systemic inflammation	Gout	1.15	0.97	1.09	1.28*	1.40*	1.44*	1.30*	2.04*	1.64*	1.73*
		[1.00, 1.33]	[0.81, 1.15]	[0.98, 1.22]	[1.18, 1.38]	[1.27, 1.55]	[1.31, 1.57]	[1.12, 1.50]	[1.55, 2.67]	[1.29, 2.07]	[1.18, 2.54]
		0.0476	0.7152	0.13	1.78x10-9	7.21x10-11	2.22x10-15	4.12x10-4	2.77x10-7	4.61x10-5	0.005

Category	Condition	Stroke	Dementia	Myocardial infarction	Atrial fibrillation	Heart failure	CKD (3+)	Fatty liver disease	Alcoholic liver disease	Liver cirrhosis	Liver failure
	Rheumatoid arthritis	1.46*	1.61*	1.66*	1.30*	1.77*	1.38*	1.39*	1.29	1.53*	1.79
		[1.20, 1.77]	[1.30, 1.99]	[1.42, 1.95]	[1.15, 1.48]	[1.52, 2.07]	[1.22, 1.57]	[1.13, 1.71]	[0.71, 2.34]	[1.05, 2.24]	[0.98, 3.27]
		1.90x10-4	1.50x10-5	1.68x10-10	5.97x10-5	1.47x10-13	7.47x10-7	0.0015	0.4096	0.0267	0.0595
	Systemic lupus	2.85*	0.87	2.85*	1.62*	2.10*	2.40*	1.64		2.69	
	erythematosus	[1.77, 4.60]	[0.32, 2.31]	[1.86, 4.38]	[1.07, 2.44]	[1.29, 3.44]	[1.73, 3.31]	[0.91, 2.97]		[1.01, 7.20]	
		1.68x10-5	0.776	1.72x10-6	0.0211	0.003	1.17x10-7	0.1016		0.0488	
Mental illness	Anxiety disorders	1.12*	1.42*	1.08	1.07*	1.05	1.09*	1.42*	1.75*	1.36*	1.45*
		[1.03, 1.22]	[1.29, 1.57]	[1.00, 1.16]	[1.01, 1.13]	[0.97, 1.14]	[1.03, 1.16]	[1.31, 1.54]	[1.43, 2.15]	[1.16, 1.61]	[1.11, 1.91]
		0.0105	3.16x10-12	0.0422	0.0168	0.2104	0.0023	5.18x10-17	5.62x10-8	2.12x10-4	0.0074
	Serious mental illness	1.52*	3.17*	1.06	1.25*	1.44*	1.74*	1.01	1.73*	1.45	1.8
		[1.21, 1.92]	[2.58, 3.90]	[0.86, 1.31]	[1.06, 1.48]	[1.18, 1.77]	[1.49, 2.02]	[0.77, 1.31]	[1.04, 2.85]	[0.94, 2.25]	[0.93, 3.51]
		3.89x10-4	9.66x10-28	0.5902	0.0078	4.16x10-4	6.78x10-13	0.9697	0.0332	0.0912	0.0833
	Depression	1.17*	1.71*	1.19*	1.09*	1.20*	1.15*	1.49*	2.35*	1.50*	1.67*
		[1.09, 1.27]	[1.57, 1.86]	[1.12, 1.27]	[1.04, 1.15]	[1.12, 1.28]	[1.10, 1.21]	[1.39, 1.61]	[1.97, 2.81]	[1.29, 1.73]	[1.31, 2.12]
		4.46x10-5	1.58x10-34	6.68x10-8	5.63x10-4	1.44x10-7	5.03x10-8	1.01x10-26	4.55x10-21	4.72x10-8	2.78x10-5

Entries are hazard ratios, 95% confidence intervals and p-values for incident outcomes (outcomes shown along the top) associated with the presence of existing risk factors, diagnoses and medication at baseline (shown down the left-hand side) in the whole cohort (n= 228,240), using Cox-proportional hazards regression. For example, pre-existing hypertension increases the 10-year risk of stroke by 46%. Models are adjusted by age, sex, post-secondary education, ethnicity, smoking, physical activity, alcohol intake frequency, body mass index, Townsend deprivation index, family history (of heart disease, stroke and dementia), any cancer diagnosis, hypertension, high cholesterol and diabetes. Hazard ratio significance was adjusted for multiple testing with a false discovery rate of 5%, where significant results are indicated with an asterisk (*).

Appendix 17: Chapter 6 - Performance of existing risk indices in the whole sample

Outcome	Type	Risk score	Events / N	Prev	Thresh	AUC / C-statistic	Sens	Spec	Brier	Dxy	Missing
Stroke	Remote	QKidney 5	3,953 / 223,956	0.018	0.14	0.705 [0.697, 0.712]	0.682	0.628	0.018	0.406	4,284 (1.9%)
		CHARGE-AF			1.63	0.703 [0.695, 0.711]	0.682	0.626	0.019	0.406	
		Framingham (without blood)			15.35	0.701 [0.693, 0.709]	0.718	0.582	0.053	0.402	
	Standard	QStroke			4.58	0.726 [0.719, 0.734]	0.689	0.646	0.018	0.453	
		QRISK3			12.48	0.717 [0.709, 0.725]	0.697	0.627	0.034	0.434	
		QKidney 5			0.14	0.705 [0.697, 0.712]	0.682	0.628	0.018	0.406	
	Extended	QStroke			4.58	0.726 [0.719, 0.734]	0.689	0.646	0.018	0.453	
		QRISK3			12.48	0.717 [0.709, 0.725]	0.697	0.627	0.034	0.434	
		PCP-HF			2.53	0.705 [0.698, 0.713]	0.712	0.602	0.019	0.411	
Dementia	Remote	UKB-DRS	2,720 / 227,894	0.012	0.03	0.801 [0.794, 0.809]	0.788	0.682	0.014	0.603	346 (0.2%)
		CHARGE-AF			1.70	0.763 [0.755, 0.771]	0.776	0.637	0.014	0.525	
		QKidney 3			2.35	0.762 [0.755, 0.770]	0.780	0.626	0.015	0.525	
	Standard	UKB-DRS			0.03	0.801 [0.794, 0.809]	0.788	0.682	0.014	0.603	
		QStroke			4.70	0.781 [0.773, 0.788]	0.786	0.650	0.014	0.561	
		CHARGE-AF			1.70	0.763 [0.755, 0.771]	0.776	0.637	0.014	0.525	
	Extended	UKB-DRS			0.03	0.801 [0.794, 0.809]	0.788	0.682	0.014	0.603	
		QStroke			4.70	0.781 [0.773, 0.788]	0.786	0.650	0.014	0.561	
		CHARGE-AF			1.70	0.763 [0.755, 0.771]	0.776	0.637	0.014	0.525	
Myocardial infarction	Remote	Framingham (without blood)	5,953 / 221,576	0.027	17.23	0.730 [0.725, 0.736]	0.691	0.647	0.055	0.461	6,664 (3.0%)
		QKidney 5			0.11	0.707 [0.701, 0.714]	0.729	0.566	0.027	0.414	
		Cambridge Diabetes Score			27.03	0.690 [0.683, 0.696]	0.609	0.661	0.120	0.379	
	Standard	QRISK3			12.66	0.749 [0.743, 0.754]	0.727	0.645	0.039	0.497	
		Framingham (with blood)			14.68	0.737 [0.731, 0.743]	0.728	0.625	0.047	0.474	
		Framingham (without blood)			17.23	0.730 [0.725, 0.736]	0.691	0.647	0.055	0.461	
	Extended	QRISK3			12.66	0.749 [0.743, 0.754]	0.727	0.645	0.039	0.497	
		Framingham (with blood)			14.68	0.737 [0.731, 0.743]	0.728	0.625	0.047	0.474	
		Framingham (without blood)			17.23	0.730 [0.725, 0.736]	0.691	0.647	0.055	0.461	
Atrial fibrillation	Remote	CHARGE-AF	9,997 / 224,008	0.045	1.73	0.760 [0.755, 0.764]	0.729	0.663	0.041	0.519	4,232 (1.9%)
		QKidney 5			0.11	0.733 [0.728, 0.737]	0.782	0.574	0.044	0.463	
		Framingham (without blood)			18.20	0.728 [0.723, 0.732]	0.667	0.670	0.065	0.455	
	Standard	CHARGE-AF			1.73	0.760 [0.755, 0.764]	0.729	0.663	0.041	0.519	
		QStroke			4.06	0.746 [0.742, 0.751]	0.765	0.610	0.041	0.493	
		QKidney 5			0.11	0.733 [0.728, 0.737]	0.782	0.574	0.044	0.463	
	Extended	CHARGE-AF			1.73	0.760 [0.755, 0.764]	0.729	0.663	0.041	0.519	
		QStroke			4.06	0.746 [0.742, 0.751]	0.765	0.610	0.041	0.493	
		PCP-HF			2.56	0.740 [0.736, 0.745]	0.749	0.618	0.042	0.481	

Outcome	Type	Risk score	Events / N	Prev	Thresh	AUC / C-statistic	Sens	Spec	Brier	Dxy	Missing
Heart failure	Remote	QKidney 5	4,988 / 226,563	0.022	0.15	0.795 [0.789, 0.801]	0.777	0.659	0.022	0.589	1,677 (0.7%)
		QKidney 3			3.14	0.783 [0.777, 0.790]	0.697	0.720	0.021	0.567	
		CHARGE-AF			1.82	0.776 [0.769, 0.782]	0.743	0.670	0.024	0.551	
	Standard	QStroke			5.29	0.803 [0.797, 0.809]	0.751	0.710	0.022	0.606	
		QKidney 5			0.15	0.795 [0.789, 0.801]	0.777	0.659	0.022	0.589	
		QRISK3			13.45	0.785 [0.779, 0.791]	0.769	0.663	0.035	0.570	
	Extended	QStroke			5.29	0.803 [0.797, 0.809]	0.751	0.710	0.022	0.606	
		QKidney 5			0.15	0.795 [0.789, 0.801]	0.777	0.659	0.022	0.589	
		QRISK3			13.45	0.785 [0.779, 0.791]	0.769	0.663	0.035	0.570	
Chronic kidney disease	Remote	QKidney 3	8,698 / 222,630	0.039	2.65	0.759 [0.754, 0.764]	0.700	0.684	0.036	0.518	5,610 (2.5%)
		QKidney 5			0.11	0.742 [0.737, 0.747]	0.772	0.591	0.038	0.484	
		UKB-DRS			0.02	0.731 [0.726, 0.736]	0.717	0.631	0.037	0.462	
	Standard	QKidney 3			2.65	0.759 [0.754, 0.764]	0.700	0.684	0.036	0.518	
		QKidney 5			0.11	0.742 [0.737, 0.747]	0.772	0.591	0.038	0.484	
		QStroke			4.41	0.741 [0.736, 0.746]	0.711	0.645	0.036	0.483	
	Extended	Kidney risk score			14.81	0.856 [0.852, 0.860]	0.785	0.777	0.051	0.711	
		QKidney 3			2.65	0.759 [0.754, 0.764]	0.700	0.684	0.036	0.518	
		QKidney 5			0.11	0.742 [0.737, 0.747]	0.772	0.591	0.038	0.484	
Fatty liver disease	Remote	Cambridge Diabetes Score	3,585 / 227,177	0.016	18.10	0.690 [0.682, 0.698]	0.755	0.536	0.124	0.380	1,063 (0.5%)
		LIBRA	3,585 / 227,177	0.016	2.65	0.680 [0.671, 0.688]	0.663	0.608	0.052	0.359	1,063 (0.5%)
		QKidney 5	3,585 / 227,177	0.016	0.21	0.626 [0.617, 0.636]	0.453	0.738	0.016	0.249	1,063 (0.5%)
	Standard	QDiabetes Model A	3,529 / 223,775	0.016	5.98	0.709 [0.701, 0.717]	0.733	0.576	0.028	0.419	4,465 (2.0%)
		QDiabetes Model C	3,585 / 227,177	0.016	3.92	0.692 [0.683, 0.701]	0.666	0.626	0.057	0.384	1,063 (0.5%)
		Cambridge Diabetes Score	3,585 / 227,177	0.016	18.10	0.690 [0.682, 0.698]	0.755	0.536	0.124	0.380	1,063 (0.5%)
	Extended	Dallas Steatosis Index	3,585 / 227,177	0.016	42.76	0.761 [0.754, 0.769]	0.742	0.656	0.175	0.522	1,063 (0.5%)
		Fatty liver index	3,585 / 227,177	0.016	59.72	0.759 [0.752, 0.766]	0.777	0.617	0.316	0.518	1,063 (0.5%)
		QDiabetes Model A	3,529 / 223,775	0.016	5.98	0.709 [0.701, 0.717]	0.733	0.576	0.028	0.419	4,465 (2.0%)
Alcoholic liver disease	Remote	Framingham (without blood)	561 / 227,806	0.002	15.80	0.711 [0.690, 0.731]	0.731	0.586	0.046	0.421	434 (0.2%)
		AUDIT-C (first question)	551 / 227,407	0.002	3.50	0.708 [0.684, 0.732]	0.601	0.804	0.451	0.416	833 (0.4%)
		LIBRA	561 / 227,806	0.002	2.10	0.700 [0.681, 0.719]	0.766	0.546	0.045	0.400	434 (0.2%)
	Standard	Framingham (without blood)	561 / 227,806	0.002	15.80	0.711 [0.690, 0.731]	0.731	0.586	0.046	0.421	434 (0.2%)
		AUDIT-C (first question)	551 / 227,407	0.002	3.50	0.708 [0.684, 0.732]	0.601	0.804	0.451	0.416	833 (0.4%)
		LIBRA	561 / 227,806	0.002	2.10	0.700 [0.681, 0.719]	0.766	0.546	0.045	0.400	434 (0.2%)
	Extended	AUDIT-C (three questions)	47 / 63,981	0.001	6.25	0.846 [0.783, 0.909]	0.830	0.777	0.187	0.692	164,259 (72%)
		APRI (AST / platelet ratio)	561 / 227,806	0.002	0.37	0.784 [0.761, 0.808]	0.620	0.857	0.005	0.568	434 (0.2%)
		Fatty liver index	561 / 227,806	0.002	70.08	0.731 [0.710, 0.752]	0.656	0.698	0.324	0.462	434 (0.2%)
Liver cirrhosis	Remote	LIBRA	951 / 227,742	0.004	2.55	0.693 [0.676, 0.710]	0.697	0.597	0.046	0.386	498 (0.2%)
		QKidney 5			0.15	0.693 [0.675, 0.710]	0.639	0.637	0.004	0.383	

Outcome	Type	Risk score	Events / N	Prev	Thresh	AUC / C-statistic	Sens	Spec	Brier	Dxy	Missing
		Cambridge Diabetes Score			38.45	0.686 [0.670, 0.703]	0.533	0.743	0.122	0.373	
	Standard	LIBRA			2.55	0.693 [0.676, 0.710]	0.697	0.597	0.046	0.386	
		QKidney 5			0.15	0.693 [0.675, 0.710]	0.639	0.637	0.004	0.383	
		Cambridge Diabetes Score			38.45	0.686 [0.670, 0.703]	0.533	0.743	0.122	0.373	
	Extended	APRI (AST / platelet ratio)			0.37	0.755 [0.736, 0.773]	0.569	0.856	0.006	0.509	
		Fatty liver index			69.24	0.730 [0.714, 0.747]	0.652	0.691	0.324	0.460	
		FIB-4			1.65	0.715 [0.696, 0.733]	0.533	0.798	0.050	0.429	
Liver failure	Remote	QKidney 5	340 / 227,985	0.001	0.21	0.701 [0.673, 0.729]	0.568	0.733	0.002	0.399	255 (0.1%)
		Framingham (without blood)			22.29	0.693 [0.665, 0.721]	0.553	0.738	0.046	0.385	
		Cambridge Diabetes Score			35.80	0.674 [0.645, 0.703]	0.541	0.721	0.122	0.348	
	Standard	QRISK3			10.43	0.701 [0.674, 0.728]	0.762	0.535	0.025	0.403	
		QKidney 5			0.21	0.701 [0.673, 0.729]	0.568	0.733	0.002	0.399	
		Framingham (without blood)			22.29	0.693 [0.665, 0.721]	0.553	0.738	0.046	0.385	
	Extended	QRISK3			10.43	0.701 [0.674, 0.728]	0.762	0.535	0.025	0.403	
		QKidney 5			0.21	0.701 [0.673, 0.729]	0.568	0.733	0.002	0.399	
		NAFLD Fibrosis Score			-1.05	0.698 [0.666, 0.730]	0.494	0.821	0.439	0.396	

AUC= area under the curve, Prev = prevalenc, Thresh = the threshold at which the listed index showed the highest balanced accuracy in the development cohort. Sens= sensitivity at given threshold, Spec= specificity at given threshold, Brier = Brier score, the average squared difference between predicted probabilities and outcomes, values closer to zero indicate better performance. Dxy = Somer's Dxy statistic, the rank correlation between predicted probabilities and outcomes, values closer to one indicate better performance.

Appendix 18: Chapter 6 - Model performance in the validation cohort

Outcome	Type	Model	AUC / C-statistic	Brier score	Somers' Dxy	False negatives	False positives	Sensitivity	Specificity
Stroke	Remote	New	0.725 [0.711, 0.739]	0.018 [0.017, 0.019]	0.451 [0.423, 0.479]	390 [350, 430]	23,357 [23,107, 23,607]	0.682 [0.655, 0.708]	0.646 [0.642, 0.650]
		QKidney 5	0.701 [0.687, 0.715]	0.018 [0.017, 0.019]	0.309 [0.255, 0.363]	415 [374, 456]	23,629 [23,386, 23,872]	0.661 [0.635, 0.688]	0.642 [0.638, 0.645]
		Difference	0.024 [0.016, 0.033]	-0.000 [-0.001, 0.000]	0.142 [0.091, 0.193]	-25 [-52, 2]	-272 [-474, -70]	0.020 [-0.002, 0.043]	0.004 [0.001, 0.007]
	Standard	New	0.727 [0.713, 0.740]	0.018 [0.017, 0.019]	0.453 [0.426, 0.481]	388 [349, 427]	23,259 [23,020, 23,498]	0.683 [0.657, 0.709]	0.647 [0.644, 0.651]
		QStroke	0.727 [0.714, 0.741]	0.018 [0.017, 0.019]	0.455 [0.428, 0.481]	381 [344, 418]	23,236 [22,998, 23,474]	0.689 [0.664, 0.714]	0.648 [0.644, 0.651]
		Difference	-0.001 [-0.007, 0.005]	-0.000 [-0.001, 0.000]	-0.001 [-0.013, 0.011]	7.000 [-16, 30]	23 [-132, 178]	-0.006 [-0.025, 0.013]	-0.000 [-0.003, 0.002]
	Extended	New	0.732 [0.718, 0.746]	0.018 [0.017, 0.019]	0.464 [0.437, 0.492]	348 [313, 383]	24,458 [24,217, 24,699]	0.716 [0.691, 0.741]	0.629 [0.626, 0.633]
		QStroke	0.727 [0.714, 0.741]	0.018 [0.017, 0.019]	0.455 [0.427, 0.482]	381 [344, 418]	23,236 [22,999, 23,473]	0.689 [0.663, 0.715]	0.648 [0.644, 0.651]
		Difference	0.005 [-0.001, 0.011]	-0.000 [-0.001, -0.000]	0.010 [-0.003, 0.022]	-33 [-56, -10]	1,222 [1,054, 1,390]	0.027 [0.008, 0.046]	-0.019 [-0.021, -0.016]
Dementia	Remote	New	0.822 [0.810, 0.835]	0.011 [0.011, 0.012]	0.644 [0.620, 0.669]	184 [158, 210]	19,116 [18,890, 19,342]	0.773 [0.744, 0.801]	0.717 [0.714, 0.720]
		UKB-DRS	0.807 [0.793, 0.820]	0.012 [0.011, 0.012]	0.612 [0.586, 0.638]	202 [175, 229]	19,081 [18,859, 19,303]	0.750 [0.721, 0.779]	0.718 [0.714, 0.721]
		Difference	0.016 [0.009, 0.022]	-0.000 [-0.000, -0.000]	0.032 [0.019, 0.045]	-18 [-34, -2]	35 [-101, 171]	0.022 [0.003, 0.042]	-0.001 [-0.003, 0.001]
	Standard	New	0.823 [0.810, 0.836]	0.011 [0.011, 0.012]	0.645 [0.619, 0.671]	210 [182, 238]	17,160 [16,947, 17,373]	0.740 [0.711, 0.770]	0.746 [0.743, 0.749]
		UKB-DRS	0.807 [0.793, 0.820]	0.012 [0.011, 0.012]	0.612 [0.585, 0.640]	202 [174, 230]	19,081 [18,860, 19,302]	0.750 [0.720, 0.781]	0.718 [0.714, 0.721]
		Difference	0.016 [0.009, 0.023]	-0.000 [-0.000, -0.000]	0.033 [0.020, 0.046]	8 [-10, 26]	-1,921 [-2,061, -1,781]	-0.010 [-0.032, 0.013]	0.028 [0.026, 0.031]
	Extended	New	0.830 [0.818, 0.842]	0.011 [0.011, 0.012]	0.660 [0.636, 0.685]	226 [198, 254]	15,670 [15,443, 15,897]	0.721 [0.691, 0.750]	0.768 [0.765, 0.771]
		UKB-DRS	0.807 [0.793, 0.820]	0.012 [0.011, 0.012]	0.612 [0.586, 0.639]	202 [175, 229]	19,081 [18,849, 19,313]	0.750 [0.721, 0.780]	0.718 [0.714, 0.721]
		Difference	0.023 [0.015, 0.032]	-0.000 [-0.000, -0.000]	0.048 [0.032, 0.064]	24 [3, 45]	-3,411 [-3,569, -3,253]	-0.030 [-0.055, -0.004]	0.050 [0.048, 0.053]
Myocardial infarction	Remote	New	0.775 [0.765, 0.785]	0.026 [0.025, 0.027]	0.549 [0.529, 0.570]	491 [447, 535]	20,873 [20,640, 21,106]	0.732 [0.711, 0.752]	0.677 [0.674, 0.681]
		FRS (BMI)	0.736 [0.726, 0.747]	0.027 [0.026, 0.028]	0.472 [0.451, 0.493]	556 [508, 604]	22,769 [22,525, 23,013]	0.696 [0.675, 0.718]	0.648 [0.644, 0.652]
		Difference	0.039 [0.032, 0.045]	-0.001 [-0.002, -0.001]	0.077 [0.064, 0.090]	-65 [-99, -31]	-1,896 [-2,082, -1,710]	0.035 [0.017, 0.054]	0.029 [0.026, 0.032]
	Standard	New	0.785 [0.775, 0.795]	0.026 [0.025, 0.027]	0.570 [0.551, 0.589]	539 [496, 582]	18,902 [18,676, 19,128]	0.706 [0.686, 0.726]	0.708 [0.704, 0.711]
		QRISK3	0.757 [0.747, 0.767]	0.026 [0.025, 0.028]	0.514 [0.494, 0.535]	480 [438, 522]	23,306 [23,063, 23,549]	0.738 [0.718, 0.758]	0.640 [0.636, 0.643]
		Difference	0.028 [0.022, 0.034]	-0.001 [-0.001, -0.000]	0.055 [0.044, 0.067]	59 [27, 91]	-4,404 [-4,586, -4,222]	-0.032 [-0.050, -0.014]	0.068 [0.065, 0.071]
	Extended	New	0.788 [0.778, 0.798]	0.026 [0.025, 0.027]	0.576 [0.556, 0.596]	424 [385, 463]	22,106 [21,867, 22,345]	0.768 [0.749, 0.788]	0.658 [0.655, 0.662]
		QRISK3	0.757 [0.747, 0.768]	0.026 [0.025, 0.027]	0.514 [0.494, 0.535]	480 [439, 521]	23,306 [23,065, 23,547]	0.738 [0.718, 0.758]	0.640 [0.636, 0.643]
		Difference	0.031 [0.025, 0.037]	-0.001 [-0.001, -0.000]	0.062 [0.049, 0.074]	-56 [-88, -24]	-1,200 [-1,380, -1,020]	0.031 [0.013, 0.048]	0.019 [0.016, 0.021]
Atrial fibrillation	Remote	New	0.776 [0.768, 0.784]	0.041 [0.039, 0.042]	0.551 [0.535, 0.567]	793 [738, 848]	20,768 [20,528, 21,008]	0.737 [0.722, 0.753]	0.676 [0.673, 0.680]
		CHARGE-AF	0.759 [0.751, 0.767]	0.043 [0.041, 0.044]	0.518 [0.502, 0.534]	826 [770, 882]	21,457 [21,221, 21,693]	0.726 [0.710, 0.743]	0.666 [0.662, 0.669]
		Difference	0.017 [0.013, 0.020]	-0.002 [-0.003, -0.002]	0.034 [0.026, 0.041]	-33 [-67, 1]	-689 [-841, -537]	0.011 [-0.000, 0.022]	0.011 [0.008, 0.013]

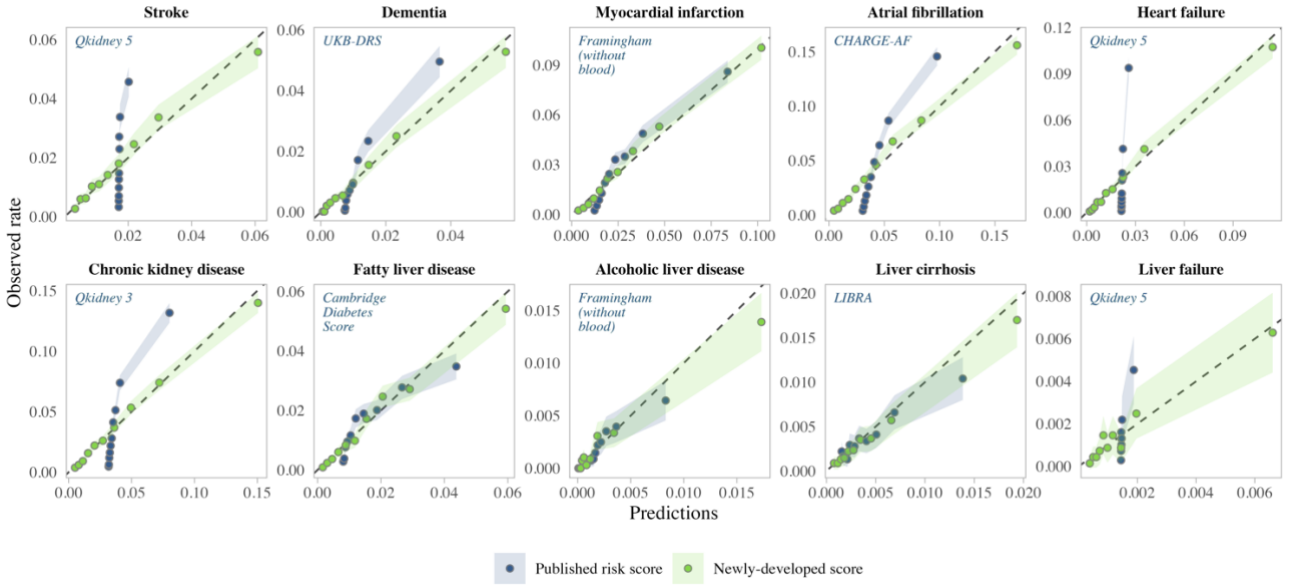
Outcome	Type	Model	AUC / C-statistic	Brier score	Somers' Dxy	False negatives	False positives	Sensitivity	Specificity
	Standard	New	0.777 [0.768, 0.785]	0.041 [0.039, 0.042]	0.553 [0.537, 0.569]	822 [764, 880]	20,150 [19,923, 20,377]	0.728 [0.712, 0.744]	0.686 [0.683, 0.690]
		CHARGE-AF	0.759 [0.751, 0.767]	0.043 [0.041, 0.044]	0.518 [0.501, 0.535]	826 [769, 883]	21,457 [21,224, 21,690]	0.726 [0.710, 0.743]	0.666 [0.662, 0.669]
		Difference	0.018 [0.014, 0.021]	-0.002 [-0.003, -0.002]	0.035 [0.028, 0.043]	-4 [-39, 31]	-1,307 [-1,454, -1,160]	0.001 [-0.010, 0.013]	0.020 [0.018, 0.023]
	Extended	New	0.781 [0.773, 0.788]	0.041 [0.039, 0.042]	0.561 [0.546, 0.577]	813 [757, 869]	19,280 [19,046, 19,514]	0.731 [0.715, 0.746]	0.700 [0.696, 0.703]
		CHARGE-AF	0.759 [0.751, 0.767]	0.043 [0.041, 0.044]	0.518 [0.502, 0.534]	826 [769, 883]	21,457 [21,219, 21,695]	0.726 [0.710, 0.743]	0.666 [0.662, 0.669]
		Difference	0.022 [0.018, 0.026]	-0.002 [-0.003, -0.002]	0.044 [0.036, 0.052]	-13 [-51, 25]	-2,177 [-2,339, -2,015]	0.004 [-0.008, 0.017]	0.034 [0.031, 0.036]
Heart failure	Remote	New	0.828 [0.818, 0.838]	0.020 [0.019, 0.021]	0.656 [0.637, 0.676]	356 [317, 395]	17,580 [17,372, 17,788]	0.761 [0.738, 0.783]	0.736 [0.733, 0.739]
		QKidney 5	0.798 [0.787, 0.809]	0.022 [0.021, 0.023]	0.580 [0.555, 0.604]	381 [344, 418]	20,130 [19,898, 20,362]	0.744 [0.722, 0.765]	0.697 [0.694, 0.701]
		Difference	0.030 [0.024, 0.036]	-0.002 [-0.002, -0.001]	0.077 [0.061, 0.093]	-25 [-53, 3]	-2,550 [-2,745, -2,355]	0.017 [-0.002, 0.036]	0.038 [0.035, 0.041]
	Standard	New	0.828 [0.818, 0.838]	0.020 [0.019, 0.021]	0.656 [0.636, 0.676]	438 [398, 478]	14,303 [14,084, 14,522]	0.706 [0.683, 0.729]	0.785 [0.782, 0.788]
		QStroke	0.806 [0.795, 0.817]	0.021 [0.020, 0.022]	0.612 [0.590, 0.634]	363 [325, 401]	19,291 [19,054, 19,528]	0.756 [0.734, 0.778]	0.710 [0.706, 0.713]
		Difference	0.022 [0.016, 0.028]	-0.001 [-0.001, -0.000]	0.044 [0.033, 0.055]	75 [45, 105]	-4,988 [-5,173, -4,803]	-0.050 [-0.070, -0.031]	0.075 [0.072, 0.078]
	Extended	New	0.835 [0.825, 0.845]	0.020 [0.019, 0.021]	0.670 [0.650, 0.689]	365 [327, 403]	16,557 [16,336, 16,778]	0.755 [0.733, 0.776]	0.751 [0.748, 0.754]
		QStroke	0.806 [0.795, 0.817]	0.021 [0.020, 0.022]	0.612 [0.591, 0.633]	363 [326, 400]	19,291 [19,060, 19,522]	0.756 [0.735, 0.777]	0.710 [0.706, 0.713]
		Difference	0.029 [0.023, 0.035]	-0.001 [-0.001, -0.001]	0.058 [0.046, 0.070]	2 [-27, 31]	-2,734 [-2,913, -2,555]	-0.001 [-0.021, 0.018]	0.041 [0.038, 0.044]
Chronic kidney disease	Remote	New	0.773 [0.764, 0.782]	0.035 [0.034, 0.037]	0.546 [0.528, 0.563]	667 [618, 716]	21,425 [21,194, 21,656]	0.742 [0.725, 0.758]	0.666 [0.663, 0.670]
		QKidney 3	0.760 [0.751, 0.769]	0.037 [0.036, 0.039]	0.520 [0.502, 0.538]	790 [736, 844]	20,214 [19,983, 20,445]	0.694 [0.677, 0.711]	0.685 [0.681, 0.689]
		Difference	0.013 [0.009, 0.016]	-0.002 [-0.003, -0.002]	0.026 [0.018, 0.033]	-123 [-157, -89]	1,211 [1,052, 1,370]	0.048 [0.035, 0.061]	-0.019 [-0.021, -0.016]
	Standard	New	0.774 [0.765, 0.783]	0.035 [0.034, 0.037]	0.547 [0.530, 0.565]	795 [743, 847]	18,227 [17,992, 18,462]	0.692 [0.675, 0.709]	0.716 [0.712, 0.720]
		QKidney 3	0.760 [0.751, 0.769]	0.037 [0.036, 0.039]	0.520 [0.502, 0.538]	790 [734, 846]	20,214 [19,979, 20,449]	0.694 [0.677, 0.712]	0.685 [0.681, 0.689]
		Difference	0.014 [0.010, 0.017]	-0.002 [-0.003, -0.002]	0.027 [0.020, 0.035]	5 [-29, 39]	-1,987 [-2,140, -1,834]	-0.002 [-0.015, 0.011]	0.031 [0.029, 0.033]
	Extended	New	0.875 [0.868, 0.881]	0.031 [0.030, 0.032]	0.749 [0.736, 0.763]	500 [454, 546]	13,864 [13,670, 14,058]	0.806 [0.790, 0.823]	0.784 [0.781, 0.787]
		KRS	0.858 [0.851, 0.866]	0.035 [0.034, 0.036]	0.717 [0.702, 0.732]	539 [493, 585]	14,138 [13,931, 14,345]	0.791 [0.775, 0.807]	0.780 [0.776, 0.783]
		Difference	0.016 [0.013, 0.020]	-0.004 [-0.004, -0.004]	0.033 [0.025, 0.040]	-39 [-70, -8]	-274 [-423, -125]	0.015 [0.003, 0.027]	0.004 [0.002, 0.007]
Fatty liver disease	Remote	New	0.765 [0.752, 0.778]	0.017 [0.016, 0.019]	0.530 [0.504, 0.557]	295 [262, 328]	21,282 [21,037, 21,527]	0.719 [0.692, 0.746]	0.683 [0.679, 0.686]
		Cambridge	0.684 [0.670, 0.699]	0.057 [0.056, 0.059]	0.369 [0.340, 0.398]	276 [245, 307]	31,021 [30,762, 31,280]	0.737 [0.712, 0.763]	0.538 [0.534, 0.541]
		Difference	0.081 [0.068, 0.094]	-0.040 [-0.041, -0.038]	0.161 [0.136, 0.187]	19 [-11, 49]	-9,739 [-9,975, -9,503]	-0.018 [-0.046, 0.010]	0.145 [0.142, 0.149]
	Standard	New	0.766 [0.753, 0.779]	0.017 [0.015, 0.018]	0.532 [0.506, 0.558]	315 [280, 350]	19,786 [19,555, 20,017]	0.695 [0.667, 0.723]	0.701 [0.697, 0.704]
		QDiabetes A	0.704 [0.690, 0.719]	0.016 [0.015, 0.017]	0.409 [0.379, 0.438]	309 [274, 344]	26,804 [26,556, 27,052]	0.701 [0.673, 0.728]	0.594 [0.591, 0.598]
		Difference	0.061 [0.050, 0.073]	0.001 [-0.000, 0.001]	0.123 [0.101, 0.145]	6 [-25, 37]	-7,018 [-7,240, -6,796]	-0.006 [-0.036, 0.024]	0.106 [0.103, 0.110]
	Extended	New	0.809 [0.797, 0.822]	0.015 [0.014, 0.016]	0.618 [0.593, 0.643]	278 [246, 310]	18,646 [18,414, 18,878]	0.735 [0.708, 0.763]	0.722 [0.719, 0.725]
		Dallas SI	0.761 [0.747, 0.775]	0.049 [0.048, 0.051]	0.522 [0.493, 0.550]	277 [247, 307]	22,891 [22,647, 23,135]	0.736 [0.710, 0.763]	0.659 [0.655, 0.662]

Outcome	Type	Model	AUC / C-statistic	Brier score	Somers' Dxy	False negatives	False positives	Sensitivity	Specificity
		Difference	0.048 [0.039, 0.058]	-0.035 [-0.036, -0.033]	0.096 [0.078, 0.115]	1 [-27, 29]	-4,245 [-4,464, -4,026]	-0.001 [-0.027, 0.025]	0.063 [0.060, 0.067]
Alcoholic liver disease	Remote	New	0.868 [0.842, 0.895]	0.002 [0.002, 0.003]	0.734 [0.680, 0.787]	41 [29, 53]	13,485 [13,279, 13,691]	0.742 [0.674, 0.810]	0.802 [0.799, 0.805]
		FRS (BMI)	0.703 [0.656, 0.750]	0.005 [0.002, 0.007]	0.407 [0.312, 0.501]	46 [29, 63]	28,597 [28,399, 28,795]	0.711 [0.633, 0.788]	0.581 [0.578, 0.583]
		Difference	0.165 [0.118, 0.212]	-0.002 [-0.005, 0.000]	0.327 [0.233, 0.422]	-5.000 [-19, 8]	-15,112 [-15,307, -14,917]	0.031 [-0.046, 0.109]	0.222 [0.219, 0.225]
	Standard	New	0.864 [0.835, 0.894]	0.002 [0.002, 0.003]	0.726 [0.666, 0.787]	23 [14, 32]	17,876 [17,663, 18,089]	0.855 [0.799, 0.912]	0.738 [0.735, 0.741]
		FRS (BMI)	0.703 [0.656, 0.751]	0.005 [0.002, 0.007]	0.407 [0.312, 0.501]	46 [30, 62]	28,597 [28,394, 28,800]	0.711 [0.632, 0.790]	0.581 [0.578, 0.584]
		Difference	0.161 [0.110, 0.212]	-0.002 [-0.005, 0.000]	0.320 [0.217, 0.423]	-23 [-37, -8.623]	-10,721 [-10,930, -10,512]	0.145 [0.064, 0.225]	0.157 [0.154, 0.160]
	Extended	New	0.922 [0.899, 0.944]	0.002 [0.002, 0.003]	0.844 [0.801, 0.888]	37 [25, 49]	5,578 [5,443, 5,713]	0.767 [0.703, 0.831]	0.918 [0.916, 0.920]
		APRI	0.780 [0.735, 0.824]	0.002 [0.002, 0.003]	0.558 [0.471, 0.646]	67 [51, 83]	9,568 [9,380, 9,756]	0.579 [0.502, 0.655]	0.860 [0.857, 0.862]
		Difference	0.142 [0.101, 0.183]	-0.000 [-0.000, 0.000]	0.286 [0.206, 0.367]	-30 [-44, -16]	-3,990 [-4,191, -3,789]	0.189 [0.109, 0.268]	0.059 [0.056, 0.061]
Liver cirrhosis	Remote	New	0.762 [0.730, 0.793]	0.004 [0.003, 0.004]	0.523 [0.461, 0.585]	83 [65, 101]	21,445 [21,203, 21,687]	0.688 [0.631, 0.745]	0.685 [0.681, 0.688]
		LIBRA	0.662 [0.628, 0.696]	0.008 [0.007, 0.008]	0.324 [0.256, 0.392]	107 [87, 127]	25,448 [25,189, 25,707]	0.598 [0.542, 0.654]	0.626 [0.622, 0.630]
		Difference	0.100 [0.070, 0.129]	-0.004 [-0.004, -0.003]	0.199 [0.141, 0.257]	-24 [-41, -7]	-4,003 [-4,255, -3,751]	0.090 [0.029, 0.151]	0.059 [0.055, 0.063]
	Standard	New	0.763 [0.734, 0.793]	0.004 [0.003, 0.004]	0.526 [0.467, 0.586]	102 [83, 121]	15,368 [15,149, 15,587]	0.617 [0.559, 0.674]	0.774 [0.771, 0.777]
		LIBRA	0.662 [0.626, 0.698]	0.008 [0.007, 0.008]	0.324 [0.252, 0.396]	107 [86, 128]	25,448 [25,197, 25,699]	0.598 [0.535, 0.660]	0.626 [0.622, 0.630]
		Difference	0.101 [0.070, 0.133]	-0.004 [-0.004, -0.003]	0.202 [0.140, 0.265]	-5 [-21, 11]	-10,080 [-10,332, -9,828]	0.019 [-0.042, 0.080]	0.148 [0.144, 0.152]
	Extended	New	0.862 [0.837, 0.888]	0.004 [0.003, 0.004]	0.723 [0.672, 0.774]	79 [62, 96]	8,973 [8,806, 9,140]	0.703 [0.647, 0.759]	0.868 [0.866, 0.871]
		APRI	0.743 [0.711, 0.774]	0.004 [0.002, 0.006]	0.483 [0.420, 0.545]	113 [94, 132]	9,661 [9,425, 9,897]	0.575 [0.517, 0.633]	0.858 [0.855, 0.861]
		Difference	0.120 [0.091, 0.148]	-0.000 [-0.002, 0.002]	0.241 [0.183, 0.298]	-34 [-50, -18]	-688 [-938, -438]	0.128 [0.067, 0.188]	0.010 [0.006, 0.014]
Liver failure	Remote	New	0.749 [0.698, 0.800]	0.002 [0.001, 0.002]	0.489 [0.386, 0.593]	42 [30, 54]	15,874 [15,657, 16,091]	0.596 [0.501, 0.691]	0.768 [0.764, 0.771]
		QKidney 5	0.669 [0.616, 0.722]	0.002 [0.001, 0.002]	0.137 [-0.013, 0.287]	52 [39, 65]	17,896 [17,670, 18,122]	0.500 [0.402, 0.598]	0.738 [0.735, 0.741]
		Difference	0.080 [0.025, 0.134]	0.000 [-0.000, 0.000]	0.353 [0.189, 0.516]	-10 [-22, 2]	-2,022 [-2,286, -1,758]	0.096 [-0.023, 0.215]	0.030 [0.026, 0.033]
	Standard	New	0.746 [0.695, 0.796]	0.002 [0.001, 0.002]	0.494 [0.392, 0.596]	53 [39, 67]	11,372 [11,181, 11,563]	0.490 [0.396, 0.584]	0.833 [0.831, 0.836]
		QRISK3	0.686 [0.632, 0.740]	0.002 [0.002, 0.002]	0.373 [0.224, 0.521]	31 [17, 45]	31,779 [31,556, 32,002]	0.702 [0.607, 0.797]	0.535 [0.531, 0.538]
		Difference	0.059 [0.008, 0.111]	-0.000 [-0.000, -0.000]	0.121 [-0.035, 0.277]	22 [10, 34]	-20,407 [-20,645, -20,169]	-0.212 [-0.327, -0.096]	0.299 [0.295, 0.302]
	Extended	New	0.766 [0.714, 0.818]	0.001 [0.001, 0.002]	0.526 [0.421, 0.631]	50 [36, 64]	9,534 [9,359, 9,709]	0.519 [0.425, 0.614]	0.860 [0.858, 0.863]
		QRISK3	0.686 [0.626, 0.746]	0.002 [0.002, 0.002]	0.373 [0.253, 0.492]	31 [16, 46]	31,779 [31,590, 31,968]	0.702 [0.611, 0.793]	0.535 [0.532, 0.537]
		Difference	0.080 [0.030, 0.129]	-0.000 [-0.001, -0.000]	0.153 [0.053, 0.253]	19 [10, 28]	-22,245 [-22,456, -22,034]	-0.183 [-0.266, -0.099]	0.326 [0.323, 0.329]

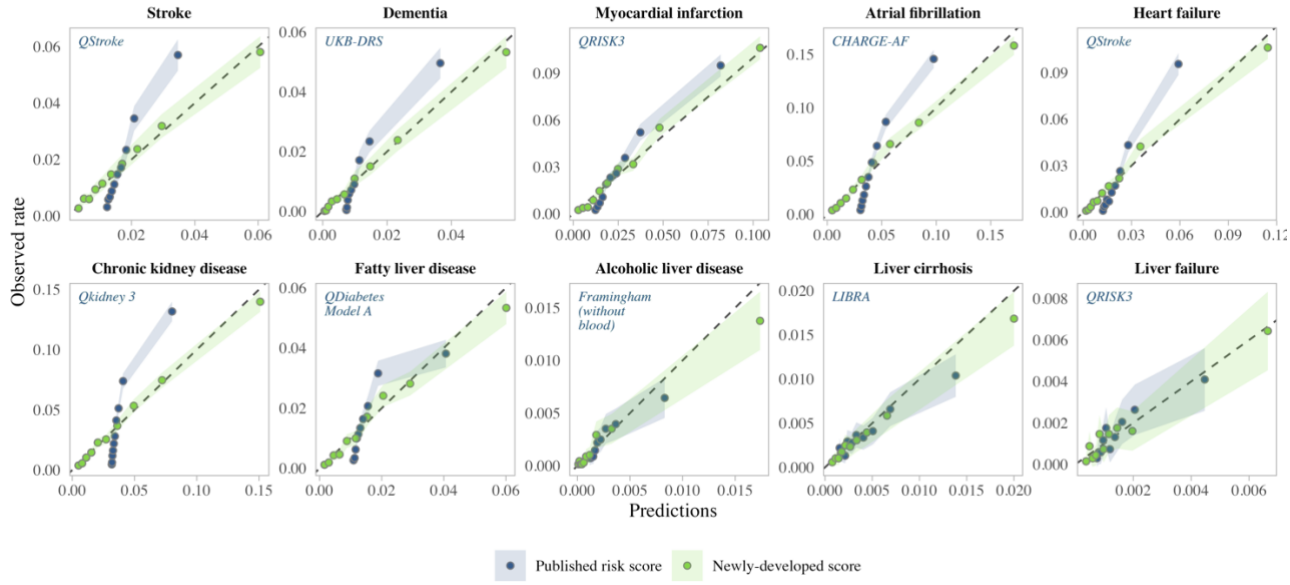
AUC= area under the curve, Thresh = the threshold at which the listed index showed the highest balanced accuracy in the development cohort. Sens= sensitivity at given threshold, Spec= specificity at given threshold, Brier = Brier score, the average squared difference between predicted probabilities and outcomes, values closer to zero indicate better performance. Dxy = Somer's Dxy statistic, the rank correlation between predicted probabilities and outcomes, values closer to one indicate better performance. Significant higher difference is shown in orange, while significantly lower difference is shown in green.

Appendix 19: Chapter 6 - Calibration plots

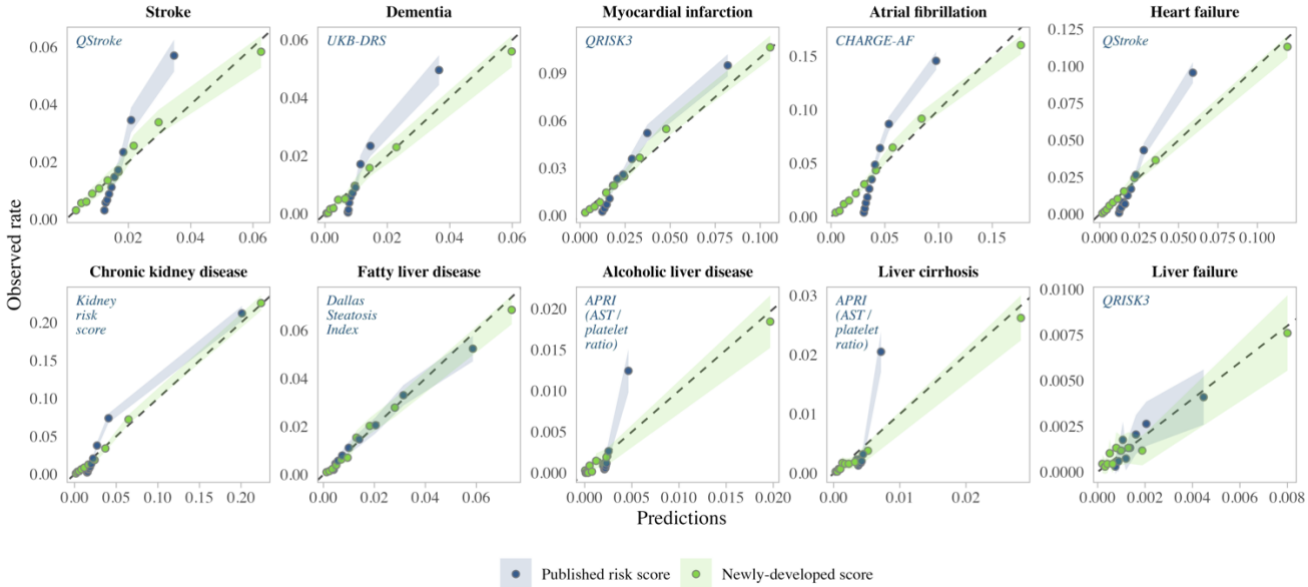
Remote models: Models that can be applied fully remotely



Standard models: Models limited to NHS Health Check / QRISK3 inputs



Extended models: Models including additional blood tests



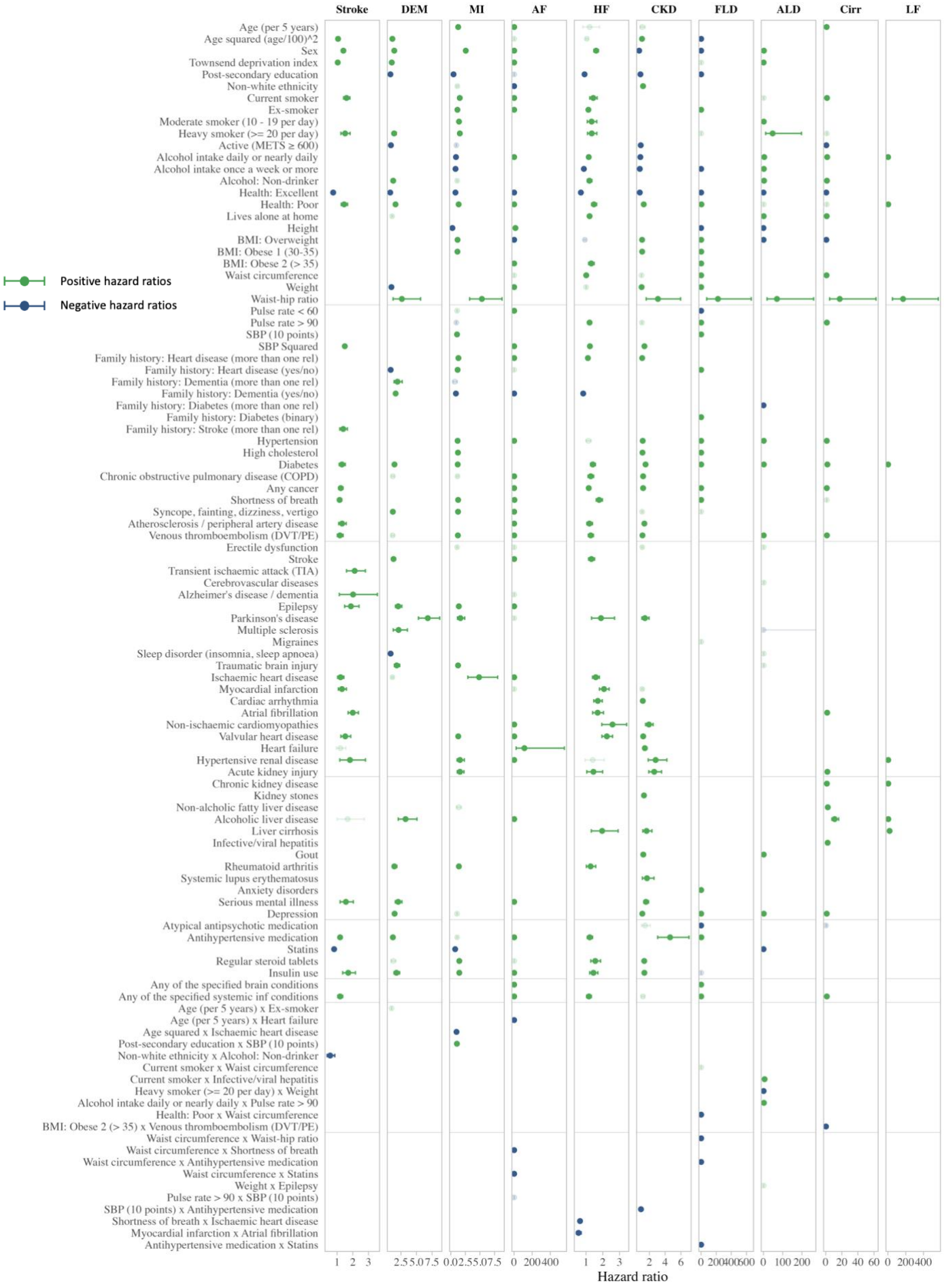
Appendix 20: Chapter 6 - Reclassification indices

Comparing newly-developed risk models with best existing risk model of the same type. Entries are index values and 95% confidence intervals.

Outcome	Index	Remote models	Standard models	Extended models
Stroke	IDI	0.017* [0.015, 0.019]	0.011* [0.009, 0.013]	0.013* [0.010, 0.015]
	NRI events	0.337* [0.284, 0.390]	0.290* [0.236, 0.343]	0.311* [0.258, 0.364]
	NRI non-events	0.325* [0.318, 0.333]	0.319* [0.312, 0.326]	0.337* [0.330, 0.344]
	NRI overall	0.662* [0.609, 0.716]	0.609* [0.555, 0.663]	0.648* [0.594, 0.702]
Dementia	IDI	0.014* [0.009, 0.018]	0.014* [0.009, 0.018]	0.018* [0.013, 0.023]
	NRI events	0.473* [0.413, 0.534]	0.459* [0.397, 0.520]	0.434* [0.372, 0.496]
	NRI non-events	0.363* [0.356, 0.370]	0.367* [0.360, 0.374]	0.407* [0.400, 0.414]
	NRI overall	0.836* [0.775, 0.897]	0.826* [0.764, 0.887]	0.841* [0.778, 0.903]
Myocardial infarction	IDI	0.019* [0.016, 0.021]	0.014* [0.011, 0.017]	0.016* [0.013, 0.019]
	NRI events	0.253* [0.209, 0.297]	0.293* [0.249, 0.337]	0.290* [0.246, 0.334]
	NRI non-events	0.364* [0.357, 0.371]	0.339* [0.332, 0.347]	0.356* [0.349, 0.363]
	NRI overall	0.617* [0.572, 0.662]	0.633* [0.588, 0.677]	0.646* [0.602, 0.691]
Atrial fibrillation	IDI	0.038* [0.035, 0.040]	0.038* [0.036, 0.041]	0.043* [0.040, 0.046]
	NRI events	0.445* [0.413, 0.477]	0.446* [0.414, 0.478]	0.442* [0.410, 0.474]
	NRI non-events	0.344* [0.337, 0.351]	0.346* [0.339, 0.353]	0.369* [0.361, 0.376]
	NRI overall	0.789* [0.756, 0.822]	0.792* [0.759, 0.825]	0.810* [0.778, 0.843]
Heart failure	IDI	0.076* [0.069, 0.083]	0.043* [0.038, 0.049]	0.053* [0.046, 0.059]
	NRI events	0.464* [0.419, 0.509]	0.293* [0.244, 0.342]	0.337* [0.290, 0.385]
	NRI non-events	0.518* [0.511, 0.524]	0.554* [0.548, 0.560]	0.559* [0.553, 0.566]
	NRI overall	0.981* [0.936, 1.027]	0.847* [0.798, 0.896]	0.897* [0.848, 0.945]
Chronic kidney disease (Stages 3, 4 and 5)	IDI	0.031* [0.028, 0.034]	0.031* [0.028, 0.035]	0.032* [0.028, 0.037]
	NRI events	0.414* [0.379, 0.450]	0.398* [0.363, 0.434]	0.338* [0.301, 0.374]
	NRI non-events	0.337* [0.330, 0.345]	0.338* [0.331, 0.345]	0.395* [0.388, 0.402]
	NRI overall	0.752* [0.716, 0.788]	0.736* [0.700, 0.772]	0.732* [0.695, 0.769]
Fatty liver disease	IDI	0.013* [0.011, 0.015]	0.013* [0.011, 0.015]	0.020* [0.017, 0.023]
	NRI events	0.302* [0.244, 0.359]	0.388* [0.332, 0.444]	0.235* [0.176, 0.294]
	NRI non-events	0.341* [0.334, 0.349]	0.329* [0.321, 0.336]	0.312* [0.305, 0.319]
	NRI overall	0.643* [0.585, 0.701]	0.717* [0.660, 0.773]	0.547* [0.488, 0.606]
Alcoholic liver disease	IDI	0.019* [0.013, 0.025]	0.019* [0.013, 0.026]	0.071* [0.048, 0.094]
	NRI events	0.497* [0.362, 0.632]	0.371* [0.227, 0.515]	0.648* [0.529, 0.766]
	NRI non-events	0.603* [0.597, 0.609]	0.615* [0.609, 0.621]	0.726* [0.721, 0.731]
	NRI overall	1.100* [0.964, 1.235]	0.986* [0.841, 1.130]	1.374* [1.255, 1.492]
Liver cirrhosis	IDI	0.009* [0.004, 0.014]	0.009* [0.005, 0.014]	0.094* [0.069, 0.120]
	NRI events	0.301* [0.186, 0.415]	0.331* [0.217, 0.444]	0.466* [0.360, 0.572]
	NRI non-events	0.323* [0.316, 0.330]	0.335* [0.328, 0.343]	0.641* [0.635, 0.647]
	NRI overall	0.624* [0.509, 0.739]	0.666* [0.553, 0.780]	1.107* [1.001, 1.214]
Liver failure	IDI	0.007* [0.003, 0.011]	0.005* [0.002, 0.008]	0.035* [0.013, 0.057]
	NRI events	0.154 [-0.036, 0.344]	0.096 [-0.095, 0.287]	0.096 [-0.095, 0.287]
	NRI non-events	0.529* [0.522, 0.535]	0.400* [0.393, 0.406]	0.539* [0.533, 0.546]
	NRI overall	0.682* [0.492, 0.872]	0.496* [0.304, 0.687]	0.636* [0.444, 0.827]

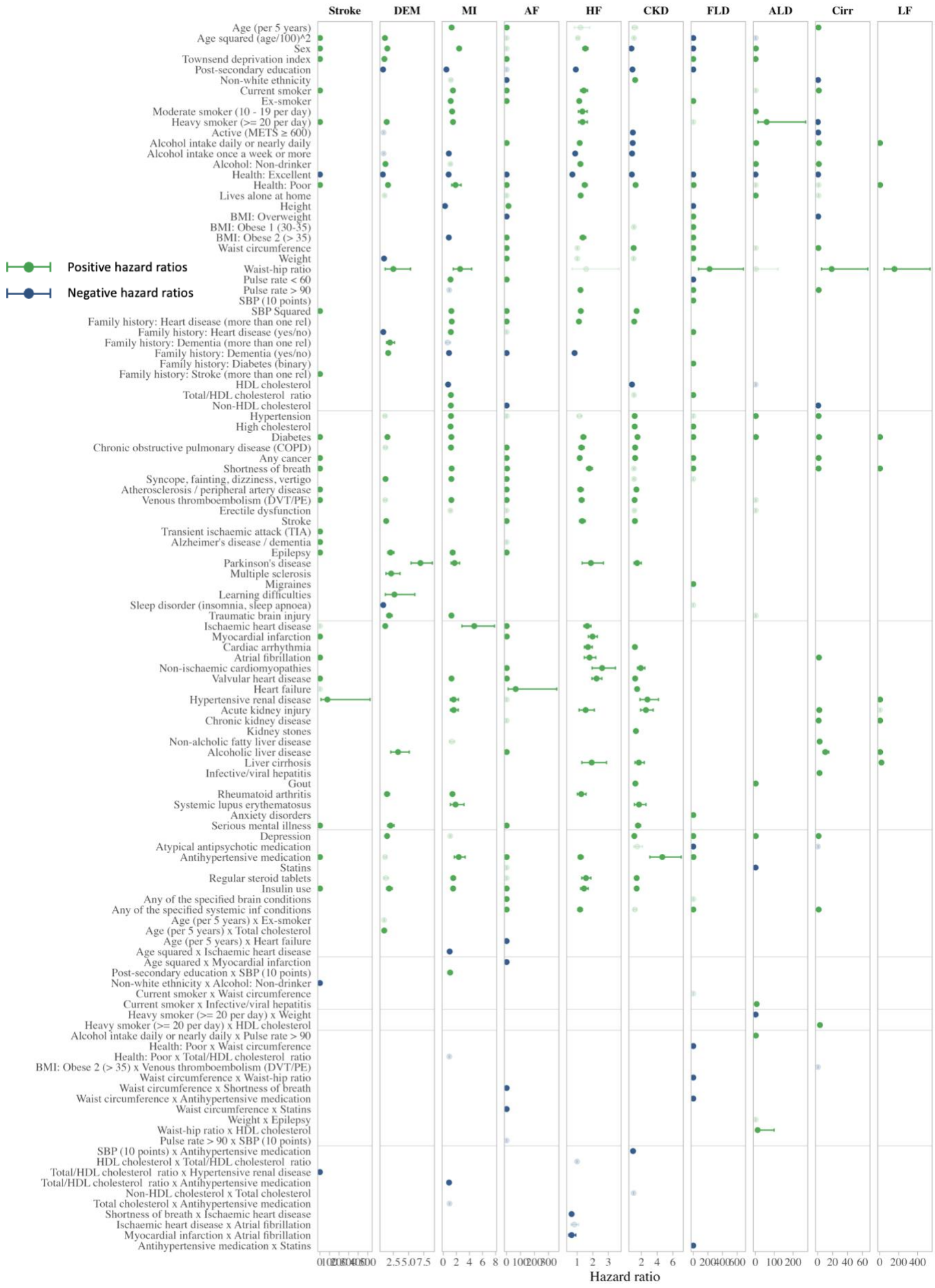
IDI = integrated discrimination index , NRI = net reclassification improvement. An asterisk (*) indicates where the 95% confidence interval for the index does not contain zero. For all indices, a positive value indicates improvement in discrimination provided by the newly-developed risk score compared with the existing risk score. Statistics are calculated with the improveProb() function from the Hmisc r package.

Appendix 21: Chapter 6 - Remote model coefficients



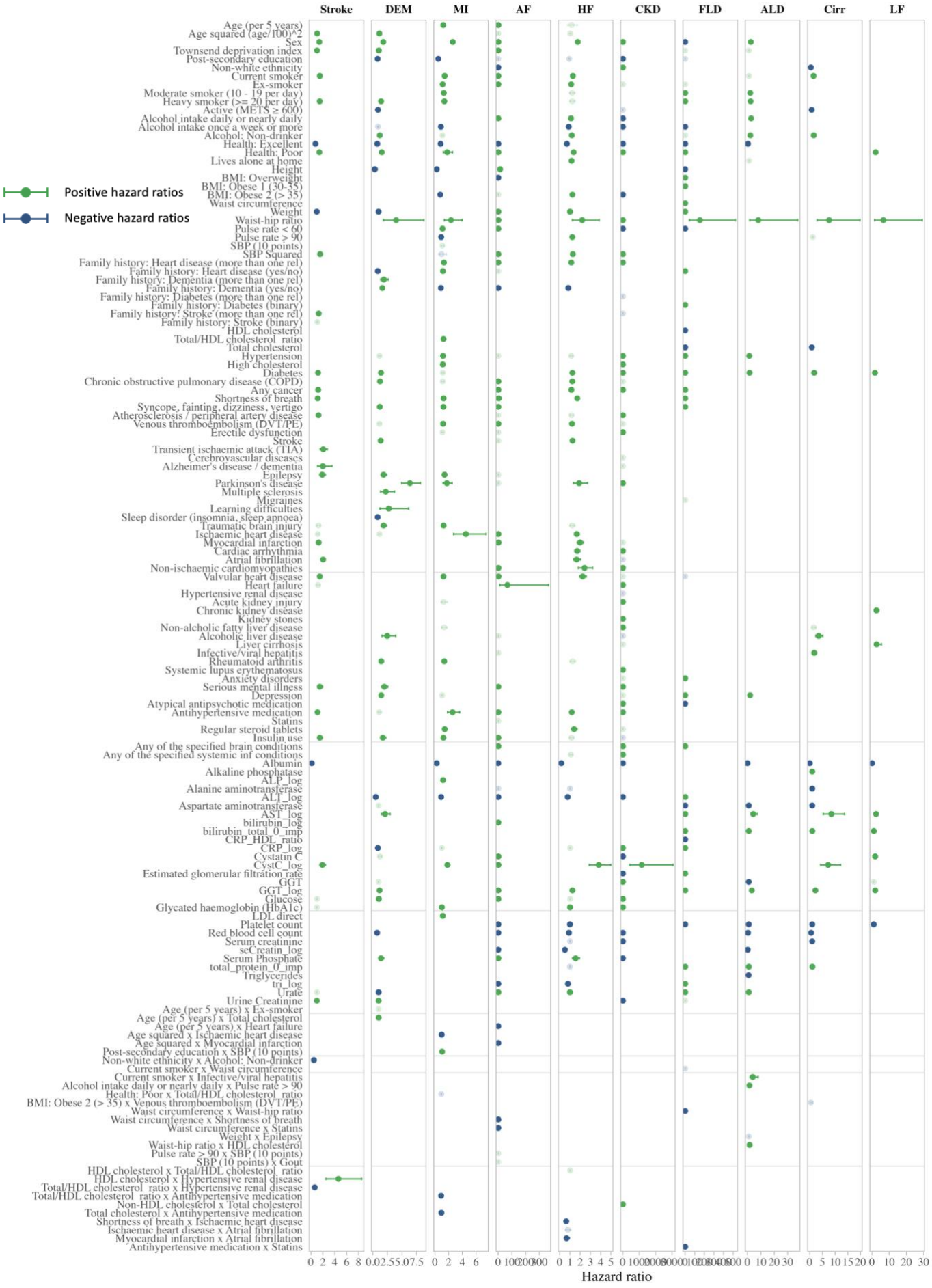
Model coefficients are shown as hazard ratios. Effects that are not significant after multiple testing adjustment (false discovery rate of 5%) has been applied are shown in greyed out colour.

Appendix 22: Chapter 6 - Standard model coefficients



Model coefficients are shown as hazard ratios. Effects that are not significant after multiple testing adjustment (false discovery rate of 5%) has been applied are shown in greyed out colour.

Appendix 23: Chapter 6 - Extended model coefficients



Model coefficients are shown as hazard ratios. Effects that are not significant after multiple testing adjustment (false discovery rate of 5%) has been applied are shown in greyed out colour.

Appendix 24: Chapter 7 - Hazard ratios (imaging vs non-imaging)

Outcome	Model	Variable	Hazard ratio (95% CI)	p-value
Stroke	Index only	QStroke	1.54* [1.43, 1.66]	< 0.001
Stroke	With imaging	QStroke	1.07 [0.92, 1.25]	0.3783
		White matter ISOVF	1.22* [1.08, 1.38]	0.0013
		White matter hyperintensities (cube root)	1.31* [1.17, 1.46]	< 0.001
		Carotid IMT at 120-150 degrees	1.13 [1.01, 1.27]	0.0329
		LVMi	1.28* [1.14, 1.44]	< 0.001
		LAEF	0.86* [0.77, 0.95]	0.0047
All-cause dementia	Index only	UKB-DRS	1.49* [1.40, 1.58]	< 0.001
All-cause dementia	With imaging	UKB-DRS	1.09 [0.95, 1.25]	0.2299
		White matter FA	0.83 [0.70, 0.98]	0.0258
		Hippocampus volume	0.60* [0.49, 0.74]	< 0.001
		CSF volume	1.17 [1.01, 1.36]	0.0375
		Peripheral brain volume	0.67* [0.54, 0.84]	< 0.001
		Carotid IMT at 210-240 degrees	1.18 [1.01, 1.37]	0.0411
		Liver cT1 > 680 ms	1.65* [1.12, 2.42]	0.0114
		RAEF	0.80* [0.67, 0.94]	0.0082
		LV cardiac index	1.33* [1.13, 1.55]	< 0.001
		Height (m)	0.79 [0.61, 1.03]	0.0843
		Body mass index (kg/m2)	0.74* [0.61, 0.90]	0.0021
Atherosclerosis / Peripheral artery disease	Index only	QStroke	1.59* [1.51, 1.68]	< 0.001
	With imaging	QStroke	1.30* [1.17, 1.44]	< 0.001
		White matter hyperintensities	1.08 [1.00, 1.16]	0.0534
		Carotid IMT at 120-150 degrees	1.15* [1.04, 1.27]	0.0065
		Wall thickness indexed	1.31* [1.19, 1.45]	< 0.001
		LVESV	1.17* [1.09, 1.26]	< 0.001
		Heart rate (bpm)	1.10 [1.00, 1.22]	0.0496
Venous thromboembolism	Index only	PCP-HF	1.26* [1.17, 1.37]	< 0.001
	With imaging	PCP-HF	1.00 [0.84, 1.20]	0.9634
		GLS	1.25* [1.12, 1.40]	< 0.001
		Diabetes	0.56 [0.31, 1.01]	0.0524
		Red blood cell count (10^{12} cells/Litre)	1.14 [1.00, 1.31]	0.0504
		Heart rate (bpm)	1.17* [1.05, 1.31]	0.0037
		Height (m)	1.25* [1.06, 1.49]	0.0098
		Body mass index (kg/m2)	1.26* [1.12, 1.41]	< 0.001
		Townsend deprivation index	1.13 [1.01, 1.25]	0.0296
Myocardial infarction	Index only	QRISK3	1.89* [1.76, 2.02]	< 0.001
Myocardial infarction	With imaging	QRISK3	1.22* [1.07, 1.40]	0.0036
		Carotid IMT at 210-240 degrees	1.14* [1.04, 1.26]	0.0060
		Liver cT1 > 680 ms	1.25 [1.00, 1.56]	0.0483
		Cardiac index	0.78* [0.69, 0.87]	< 0.001
		LVMi	1.27* [1.15, 1.41]	< 0.001
		Family history: Heart	1.45* [1.13, 1.86]	0.0034
		Hypertension	1.33* [1.07, 1.65]	0.0105
		Current smoker	1.60 [1.06, 2.41]	0.0248
		SBP (mmHg)	1.20* [1.08, 1.34]	< 0.001
		Height (m)	0.86 [0.74, 1.00]	0.0555
		Post-secondary education	0.73* [0.59, 0.89]	0.0026
Atrial fibrillation	Index only	CHARGE-AF	1.51* [1.46, 1.55]	< 0.001
Atrial fibrillation	With imaging	CHARGE-AF	1.02 [0.94, 1.11]	0.5720
		Liver cT1 > 720 ms	1.31* [1.13, 1.53]	< 0.001
		Max wall thickness	1.26* [1.17, 1.37]	< 0.001
		RAV max	1.10* [1.02, 1.18]	0.0091
		LAVi min	1.39* [1.28, 1.50]	< 0.001
		LAEF	0.84* [0.75, 0.94]	0.0022
		Family history: Heart	1.18 [1.00, 1.39]	0.0539
		Hypertension	1.34* [1.13, 1.58]	< 0.001
		Red blood cell count (10^{12} cells/Litre)	0.92 [0.84, 0.99]	0.0369
		Height (m)	1.21* [1.08, 1.37]	0.0016
		Townsend deprivation index	1.09 [1.01, 1.17]	0.0203
Non-ischaemic cardiomyopathy	Index only	Framingham	1.80* [1.54, 2.09]	< 0.001
	With imaging	Framingham	1.10 [0.84, 1.43]	0.4851
		Max wall thickness indexed	1.65* [1.44, 1.91]	< 0.001
		Volume ratio	1.23* [1.05, 1.44]	0.0097
		LVESV	1.22* [1.05, 1.43]	0.0095
		LAV min	1.15* [1.05, 1.27]	0.0039
Valvular heart disease	Index only	QStroke	1.81* [1.73, 1.89]	< 0.001
Valvular heart disease	With imaging	QStroke	1.29* [1.18, 1.41]	< 0.001
		White matter hyperintensities	1.08* [1.02, 1.14]	0.0052
		Carotid IMT at 210-240 degrees	1.09 [1.01, 1.18]	0.0334

Outcome	Model	Variable	Hazard ratio (95% CI)	p-value
		Wall thickness indexed	1.14* [1.03, 1.27]	0.0098
		Volume ratio	1.12* [1.05, 1.20]	< 0.001
		LVMi	1.37* [1.22, 1.53]	< 0.001
		LAVi min	1.10* [1.05, 1.15]	< 0.001
		Post-secondary education	0.81 [0.68, 0.96]	0.0158
Heart failure	Index only	QStroke	1.78* [1.70, 1.86]	< 0.001
Heart failure	With imaging	QStroke	1.28* [1.15, 1.43]	< 0.001
		Volume ratio	1.14* [1.05, 1.23]	< 0.001
		LVMi	1.38* [1.24, 1.53]	< 0.001
		LVEF	0.72* [0.65, 0.79]	< 0.001
		LAEF	0.86* [0.79, 0.94]	0.0012
		Hypertension	1.44* [1.11, 1.85]	0.0051
		Body mass index (kg/m2)	1.20* [1.08, 1.34]	< 0.001
Kidney combined	Index only	PCP-HF	1.47* [1.42, 1.51]	< 0.001
Kidney combined	With imaging	PCP-HF	1.10* [1.03, 1.18]	0.0051
		White matter hyperintensities (cube root)	1.11* [1.04, 1.18]	< 0.001
		Very low liver iron (< 1.1mg)	1.29 [1.04, 1.59]	0.0212
		Liver cT1	1.08* [1.02, 1.15]	0.0136
		LV interventricular septum T1	1.09* [1.02, 1.16]	0.0085
		LVM	1.10 [1.01, 1.21]	0.0383
		Global function index	0.91* [0.86, 0.98]	0.009
		Family history: Liver	11.91* [2.94, 48.27]	< 0.001
		High cholesterol	1.25* [1.08, 1.44]	0.002
		Hypertension	1.37* [1.18, 1.60]	< 0.001
		SBP (mmHg)	0.92 [0.86, 0.99]	0.0242
		Body mass index (kg/m2)	1.11* [1.03, 1.19]	0.004
		Post-secondary education	0.79* [0.70, 0.91]	< 0.001
Chronic kidney	Index only	QKidney (V3)	1.49* [1.44, 1.54]	< 0.001
disease	With imaging	QKidney (V3)	1.07 [0.99, 1.15]	0.0835
		Very low liver fat (< 2%)	1.39 [1.07, 1.81]	0.0146
		Low liver iron (<1.3mg)	1.23 [1.00, 1.50]	0.0495
		Very low liver iron (< 1.1mg)	1.94* [1.47, 2.57]	< 0.001
		Cardiac index	0.88* [0.79, 0.97]	0.0142
		RAVi max	0.82* [0.74, 0.91]	< 0.001
		LAV min	1.14* [1.07, 1.23]	< 0.001
		Family history: Brain	1.22 [1.01, 1.47]	0.0442
		High cholesterol	1.28 [1.04, 1.59]	0.0221
		Hypertension	2.02* [1.61, 2.53]	< 0.001
		Red blood cell count (10^12 cells/Litre)	0.85* [0.76, 0.95]	0.0054
		Height (m)	1.20 [1.04, 1.39]	0.0144
		Body mass index (kg/m2)	1.18* [1.06, 1.31]	0.0020
		Post-secondary education	0.81 [0.66, 0.99]	0.0358
		Townsend deprivation index	1.10 [1.00, 1.20]	0.0433
Liver disease	Index only	Fatty liver index	1.89* [1.70, 2.10]	< 0.001
Liver disease	With imaging	Fatty liver index	2.13* [1.71, 2.67]	3.07x10-11
		Liver cT1	1.19* [1.05, 1.35]	0.0056
		Liver PDFF	1.12 [1.01, 1.24]	0.0266
		RVSV	0.87 [0.77, 0.99]	0.0300
		Diabetes	1.48* [1.10, 2.00]	0.0103
		Body mass index (kg/m2)	0.74* [0.62, 0.89]	9.73x10-4
		Health: Poor	1.70* [1.12, 2.57]	0.0119
		Health: Good	0.58* [0.45, 0.74]	1.16x10-5
		Health: Excellent	0.49* [0.33, 0.73]	4.00x10-4
		Post-secondary education	0.75* [0.60, 0.93]	0.0091
		Townsend deprivation index	1.11 [1.01, 1.22]	0.0343
Fatty liver disease	Index only	Fatty liver index	2.49* [2.15, 2.88]	< 0.001
Fatty liver disease	With imaging	Fatty liver index	2.34* [1.79, 3.05]	< 0.001
		White matter hyperintensities	1.14 [1.02, 1.27]	0.0163
		Liver PDFF (log)	1.51* [1.32, 1.72]	< 0.001
		RVEDVi	0.81* [0.69, 0.96]	0.0122
		Diabetes	1.54 [1.08, 2.20]	0.0180
		Height (m)	0.73* [0.59, 0.89]	0.0026
		Body mass index (kg/m2)	0.75* [0.62, 0.92]	0.0059
Liver cirrhosis	Index only	Fatty liver index	2.48* [1.79, 3.43]	< 0.001
Liver cirrhosis	With imaging	Fatty liver index	4.19* [2.26, 7.78]	< 0.001
		Liver cT1	1.53* [1.20, 1.96]	< 0.001
		Total/HDL cholesterol ratio	0.60* [0.42, 0.84]	0.0033
		Body mass index (kg/m2)	0.54 [0.33, 0.89]	0.0160
Combined heart,	Index only	QStroke	1.55* [1.52, 1.58]	< 0.001
brain, liver	With imaging	QStroke	1.10* [1.05, 1.15]	< 0.001

Outcome	Model	Variable	Hazard ratio (95% CI)	p-value
or kidney		White matter hyperintensities (cube root)	1.10* [1.06, 1.14]	< 0.001
		Carotid IMT at 210-240 degrees	1.05* [1.01, 1.08]	0.0071
		Liver cT1 > 700 ms	1.15* [1.07, 1.24]	< 0.001
		Liver iron	0.96 [0.93, 1.00]	0.0505
		Max wall thickness	1.17* [1.12, 1.22]	< 0.001
		Volume ratio	1.06* [1.03, 1.09]	< 0.001
		LVEDV	1.12* [1.08, 1.17]	< 0.001
		LAEF	0.91* [0.88, 0.94]	< 0.001
		Global function index	0.94* [0.90, 0.98]	0.0017
		High cholesterol	1.10 [1.01, 1.19]	0.0246
		Hypertension	1.24* [1.14, 1.35]	< 0.001
		Current smoker	1.22 [1.03, 1.44]	0.0218
		Post-secondary education	0.86* [0.80, 0.93]	< 0.001
		Townsend deprivation index	1.04 [1.00, 1.07]	0.0368

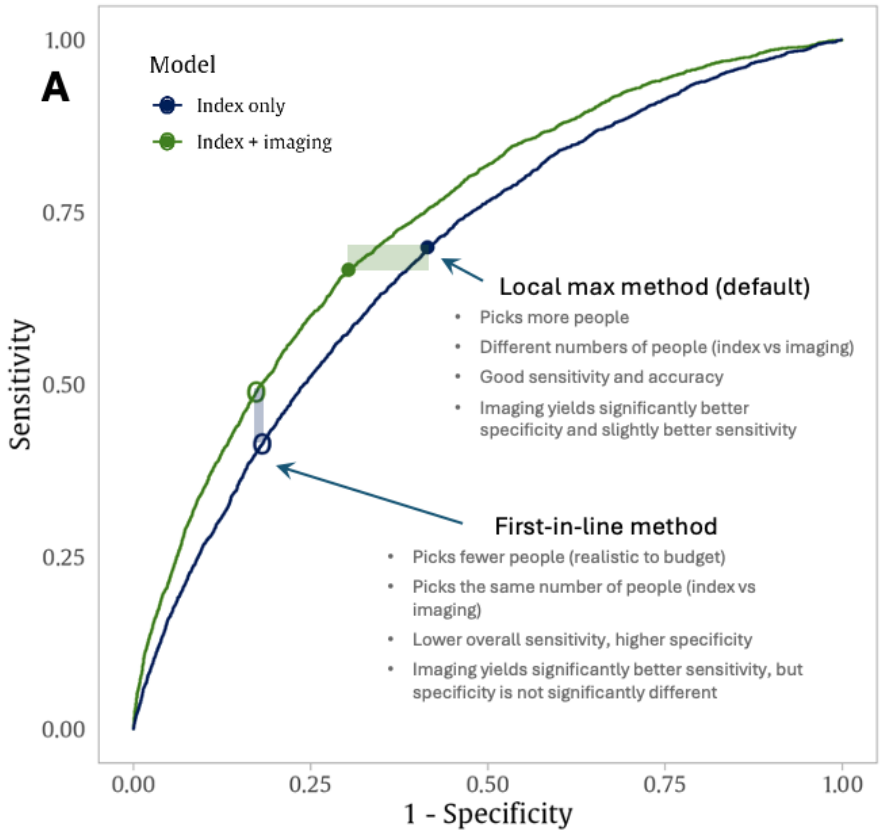
* Significant following multiple testing adjustment for a false discovery rate of 5%

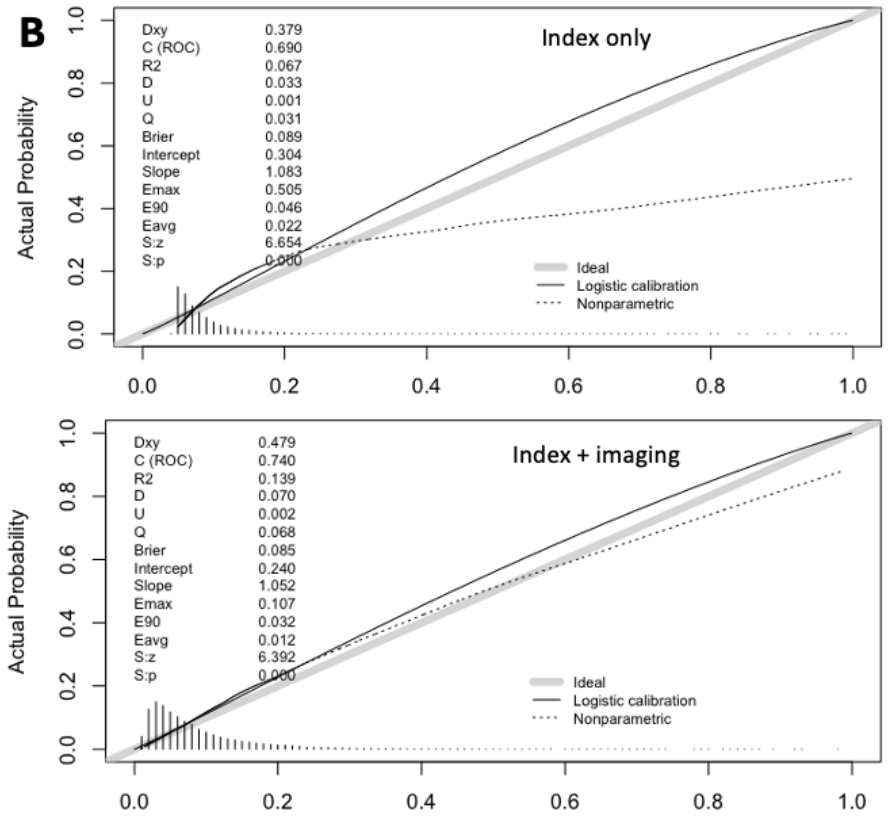
Appendix 25: Chapter 7 - Global performance scores

Outcome r = outcome rate	**Metric**	**Index only** performance metric (95% confidence interval)	**Index + Imaging** performance metric (95% confidence interval)	**Difference** difference (95% confidence interval)	**p-value**	**N**
Stroke	AUC	0.675 [0.663, 0.687]	0.718 [0.705, 0.731]	0.043* [0.023, 0.063]	< 1.0x10-20	30,441
r = 1.0%	AUC-PR	0.020 [0.016, 0.025]	0.033 [0.029, 0.037]	0.012* [0.006, 0.019]	9.98x10-4	
	Balanced accuracy	0.519 [0.509, 0.529]	0.538 [0.527, 0.548]	0.019* [0.002, 0.035]	0.0349	
	Sensitivity	0.057 [0.037, 0.077]	0.094 [0.073, 0.115]	0.037* [0.004, 0.070]	0.0279	
	Specificity	0.981 [0.981, 0.981]	0.981 [0.981, 0.981]	0.000* [0.000, 0.001]	0.0349	
	PPV	0.029 [0.018, 0.039]	0.047 [0.037, 0.057]	0.018* [0.002, 0.035]	0.0269	
All-cause	AUC	0.757 [0.739, 0.776]	0.866 [0.848, 0.885]	0.109* [0.078, 0.140]	< 1.0x10-20	31,004
dementia	AUC-PR	0.017 [0.000, 0.035]	0.077 [0.060, 0.095]	0.060* [0.032, 0.088]	< 1.0x10-20	
r = 0.5%	Balanced accuracy	0.527 [0.506, 0.547]	0.589 [0.568, 0.610]	0.062* [0.028, 0.096]	< 1.0x10-20	
	Sensitivity	0.062 [0.022, 0.103]	0.186 [0.145, 0.228]	0.124* [0.057, 0.192]	< 1.0x10-20	
	Specificity	0.991 [0.991, 0.991]	0.991 [0.991, 0.992]	0.000* [0.000, 0.001]	0.0090	
	PPV	0.031 [0.011, 0.052]	0.093 [0.072, 0.114]	0.062* [0.028, 0.095]	< 1.0x10-20	
Atherosclerosis /	AUC	0.691 [0.682, 0.700]	0.734 [0.725, 0.743]	0.043* [0.028, 0.058]	< 1.0x10-20	30,400
Peripheral artery	AUC-PR	0.029 [0.026, 0.033]	0.043 [0.039, 0.047]	0.014* [0.007, 0.020]	< 1.0x10-20	
disease	Balanced accuracy	0.535 [0.524, 0.545]	0.556 [0.546, 0.566]	0.021* [0.005, 0.038]	0.0150	
r = 1.2%	Sensitivity	0.092 [0.072, 0.112]	0.134 [0.114, 0.154]	0.042* [0.009, 0.074]	0.0120	
	Specificity	0.977 [0.977, 0.977]	0.978 [0.977, 0.978]	0.000* [0.000, 0.001]	0.0130	
	PPV	0.046 [0.036, 0.056]	0.067 [0.057, 0.077]	0.021* [0.005, 0.037]	0.0130	
Venous	AUC	0.610 [0.596, 0.625]	0.686 [0.671, 0.700]	0.075* [0.051, 0.099]	< 1.0x10-20	30,007
thromboembolism	AUC-PR	0.016 [0.012, 0.020]	0.029 [0.025, 0.033]	0.013* [0.007, 0.019]	< 1.0x10-20	
r = 1.0%	Balanced accuracy	0.501 [0.491, 0.511]	0.532 [0.522, 0.542]	0.031* [0.015, 0.047]	< 1.0x10-20	
	Sensitivity	0.023 [0.003, 0.043]	0.084 [0.065, 0.104]	0.062* [0.030, 0.093]	< 1.0x10-20	
	Specificity	0.979 [0.979, 0.980]	0.980 [0.980, 0.980]	0.001* [0.000, 0.001]	< 1.0x10-20	
	PPV	0.011 [0.001, 0.021]	0.042 [0.032, 0.052]	0.031* [0.015, 0.047]	< 1.0x10-20	
Myocardial	AUC	0.724 [0.717, 0.732]	0.765 [0.758, 0.773]	0.041* [0.028, 0.054]	< 1.0x10-20	30,225
infarction	AUC-PR	0.035 [0.032, 0.038]	0.044 [0.041, 0.047]	0.009* [0.004, 0.014]	< 1.0x10-20	
r = 1.3%	Balanced accuracy	0.538 [0.528, 0.547]	0.556 [0.547, 0.566]	0.019* [0.003, 0.034]	0.0230	
	Sensitivity	0.101 [0.082, 0.119]	0.138 [0.120, 0.156]	0.037* [0.007, 0.067]	0.0220	
	Specificity	0.974 [0.974, 0.974]	0.975 [0.974, 0.975]	0.001* [0.000, 0.001]	0.0230	
	PPV	0.050 [0.041, 0.060]	0.069 [0.060, 0.078]	0.018* [0.003, 0.034]	0.0180	
Atrial fibrillation	AUC	0.733 [0.725, 0.741]	0.788 [0.780, 0.795]	0.055* [0.042, 0.067]	< 1.0x10-20	30,160
r = 2.4%	AUC-PR	0.065 [0.054, 0.077]	0.147 [0.136, 0.158]	0.081* [0.063, 0.100]	< 1.0x10-20	
	Balanced accuracy	0.563 [0.553, 0.573]	0.636 [0.626, 0.646]	0.073* [0.057, 0.089]	< 1.0x10-20	
	Sensitivity	0.172 [0.153, 0.192]	0.315 [0.296, 0.334]	0.143* [0.111, 0.174]	< 1.0x10-20	
	Specificity	0.953 [0.953, 0.954]	0.957 [0.957, 0.958]	0.004* [0.003, 0.004]	< 1.0x10-20	
	PPV	0.086 [0.076, 0.096]	0.158 [0.148, 0.167]	0.071* [0.056, 0.087]	< 1.0x10-20	
Non-ischaemic	AUC	0.709 [0.681, 0.737]	0.839 [0.812, 0.866]	0.130* [0.084, 0.175]	< 1.0x10-20	30,976
cardiomyopathy	AUC-PR	0.012 [0.000, 0.029]	0.047 [0.030, 0.064]	0.035* [0.008, 0.062]	0.0030	
r = 0.3%	Balanced accuracy	0.508 [0.486, 0.530]	0.578 [0.556, 0.600]	0.070* [0.035, 0.105]	< 1.0x10-20	
	Sensitivity	0.022 [0.000, 0.066]	0.161 [0.118, 0.205]	0.140* [0.070, 0.210]	< 1.0x10-20	
	Specificity	0.994 [0.994, 0.994]	0.994 [0.994, 0.995]	0.000* [0.000, 0.001]	< 1.0x10-20	
	PPV	0.011 [0.000, 0.033]	0.081 [0.059, 0.102]	0.070* [0.035, 0.105]	< 1.0x10-20	
Valvular heart	AUC	0.745 [0.739, 0.751]	0.782 [0.775, 0.789]	0.037* [0.026, 0.048]	< 1.0x10-20	30,465
disease	AUC-PR	0.060 [0.052, 0.067]	0.100 [0.093, 0.108]	0.041* [0.029, 0.053]	< 1.0x10-20	
r = 2.0%	Balanced accuracy	0.560 [0.551, 0.569]	0.599 [0.590, 0.608]	0.039* [0.024, 0.053]	< 1.0x10-20	
	Sensitivity	0.158 [0.141, 0.175]	0.234 [0.216, 0.251]	0.076* [0.048, 0.104]	< 1.0x10-20	
	Specificity	0.962 [0.962, 0.963]	0.964 [0.964, 0.964]	0.002* [0.001, 0.002]	< 1.0x10-20	
	PPV	0.079 [0.070, 0.088]	0.117 [0.108, 0.125]	0.038* [0.024, 0.052]	< 1.0x10-20	
Heart failure	AUC	0.769 [0.758, 0.779]	0.838 [0.827, 0.849]	0.069* [0.052, 0.087]	< 1.0x10-20	30,840
r = 1.1%	AUC-PR	0.049 [0.032, 0.065]	0.131 [0.115, 0.148]	0.082* [0.056, 0.109]	< 1.0x10-20	
	Balanced accuracy	0.571 [0.558, 0.585]	0.633 [0.620, 0.646]	0.062* [0.040, 0.083]	< 1.0x10-20	
	Sensitivity	0.163 [0.137, 0.190]	0.285 [0.258, 0.311]	0.122* [0.079, 0.165]	< 1.0x10-20	
	Specificity	0.980 [0.979, 0.980]	0.981 [0.981, 0.981]	0.001* [0.001, 0.002]	< 1.0x10-20	
	PPV	0.082 [0.068, 0.095]	0.142 [0.129, 0.156]	0.061* [0.039, 0.082]	< 1.0x10-20	
Kidney combined	AUC	0.688 [0.682, 0.693]	0.757 [0.751, 0.763]	0.070* [0.060, 0.079]	< 1.0x10-20	29,109
r = 3.3%	AUC-PR	0.078 [0.072, 0.084]	0.126 [0.120, 0.132]	0.048* [0.038, 0.058]	< 1.0x10-20	
	Balanced accuracy	0.563 [0.556, 0.570]	0.606 [0.599, 0.614]	0.043* [0.031, 0.056]	< 1.0x10-20	

Outcome r = outcome rate	**Metric**	**Index only** performance metric (95% confidence interval)	**Index + Imaging** performance metric (95% confidence interval)	**Difference** difference (95% confidence interval)	**p-value**	**N**
	Sensitivity	0.192 [0.178, 0.206]	0.276 [0.261, 0.290]	0.084* [0.060, 0.107]	< 1.0x10-20	
	Specificity	0.934 [0.933, 0.934]	0.937 [0.936, 0.938]	0.003* [0.002, 0.004]	< 1.0x10-20	
	PPV	0.096 [0.089, 0.103]	0.138 [0.131, 0.145]	0.042* [0.030, 0.054]	< 1.0x10-20	
Chronic kidney	AUC	0.755 [0.746, 0.764]	0.796 [0.787, 0.804]	0.041* [0.027, 0.055]	< 1.0x10-20	30,456
disease	AUC-PR	0.050 [0.042, 0.057]	0.078 [0.070, 0.086]	0.028* [0.016, 0.041]	< 1.0x10-20	
r = 1.4%	Balanced accuracy	0.552 [0.542, 0.562]	0.574 [0.564, 0.584]	0.022* [0.005, 0.038]	0.0080	
	Sensitivity	0.132 [0.112, 0.152]	0.174 [0.155, 0.194]	0.043* [0.010, 0.075]	0.0080	
	Specificity	0.972 [0.972, 0.972]	0.973 [0.973, 0.973]	0.001* [0.000, 0.001]	0.0090	
	PPV	0.066 [0.056, 0.076]	0.087 [0.077, 0.097]	0.021* [0.005, 0.037]	0.0090	
Liver disease	AUC	0.680 [0.671, 0.689]	0.743 [0.734, 0.752]	0.063* [0.049, 0.078]	< 1.0x10-20	30,306
r = 1.1%	AUC-PR	0.028 [0.020, 0.036]	0.054 [0.046, 0.062]	0.026* [0.013, 0.039]	< 1.0x10-20	
	Balanced accuracy	0.535 [0.524, 0.546]	0.556 [0.545, 0.568]	0.021* [0.003, 0.040]	0.0180	
	Sensitivity	0.092 [0.070, 0.115]	0.134 [0.112, 0.157]	0.042* [0.005, 0.079]	0.0180	
	Specificity	0.977 [0.977, 0.978]	0.978 [0.977, 0.978]	0.001* [0.000, 0.001]	0.0180	
	PPV	0.046 [0.035, 0.057]	0.067 [0.056, 0.079]	0.021* [0.003, 0.039]	0.0140	
Fatty liver disease	AUC	0.745 [0.733, 0.756]	0.821 [0.810, 0.832]	0.076* [0.058, 0.095]	< 1.0x10-20	30,816
r = 0.7%	AUC-PR	0.025 [0.014, 0.036]	0.056 [0.046, 0.067]	0.032* [0.014, 0.049]	< 1.0x10-20	
	Balanced accuracy	0.532 [0.516, 0.547]	0.582 [0.567, 0.597]	0.050* [0.026, 0.074]	< 1.0x10-20	
	Sensitivity	0.077 [0.047, 0.107]	0.176 [0.147, 0.206]	0.100* [0.051, 0.148]	< 1.0x10-20	
	Specificity	0.986 [0.986, 0.986]	0.987 [0.987, 0.987]	0.001* [0.000, 0.001]	< 1.0x10-20	
	PPV	0.038 [0.024, 0.053]	0.088 [0.073, 0.103]	0.050* [0.026, 0.074]	< 1.0x10-20	
Liver cirrhosis	AUC	0.740 [0.708, 0.771]	0.816 [0.785, 0.847]	0.076* [0.024, 0.129]	0.0030	30,975
r = 0.1%	AUC-PR	0.016 [0.000, 0.043]	0.044 [0.018, 0.071]	0.029 [-0.014, 0.071]	0.1946	
	Balanced accuracy	0.499 [0.475, 0.522]	0.543 [0.520, 0.566]	0.045* [0.007, 0.082]	0.0259	
	Sensitivity	0.000 [0.000, 0.048]	0.089 [0.042, 0.135]	0.089* [0.015, 0.163]	0.0250	
	Specificity	0.997 [0.997, 0.997]	0.997 [0.997, 0.997]	0.000* [0.000, 0.000]	0.0389	
	PPV	0.000 [0.000, 0.024]	0.044 [0.021, 0.068]	0.044* [0.007, 0.082]	0.0389	
Combined heart,	AUC	0.690 [0.686, 0.693]	0.740 [0.737, 0.743]	0.050* [0.045, 0.055]	< 1.0x10-20	31,048
brain, liver	AUC-PR	0.201 [0.196, 0.207]	0.266 [0.261, 0.271]	0.065* [0.056, 0.073]	< 1.0x10-20	
or kidney	Balanced accuracy	0.616 [0.611, 0.620]	0.658 [0.654, 0.662]	0.042* [0.035, 0.049]	< 1.0x10-20	
r = 10.3%	Sensitivity	0.413 [0.406, 0.421]	0.489 [0.481, 0.497]	0.076* [0.063, 0.088]	< 1.0x10-20	
	Specificity	0.818 [0.817, 0.819]	0.827 [0.826, 0.828]	0.009* [0.007, 0.010]	< 1.0x10-20	
	PPV	0.207 [0.203, 0.211]	0.245 [0.241, 0.249]	0.038* [0.032, 0.044]	< 1.0x10-20	

Appendix 26: Chapter 7 - Why is the sensitivity lower than expected?





C

Method	Model	AUC	Sens	Spec	Balanced accuracy	True Neg	True Pos	Event rate (*r*)	Events (*p*)	N	Picked
Local max	Index only	0.690	0.699	0.585	0.642	22,789	2,232	0.103	3,193	31,048	13,786
	Index + imaging	0.740	0.666	0.697	0.682	23,031	2,128	0.103	3,193	31,048	10,574
First-in-line	Index only	0.690	0.413	0.818	0.616	16,301	1,320	0.103	3,193	31,048	6,386
	Index + imaging	0.740	0.489	0.827	0.658	19,409	1,562	0.103	3,193	31,048	6,386

The purpose of this figure is to help explain why the performance values for this comparison may seem significantly lower than typically reported in binary classification studies. **Panel A**: Receiver operating curves (ROCs) showing discriminative performance of non-imaging risk index (in blue) compared with risk index plus imaging (in green) for combined heart, brain, liver and kidney outcomes. The "first-in-line" method results in classification cut-off thresholds that are significantly more conservative than the default method for finding maximum sensitivity/specificity. The underlying models are the same, but as shown with calibration plots (**Panel B**) and numerical results (**Panel C**), the "First-in-line" method ensures the same number of positive predictions ("number picked"), at a rate proportional to the number of expected events. Please note the AUC is the same in both cases, because AUC is agnostic to clinical cutoff method.

Appendix 27: Chapter 7 - Decomposition of effects (AUC)

Outcome	Non-imaging index baseline	Pruned index + imaging + covariates	Whole effect (covariates + imaging + pruning)	Whole effect - pruning (covariates + imaging)	Effect of Covariates	Effect of Imaging	Effect of pruning	N
Athero / Peripheral artery disease	0.691 [0.682, 0.700]	0.734 [0.725, 0.743]	0.051* [0.036, 0.066]	0.043* [0.028, 0.058]	0.026* [0.012, 0.041]	0.017* [0.003, 0.031]	0.008 [-0.007, 0.023]	30,400
Venous thromboembolism	0.610 [0.596, 0.625]	0.686 [0.671, 0.700]	0.088* [0.064, 0.113]	0.075* [0.051, 0.099]	0.057* [0.033, 0.082]	0.018 [-0.006, 0.042]	0.013 [-0.011, 0.037]	30,007
Stroke	0.675 [0.663, 0.687]	0.718 [0.705, 0.731]	0.055* [0.035, 0.075]	0.043* [0.023, 0.063]	0.014 [-0.006, 0.034]	0.029* [0.008, 0.049]	0.012 [-0.009, 0.033]	30,441
All-cause dementia	0.757 [0.739, 0.776]	0.866 [0.848, 0.885]	0.118* [0.088, 0.148]	0.109* [0.078, 0.140]	0.041* [0.011, 0.071]	0.068* [0.037, 0.099]	0.009 [-0.021, 0.039]	31,004
Myocardial infarction	0.724 [0.717, 0.732]	0.765 [0.758, 0.773]	0.044* [0.032, 0.057]	0.041* [0.028, 0.054]	0.028* [0.015, 0.040]	0.013* [0.001, 0.025]	0.003 [-0.009, 0.015]	30,225
Atrial fibrillation	0.733 [0.725, 0.741]	0.788 [0.780, 0.795]	0.058* [0.045, 0.071]	0.055* [0.042, 0.067]	0.009 [-0.003, 0.022]	0.045* [0.033, 0.058]	0.003 [-0.009, 0.015]	30,160
Non-ischaemic cardiomyopathy	0.709 [0.681, 0.737]	0.839 [0.812, 0.866]	0.145* [0.101, 0.190]	0.130* [0.084, 0.175]	0.033 [-0.013, 0.079]	0.097* [0.053, 0.141]	0.016 [-0.029, 0.060]	30,976
Valvular heart disease	0.745 [0.739, 0.751]	0.782 [0.775, 0.789]	0.041* [0.030, 0.051]	0.037* [0.026, 0.048]	0.004 [-0.007, 0.015]	0.033* [0.023, 0.044]	0.004 [-0.007, 0.015]	30,465
Heart failure	0.769 [0.758, 0.779]	0.838 [0.827, 0.849]	0.073* [0.055, 0.091]	0.069* [0.052, 0.087]	0.024* [0.007, 0.042]	0.045* [0.027, 0.063]	0.004 [-0.013, 0.021]	30,840
Kidney combined	0.688 [0.682, 0.693]	0.757 [0.751, 0.763]	0.073* [0.063, 0.083]	0.070* [0.060, 0.079]	0.029* [0.020, 0.039]	0.040* [0.030, 0.050]	0.003 [-0.007, 0.013]	29,109
Chronic kidney disease	0.755 [0.746, 0.764]	0.796 [0.787, 0.804]	0.043* [0.029, 0.058]	0.041* [0.027, 0.055]	0.022* [0.007, 0.036]	0.019* [0.005, 0.033]	0.003 [-0.012, 0.017]	30,456
Liver disease	0.680 [0.671, 0.689]	0.743 [0.734, 0.752]	0.066* [0.051, 0.081]	0.063* [0.049, 0.078]	0.050* [0.035, 0.065]	0.013 [-0.001, 0.027]	0.003 [-0.011, 0.016]	30,306
Fatty liver disease	0.745 [0.733, 0.756]	0.821 [0.810, 0.832]	0.084* [0.066, 0.103]	0.076* [0.058, 0.095]	0.051* [0.032, 0.070]	0.025* [0.007, 0.044]	0.008 [-0.010, 0.026]	30,816
Liver cirrhosis	0.740 [0.708, 0.771]	0.816 [0.785, 0.847]	0.114* [0.064, 0.163]	0.076* [0.024, 0.129]	0.081* [0.031, 0.132]	-0.005 [-0.055, 0.045]	0.037 [-0.013, 0.088]	30,975
Combined HBLK	0.690 [0.686, 0.693]	0.740 [0.737, 0.743]	0.051* [0.046, 0.056]	0.050* [0.045, 0.055]	0.017* [0.012, 0.023]	0.033* [0.028, 0.038]	0.001 [-0.003, 0.006]	31,048

Entries are AUC values for final Cox proportional hazards models with 95% confidence intervals. The table shows how we can use the first-in-line method to calculate the incremental effect of adding imaging variables on model performance. Cells highlighted in yellow (marked with an asterisk *) show outcomes where the incremental effect is significantly different from zero.

Appendix 28: Chapter 7 - Decomposition of effects (True positives)

Outcome	Non-imaging index baseline	Pruned index + imaging + covariates	Whole effect (covariates + imaging + pruning)	Whole effect - pruning (covariates + imaging)	Effect of Covariates	Effect of Imaging	Effect of pruning	N
Athero / Peripheral artery disease	33 [26, 40]	48 [41, 55]	16* [4, 28]	15* [3, 27]	8 [-4, 20]	7 [-5, 19]	1 [-11, 13]	30,400
Venous thromboembolism	7 [1, 13]	26 [20, 32]	21* [11, 31]	19* [9, 29]	15* [5, 25]	4 [-6, 14]	2 [-8, 12]	30,007
Stroke	17 [11, 23]	28 [22, 34]	14* [4, 24]	11* [1, 21]	1 [-9, 11]	10 [-0, 20]	3 [-7, 13]	30,441
All-cause dementia	9 [3, 15]	27 [21, 33]	19* [9, 29]	18* [8, 28]	0 [-9, 9]	18* [9, 27]	1 [-9, 11]	31,004
Myocardial infarction	41 [33, 49]	56 [49, 63]	22* [10, 34]	15* [3, 27]	7 [-5, 19]	8 [-4, 20]	7 [-5, 19]	30,225
Atrial fibrillation	129 [114, 144]	236 [222, 250]	110* [86, 134]	107* [84, 130]	22 [-2, 46]	85* [61, 109]	3 [-20, 26]	30,160
Non-ischaemic cardiomyopathy	2 [-2, 6]	15 [11, 19]	13* [6, 20]	13* [7, 19]	2 [-5, 9]	11* [4, 18]	0 [-7, 7]	30,976
Valvular heart disease	96 [85, 107]	142 [131, 153]	51* [34, 68]	46* [29, 63]	18* [1, 35]	28* [11, 45]	5 [-12, 22]	30,465
Heart failure	55 [46, 64]	96 [87, 105]	46* [32, 60]	41* [26, 56]	4 [-11, 19]	37* [22, 52]	5 [-9, 19]	30,840
Kidney combined	197 [182, 212]	283 [268, 298]	87* [63, 111]	86* [62, 110]	46* [23, 69]	40* [15, 65]	1 [-22, 24]	29,109
Chronic kidney disease	59 [50, 68]	78 [69, 87]	24* [9, 39]	19* [5, 33]	15 [1, 29]	4 [-10, 18]	5 [-9, 19]	30,306
Liver disease	33 [25, 41]	48 [40, 56]	18* [5, 31]	15* [2, 28]	12 [-1, 25]	3 [-10, 16]	3 [-10, 16]	30,816
Fatty liver disease	17 [10, 24]	39 [32, 46]	18* [7, 29]	22* [11, 33]	15* [4, 26]	7 [-4, 18]	-4 [-15, 7]	30,975
Liver cirrhosis	0 [-2, 2]	4 [2, 6]	3 [-0, 6]	4* [1, 7]	0 [-4, 4]	4* [1, 7]	-1 [-4, 2]	31,048
Combined HBLK	1,320 [1,295, 1,345]	1,562 [1,537, 1,587]	248* [207, 289]	242* [202, 282]	74* [33, 115]	168* [127, 209]	6 [-35, 47]	30,400

Entries are counts of true positives (true outcomes correctly identified) for final Cox proportional hazards models with 95% confidence intervals. The table shows how we can use the first-in-line method to calculate the incremental effect of adding imaging variables on model performance. Cells highlighted in yellow (marked with an asterisk *) show outcomes where the incremental effect is significantly different from zero.

Appendix 29: Chapter 7 - Decomposition of effects (Sensitivity)

Outcome	Non-imaging index baseline	Pruned index + imaging + covariates	Whole effect (covariates + imaging + pruning)	Whole effect - pruning (covariates + imaging)	Effect of Covariates	Effect of Imaging	Effect of pruning	N
Athero / Peripheral artery disease	0.092 [0.072, 0.112]	0.134 [0.114, 0.154]	0.045* [0.011, 0.078]	0.042* [0.009, 0.074]	0.022 [-0.010, 0.055]	0.019 [-0.013, 0.052]	0.003 [-0.030, 0.035]	30,400
Venous thromboembolism	0.023 [0.003, 0.043]	0.084 [0.065, 0.104]	0.068* [0.035, 0.101]	0.062* [0.030, 0.093]	0.049* [0.016, 0.081]	0.013 [-0.019, 0.045]	0.006 [-0.026, 0.039]	30,007
Stroke	0.057 [0.037, 0.077]	0.094 [0.073, 0.115]	0.047* [0.014, 0.080]	0.037* [0.004, 0.070]	0.003 [-0.032, 0.038]	0.034 [-0.002, 0.069]	0.010 [-0.023, 0.044]	30,441
All-cause dementia	0.062 [0.022, 0.103]	0.186 [0.145, 0.228]	0.131* [0.065, 0.197]	0.124* [0.057, 0.192]	0.000 [-0.065, 0.065]	0.124* [0.060, 0.188]	0.007 [-0.062, 0.075]	31,004
Myocardial infarction	0.101 [0.082, 0.119]	0.138 [0.120, 0.156]	0.054* [0.024, 0.084]	0.037* [0.007, 0.067]	0.017 [-0.012, 0.047]	0.020 [-0.010, 0.049]	0.017 [-0.013, 0.047]	30,225
Atrial fibrillation	0.172 [0.153, 0.192]	0.315 [0.296, 0.334]	0.147* [0.115, 0.179]	0.143* [0.111, 0.174]	0.029 [-0.002, 0.061]	0.113* [0.082, 0.145]	0.004 [-0.027, 0.035]	30,160
Non-ischaemic cardiomyopathy	0.022 [0.000, 0.066]	0.161 [0.118, 0.205]	0.140* [0.067, 0.212]	0.140* [0.070, 0.210]	0.022 [-0.051, 0.094]	0.118* [0.047, 0.190]	0.000 [-0.072, 0.072]	30,976
Valvular heart disease	0.158 [0.141, 0.175]	0.234 [0.216, 0.251]	0.084* [0.056, 0.112]	0.076* [0.048, 0.104]	0.030* [0.001, 0.058]	0.046* [0.018, 0.074]	0.008 [-0.020, 0.037]	30,465
Heart failure	0.163 [0.137, 0.190]	0.285 [0.258, 0.311]	0.136* [0.094, 0.179]	0.122* [0.079, 0.165]	0.012 [-0.032, 0.056]	0.110* [0.066, 0.153]	0.015 [-0.028, 0.058]	30,840
Kidney combined	0.192 [0.178, 0.206]	0.276 [0.261, 0.290]	0.085* [0.061, 0.108]	0.084* [0.060, 0.107]	0.045* [0.022, 0.068]	0.039* [0.015, 0.063]	0.001 [-0.022, 0.024]	29,109
Chronic kidney disease	0.132 [0.112, 0.152]	0.174 [0.155, 0.194]	0.054* [0.021, 0.087]	0.043* [0.010, 0.075]	0.034* [0.001, 0.066]	0.009 [-0.023, 0.041]	0.011 [-0.021, 0.043]	30,306
Liver disease	0.092 [0.070, 0.115]	0.134 [0.112, 0.157]	0.050* [0.014, 0.086]	0.042* [0.005, 0.079]	0.034 [-0.004, 0.071]	0.008 [-0.028, 0.045]	0.008 [-0.029, 0.046]	30,816
Fatty liver disease	0.077 [0.047, 0.107]	0.176 [0.147, 0.206]	0.081* [0.032, 0.131]	0.100* [0.051, 0.148]	0.068* [0.020, 0.116]	0.032 [-0.016, 0.080]	-0.018 [-0.068, 0.032]	30,975
Liver cirrhosis	0.000 [0.000, 0.048]	0.089 [0.042, 0.135]	0.067 [-0.008, 0.142]	0.089* [0.015, 0.163]	0.000 [-0.079, 0.079]	0.089* [0.013, 0.164]	-0.022 [-0.098, 0.054]	31,048
Combined HBLK	0.413 [0.406, 0.421]	0.489 [0.481, 0.497]	0.078* [0.065, 0.090]	0.076* [0.063, 0.088]	0.023* [0.010, 0.036]	0.053* [0.040, 0.066]	0.002 [-0.011, 0.015]	30,400

Entries are sensitivity statistics for final Cox proportional hazards models with 95% confidence intervals. The table shows how we can use the first-in-line method to calculate the incremental effect of adding imaging variables on model performance. Cells highlighted in yellow (marked with an asterisk *) show outcomes where the incremental effect is significantly different from zero.

Appendix 30: Chapter 8 - Subgroup structure

QALYs lost are calculated from deaths before average life expectancy with a primary cause associated with the heart, brain, liver or kidney (HBLK) cause, plus the diagnosed HBLK disease time periods during the follow-up multiplied by 1- quality-of-life disease weights given in Table 8.1. Ninety-five percent confidence intervals are not given here because QALYs are calculated quantities derived from the sample and are not estimates. The total QALYs lost in the sample is 3,019.62, which can be checked across subgroup decompositions.

Group-ing factors	Subgroup	Subgroup description	Participants	HBLK events	QALYs lost
1	001	Men	14,870	1,952	1,846.33
1	002	Women	16,178	1,241	1,173.29
1	003	People aged less than 60yrs	10,144	546	482.42
1	004	People aged from 60 to 69yrs	13,780	1,398	1,370.36
1	005	People aged 70yrs or more	7,124	1,249	1,166.84
1	006	People with hypertension	10,350	1,670	1,673.25
1	007	People with diabetes	1,790	357	378.60
1	008	People with high cholesterol	8,847	1,431	1,356.54
1	009	People with higher local deprivation	7,074	766	731.22
1	010	People with metabolic syndrome	5,301	829	800.80
1	011	People with family history	12,821	1,370	1,316.52
2	012	Men aged less than 60yrs	4,435	297	268.66
2	013	Men aged from 60 to 69yrs	6,492	835	833.61
2	014	Men aged 70yrs or more	3,943	820	744.06
2	015	Men with hypertension	5,989	1,112	1,096.36
2	016	Men with diabetes	1,137	258	267.77
2	017	Men with high cholesterol	5,517	1,008	939.46
2	018	Men with higher local deprivation	3,329	462	441.45
2	019	Men with metabolic syndrome	3,547	617	575.39
2	020	Men with family history	5,818	787	744.96
2	021	Women aged less than 60yrs	5,709	249	213.76
2	022	Women aged from 60 to 69yrs	7,288	563	536.75
2	023	Women aged 70yrs or more	3,181	429	422.78
2	024	Women with hypertension	4,361	558	576.89
2	025	Women with diabetes	653	99	110.82
2	026	Women with high cholesterol	3,330	423	417.08
2	027	Women with higher local deprivation	3,745	304	289.77
2	028	Women with metabolic syndrome	1,754	212	225.41
2	029	Women with family history	7,003	583	571.56
2	030	People aged less than 60yrs with hypertension	2,125	203	203.09
2	031	People aged less than 60yrs with diabetes	396	51	55.31
2	032	People aged less than 60yrs with high cholesterol	1,324	143	140.87
2	033	People aged less than 60yrs with higher local deprivation	2,705	172	164.64
2	034	People aged less than 60yrs with metabolic syndrome	1,415	146	131.46
2	035	People aged less than 60yrs with family history	3,428	190	169.50
2	036	People aged from 60 to 69yrs with hypertension	4,843	706	738.43
2	037	People aged from 60 to 69yrs with diabetes	806	144	165.40
2	038	People aged from 60 to 69yrs with high cholesterol	4,096	588	561.19
2	039	People aged from 60 to 69yrs with higher local deprivation	2,956	325	318.16
2	040	People aged from 60 to 69yrs with metabolic syndrome	2,434	368	372.11
2	041	People aged from 60 to 69yrs with family history	6,287	631	626.83
2	042	People aged 70yrs or more with hypertension	3,382	761	731.73
2	043	People aged 70yrs or more with diabetes	588	162	157.88
2	044	People aged 70yrs or more with high cholesterol	3,427	700	654.48
2	045	People aged 70yrs or more with higher local deprivation	1,413	269	248.42
2	046	People aged 70yrs or more with metabolic syndrome	1,452	315	297.24
2	047	People aged 70yrs or more with family history	3,106	549	520.20
2	048	People with hypertension with diabetes	1,236	283	292.17
2	049	People with hypertension with high cholesterol	5,472	1,030	996.94

Grouping factors	Subgroup	Subgroup description	Participants	HBLK events	QALYs lost
2	050	People with hypertension with higher local deprivation	2,473	422	428.30
2	051	People with hypertension with metabolic syndrome	3,185	594	577.47
2	052	People with hypertension with family history	4,625	749	741.82
2	053	People with diabetes with high cholesterol	1,365	281	299.20
2	054	People with diabetes with higher local deprivation	521	121	139.72
2	055	People with diabetes with metabolic syndrome	1,367	296	303.68
2	056	People with diabetes with family history	755	155	156.71
2	057	People with high cholesterol with higher local deprivation	2,099	361	361.92
2	058	People with high cholesterol with metabolic syndrome	2,781	522	502.18
2	059	People with high cholesterol with family history	3,994	631	587.63
2	060	People with higher local deprivation with metabolic syndrome	1,401	252	269.18
2	061	People with higher local deprivation with family history	2,875	344	339.75
2	062	People with metabolic syndrome with family history	2,251	345	325.77
3	063	Men aged less than 60yrs with hypertension	1,165	123	125.15
3	064	Men aged less than 60yrs with diabetes	223	33	36.21
3	065	Men aged less than 60yrs with high cholesterol	812	96	97.75
3	066	Men aged less than 60yrs with higher local deprivation	1,240	94	93.03
3	067	Men aged less than 60yrs with metabolic syndrome	973	105	89.19
3	068	Men aged less than 60yrs with family history	1,460	95	86.08
3	069	Men aged from 60 to 69yrs with hypertension	2,731	458	481.52
3	070	Men aged from 60 to 69yrs with diabetes	520	105	114.53
3	071	Men aged from 60 to 69yrs with high cholesterol	2,499	403	386.00
3	072	Men aged from 60 to 69yrs with higher local deprivation	1,345	194	191.43
3	073	Men aged from 60 to 69yrs with metabolic syndrome	1,600	273	272.62
3	074	Men aged from 60 to 69yrs with family history	2,774	354	356.32
3	075	Men aged 70yrs or more with hypertension	2,093	531	489.69
3	076	Men aged 70yrs or more with diabetes	394	120	117.03
3	077	Men aged 70yrs or more with high cholesterol	2,206	509	455.70
3	078	Men aged 70yrs or more with higher local deprivation	744	174	156.99
3	079	Men aged 70yrs or more with metabolic syndrome	974	239	213.58
3	080	Men aged 70yrs or more with family history	1,584	338	302.56
3	081	Men with hypertension and diabetes	812	204	211.32
3	082	Men with hypertension and high cholesterol	3,622	740	707.18
3	083	Men with hypertension and higher local deprivation	1,385	274	272.06
3	084	Men with hypertension and metabolic syndrome	2,132	435	412.75
3	085	Men with hypertension and family history	2,521	466	448.70
3	086	Men with diabetes and high cholesterol	900	207	218.60
3	087	Men with diabetes and higher local deprivation	319	81	97.01
3	088	Men with diabetes and metabolic syndrome	896	218	215.92
3	089	Men with diabetes and family history	446	106	108.54
3	090	Men with high cholesterol and higher local deprivation	1,261	241	249.10
3	091	Men with high cholesterol and metabolic syndrome	1,952	403	383.02
3	092	Men with high cholesterol and family history	2,344	408	362.57
3	093	Men with higher local deprivation and metabolic syndrome	899	174	179.78
3	094	Men with higher local deprivation and family history	1,276	195	188.00
3	095	Men with metabolic syndrome and family history	1,411	237	212.96
3	096	Women aged less than 60yrs with hypertension	960	80	77.95
3	097	Women aged less than 60yrs with diabetes	173	18	19.10
3	098	Women aged less than 60yrs with high cholesterol	512	47	43.11
3	099	Women aged less than 60yrs with higher local deprivation	1,465	78	71.61
3	100	Women aged less than 60yrs with metabolic syndrome	442	41	42.27
3	101	Women aged less than 60yrs with family history	1,968	95	83.42
3	102	Women aged from 60 to 69yrs with hypertension	2,112	248	256.90
3	103	Women aged from 60 to 69yrs with diabetes	286	39	50.87
3	104	Women aged from 60 to 69yrs with high cholesterol	1,597	185	175.19
3	105	Women aged from 60 to 69yrs with higher local deprivation	1,611	131	126.73

Group-ing factors	Subgroup	Subgroup description	Participants	HBLK events	QALYs lost
3	106	Women aged from 60 to 69yrs with metabolic syndrome	834	95	99.49
3	107	Women aged from 60 to 69yrs with family history	3,513	277	270.51
3	108	Women aged 70yrs or more with hypertension	1,289	230	242.04
3	109	Women aged 70yrs or more with diabetes	194	42	40.85
3	110	Women aged 70yrs or more with high cholesterol	1,221	191	198.77
3	111	Women aged 70yrs or more with higher local deprivation	669	95	91.43
3	112	Women aged 70yrs or more with metabolic syndrome	478	76	83.66
3	113	Women aged 70yrs or more with family history	1,522	211	217.64
3	114	Women with hypertension and diabetes	424	79	80.85
3	115	Women with hypertension and high cholesterol	1,850	290	289.77
3	116	Women with hypertension and higher local deprivation	1,088	148	156.24
3	117	Women with hypertension and metabolic syndrome	1,053	159	164.71
3	118	Women with hypertension and family history	2,104	283	293.12
3	119	Women with diabetes and high cholesterol	465	74	80.60
3	120	Women with diabetes and higher local deprivation	202	40	42.71
3	121	Women with diabetes and metabolic syndrome	471	78	87.76
3	122	Women with diabetes and family history	309	49	48.17
3	123	Women with high cholesterol and higher local deprivation	838	120	112.82
3	124	Women with high cholesterol and metabolic syndrome	829	119	119.16
3	125	Women with high cholesterol and family history	1,650	223	225.06
3	126	Women with higher local deprivation and metabolic syndrome	502	78	89.40
3	127	Women with higher local deprivation and family history	1,599	149	151.75
3	128	Women with metabolic syndrome and family history	840	108	112.81
3	129	People aged less than 60yrs with hypertension and diabetes	226	33	31.86
3	130	People aged less than 60yrs with hypertension and high cholesterol	687	87	90.25
3	131	People aged less than 60yrs with hypertension and higher local deprivation	617	69	76.25
3	132	People aged less than 60yrs with hypertension and metabolic syndrome	672	80	76.11
3	133	People aged less than 60yrs with hypertension and family history	788	75	74.61
3	134	People aged less than 60yrs with diabetes and high cholesterol	256	34	35.52
3	135	People aged less than 60yrs with diabetes and higher local deprivation	147	20	24.17
3	136	People aged less than 60yrs with diabetes and metabolic syndrome	290	45	47.32
3	137	People aged less than 60yrs with diabetes and family history	131	21	22.70
3	138	People aged less than 60yrs with high cholesterol and higher local deprivation	428	52	63.66
3	139	People aged less than 60yrs with high cholesterol and metabolic syndrome	486	65	60.24
3	140	People aged less than 60yrs with high cholesterol and family history	537	58	53.55
3	141	People aged less than 60yrs with higher local deprivation and metabolic syndrome	463	62	60.17
3	142	People aged less than 60yrs with higher local deprivation and family history	912	65	68.57
3	143	People aged less than 60yrs with metabolic syndrome and family history	508	54	44.75
3	144	People aged from 60 to 69yrs with hypertension and diabetes	570	115	125.72
3	145	People aged from 60 to 69yrs with hypertension and high cholesterol	2,518	419	413.18
3	146	People aged from 60 to 69yrs with hypertension and higher local deprivation	1,145	181	188.96
3	147	People aged from 60 to 69yrs with hypertension and metabolic syndrome	1,524	272	273.78
3	148	People aged from 60 to 69yrs with hypertension and family history	2,316	329	336.77
3	149	People aged from 60 to 69yrs with diabetes and high cholesterol	640	119	134.93
3	150	People aged from 60 to 69yrs with diabetes and higher local deprivation	235	56	62.70
3	151	People aged from 60 to 69yrs with diabetes and metabolic syndrome	638	120	130.23
3	152	People aged from 60 to 69yrs with diabetes and family history	373	60	63.03
3	153	People aged from 60 to 69yrs with high cholesterol and higher local deprivation	972	147	138.39
3	154	People aged from 60 to 69yrs with high cholesterol and metabolic syndrome	1,337	230	220.25
3	155	People aged from 60 to 69yrs with high cholesterol and family history	1,929	261	244.02
3	156	People aged from 60 to 69yrs with higher local deprivation and metabolic syndrome	610	113	128.10
3	157	People aged from 60 to 69yrs with higher local deprivation and family history	1,333	161	157.61
3	158	People aged from 60 to 69yrs with metabolic syndrome and family history	1,106	153	151.83
3	159	People aged 70yrs or more with hypertension and diabetes	440	135	134.59
3	160	People aged 70yrs or more with hypertension and high cholesterol	2,267	524	493.51

Grouping factors	Subgroup	Subgroup description	Participants	HBLK events	QALYs lost
3	161	People aged 70yrs or more with hypertension and higher local deprivation	711	172	163.08
3	162	People aged 70yrs or more with hypertension and metabolic syndrome	989	242	227.59
3	163	People aged 70yrs or more with hypertension and family history	1,521	345	330.45
3	164	People aged 70yrs or more with diabetes and high cholesterol	469	128	128.75
3	165	People aged 70yrs or more with diabetes and higher local deprivation	139	45	52.84
3	166	People aged 70yrs or more with diabetes and metabolic syndrome	439	131	126.13
3	167	People aged 70yrs or more with diabetes and family history	251	74	70.98
3	168	People aged 70yrs or more with high cholesterol and higher local deprivation	699	162	159.87
3	169	People aged 70yrs or more with high cholesterol and metabolic syndrome	958	227	221.68
3	170	People aged 70yrs or more with high cholesterol and family history	1,528	312	290.05
3	171	People aged 70yrs or more with higher local deprivation and metabolic syndrome	328	77	80.91
3	172	People aged 70yrs or more with higher local deprivation and family history	630	118	113.57
3	173	People aged 70yrs or more with metabolic syndrome and family history	637	138	129.20
3	174	People with hypertension with diabetes and high cholesterol	1,031	230	235.67
3	175	People with hypertension with diabetes and higher local deprivation	365	102	117.55
3	176	People with hypertension with diabetes and metabolic syndrome	1,025	241	243.31
3	177	People with hypertension with diabetes and family history	554	126	121.25
3	178	People with hypertension with high cholesterol and higher local deprivation	1,354	267	274.65
3	179	People with hypertension with high cholesterol and metabolic syndrome	2,110	423	396.94
3	180	People with hypertension with high cholesterol and family history	2,528	463	437.09
3	181	People with hypertension with higher local deprivation and metabolic syndrome	850	178	193.14
3	182	People with hypertension with higher local deprivation and family history	1,096	199	199.50
3	183	People with hypertension with metabolic syndrome and family history	1,416	255	240.51
3	184	People with diabetes with high cholesterol and higher local deprivation	415	99	114.16
3	185	People with diabetes with high cholesterol and metabolic syndrome	1,089	233	243.44
3	186	People with diabetes with high cholesterol and family history	583	117	115.25
3	187	People with diabetes with higher local deprivation and metabolic syndrome	407	106	126.08
3	188	People with diabetes with higher local deprivation and family history	208	51	59.39
3	189	People with diabetes with metabolic syndrome and family history	582	128	119.92
3	190	People with high cholesterol with higher local deprivation and metabolic syndrome	764	160	173.46
3	191	People with high cholesterol with higher local deprivation and family history	936	162	162.89
3	192	People with high cholesterol with metabolic syndrome and family history	1,253	212	187.66
3	193	People with higher local deprivation with metabolic syndrome and family history	605	107	115.60

Appendix 31: Subgroup CE results for Combined HBLK (single model), with no filter

HBLK status 4

			QALYs picked up in positive predictions							
A	B	C	D	E	F	G	H	I	J	K
Sub-group	Subgroup description	N	Non-imaging index only	Index + imaging	Difference in QALYs picked up	Grouping factors	Cost of imaging (£)	ICER (£/QALY)	Outcome rate	Picked
109	Women aged 70yrs or more with diabetes	194	22 [17, 27]	31 [26, 36]	9 [1, 17]	3	112,714	11,988	21.6%	84
164	People aged 70yrs or more with diabetes and high cholesterol	469	80 [72, 89]	102 [93, 110]	22 [8, 35]	3	272,489	12,624	27.3%	256
136	People aged less than 60yrs with diabetes and MetS	290	16 [10, 22]	29 [23, 35]	13 [3, 23]	3	168,490	12,858	15.5%	90
144	People aged from 60 to 69yrs with hypertension and diabetes	570	65 [54, 76]	91 [80, 102]	26 [8, 43]	3	331,170	12,970	20.2%	230
069	Men aged from 60 to 69yrs with hypertension	2,731	207 [184, 230]	324 [301, 346]	117 [80, 153]	3	1,586,711	13,619	16.8%	916
159	People aged 70yrs or more with hypertension and diabetes	440	83 [74, 91]	101 [92, 110]	18 [5, 32]	3	255,640	13,963	30.7%	270
181	People with hypertension with higher local deprivation and MetS	850	109 [97, 121]	143 [131, 155]	34 [14, 53]	3	493,850	14,587	20.9%	356
147	People aged from 60 to 69yrs with hypertension and MetS	1,524	121 [105, 136]	181 [165, 197]	60 [35, 85]	3	885,444	14,671	17.8%	544
154	People aged from 60 to 69yrs with high cholesterol and MetS	1,337	95 [82, 108]	148 [135, 160]	53 [32, 73]	3	776,797	14,757	17.2%	460
043	People aged 70yrs or more with diabetes	588	100 [91, 109]	122 [114, 131]	22 [8, 37]	2	341,628	15,185	27.6%	324
097	Women aged less than 60yrs with diabetes	173	5 [1, 9]	11 [8, 15]	6 [0, 12]	3	100,513	15,976	10.4%	36
151	People aged from 60 to 69yrs with diabetes and MetS	638	64 [53, 75]	87 [76, 98]	23 [4, 41]	3	370,678	16,154	18.8%	240
073	Men aged from 60 to 69yrs with MetS	1,600	118 [104, 132]	176 [161, 190]	58 [34, 81]	3	929,600	16,163	17.1%	546
176	People with hypertension with diabetes and MetS	1,025	144 [130, 157]	179 [166, 192]	35 [14, 57]	3	595,525	16,857	23.5%	482
172	People aged 70yrs or more with higher local deprivation and FH	630	60 [50, 71]	82 [72, 92]	21 [4, 39]	3	366,030	17,048	18.7%	236
085	Men with hypertension and family history	2,521	215 [198, 232]	299 [281, 317]	84 [55, 113]	3	1,464,701	17,394	18.5%	932
166	People aged 70yrs or more with diabetes and MetS	439	86 [79, 94]	101 [93, 109]	14 [1, 28]	3	255,059	17,619	29.8%	262
076	Men aged 70yrs or more with diabetes	394	78 [70, 86]	91 [83, 98]	13 [0, 25]	3	228,914	18,069	30.5%	240
015	Men with hypertension	5,989	541 [513, 569]	734 [706, 761]	192 [147, 238]	2	3,479,609	18,086	18.6%	2,224
077	Men aged 70yrs or more with high cholesterol	2,206	261 [241, 281]	331 [310, 352]	70 [37, 103]	3	1,281,686	18,247	23.1%	1,018
070	Men aged from 60 to 69yrs with diabetes	520	62 [53, 71]	79 [70, 88]	16 [2, 31]	3	302,120	18,544	20.2%	210
081	Men with hypertension and diabetes	812	131 [120, 143]	156 [145, 168]	25 [6, 44]	3	471,772	18,960	25.1%	408
084	Men with hypertension and MetS	2,132	223 [207, 239]	288 [272, 304]	65 [39, 91]	3	1,238,692	19,052	20.4%	870
145	People aged from 60 to 69yrs with hypertension and high cholesterol	2,518	198 [179, 216]	274 [255, 294]	77 [46, 108]	3	1,462,958	19,058	16.6%	838
121	Women with diabetes and MetS	471	38 [30, 47]	53 [44, 61]	14 [1, 28]	3	273,651	19,079	16.6%	156
055	People with diabetes and MetS	1,367	172 [159, 185]	213 [199, 227]	41 [19, 64]	2	794,227	19,261	21.7%	592
108	Women aged 70yrs or more with hypertension	1,289	108 [94, 123]	147 [133, 162]	39 [16, 62]	3	748,909	19,267	17.8%	460
048	People with hypertension with diabetes	1,236	175 [161, 189]	212 [198, 226]	37 [14, 59]	2	718,116	19,527	22.9%	566
051	People with hypertension with MetS	3,185	289 [270, 309]	384 [364, 403]	94 [63, 126]	2	1,850,485	19,605	18.6%	1,188
080	Men aged 70yrs or more with family history	1,584	157 [143, 171]	204 [190, 219]	47 [24, 70]	3	920,304	19,672	21.3%	676
006	People with hypertension	10,350	805 [771, 839]	1,046 [1,014, 1,078]	241 [187, 295]	1	6,013,350	24,946	16.1%	3,340

Subgroup cost-effectiveness results for the lowest 30 subgroup ICERs for this outcome. In columns D, E and F, entries are QALYs picked up in positive predictions with 95% confidence intervals. Rows with no shading show subgroups with 3 grouping factors, rows with green shading show subgroups with 2 grouping factors and the most cost-effective subgroup with a single grouping factor is provided in grey in the bottom row of the table. Img = Imaging, QALY = quality adjusted life year, ICER = incremental cost-effectiveness ratio, GF= grouping factors, MetS= metabolic syndrome, FH= family history, high chol.= high cholesterol, HTN = hypertension.

Appendix 32: Subgroup CE results for Combined HBLK (single model), above median risk

HBLK status 4 HIGH

			QALYs picked up in positive predictions							
A	B	C	D	E	F	G	H	I	J	K
Sub-group	Subgroup description	N	Non-imaging index only	Index + imaging	Difference in QALYs picked up	GF	Cost of imaging (£)	ICER (£/QALY)	Outcome rate	Picked
137	People aged less than 60yrs with diabetes and family history	70	6 [1, 10]	13 [9, 17]	7 [0, 14]	3	40,670	5,682	21.4%	30
181	People with hypertension with higher local deprivation and MetS	694	100 [88, 112]	136 [123, 148]	35 [15, 55]	3	403,214	11,455	23.5%	326
151	People aged from 60 to 69yrs with diabetes and MetS	598	57 [46, 68]	87 [76, 98]	30 [12, 48]	3	347,438	11,599	19.6%	234
109	Women aged 70yrs or more with diabetes	193	22 [17, 27]	31 [26, 36]	9 [1, 18]	3	112,133	11,926	21.8%	84
144	People aged from 60 to 69yrs with hypertension and diabetes	547	65 [54, 76]	90 [79, 102]	25 [7, 44]	3	317,807	12,574	20.5%	224
164	People aged 70yrs or more with diabetes and high cholesterol	468	80 [72, 89]	102 [93, 110]	22 [8, 35]	3	271,908	12,597	27.4%	256
140	People aged less than 60yrs with high cholesterol and family history	136	5 [2, 8]	12 [8, 15]	6 [1, 11]	3	79,016	12,640	16.9%	46
069	Men aged from 60 to 69yrs with hypertension	2,516	202 [179, 225]	318 [295, 340]	116 [79, 152]	3	1,461,796	12,652	17.6%	888
147	People aged from 60 to 69yrs with hypertension and MetS	1,363	118 [102, 133]	175 [160, 191]	58 [32, 83]	3	791,903	13,762	18.4%	502
138	People aged less than 60yrs with high chol. and higher deprivation	132	11 [8, 15]	17 [13, 20]	6 [0, 11]	3	76,692	13,841	18.9%	50
159	People aged 70yrs or more with hypertension and diabetes	440	83 [74, 91]	101 [93, 109]	18 [5, 32]	3	255,640	13,963	30.7%	270
073	Men aged from 60 to 69yrs with MetS	1,411	114 [100, 129]	171 [157, 185]	57 [33, 80]	3	819,791	14,490	18.3%	516
193	People with higher local deprivation with MetS and family history	446	50 [42, 58]	68 [60, 76]	18 [5, 31]	3	259,126	14,529	20.2%	180
154	People aged from 60 to 69yrs with high cholesterol and MetS	1,221	93 [80, 107]	142 [128, 156]	49 [26, 71]	3	709,401	14,591	17.7%	432
068	Men aged less than 60yrs with family history	147	7 [4, 10]	13 [10, 16]	6 [1, 11]	3	85,407	14,602	15.0%	44
043	People aged 70yrs or more with diabetes	587	100 [91, 109]	122 [113, 131]	22 [8, 37]	2	341,047	15,159	27.6%	324
117	Women with hypertension and MetS	771	53 [42, 64]	82 [71, 92]	28 [11, 46]	3	447,951	15,724	16.5%	254
094	Men with higher local deprivation and family history	830	77 [68, 86]	107 [98, 116]	30 [16, 45]	3	482,230	15,881	19.9%	330
187	People with diabetes with higher local deprivation and MetS	363	81 [73, 89]	94 [86, 102]	13 [0, 26]	3	210,903	15,953	28.7%	208
121	Women with diabetes and MetS	383	36 [28, 45]	50 [42, 59]	14 [0, 28]	3	222,523	16,135	18.3%	140
060	People with higher local deprivation with MetS	963	132 [119, 145]	167 [154, 180]	35 [13, 56]	2	559,503	16,141	21.7%	418
091	Men with high cholesterol and MetS	1,709	205 [188, 222]	266 [250, 282]	61 [35, 88]	3	992,929	16,225	22.1%	756
182	People with hypertension with higher deprivation and family history	847	91 [82, 100]	121 [112, 131]	30 [15, 45]	3	492,107	16,225	20.5%	348
130	People aged less than 60yrs with hypertension and high cholesterol	261	18 [13, 22]	27 [22, 31]	9 [2, 16]	3	151,641	16,314	17.2%	90
052	People with hypertension with family history	3,561	305 [284, 326]	430 [408, 452]	125 [90, 161]	2	2,068,941	16,512	18.6%	1,328
156	People aged from 60 to 69yrs with higher deprivation and MetS	526	73 [62, 85]	92 [81, 103]	18 [0, 37]	3	305,606	16,542	20.2%	212
018	Men with higher local deprivation	1,984	183 [169, 198]	253 [239, 267]	70 [46, 93]	2	1,152,704	16,554	19.2%	762
176	People with hypertension with diabetes and MetS	937	139 [126, 152]	172 [159, 185]	33 [12, 54]	3	544,397	16,588	24.4%	458
190	People with high cholesterol with higher local deprivation and MetS	641	99 [89, 109]	121 [111, 131]	22 [6, 39]	3	372,421	16,590	22.9%	294
081	Men with hypertension and diabetes	756	129 [118, 141]	156 [144, 167]	26 [7, 45]	3	439,236	16,705	26.3%	398
006	People with hypertension	7,653	705 [671, 740]	972 [938, 1,005]	266 [211, 321]	1	4,446,393	16,707	19.0%	2,908

Subgroup cost-effectiveness results for the lowest 30 subgroup ICERs for this outcome. In columns D, E and F, entries are QALYs picked up in positive predictions with 95% confidence intervals. Rows with no shading show subgroups with 3 grouping factors, rows with green shading show subgroups with 2 grouping factors and the most cost-effective subgroup with a single grouping factor is provided in grey in the bottom row of the table. Img = Imaging, QALY = quality adjusted life year, ICER = incremental cost-effectiveness ratio, GF= grouping factors, MetS= metabolic syndrome, FH= family history, high chol.= high cholesterol, HTN = hypertension

Appendix 33: Subgroup CE results for Aggregated HBLK risk (multi-model), with no filter

			QALYs picked up in positive predictions							
A	B	C	D	E	F	G	H	I	J	K
Sub-group	Subgroup description	N	Non-imaging index only	Index + imaging	Difference in QALYs picked up	GF	Cost of imaging (£)	ICER (£/QALY)	Outcome rate	Picked
109	Women aged 70yrs or more with diabetes	194	19 [13, 24]	30 [24, 35]	11 [3, 19]	3	112,714	10,078	21.6%	64
069	Men aged from 60 to 69yrs with hypertension	2,731	127 [108, 147]	279 [258, 299]	151 [119, 184]	3	1,586,711	10,486	16.8%	486
159	People aged 70yrs or more with hypertension and diabetes	440	81 [73, 90]	106 [97, 115]	24 [10, 39]	3	255,640	10,493	30.7%	246
166	People aged 70yrs or more with diabetes and MetS	439	83 [74, 91]	105 [97, 113]	22 [9, 36]	3	255,059	11,396	29.8%	230
169	People aged 70yrs or more with high cholesterol and MetS	958	115 [103, 127]	164 [150, 177]	49 [29, 68]	3	556,598	11,455	23.7%	379
043	People aged 70yrs or more with diabetes	588	93 [82, 104]	119 [109, 130]	26 [10, 43]	2	341,628	13,084	27.6%	273
168	People aged 70yrs or more with high chol. and higher deprivation	699	85 [75, 94]	115 [105, 126]	30 [14, 47]	3	406,119	13,319	23.2%	246
147	People aged from 60 to 69yrs with hypertension and MetS	1,524	113 [99, 128]	179 [164, 194]	66 [42, 90]	3	885,444	13,458	17.8%	474
145	People aged from 60 to 69yrs with hypertension and high cholesterol	2,518	133 [115, 152]	239 [219, 260]	106 [73, 139]	3	1,462,958	13,798	16.6%	517
078	Men aged 70yrs or more with higher local deprivation	744	72 [62, 82]	103 [92, 113]	31 [14, 47]	3	432,264	14,031	23.4%	225
114	Women with hypertension and diabetes	424	31 [22, 40]	48 [40, 57]	17 [4, 31]	3	246,344	14,105	18.6%	119
148	People aged from 60 to 69yrs with hypertension and family history	2,316	70 [54, 86]	162 [145, 180]	92 [65, 119]	3	1,345,596	14,603	14.2%	312
071	Men aged from 60 to 69yrs with high cholesterol	2,499	109 [91, 126]	207 [189, 226]	99 [69, 128]	3	1,451,919	14,727	16.1%	455
161	People aged 70yrs or more with HTN and higher local deprivation	711	89 [79, 98]	116 [107, 126]	28 [13, 43]	3	413,091	14,916	24.2%	271
036	People aged from 60 to 69yrs with hypertension	4,843	174 [151, 197]	360 [337, 384]	187 [150, 223]	2	2,813,783	15,086	14.6%	652
073	Men aged from 60 to 69yrs with MetS	1,600	106 [92, 121]	167 [153, 181]	61 [39, 83]	3	929,600	15,276	17.1%	424
077	Men aged 70yrs or more with high cholesterol	2,206	209 [188, 230]	293 [271, 314]	84 [51, 117]	3	1,281,686	15,284	23.1%	778
075	Men aged 70yrs or more with hypertension	2,093	245 [226, 264]	324 [305, 344]	79 [47, 111]	3	1,216,033	15,306	25.4%	881
160	People aged 70yrs or more with hypertension and high cholesterol	2,267	239 [221, 258]	320 [301, 339]	81 [51, 111]	3	1,317,127	16,263	23.1%	890
163	People aged 70yrs or more with hypertension and family history	1,521	143 [127, 160]	197 [180, 214]	54 [27, 82]	3	883,701	16,324	22.7%	522
176	People with hypertension with diabetes and MetS	1,025	123 [111, 136]	160 [146, 173]	36 [15, 57]	3	595,525	16,453	23.5%	403
156	People aged from 60 to 69yrs with higher deprivation and MetS	610	70 [59, 81]	91 [80, 103]	21 [3, 40]	3	354,410	16,625	18.5%	190
042	People aged 70yrs or more with hypertension	3,382	310 [285, 334]	428 [402, 454]	118 [77, 159]	2	1,964,942	16,636	22.5%	1,168
080	Men aged 70yrs or more with family history	1,584	112 [95, 128]	167 [150, 184]	55 [28, 82]	3	920,304	16,760	21.3%	428
158	People aged from 60 to 69yrs with MetS and family history	1,106	47 [36, 59]	85 [74, 95]	38 [21, 55]	3	642,586	17,080	13.8%	247
164	People aged 70yrs or more with diabetes and high cholesterol	469	83 [74, 92]	99 [90, 107]	16 [1, 31]	3	272,489	17,098	27.3%	228
144	People aged from 60 to 69yrs with hypertension and diabetes	570	51 [40, 63]	70 [59, 81]	19 [1, 37]	3	331,170	17,687	20.2%	140
040	People aged from 60 to 69yrs with MetS	2,434	134 [118, 149]	213 [196, 230]	80 [53, 107]	2	1,414,154	17,727	15.1%	549
170	People aged 70yrs or more with high cholesterol and family history	1,528	115 [101, 130]	165 [151, 180]	50 [26, 73]	3	887,768	17,846	20.4%	458
121	Women with diabetes and MetS	471	29 [20, 38]	44 [35, 52]	15 [1, 29]	3	273,651	18,149	16.6%	114
006	People with hypertension	10,350	677 [643, 711]	964 [927, 1,000]	287 [228, 346]	1	6,013,350	20,946	16.1%	2,664

Subgroup cost-effectiveness results for the lowest 30 subgroup ICERs for this outcome. In columns D, E and F, entries are QALYs picked up in positive predictions with 95% confidence intervals. Rows with no shading show subgroups with 3 grouping factors, rows with green shading show subgroups with 2 grouping factors and the most cost-effective subgroup with a single grouping factor is provided in grey in the bottom row of the table. Img = Imaging, QALY = quality adjusted life year, ICER = incremental cost-effectiveness ratio, GF= grouping factors, MetS= metabolic syndrome, FH= family history, high chol.= high cholesterol, HTN = hypertension.

Appendix 34: Subgroup CE results for Aggregated HBLK risk (multi-model), risk ≥ 8

			QALYs picked up in positive predictions							
A	B	C	D	E	F	G	H	I	J	K
Sub-group	Subgroup description	N	Non-imaging index only	Index + imaging	Difference in QALYs picked up	GF	Cost of imaging (£)	ICER (£/QALY)	Outcome rate	Picked
138	People aged less than 60yrs with high chol. and higher deprivation	125	6 [2, 10]	16 [12, 20]	10 [4, 16]	3	72,625	7,382	19.2%	34
141	People aged less than 60yrs with higher local deprivation and MetS	115	8 [4, 12]	15 [11, 19]	7 [1, 13]	3	66,815	9,691	23.5%	35
069	Men aged from 60 to 69yrs with hypertension	2,533	127 [105, 149]	278 [256, 299]	151 [115, 187]	3	1,471,673	9,751	17.5%	479
109	Women aged 70yrs or more with diabetes	193	19 [13, 24]	30 [25, 35]	11 [3, 19]	3	112,133	10,026	21.8%	64
159	People aged 70yrs or more with hypertension and diabetes	440	81 [72, 91]	106 [97, 115]	24 [10, 39]	3	255,640	10,493	30.7%	246
166	People aged 70yrs or more with diabetes and MetS	439	83 [74, 92]	105 [96, 114]	22 [8, 37]	3	255,059	11,396	29.8%	230
169	People aged 70yrs or more with high cholesterol and MetS	957	114 [102, 127]	163 [151, 175]	49 [30, 68]	3	556,017	11,443	23.6%	378
148	People aged from 60 to 69yrs with hypertension and family history	1,888	70 [54, 87]	161 [144, 178]	91 [64, 118]	3	1,096,928	12,039	15.6%	305
036	People aged from 60 to 69yrs with hypertension	3,901	173 [149, 197]	353 [330, 376]	180 [142, 219]	2	2,266,481	12,582	16.2%	631
139	People aged less than 60yrs with high cholesterol and MetS	199	10 [6, 14]	19 [15, 23]	9 [2, 16]	3	115,619	12,645	18.6%	48
145	People aged from 60 to 69yrs with hypertension and high cholesterol	2,257	133 [114, 152]	236 [217, 255]	103 [72, 133]	3	1,311,317	12,751	17.6%	511
043	People aged 70yrs or more with diabetes	587	93 [83, 104]	119 [109, 130]	26 [10, 43]	2	341,047	13,062	27.6%	273
168	People aged 70yrs or more with high chol. and higher deprivation	698	85 [74, 95]	115 [105, 126]	30 [13, 48]	3	405,538	13,300	23.2%	245
071	Men aged from 60 to 69yrs with high cholesterol	2,265	109 [91, 126]	207 [189, 225]	99 [70, 127]	3	1,315,965	13,348	17.0%	452
073	Men aged from 60 to 69yrs with MetS	1,425	106 [91, 120]	166 [152, 181]	61 [37, 84]	3	827,925	13,605	18.1%	417
078	Men aged 70yrs or more with higher local deprivation	744	72 [62, 82]	103 [93, 113]	31 [14, 48]	3	432,264	14,031	23.4%	225
158	People aged from 60 to 69yrs with MetS and family history	927	47 [37, 58]	85 [74, 95]	38 [21, 55]	3	538,587	14,316	15.1%	240
114	Women with hypertension and diabetes	373	31 [23, 39]	46 [38, 54]	15 [2, 28]	3	216,713	14,429	19.6%	119
156	People aged from 60 to 69yrs with higher deprivation and MetS	535	70 [59, 81]	91 [80, 102]	21 [4, 39]	3	310,835	14,581	19.8%	187
161	People aged 70yrs or more with hypertension and higher deprivation	710	89 [79, 98]	116 [107, 126]	28 [13, 43]	3	412,510	14,895	24.2%	270
155	People aged from 60 to 69yrs with high cholesterol and FH	1,540	58 [46, 71]	117 [104, 130]	59 [38, 79]	3	894,740	15,233	14.3%	266
074	Men aged from 60 to 69yrs with family history	2,217	62 [45, 78]	146 [130, 162]	84 [58, 111]	3	1,288,077	15,249	14.1%	251
013	Men aged from 60 to 69yrs	5,023	155 [131, 178]	346 [321, 371]	191 [152, 231]	2	2,918,363	15,252	14.6%	566
077	Men aged 70yrs or more with high cholesterol	2,205	208 [189, 228]	292 [271, 313]	84 [51, 117]	3	1,281,105	15,277	23.0%	777
075	Men aged 70yrs or more with hypertension	2,092	244 [225, 264]	324 [306, 342]	79 [49, 110]	3	1,215,452	15,298	25.3%	880
040	People aged from 60 to 69yrs with MetS	2,021	133 [117, 149]	209 [193, 225]	76 [50, 102]	2	1,174,201	15,396	16.4%	530
146	People aged from 60 to 69yrs with HTN and higher deprivation	964	73 [61, 85]	109 [97, 121]	35 [16, 54]	3	560,084	15,859	17.3%	213
038	People aged from 60 to 69yrs with high cholesterol	3,232	147 [127, 167]	265 [245, 285]	118 [84, 151]	2	1,877,792	15,978	16.1%	579
072	Men aged from 60 to 69yrs with higher local deprivation	1,097	59 [47, 71]	98 [87, 110]	39 [20, 59]	3	637,357	16,168	16.3%	180
160	People aged 70yrs or more with hypertension and high cholesterol	2,265	239 [220, 258]	320 [300, 339]	81 [50, 112]	3	1,315,965	16,248	23.1%	888
001	Men	9,312	620 [587, 653]	916 [882, 950]	296 [242, 350]	1	5,410,272	18,269	17.3%	2,421

Subgroup cost-effectiveness results for the lowest 30 subgroup ICERs for this outcome. In columns D, E and F, entries are QALYs picked up in positive predictions with 95% confidence intervals. Rows with no shading show subgroups with 3 grouping factors, rows with green shading show subgroups with 2 grouping factors and the most cost-effective subgroup with a single grouping factor is provided in grey in the bottom row of the table. Img = Imaging, QALY = quality adjusted life year, ICER = incremental cost-effectiveness ratio, GF= grouping factors, MetS= metabolic syndrome, FH= family history, high chol.= high cholesterol, HTN = hypertension.

Appendix 35: Subgroup CE results for Aggregated HBLK risk (multi-model), risk ≥ 12

			QALYs picked up in positive predictions							
A	B	C	D	E	F	G	H	I	J	K
Sub-group	Subgroup description	Img N	Non-imaging index only	Index + imaging	Difference in QALYs picked up	GF	Cost of imaging (£)	ICER (£/QALY)	Outcome rate	Picked N
120	Women with diabetes and higher local deprivation	131	13 [6, 20]	25 [18, 32]	12 [0, 23]	3	76,111	6,529	20.6%	38
159	People aged 70yrs or more with hypertension and diabetes	389	67 [59, 75]	92 [84, 100]	25 [12, 38]	3	226,009	8,972	29.8%	206
069	Men aged from 60 to 69yrs with hypertension	2,086	99 [79, 119]	233 [212, 254]	134 [101, 166]	3	1,211,966	9,071	17.6%	395
148	People aged from 60 to 69yrs with hypertension and family history	1,414	53 [38, 68]	132 [117, 148]	80 [55, 104]	3	821,534	10,316	16.2%	242
166	People aged 70yrs or more with diabetes and MetS	408	67 [59, 75]	90 [82, 97]	22 [10, 35]	3	237,048	10,591	28.4%	203
114	Women with hypertension and diabetes	301	24 [16, 32]	41 [33, 48]	16 [3, 29]	3	174,881	10,687	18.9%	87
036	People aged from 60 to 69yrs with hypertension	2,906	132 [110, 153]	287 [266, 308]	155 [122, 188]	2	1,688,386	10,877	16.7%	516
169	People aged 70yrs or more with high cholesterol and MetS	906	92 [80, 105]	139 [126, 152]	47 [27, 67]	3	526,386	11,269	22.7%	338
145	People aged from 60 to 69yrs with hypertension and high cholesterol	1,768	92 [75, 109]	182 [165, 200]	90 [61, 119]	3	1,027,208	11,367	17.4%	410
072	Men aged from 60 to 69yrs with higher local deprivation	777	47 [36, 58]	85 [73, 98]	38 [18, 59]	3	451,437	11,768	17.1%	149
071	Men aged from 60 to 69yrs with high cholesterol	1,809	78 [62, 94]	167 [150, 184]	89 [62, 116]	3	1,051,029	11,790	16.9%	369
074	Men aged from 60 to 69yrs with family history	1,595	47 [31, 63]	125 [110, 141]	78 [52, 104]	3	926,695	11,843	15.1%	198
064	Men aged less than 60yrs with diabetes	80	4 [2, 7]	8 [6, 11]	4 [0, 8]	3	46,480	11,957	21.3%	22
168	People aged 70yrs or more with high chol. and higher deprivation	572	62 [53, 71]	89 [80, 98]	28 [13, 42]	3	332,332	12,060	22.2%	200
165	People aged 70yrs or more with diabetes and higher local deprivation	125	29 [25, 33]	35 [31, 39]	6 [0, 12]	3	72,625	12,482	28.0%	69
073	Men aged from 60 to 69yrs with MetS	1,255	91 [77, 104]	149 [135, 163]	58 [36, 80]	3	729,155	12,521	18.2%	370
013	Men aged from 60 to 69yrs	3,582	120 [94, 146]	286 [262, 309]	166 [126, 205]	2	2,081,142	12,564	15.5%	466
155	People aged from 60 to 69yrs with high chol. and family history	1,110	41 [30, 52]	92 [80, 104]	51 [33, 69]	3	644,910	12,619	15.0%	204
076	Men aged 70yrs or more with diabetes	362	60 [52, 68]	76 [68, 84]	16 [4, 29]	3	210,322	12,846	28.5%	180
146	People aged from 60 to 69yrs with HTN and higher local deprivation	708	58 [47, 70]	90 [79, 101]	32 [13, 50]	3	411,348	12,957	17.8%	178
038	People aged from 60 to 69yrs with high cholesterol	2,355	103 [84, 121]	208 [191, 225]	105 [76, 134]	2	1,368,255	12,987	16.6%	463
167	People aged 70yrs or more with diabetes and family history	225	37 [31, 43]	47 [42, 52]	10 [2, 18]	3	130,725	13,054	28.0%	124
090	Men with high cholesterol and higher local deprivation	841	67 [55, 79]	105 [94, 116]	37 [19, 56]	3	488,621	13,070	20.9%	223
121	Women with diabetes and MetS	332	22 [15, 30]	37 [29, 45]	15 [2, 27]	3	192,892	13,218	16.9%	89
139	People aged less than 60yrs with high cholesterol and MetS	118	7 [3, 10]	12 [8, 15]	5 [0, 10]	3	68,558	13,277	19.5%	31
041	People aged from 60 to 69yrs with family history	2,229	66 [48, 85]	163 [145, 181]	97 [66, 127]	2	1,295,049	13,420	14.5%	278
163	People aged 70yrs or more with hypertension and family history	1,267	113 [99, 128]	165 [149, 181]	52 [27, 76]	3	736,127	14,184	22.7%	406
176	People with hypertension with diabetes and MetS	843	100 [86, 113]	134 [122, 146]	34 [14, 55]	3	489,783	14,257	23.5%	340
025	Women with diabetes	401	26 [18, 35]	43 [35, 50]	16 [3, 30]	2	232,981	14,270	17.5%	99
040	People aged from 60 to 69yrs with MetS	1,740	116 [101, 131]	187 [172, 201]	70 [45, 96]	2	1,010,940	14,346	16.7%	470
004	People aged from 60 to 69yrs	4,776	158 [134, 182]	347 [321, 373]	189 [148, 231]	1	2,774,856	14,668	14.8%	598

Subgroup cost-effectiveness results for the lowest 30 subgroup ICERs for this outcome. In columns D, E and F, entries are QALYs picked up in positive predictions with 95% confidence intervals. Rows with no shading show subgroups with 3 grouping factors, rows with green shading show subgroups with 2 grouping factors and the most cost-effective subgroup with a single grouping factor is provided in grey in the bottom row of the table. Img = Imaging, QALY = quality adjusted life year, ICER = incremental cost-effectiveness ratio, GF= grouping factors, MetS= metabolic syndrome, FH= family history, high chol.= high cholesterol, HTN = hypertension.